ANNUAL REVIEW OF NUCLEAR SCIENCE

VOLUME 2

1953

PUBLISHED BY

ANNUAL REVIEWS, INC.
IN CO-OPERATION WITH THE
NATIONAL RESEARCH COUNCIL
OF THE NATIONAL ACADEMY OF SCIENCES

ON SALE BY

ANNUAL REVIEWS, INC.
STANFORD, CALIFORNIA, U.S.A.

Engin. Library
QC
770
A65
v. 2

ANNUAL REVIEWS, INC.
STANFORD, CALIFORNIA, U.S.A.

FOREIGN AGENCIES

H. K. Lewis & Company, Ltd.
136 Gower Street
London, W.C. 1

Maruzen Company, Ltd.
6 Tori-Nichome Nihonbashi
Tokyo

PRINTED AND BOUND IN THE UNITED STATES OF AMERICA BY
THE GEORGE BANTA PUBLISHING COMPANY

PREFACE

This is the second in a series of annual review volumes planned to cover the most important developments in the fields of nuclear science each year. The original plans for this volume were drawn up by the Committee on Nuclear Science of the National Research Council. Early in 1952, arrangements were concluded between the National Research Council and Annual Reviews, Inc. providing for Annual Reviews to assume the responsibility for the volumes of this series. Accordingly, the editing of this volume has been the responsibility of James G. Beckerley, Editor of the series, assisted by Martin D. Kamen, Donald F. Mastick, and Leonard I. Schiff, Associate Editors.

Most of the work of planning this volume and arranging for the preparation of manuscripts was accomplished by Donald F. Mastick of the Subcommittee on Publications and Information, Committee on Nuclear Science.

It is a pleasure to acknowledge the assistance of Carol F. Kupke of the staff of Annual Reviews, Inc. in the editorial preparation of this material for the printer.

The contents of this volume have been cleared with respect to security by the proper authorities.

JAMES G. BECKERLEY, *Editor*
ALBERTO F. THOMPSON, *Chairman,*
Subcommittee on Publications and Information Committee on Nuclear Science

TOPICS AND AUTHORS
ANNUAL REVIEW OF NUCLEAR SCIENCE
VOLUME 3 (1954)

PHOTOGRAPHIC EMULSIONS, *Y. Goldschmidt-Clermont*

EXTRANUCLEAR INTERACTIONS OF ELECTRONS AND GAMMA RADIATIONS WITH MATTER, *D. R. Corson and A. O. Hanson*

NUCLEAR REACTIONS OF INTERMEDIATE ENERGY HEAVY PARTICLES, *V. F. Weisskopf*

NUCLEAR REACTORS, *H. Brooks*

INTERACTION OF NEUTRONS WITH MATTER, *D. J. Hughes*

MESONS, *J. Steinberger*

COSMIC RAYS, *L. Leprince-Ringuet*

STANDARDIZATION OF NEUTRON MEASUREMENTS, *A. Wattenberg*

RADIATION DOSIMETRY AND PROTECTION, *L. D. Marinelli*

RADIATION CHEMISTRY, *J. L. Magee*

CHEMICAL EFFECTS FOLLOWING NUCLEAR TRANSFORMATIONS, *J. E. Willard*

CHEMICAL TECHNIQUES FOR RADIOACTIVE PREPARATIONS, *P. Stevenson and H. G. Hicks*

VERTEBRATE RADIOBIOLOGY: EMBRYOLOGY, *B. Rugh*

VERTEBRATE RADIOBIOLOGY: CARCINOGENESIS AND HISTOPATHOLOGY, *J. Furth and A. C. Upton*

CELLULAR RADIOBIOLOGY, *A. H. Sparrow and F. Forro*

MEDICINE IN NUCLEAR SCIENCE, *L. H. Hempelmann*

ISOTOPE EFFECT IN CHEMICAL REACTIONS, *M. Calvin and P. Yankwich*

CONTENTS

PAGE

THE ORIGIN AND ABUNDANCE DISTRIBUTION OF THE ELEMENTS, *R. A. Alpher and R. C. Herman* 1

ENERGY PRODUCTION IN STARS, *E. E. Salpeter* 41

THE PRODUCTION AND DISTRIBUTION OF NATURAL RADIOCARBON, *E. C. Anderson*. 63

RECENT PROGRESS IN ACCELERATORS, *E. L. Chu and L. I. Schiff* . . 79

NUCLEAR REACTIONS INDUCED BY HIGH ENERGY PARTICLES, *D. H. Templeton* 93

RECENT STUDIES OF PHOTONUCLEAR REACTIONS, *K. Strauch* . . . 105

ANGULAR CORRELATION OF NUCLEAR RADIATION, *H. Frauenfelder* . 129

SUBNUCLEAR PARTICLES, *J. S. Blair and G. F. Chew* 163

RADIATION EFFECTS IN SOLIDS, *G. J. Dienes* 187

ISOTOPES, *J. Bigeleisen* 221

NUCLEAR MOMENTS, *B. T. Feld* 239

THE EXPERIMENTAL CLARIFICATION OF THE THEORY OF β-DECAY, *E. J. Konopinski and L. M. Langer* 261

β-DECAY ENERGETICS, *C. D. Coryell* 305

ORIGIN AND PROPAGATION OF COSMIC RAYS, *L. Biermann* 335

ADVANCES IN NUCLEON-NUCLEON SCATTERING EXPERIMENTS AND THEIR THEORETICAL CONSEQUENCES, *G. Breit and R. L. Gluckstern* 365

HIGH ENERGY FISSION, *R. W. Spence and G. P. Ford* 399

INDEXES 411

Annual Reviews, Inc., the National Research Council, and the Editors of this publication assume no responsibility for the statements expressed by the contributors to this *Review*.

THE ORIGIN AND ABUNDANCE DISTRIBUTION OF THE ELEMENTS[1,2]

By Ralph A. Alpher and Robert C. Herman[3]

Applied Physics Laboratory, The Johns Hopkins University, Silver Spring, Maryland

Introduction

During the past two decades there has been a considerable effort made toward understanding the origin and relative abundance distribution of nuclear species. This has been made possible by advances in nuclear physics and astrophysics which indicate that the origin and the observed abundance distribution must be closely connected. On the one hand, nuclear physics suggests a generic relationship between nuclear species in that they are composed of the same constituents and exhibit significant correlations between their systematic properties and abundances. On the other hand, astrophysics suggests that our present universe has a definite age, that the observed relative abundances appear to be universal quantities, and that the physical conditions required for nuclear synthesis might be found in the early stages of the universe or in the interiors of special types of stars.

The principal stimulus for theoretical speculation has been the recent analysis and compilation of adequate relative abundance data. Several very different theories have been developed to explain the origin and abundance distribution of the elements. One of the earliest of these describes the observed abundances as a "frozen-in" thermodynamic equilibrium distribution of an assembly of nuclei and elementary particles, where the fundamental parameters are nuclear binding energies, temperature and density. In a recent theory the abundances of the elements are considered as resulting from non-equilibrium processes, involving the formation of the lightest nuclei by thermonuclear processes with both neutrons and charged particles, and formation of the remaining nuclei principally by the successive radiative capture of neutrons, with intervening β-decay. In a third type of theory the formation of elements involves the fission of one or many supernuclei or polyneutron complexes. Finally, another attack on this problem which leads to a steady-state cosmology involves either the continuous and spontaneous creation of matter uniformly throughout the universe at a rate such as to maintain the mean density of the universe at a constant value, or the sudden appearance in the universe of stars, identified as supernovae. The foregoing theories, differing in the proposed mechanisms and in the associated cosmological models, are all confronted with sundry difficulties, and it is not evident as yet that any one of them represents a final solution of this ancient problem.

[1] The survey of the literature pertaining to this review was concluded in July 1952.

[2] This work was supported by the U. S. Navy Bureau of Ordnance.

[3] For a more detailed review through 1950 by the authors see reference (10).

Recent reviews of this problem which are in various ways limited in scope include those of Gamow (65, 67), Gamow & Critchfield (68), and ter Haar (82, 83, 84). A more complete review was given by the present authors several years ago [Alpher & Herman (10)], and it is the purpose of this chapter to cover the material of this former review somewhat more succinctly, and to include the work done in the past several years.

The Cosmic Relative Abundances of the Elements

The nature of the Data.—There have been both direct and indirect determinations of the relative abundances of the elements in various locales in the universe. Direct measurements include the lithosphere, hydrosphere, and atmosphere of the earth [e.g. (147)], meteorites [e.g. (34, 35, 147)], interstellar matter [e.g. (156); Greenstein (76)], the surfaces and atmospheres of the planets and their satellites [e.g. (95, 186); Kuiper (120)], stellar atmospheres [e.g. (168); Aller (4)], and extragalactic nebulae [e.g. (20, 101)]. Indirectly, i.e., by calculation rather than by direct measurement chemically or spectroscopically, the composition of the interiors of the earth and other planets [e.g. (186)], and of various types of stars [e.g. Chandrasekhar (39, 40)] have been obtained. Ideally, cosmic relative abundances should be determined from stellar spectra, and indeed, stellar spectra do provide much data. However, the main difficulties are conversion from spectral intensities to relative abundances, and prediction of composition of stellar interiors from spectra of stellar atmospheres and representation by stellar models [see bibliography in (34)]. Among the possible difficulties with many stellar models is the assumption of homogeneity of composition and, in particular, maintenance of this homogeneity by mixing. This latter question has been extensively argued.[4] As a result of the foregoing difficulties, meteoritic data have been given the greatest statistical weight in abundance tabulations. The assumption that meteoritic abundances are representative of stellar matter, except primarily for volatile constituents, appears to be reasonably well founded.[5]

The first adequate and complete tabulation of modern universal relative abundance data[6] is that of Goldschmidt (72) in 1938. Brown (34, 120) recently published a new tabulation as required by general improvement of the data from various sources and by his specific work in the analysis and interpretation of the composition of meteorities. Brown's tabulation includes new tables of stellar abundances of the lighter elements, meteoritic abundances and cosmic abundances of the elements and of the nuclear spe-

[4] For example, see Greenstein & Richardson (77) on the requirement of a slow convection current to explain the low abundance of Li in the sun and also Öpik (140) who finds negligible mixing except for the innermost 20 per cent of the mass of the sun.

[5] These and other questions involved in abundance tabulations are discussed by Brown (34).

[6] For a complete account of this subject through 1932 see von Klüber (119) and von Hevesy (96).

cies. While there are many differences in detail from the earlier listings of Goldschmidt, the major features of the data have not been altered.

That the so-called cosmic abundances given by Goldschmidt or Brown are indeed cosmic is believed to be firmly founded, since the agreement between the relative abundances determined in various regions of the universe is reasonably good. Thus as long ago as 1925, Payne (141) showed that stars of different spectral types have marked similarities of composition and, particularly for the heavier elements, resemble the earth's crust. Russell (150) has remarked that it is difficult to find a single case where a metal is more or less abundant in the sun than on earth. More recently, Unsöld (182, 184) has shown that the relative amounts of hydrogen, helium, and heavier elements are the same for essentially all main sequence stars. Similarly, Greenstein (74), studying abundances in a group of F-type stars, found no significant variations except in one peculiar case. While quantitative determination of relative abundances in the extragalactic nebulae is not yet possible except perhaps for such nearby ones as Andromeda, nevertheless, as pointed out by Hubble (101), the spectra of the distant nebulae appear to have the same characteristics as spectra of stars such as the sun. Of the relatively few variations in relative abundance which have been observed, most can be explained in terms of the present or past physical conditions in the locale of observation. For example, meteoritic and terrestrial material differ from solar material in the relative scarcity of the volatile elements, i.e., H and the noble gases, as well as of those elements which probably were contained in volatile compounds at the time of planet formation. Such disparities would appear to result from the physical conditions associated with the origin of the solar system (80, 81, 84, 120, 186). Variations in the abundances of Li, Be, B, C, N, O, as well as H, D, and He, are probably associated with thermonuclear reactions, particularly those responsible for stellar energy production [(26, 27, 68, 75, 77); Aller (4)]. Pecularities in the He, C, N, and O abundances in hot Wolf-Rayet stars also arise from special features of thermonuclear reactions [(62); Aller (4)]. Differences in composition between population I and II type stars recently have been explained by Schwarzschild, Spitzer & Wildt (154). The population I stars probably formed later out of denser interstellar clouds in which grains had accumulated preferentially and therefore exhibit enhanced abundances of the heavier elements relative to population II stars. The latter are supposed to have formed earlier out of the more uniform interstellar medium. Some isotopic abundance ratios also vary with locale. These include, for example, the ratio He^3/He^4, which differs with locale terrestrially because of cosmic ray processes (136), H^2/H^1 ratios which appear to be much smaller in stellar atmospheres than terrestrially and even vary terrestrially [(92); 4, 92, 172a], and the C^{13}/C^{12} ratio which is excessively large in some stellar atmospheres (126). The last variation is as yet unexplained. Many terrestrial variations in isotopic abundance ratios have been found and in general are understood to be the result of the effect of nuclear mass differences in chemical reactions during the earth's long history (166, 174, 185).

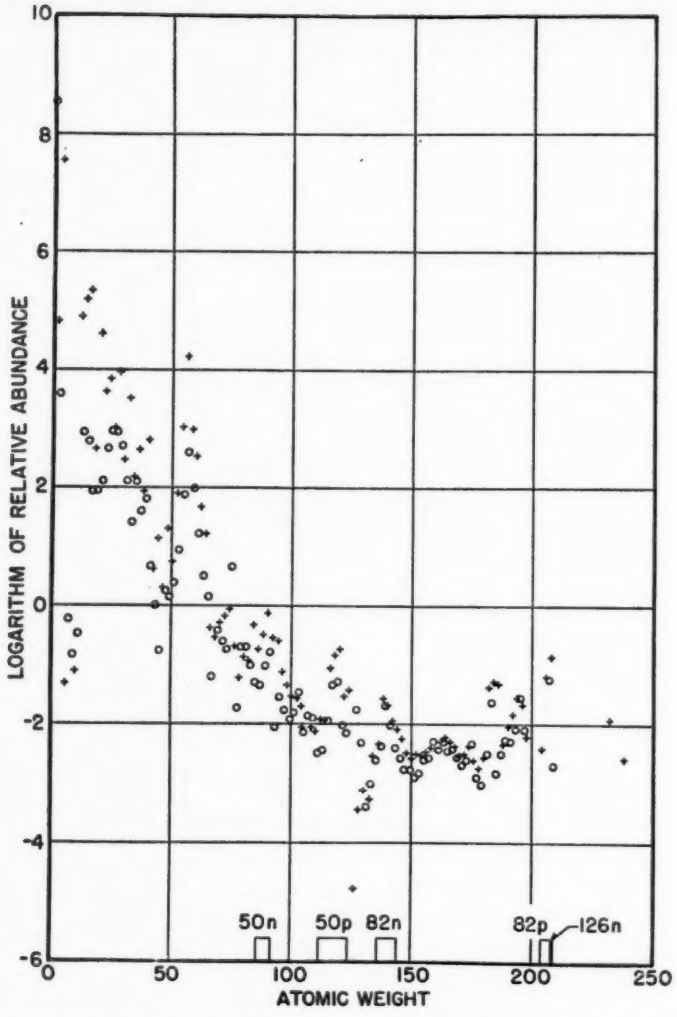

FIG. 1. Relative isobaric abundances of nuclear species, normalized to 10,000 atoms of silicon, versus atomic weight, as derived from the tabulation of Brown (34). Odd and even A (atomic weight) are denoted by O and +, respectively. Regions of A for closed shell nuclei are indicated.

The cosmic relative abundances of the nuclear species as given by Brown are used here with slight modification as the basic experimental data for comparison with theory.[7] Since Brown does not give the abundances of nu-

[7] We understand from Dr. H. Brown that there have been some changes in the abundance data since his tabulation in (34). However, these changes do not alter the major features of the data and therefore do not affect the discussions in this review.

clear species below oxygen, his tables of cosmic elemental abundances were employed for the lighter nuclei, including those for Li, Be, and B. Although there are uncertainties in abundance and isotopic abundance ratios for these light elements, mainly because of their participation in thermonuclear reactions, the appropriate elemental abundances were converted to nuclear abundances by means of terrestrially observed isotopic abundance ratios (155). Values of noble gas abundances which are difficult to determine on a cosmic abundance scale have been interpolated by Brown and are included as basic data in this review. However, unstable nuclei are not included. With these qualifications all the available data are shown in Figure 1, where logarithms of the cosmic relative abundances of nuclear species, stated as the number of nuclei of a given atomic weight (i.e., isobars) per 10,000 atoms of silicon, are plotted versus atomic weight.[8] Since data are not yet available for several nuclear species, some points plotted in Figure 1 may be shifted upward slightly as new isobaric abundances are added. This method of presenting the relative abundance data is employed because most of the theories deal with the abundance distribution as a function of atomic weight (i.e., nucleon content), rather than of atomic or neutron number. Furthermore, the abundance distribution in atomic weight is important in at least one of the theories of element formation in that the present distribution with isobars added probably most nearly resembles an original abundance distribution prior to the changes caused by long-lived β-decay.

The role of cosmic relative abundances in the systematics of nuclear species has been extensively studied by a number of investigators [(17, 33, 52, 72, 89, 106, 107, 110, 161, 169, 170, 171). Correlations have been made between relative abundance and mass number, isotopic number, neutron content, shell structure, and the parity of the nucleon number. The reader is referred to the original papers for these discussions of many of the detailed features of the data and, in particular, for the interesting correction factors which Suess (171) has estimated as required to smooth the observed abundance data on the basis of reasonableness and continuity. These discussions of details will be of great value when theories of element formation are advanced to the point where one may attempt the explanation of abundances of particular species.

The most prominent feature of the distribution of cosmic abundances based on atomic weight is the approximately exponential decrease of abundance with increasing atomic weight up to $A \cong 100$, and the essentially constant abundances for species with $A > 100$. It seems reasonable to expect that a correct theory of the relative abundance of nuclear species will reproduce this behavior at least in first approximation. This general behavior as well as the systematic details of the abundance data emphasizes that there must be a close correlation between the properties of atomic nuclei on an atomic

[8] A similar plot of Goldschmidt's tabulation of abundances (72) is given in Figure 1 of Reference (6).

weight basis and their relative abundances. The manner in which the abundance data are presented can tend to obscure the essential features of the distribution. Thus some investigators have used a contracted abundance scale while others have connected plotted abundance points. Either may give a misleading appearance to the data.

Detailed features.—There are a number of detailed features of the cosmic abundance data which are discussed because they may bear on the theories of element formation thus far developed. In tabulations of cosmic abundances the many radioactive species between Pb and the parent elements U and Th are generally not included because the relative abundances are explained by the statistical laws of radioactive decay (170). The observed abundances of the long-lived parent elements and perhaps the abundances of the decay products if originally formed by processes other than the disintegration of parent elements require theoretical explantion.

An examination of Figure 1 reveals rather large fluctuations in abundance compared with the general trend, particularly among the very light elements. The fluctuations for species up to and including F^{19} may reflect the participation of these nuclei in thermonuclear reactions in stars or in the prestellar state of the universe. Perhaps the most striking irregularity in abundance is the iron peak which lies in the region $53 \lesssim A \lesssim 63$. This abundance peak, which consists of only several elements, is above the general abundance trend by a factor of $\backsim 10^4$. In the region of the heavy elements there are several abundance peaks which deviate from the trend by a factor of about 10. Their location can be correlated with the atomic weight of nuclei of the closed shell or magic number variety [Feenberg (55)]. Nuclei containing 50 or 82 protons, or 50, 82, or 126 neutrons exhibit stability and other nuclear properties which can be associated with completed shell structure and, in particular, are more abundant in general than isotopes and/or neighboring elements [Harkins (89)]. In this connection a recent estimate of primeval lead isotopic abundances appears to show the effects of both neutron and proton shell closure (13); thus there is an abundance peak at ${}_{82}Pb$ and the calculated primeval Pb isotopic increase abundances as neutron number increases from 122 to 126. It may be noted that two of the closed shell peaks occur at atomic weights corresponding quite closely to those of the mass yield peaks for the fission of U and Th (6, 73, 110).

The analysis of relative abundance data in terms of the systematic properties of nuclei has led to many abundance rules,[9] some of which are of particular interest in the problem of the origin of the elements. As a result of the closure of a sub-shell by a pair of neutrons or protons, nuclei of the even $Z-$ even A type are both more numerous and more abundant than any of the other types. Nuclei of the odd $Z-$ even A or even $Z-$ odd A types are

[9] Harkins, (87, 90) and Oddo (138) appear to have first pointed out that the relative abundances of the elements involve nuclear rather than chemical properties. More complete discussions of abundance rules are given, e.g., by Mattauch & Fluegge (132) and Rankama & Sahama (147).

about equally numerous and abundant, while nuclei of the odd $Z-$ odd A type are rare in number and scarce in nature. In general even Z or even A species are about an order of magnitude more abundant than adjacent odd species.[10] The odd-even A abundance variation is quite noticeable, particularly near the iron peak. It should also be noted that nuclei which might have a completed shell structure according to an α-particle model exhibit rather large abundances, e.g., He, C, and O. With reference to isobars, stable nuclei of odd A all have only one isobar and stable isobars of adjacent elements are very rare[11] (131).

Odd Z species have as a rule only one or two stable isotopes while the even Z species usually have many more, and where there are two isotopes of an odd Z species, the lighter is usually more abundant (15, 88). Elements possess, in general, only one or two stable odd A isotopes. When there are two such isotopes they are nearly equal in abundance, whereas even A isotopic abundances may differ by as much as two orders of magnitude (131). Furthermore, odd A isotopes of even Z species have relatively low abundances. When an odd isotope occurs between two even isotopes, the abundance of the former is always less than the sum of the abundances of the latter, except for Xe^{129} (16). There is a considerable variation with Z of the number of odd A isotopes of even Z nuclei (134). The abundances of the isotopes of a given element show less spread among themselves than the elemental abundances show. The number of isotopes, as well as their spread in atomic weight, increases quite noticeably in the vicinity of $Z=28$ and then does not decrease until very high Z (133, 147). Also, for $Z>28$ one of the isotopes, usually the lightest, is predominately abundant, whereas for $Z>28$ several isotopes may be equally abundant (147). Furthermore, as a rule for the even Z elements above ${}_{34}Se$ the heaviest stable isotope is quite abundant while below ${}_{34}Se$ the trend seems to be reversed (134). Thus a plot of relative even A isotopic abundances for even Z species versus A yields roughly bell-shaped curves skewed toward the heavier isotopes (133, 147). The lightest isotopes of a given element appear to form a less regular abundance sequence than do the heavier isotopes, suggesting the possible existence in nature of extremely small amounts of stable isotopes lighter than those now known (133). Recently, Way (191) has noted a regularity in the abundances of the lightest and heaviest isotopes of even Z elements for $Z>34$. Consider the ratio of abundances of species $[Z, N]$ to species $[Z, N+2]$. Taking the lightest of such pairs for various elements, one finds 10 cases where the ratio lies between 0.6 and 3 and 14 cases where it lies between 0.005 and 0.15. For the heaviest of such pairs, the ratio lies, with two exceptions, between 0.5 and 8. The three groups are apparently closely connected with the degree of shield-

[10] The odd-even Z rule was first stated by Harkins (87, 88, 91, 169) on the basis of the early data of Noddack & Noddack (137).

[11] Of the four cases, all pairs, it is very likely that one member of each isobaric pair is radioactive (130, 131).

ing,[12] for in the first group, in 8 of the 10 cases both members are completely shielded, in the second group 12 of the 14 members have the $[Z, N]$ species completely shielded and the $[Z, N+2]$ species partially shielded, while of the third group, in 22 cases both members of the pairs are completely unshielded. Of the two exceptions in the latter group, in each one member of the pair is partially shielded.

There are several indications of the possible high concentration of neutrons during the process of element formation. Not only are neutron-rich isotopes more abundant but also there appears to be an isobaric abundance rule indicating the possible importance of β-decay in element formation (6, 38, 59, 169). An examination of the abundance data shows that of 51 sets of stable isobars the isobar of lowest Z is more abundant in 44 cases as might be expected if β-decay played a role.

The presence of nuclei other than protons in the primary cosmic radiation provides an interesting comparison with the cosmic relative abundances of the elements (31, 60, 145). Particles having a charge up to $Z \cong 53$ have been detected (197) and the relative numbers of such particles determined as a function of Z. The cosmic ray relative abundances decrease with Z in remarkable accord with the cosmic abundance data discussed earlier, although it would appear that there is some overabundance of the heavier elements. The H/He abundance ratio of 10 in cosmic radiation [Peters (145)] is in excellent agreement with Brown's cosmic value. It is also interesting that the high cosmic abundances of the C, N, and O group and of Fe are also found in the cosmic ray flux. Furthermore, Yagoda[13] (196, 197) has detected a nucleus with $Z = 49 \pm 3$, probably reflecting the high abundance of Sn. According to Bradt & Peters (32), Li, Be, and B are almost or entirely absent from the primary cosmic radiation. This is consistent with their cosmic scarcity. However, Dainton & Kent (44) report the presence of B in the primary flux in amounts in excess of C, N, and O, while Hoang (97) has reported appreciable quantities of Be. The general similarity of cosmic and cosmic ray relative abundances suggests that the problem of cosmic ray origin may be connected with more general cosmological problems, including perhaps the formation of the chemical elements.

The fact that there appears to be an intimate relationship between some of the systematic features of the abundance data and the stability properties of atomic nuclei, in particular the even-odd rules, has led many investigators to study the possibility of element formation under equilibrium conditions. However, properties other than nuclear stability per se may also be correlated

[12] Shielding is descriptive of the possibility of direct formation of species by neutron capture or β-decay from adjacent species. Both are possible for unshielded species, one or the other is forbidden in partial shielding, and neither is allowed in complete shielding. Thus a species $[Z, N]$ is said to be shielded if $[Z-1, N+1]$ is stable, or if $[Z, N-1]$ does not exist.

[13] H. Yogoda informs us that a nucleus incorrectly identified (196) as $Z = 53 \pm 6$ probably represents Zr or a nucleus between Zr and Sn.

with the systematic features of the abundance data. Thus, recently a non-equilibrium theory of element formation was developed which depends upon the behavior of the radiative capture cross sections of nuclei for fast neutrons. In any event all theories of the abundance of nuclei should probably reflect the stability properties of nuclei in the detailed variation of relative abundances from one species to another (68).

Equilibrium Theories

The apparent connection between relative abundances and the stability properties of nuclei (10, 87, 108), particularly their binding energies, stimulated study of the observed abundance data on the basis of equilibrium theories. Well-known methods of thermodynamics and statistical mechanics can be applied to calculate equilibrium concentrations of the nuclear species. These concentrations depend on the temperature and density of the assembly as well as on the nature of the constituents and nuclear binding energies. It is assumed that there exist all the reactions necessary to establish equilibrium. High temperatures and densities are required to attain equilibrium in a reasonable time since nuclear binding energies reach values of $\sim$2000 Mev. The question of where and when such an assembly may have existed, what constitutes a reasonable length of time for the attainment of equilibrium, and the manner in which the equilibrium distribution may have been "frozen-in" are perhaps cosmological problems which cannot be ignored. Thus it is found that no single assignment of density and temperature leads to the correct abundance distribution so that one must resort to either special stellar models or different processes for light and heavy element formation.

The earliest equilibrium studies appear to be those of Tolman (176) and Suzuki (173) who investigated the H/He abundance ratio and found that temperatures above those of ordinary stellar interiors were indicated. Urey & Bradley (187) concluded that relative isotopic abundances did not correspond to equilibrium under a single set of physical conditions. Farkas & Harteck (53) and Pokrowski (146) first applied equilibrium theory to the abundance distribution in atomic weight. The former authors first mentioned the necessity of understanding the "freezing-in" of the distribution while the latter noted the difficulty of forming a sufficient relative quantity of heavy elements with specification of a single density and temperature and suggested the need for a different process in building the heavy species. In general, the early equilibrium theories are of historical interest because both nuclear and abundance data were inadequate, and the theory was not fully developed. A more complete discussion of both the historical development and detailed treatment of equilibrium theories has been given recently by the authors (10).

Basic theory.—The detailed development of equilibrium theories of relative abundance are based on one statistical approach or another, involving, e.g., the classical Gibbs grand canonical ensemble (70, 116, 178), the method of Darwin and Fowler (58, 165), or, the analogue of Saha's ionization equation (151), all of which are necessarily equivalent.

Applying the Gibbs method of the grand cononical ensemble to the problem of nuclear equilibrium, one may write for the probability of finding a nucleus of given composition, i.e., Z protons and N neutrons, in an energy state E_j'

$$P(N, Z, E_j') = \exp\left[(\Omega + \mu_n N + \mu_p Z - E_j')/kT\right], \quad 1.$$

where E_j' includes both binding and excitation energy, μ_n and μ_p are the Gibbs or intrinsic potentials per neutron and proton, respectively, referred to rest mass as zero-point energy, and where $\exp(\Omega/kT)$ is the density-in-phase. Then, in the nonrelativistic nondegenerate case the concentrations, C_j, of nuclear species of mass $m_j (j = N+Z)$ is given by

$$C_j(N, Z) = (2\pi m_j kT/h^2)^{3/2} \Phi_j(N, Z) \exp\left[(\mu_n N + \mu_p Z - E_j)/kT\right], \quad 2.$$

where Φ_j is the partition sum for the internal degrees of freedom and E_j, the binding energy, is defined as

$$E_j = c^2(m_j - Nm_n - Zm_p). \quad 3.$$

If only the ground state is considered then $\Phi_j = 2i_j + 1$, where i_j is the nuclear spin quantum number. At equilibrium, for the proton-neutron-electron-neutrino reaction, assuming equality of the electron and neutrino intrinsic potentials, one has (25, 118)

$$2(\mu_{e-} + m_e c^2) = (\mu_n + m_n c^2) - (\mu_p + m_p c^2), \quad 4.$$

where μ_{e-} is the electron intrinsic potential. Similarly the equilibrium condition for nuclei, neutrons, and protons is

$$(\mu_j + m_j c^2) = N(\mu_n + m_n c^2) + Z(\mu_p + m_p c^2). \quad 5.$$

It is a reasonable physical assumption that the assembly be electrically neutral, whence the C_j must satisfy

$$C_{e-} = \sum_j Z_j C_j. \quad 6.$$

where the electron concentration, C_{e-}, is calculated from Fermi-Dirac statistics. While it would appear from the foregoing that the quantities μ_n, μ_p and T are arbitrary parameters, electrical neutrality limits the free choice to T and either μ_n or μ_p. The latter choice can be shown to be completely equivalent to specifying the density of matter, ρ_m, in the assembly. In calculations it proves expedient to specify the μ and compute ρ_m from

$$\rho_m = \sum_j m_j C_j + m_e C_{e-}. \quad 7.$$

The foregoing results require modification for high T where energies are relativistic and phenomena such as pair production occur, for high ρ_m where degeneracy may arise, and for equilibrium in gravitational or electrostatic fields, where the Gibbs equilibrium condition is modified (70, 117).

As has been indicated, equilibrium theory can be applied to determine whether isotopic abundance ratios of various elements are consistent with

equilibrium at a single ρ_m and T.[14] The original work of Urey & Bradley (187) indicated that there was no consistency, a result independently confirmed later by a considerable number of investigators (1, 21, 41, 109, 110, 157, 192).[15]

Despite the difficulty of understanding isotope abundance ratios, Chandrasekhar & Henrich (41) applied equilibrium theory to the abundance distribution in atomic weight using modern binding energy data. General agreement in trend was obtained from O^{16} to A^{40} with $T=8\times10^{9}$° K. and $\rho_m=10^7$ gm./cm.^{3} although beyond sulfur the computed abundances become progressively lower. These authors pointed up the difficulty of obtaining overall agreement with a single set (ρ_m, T), as was also indicated earlier by Pokrowski (146) and Weizsäcker (192), and suggested the possibility that the light and heavy elements might have been formed separately during different stages of the universal expansion. However, the universal expansion appears to have been too rapid during its early stages to permit element formation in this manner. As is well known, there has been a great deal of work on the problem of stellar energy generation which has touched on the problem of element formation [e.g. (18, 19, 26, 27, 152, 163, 167, 189, 192, 195); Salpeter (153)]. The general conclusion is that except for the very light elements no synthesis of elements can take place in ordinary stellar interiors, and that either a prestellar locale or very special stellar types must be introduced.

One of the most recent independent and complete calculations of equilibrium relative abundances for a single set of physical conditions was made by Klein, Beskow & Treffenberg (118). Using the Gibbs formulation but ignoring spin multiplicity and excited states, they found the best representation for the light elements, $1\leqq A\leqq40$, with the parameters $kT=1$ Mev, $\mu_n=-7.6$ Mev and $\mu_p=-11.6$ Mev, corresponding to a density $\rho_m\cong4\times10^8$ gm./cm.^{3}. The equilibrium abundances have been recomputed by us using binding energies from Rosenfeld (149) and the parameters given above. The results are compared in detail up to $A=80$ in Figure 2 with Brown's observed abundances (34). There is general agreement in trend for $A<50$ although the agreement in detail is poor. In the region $A>50$ the iron peak is not reproduced. The abundances computed for the heavier elements become extraordinarily small, e.g., they are below the observed abundances by a factor $\backsim10^{50}$ by $A=150$ and become progressively smaller. It would appear that the conditions required to fit light and heavy element abundances are quite different.[16] It has been shown (25, 165) that for every choice of a μ only nu-

[14] It has been suggested that since isotopic ratios are apparently independent of locale the elements must have been formed in equilibrium and therefore one should in principle be able to compute binding energies from relative abundance data (79, 132).

[15] See Ref. (181) for the opposite interpretation on the basis of the same data.

[16] Demeur (46) has discussed, apparently erroneously, the role of temperature in increasing heavy element abundances [see (10)].

clei in a rather narrow range of atomic weights will be predominant and that the larger μ_n, the larger the A of the predominant nuclei.

Equilibrium theory calculations of abundance distributions for a given ρ_m and T, again neglecting nuclear excited states, have also been made by a number of other investigators. Wataghin and collaborators (122, 175, 190) have obtained a fit to the abundance distribution in A but a re-examination

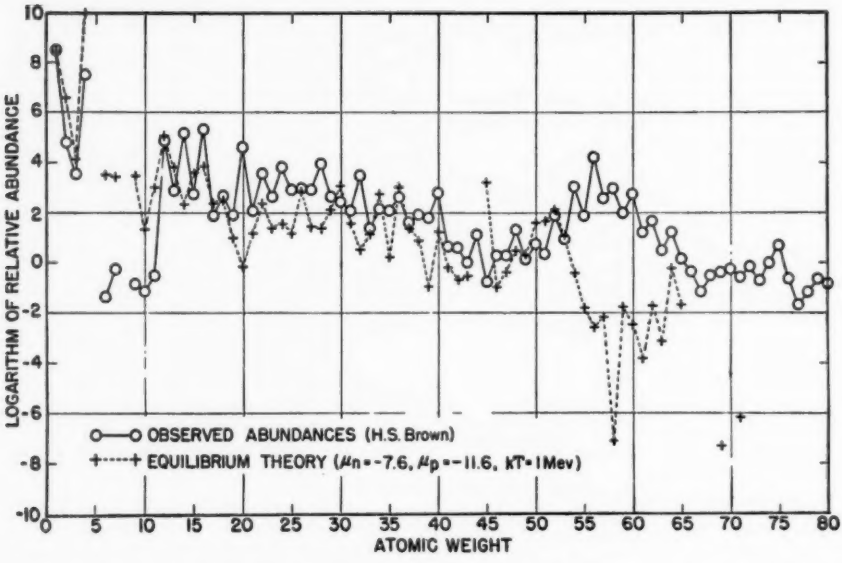

FIG. 2. Relative isobaric abundances versus atomic weight according to the simple equilibrium theory (10, 118). Theoretical and observed points are normalized to 10,000 atoms of silicon. The computed abundance for $A=78$ is -11.73 and the neutron concentration is not included at $A=1$. For higher A the computed abundances become extraordinarily small (10).

by us of these calculations indicates that nuclear density is exceeded and electrical neutrality is not satisfied (10). Cherdyncev (42, 43) has also obtained a general fit to the data, but with the postulation of physically unreasonable pure neutron nuclei. Steinwedel & Jensen (164) have examined the equilibrium problem in considerable detail, including relativistic and degeneracy effects as well as excited states and confirmed the earlier conclusion of Jensen & Suess (110) that the abundance distribution must reflect nonequilibrium processes. A recent detailed equilibrium calculation by Singwi & Agarwala (156a) appears to cover the same ground reported earlier in references (24, 25, 164) among others.

Detailed modifications.— There have been a variety of specific modifications of the simple equilibrium theory suggested to repair the difficulties

noted. Among these is the effect of excited nuclear states, for as Chandrasekhar & Henrich (41) have remarked, nuclear level densities increase with increasing A so that proper evaluation of $\Phi_j = (2i_j+1)\Phi_j(\text{rot})\Phi_j(\text{vib})$ in Equation 2 should lead to increased abundances of the heavier elements. The general nature of these evaluations of Φ is to treat the nucleus as a rigid sphere (24, 25, 183) in determining the rotational partition sum $\Phi_j(\text{rot})$ while various vibrational level density formulae (24, 25, 85) have been used in finding a vibrational partition sum $\Phi_j(\text{vib})$. Neither the inclusion of Φ_j calculated in this manner nor estimates of Φ_j based on physically less reasonable assumptions (69) lead to an increase in abundance by, say, a factor of more than $\backsim 10^{20}$ at $A = 250$ where $\backsim 10^{100}$ is required. Nevertheless, the inclusion of excited states has an important effect on the resulting abundances in the more complex equilibrium calculations involved in special stellar models and in the "freezing-in" problem.

It would appear that in a successful equilibrium theory one would require higher ρ_m and perhaps higher T to form the heavier elements than is required for the lighter elements. Since conditions for the lighter elements are already severe, Albada (1, 2) and Hoyle (98, 99) suggested that electron degeneracy and electrostatic effects be considered in the element-formation problem [see also (164)]. It is shown that electron degeneracy lowers the Z/A and increases the A of that nucleus having the maximum binding energy per nucleon, thereby indicating possible improvement of the equilibrium abundances of heavy elements. There appear to be certain difficulties with the calculations of these investigators associated with the statistics required under the conditions considered, particularly the presence and degeneracy of neutrons (10, 121). In any event no abundance distribution calculations were made, and the reader is referred to a recent detailed discussion of this problem elsewhere (10).

In view of the failure of explaining the abundance distribution with a single set (ρ_m, T), and since it appeared that neither the expanding universe nor the interiors of ordinary stars (39, 68) were suitable locales for element formation in equilibrium (41, 164), various investigators have considered special stellar models (2, 25, 42, 98, 99, 115, 117, 177). In a qualitative discussion, Albada (2) proposed a kind of white dwarf with a degenerate core which rotates nonuniformly. Presumably the abundances of heavier elements might be enchanced in the core and the various species subsequently distributed in space by virtue of a supernova-like outburst of this model which has evolved into rotational instability. The lighter elements are supposed to form in nondegenerate cores of red giant-like stars. A more detailed study of this question was carried out by Hoyle (98, 99) who also proposed that elements be formed at equilibrium in dehydrogenized stars [see also (66)]. Such stars contract with consequent increase of ρ_m and T at the center and, if they rotate, will become rotationally unstable and explode. During the contraction, successively different abundance distributions would develop in the core as ρ_m and T increased. The time of explosion, which depends on

the exact nature of the model, determines the particular heavy element distribution ejected into space. Hoyle has identified these models as O-, B- and A-type stars whose lifetimes are small compared with the age of the universe.

The problem of element formation in stellar models in which the effect of the gravitational potential on nuclear equilibrium is taken into account explicitly has been discussed by Beskow & Treffenberg (25) and Klein (115, 117). The model studied is an isothermal star with $kT=1$ Mev, which temperature proved satisfactory for the prediction of the general abundance trend for the ligher elements with a single ρ_m. In such a model it was expected that proper equilibrium conditions for various nuclei could be realized simultaneously at different radial positions. The basic calculation involves the determination of the Gibbs intrinsic potentials for neutrons and protons as a function of radial position. If ϕ_g and ϕ_e are the gravitational and electrostatic potentials then the conditions for equilibrium are (116, 117)

$$\mu_n + m_n\phi_g = \text{constant} \qquad 8a.$$

for the neutron, and

$$\mu_p = m_p\phi_g + e\phi_e = \text{constant} \qquad 8b.$$

for the proton.

The procedure followed by Beskow & Treffenberg, involving Poisson's equation, has been shown by Klein [see (10)] to be equivalent to using Equation 8a as follows:

$$\frac{d\mu_n(r)}{dr} = -\frac{GM(r)m_n}{r^2}\left[= -m_n\frac{d\phi_g(r)}{dr}\right], \qquad 9.$$

and

$$\frac{dM(r)}{dr} = 4\pi r^2\rho_m(\mu_n). \qquad 10.$$

One chooses a central uniform core of radius r_0, density ρ_0 and intrinsic potential $(\mu_n)_0$. Then one adjusts μ_n as a function of r in such a way that together with ρ_m determined from Equation 7 one is led to the desired total abundance distribution for the star. The calculation is carried out subject to the requirements of electrical neutrality and also the equilibrium relationships stated earlier in Equations 4, 5, and 8. Beskow & Treffenberg considered models with cores of nuclear density having radii varying from 10^5 to 10^6 cm. and $(\mu_n)_0=5.68$ Mev (an upper limit corresponding to nuclear density) as well as one case of a less dense core with $r_0=10^5$ cm. and $(\mu_n)_0=3$ Mev. In determining the total abundances over the model they did not include core material and the superheavy nuclei predicted by the theory, while the rather considerable neutron concentration exterior to the core was added to the proton concentration. Their computed abundances for the 10 atomic weights chosen are shown in Figure 3 for the various models and are compared with Brown's data (34) adjusted to 1 $M_\odot$ (solar mass). The theoretical

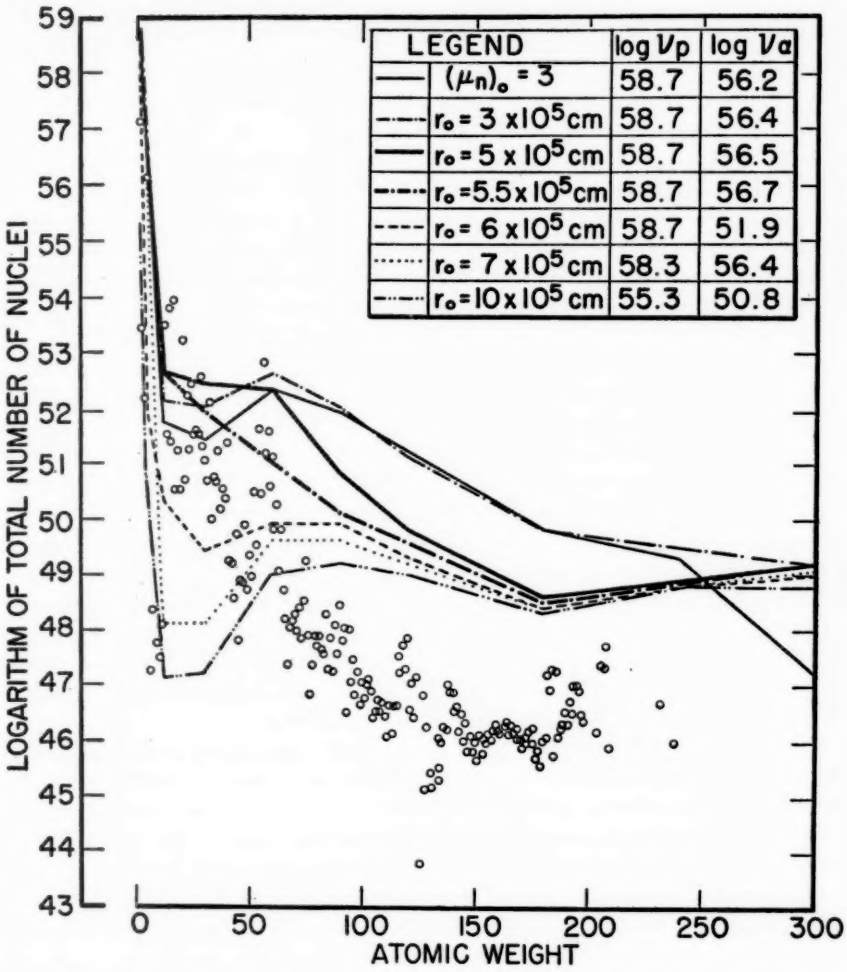

FIG. 3. Isobaric abundances versus atomic weight in the isothermal star models of Beskow & Treffenberg (25) compared with Brown's observed abundances (34) adjusted to give 1 $M_\odot$. The proton and α-particle contents, ν_p and ν_α, make up the bulk of the star masses.

values lie above the data for the reason that with the exception of two models the total masses are $\backsim 40 M_\odot$. If the computed abundances are considered as relative, the curves for $r_0 < 6 \times 10^5$ cm. could be adjusted to fit the data fairly well although there appears to be an overabundance of the heavier elements.

Beskow & Treffenberg suggest that these "prestellar" stars explode and distribute the equilibrium distribution through space, and that the present universe evolved from these prestellar explosion products. Assuming that

the equilibrium distribution could survive the explosion and freeze in without major modification, one must determine the properties of these isothermal prestellar bodies in more detail. Klein has constructed a spherically symmetric static solution of Einstein's field equations representing a mass of gravitating radiation (115). For this model $kT \cong 1$ Mev up to $r \cong 2.6 \times 10^{10}$ cm. so that a "prestellar" material body of $\backsim 40 M_{\odot}$ might be embedded under essentially isothermal conditions. To preserve equilibrium the radiation field must be large compared with the material star and contain photons, electron-proton pairs, and neutrinos. Because Klein's radiation star model is infinite in mass and extent, and static as well, it falls short of providing a satisfactory hypothesis without modification. However, it appears that recent work of Vaidya (188) may provide the desired model for element formation in equilibrium since he has obtained solutions of the Einstein field equations representing nonstatic radiating spherical distributions. This specific application of his work to this problem has not yet been made.

Discussion.—From an historical point of view it was natural to attempt to describe element formation in terms of a frozen-in equilibrium distribution. If, and it appears necessary to do so, one rejects as a locale for equilibrium formation of elements the prestellar homogeneous expanding universe and the interiors of ordinary stars, one is led to the introduction of "prestellar" bodies or special stellar models continuously producing elements. While the general abundance trend can be reproduced by equilibrium theory, the detailed agreement is not satisfactory, particularly when it is recalled that the basic premise of an equilibrium theory is the detailed correlation between nuclear stability properties and abundances.

All of the investigators who have introduced special stellar models as the locale have assumed that the star will explode in a sufficiently violent manner to freeze-in effectively the established abundance distribution (1, 2, 25, 42, 98, 99). This assumption requires more careful examination because it is difficult to see how the explosion could be sufficiently rapid to avoid modification of the distribution by nuclear reactions. In particular, large neutron concentrations are associated with all the models suggested and, at the temperatures and densities required, neutron reactions would be expected to alter the abundance distribution completely[17] (10, 110). In addition, the increase of heavy element abundances by a factor of at least 10^3 and perhaps more than 10^{20} resulting from the effect of excited states would rapidly disappear with the expansion and cooling of the exploding material, again altering the original distribution. One is faced with the problem of specifying an initial equilibrium distribution which as the result of nonequilibrium processes during the freezing-in would have evolved into the presently ob-

[17] In the nonequilibrium theory to be described, a T and ρ_m of ~ 0.1 Mev and $\sim 10^{-7}$ gm./cm.^{3}, respectively, suffices with nonequilibrium neutron-capture reactions in an expanding universe to explain the observed abundance distribution starting with neutrons and protons only. In the equilibrium stellar models, one has about the same T and $\sim 10^{15}$ times the ρ_m.

served distribution. Difficulties of the type mentioned (10), especially the freezing-in problem, have led to the development of nonequilibrium theories of element formation.

Nonequilibrium Theories

It appears to be a reasonable supposition that the elements were formed during the early prestellar state of the universe—a period when, according to an extrapolation backward of the present universal expansion, physical conditions would have been of too transient a nature to admit of an equilibrium among nuclei. The existence of radioactive species indicates that the elements have not had their present form for all time (5, 68). Furthermore, relative abundance ratios in families of radioactive elements yield an apparent age of the elements in remarkable agreement with values for the age of the universe. In the former case, one makes use of nuclear systematics to estimate the relative abundance of a nuclear species when formed, and then one may compute the time required for the reduction of original abundances to their present values. With K, Sm, Rb, Th, and U the ages obtained are of the order of two to five billion years. Species with half-lives short compared with $\backsim 3 \times 10^9$ years are not found in nature, while those with long half-lives show no anomalous abundance (10, 143). On the other hand, the expansion rate of the universe, the presently proposed evolutionary theories for stars, galaxies, and our solar system (193), the departures from dynamical equilibrium in stellar clusters (28), as well as other astronomical data suggest an age, the time of a "great event", of the order of 2 to 5 billion years (22, 28, 127, 179). This agreement in apparent age between the elements and the universe, together with the excellent cosmic uniformity in relative abundances, suggests that the elements may have been formed in the prestellar state at one time uniformly throughout the universe (13, 36, 113, 172). The restriction to the prestellar state is emphasized for the reasons already described, namely, that element synthesis in the interior of common stellar types does not appear possible, and that the "freezing-in" problem associated with the special stellar types suggested appears to be a very difficult one indeed.

The probable rapid change of physical conditions during the early universal expansion suggests a nonequilibrium theory of element formation, intimately connected with a cosmological model (63). A number of investigators[18] (10, 59, 61, 110, 189, 192) have proposed that neutron-capture reactions played an important role in the formation of heavy elements in particular. In the main, these authors were seeking to explain stellar energy production, or to overcome the difficulties of equilibrium theories in explaining the existence of the heavier elements. The combination of neutron-capture reactions with nonequilibrium processes in the universal prestellar state

[18] It has been suggested that there might be cyclic light element reactions which would at the same time provide a source of stellar energy and a continuing supply of neutrons for heavy element synthesis (39, 50, 192).

appears to have been first suggested by Gamow (63). This concept has been developed into a nonequilibrium theory of element formation by Alpher, Herman, Gamow, Smart, Fermi, and Turkevich, and this theory is discussed in the following sections.

Cosmological model.—An estimate of the physical conditions during the early stages of the expanding universe can be made with the aid of cosmological theory (10, 11, 177). The premises upon which the model is based are that the universe is homogeneous and isotropic on the large scale, that one therefore may speak of a smeared-out density of matter in the universe which is of the order of 10^{-29} gm./cm.^{3} (22, 162), and that the observed red shift in the spectra of extragalactic nebulae is, indeed, indication of true recession (101). The universal expansion revealed by the red shift can be expressed through

$$v = Hl, \qquad 11.$$

where l is the proper distance, and Hubble's constant $H = 1.8 \times 10^{-17}$ cm. sec.$^{-1}$cm.$^{-1}$. If the universal expansion had always proceeded as described by Equation 11, the apparent age of the universe would be the reciprocal of Hubble's constant, or $\backsim 2 \times 10^9$ years. This value is on the low side of the various age estimates, probably because Equation 11 is only a first approximation to the relativistic expression (177) and, further, it appears that the galactic distance scale may require change, and this would alter Hubble's constant (22). Both could greatly modify the apparent age of the expansion (11, 65). A more serious question about the premises given is the assumption of homogeneity. A reasonably satisfactory non-homogeneous cosmological model has been constructed (139), but it does not appear feasible as yet to extrapolate this model back to the prestellar epoch. A more nearly correct cosmology may involve homogeneity in the early epochs and inhomogeneity now, with a transition epoch associated with the formation of galaxies from a homogeneous medium. Smearing out the present universal properties in order to extrapolate back to the prestellar epoch may then be a quite reasonable procedure. In the following, the general nonstatic cosmological model is employed.

Assuming that the expanding universe contains a homogeneous isotropic mixture of noninterconverting radiation and matter which behaves as an ideal fluid, one may obtained from the Einstein field equations the following differential equation, in c.g.s. units, describing the expansion:

$$\frac{dl}{dt} = + \left[\gamma \rho l^2 - \frac{c^2 l_0^2}{R_0^2} \right]^{1/2}, \qquad 12.$$

where l is proper distance and l_0, the unit of length, together with R_0, the unit measure for radius of curvature ($R/R_0 = l/l_0$), are determined from the boundary conditions, $\gamma = 8\pi G/3$ and G and c are the universal constant of gravitation and velocity of light. The density of mass, ρ, which fixes the geometry, is the sum of the densities of matter, ρ_m, radiation, ρ_r, and kinetic energy, the

last named being negligible under the conditions to be discussed. The conservation of matter requires that $\rho_m l^3 = \text{constant}$. Furthermore, if the universal expansion is adiabatic so that $T \propto 1/l$, then the assumption that the radiation has a black body distribution requires $\rho_r l^4 = \text{constant}$. Energy is not conserved in a cosmological model of this kind. Equation 12 can be integrated and the solution obtained can be reduced for very early times to the following (10): for $\rho_r \gg \rho_m$,

$$\rho_r = (4\gamma t^2)^{-1} = 4.48 \times 10^5\, t^{-2} \text{ gm./cm.}^3, \qquad 13a.$$

$$\rho_m = \rho_0 t^{-3/2} \text{ gm./cm.}^3, \qquad 13b.$$

and

$$T = 1.52 \times 10^{10}\, t^{-1/2} \text{ °K.}; \qquad 13c.$$

for $\rho_m \gg \rho_r$,

$$\rho_r = \rho_0' t^{-8/3} \text{ gm./cm.}^3, \qquad 14a.$$

$$\rho_m = 4(9\gamma t^2)^{-1} = 7.94 \times 10^5\, t^{-2} \text{ gm./cm.}^3, \qquad 14b.$$

and

$$T = T_0 t^{-2/3} \text{ °K.}; \qquad 14c.$$

where ρ_0, ρ_0', and T_0 are parameters whose choice fixes the model. A comparison of Equations 13a, b, c with a complete solution of Equation 12 shows that Equations 13a and 13b are good approximations up to about the time when $\rho_m = \rho_r$ (or $\backsim 10^{14}$ sec. for the ρ_0 required by the neutron capture process).

The relationships $\rho = \rho(t)$ are of questionable validity in the immediate vicinity of the singularity at $t = 0$ when the interconversion of matter and radiation might have been important (10, 51). While the nonequilibrium theory of element formation is, in the main, not concerned with times so early that the validity of the cosmological model need be questioned, it does involve sufficiently early times and densities such that the term in Equation 12 containing R_0 may be neglected. Thus the nature of the radius of curvature of the universe need not be specified. As will become evident, the neutron capture theory requires that the universal expansion be controlled by radiation at early times. In this case, ρ_r is fixed by the cosmological model whereas the ρ_m is adjusted by proper choice of the constant ρ_0 in Equation 13b to yield agreement between theoretical and observed relative abundances of the elements.

Neutron-capture cross-section data.—There appears to be a strong connection between the relative abundances of nuclear species and their systematic properties. Thus nuclear binding energies form the principal basis of equilibrium theories of element formation. On the other hand, the neutron-capture theory had as its basis the correlation of fast neutron-capture cross sections with relative abundances. The essence of this relationship is that while abundances decrease exponentially with increasing atomic weight up to $A \cong 100$, radiative neutron-capture cross sections increase exponentially up to $A \cong 100$ and both remain essentially constant thereafter.

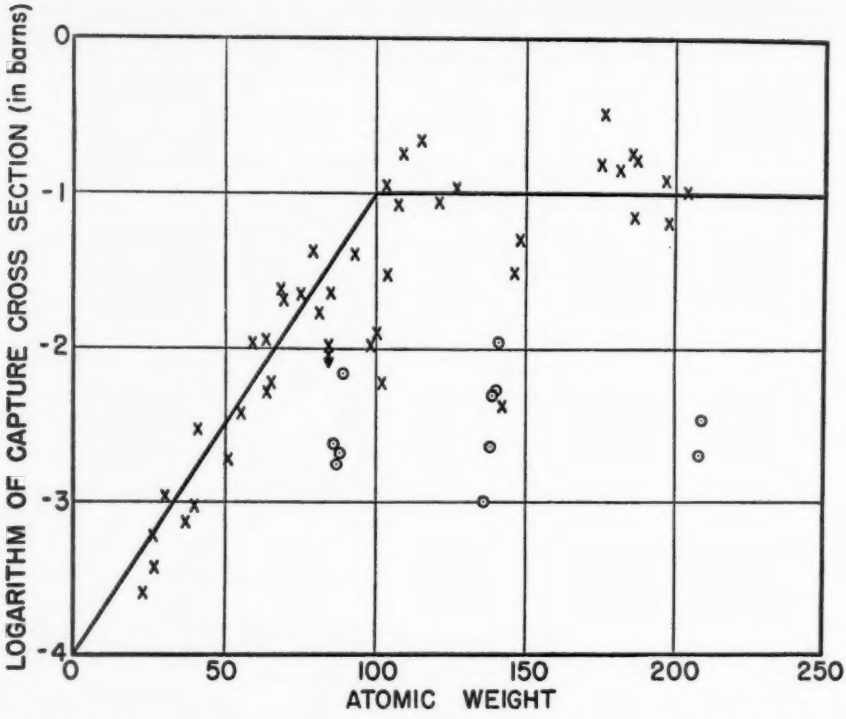

FIG. 4. Neutron capture cross sections at 1 Mev versus atomic weight after Hughes *et al.* (102). Data for nuclei with 50 ± 1, 82 ± 1 and 126 ± 1 neutrons are shown as circles. The point for Kr^{84} is an upper limit.

The relative abundance data permit one to estimate roughly within what range the temperature must have varied during a neutron-capture process of element formation. The temperature must have exceeded $\backsim 10^3 - 10^4$ ev because one finds no correlation of abundances with the enormous resonances observed in the cross sections of certain nuclei below these energies. On the other hand, the temperature must have been somewhat less than the smallest mean binding energies per nucleon in order that stable nuclei might be formed. We have assumed a temperature for the start of the element-forming process of $\backsim 10^{9°}$ K. The effect of temperature variation during the universal expansion on capture reaction rates is discussed later. The possibility cannot yet be excluded that neutron-rich unstable nuclei, which may have existed during the formation process, led to abundance deviations in the presently observed abundance data because of resonance capture. However, it seems reasonable that during the element-forming process the species were not too different from the stable nuclei.

The most important evidence for the correlation of abundance with cap-

ture cross section is the work of Hughes and collaborators (102, 103) in which the activation cross sections of a number of species were determined for 1 Mev fission neutrons.

The cross-section data of Hughes and collaborators (102) are given in Figure 4 where the logarithms of neutron-capture cross sections, σ, at 1 Mev are plotted versus atomic weight.[19] The capture cross sections exhibit, except for "magic" and "near-magic" number nuclei, a remarkably regular dependence on A. Nuclei containing 50, 82, or 126 neutrons have completed nuclear shells and have cross sections much lower than neighboring nuclei. This depression in cross section is shared by near-magic nuclei. It may be noted that, particularly with respect to cross section, there appears to be evidence for a closed shell at 58 neutrons (102). A similar effect has not been observed for proton shell closure at $Z = 20$, 50, and 82. The principal features of the data excluding the magic and near-magic nuclei are well represented by the two straight lines shown in Figure 4, viz., (6)

$$\log \sigma = 0.03A - 4.00, \; A < 100 \qquad 15a.$$

and

$$\log \sigma = -1.00, \; A > 100, \qquad 15b.$$

where σ at 1 Mev is given in barns (10^{-24}cm.^{2}). According to Hughes *et al.* (102) the experimental error in σ lies within a factor of $\backsim 2$ of the measured values, and, as may be seen in Figure 4, the measured cross sections, except for the closed shell nuclei, also lie within a factor of about two from the straight lines shown.

In the neutron-capture theory to be described, Equations 15a and 15b are taken as defining the neutron-capture cross sections of the elements at 1 Mev. This approximation ignores such detailed features as the smaller cross sections of the "magic" and "near-magic" number nuclei and the more complicated behavior of the light element cross sections. It might follow from the abundance rules discussed that there should be even-odd variations in cross section both with respect to Z and N. The expected even Z—odd Z variation, recently discussed by Hurwitz & Bethe (104), has not been observed by Hughes *et al.* (102), either because of experimental error or because, as Hughes *et al.* suggest, the value of σ is determined by the excitation energy of the compound nucleus which in turn depends on the neutron binding energy.[20] However, odd N nuclei might be expected to have relatively large σ (54) and it is interesting to note the one example measured (102), namely Lu^{176}, is the highest point in Figure 4. It may also be noted in Figure 4 that

[19] Several other investigators have also studied capture cross sections [e.g. (3, 45, 78, 86, 94, 135)]. Their results are in good agreement with the more extensive work of Hughes *et al.* and are discussed in (10, 103).

[20] MacNamara & Thode (129) have observed an even A—odd A variation with thermal pile neutrons, while Kempton (114) has discussed the possible connection of isotopic abundance ratios with thermal activation cross sections.

the regular increase of σ with Z among the 82 neutron group of nuclei has been interpreted as arising from a decrease in stability as protons are added (103).

A logarithmic plot of neutron-capture cross section against relative abundance, for all but closed shell nuclei, yields a good linear inverse correlation. In the case of the closed shell nuclei, this correlation is greatly magnified. It is this type of correlation which suggested the possibility that the elements were formed by a neutron-capture process. If the various atomic species were indeed formed by the successive capture of neutrons, then β-decay should have played a role in establishing the present abundance distribution from neutron-rich isobars. Starting from an unstable neutron-rich nucleus β-decay would terminate at the stable nucleus having the lowest possible Z. In this connection, then, it will be recalled that the most abundant of a group of isobars is usually the one with lowest charge, a fact which lends credence to the role of β-decay in establishing the abundance distribution with respect to Z.

The general behavior of σ as a function of A, approximately represented by Equations 15a and 15b, has been employed by Alpher & Herman (10, 12) in the formulation of a neutron-capture theory of element formation. Detailed consideration has been given to the formation of the very light elements by Fermi & Turkevich (56) who have taken into account the actual cross-section variations and reactions other than neutron capture.

Neutron-capture process.—The process of element formation is considered to be an integral part of the early stages of the expanding universe, and the following qualitative picture has been suggested. Immediately following the start of the universal expansion, the material universe consisted of elementary particles. While the matter density was sufficiently low to permit neutron decay, it is supposed that for some time after the expansion started the temperature was so high as to prevent significant formation of nuclei because of thermal dissociation and photodisintegration processes. When the universe had expanded and cooled sufficiently, deuterons were formed by the process $H(n, \gamma)D$, and successive neutron captures built the heavier nuclei. The density of matter was sufficiently low so that the time between successive captures was long enough to allow charge adjustment by β-decay of the excited nuclei being formed. The densities required by the theory are such that β-decay and neutron capture probabilities during the formation process were about equal (160). The relative concentrations of the various nuclei depend on the matter density assigned, the rate of the dilution of matter resulting from the universal expansion, and the rate of decrease of the neutron concentration because of neutron decay. The neutron-capture theory developed requires that $\rho_r \gg \rho_m$, and the specification of ρ_0 in Equation 13b as well as a starting time for the process. Qualitatively, a very low value of ρ_m would have yielded principally hydrogen, while a very high ρ_m would have led to an overabundance of the heaviest elements as end products. The reduction of the neutron concentration caused by capture and decay, together

with the reduction of reaction rates as matter diluted in the expansion, terminated the element-building process in a time of the order of several neutron half-lives.

In the formulation of the neutron capture theory, the radiative capture of neutrons is taken to be the only important reaction. In particular the smoothed-out dependence of σ on A given by the two straight lines in Figure 4 is used, rather than detailed cross sections. Reactions involving photons, thermal dissociation, and particle reactions other than the (n, γ) type are expected to contribute only to establishing the finer details of the relative abundance distribution. The mathematical formulation is then the following (10):

Let V be any finite volume element in the universe, N_j the number of nuclei composed of $j(=A)$ nucleons in that volume, and let the concentration $C_j = N_j/V$. Assuming homogeneity in composition, one may write

$$\frac{dC_j}{dt} = \frac{1}{V}\frac{dN_j}{dt} - \frac{C_j}{V}\frac{dV}{dt}. \tag{16.}$$

In the cosmological model discussed earlier, the density of matter at early times is given by

$$\rho_m \propto t^{-\psi}, \tag{17.}$$

where $\psi = 2$ for $\rho_m \gg \rho_r$ and $\psi = 3/2$ for $\rho_r \gg \rho_m$. Since $\rho_m = M/V$, where M is the mass of matter in the volume V, it follows that

$$\frac{1}{\rho_m}\frac{d\rho_m}{dt} = -\frac{1}{V}\frac{dV}{dt} = -\frac{\psi}{t}. \tag{18.}$$

Combining Equations 16 and 18 yields

$$\frac{dC_j}{dt} = \frac{1}{V}\frac{dN_j}{dt} - \frac{\psi C_j}{t}. \tag{19.}$$

The rates of change of the numbers of neutrons, N_n, protons, N_1, and nuclei of nucleon content j, N_j, in the volume V are given by

$$\frac{dN_n}{dt} = -\lambda N_n - \sum_{j=1}^{J} p_j C_n N_j, \tag{20a.}$$

$$\frac{dN_1}{dt} = +\lambda N_n - p_1 C_n N_1, \tag{20b.}$$

and, in general for $j > 1$,

$$\frac{dN_j}{dt} = p_{j-1} C_n N_{j-1} - p_j C_n N_j, \tag{20c.}$$

where λ is the neutron decay constant, p_j is the effective neutron capture volume swept out per second by nuclei of species j, and J is the total number of nuclear species differing only in nucleon content j. If one sets $\tau = \lambda t$, substitutes Equation 19 into Equation 20 and normalizes the particle concentrations C_n, C_1, and C_j with respect to the nucleon concentration C_0 at time

$t=t_0$, then the following expressions describing the neutron-capture process result:[21]

$$\frac{d\xi_n}{d\tau} = -\left[1+\frac{\psi}{\tau}\right]\xi_n - \sum_{j=1}^{J} P_j\xi_n\xi_j \qquad 21a.$$

$$\frac{d\xi_1}{d\tau} = \xi_n - P_1\xi_n\xi_1 - \frac{\psi\xi_1}{\tau}, \qquad 21b.$$

and for the remaining species

$$\frac{d\xi_j}{d\tau} = P_{j-1}\xi_n\xi_{j-1} - P_j\xi_n\xi_j - \frac{\psi\xi_j}{\tau}, \qquad 21c.$$

where

$$\xi_j = C_j/C_0, \qquad 21d.$$

and

$$P_j = p_jC_0/\lambda. \qquad 21e.$$

These equations state that the neutron concentration is decreased by decay and capture, the proton concentration is increased by neutron decay and decreased by deuteron formation, the concentration of species j is increased by neutron capture in species $(j-1)$ and decreased as it captures neutrons, and finally, all concentrations decrease according to the universal expansion. Equations 21a, b, and c, can be solved only by numerical integration as they stand.

The singular nature of Equations 21a, b, and c, at $\tau=0$ requires the choice of a finite starting time $\tau_0=\lambda t_0$ for the element-forming process. It does not appear to be physically correct to select a starting time, since the element-forming process builds up as dissociative processes die out. However, since this occurs rapidly it appears to be reasonable to assume that the process started at a time when the temperature in the expansion has fallen well below the deuteron binding energy. For this time one must specify C_0 as well as the coefficients P_j. In order to calculate the p_j, it is assumed that one may use classical ideal gas statistics (10), with the result that

$$p_j = B\left(\frac{1+j}{j}\right)^{1/2}\int_0^\infty \sigma(j,E)E\exp\left(-\frac{E}{kT}\right)dE, \qquad 22a.$$

where

$$B = \left(\frac{8}{\pi m_n}\right)^{1/2}(kT)^{-3/2}, \qquad 22b.$$

[21] If Equations 21a, b, c, d, e are formulated in terms of concentrations by weight [see (10)], the explicit term for the universal expansion effect is eliminated. However the coefficients P then contain the time explicitly through a factor ρ_m. Only if all the reactions in Equations 21 were of the same order would it be possible to completely eliminate the explicit τ dependence, and to determine ratios of concentrations independently of the nature of the expansion.

E is the collision energy, and m_n is the mass of a nucleon. Evaluation of Equation 22 requires insertion of the capture cross section, σ, as a function of j and of E. The energy dependence of σ is about as $E^{-1/2}$ for low and medium energies, and E^{-1} for Mev energies (102, 194). However, if $kT \backsim 0.1$ Mev in Equation 22, the main contribution from σ will be in this energy region so that $\sigma \propto E^{-1/2}$ should be an adequate approximation.[22] With this energy dependence and with the smoothed-out j dependence given by Equation 15, the possible time dependence of p_j which enters through E and T in Equation 22 vanishes and one obtains

$$p_j \cong 1.4 \times 10^{-19+0.03j} \left(\frac{1+j}{j}\right)^{1/2} \text{cm.}^3/\text{sec.}, \; j < 100, \qquad 23a.$$

and

$$p_j \cong 1.4 \times 10^{-16} \text{ cm.}^3/\text{sec.}, \; j > 100. \qquad 23b.$$

The neutron-capture process has been studied quantitatively in several successively improved approximations.[23] The simplest of these involved neglecting the universal expansion and taking neutron and proton concentrations as constant during the process (5, 6, 7, 10). In addition to demonstrating that the neutron-capture process did yield the correct general trend for the relative abundance distribution, this work also showed that the universal expansion should involve a radiation universe containing a trace of matter.

In an improved approximation Equations 21a, b, and c, were taken without the expansion terms, i.e., the process was calculated for a static universe. Because of the almost exponential decrease in relative abundance with increasing A, it was assumed in this calculation, and in the calculation involving the expansion to be described, that the summation term $\sum P_j \xi_n \xi_j$ could be neglected for $j > 4$. In order to reduce the labor involved in the numerical integration of Equations 21a, b, and c, even with the expansion terms deleted, the nuclear species were grouped (10) by appropriate averaging of the coefficients p_j over sets of 5 or 20 in j, thereby reducing the number of equations to be solved to 27. For the first five equations, the coefficients were taken as in Equation 21e while for the remainder of the species the grouped coefficients were

$$\prod(\bar{j}) = \frac{2}{q(q+q')} \sum{}' P_j, \qquad 24.$$

[22] If $\sigma \propto E^{-1}$ were used, then the p_j calculated would differ by a factor of $\sim\frac{1}{3}$ to $\sim\frac{1}{2}$ of those given by Equation 22. This is a trivial difference in view of the approximate form of σ used, in terms of both j and E dependence.

[23] In a very rough approximation, one may write on the basis of the inverse correlation of abundance and cross section that $\log \sigma = a_1 \log \alpha + a_2$, where α is relative abundance and the a's are constants. Then using Equation 15, one may derive that $\log \alpha = a_3 A + a_4$ for $A < 100$ and $\log \alpha =$ constant for $A > 100$, two straight lines approximately representing the $\log \alpha$ versus A distribution. It is interesting to note in this connection that Goldschmidt (71) suggested that the relative abundances appear to be described by $\alpha \propto Z^7$ or Z^8, while Mattauch & Fluegge (132) suggested $\alpha \propto 1.2^Z$.

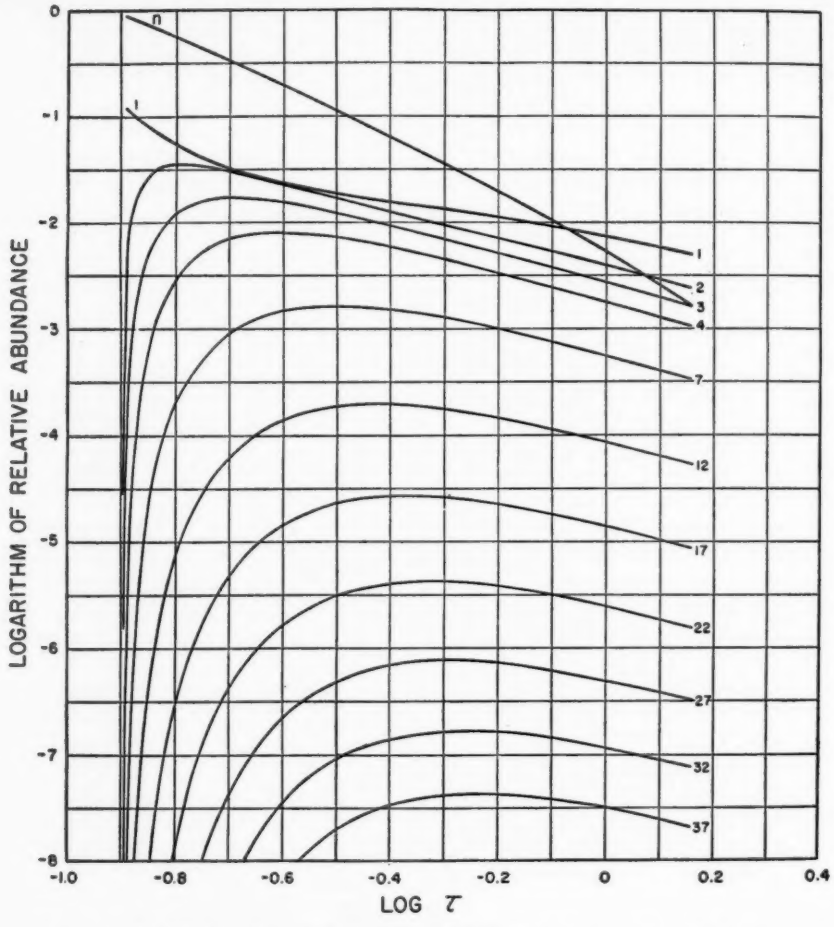

FIG. 5. Relative abundance as a function of time ($\tau = \lambda t$) according to the neutron-capture theory including expansion (12). Curves are labeled to indicate atomic weight. The nucleon concentration at τ_0 for this case is 1.07×10^{17} cm.$^{-3}$

where $\sum'$ denotes summation over the group of size q, and q' is the number of species in the succeeding group. In the integration, group sizes of 5 and 20 were taken for values of j below and above 100, respectively. Neglecting the expansion terms removed the singular nature of Equation 21 so that one could take $\tau = 0$ as the starting time with $\xi_n = 1$ and $\xi_j = 0$ at this τ for all j. Again it was found possible in this approximation to fit the general trend of the relative abundance data by proper choice of the arbitrary parameter ρ_m (9, 10). More recently, Berlin (23) has obtained an exact analytical solution to the equations describing the neutron-capture process in a static universe, i.e., Equation 21 with the expansion terms deleted [see (12)].

The solution of Equations 21a, b, and c, for an expanding universe was obtained recently by means of the SEAC computer (12). The results of this work would appear to provide the best available estimate of the physical conditions associated with element formation. Equations 21, reduced to 27 in number by grouping, were solved for a variety of initial conditions. One of the solutions obtained is illustrated in Figure 5 where $\xi_n(\tau_0)=0.88$, $\xi_1(\tau_0)=0.12$ and $\tau_0=\lambda t_0=0.128$. For a neutron half-life of 12.8 min. (148), the initial temperature and time are $\backsim 1.28\times10^{9}$° K (0.11 Mev) and $\backsim 142$ sec., respectively. The growth curves in Figure 5 show, as expected, that after a sufficiently long τ the relative abundances of all species other than neutrons decrease as $\tau^{-3/2}$, i.e., the only further changes in abundances are those resulting from dilution in the continuing universal expansion. The abundances for large τ therefore no longer change relative to one another, and may be compared with observed universal abundance data if one adds the small percentage residual of decaying neutrons to the proton concentration, since capture reactions are no longer important.

The character of the growth curves depends strongly on the value of C_0. For $C_0 > C_0' = 1.07\times10^{17}$ cm.$^{-3}$ (that used in Fig. 5) the relative abundances go through a sharper peak, whereas for $C_0 < C_0'$ the growth peaks are broadened. The final relative abundances obtained for different values of C_0 are shown in Figure 6, where all abundances are normalized to protons and the solutions joined with the data at $j=1$. The best representation of the observed data (34) is given by the curve labeled C_0' which corresponds to a nucleon concentration of 1.07×10^{17} cm.$^{-3}$ at τ_0. The solutions[24] shown cover a range 2.13×10^{16} cm.$^{-3} \leqq C_0 \leqq 2.13\times10^{18}$ cm.$^{-3}$. For $C_0 > C_0'$ the heavier elements are relatively overabundant, while for $C_0 < C_0'$ only the lightest elements are present in appreciable relative abundance.

The effect of grouping nuclear species in order to reduce the number of Equations 21c has been investigated and can be compensated if a new C_0 is taken which is approximately five times the value in the case of grouping. Hence a better estimate of the C_0 required to represent the general trend of the observed data is $\backsim 5.4\times10^{17}$ cm.$^{-3}$, which corresponds to $\rho_m = 8.9\times10^{-7}$ gm./cm.^{3} at $\tau_0=0.128$, or $\rho_0 = 1.5\times10^{-3}$ gm. cm.$^{-3}$ sec.$^{3/2}$ in Equation 13b. The value of ρ_0 in the nonstatic case is about 25 times larger than the average ρ_m required in the static case. The neutron-capture theory is thus seen to adequately describe the general trend of the observed relative abundance data when the universal expansion is explicitly taken into account.

The formation of light nuclei.—The use of smoothed neutron-capture cross sections for the lightest elements is a very rough approximation. A study of the formation of very light nuclei in terms of specific reactions has been made

[24] The case 0.2 C_0' runs out because of the limitations of a single-precision calculation. The dashed portion of the C_0' curve in Figure 6 reflects the fact that for $j > \sim 90$ the accuracy of solution is reduced to about one significant figure. All curves can be linearly extrapolated for $j > \sim 185$.

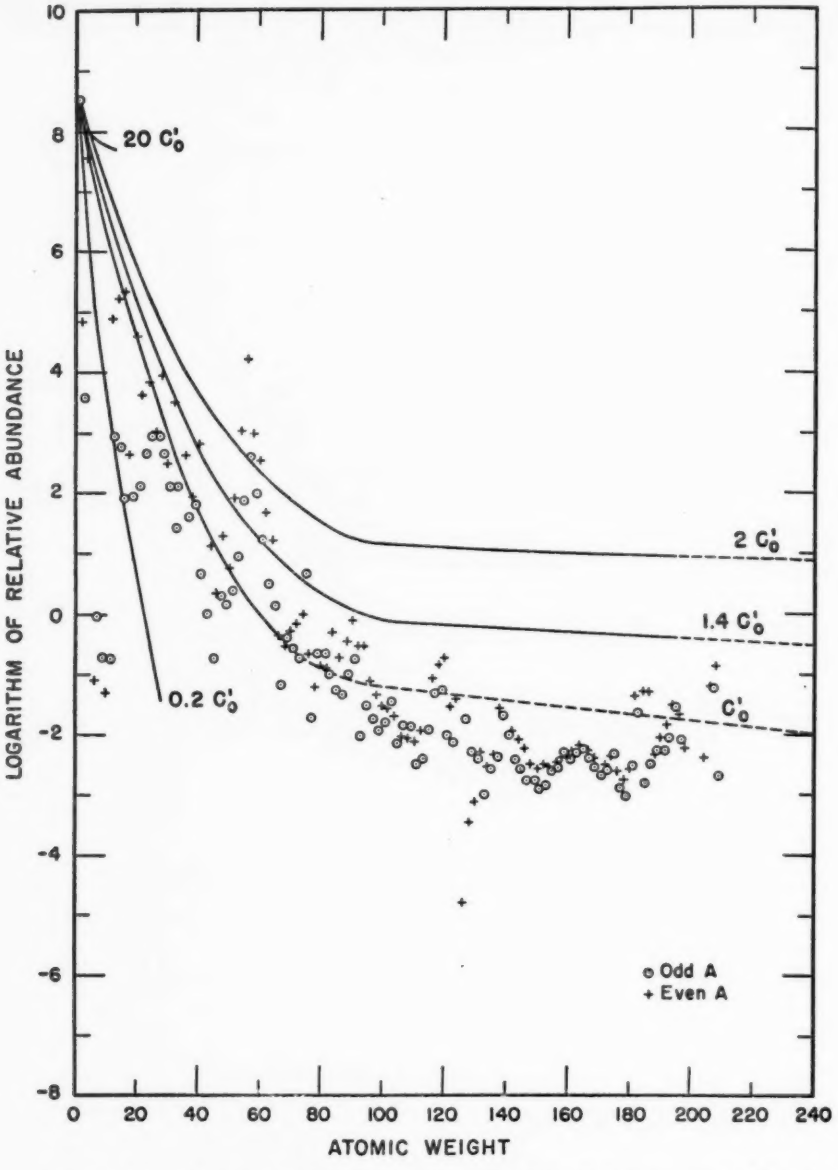

FIG. 6. Comparison with observed abundances (34) of those computed for the neutron capture theory in an expanding universe (12). The effect of varying the initial nucleon concentration is shown by the several curves, where $C_0' = 1.07 \times 10^{17}$ cm.$^{-3}$.

by Gamow (8, 64, 68), Fermi & Turkevich (56) and Carson (37). Gamow investigated the building of deuterons by neutron-proton capture. More recently Fermi & Turkevich examined all the thermonuclear reactions which are less endothermic than the disintegration of the deuteron, and which can go on between n, H, D, T, He^3, and He^4, as well as the radioactive decay of n and H^3. These reactions, 28 in number, were followed in the nonstatic cosmological model containing radiation with a trace of matter, as discussed earlier. Fermi & Turkevich found that among these reactions only neutron decay was important up to $\backsim$300 sec., when the neutron-proton ratio is $\backsim 7/3$ if one started at $t=0$ with neutrons only. After this time the important reactions in addition to neutron decay are $H(n, \gamma)D$, $D(d, \gamma)He^4$, $D(d, n)He^3$, $D(d, p)T$, $T(d, n)He^4$ and $D(\gamma, n)H$. The ρ_0 required was found to be in agreement with that obtained in the neutron-capture theory and the computed relative abundances in qualitative agreement with observation.

One of the difficulties of the nonequilibrium theory is the question of the existence of specific reactions that might carry the formation process past $A=5$ and 8 for which there are no stable nuclei. Fermi & Turkevich did not find sufficient improvement by increasing ρ_0 and up to the present no specific resonance reactions or cyclic reactions involving "seed" nuclei have been successful (10, 65). Recently Turkevich (180) suggested that the fast product particles probably do not become thermalized between successive reactions so that reaction rates might be increased. However, his preliminary calculation yielded negative results. Carson has currently re-examined this question of specific reactions, taking into particular account the fact that the matter temperature may lag the radiation temperature in the universal expansion at early times. This lag results from the time required for thermalization of fast product particles. Furthermore, associated with the initiation of reactions building up nuclei there might be the sudden release of a large amount of energy. A preliminary calculation shows that the resulting momentary increase in reaction rate does not yet provide a mechanism to bridge the gaps.

As has been indicated, Li, Be, and B are at present much less abundant than the general trend in their vicinity and therefore are below the curve predicted by the neutron-capture theory. While it is clear that these species would be depleted in stars, it is also interesting to note that thermonuclear reactions with protons during and following the formation process in the homogeneous expanding universe could yield the observed lowering in relative abundance of these species as well as F^{19}, since they have rather high cross sections for such reactions[25] (14).

Detailed problems.—There are a number of detailed problems associated with the neutron-capture theory, some of which are discussed here briefly. In the theory of the neutron-capture process presented thus far, it has been assumed that the time between successive captures was long enough to allow

[25] Since the depletion would be most rapid at early times this implies that Li, Be, etc., may not have been present in appreciable quantities during stellar formation and, therefore may not have been involved in stellar energy sources.

any necessary adjustment of charge by β-decay. The validity of this assumption depends upon the ρ_m and upon the β-decay rates. Smart (158, 160) has examined this problem in detail and finds that at the densities required by the neutron-capture theory the probabilities of β-decay and of neutron capture should be about equal for the somewhat neutron-rich nuclei involved. This conclusion does not alter the validity of the representation of the general trend of the abundance data by the basic neutron-capture theory, although it does bear directly on detailed calculation of abundances. By following a

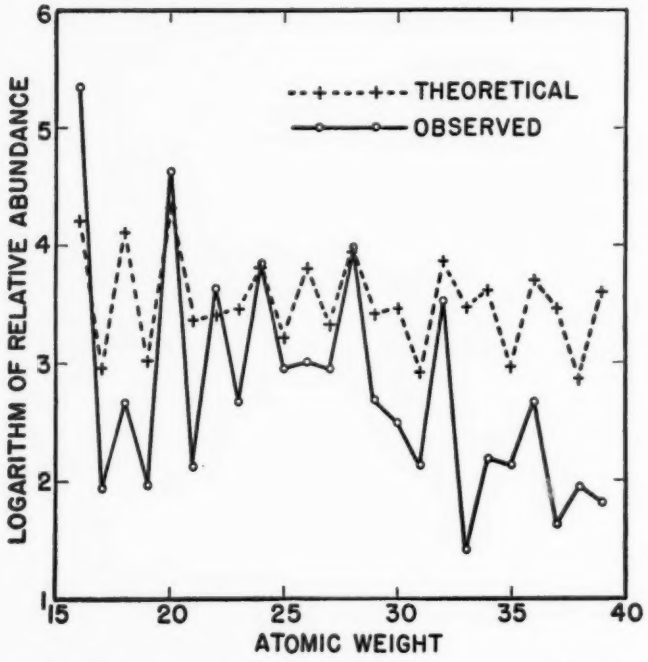

FIG. 7. Relative abundances of the light elements versus atomic weight according to the steady-state formation chain of Smart (158), fitted to Brown's data (34) at Si^{28}.

detailed formation chain and estimating at each step the relative probabilities of β-decay and neutron capture, Smart has calculated the steady state relative abundances of the lighter elements, as shown in Figure 7. It is interesting to compare this with the results of equilibrium theory since there is agreement not only in trend but also most of the computed abundances follow detailed variations in the observed data (compare Fig. 2). Furthermore, Smart's work appears to place the even-odd abundance rules in the framework of the nonequilibrium theory.

Since the neutron-capture theory would appear to involve β-decay as well as neutron-capture reactions, it seems reasonable to suppose that the

final abundance distribution in Z is strongly influenced by β-decay subsequent to the formation process. This raises the question of forming shielded nuclear species, since most sets of stable isobars are of the form ${}_{Z}X^{A}$ and ${}_{Z+2}X^{A}$ and it is the latter or shielded isobars which apparently cannot be reached by β-decay. This problem has not yet been satisfactorily settled, although one must further examine the role of additional reactions such as (γ, n) and $(n, 2n)$ (10, 111, 134, 159).

An outstanding feature of the abundance data is the large peak at iron which has yet to receive quantitative explanation in any theory of element formation. The fact that the elements around iron are most stable makes the explanation of this peak according to an equilibrium theory quite attractive, although not yet successful. On the other hand, in a nonequilibrium theory, the iron peak might be enhanced by thermal dissociation and photodisintegration processes not included in the basic theory. Since the probability of thermal dissociation is an exponential function of binding energy per nucleon, the elements lighter than iron will tend to be depressed in abundance, whereas the large increase in (γ, n) probabilities for $Z \geqq 29$ (30, 111, 144) would tend to depress the abundances of elements heavier than iron, the net result being an emphasis of abundance near iron.

Qualitatively the neutron-capture theory indicates that because of the low neutron-capture cross sections there should be relatively high abundances in the vicinity of the magic number nuclei. Rough calculations do indeed indicate that such would be the case except that in these calculations the relative abundance of the species next following the magic numbers are so depressed that the picture is undoubtedly more complex (10). It has been suggested (9) that one has to include by-passing reactions through isobaric nuclei to remove this difficulty. In the vicinity of the magic numbers would also lie the peaks in mass yield curves due to fission of heavy nuclei [(68); Deutsch (47)]. The fission process would tend to cycle material through the heavy element region during the time of formation, building up mass yield peaks and acting as a terminus in A for the formation process.

One of the most important special problems in the neutron-capture theory is the determination of the proper initial conditions. The authors' work is predicated on the simplified assumption that the neutron-proton ratio at the start of the element-forming process was that determined by the β-decay of a pure neutron ylem up to that time. This assumption ignores the many processes which must have gone on in the expanding universe for, say, the first several hundred critical seconds. While such processes as (γ, n) reactions prevented the building of nuclei in appreciable numbers during this period [see (10)], there may have been other phenomena seriously affecting the relative amounts of neutrons and protons. Recently Hayashi (93) examined this problem and found that the ylem should have an equilibrium proton-neutron ratio of unity, and that by the time of element formation, neutrino-induced β-decay of the neutron should have increased this ratio to about four. With this initial condition in the basic neutron-capture theory, the authors have

not found it possible to reproduce the general trend of the observed data (12). A recalculation of the initial neutron-proton ratio after the method of Hayashi, with more detailed consideration of the relativistic model and of the fundamental processes involved, leads to a ratio not significantly different from that calculated by Hayashi.[26] It would appear necessary to re-examine all of the nonequilibrium processes without the assumption of a specific starting time.

Discussion.—The neutron-capture theory within the framework of a cosmological model predicts not only the general trend of the abundance data but also some of the detailed features when β-decay and other specific processes are taken into account. However, the principal difficulties still extant are those associated with the gaps at $A=5$ and 8, shielded isobars, and the initial conditions. While the theory is in a quite approximate state at the present time, it is hoped that the inclusion of the growing knowledge of the properties of nuclei and nuclear reactions will satisfactorily explain the detailed features of the abundance data, provided, of course, that the extremely difficult detailed calculations can be carried out.

The Polyneutron Fission Theory

A rather different approach to the problem of element origin is the formation of nuclei as the result of the fission of supernuclei. While the properties of such supernuclei have been examined rather extensively, there has not been any successful calculation of the resulting relative abundance distribution as a function of atomic weight. The originator of these ideas was Lemaître (123), who suggested that in the "beginning" the entire universe consisted of one huge nucleus and that the disruption of this "primeval atom" marked the start of the time scale and of the universal expansion as well as the mechanism for element formation by evaporation. More recently Cherdyncev (42) applied equilibrium notions to neutron nuclei in large neutron aggregates of stellar dimensions. Here again the breakup hypothesis is invoked with the common nuclei produced by the β-decay of the pure neutron fragments. Mayer & Teller (133, 134) have suggested as a source for heavy elements the fragments resulting from the breakup of a polyneutron—a cold nuclear fluid consisting primarily of neutrons and of somewhat less than stellar dimensions. They have calculated some of the properties of the polyneutron and give a theory for its fission into highly excited fragments. A mechanism for the formation of such original polyneutrons has been suggested by Peierls, Singwi & Wroe (142),[26] who consider a cool homogeneous expanding universe of very high ρ_m which initially consists of neutrons and in which cavities form because of the development of tension. The cavities are shown to grow in a regular manner so that the nuclear fluid ultimately separates into lumps identified with the Mayer-Teller polyneutrons.

As a consequence of the polyneutron theory, there have been several attempts to describe the relative abundance distribution. Mayer & Teller

[26] This work is currently being carried on by the authors with J. W. Follin, Jr.

(134) have had a measure of success in predicting relative isotopic abundances for some species by assuming that for a given Z the isotopic abundances obey a Gaussian distribution weighted according to the binding energy of the last neutron. While they show that the polyneutron fission fragments will more than cover the range required in Z above $Z=37$, they have not estimated the relative frequency of fragments of given sizes. Thus there does not appear to be a direct tie-up between the isotopic abundance calculation and the break-up hypothesis, and in particular the abundance distribution in A does not result from their work. Peierls, Singwi & Wroe (142) have shown that, principally because of the low temperature involved in the formation and subsequent fission of the polyneutrons, the mass of material which would remain as heavy nuclei greatly exceeds that left over as free neutrons which it has been assumed would combine to form the light elements. They have been unable to find any simple modification of the theory such as a higher temperature which would solve the light element difficulty and at the same time preserve the conditions required for the formation and evolution of polyneutrons.

In an attempt to explain light element abundances in connection with the polyneutron theory, Band (21) has used the quantum statistics of a dissociative clustering nucleon gas. His formal result for equilibrium concentrations differs negligibly from that given by the Gibbs grand canonical ensemble and his work appears essentially to reproduce the many earlier equilibrium calculations. A fit for the light elements only was obtained to the observed abundance data for $kT \cong 5$ Mev. Band suggests that the primordial fluid first separated into two phases, one being superclusters which eventually cooled and became polyneutrons, the other being the atmosphere of polyneutrons which yields the light elements. This suggestion is not in agreement with the evolutionary model for polyneutrons proposed by Peierls, Singwi & Wroe.

The various investigations of the polyneutron model are interesting and provocative. However, they suffer from two main difficulties, namely, they appear to raise difficult cosmological questions and they have not been successful as yet in predicting the over-all trend of the relative abundance distribution.

Matter Creation Theory

From the earlier discussions it is clear that the cosmological problem should be considered as an integral part of the framework of theories of element formation. While it is beyond the scope of this work to review the large subject of cosmological theory, the recently proposed steady state theory of the expanding universe involves matter creation and is therefore pertinent for discussion here. Perhaps the earliest suggestion along these lines was that of Jeans (105) who conjectured that in the center of galaxies there might be singular points through which matter entered the universe from "elsewhere." More recently Dirac (48) suggested the time variation of some of the universal constants as a new basis for cosmology. In particular he

proposed that the constant of gravitation decrease with time, requiring an increase with time of the amount of matter in the universe. Dirac (49) later modified this theory to preserve the conservation of matter. Jordan (112) has also described a cosmology involving time-dependent universal constants in which matter somehow enters the universe in the form of "drops" of the dimensions of giant stars, which events are suggested as being supernovae outbursts. The most extensively developed ideas along these lines are those of Bondi & Gold (29) and Hoyle (100) who have suggested

> that the creation of matter is a continuing process operating at the same statistical rate at all epochs, a statistically constant density being preserved by the dispersal of matter known as the expansion of the universe.[27]

Hoyle has formalized these ideas by considering field equations as nearly as possible like those of Einstein without requiring the conservation of matter, while McCrea (125) more recently has shown that one may use the Einstein theory without any modification other than the introduction of a zero-point stress in the energy-momentum tensor. According to McCrea the matter created is the mass equivalent of the work done by this stress in the universal expansion. The process proposed is the spontaneous creation of either neutrons, hydrogen atoms, or protons and electrons, or neutrons at a rate of about 3×10^{-44} gm. cm^{-3} sec.$^{-1}$ which would maintain a $\rho_m=6\times10^{-28}$ gm. cm.$^{-3}$ at a constant value according to the present expansion rate.

The mechanism suggested by Hoyle (98, 99) for the formation of all the elements from the continually created hydrogen involves the formation of stars by accretion. These stars are supposed eventually to dehydrogenize and during subsequent collapse heavier elements are synthesized. The difficulties associated with this mode of element formation, and in particular the problem of freezing-in an equilibrium distribution from an exploding star, have been described in the earlier discussion of the equilibrium theory (10).

Conclusion

The abbreviated nature of this review makes it impractical to bring together here a more detailed discussion than has already been given of the successes and failures of the theories of the origin and relative abundance of the elements. None of the theories presented is without serious difficulties. However, it is the belief of the authors, and perhaps not without prejudice, that the theory of element formation principally by neutron-capture reactions in the expanding universe may suffer from fewer difficulties than other theories. In addition, this theory has as a minimum provided a fit to the general trend of the relative abundance data with relatively few adjustable parameters within the framework of what at present appears to be a reasonable cosmological theory. The authors have attempted to give as objective a

[27] Quoted from a review of this subject by McCrea (124) q.v. for general references. See also McVittie (128).

survey as possible of the present status of this problem and hope that it will serve to point up the many interesting and provocative questions that remain in this unsettled field.

LITERATURE CITED

1. Albada, G. B. van, *Bull. Astron. Inst. Netherlands*, **10**, 161 (1946)
2. Albada, G. B. van, *Astrophys. J.*, **105**, 393 (1947)
3. Allen, R., Bishop, G. R., Demers, P., and Halban, H. von, *Nature*, **161**, 727 (1948)
4. Aller, L. H., in *Astrophysics*, 29 (Hynek, J. A., Ed., McGraw-Hill Book Co., Inc., New York, N. Y., 703 pp., 1951)
5. Alpher, R. A., *On the Origin and Relative Abundance of the Elements* (Doctoral thesis, George Washington Univ., Washington, D. C., 1948)
6. Alpher, R. A., *Phys. Rev.*, **74**, 1577 (1948)
7. Alpher, R. A., Bethe, H. A., and Gamow, G., *Phys. Rev.*, **73**, 803 (1948)
8. Alpher, R. A., and Herman, R. C., *Nature*, **162**, 774 (1948)
9. Alpher, R. A., and Herman, R. C., *Phys. Rev.*, **74**, 1737 (1948)
10. Alpher, R. A., and Herman, R. C., *Revs. Modern Phys.*, **22**, 153 (1950); **22**, 406 (1950)
11. Alpher, R. A., and Herman, R. C., *Phys. Rev.*, **75**, 1089 (1949)
12. Alpher, R. A., and Herman, R. C., *Phys. Rev.*, **84**, 60 (1951)
13. Alpher, R. A., and Herman, R. C., *Phys. Rev.*, **84**, 1111 (1951)
14. Alpher, R. A., Herman, R. C., and Gamow, G., *Phys. Rev.*, **74**, 1198 (1948); **75**, 701 (1949)
15. Aston, F. W., *Phil. Mag.*, **45**, 400 (1923)
16. Aten, A. H. W., Jr., *Phys. Rev.*, **73**, 1206 (1948)
17. Aten, A. H. W., Jr., *Science*, **110**, 260 (1949)
18. Atkinson, R. d'E., *Astrophys. J.*, **73**, 250 (1931); **73**, 308 (1931); **84**, 73 (1936)
19. Atkinson, R. d'E., and Houtermans, F. G., *Z. Physik.*, **54**, 656 (1929)
20. Baade, W., *Extragalactic Nebulae* (Univ. of Chicago Press, Chicago, Ill., 1952)
21. Band, W., *Phys. Rev.*, **79**, 871 (1950); **80**, 813 (1950)
22. Behr, A., *Astron. Nachr.*, **279**, 97 (1951)
23. Berlin, T. H., in Ref. (12)
24. Beskow, G., and Treffenberg, L., *Arkiv Mat. Astron. Fysik*, [A]**34**, No. 13 (1947)
25. Beskow, G., and Treffenberg, L., *Arkiv Mat. Astron. Fysik*, [A]**34**, No. 17 (1947)
26. Bethe, H. A., *Phys. Rev.*, **55**, 434 (1939)
27. Bethe, H. A., and Critchfield, C. L., *Phys. Rev.*, **54**, 248 (1938)
28. Bok, B. J., *Monthly Notices Roy. Astron. Soc.*, **106**, 61 (1946)
29. Bondi, H., and Gold, T., *Monthly Notices Roy. Astron. Soc.*, **108**, 252 (1948)
30. Bowers, W. A., *Phys. Rev.*, **74**, 1538 (1948)
31. Bradt, H. L., Freier, P. S., Lofgren, E. J., Ney, E. P., Oppenheimer, F., and Peters, B., *Revs. Modern Phys.*, **21**, 101 (1949)
32. Bradt, H. L., and Peters, B., *Phys. Rev.*, **80**, 943 (1950)
33. Brightsen, R. A., *Nucleonics*, **6**, (4), 14 (1950)
34. Brown, H., *Revs. Modern Phys.*, **21**, 625 (1949)
35. Brown, H., and Patterson, C., *J. Geol.*, **55**, 405 (1947); **55**, 508 (1947); **56**, 85 (1948)
36. Burling, R. L., *Phys. Rev.*, **84**, 839 (1951)
37. Carson, A. N. (Personal communication)

38. Chackett, K. F., and Martin, G. R., *Proc. Phys. Soc.* (*London*), [A]**61**, 197 (1948)
39. Chandrasekhar, S., *An Introduction to the Study of Stellar Structure* (Univ. of Chicago Press, Chicago, Ill., 509 pp., 1939)
40. Chandrasekhar, S., in *Astrophysics*, p. 598 (Hynek, J. A., Ed., McGraw-Hill Book Co., Inc., New York, N. Y., 703 pp., 1951)
41. Chandrasekhar, S., and Henrich, L. R., *Astrophys. J.*, **95**, 288 (1942)
42. Cherdyncev, V., *Astron. J. Soviet Union*, **17**, 1 (1940); **17**, 12 (1940); **18**, 1 (1941)
43. Cherdyncev, V., *Compt. rend. acad. sci. U.R.S.S.*, **33**, 22 (1941)
44. Dainton, A. D., and Kent, D. W., *Phil. Mag.*, **41**, 963 (1950); Dainton, A. D., Fowler, P. H., and Kent, D. W., *Phil. Mag.*, **43**, 729 (1952)
45. Dementi, V. S., and Timoshuk, D. V., *Compt. rend. acad. sci. U.R.S.S.*, **27**, 926, (1940)
46. Demeur, M., *Physica*, **13**, 321 (1947)
47. Deutsch, M., in *The Science and Engineering of Nuclear Power*, **1** (Goodman, C., Ed., Addison-Wesley Press, Inc., Cambridge, Mass., 536 pp., 1947)
48. Dirac, P. A. M., *Nature*, **139**, 323 (1937)
49. Dirac, P. A. M., *Proc. Roy. Soc.* (*London*), [A]**165**, 199 (1938)
50. Döpel, R., and Döpel, K., *Z. Astrophys.*, **14**, 139 (1937)
51. Einstein, A., *The Meaning of Relativity* (Princeton Univ. Press, Princeton, N. J., 135 pp., 1945)
52. Elsasser, W. M., *J. phys. radium*, **4**, 549 (1933); **5**, 389 (1934); **5**, 635 (1934); *Compt. rend.*, **199**, 46 (1934); **199**, 1213 (1934)
53. Farkas, L., and Harteck, P., *Naturwissenschaften*, **19**, 705 (1931)
54. Feenberg, E., *Revs. Modern Phys.*, **19**, 239 (1947)
55. Feenberg, E., *Ann. Rev. Nuclear Sci.*, **1**, 43 (1952)
56. Fermi, E., and Turkevich, A., in Ref. (10)
57. Follin, J. W., Jr. (Personal communication)
58. Fowler, R. H., *Statistical Mechanics* (Cambridge Univ. Press, Cambridge, England, 570 pp., 1929)
59. Frank, F. C., *Proc. Phys. Soc.* (*London*), **60**, 211 (1948)
60. Freier, P. S., Anderson, G. W., Naugle, J. E., and Ney, E. P., *Phys. Rev.*, **84** 322 (1951)
61. Gamow, G., *Ohio J. Sci.*, **35**, 406 (1935)
62. Gamow, G., *Astrophys. J.*, **98**, 500 (1943)
63. Gamow, G., *Phys. Rev.*, **70**, 572 (1946)
64. Gamow, G., *Nature*, **162**, 680 (1948)
65. Gamow, G., *Revs. Modern Phys.*, **21**, 367 (1949)
66. Gamow, G., *Nature*, **168**, 72 (1951)
67. Gamow, G., *Creation of the Universe* (Viking Press, New York, N. Y., 167 pp., 1952)
68. Gamow, G., and Critchfield, C. L., *Theory of Atomic Nucleus and Nuclear Energy-Sources* (The Clarendon Press, Oxford, England, 344 pp., 1949)
69. Géhéniau, J., Prigogine, I., and Demeur, M., *Physica*, **13**, 429 (1947)
70. Gibbs, J. W., *Collected Works* (Yale Univ. Press, New Haven, Conn., 1948)
71. Goldschmidt, V. M., *Naturwissenschaften*, **18**, 999 (1930)
72. Goldschmidt, V. M., *Skrifter Norske Videnskaps-Akad. Oslo*, **I**, *Mat.-Naturv. Klasse*, No. 4, 148 (1938)
73. Goodman, C., Ed., *The Science and Engineering of Nuclear Power*, **1** (Addison-Wesley Press, Inc., Cambridge, Mass., 536 pp., 1947)

74. Greenstein, J. L., *Astrophys. J.*, **107**, 151 (1948)
75. Greenstein, J. L., *Astrophys. J.*, **113**, 531 (1951)
76. Greenstein, J. L., in *Astrophysics* p. 526 (Hynek, J. A., Ed., McGraw-Hill Book Co., Inc., New York, N. Y., 703 pp., 1951)
77. Greenstein, J. L., and Richardson, R. S., *Astrophys. J.*, **113**, 536 (1951)
78. Griffiths, J. H. E., *Proc. Roy. Soc.* (*London*), [A]**170**, 513 (1939)
79. Guggenheimer, K., *J. phys. radium*, **5**, 253 (1934); **5**, 475 (1934)
80. Haar, D. ter, *Kgl. Danske. Videnskab. Selskab. Mat.-fys. Medd.*, **25**, No. 3 (1948)
81. Haar, D. ter, *Science*, **107**, 405 (1948)
82. Haar, D. ter, *Science*, **109**, 81 (1949)
83. Haar, D. ter, *Am. J. Phys.*, **17**, 282 (1949)
84. Haar, D. ter, *Revs. Modern Phys.*, **22**, 119 (1950)
85. Haar, D. ter, *Phys. Rev.*, **76**, 1525 (1949)
86. Halban, H. von, and Kowarski, L., *Nature*, **142**, 392 (1938)
87. Harkins, W. D., *J. Am. Chem. Soc.*, **39**, 856 (1917)
88. Harkins, W. D., *Phys. Rev.*, **38**, 1270 (1931)
89. Harkins, W. D., in *Colloid Chem.*, **7**, 3 (1951)
90. Harkins, W. D., and Popolka, M., Jr., *Phys. Rev.*, **76**, 989 (1949)
91. Harkins, W. D., and Wilson, E. D., *Phil. Mag.*, **30**, 723 (1915)
92. Harteck, P., and Suess, H. E., *Naturwissenschaften*, **36**, 218 (1949)
93. Hayashi, C., *Progress Theoret. Phys.*, **5**, 225 (1950)
94. Henkel, R. L., and Barschall, H. H., *Phys. Rev.*, **80**, 145 (1950)
95. Herzberg, G., *J. Roy. Astron. Soc. Can.*, **45**, 100 (1951)
96. Hevesy, G. von, *Chemical Analysis by X-Rays and Its Applications* (McGraw-Hill Book Co., Inc., New York, N. Y., 333 pp., 1932)
97. Hoang, T.-F., *Compt. rend.*, **230**, 292 (1950); *Ann. phys.*, **5**, 537 (1950)
98. Hoyle, F., *Monthly Notices Roy. Astron. Soc.*, **106**, 343 (1946)
99. Hoyle, F., *Proc. Phys. Soc.* (*London*), **59**, 972 (1947)
100. Hoyle, F., *Monthly Notices Roy. Astron. Soc.*, **108**, 372 (1948); *Nature*, **163**, 196 (1949); *Monthly Notices Roy. Astron. Soc.*, **109**, 365 (1949)
101. Hubble, E. P., *The Realm of the Nebulae* (Yale Univ. Press, New Haven, Conn., 210 pp., 1936); *The Observational Approach to Cosmology* (The Clarendon Press, Oxford, England, 1937); *Sigma Xi Quart.*, **30**, 99 (1942)
102. Hughes, D. J., Garth, R. C., and Eggler, C., *Phys. Rev.* (In press)
103. Hughes, D. J., Spatz, W. B., and Goldstein, N., *Phys. Rev.*, **75**, 1781 (1949)
104. Hurwitz, H., Jr., and Bethe, H. A., *Phys. Rev.*, **81**, 898 (1951)
105. Jeans, J. H., *Astronomy and Cosmogony* (Cambridge Univ. Press, London, England, 420 pp., 1929)
106. Jensen, H., *Naturwissenschaften*, **27**, 793 (1939)
107. Jensen, H., *Naturwissenschaften*, **27**, 841 (1939)
108. Jensen, J. H. D., and Steinwedel, H., *Naturwissenschaften*, **33**, 249 (1946)
109. Jensen, J. H. D., and Suess, H. E., *Naturwissenschaften*, **32**, 374 (1944)
110. Jensen, J. H. D., and Suess, H. E., *Naturwissenschaften*, **34**, 131 (1947)
111. Jensen, P., *Proc. Phys. Soc.* (*London*), **61**, 579 (1948)
112. Jordan, P., *Nature*, **164**, 637 (1949)
113. Katcoff, S., Schaeffer, O. A., and Hastings, J. M., *Phys. Rev.*, **82**, 688 (1951)
114. Kempton, A. E., *Nature*, **165**, 801 (1950)
115. Klein, O., *Arkiv Mat. Astron. Fysik*, [A]**34**, No. 19 (1947)
116. Klein, O., *Nuovo cimento*, **6**, Suppl. 2, 171 (1949)
117. Klein, O., *Revs. Modern Phys.*, **21**, 531 (1949)

118. Klein, O., Beskow, G., and Treffenberg, L., *Arkiv Mat. Astron. Fysik*, [B]**33**, No. 1 (1946)
119. Klüber, H. von, *Das Vorkommen der Chemischen Elemente im Kosmos* (J. A. Barth, Leipzig, Germany, 170 pp., 1931)
120. Kuiper, G. P., Ed., *The Atmospheres of the Earth and Planets* (Univ. of Chicago Press, Chicago, Ill., 366 pp., 1949)
121. Lacroute, P., *Compt. rend.*, **224**, 1481 (1947)
122. Lattes, C., and Wataghin, G., *Acad. Brasil. Cien., Anais*, **17**, 269 (1945); *Phys. Rev.*, **69**, 237 (1946)
123. Lemaître, G., *The Primeval Atom* (D. Van Nostrand Company, Inc., New York, N. Y., 186 pp., 1950); *Nature*, **127**, 706 (1931)
124. McCrea, W. H., *Endeavour*, **9**, 3 (1950)
125. McCrea, W. H., *Proc. Roy. Soc.* (*London*), [A]**206**, 562 (1951)
126. McKellar, A., *Pubs. Astron. Soc. Pacific*, **62**, 110 (1950)
127. McVittie, G. C., *Nature*, **154**, 477 (1944)
128. McVittie, G. C., *Proc. Roy. Soc.* (*London*), [A]**211**, 295 (1952)
129. MacNamara, J., and Thode, H. G., *Phys. Rev.*, **80**, 296 (1950)
130. Martell, E. A., and Libby, W. F., *Phys. Rev.*, **80**, 977 (1950)
131. Mattauch, J., *Z. Physik.*, **91**, 361 (1934); *Physik. Z.*, **35**, 567 (1934); *Naturwissenschaften*, **25**, 738 (1937)
132. Mattauch, J., and Fluegge, S., *Nuclear Physics Tables and an Introduction to Nuclear Physics* (Interscience Publishers, Inc., New York, N. Y., 173 pp., 1946)
133. Mayer, M. G., and Teller, E., *Rept. Solvay Congr., Brussels*, (1948)
134. Mayer, M. G., and Teller, E., *Phys. Rev.*, **76**, 1226 (1949)
135. Mescheryakov, M. G., *Compt. rend. acad. sci. U.R.S.S.*, **48**, 555 (1948)
136. Morrison, P., and Beard, D. B., *Phys. Rev.*, **75**, 1332A (1949)
137. Noddack, I., and Noddack, W., *Naturwissenschaften*, **18**, 757 (1930)
138. Oddo, G., *Z. anorg. chem.*, **87**, 253 (1914)
139. Omer, G. C., Jr., *Astrophys. J.*, **109**, 164 (1949)
140. Öpik, E. J., *Monthly Notices Roy. Astron. Soc.*, **111**, 278 (1951)
141. Payne, C. H., *Harvard Observatory Monograph*, **1** (1925)
142. Peierls, R. E., Singwi, K. S., and Wroe, D., *Phys. Rev.*, **87**, 46 (1952)
143. Perlman, I., *Nucleonics*, **7**(2), 3 (1950)
144. Perlman, M. L., and Friedlander, G., *Phys. Rev.*, **74**, 442 (1948)
145. Peters, B., in *Progress in Cosmic Ray Physics* p. 191 (Wilson, J. G., Ed., Interscience Publishers, Inc., New York, N. Y., 557 pp., 1951)
146. Pokrowski, G. I., *Physik. Z.*, **32**, 374 (1931)
147. Rankama, K., and Sahama, T. G., *Geochemistry* (Univ. of Chicago Press, Chicago, Ill., 1950)
148. Robson, J. M., *Phys. Rev.*, **83**, 349 (1951)
149. Rosenfeld, L., *Nuclear Forces* (Interscience Publishers, Inc., New York, N. Y., 543 pp., 1949)
150. Russell, H. N., *Science*, **94**, 375 (1941)
151. Saha, M. N., *Phil. Mag.*, **40**, 809 (1920); *Proc. Roy. Soc.* (*London*), [A]**99**, 135 (1921); *Z. Physik.*, **6**, 40 (1921)
152. Salpeter, E. E., *Astrophys. J.*, **112**, 526 (1952)
153. Salpeter, E. E., *Ann. Rev. Nuclear Sci.*, **2**, 41 (1953)
154. Schwarzschild, M., Spitzer, L., Jr., and Wildt, R., *Astrophys. J.*, **114**, 398 (1951)

155. Seaborg, G. T., and Perlman, I., *Revs. Modern Phys.*, **20**, 585 (1948)
156. Seaton, M. F., *Monthly Notices Roy. Astron. Soc.*, **111**, 368 (1951)
156a. Singwi, K. S., and Agarwala, B. K., *Proc. Natl. Inst. Sci.* India, **17**, 425 (1951)
157. Singwi, K. S., and Rai, R. N., *Proc. Natl. Inst. Sci. India*, **12**, 291 (1946)
158. Smart, J. S., *on the Formation and Relative Abundances of the Chemical Elements* (Doctoral thesis, Univ. of Minnesota, 1948)
159. Smart, J. S., *Phys. Rev.*, **74**, 1882 (1948)
160. Smart, J. S., *Phys. Rev.*, **75**, 1379 (1949)
161. Sonder, R. A., *Schweiz. mineralog. petrog. Mitt.*, **28**, 528 (1948)
162. Stebbins, J., and Whitford, A. E., *Astrophys. J.*, **108**, 413 (1948); *Proc. Am. Phil. Soc.*, **93**, 45 (1949)
163. Steensholt, G., *Z. Astrophys.*, **5**, 140 (1932); *Pubs. Oslo Univ. Observatory*, **1**, No. 4 (1931–34)
164. Steinwedel, H., and Jensen, J. H. D., *Z. Physik*, **125**, 394 (1949)
165. Sterne, T. E., *Monthly Notices Roy. Astron. Soc.*, **93**, 736 (1933); **93**, 767 (1933); **93**, 770 (1933); *Trans. Am. Electrochem. Soc.*, **68**, 73 (1935)
166. Stewart, D. W., *Ann. Rev. Phys. Chem.*, **2**, 67 (1951)
167. Strömgren, B., *Ergeb. exakt. Naturw.*, **16**, 465 (1937)
168. Struve, O., *Stellar Evolution* (Princeton Univ. Press, Princeton, N. J., 266 pp., 1950)
169. Suess, H. E., *Z. Naturforsch.*, [A]**2**, 311 (1947); [A]**2**, 604 (1947)
170. Suess, H. E., *Z. physik*, **125**, 386 (1949)
171. Suess, H. E., *Experientia*, **5**, 266 (1949)
172. Suess, H. E., and Brown, H., *Phys. Rev.*, **83**, 1254 (1951)
172a. Swings, P., in *Astrophysics*, p. 145 (Hynek, J. A., Ed., McGraw-Hill Book Co., New York, N. Y., 703 pp., 1951)
173. Suzuki, S., *Proc. Phys.-Math. Soc. Japan*, **10**, 166 (1928); **11**, 119 (1929); **13**, 277 (1931)
174. Thode, H. G., *Research* (*London*), **21**, 155 (1949)
175. Toledo, P. S. de, and Wataghin, G., *Phys. Rev.*, **73**, 79 (1948)
176. Tolman, R. C., *J. Am. Chem. Soc.*, **44**, 1902 (1922)
177. Tolman, R. C., *Relativity, Thermodynamics and Cosmology* (The Clarendon Press, Oxford, England, 501 pp., 1934)
178. Tolman, R. C., *The Principles of Statistical Mechanics* (The Clarendon Press, Oxford, England, 660 pp., 1938)
179. Tolman, R. C., *Revs. Modern Phys.*, **21**, 374 (1949)
180. Turkevich, A. (Personal communication)
181. Ubbleohde, A. R., *Proc. Phys. Soc.* (*London*), **59**, 139 (1947); **61**, 96 (1948)
182. Unsöld, A., *Himmelswelt*, **55**, 12 (1947); **55**, 59 (1948)
183. Unsöld, A., *Z. Astrophys.*, **24**, 278 (1948)
184. Unsöld, A., *Z. Astrophys.*, **24**, 306 (1948)
185. Urey, H. C., *J. Chem. Soc.*, 562 (1947)
186. Urey, H. C., *The Planets* (Yale Univ. Press, New Haven, Conn., 254 pp., 1952); *Geochimica et Cosmochimica Acta*, **1**, 209 (1951)
187. Urey, H. C., and Bradley, C. A., Jr., *Phys. Rev.*, **38**, 718 (1931)
188. Vaidya, P. C., *Nature*, **166**, 565 (1950); *Proc. Indian Acad. Sci.*, **33**, 264 (1951); *Phys. Rev.*, **83**, 10 (1951)
189. Walke, H. J., *Phil. Mag.*, **18**, 795 (1934); **19**, 33 (1935); **19**, 341 (1935)
190. Wataghin, G., *Phil. Mag.*, **17**, 910 (1934); *Compt. rend.*, **200**, 909 (1935); *Phys.*

Rev., **63**, 137 (1943); **66**, 149 (1944); **69**, 33 (1946); **70**, 430 (1946); *Compt. rend.*, **226**, 633 (1948); *Phys. Rev.*, **73**, 79 (1948); *Nuovo cimento*, **6**, Suppl. 2, 241 (1949)

191. Way, K. (Personal communication)
192. Weizsäcker, C. F. von, *Physik. Z.*, **38**, 176 (1937); **39**, 633 (1938)
193. Weizsäcker, C. F. von, *Astrophys. J.*, **114**, 165 (1951)
194. Wigner, E. P., *Am. J. Phys.*, **17**, 99 (1949)
195. Wilson, A. H., *Monthly Notices Roy. Astron. Soc.*, **91**, 283 (1931)
196. Yagoda, H., *Phys. Rev.*, **80**, 753 (1950)
197. Yagoda, H., *Phys. Rev.*, **85**, 720A (1952)

ENERGY PRODUCTION IN STARS[1]

By E. E. Salpeter

Newman Laboratory of Nuclear Studies, Cornell University, Ithaca, New York

Introduction

The most apparent astrophysical fact is that stars emit electromagnetic radiation and hence are continuously losing energy to their surroundings. The mean rate $\bar{\epsilon}$ at which energy is emitted in the form of radiation, per unit mass of the star, is not very large. For the sun, for instance, $\bar{\epsilon}$ is only 2 ergs per gm. per sec., which is much less than 1 per cent of the rate of heat generation during animal metabolism. On the other hand, we know from geological evidence that the sun has been emitting radiation at approximately its present rate for several billions of years. There is also strong astrophysical evidence that the age of our galaxy is of the same order of magnitude.

Chemical sources of energy production could not supply the observed energy emission of a star for more than a few thousand years. The gravitational energy gained by the gradual contraction of a star is a more important source of energy, but if this were the only energy source our sun could not be older than 2×10^7 years. On the other hand, many exothermic nuclear reactions liberate energies of several Mev per nucleon, or about 10^{19} ergs per gm. Such nuclear reactions could sustain the energy loss of the sun for about 10^{11} years and are the only type of reactions which can supply a sufficiently large amount of energy.

Almost 15 years ago the actual nuclear reactions of importance under stellar conditions were discussed and their reaction rates calculated in the classic papers by Bethe & Critchfield (1) and by Bethe (2), as well as by Weizsäcker and Atkinson & Houtermans (3). These classic results have since been applied to different specific stellar problems by various authors. A review of some of the aspects of these problems has been given previously by Gamow & Critchfield (4), Ter Haar (5), Chandrasekhar (6), and Bethe & Marshak (7).

The biggest advance in the field of stellar energy production in the last few years has come from a great increase in accuracy and completeness of experimental determinations of nuclear energy levels and cross sections of nuclear reactions. A summary of most of these determinations has been given by Hornyak *et al.* (8). In the sections, Proton-Proton Chain and Carbon-Nitrogen Cycle, of the present review, we give a summary of the chains of nuclear reactions which are of importance in the interior of a normal main sequence star, and the reaction rates as a function of temperature and density, as obtained from our present quantitative knowledge of nuclear physics. In the section, Stars Which Have Exhausted Their Hydrogen Supply, we summarize the reactions of importance for such stars.

[1] The survey of the literature pertaining to this review was concluded in April, 1952.

To draw quantitative conclusions about stellar energy production and the evolution of stars we need two types of information. Firstly, we need to know the relevant reaction rates as a function of temperature and density; secondly, we need to know the details of stellar structure, i.e., chemical composition, state of mixing, distribution of mass and temperature, rotation, interaction with the surrounding, etc. The problem of stellar structure is a very difficult one and, in spite of a large amount of work done in this subject it is still in a controversial state. In the sections, EMPIRICAL ASTROPHYSICAL DATA and STELLAR STRUCTURE AND EVOLUTION, we summarize, in a highly schematic form, some of the relevant conclusions on which there is at least moderate agreement, without discussing in detail the reliability and range of validity of these conclusions. In the sections, ENERGY PRODUCTION IN MAIN SEQUENCE STARS, STARS WHICH HAVE EXHAUSTED THEIR HYDROGEN SUPPLY; WHITE DWARFS, RED GIANTS, AND VARIABLES, and SUPERNOVAE, we discuss briefly some tentative conclusions about energy production in different types of stars to which the astrophysical and nuclear data might lead.

The bibliography is by no means complete. Of a large number of equally important papers on a particular topic only the most recent ones, or those having the most extensive review of the literature, will be quoted.

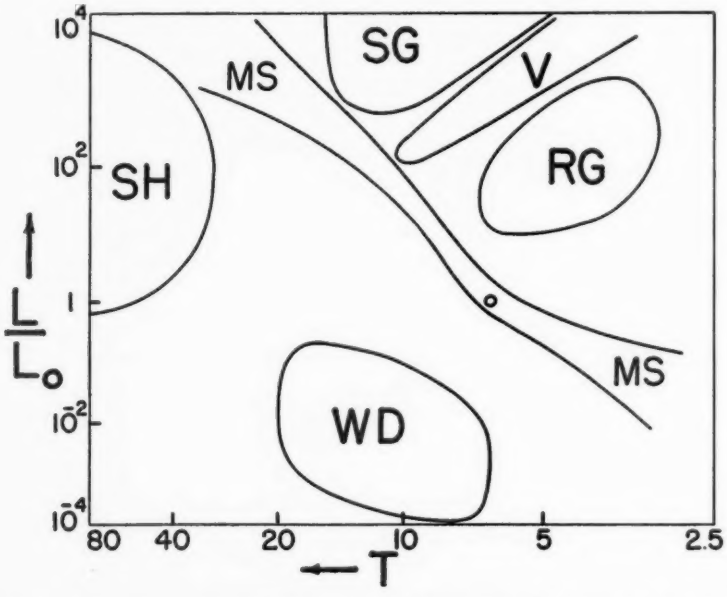

FIG. 1. Hertzsprung-Russell Diagram. L is the luminosity and T_S the effective surface temperature of the star, in units of $10^{3°}$ K. **MS** denotes "Main Sequence"; **SG** "super giants"; **V** "variable stars"; **RG** "red giants"; **WD** "white dwarfs"; **SH** "superhot stars." The symbol ⊙ denotes the position of the sun.

Empirical Astrophysical Data

We give in this section a brief account of some of the astrophysical data which can be obtained fairly directly from astronomical observations. For a fuller account see Strömgren (9), Kienle (10), and Hynek *et al.* (11).

The distance from the earth of a few thousand stars is known observationally. For these stars then the absolute luminosity L (total energy radiated per second) can be obtained from a measurement of their apparent (visible) luminosity, after the appropriate bolometric correction has been estimated. From a detailed spectral analysis of the light emitted by any star, its effective surface temperature T_S can be calculated. If L is plotted against T_S (Hertzsprung-Russell diagram) one finds stars only in certain regions of this diagram. The most conspicuous region is the "main sequence," a fairly narrow band ranging from hot and luminous stars (white giants) to cool and faint stars (red dwarfs). The main sequence stars are the best understood at the present time, and this paper will deal mostly with them. The majority of the stars of our galaxy are white dwarfs and main sequence stars less luminous than the sun. The most luminous stars form a small fraction of a galaxy, but are of course visible over larger distances. A highly schematic representation of the Hertzsprung-Russell diagram is given in Figure 1. If L and T_S are known for a star, its surface area, and hence its radius R, can be deduced from the laws of thermal radiation.

TABLE I

Properties of Main Sequence Stars*

$M/M_\odot$	$R/R_\odot$	$\bar{\rho}$	$\bar{\epsilon}$	T_S	T_c	Spectral Type
0.2	0.3	7 gm. cm.$^{-3}$	0.2 ergs gm.$^{-1}$ sec^{-1}	3×10^3	10×10^6	M2
1	1	1.4 gm. cm.$^{-3}$	2 ergs gm.$^{-1}$ sec^{-1}	6×10^3	15×10^6	G2
5	3	0.3 gm. cm.$^{-3}$	100 ergs gm.$^{-1}$ sec^{-1}	14×10^3	20×10^6	B6

* $(M/M_\odot)$ and $(R/R_\odot)$ are the mass and radius of the star, respectively, in solar units; $\bar{\rho}$ the mean density in grams per cubic centimeter; $\bar{\epsilon}$ the mean energy radiated in ergs per gram per second; T_S and T_c the effective surface temperature and central temperature, respectively, in ° K.

If a star, whose distance is known, forms part of a binary then its mass M can sometimes be determined from observations (mainly spectroscopic) of the motion of the binary. About 100 such determinations of stellar masses M have been made, mainly for the main sequence. (For stars much more massive than the sun, the data is poor.) There seems to be a tendency for a definite mass M to correspond to each point on the Hertzsprung-Russell diagram.

One important fact is that the luminosities vary very much more from star to star than do the other quantities. Thus, in most cases, T_S varies by a factor of less than 20, M by less than 100, and R by less than 1000. On the other hand L may vary by a factor of as much as 10^8. The (rough) order of

magnitudes of these quantities for three typical main sequence stars is given in Table I.

A detailed analysis of the relative intensities of spectral lines in stellar spectra leads to information about the chemical composition of the surface layers of stars [for reviews, see Alpher & Herman (12); Aller (13)]. For most main sequence (and many other) stars one finds that the outer layers consist mainly of hydrogen and a moderate amount (about 20 per cent by mass) of helium. The abundance of carbon, nitrogen, and oxygen together is of the order of 1 per cent (by mass), the abundance of all heavier elements together being of the same order. There is some evidence for a smaller ratio of hydrogen to helium abundance in white dwarfs and some "superhot" stars, for a higher abundance of some of the heavier elements (notably nitrogen and carbon) in some of the superhot stars, and for some abundance peculiarities of metals in red giants. There is at present no reliable direct information as to whether the chemical composition of the interior of a star is similar to that of its surface layers.

Some information about the rotational velocity of a star can be obtained from a systematic Doppler broadening of all its spectral lines. There is some indication that most of the very hot stars have high rotational velocities (100 km. per sec. or more, at the surface), while most of the cooler stars have small rotational velocities (less than 50 km. per sec.).

Stellar Structure and Evolution

Valuable information about the structure and course of development of a star can also be obtained from purely theoretical considerations. For a detailed account, see Strömgren (9) and Chandrasekhar (6, 14).

Let us consider a star as having originated from a relatively cold and dilute gas cloud of stellar mass. Such a gas cloud will contract under its own gravitation, and the central portions will heat up as a result of the release of gravitational energy. The inward temperature gradient will result in an outward flow of energy, and the surface will begin to radiate this energy into space. The rate of energy emission depends mainly on the mass and opacity of the star. This loss of energy leads to further gradual contraction and increase in temperature and this process continues until a central temperature T_c of 10 to 20 million degrees is reached, after a few million years. At these high temperatures the nuclear reactions, to be discussed in the next three sections, proceed at a fast enough rate to balance the radiative energy loss and equilibrium will be established.

If a star is in complete equilibrium, both its temperature and density distribution remaining constant in time, two relations can be set up between density, temperature, chemical composition, and energy production as a function of radial distance. One relation (Lane's law) is obtained from the fact that the gravitational attraction must balance the outward force due to the pressure gradient, at every point in the star. A consequence of this equation is the approximate similarity relation,

$$T_c \propto (M/R). \qquad 1.$$

The second relation gives an expression, at every point in the star, for the outward flow of heat energy in terms of the temperature gradient and the opacity (if convection is assumed to be absent). The opacity in turn is a definite function of temperature, density, and chemical composition (dependent mainly on the concentration of helium and of all heavier elements together), but the form of this function is not yet known very accurately.

If the total luminosity L and radius R are known and if a particular distribution of the chemical elements and the energy production throughout the star (stellar model) is assumed, then the distribution of temperature and density can, in principle, be calculated. Such a calculation then furnishes values for the mass M, and central temperature T_c of the star, which depend, however, fairly strongly on the assumed stellar model and chemical abundances. If a uniform chemical composition throughout the star, similar to that observed spectroscopically in the surface layers, and a concentration of the energy production in the central regions is assumed, then the values calculated for M (from given values of L and R) agree fairly well with the values observed for main sequence stars. These calculations explain the tendency for a definite relation between M, L, and R for the main sequence and furnish values for T_c, independent of any knowledge of energy production as a function of temperature and density. Rough values for T_c, calculated in this manner, are given in Table I. Note the small variations in T_c accompanying very large changes in L ($L = \bar{\epsilon} M$).

On the other hand, if the rate of energy production as a function of temperature, density, and chemical composition is known, another expression for T_c can be obtained from L, which depends on the distribution of density and of chemical composition but not directly on opacity. A comparison of these two values for T_c thus provides a rough check for the law of energy production. Or, if the law of energy production is known accurately, a comparison of the two expressions for T_c can yield new information about the chemical composition, stellar model, and opacity.

Calculations show that, under normal main sequence conditions (uniform chemical composition), the star will be stable against density and temperature fluctuations unless the rate of energy production is extremely temperature sensitive. If the rate of energy production increases fairly strongly with increasing temperature, calculations show that the star will possess a convective core, in which heat can be transferred very much more rapidly by convection than by radiation.[2] Most of the energy production in such a star takes place well inside the convective core, which contains of the order of 10 per cent of the stellar mass. Typical graphs for temperature, density, and rate of energy production for a star possessing a convective core are given in Figure 2 [Chandrasekhar (6); Harrison (15)].

[2] The relation between energy flow and temperature gradient, obtained in this case of convective equilibrium, differs from that mentioned above for radiative equilibrium (no convection).

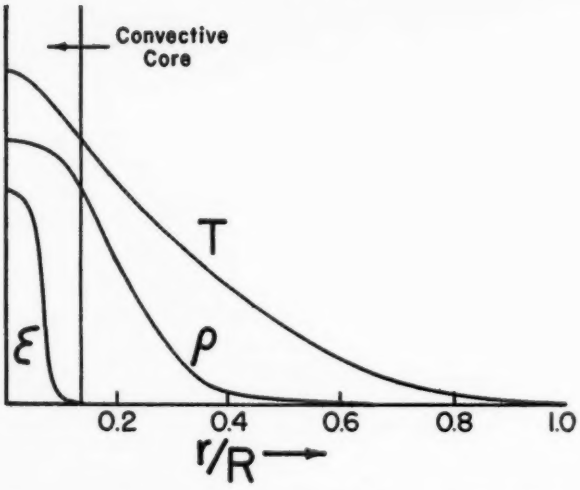

FIG. 2. Stellar properties as functions of radial distance. Distribution of temperature (T), density (ρ), and rate of energy production by the carbon cycle (ϵ) as a function of distance from the center (r) for a typical star of radius R with a convective core. The units of T, ρ, ϵ are arbitrary.

If, for any cause, the nuclear energy production stops, the star will again contract under its own gravitational field and the central temperature will increase, following Equation 1 approximately. If the star already had a high rotational velocity before the contraction, this velocity will increase as the radius decreases and the star becomes flattened. When this flattening reaches a certain point, the star becomes unstable and begins to lose matter. For a star with no (or little) rotation its fate depends on whether its mass is smaller or greater than the "Chandrasekhar limit,"

$$M_{CL} = 5.8 M_\odot / \mu_e^2 \qquad 2.$$

where μ_e is the mean molecular weight for the star and $M_\odot$ is the solar mass. If the mass M is greater than M_{CL} a star without rotation can contract almost indefinitely. If M is less than M_{CL} the star can only shrink down to a certain equilibrium radius, and its electrons will form a degenerate Fermi gas. The increase in gravitational energy will thus stop and the star will eventually cool.

THERMONUCLEAR REACTIONS

In this and the next three sections we shall be mainly concerned with main sequence stars. These stars consist to a large extent of hydrogen and a few other reasonably light elements. It is a well-known fact that the nuclear packing fraction increases with increasing atomic number Z, up to Z about 25. Hence any reaction, in which a heavier nucleus is built up out of two

very light nuclei, will be exothermic, to the extent of several Mev in most cases.

At "stellar" temperatures of ten to twenty million degrees the mean kinetic energies resulting from thermal motion are only of the order of magnitude of $kT \sim 1$ kev. In the stellar interior all atoms are ionized and no free neutrons are available. Two colliding nuclei then experience a very strong Coulomb repulsion (of the order of 1 Mev at a separation small enough for nuclear forces to come into play, say 5×10^{-13} cm.). The probability of a nuclear reaction is thus reduced greatly by a barrier penetration factor, even for two nuclei whose relative kinetic energy is considerably larger than the mean thermal energy.

The contribution to the rate of such a reaction between two nuclei from a value E of the relative kinetic energy (relative velocity v) is proportional to a factor

$$\exp(-E/kT) \exp(-2\pi Z_1 Z_2 e^2/\hbar v) \qquad 3.$$

where Z_1 and Z_2 are the two atomic numbers. The first factor in Equation 3 comes from the Maxwell distribution of energies; the second is due to the effect of the Coulomb repulsion. After integrating over all values of E one finds that the total reaction rate is approximately proportional to

$$\tau^2 e^{-\tau} \qquad 4.$$

where

$$\tau = 3(\pi^2 m e^4 Z_1^2 Z_2^2/2\hbar kT)^{1/3} \qquad 5.$$

and m is the reduced mass. The main contribution to this integral comes from the neighborhood of the value of E for which the expression 3 has a maximum, about 5 to 50 kev under stellar conditions.

The quantity τ is large compared with unity for most cases. Because of the presence of the factor $e^{-\tau}$ the mean reaction rate (*a*) increases very strongly with increasing temperature, (*b*) decreases very strongly with increasing Z, and (*c*) is numerically rather small. This strong temperature dependence explains why the luminosities of different main sequence stars vary so much more than the central temperatures.

Because of the small atomic number Z and high abundance of hydrogen, reactions involving the radiative absorption of a proton by various nuclei, (p, γ) reactions, are likely to be the most important ones.[3] It was shown by Bethe (2) that such (p, γ) reactions are of importance for only a few kinds of nuclei. For hydrogen and He^4 no direct (p, γ) reactions are possible. For Li, Be, and B, concentrations are so low and reaction rates so high that these elements are used up very quickly at an early stage of development of a star, except possibly for very cool stars. On the other hand, for nuclei heavier than

[3] Because of the slope of the packing fraction curve, reactions involving the emission of particles, such as (p, α) reactions, etc., are not exothermic in most (but not all) cases and hence cannot occur under stellar conditions. But, if such reactions are exothermic, they are generally much faster than (p, γ) reactions.

oxygen, the reaction rates at stellar temperatures are so low that the rates of energy production are much smaller than the rate at which the star radiates energy. The only reactions of interest in main sequence stars thus either involve carbon, nitrogen, and oxygen or are reactions other than (p, γ) involving some of the isotopes of hydrogen and helium.

As shown by Bethe (2), the bulk of the energy production in main sequence stars is due to two chains of nuclear reactions, the proton-proton chain and the carbon-nitrogen cycle. In each of these chains the net result is the conversion of four protons into one He^4 nucleus, two positrons, and two neutrinos. The two positrons are quickly annihilated in collisions with two

TABLE II

MEAN LIFETIME OF HYDROGEN ON THE PROTON-PROTON CHAIN AND C-N CYCLE AND MEAN REACTION TIME FOR TWO OTHER REACTIONS*

	$T=8$	$T=15$	$T=25$
p-p chain	2×10^{11} years	5×10^{9} years	5×10^{8} years
C-N cycle	10^{14} to 10^{16} years	5×10^{8} to 10^{10} years	5×10^{4} to 5×10^{5} years
$Be^9+H^1\rightarrow Li^6+He^4$	5×10^{3} years	1 year	1 day
$F^{19}+H^1\rightarrow O^{16}+He^4$	10^{17} years	2×10^{10} years	2×10^{5} years

* For a density of 125 gm./cc. and hydrogen abundance of 0.8, carbon plus nitrogen abundance 0.01 (by mass). T is temperature in 10^6 °K.

of the free electrons (from the ionized atoms which constitute the stellar interior); the two neutrinos escape from the star and carry away a small fraction of the energy release. For each helium nucleus produced about 26 Mev of thermal energy is released. If a star consisting entirely of hydrogen is converted completely into helium, a fraction of 7×10^{-3} of the rest-mass energy of the star is converted into thermal energy. For the sun, such a process could maintain its present rate of radiation for about 10^{11} years.

Details of the proton-proton chain and of the carbon-nitrogen cycle are given in the next two sections. In Table II we give the approximate mean life of hydrogen according to the proton-proton chain and C-N cycle respectively for densities and chemical composition corresponding roughly to stellar conditions. The temperatures of 8 and 25 million degrees are the approximate limits of central temperatures in main sequence stars. We also give the mean reaction times (lifetime of the heavier and rarer atom, not lifetime of hydrogen) for two other reactions. The reaction involving Be^9 is the slowest of the reactions involving Li, B, and Be. As seen from Table II these elements have a very short life even at 8×10^6 °K. and are probably used up during the gravitational contraction before central temperatures of this order of mag-

nitude are attained. The reaction involving F^{19} is by far the fastest of the reactions involving nuclei heavier than N^{15}. The abundance of fluorine is only about 10^{-5} (by mass), and the energy generation resulting from its combination with hydrogen, even at a temperature of 25×10^6 °K., is only about 20 ergs/gm. sec. compared with at least 5×10^6 ergs/gm. sec. for the carbon-nitrogen cycle.[4]

Proton-Proton Chain

Since He^2 does not exist at all, two protons cannot combine with each other with the emission of radiation alone. But, because of the low charge Z and high abundance of hydrogen, close collisions (to within 5×10^{-13} cm., say) between two protons are very much more frequent under stellar conditions than any other close collision of nuclei. During a small fraction of these collisions a β-decay, involving the emission of a positron and a neutrino, can take place. The resulting nucleus is then a deuteron, which is stable.

The reaction rate of this conversion of two protons into a deuteron plus a positron was estimated in the original paper of Bethe & Critchfield (1). For two protons with relatively low kinetic energies to be able to approach each other closely, they must collide with zero orbital angular momentum and, since protons obey the Pauli exclusion principle, the initial state must be a singlet S-state (antiparallel spin). The deuteron ground state, on the other hand, is a triplet S-state (parallel spin) and the β-transition involves a reversal of one nucleon spin direction. This requires Gamow-Teller selection rules, which are now known to be correct. Our knowledge of two-nucleon wave functions and of β-decay theory has increased greatly in the last few years and the reaction rate for the proton-proton reaction can now be calculated to an accuracy of 15 per cent. Such calculations have been carried out by Frieman & Motz (16) and by Salpeter (17).

Once a deuteron has been formed, the remaining reactions of the proton-proton chain proceed at a much faster rate, since no β-decays are involved and since the nuclear charges involved are still quite low. He^3 is a stable nucleus; consequently the reaction $H^2(p, \gamma)He^3$ is possible and proceeds so rapidly that any competing reactions involving a deuteron are quite unimportant. Li^4, however, is unstable to particle disintegration so that no (p, γ) reaction involving He^3 is possible. There is a variety of other competing reactions which He^3 can undergo, the one originally suggested by Bethe (2) involving a collision between He^3 and He^4. The rates of these competing reactions can now be estimated fairly accurately [Chandrasekhar (6); Salpeter (17)]. Under conditions existing in the interior of main sequence stars (electron gas not degenerate), a collision between two He^3 nuclei, resulting in one He^4 nucleus and two protons (suggested first by Fowler & Lauritsen and by Schatzman), is the fastest and most important reaction involving He^3. This reaction predominates in spite of the low concentration of He^3, since particle

[4] For a more detailed table of reaction rates, see the unpublished calculations of Fermi & Turkevitch [see (12, p. 194)].

reactions, if energetically possible, are generally faster than reactions involving emission of radiation or neutrinos.

As discussed in the section, THERMONUCLEAR REACTIONS, the net effect of the proton-proton chain is the conversion of four H^1 atoms into one He^4 atom with an energy release of about 26 Mev per He^4 atom. The mean reaction times for the three reactions involved are given in Table III for typical stellar conditions. The estimated reaction rates for the two reactions following the formation of a deuteron might be in error by a factor of as much as two or three. But the rates are quite certainly much faster than for the first reaction, which therefore governs the reaction rate for the proton-proton chain as a whole. The rate of energy generation ϵ_p from this reaction chain is, assuming a normal Maxwell distribution of thermal energies,

$$\epsilon_p = (50 \pm 10)\left(\frac{\rho}{100}\right) x_H^2 \left(\frac{T}{15 \times 10^6\ °K.}\right)^4 \text{ergs/gm. sec.} \qquad 6.$$

where x_H is the hydrogen concentration and ρ the density in gm./cc. This value for ϵ_p is much larger than the original estimate of Bethe & Critchfield (1). This is due largely to the fact that the value assumed for the Fermi β-decay constant 10 years ago was almost one-tenth of the present value (which is now accurate to about 15 per cent).

TABLE III

MEAN REACTION TIMES IN PROTON-PROTON CHAIN AND CARBON-NITROGEN CYCLE FOR TYPICAL STELLAR CONDITIONS*

Reaction	t_r
$H^1+H^1 \rightarrow H^2+e+\nu$	7×10^9 years
$H^2+H^1 \rightarrow He^3+\gamma$	4 sec.
$He^3+H+e^3 \rightarrow He^4+2H^1$	4×10^5 years
$C^{12}+H^1 \rightarrow N^{13}+\gamma$	10^6 years
$N^{13} \rightarrow C^{13}+e+\nu$	10 min.
$C^{13}+H^1 \rightarrow N^{14}+\gamma$	2×10^5 years
$N^{14}+H^1 \rightarrow O^{15}+\gamma$	$<3\times10^7$ years
$O^{15} \rightarrow N^{15}+e+\nu$	2 min.
$N^{15}+H^1 \rightarrow C^{12}+He^4$	10^4 years

* Mean reaction time t_r for a temperature T of 15×10^6 °K., density of 125 gm./cc., hydrogen concentration x_H of 0.8, and total concentration x_{CN} of C and N of 0.01 (by mass).

CARBON-NITROGEN CYCLE

The stable isotopes of carbon and nitrogen constitute of the order of 1 per cent of the mass of a normal star; (p, γ) reactions are possible for each of these four stable isotopes and, as discussed in THERMONUCLEAR REACTIONS,

their reaction rates are of the right order of magnitude for contributing to stellar energy generation.

Starting with one C^{12} nucleus, a N^{13} nucleus and about 2 Mev of energy in the form of radiation, are produced by a (p, γ) reaction. The N^{13} nucleus β-decays to C^{13} so quickly (10 min.), that nuclear reactions involving N^{13} are completely unimportant. About 1 Mev is converted into kinetic energies of the positron and neutrino. The C^{13} nucleus, being stable, undergoes a (p, γ) reaction with an energy release of 8 Mev and the resulting nucleus (again stable), N^{14}, undergoes another (p, γ) reaction with an energy release of about 7 Mev. The resulting O^{15} nucleus quickly β-decays to N^{15} (kinetic energies of 1.7 Mev for positron and neutrino). A (p, γ) reaction on N^{15} is possible, but here a (p, α) reaction is also energetically possible, resulting in one C^{12} and one He^4 nucleus plus 5 Mev. This second reaction, involving only the emission of particles and not radiation, is faster than the first by a factor of about 10,000.

In most cases then, this chain of reactions represents a complete cycle; for each C^{12} nucleus present originally, four hydrogen atoms are converted into one He^4 atom and the C^{12} nucleus reappears. The carbon and nitrogen thus merely act as catalysts, the rate of conversion of hydrogen into helium being proportional to their concentration. For a concentration (by mass) of 1 per cent, about 0.3 per cent of the hydrogen is then converted for each complete cycle. The mean life of hydrogen, according to the carbon-nitrogen cycle alone, is given in Table II for various temperatures.

In Table III estimated reaction times are given for the four nuclear reactions involved in the cycle. These estimates are usually obtained by measuring directly in the laboratory the cross sections for these reactions for the lowest proton energies (about 100 kev) which still yield measurable cross sections [Fowler (18); Woodbury & Fowler (19); Hornyak *et al.* (8)]. An extrapolation of these cross sections to the "stellar" energy region (5 to 50 kev) is then required. If there are no nuclear resonances near this energy region, this extrapolation can be carried out quite simply and the numbers quoted in Table III are based on these extrapolations [Epstein (20); Salpeter (17); Chandrasekhar (6)]. It is not easy to investigate resonance levels directly in this low energy region and the following procedure is usually adopted: Assuming the absence of levels near the stellar energy region, cross sections are calculated for, say 100 kev protons using the Breit-Wigner formulae and experimental values for the width and position of all resonance levels at more than about 250 kev (almost all of which are known). The calculated and experimental values are then compared.

For the reactions involving C^{12}, C^{13}, and N^{15} these calculated cross sections at about 100 kev agree fairly well with the experimental values. It is therefore likely that there are no resonance levels near the stellar region, and the extrapolation values given in Table III should be fairly reliable, at least to within a factor of two or three. But for the $N^{14}(p, \gamma)O^{15}$ reaction the experimental value at 100 kev is about seven times larger than the calculated

one [Duncan & Perry (21)]. This discrepancy is most probably due to the presence of a resonance level somewhere in the vicinity of this energy region. If this resonance level happens to be right in the stellar energy region, the reaction rate in stars for this reaction would be increased enormously (factor of 100 or more). The reaction time quoted in Table III is thus only an upper limit. At the moment we can thus only give limits to the mean time required for a single cycle: It is at least as long as the reaction time of $C^{12}(p, \gamma)N^{13}$ and shorter than the upper limit for the $N^{14}(p, \gamma)O^{15}$ reaction.

The rate of energy generation ϵ_C resulting from the carbon-nitrogen cycle in the neighborhood of fifteen million degrees is, again assuming a normal Maxwell distribution.

$$\epsilon_C = (30 \text{ to } 700)\left(\frac{\rho X_H}{100}\right)\left(\frac{X_{CN}}{0.01}\right)\left(\frac{T}{15 \times 10^6 \text{ °K.}}\right)^{20} \text{ ergs/gm. sec.,} \qquad 7.$$

where X_{CN} is the concentration (by mass) of carbon and nitrogen. The upper limit for the rate of energy production is more likely.

Energy Production in Main Sequence Stars

We shall assume the upper limit of the rate of energy generation for the carbon-nitrogen cycle to be correct. As discussed before, values of the central temperature T_c can be obtained from a knowledge of the luminosity and the rates of energy production if a particular stellar model and chemical composition are assumed [Schwarzschild (22); Harrison (15); Epstein (20)]. These calculations lead to a value in the neighborhood of 14×10^6 °K. for T_c for the sun. The carbon cycle is much more temperature sensitive than the proton chain, and the temperature decreases very rapidly with increasing distance from the center. Therefore energy generation by means of the carbon cycle takes place to an appreciable extent only over a very small central volume of the star, generation by means of the proton chain over a much larger volume. If one assumes a uniform concentration of helium of 10 to 20 per cent and a Maxwell distribution, one finds that the total energy production in the sun by means of the proton chain is roughly five times larger than that by means of the carbon cycle.[5] In main sequence stars very much more luminous than the sun, the central temperatures are higher and the carbon cycle produces more total energy than the proton chain. For main sequence stars less luminous than the sun the proton chain contributes overwhelmingly more energy.

As discussed in the section Stellar Structure and Evolution, an independent value for T_c can also be obtained from purely astrophysical considerations, without any previous knowledge of the law of energy production. Qualitatively, there is fairly good agreement between these two types of calculations. For the sun the two values agree to within about one million degrees and there is rough agreement for the other parts of the main sequence. For stars other than the sun, the observational astrophysical data

[5] If a helium concentration of about forty per cent is assumed for the central regions, however, the carbon cycle predominates slightly for the sun.

are not very accurate, but there is some evidence from a detailed study of the luminosity-temperature diagram that the rate of energy production is very temperature sensitive for the more luminous main sequence stars (which checks roughly with the temperature sensitivity of the carbon cycle) and less sensitive for the low luminosity stars [Bondi (23)].

Quantitatively, however, there are some disagreements: The proton chain and carbon cycle produce equal amounts of energy for stars somewhat more luminous than the sun, according to the nuclear data alone (if a low central concentration of helium is assumed) [Epstein (20)]. But according to the conclusions of Bondi (23) from astrophysical data, the carbon cycle dominates already for stars slightly less luminous than the sun. This disagreement could however be due to a strongly nonuniform distribution of helium throughout the star (build-up of the helium formed in the central regions depresses the proton chain more than the carbon cycle) or to the inaccuracies and scatter of total luminosity measurements (involving somewhat uncertain bolometric corrections) on which Bondi's work and conclusion is based.

Another related disagreement is found in the case of the very low luminosity stars (red dwarfs) of the main sequence [Aller (24); Aller *et al.* (25)]. Here the astrophysical calculations, based on a radiative model, give distinctly higher values for T_c than is required according to the proton chain for the observed luminosities.

Some possible sources of this discrepancy are: (*a*) A large error in the expressions assumed for opacity; (*b*) a large error in the bolometric corrections used to obtain total luminosity; (*c*) convective equilibrium (suggested by B. Strömgren) which would give lower values for T_c than the radiative model used; (*d*) a very small concentration (say 20 per cent) of hydrogen throughout most of the interior, which would yield a much lower rate of energy production (proportional to x_H^2 for the proton chain;[6] (*e*) some large (factor of more than 10) and unexpected error in the nuclear calculations for the rate of the proton-proton reaction (claimed to be accurate to within 15 per cent).

It should be pointed out that the calculations of nuclear reaction rates, summarized in the preceding two sections, are accurate only if the distribution of kinetic energies of nuclei in stellar interiors follows accurately a Maxwell distribution law. The main contribution to the calculated reaction rates (especially for the carbon cycle, less so for the proton chain) comes from kinetic energies far out in the small "exponential tail" of the Maxwell distribution. Small deviations from a Maxwell distribution could thus alter the reaction rates drastically. Although the Maxwell distribution is certainly a very good approximation in stellar interiors [Bohm & Aller (26)], a slight increase of the "Maxwell tail" resulting from turbulence or a slight decrease from cooperative phenomena cannot yet be ruled out completely.

Stars Which Have Exhausted Their Hydrogen Supply

Main sequence stars of mass greater than about five solar masses have

[6] There is, however, no spectroscopic evidence for a low hydrogen concentration in red dwarfs.

such a high luminosity, and therefore high rate of conversion of hydrogen into helium, that they exhaust their hydrogen supply in times of the order of 10^9 years or less. Since this time is shorter than the age of our galaxy, a galaxy should contain a proportion of such luminous stars, whose interior regions consist mainly of helium. The energy production from the conversion of hydrogen into helium then ceases to be a sufficient source of energy. If good mixing is assumed, the star will begin to contract gravitationally, its central temperature increasing, approximately following Equation 1, and the star probably moves off the main sequence.

Such a star has a mass larger than Chandrasekhar's limit (Equation 2), and can thus keep on contracting until rotational (or some other) instability sets in or until the temperatures and densities become high enough for new nuclear reactions to set in. We consider in this section a star with zero (or very small) rotational velocity, good mixing and generally high stability. Such a star will contract until its radius has decreased by a factor of about 10 in a few million years. At this stage of its contraction its central density is about 2×10^4 gm./cc. and its central temperature T_c about 2×10^8 °K. Although, for ordinary main sequence stars, reactions involving triple collisions are quite unimportant, at these high densities and temperatures the exothermic conversion of three He^4 nuclei into one C^{12} nucleus becomes frequent enough to be able to supply the energy radiated away by the star [Öpik (27); Salpeter (28)].

The reaction proceeds in two steps

$$\left.\begin{aligned} &He^4 + He^4 + 95\ \text{kev} \rightarrow Be^8 + \gamma \\ &He^4 + Be^8 \rightarrow C^{12} + \gamma + 7.4\ \text{Mev} \end{aligned}\right\} \qquad 8.$$

The nucleus Be^8 is unstable to disintegration into two He^4 nuclei. But the energy required for its formation from two helium nuclei is only (95 ± 5) kev which is not very much larger than the mean thermal energies at temperatures over 10^8 °K. Thus a small fraction (about 1 in 10^{10}) of the material in the interior of the star is constantly in the form of Be^8 in a state of dynamic equilibrium. The Be^8 present then easily undergoes a (α, γ) reaction and over 7 Mev per C^{12} nucleus is liberated in the form of radiation.[7]

Once a C^{12} nucleus has been produced, it can undergo a further (α, γ) reaction, yielding an O^{16} nucleus and about 7 Mev. Another exothermic reaction, O^{16} (α, γ) Ne^{20}, is then possible, and so on. Because of the increasing Coulomb barrier, the reaction rates for these (α, γ) reactions decrease with increasing atomic number. The helium is probably converted mainly into C^{12}, O^{16}, and Ne^{20} and decreasing amounts of Mg^{24}, Si^{28}, etc., and energies of 3 to 4 Mev per He^4 nucleus are produced in these reactions.

The nuclear resonance levels of C^{12} are not yet known well enough to calculate reaction rates accurately, but a rough estimate can be obtained.

[7] The conversion of three He^4 nuclei into one C^{12} nucleus could also proceed directly (without the temporary formation of Be^8), but at a much lower rate [calculated by Öpik (27)].

At temperatures T near 2×10^8 °K. the estimate for the rate of energy production ϵ is, again assuming a Maxwell distribution [Salpeter (28)],

$$\epsilon \approx 10^3 \left(\frac{\rho}{2.5\times10^4}\right)^2 x_\alpha^3 \left(\frac{T}{2\times10^8\ °\text{K.}}\right)^{18} \text{ergs/gm. sec.,} \qquad 9.$$

where x_α is the concentration of helium. Although Equation 9 is only a rough estimate and no work has yet been done on stellar models appropriate for such a star, the rate of energy production is so temperature sensitive that the total energy production will certainly balance the total luminosity for some temperature between 10^8 °K. and 3×10^8 °K.

The energy release per unit mass in the conversion of helium into carbon, oxygen, etc., is about one-seventh of the energy release in the conversion of hydrogen into helium and much larger than the energy released in the preceding gravitational contraction. Such a star should then be able to stay in equilibrium, at an almost constant temperature and luminosity, for several times 10^7 years until most of the helium is used up.[8] There is a possibility that some or all of the "superhot" stars of Figure 1 (Wolf-Rayet stars, nuclei of planetary nebulae, etc.) receive their energy from such a process. This hypothesis has not yet been tested in detail but is supported by the fact that the atmospheres of some hydrogen-deficient stars have an abnormally high abundance of C^{12}, but not of C^{13} [Bidelman (29)].

White Dwarfs, Red Giants, and Variables

The white dwarfs, red giants, the various types of variable stars and novae are not as well understood at present as main sequence stars. There is a general belief, however, that the primary cause for their different behavior lies in peculiarities of their stellar structure and not in the type of energy production taking place.

White dwarfs.—White dwarfs are characterized by having a very high density and consequently a small radius, and a very low luminosity. Their surface temperature is somewhat higher than that of the sun, their mass is similar to that of the sun and they are very abundant in our galaxy (see Fig. 1). It is generally believed that their high densities are connected with the fact that their mass is less than the Chandrasekhar limit (Equation 2), and that they probably contain little hydrogen. Calculations show that, if a main sequence star of mass less than this limit has exhausted most of its hydrogen supply and consists mainly of helium, it will contract gravitationally for a while until it reaches a state of equilibrium with density comparable to that of a white dwarf [Chandrasekhar (6, 14)]. It was pointed out by

[8] The development of a massive star with no (or very poor) mixing is rather different, according to calculations being carried out by A. Sandage and M. Schwarzschild. After the hydrogen in the central core (only about 10 per cent of the stellar mass) has been converted into helium, the core may begin to contract gravitationally but the outer layers of the star expand. High densities and temperatures over 10^8 °K. may be reached in the center of the core after only a small fraction of the hydrogen outside the core (now the most important energy source) has been converted into helium.

Schatzman (30, 31) that, owing to the large gravitational fields, there is a possibility that the helium and heavier nuclei will occupy the central regions of the star, while all the hydrogen will move towards the outer layers. The central temperatures are calculated to be similar to that of the sun, and the electrons in the central, dense, region form a degenerate Fermi gas [Marshak (32)].

The only nuclear energy production in such a star, in which the helium and remaining hydrogen are poorly mixed, then takes place in a relatively thin spherical shell in the transition region from the helium core to the hydrogen layers, where both the hydrogen concentration and temperature are large enough for an appreciable conversion of hydrogen into helium to take place. The thinness of this shell explains the puzzling fact that the luminosity of a white dwarf is very low in spite of its fairly high surface and central temperature and very high density [Schatzman (30, 31)].[9]

It is reasonably certain now that the interior of white dwarf stars cannot contain any appreciable amount of hydrogen [Ledoux & Sauvenier-Goffin (33); Lee (34)], and calculations based on this assumption seem to explain their structure fairly well and do not depend appreciably on the mode of energy production. In fact it is even possible that the nuclear energy production in white dwarfs only accounts for a small fraction of the observed luminosities and that these stars derive their energy from gravitational contraction or are actually cooling down.

A star of the luminosity of a white dwarf can convert only a fairly small fraction of its mass from hydrogen into helium in a few billion years. This suggests that white dwarfs were originally formed from hydrogen-poor material or are the remnants of more massive and luminous stars which have exhausted most of their hydrogen supply and have lost a large fraction of their mass (possibly novae).

Red giants.—Red giant stars are characterized by having a very large radius and fairly large luminosity, but a very low surface temperature. No complete explanation for this phenomenon has been found yet, but the following hypothesis has been suggested by various authors: The essential part of a red giant is supposed to consist of a fairly dense and hot star with considerable energy production taking place in its central regions by means of the carbon-nitrogen cycle. This main part of the red giant is surrounded by a very extended, tenuous, and rather cool envelope which contains only a small fraction of the stellar mass.

Various mechanisms have been suggested for the maintenance of such a tenuous envelope: (*a*) A discontinuity in chemical composition between the main part of the star and the envelope leading to a very large radius [Öpik (35); Hoyle & Lyttleton (36); Li & Schwarzschild (37); Bondi & Bondi (38)]. This discontinuity might arise from the helium produced in the core of the

[9] The He^3 may be used up in a white dwarf by a reaction different from that discussed in the section PROTON-PROTON CHAIN, involving an inverse β-decay (because of the high density and high Fermi energy of the degenerate electron gas). The end result is again He^4, and Equation 6 is only altered by a factor of two.

main part of the star not penetrating into the envelope and also from accretion of hydrogen into the envelope from interstellar gas clouds. (*b*) Electron degeneracy in the stellar core, caused by partial depletion of hydrogen, might lead to an extended envelope [Gamow & Keller (39); Gamow & Longmire (40)]. (*c*) The envelope might be maintained by magneto-hydrodynamic forces, if the star possesses strong magnetic fields [Menzel (40a, 41)].

Variables.—A number of stars show recurring (periodic or irregular) variations in luminosity and surface temperature [Payne-Gaposchkin (42)]. The best known of these stars are the Cepheids and cluster type variables, which show periodic variations. The detailed mechanism of these variations is not yet understood, but it is widely believed that they are connected with dynamic pulsations of the star as a whole or of its outer layers [Rosseland (43)]. Such pulsations may be more likely to occur if the chemical composition is not uniform throughout the star.

One possibility is a massive star with a central helium core of about 10 per cent of the stellar mass, the energy production taking place in the transition region between the central helium-core and the hydrogen-rich bulk of the star [Gamow & Longmire (40)].

Another type of stars, the novae, show sudden increases in their luminosity by factors of up to 10^4. There seems to be no satisfactory explanation for these stars. One attractive hypothesis is that novae are an extreme form of variable stars [e.g., see Gamow (44)]. The star is supposed to shed explosively its expanding, fairly cool envelope, at least temporarily. The large increase in luminosity would then be due merely to the fact that the inner, hot regions become exposed and not to any drastic nuclear (or dynamic) catastrophe. This hypothesis is supported by the fact that there are some recurrent novae but there are some difficulties in its more detailed predictions. The possibility of the intimate connection of nova outbursts with specific rapid nuclear reactions cannot be ruled out however [Schatzman (45)].

For a more detailed discussion and bibliography for the stars discussed in this section, see Ter Haar (5) and Chandrasekhar (6).

Supernovae

A very small fraction of the stars (about one star per galaxy every few hundred years) show a very sudden and enormous increase of luminosity (by factors of up to 10^8) accompanied by the expulsion of a large fraction of the stellar mass. There are two types of supernovae. Type I show the largest sudden increases in luminosity, followed by an exponential decrease of luminosity with a remarkably constant half life of (55 ± 5) days. In our own galaxy the supernova observed by Tycho Brahe was of this type [Baade (46)]. The expelled parts of the star expand rapidly and later form tenuous nebulae illuminated by the central stellar remnant, which has a very high density and surface temperature. The crab nebula in our galaxy is the result of such a supernova [Minkowski (47)]. Supernovae of type II show a somewhat smaller sudden increase in luminosity followed by an irregular decrease in luminosity.

There exist a large number of alternative explanations for the supernova phenomenon, none of which are entirely satisfactory. Some of these explanations suppose the catastrophe to be purely of dynamic nature, but three explanations ascribe the phenomenon primarily to the catastrophic onset of endothermic nuclear reactions [Hoyle (48); Gamow & Schönberg (49); Borst (50)]. According to these hypotheses an endothermic nuclear reaction (the actual reaction being different in the three hypotheses) sets in, whose reaction rate increases with increasing density. The energy absorbed in these reactions leads to a gravitational contraction and thus to an increase in density. The increased density in turn leads to an acceleration of the endothermic reaction and the contraction becomes a catastrophic collapse. If the star initially had any rotational velocity at all, rotational instability will be reached very rapidly during the collapse and a part of the stellar mass is suddenly expelled.

The subsequent fate of a massive star which has converted most of its matter into carbon, oxygen, and neon (as discussed in the section STARS WHICH HAVE EXHAUSTED THEIR HYDROGEN SUPPLY) depends greatly on the rotational velocity, state of mixing, neighboring matter, structural stability, and other factors. But under the simplest conditions (very little rotation, good mixing, no accretion, and good stability) the development can be considered in detail [Öpik (35); Salpeter (17)]:[10] When most of the helium has been exhausted at a temperature of a few times 10^8 °K. nuclear energy production ceases and gravitational contraction again sets in, accompanied by an increase in temperature. At temperatures of about 10^9 °K. exothermic reactions between two carbon (or oxygen, etc.) nuclei take place, resulting in various heavier nuclei. At temperatures of $(2 \text{ to } 4) \times 10^9$ °K. some dissociation of the light nuclei into protons and helium nuclei takes place. These protons and helium nuclei can undergo a large number of different reactions involving the other nuclei present, and the net result will be a building up of the most stable nuclei, especially those with atomic weight 40 to 60.

When most of the star consists of the most stable nuclei (iron region), any further nuclear reactions can only absorb energy and result in gravitational contraction without a great increase of temperature. (*a*) One such type of endothermic reaction is the Urca process of Gamow & Schönberg (49), in which energy escapes in the form of fast neutrinos, produced in cycles of β-decays and inverse β-decays. This Urca process takes place already at temperatures of $(1 \text{ to } 4) \times 10^9$ °K. and its rate increases with increasing density.

(*b*) Another endothermic process, proposed by Hoyle (48), is the building up of the very heavy nuclei (up to uranium). This building up process involves inverse β-decays, made possible by the large Fermi energies of the electrons which form a degenerate Fermi gas at high densities, and its reaction rate therefore also increases greatly with density. The relative concentrations of the various nuclear species were calculated as a function of tem-

[10] The influence of high densities on rates of nuclear reactions has been investigated by Schatzman (51).

perature and density by Hoyle (48), Albada (52), and Klein, Beskow & Treffenberg (53), assuming complete thermodynamic equilibrium. It was proposed by these authors that all the heavy elements may have originated by such processes in supernovae, but there are some difficulties connected with this hypothesis, including the problem of the "freezing in" of the equilibrium distribution in the subsequent explosion [Alpher & Herman (12)].

(*c*) Another endothermic reaction, proposed by Borst (50), is

$$He^4+He^4+19\ Mev\rightarrow Be^7+n. \qquad 10.$$

Be^7 (unless strongly ionized) β-decays with a half life of 55 days, and the presence of Be^7 in the envelope of a supernova of type I might explain the remarkably constant decay curve of the luminosity.[11] The amount of He^4 present in the interior of a star at temperatures of several times 10^9 °K. is, however, rather low and it seems rather unlikely that Be^7 should form a very large fraction of all the beta-active nuclei produced.

To summarize: Our present knowledge of stellar hydrodynamics and nuclear physics is insufficient to predict in detail the processes taking place in a supernova. It seems rather likely, however, that some catastrophic nuclear reactions take place, at least in supernovae of type I. The possible mechanisms (rotational or otherwise) for the expulsion of such a large fraction of the stellar mass following a sudden collapse have not yet been investigated in detail.

Conclusion

In the case of main sequence stars, it is well established that the main source of energy stems from exothermic nuclear reactions whose net effect is the conversion of hydrogen into helium. For the proton-proton chain the rate of energy production is now known with some accuracy from nuclear data as a function of temperature and density. For the carbon-nitrogen cycle, further nuclear experiments (now in progress) on one reaction will be necessary before reaction rates can be predicted accurately. Apart from this uncertainty in the nuclear data, the reaction rate for the carbon cycle is proportional to the concentration in stellar interiors of carbon and nitrogen, which cannot be estimated accurately from astrophysical data alone.

Quantitatively there seems to be some discrepancy between the reaction rates predicted for the proton-proton chain from nuclear physics and from astrophysical data and calculations. The rate predicted from nuclear physics seems to be somewhat higher than that required by the astrophysical data, especially for red dwarf stars. The nuclear calculations of reaction rates as a function of temperature, density, and chemical composition (for an accurately Maxwellian distribution) are now based on seemingly reliable data. It is likely that these discrepancies are due to the less accurate astrophysical data and calculations, on which the assumed chemical composition, stellar

[11] But the β-decay of Be^7 involves K-capture and the half life is radically different if an appreciable fraction of the Be^7 is completely ionized (which might be the case in a supernova envelope).

models, and stellar opacities are based. The nuclear calculations are thus (or soon will be) accurate enough (barring any unforeseen and unlikely serious errors) to supply valuable relations between the various astrophysical factors, at least for main sequence stars.

For stars other than main sequence stars both the nuclear and the astrophysical calculations are much less reliable, especially since the nuclear reactions and stellar structure seem much more interdependent for these stars. It is very probable that the peculiarities of white dwarfs and red giants are due primarily to their difference in structure and chemical composition from main sequence stars, and not to new nuclear reactions. White dwarfs almost certainly contain little hydrogen, and their basic structure is fairly well understood. The causes for the extended envelopes of red giants are not certain yet. It seems plausible that a small fraction of the more luminous stars of any galaxy have exhausted their hydrogen supply and have a low enough rotational velocity for large gravitational contractions to occur. At the high temperatures thus obtained, the conversion of helium into carbon and heavier nuclei could supply sufficient energy to maintain the luminosity for several times 10^7 years. This hypothesis is supported to some extent by the existence of some stars with very high surface temperatures and fairly high abundance of elements heavier than helium, but has not been tested in detail. Finally, the discussion given in the section SUPERNOVAE for endothermic nuclear reactions, which might take place in supernovae, is somewhat speculative.

One should perhaps discuss the possibility of stellar energy sources which are undetectable in terrestrial laboratories. The rate of nuclear reactions in stars is quite low (the energy production from one collision in about 10^{22} is sufficient to maintain the luminosity of the sun) compared with rates usually measured in the laboratory. But practically all reactions, whose rate increases strongly with relative kinetic energies of the reacting particles, can be (and have been) detected in the laboratory in view of the high energies available (a few Mev compared with a few kev in stellar interiors). Again it is known from studies involving particle counters and ionization chambers that no exothermic reactions, whose rate is independent of relative kinetic energy (faster than natural radioactivity) take place in all the elements present in the earth's crust and atmosphere. The only reactions which could have escaped detection are then reactions whose rate increases slowly with energy, but the existence of any such reactions (other than the proton-proton reaction) of importance for stars is rather unlikely on theoretical grounds.

Lack of space prevents a discussion of theories of the origin and evolution of stars and galaxies, or of the significance of interstellar matter [Greenstein (54)], and of the division of stars into populations I and II [Baade (55)]. Reviews on these important topics will be found in Ter Haar (5) and Alpher & Herman (12).

Lack of space also prevents a detailed discussion of the question of mixing in stars, which affects the properties of a star greatly, especially for white dwarfs, red giants, and variables. From a consideration of nuclear reaction

rates some quantitative conclusions can be obtained about chemical and isotopic abundances in stellar interiors (assuming temperatures of 8 to 25 million degrees, say, and the presence of a fairly large amount of hydrogen). For instance, the abundance of lithium and of He^3 should be extremely low and the abundance ratio of C^{12} to C^{13} about five. These conclusions can then be compared with detailed spectroscopic investigations on chemical and isotopic abundances in the surface of stars, which have been carried out by McKellar and others and are continuing [e.g., see Greenstein *et al.* (56, 57, 58)]. For the sun and many main sequence stars, the surface abundance of lithium and the C^{12}/C^{13} ratio are much larger than is to be expected for the interior, in which nuclear reactions occur. We can therefore conclude that there cannot be complete mixing, at least in the sun. This conclusion is also obtained from independent theoretical considerations [Öpik (59)]. Further work along these lines, for many different types of stars, should give valuable information about the constitution and hydrodynamics of stars.[12]

LITERATURE CITED

1. Bethe, H. A., and Critchfield, C. L., *Phys. Rev.*, **54**, 248–54 (1938)
2. Bethe, H. A., *Phys. Rev.*, **55**, 434–56 (1939)
3. Weizsäcker, C., *Physik. Z.*, **39**, 633–45 (1938); Atkinson, R., and Houtermans, F., *Z. Physik.*, **54**, 656–65 (1928)
4. Gamow, G., and Critchfield, C. L., *Theory of Atomic Nucleus*, 264–316 (The Clarendon Press, Oxford, England, 344 pp., 1949)
5. Ter Haar, D., *Rev. Modern Phys.*, **22**, 119–52 (1950)
6. Chandrasekhar, S., in *Astrophysics, A Topical Symposium*, Chap. 14, 598–674 (McGraw-Hill Book Co., Inc., New York, N. Y., 703 pp., 1951)
7. Bethe, H. A., and Marshak, R. E., *Rept. Progress Phys.*, **6**, 1–15 (1939)
8. Hornyak, W. F., Lauritsen, T., Morrison, P., and Fowler, W. A., *Rev. Modern Phys.*, **22**, 291–372 (1950)
9. Strömgren, B., *Ergeb. exakt. Naturwiss.*, **16**, 465 (1937)
10. Kienle, H., *Ergeb. exakt. Naturw.*, **20**, 89–120 (1942)
11. Hynek, J. A., *et al.*, *Astrophysics, A Topical Symposium* (McGraw-Hill Book Co., Inc., New York, N. Y., 674 pp., 1951)
12. Alpher, R. A., and Herman, R. C., *Rev. Modern Phys.*, **22**, 153–212 (1950)
13. Aller, L. H., in *Astrophysics*, Chap. 2, 29–84 (McGraw-Hill Book Co., Inc., New York, N. Y., 703 pp., 1951)
14. Chandrasekhar, S., *An Introduction to the Study of Stellar Structure* (Univ. of Chicago Press, Chicago, Ill., 703 pp., 1939)
15. Harrison, M. H., *Astrophys. J.*, **108**, 310–25 (1948)
16. Frieman, E., and Motz, L., *Phys. Rev.* (To be published)
17. Salpeter, E. E., *Phys. Rev.* (To be published)
18. Fowler, W. A., *Phys. Rev.*, **81**, 655 (1951)
19. Woodbury, E. J., and Fowler, W. A., *Phys. Rev.*, **85**, 51–57 (1952)

[12] I am greatly indebted to Professors L. H. Aller, R. A. Alpher, W. Baade, H. A. Bethe, W. P. Bidelman, H. Bondi, W. A. Fowler, G. Gamow, J. L. Greenstein, R. C. Herman, R. E. Marshak, D. H. Menzel, R. Minkowski, P. Morrison, L. Motz, E. Schatzman, M. Schwarzschild and O. Struve for valuable discussions, comments and communications.

20. Epstein, I., *Astrophys. J.*, **112**, 207–10 (1950); **114**, 438–42 (1951)
21. Duncan, D. B., and Perry, J. E., *Phys. Rev.*, **82**, 809–13 (1951)
22. Schwarzschild, M., *Astrophys. J.*, **104**, 203–7 (1946)
23. Bondi, H., *Monthly Notices Roy. Astron. Soc.*, **110**, 595–606 (1950)
24. Aller, L. H., *Astrophys. J.*, **111**, 173–78 (1950)
25. Aller, L. H., Chamberlain, J. W., Lewis, E. M., Liller, W. C., McDonald, J. K., Potter, W. H., and Weber, N. E., *Astrophys. J.*, **115**, 328–30 (1952)
26. Bohm, D., and Aller, L. H., *Astrophys. J.*, **105**, 131–50 (1947)
27. Öpik, E. J., *Proc. Roy. Irish Acad.*, [A]**54**, 49–77 (1951)
28. Salpeter, E. E., *Astrophys. J.*, **115**, 326–28 (1952)
29. Bidelman, W. P., *Astrophys. J.*, **116** (In press)
30. Schatzman, E., *Astrophys. J.*, **107**, 110–11 (1948)
31. Schatzman, E., *Commun. Danish Acad. Sci.*, **25**, No. 7 (1950)
32. Marshak, R. E., *Astrophys. J.*, **92**, 321–53 (1940)
33. Ledoux, P. J., and Sauvenier-Goffin, E., *Astrophys. J.*, **111**, 611–24 (1950)
34. Lee, T. D., *Astrophys. J.*, **111**, 625–40 (1950)
35. Öpik, E. J., *Tartu Obs. Publ.*, **30**, No. 4 (1938)
36. Hoyle, F., and Lyttleton, R. A., *Monthly Notices Roy. Astron. Soc.*, **102**, 218 (1942); **109**, 614–30 (1949)
37. Li, H., and Schwarzschild, M., *Monthly Notices Roy. Astron. Soc.*, **109**, 631–46 (1949)
38. Bondi, C. M., and Bondi, H., *Monthly Notices Roy. Astron. Soc.*, **110**, 287–304 (1950)
39. Gamow, G., and Keller, G., *Rev. Modern Phys.*, **17**, 125–37 (1945)
40. Gamow, G., and Longmire, C., *Phys. Rev.*, **79**, 743–44 (1950)
40a. Menzel, D. H. (Unpublished data)
41. Menzel, D. H., *Physica*, **12**, 768–74 (1946)
42. Payne-Gaposchkin, C., in *Astrophysics, A Topical Symposium*, Chap. 12, 495–525 (McGraw-Hill Book Co., Inc., New York, N. Y., 703 pp., 1951)
43. Rosseland, S., *The Pulsation Theory of Variable Stars*, 1 (Oxford Univ. Press, Oxford, England, 1949)
44. Gamow, G., *Nature*, **168**, 72–73 (1951)
45. Schatzman, E., *Ann. astrophys.*, **14**, 305–12 (1951)
46. Baade, W., *Astrophys. J.*, **102**, 309–17 (1945)
47. Minkowski, R., *Astrophys. J.*, **96**, 199–213 (1942)
48. Hoyle, F., *Monthly Notices Roy. Astron. Soc.*, **106**, 343–83 (1946)
49. Gamow, G., and Schönberg, M., *Phys. Rev.*, **59**, 539–47 (1941)
50. Borst, L., *Phys. Rev.*, **78**, 807–8 (1950)
51. Schatzman, E., *J. phys. radium*, **9**, 46–60 (1948)
52. Albada, G. B. van, *Astrophys. J.*, **105**, 393–405 (1947)
53. Klein, D., Beskow, G., and Treffenberg, L., *Arkiv. Mat. Astron. Fysik*, [B]**33**, No. 1 (1946)
54. Greenstein, J. L., in *Astrophysics, A Topical Symposium*, Chap. 13, 526–597 (McGraw-Hill Book Co., Inc., New York, N. Y., 703 pp., 1951)
55. Baade, W., *Astrophys. J.*, **100**, 137–46 (1944)
56. Greenstein, J. L., Richardson, R. S., and Schwarzschild, M., *Pubs. Astron. Soc. Pacific*, **62**, 15–18 (1950)
57. Greenstein, J. L., *Astrophys. J.*, **113**, 531–35 (1951)
58. Greenstein, J. L., and Richardson, R. S., *Astrophys. J.*, **113**, 536–46 (1951)
59. Öpik, E. J., *Monthly Notices Roy. Astron. Soc.*, **111**, 278–88 (1951)

THE PRODUCTION AND DISTRIBUTION OF NATURAL RADIOCARBON[1,2]

By Ernest C. Anderson

Zoophysiological Laboratory, University of Copenhagen, Copenhagen, Denmark

Introduction

The naturally occurring radioactive isotope of carbon is identical with the well-known artificial tracer C^{14}. While its half-life of 5570 years (1, 2, 3) is classed as long among the synthetic nuclides, it is very short indeed on a geologic time scale. Radiocarbon may be said to constitute an entirely new type of natural radioactivity in that it not only lacks a long-lived parent but also has a half-life so short that none of it now on earth was formed originally, as by primordial element genesis or by thermonuclear processes which may have occurred when the material of the earth was at stellar temperatures. The other naturally occurring nuclides fall into one of two groups: either their half-lives are sufficiently long to permit detectable survival over a period of the order of 10^9 years or, alternatively, they are produced by the radioactive decay of a nuclide of the first group and are therefore to be found in more or less close association with the parent substance.

Natural radiocarbon owes its existence to a new type of process, namely, the occurrence in nature of a transmutation reaction identical with the one used in the nuclear reactor to make synthetic C^{14}:

$$N^{14} + n \rightarrow C^{14} + p + 620 \text{ kev}$$

The neutrons are provided by the cosmic radiations (4, 5) and the nitrogen is that of the atmosphere of the earth. The probable existence of this production mechanism was first pointed out by Korff (6). However, the importance of the production of radioactive nuclides by the cosmic ray neutrons was not appreciated until Libby considered the problem in detail (7) and began an energetic search for the two principal activities produced by these neutrons, an effort which culminated successfully in the discovery of natural radiocarbon in 1947 (8, 9) and of natural tritium in 1951 (10). [The tritium is produced by the fast neutron reaction $N^{14}(n, t)\ C^{12}$; the yield is so low compared with that of C^{14} that it need not be considered here.]

As pointed out by Libby (7), if the average number of cosmic ray neutrons captured in the atmosphere per square centimeter of earth's surface

[1] The survey of the literature pertaining to this review was concluded in December, 1951.

[2] This review was prepared during a visit to the University of Copenhagen, where a radiocarbon dating laboratory was set up at the Zoophysiological Institute. Grateful acknowledgement is made of the grant of a fellowship by the Danish Rask-Ørsted Fond and of financial aid to the author by the Wenner-Gren Foundation for Anthropological Research. The Los Alamos Scientific Laboratory generously granted the author a leave of absence during the tenure of the fellowship.

and per second be represented by $\overline{Q}$, then $\overline{Q}$ is also the production rate of C^{14} since very few neutrons disappear by any other mechanism. In the steady state which prevails, $\overline{Q}$ is also identical with the disintegration rate of the total amount of C^{14} present. For a given $\overline{Q}$ the specific activity which will be observed for natural radiocarbon will depend on the quantity of inert carbon through which the radiocarbon is distributed. If this amount of carbon, which may be called the "exchange reservoir," is represented by B and expressed in units of grams of carbon per square centimeter of earth's surface, the specific activity S of this carbon in disintegrations per second and per gram is simply $\overline{Q}/B$.

In the following paragraphs we will consider the estimation of these two important quantities and the comparison of the results with the observed specific activity of carbon from the exchange reservoir.

Evaluation of $\overline{Q}/B$

Description of the cosmic ray neutron flux.—(11) The neutrons observed in the atmosphere are necessarily of local origin since the short half-life (about 13 min.) (12) of the neutron to β-decay precludes its existence in the primary radiation. The primary cosmic rays, predominantly protons with energies well above 1 Bev cause complete nuclear disruption of atoms of the atmosphere producing neutrons and protons with energies of the order of 1 Bev. These in turn lead to further nuclear disruptions (evaporation type "stars") with the emission of neutrons and protons of about 10 Mev energy. This "cascade" results in the formation of perhaps eight neutrons per primary proton. Below 10 Mev, star production ceases and moderation of the neutrons by collision with nitrogen and oxygen atoms becomes the predominating process. As the energy falls below about 1 kev, capture by N^{14} becomes important, preventing the neutrons from ever becoming truly "thermal." Moderation and capture are so effective that the neutrons are unable to travel far from their site of production. The distribution of the neutrons with altitude therefore reflects the absorption of the parent radiation. Further, it has been shown (4) that the energy spectrum is independent of the energy of production and depends only on the details of the scattering and absorption processes.

Note must also be made of the latitudinal variation of the neutron intensity resulting from the effect of the magnetic field of the earth on the approaching charged primaries. This variation is considerably greater for the neutrons than for any other component of the cosmic radiations, amounting to nearly a factor of four. Detailed measurements have been made by Simpson (11) of the latitude effect and of the altitude-intensity curve up to altitudes of 37,000 ft. (pressure = 17 cm. Hg). Over this region the neutron intensity rises exponentially with altitude, the half-thickness varying from 147 gm./sq. cm. at the geomagnetic equator to 109 gm./sq. cm. at high geomagnetic latitudes. The intensity at a given altitude shows a flat minimum at the equator, a steep rise in middle latitudes (20° to 50°) and a con-

stant intensity from about 55° to the magnetic pole. The ratio of polar maximum to equatorial minimum is about four.

Since the neutrons are a secondary component produced by atmospheric absorption of the primary protons, the intensity-altitude curve must show a maximum and fall to zero at the top of the atmosphere. Experimental confirmation of this was first obtained by Yuan (13), whose balloon flights have established the maximum in the neutron intensity to be at a pressure altitude of about 8 cm. Hg (50,000 ft.). Similar results have been obtained by Staker, Pavalow & Korff (14), Staker (15), and Davis (16).

An additional and very striking variation of the cosmic ray neutrons has been clearly demonstrated by Simpson, namely, a time variation correlated with solar flares and magnetic storms (11, 17, 18). This variation manifests itself in a continuation to higher latitudes of the rapid rise in intensity in middle latitudes. Whereas on "quiet" days the neutron intensity is constant above 55° N. latitude, on disturbed days the intensity may continue to rise toward the pole. Thus Staker, Pavalow & Korff (14) found the neutron intensity at 65° N. to be twice as great as that at 55° N. These data were obtained during the month of August, 1950, and the increase may be the result of the solar flare of August 2nd (19). Simpson reports variations of up to 30 per cent, detectable only at high latitudes, and well correlated with solar flares and magnetic storms. Similar observations have been made by Adams (20). Since these increases are relatively infrequent, the quiet-day intensity must be used to obtain the true time average.

Calculation of $\overline{Q}$.—The following symbols are used in the discussion. Functional dependences are indicated explicitly here for logical clarity but are omitted in the text.

λ = geomagnetic latitude

h = altitude

$q_{tot}(\lambda, h)$ = rate of capture per second and per gram of air of neutrons of all energies at a given latitude and altitude

$q_{th}(\lambda, h)$ = rate of capture per second and per gram of air of neutrons of energies less than the Cd cut-off (0.4 ev) at a given latitude and altitude

q_{tot}/q_{th} = ratio of total capture to "thermal" capture, assumed to be independent of λ and of h

$$Q_\lambda = \int q_{th}(\lambda, h)dh$$ = rate of capture per second and per square centimeter of neutrons of energies less than the Cd cut-off in a column atmosphere at a given latitude

$$\overline{Q} = \frac{q_{tot}}{q_{th}} \int\int q_{th}(\lambda, h) \cos \lambda d\lambda dh$$ = average rate of capture per second and per square centimeter of all neutrons

The only measurements of cosmic ray neutron intensity with counters of known absolute efficiency are those of Yuan (13) and of Simpson (21), and these measurements are not completely independent, Simpson's counters being calibrated in terms of Yuan's. The primary calibration was made by the comparison of the counting rate in a neutron beam scattered out of the

thermal column of the Argonne pile with the activity induced in indium foils exposed to the same beam (13). This calibration gives the "cross section" of the detector for thermal neutrons. To the extent that the ratio of the cross section of the counter to that of air for neutron capture is a constant, the capture rate of neutrons per gram of air will be simply a constant times the counting rate of the counter resulting from neutrons. Because a boron trifluoride counter registers additional events besides neutron capture (e.g., fast protons, "bursts," "stars") it is necessary to subtract these "background" events to obtain the true neutron-counting rate.

Two techniques have been used to this end: the "cadmium difference" method and the enriched isotope method. The former relies on the use of a cadmium filter placed around one of a pair of counters to remove all neutrons below the "Cd cut-off," e.g., the very abrupt increase of the cadmium absorption cross section at 0.4 ev. Neutrons below this energy are completely absorbed by a thin sheet of cadmium while those of greater energy are virtually completely transmitted. The other events causing counts will not be different in the two counters providing the wall masses and atomic numbers are nearly the same. Of the pair of counters, the one will detect neutrons of all energies plus "background," while the other will detect only neutrons above the Cd cut-off plus background. The difference between the two counting rates is a measure of the neutrons with energies below 0.4 ev with the background eliminated. The enriched isotope method is based on the fact that neutrons are detected by the reaction B^{10} (n, α) Li^7, the emitted alpha particle causing the count; the other isotope of boron, B^{11}, undergoes no similar reaction. If two identical counters are filled, one with boron trifluoride enriched in the isotope B^{10} and the other with boron trifluoride enriched in B^{11}, the true neutron count can be separated from the background and the measurement will be proportional to the neutron intensity over the entire part of the spectrum in which the 1/v law is operative rather than over only the low-energy portion. In view of the difficulty of evaluating the ratio of total neutron capture to capture below the Cd cut-off this constitutes a great advantage for this system. Unfortunately the only data which have been obtained by this method (14, 15, 16) have been made with uncalibrated counters constructed of boron-rich glass.

The constancy of the ratio of counter (i.e., B^{10}) capture cross section to that of N^{14} holds very well since both nuclides are absorbers which obey the 1/v law in the energy region of principal importance. The constancy of the 1/v law has been established for N^{14} up to 15 ev by Melkonian (22) and for B^{10} to 1000 ev (23). It is clear from Figure 1 that the energy region of principal importance is covered. (There is in addition a small but significant amount of resonance capture by N^{14} at energies of about 1 Mev which will be considered later.)

The Cd cut-off lies just in the middle of the region of neutron capture so that the cadmium difference measurements give about half of the total capture rate. It is therefore necessary to know with some accuracy the fraction of the neutrons which are captured at energies below 0.4 ev.

This problem was first treated by Bethe, Korff & Placzek (24). Their results were recalculated, using more recent data, by Anderson & Libby (1) and by Davis (16). A different method of calculation has been used by Bagge & Fincke (25), but this aspect of the problem appears in their paper only in an approximation.

The method of Bethe, Korff & Placzek is as follows: Let σ_a and σ_t be respectively the cross sections of air for absorption and for absorption plus scattering of neutrons. Both cross sections will in general be functions of the neutron energy. If ΔE is the neutron energy loss per scattering collision, the number of collisions necessary to reduce the neutron energy by dE is $dE/\Delta E$. The fraction of the neutrons not captured while being moderated from energy E_1 to E_2 is then

$$N_2/N_1 = \exp - \int_{E_1}^{E_2} \sigma_a dE/\sigma_t \Delta E \qquad 1.$$

The following numerical values are used:

$$\sigma_t = \sigma_a + \sigma_s$$
$$\sigma_s = 8.56 \text{ barns, independent of energy}$$
$$\sigma_a = 0.266E^{-1/2} \text{ [} E \text{ in ev, based on nitrogen}$$
$$\sigma_t = 9.96 + 0.34E^{-1/2} \text{ and oxygen}$$
$$\sigma_t = 3.73 \text{ (22)]}$$
$$\Delta E = 0.124E \text{ (26)}$$

Performing the integration we find

$$N/N_0 = \exp - (0.501E^{-1/2}) \qquad 2.$$

This function is plotted in Figure 1. Taking the Cd cut-off to be 0.4 ev and substituting in this equation gives 0.45 for the fraction of the neutrons cap-

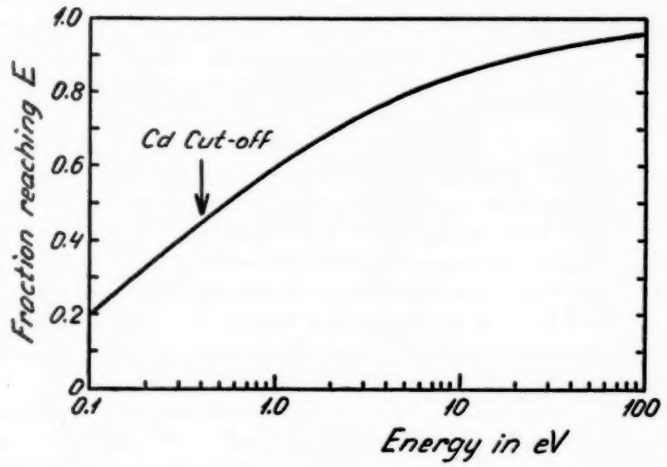

FIG. 1. Fraction of cosmic ray neutrons moderated to a given energy before capture

tured below this energy or 2.2 for q_{tot}/q_{th}, the ratio of "total" capture to "thermal" capture as measured by the Cd difference method.

Experimental check of this calculation is provided by the Cd difference data themselves, a method suggested by Ladenburg (27). It is clear that while the Cd difference count is proportional to the neutron capture rate below 0.4 ev, the counting rate in the unshielded counter is proportional (by the same factor) to the total capture rate over the 1/v region plus an additional background rate. The ratio of the unshielded counter rate to the Cd difference rate must therefore exceed the true value of the ratio q_{tot}/q_{th} by an amount determined by this unknown, additional background rate and should constitute a generous upper limit for q_{tot}/q_{th}. Simpson's data (21) at the equator under 312 gm./sq. cm. of air give 1.95 ± 0.10 for this counting ratio. Yuan's data (13) at 53° N. integrated over the atmosphere give 1.91. If the order of magnitude of Yuan's background be estimated from Staker's measurements (15) with a counter depleted in B^{10}, an estimate for q_{tot}/q_{th} of 1.75 is found.

The reason for this serious discrepancy between theory and experiment is not apparent. It seems not unlikely that the cause may be found in the neglect of the effect of vibrational excitation on the cooling process in the critical region just above the Cd cut-off. While Placzek has shown (28) that to a first approximation the energy distribution formulae will remain the same down to neutron energies of the order of the vibrational quantum (0.25 ev for N_2), a detailed analysis has not been made. The problem of the effect of chemical binding on the moderation of neutrons has been considered by several writers (29 to 32), but a detailed solution applicable to the case of interest here has not been obtained. Since the data suggest that the effect may be of appreciable magnitude, an attempt at analysis seems highly desirable.

For lack of a better alternative, we will use for q_{tot}/q_{th} a value intermediate to that given by simple theory and that indicated by the experimental results, namely 2.0. This value must be uncertain by at least 10 per cent.

This factor has been derived from a consideration of only the 1/v capture by N^{14} and correction must be made for additional capture by the resonances near 1 Mev. These n, p resonances have been investigated by Barshall & Battat (33) and by Johnson & Barshall (34). They lie at 0.5, 0.64, and 1.42 Mev with maxima of up to 0.2 barns. The scattering cross section has fallen to a value of two barns in this region (35). Graphical integration of equation 1 over these resonances gives N/N_0 equal to 0.86 from 2.0 to 0.5 Mev. No resonances have been observed below 0.5 Mev and since inelastic scattering begins above 2.3 Mev, the lowest excited state of N^{14} (36), no other resonance capture of appreciable amount is to be expected. The corrected value for q_{tot}/q_{th} is therefore taken to be 2.3.

The absolute evaluation of the average capture rate of neutrons to form C^{14} in a one square centimeter column atmosphere, $\overline{Q}$, then proceeds as follows: Simpson's result (21) for the slow neutron capture rate at the equator

and at 23 cm. Hg (8.2 ± 0.38 counts/min. Cd difference neutrons from a counter with a thermal neutron cross section of 8.8 sq. cm., i.e., $q_{th} = 3.1$ per sec. and per gm. of air) is corrected to latitude 53° and combined with the data from Yuan's third flight (13). The curve is then integrated, analytically over the exponential part (to 20 cm. Hg) using Simpson's value for the absorption coefficient (11), and graphically over the high altitude maximum. The result is 1.94 per sec. and per sq. cm. for Q_λ, the "thermal" capture rate in a column atmosphere, at the high latitude maximum ($\lambda > 55°$) on quiet days. To establish the average for all latitudes, Simpson's relative values of Q_λ (11) are plotted as $Q_\lambda \cos \lambda$ versus λ and integrated graphically. The ratio of $\overline{Q}$ to Q_λ at the polar maximum is found to be 0.58. Using this factor and the factor 2.3 for the ratio of total to Cd difference production gives $\overline{Q} = 2.6$ per sq. cm. and per sec.[3]

Note that because of the method of calculation, the capture of neutrons by mechanisms other than the $N^{14}(n, p)\ C^{14}$ reaction will not affect the accuracy of $\overline{Q}$ as a measure of radiocarbon production even though they make the actual neutron flux higher. The calculation used gives directly the ratio of radiocarbon production to BF_3 counts. It can be shown, however, that other mechanisms of neutron capture are probably negligible.

Estimation of B.—The estimation of B, the amount of carbon in exchange equilibrium with the radiocarbon produced by the cosmic ray neutrons, involves some very interesting geochemical problems which lie outside the scope of the present review. We will limit our discussion to a brief summary of the results (1, 37).

The original chemical form of the radiocarbon must be carbon dioxide. This carbon dioxide, formed mostly at high altitudes, will be mixed throughout the entire atmosphere in a time short compared with the mean life of radiocarbon, and no trace of the pronounced latitudinal variation of the neutron intensity will be reflected in the radiocarbon distribution. This has been proved by a measurement of the world-wide distribution of natural radiocarbon (1, 37, 38). From atmospheric carbon dioxide the radiocarbon finds its way into those other chemical species which are in exchange equilibrium with it. The exchange may be direct such as that between atmospheric carbon dioxide and dissolved ocean carbonate, or it may be a chemical cycle such as the one connecting carbon dioxide, plants, and animals. Cycles involving long time scales such as the solution of limestones, their transport to the sea, and their reprecipitation are so slow that the limestone cannot be considered as part of the exchange reservoir. However, cognizance must be taken of such losses of radiocarbon from the reservoir as the precipitation of ocean carbonate and the formation of peat, coal, and petroleum.

[3] The considerably higher value obtained by Yuan (13) is a result of the use of erroneous values for the cross sections. A revised calculation (to be published by Kouts and Yuan) gives a value in agreement with the one derived here. I am indebted to Dr. Yuan for allowing me to see his manuscript before publication.

The components of the exchange reservoir are three: atmospheric carbon dioxide, dissolved carbon in the hydrosphere (both inorganic and organic), and living plants and animals. On the basis of geochemical data the composition of the exchange reservoir is estimated to be that given in Table I (1, 37). The uncertainty of the total is estimated to be about 10 per cent.

TABLE I

COMPOSITION OF THE EXCHANGE RESERVOIR*

Source	Amount in grams of carbon per square centimeter
Dissolved inorganic (HCO_3^-)	7.25
Dissolved organic matter	.59
Biosphere	.33
Atmospheric carbon dioxide	.08
Total	8.25

* After Anderson & Libby (1).

The uncertainty in ocean bicarbonate can be calculated from the variations in the reported data on the pH and alkalinity of sea water. Dissolved organic matter has not been determined with much accuracy, and the figure given for the biosphere, that is, all living matter, is little more than a crude guess. It is believed to constitute an upper limit. Atmospheric carbon dioxide is known with considerable accuracy but consitutes only 1 per cent of the total. The question of the rate of loss of radiocarbon through incorporation into limestone, coal, peat, and petroleum is difficult to treat quantitatively, but it has been concluded that this loss is probably small compared with the uncertainty in B, amounting to not more than 3 per cent of the production rate.

SPECIFIC ACTIVITY OF NATURAL RADIOCARBON

Measurements on wood and shells.—An exhaustive study of the activities of all of the components of the exchange reservoir has yet to be made. However, sufficient data have accumulated to outline the general features of the distribution and to establish an over-all average for comparison with $\overline{Q}/B$. Wood has received the greatest attention because of its importance in dating applications. The Chicago results are given in Table II (1). The error given with each sample is the standard deviation as calculated from counting statistics only. An analysis of the scatter of the data shows no significant variation to be present other than this statistical one. The error given with the average of all wood samples is calculated from the sum of squares of the individual sample errors and therefore includes only random errors. On an abso-

TABLE II

ABSOLUTE SPECIFIC ACTIVITY OF CONTEMPORARY CARBON*

Source	Geomagnetic Latitude	Specific Activity (per min., per gm.)
Wood:		
White spruce, Yukon	60° N.	14.84±0.30
Norwegian spruce, Sweden	55° N.	15.37±0.54
Elm, Chicago	53° N.	14.72±0.54
Ash, Switzerland	49° N.	15.16±0.30
Honeysuckle, Tennessee	47° N.	14.60±0.30
Pine, New Mexico	44° N.	15.82±0.47
Briar, North Africa	40° N.	14.47±0.44
Oak, Palestine	34° N.	15.19±0.40
Unidentified wood, Iran	28° N.	15.57±0.31
Ash, Japan	26° N.	14.84±0.30
Unidentified wood, Panama	20° N.	15.94±0.51
Chlorophora, Liberia	11° N.	15.08±0.34
Sterculia, Bolivia	1° N.	15.47±0.50
Ironwood, Marshall Islands	0°	14.53±0.60
Unidentified wood, Ceylon	2° S.	15.29±0.67
Beech, Tierra del Fuego	45° S.	15.37±0.49
Eucalyptus, Australia	45° S.	16.31±0.43
Average		15.3 ±0.1
Animal:		
Sea Oil, Antarctica	65° S.	15.69±0.30
Shell:		
Murex, Florida		17.1 ±0.5
Contemporary sediments, Bermuda		17.4 ±0.6
Oyster, Chesapeake Bay		15.1 ±0.5
Average		16.5 ±0.5

* After Anderson & Libby (1).

lute basis systematic errors (e.g., in the determination of the counter efficiency) will increase the uncertainty to an estimated 0.5 per min. and per gm. Table III gives the results obtained at Lamont (39) for anthracite coal (i.e., a "blank"), wood, and shell. The activity is expressed in counts per minute above background since the counters were not calibrated on an absolute basis (which is unnecessary for age determinations).

Isotopic fractionation.—It is clear that both the Chicago and the Lamont results indicate a surprisingly large fractionation of the C^{14} isotope between

TABLE III

ACTIVITY OF CARBON SAMPLES (Counts per Minute)*

Anthracite Coal	Wood	Shell
$+0.15 \pm 0.12$	6.17 ± 0.07	6.60 ± 0.20
-0.31 ± 0.25	6.05 ± 0.11	6.63 ± 0.25
-0.04 ± 0.10	5.89 ± 0.13	7.08 ± 0.20
$+0.10 \pm 0.29$	6.07 ± 0.13	6.42 ± 0.17
$+0.01 \pm 0.09$	5.99 ± 0.08	6.95 ± 0.15
-0.08 ± 0.30	6.09 ± 0.06	
-0.01 ± 0.06	6.07 ± 0.04	6.72 ± 0.08

* After Kulp *et al.* (39).

wood and shell. The Lamont data give a fractionation factor $\alpha = 1.11 \pm 0.02$, the Chicago results give 1.09 ± 0.03.

The $C^{13}:C^{12}$ fractionation in the exchange reservoir system has been discussed by Urey (40), and the available information is summarized in Figure 2 together with the C^{14} result. The fractionation factor between aqueous bicarbonate ion and gaseous carbon dioxide is from the work of Urey, Aten & Keston (41), who estimated α to be at least 1.014 from the observed enrichment in a counter-current exchange column.

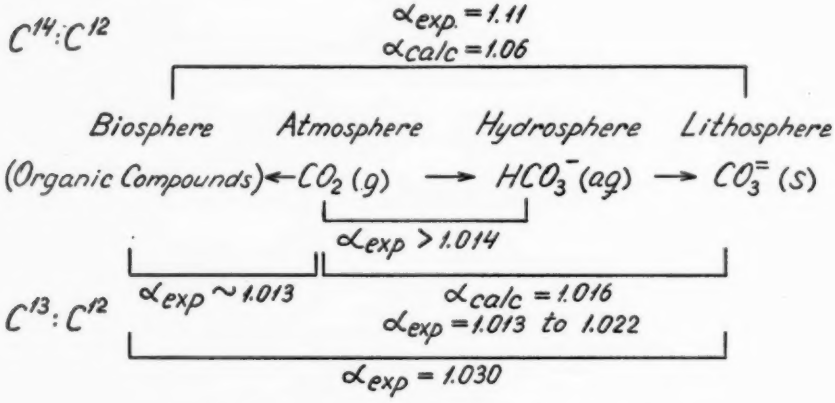

FIG. 2. Fractionation of the carbon isotopes in nature.

The isotopic ratio $C^{12}:C^{13}$ has been measured in atmospheric CO_2, in some organic compounds, and in carbonates by Nier & co-workers (42 to 45), and the results have been summarized by Rankama (46). Similar results have been reported by Wickman & co-workers (47, 48) and by Mars (49). From these data the experimental α between atmospheric CO_2 and carbonate was

calculated. The variation is due principally to the nonreproducibility of the atmospheric CO_2 value. The mean is not in serious disagreement with the theoretical value calculated by Urey. The latter result cannot be considered exact since a number of approximations and estimates were necessary to evaluate the partition functions for the carbonate ion (40).

The experimental α between organic compounds and CO_2 also suffers from the uncertainty in the $C^{12}:C^{13}$ ratio of the latter. In addition, Murphy (43, 44, 46) reported an appreciable difference in the C^{13} content of coal and wood on the one hand and of a number of diverse organic materials on the other (such as casein, linseed oil, china wood oil, rubber, spores, algae, peat, and petroleum). These materials indicated an α_{13} of about 1.01 compared to wood, having the lowest $C^{13}:C^{12}$ ratios of any which have been measured. For the over-all α_{13} given in Figure 2 between organic matter and carbonate, the $C^{12}:C^{13}$ ratio for coal and wood was used since these are the materials used in the C^{14} measurements.

The calculation of any of the factors involving biosphere material is difficult if not impossible owing to the complexity of the compounds and to the fact that the fractionation in this case is probably due to kinetic rather than to thermodynamic factors (40). Urey (50) has reported an additional result, not entered in Figure 2, on the fractionation of C^{13} between algae and the dissolved carbonate of the nutrient solution. An α of 1.031 was found, in agreement with the over-all, organic-solid carbonate factor. This indicates that, as expected, the fractionation between dissolved and crystalline carbonate may be comparatively small.

The "calculated" value for α_{14} entered in Figure 2 is derived from the experimental value of α_{13} between wood and carbonate, assuming α to vary as the first power of the isotopic mass difference (51). The result is not in good agreement with the observed C^{14} fractionation.

Further disagreement is to be found in the results reported by Weigl & Calvin (52). After allowing an algae culture to grow by a factor of 100 by photosynthesis of C^{14}-labeled CO_2, they determined the specific activities of the algae, the dissolved carbonate, and the CO_2 gas. Their results indicate α_{14} between CO_2 (g) and HCO_3^- (aq) to be about 1.07 and between algae and CO_2 (g) to be 1.22, giving an over-all α_{14} of 1.31. Weigl (53) has also reported a differential rate of uptake of 1.17 between $C^{12}O_2$ and $C^{14}O_2$ by photosynthesizing barley sprouts. Since the fractionation probably derives from differences in reaction rates, rapidly-growing young organisms may show quite different results from mature organisms which are in a more or less steady state. It is apparent that further study of both C^{13} and C^{14} abundances in the various chemical forms is indicated.

Comparison of S with $\overline{Q}/B$.—Combining the fractionation factor of 1.10 with the observed 15.3 min.$^{-1}$ gm.$^{-1}$ activity of wood, a value of 16.8 ± 0.6 is obtained for the absolute specific activity of carbonate. Taking a suitable average over the entire exchange reservoir gives 16.6 ± 0.6 for S. Using $\overline{Q} = 2.65$ sec.$^{-1}$ cm.$^{-2}$ and $B = 8.25$ gm. cm.$^{-2}$ leads to $\overline{Q}/B = 19$ min.$^{-1}$ gm.$^{-1}$

with an estimated uncertainty of 20 per cent. The agreement between the two figures is within the uncertainty of the latter. While this is all that can be safely said, one is tempted to point out that the high result for the predicted activity agrees with the Cd difference ratios in suggesting that current calculations of the rate of capture of cosmic ray neutrons as a function of energy give too high a capture rate in the region just above the Cd cut-off. A more thorough analysis of this problem is highly desirable as well as further measurements of the absolute cosmic ray neutron flux. An application of the enriched BF_3 counter method, so far used only to obtain relative values, would be most interesting because it would eliminate the Cd cut-off problem.

Counting System

Since the measurements of natural radiocarbon with a precision of a few per cent at a specific activity of the order of 10^{-12} c. per gm. involve rather special techniques, a word about the method is in order.

The screen-wall counter (54, 55, 56) is used because it provides the maximum net sample count with minimum background and long-term stability. A solid sample is mounted on the inside surface of a cylinder surrounding a Geiger-Müller tube whose "wall" consists of an open grid of wires. By a suitable electric field between the screen and the sample, electrons produced by ionization outside the screen are drawn into the counter where they produce a count. The sensitive volume therefore extends to the surface of the sample and a geometry of essentially 50 per cent is achieved. A layer of sample thicker than the range of the particle to be detected is used, and although self-absorption losses are high [over-all efficiency, including geometry, is 5.46 per cent for C^{14} (1, 37, 56)] this is compensated by the very large samples which can be accommodated. The common size of the screen-wall has a sample area of 400 sq. cm. or a capacity of 11 gm. of elemental carbon.

A detailed comparison with a gas-sample counter (57) shows that for C^{14} the greater sample accommodation of the screen-wall just compensates for the greater efficiency of the gas sample counter and the same net sample count is obtained from a pair of these counters of conventional size and having the same background. For more energetic betas the screen-wall becomes the more efficient, for less energetic betas, the gas counter. The great scarcity of elements yielding possible counter gases greatly limits the general applicability of the gas counter. Furthermore, experience seems to confirm the expectation that the screen-wall is a more stable and reproducible instrument when an attempt is being made to measure activities equal to, or less than, background.

The high background of a large and sensitive detector exposed to the cosmic radiation and to the natural radioactivities contaminating most materials of construction necessitates considerable care in shielding and in construction. The "soft" or cascade component of the cosmic radiation, consisting of a mixture of electrons and gamma rays and amounting to about 35 per

cent (particle-wise) (58) of the total intensity at sea level, can be stopped with 10 cm. of lead or 20 cm. of iron. The latter is preferable, although more bulky and massive, because of its lower contamination with natural radioactivities and because it is more economical.

The "hard" or meson component, constituting the remainder of the cosmic radiation at sea level, is so penetrating as to render impractical attempts to remove it by massive shielding. Its penetrating power and high specific ionization make it easy to eliminate by anticoincidence methods, a standard technique in cosmic ray studies (59) which was first applied to low-level activity measurements by Buch Andersen (60).[4] If a counter be surrounded

TABLE IV

NATURE OF BACKGROUND OF SCREEN-WALL COUNTER*

Shielding	Background Rate Counts per Min.	Difference	Remarks on Difference
None	450		
5 cm. lead	142	308	"Soft" plus local contamination
20 cm. iron	110	32	Contamination of the lead
20 cm. iron plus anti-coincidence	5	105	Mesons

* After Anderson (37).

with a ring of other counters, each pulse produced in the central counter by a meson will be accompanied by a simultaneous pulse from at least one counter of the surrounding ring. An electronic circuit is so arranged as to accept pulses from the central counter only if they are not accompanied by a simultaneous pulse from the shielding counters. In this way the meson background can be entirely eliminated. Massive shielding is still necessary to remove the gamma background since it does not produce coincidences with high efficiency. Some aspects of anticoincidence techniques have recently been discussed by Curran & Craggs (61), by Wilkinson (62), by Raeth, Sevold & Pederson (63), and by Putman (64); applications have been given by Martell & Libby (65), by Rusinow & Igelnitsky (66), and by Hirzel & Wäffler (67).

Table IV presents a summary of the experience at Chicago with the sources of background in a screen-wall counter of internal diameter 67 mm. and length 200 mm. The residual background is of unknown origin. Kulp (68) has recently reduced this still further to about 2.5 counts per min. by the

[4] In this interesting but apparently little-known paper, an apparatus strikingly similar to the current natural radiocarbon apparatus is described. The data presented suggest that inefficiency of the anticoincidence counters used prevented a greater background reduction than the factor of five observed.

insertion of a cylindrical shield of one inch of liquid mercury between the anticoincidence counter ring and the sample counter. Such a reduction might be the result of the removal of γ-radiation arising either from contamination of the iron used in shielding or from the decay or capture of slow mesons.

At these levels of activity, materials of construction must be chosen with extreme care since a detectable contamination is the rule rather than the exception. Aluminum and ordinary leaded brass are particularly bad (56).

The sensitivity of the apparatus for C^{14} is 10^{12} c./min. per gm. For a nuclide of medium atomic weight emitting a 1 Mev beta, the sensitivity corresponds to a maximum detectable half-life of 10^{17} years.

The applications of natural radiocarbon to archaeology and geology (38, 39, 69 to 73) are too specialized to warrant review here. The measurement of samples of known age in connection with the dating program has established the reliability of the method to the limit of the availability of reference samples (about 5000 years ago). Since the radiocarbon of a live sample is, on the average, 8000 years old, the implication is that there have been no major variations of the cosmic ray neutron flux over a period of ten to fifteen thousand years.

Summary

The principal results of the studies of natural radio-carbon from the point of view of nuclear science are:

(*a*) The absolute specific activity of natural radiocarbon is 16.6 ± 0.6 disintegrations per min. and per gm., agreeing within the errors of estimate with the value calculated from the cosmic ray neutron flux and the amount of exchangeable carbon, $\overline{Q}/B = 19 \pm 4$ min.$^{-1}$ gm.$^{-1}$.

(*b*) The fractionation factor for C^{14} between wood and shell carbonate is found to be 1.10 ± 0.02.

(*c*) The extreme latitudinal variation of the cosmic ray neutron flux is not reflected in the distribution of radiocarbon.

(*d*) The cosmic ray neutron flux has been constant for at least the past 10 or 15 thousand years.

LITERATURE CITED

1. Anderson, E. C., and Libby, W. F., *Phys. Rev.*, **81**, 64 (1951)
2. Engelkemeir, A. G., and Libby, W. F., *Rev. Sci. Instruments*, **21**, 550 (1950)
3. Engelkemeir, A. G., Hamill, W. H., Inghram, M. G., and Libby, W. F., *Phys. Rev.*, **75**, 1825 (1949)
4. Flügge, S., *Cosmic Radiation*, 144 (Heisenberg, W., Ed., Johnson, T. H., Trans., Dover Publications, New York, N. Y., 192 pp., 1946)
5. Korff, S. A., *Am. J. Phys.*, **19**, 226 (1951)
6. Korff, S. A., *Terrestrial Magnetism and Atmospheric Electricity*, **45**, 133 (1940)
7. Libby, W. F., *Phys. Rev.*, **69**, 671 (1946)
8. Anderson, E. C., Libby, W. F., Weinhouse, S., Reid, A. F., Kirshenbaum, A. D., and Grosse, A. V., *Science*, **105**, 576 (1947)
9. Anderson, E. C., Libby, W. F., Weinhouse, S., Reid, A. F., Kirshenbaum, A. D., and Grosse, A. V., *Phys. Rev.*, **72**, 931 (1947)

10. Grosse, A. V., Johnston, W. H., Wolfgang, R. L., and Libby, W. F., *Science*, **113**, 1 (1951)
11. Simpson, J. A., Jr., *Phys. Rev.*, **83**, 1175 (1951)
12. Robson, J. M., *Phys. Rev.*, **83**, 349 (1951)
13. Yuan, L. C. L., *Phys. Rev.*, **81**, 175 (1951)
14. Staker, W. P., Pavalow, M., and Korff, S. A., *Phys. Rev.*, **81**, 889 (1951)
15. Staker, W. P., *Phys. Rev.*, **80**, 52 (1950)
16. Davis, W. O., *Phys. Rev.*, **80**, 150 (1950)
17. Simpson, J. A., Jr., *Phys. Rev.*, **81**, 639 (1951)
18. Simpson, J. A., Jr., *Phys. Rev.*, **81**, 895 (1951)
19. Naugle, J. E., and Anderson, G. W., Jr., *Phys. Rev.*, **81**, 314 (1951)
20. Adams, N., *Phil. Mag.*, **41**, 503 (1950)
21. Simpson, J. A., Jr. (Unpublished data)
22. Melkonian, E., *Phys. Rev.*, **76**, 1750 (1949)
23. *The Science and Engineering of Nuclear Power*, **I**, 404 (Goodman, C., Ed., Addison-Wesley Press, Inc., Cambridge, Mass., 503 pp., 1947)
24. Bethe, H. A., Korff, S. A., and Placzek, G., *Phys. Rev.*, **57**, 573 (1940)
25. Bagge, E., and Fincke, K., *Ann. Physik*, **6**, 321 (1949)
26. Libby, W. F., *J. Am. Chem. Soc.*, **69**, 2523 (1947) (Appendix 3)
27. Ladenburg, R. (Unpublished data)
28. Placzek, G., *Phys. Rev.*, **69**, 423 (1946)
29. Bethe, H. A., *Revs. Modern Phys.*, **9**, 122 (1937)
30. Arley, N., *Kgl. Danske Videnskab. Selskab, Math.-fys. Medd.*, **16**(1) 1 (1938)
31. Sachs, R. G., and Teller, E., *Phys. Rev.*, **60**, 18 (1941)
32. Messiah, A. M. L., *Phys. Rev.*, **84**, 204 (1951)
33. Barshall, H. H., and Battat, M. E., *Phys. Rev.*, **70**, 245 (1946)
34. Johnson, C. H., and Barshall, H. H., *Phys. Rev.*, **80**, 818 (1950)
35. Johnson, C. H., Petree, B., and Adair, R. K., *Phys. Rev.*, **84**, 775 (1951)
36. Hornyak, W. F., Lauritsen, T., Morrison, P., and Fowler, W. A., *Revs. Modern Phys.*, **22**, 334 (1950)
37. Anderson, E. C., *Natural Radiocarbon* (Doctoral thesis, Univ. of Chicago, Chicago, Ill., 1949)
38. Libby, W. F., Anderson, E. C., and Arnold, J. R., *Science*, **109**, 227 (1949)
39. Kulp, J. L., Feeley, H. W., and Tryon, L. E., *Science*, **114**, 565 (1951)
40. Urey, H. C., *J. Chem. Soc.*, 562 (1947)
41. Urey, H. C., Aten, A. H. W., Jr., and Keston, A. S., *J. Chem. Phys.*, **4**, 622 (1936)
42. Nier, A. O., *Phys. Rev.*, **77**, 789 (1950)
43. Murphey, B. F., and Nier, A. O., *Phys. Rev.*, **59**, 771 (1941)
44. Murphey, B. F. (Master's thesis, Univ. of Minnesota, Minneapolis, Minn., 1941)
45. Nier, A. O., and Gulbransen, E. A., *J. Am. Chem. Soc.*, **61**, 697 (1939)
46. Rankama, K., *J. Geol.*, **56**, 199 (1948)
47. Wickman, J. E., Blix, R., and Ubisch, H. von, *J. Geol.*, **59**, 142 (1951)
48. Wickman, J. E., and Ubisch, H. von, *Geochim. Cosmochim. Acta.*, **1**, 119 (1951)
49. Mars, K. E., *J. Geol.*, **59**, 131 (1951)
50. Urey, H. C., *Science*, **108**, 489 (1948)
51. Bigeleisen, J., and Mayer, M. G., *J. Chem. Phys.*, **15**, 261 (1947)
52. Weigl, J. W., and Calvin, M., *J. Chem. Phys.*, **17**, 210 (1949)
53. Weigl, J. W., *U. S. Atomic Energy Commission Document, UCRL-590* (1950)
54. Libby, W. F., *Phys. Rev.*, **46**, 196 (1934)
55. Libby, W. F., and Lee, D. D., *Phys. Rev.*, **55**, 245 (1939)

56. Anderson, E. C., Arnold, J. R., and Libby, W. F., *Rev. Sci. Instruments*, **22**, 225 (1951)
57. Anderson, E. C., and Levi, H., *Kgl. Danske Videnskab. Selskab, Math.-fys. Medd.* (In press)
58. Montgommery, D. J. X., *Cosmic Ray Physics*, 131 (Princeton University Press, Princeton, N. J., 370 pp., 1949)
59. Leprince-Ringuet, L., *Cosmic Rays*, 49 (Prentice-Hall, Inc., New York, N. Y., 290 pp., 1950)
60. Anderson, E. B., *Z. Physik*, **98**, 597 (1935)
61. Curran, S. C., and Craggs, J. D., *Counting Tubes*, 135, 188, 197 (Academic Press, Inc., New York, N. Y., 238 pp., 1949)
62. Wilkinson, D. H., *Ionization Chambers and Counters*, 239 (Cambridge University Press, Cambridge, Mass., 266 pp., 1950)
63. Raeth, C. H., Sevold, B. J., Pedersen, C. N., *Rev. Sci. Instruments*, **22**, 461 (1951)
64. Putman, J. L., *J. Sci. Instruments*, **26**, 198 (1949)
65. Martell, E. A., and Libby, W. F., *Phys. Rev.*, **80**, 977 (1950)
66. Rusinov, L. I., and Igelnitsky, J. M., *Doklady Akad. Nauk S.S.S.R.*, **47**, 333 (1945); **49**, 343 (1945)
67. Hirzel, O., and Wäffler, H., *Helv. Phys. Acta*, **20**, 373 (1947)
68. Kulp, J. L. (Personal communication, 1951)
69. Arnold, J. R., and Libby, W. F., *Science*, **113**, 111 (1951)
70. Libby, W. F., *Science*, **144**, 291 (1951)
71. Johnson, F., *et al.*, *Mem. Soc. Am. Archaeol.*, No. 8 (1951); *Am. Antiquity*, **17**(1), Part 2, 65 pp., (1951)
72. Flint, R. F., and Deevey, E. S., Jr., *Am. J. Sci.*, **249**, 257 (1951)
73. Flint, R. F., *Nature*, **167**, 833 (1951)

RECENT PROGRESS IN ACCELERATORS[1]

By E. L. Chu and L. I. Schiff

Microwave Laboratory and Physics Department,
Stanford University, Stanford, California

This chapter is intended as a survey of recent progress in accelerators, mainly that which occurred during 1951. A few references to earlier work and to more recent work are included where warranted by inadequate earlier discussion or by current interest. For the most part, work on accelerators up to early 1951 is covered in a number of recent review articles which are listed in part A of the bibliography (1 to 8). Two excellent bibliographies dealing with accelerators have also been published [Thomas, Mittelman & Goldsmith (9); Cushman (10)]. Cushman's listing of accelerators and their status as of late 1950 was found especially helpful by the present authors in gathering information for this chapter.

The following discussion is divided into ten sections, which deal with particular types of accelerators. Needless to say, the space devoted to each type does not reflect the level of current activity, but rather the authors' estimate of the importance and interest of new developments, based on an earnest but probably not completely successful attempt to learn of and properly appreciate all current activities. Each section starts with a reference to the appropriate review articles listed in part A of the bibliography.

Kevatron

The term kevatron is coming into general use to designate accelerators that make use of transformers or cascading rectifier circuits to attain particle energies in the range from 50 to 1000 kev. A review of DC machines of this type has been given by Fortescue (4). Kevatrons are most used as fast neutron sources, in which advantage is taken of the deuteron-deuteron, deuteron-beryllium, or deuteron-triton reactions, which give good neutron yields at relatively low bombarding deuteron energies. With careful voltage control, the DC type of machine has been used to study both the nuclear and extranuclear interactions of charged particles, as well as to produce fast neutrons of homogeneous and variable energy.

A cascade or Cockcroft-Walton DC generator built by Philips has recently been installed at the University of Istanbul [Yenicay (11)], and yields energies up to 800 kev and proton or deuteron currents up to about 170 μamp. Similar Philips type machines for 500 and 1000 kev have also been built at the Clarendon Laboratory, Oxford [Collie (12)]; the latter has the power ripple suppressed to 50 v., and long-period stabilization is provided within 300 v. A much larger number of stages, with corresponding reduction in the number of volts per stage, is achieved at the State University of Iowa, where

[1] The survey of the literature pertaining to this review was concluded in March' 1952.

dry-disk selenium rectifiers are employed in a 500 kv. accelerator [Arnold (13)]. Another 500 kv. Cockcroft-Walton type accelerator has been built at the University of California in Berkeley as the injector to the 10 Mv. linear accelerator that will serve as the injector to the bevatron [Woodyard (14)]. This machine has 26 stages and operates at the unusually high frequency of 100 kc.

With careful design, accelerators of this type can be made portable. A 250 kv. Cockcroft-Walton type generator has been built at the U. S. Naval Research Laboratory, and can be moved in four units: power supply (Beta Electronic Corporation), high voltage terminal, accelerating tube, and pumping system [Bergstralh *et al.* (15)]. A similar machine at Los Alamos was designed as a portable source of 14 Mev neutrons from the deuteron-triton reaction [Forbes, Graves & Little (16)]. It was originally powered with a transformer that gave 70 kv. peak AC, but since has been changed to 120 kv. DC operation by installation of a Beta Electronic Corporation voltage doubler circuit.

An interesting method for doubling the energy of the particles produced by a DC accelerator has recently been suggested by Alvarez (17), independently of an earlier mention by Bennett (18). This consists in accelerating negative hydrogen or deuterium ions from ground potential to a positive high voltage electrode, passing them through a thin foil that strips off the electrons, and accelerating them back to ground potential. The success of such a device will depend on the efficiency of the negative ion source, which has been greatly improved in the last two years. An attractive feature of this arrangement is that the ion source and target are at ground potential, so that no electronic or electromechanical devices need be operated at high potential. An accelerator of this type, to give 4 Mev protons, is now being designed at the University of California in Berkeley, and will make use of a Cockcroft-Walton type high voltage supply.

Electrostatic Generator

An electrostatic generator makes use of a moving insulator that transports electric charge by mechanical means from a low to a high potential. The type most widely used now employs an endless belt as the moving insulator; it was first introduced as a practical generator by Van de Graaff, and further developed by many other workers, notably Herb. Review articles have been written by Fortescue (4) and by Shire (5).

One of the most significant recent developments in this field is the appearance of a line of thoroughly reliable, commercially-produced Van de Graaff generators, manufactured by the High Voltage Engineering Corporation. One of these, the vertical accelerator at the Oak Ridge National Laboratory, has produced 6 to 8 μamp. of analyzed protons in a continuous beam throughout the operating range of 0.5 to 5.5 Mev energy, with a voltage stability of better than ± 0.1 per cent. The acceleration tube of this machine is 12 ft. long, so that the voltage can be maintained at nearly half a million

volts per foot. This accelerator has been in almost daily operation for many months with practically no maintenance [Willard (19)].

Progress continues with the 12 Mev vertical Van de Graaff accelerator at Los Alamos. The acceleration tube is assembled from 2-ft. sections, each of which can withstand 1.7 Mv. [McKibben (20)]. However, the voltage does not go up in proportion to the number of sections, and the 12 of the eventual 20 ft. of tube that have been tried thus far will carry a little over 5 Mv. The tube will be redesigned, and in the meantime the machine is being started on research. This generator has a separation column, which enables the pressure tank and the high voltage electrodes to be lifted off without pumping off the main insulating gas (which will be SF_6). This exposes the apparatus within the highest potential electrode; decompression of the nitrogen within the separation column and access to the electrode interior can be accomplished in about half an hour.

The horizontal electrostatic generator at the University of Kansas incorporates a novel feature that makes it particularly well-suited to a small laboratory space [Seagondollar (21)]. The free space in the room (difference between the length of the laboratory and that of the pressure tank) is put at the target end. It is then not possible to roll the tank back for maintenance. Instead, the entire generator structure can be rolled out of the tank, which remains fixed. This arrangement allows a maximum of working space in the target area.

An electrostatic generator is being built at the Commisariat à l'Énergie Atomique in Paris that has a much larger tube than existing machines and consequent greater pumping speed [Kowarski (22)]. It also incorporates two types of voltage stabilization: a slow control that adjusts the current on the charging belt, and a faster control that varies the potential of a capacitive lining of the pressure tank. The combination is expected to yield stabilization to between 0.1 and 0.01 per cent.

A factor that has received considerable attention lately is that of electron loading. This is the name given to the very large electron current that is drawn up the tube into the high voltage electrode, and which seriously limits the voltage attainable with given belt current capacity. This factor also provides the principal limitation on the ion current now that high-performance ion sources are available. Blewett (23) has studied this effect with the Brookhaven accelerators, and has found indications that it arises from a surface insulating layer, probably of organic material, that produces a Malter effect. Such a layer, a few thousand Ångstrom units thick, deposited on metal surfaces in the lower part of the tube, collects positive charge which pulls electrons out of the underlying metal surface. These electrons are then emitted copiously at moderate field strengths. Similar conclusions have been reached at High Voltage Engineering Corporation [Robinson, McIntosh & Nygard (24)] and at Los Alamos [McKibben & Boyer (25)], where the tubes are so designed as to minimize this effect.

An interesting variation of the electrostatic generator was developed in

Belgium before the war, and has since been rebuilt at the Université de Liége [Morand & Raskin, & Winand (26)]. The charge-carrying belt of the Van de Graaff machine is replaced by a closed aerodynamic circuit that carries very small charged dust particles. This generator, operating in 1939, was destroyed during the war and redesigned in 1947. A potential of 1 Mv. has been achieved with a charging current of 1 m. amp., and the tube sections thus far assembled accelerate protons and deuterons to 300 kev energy.

Cyclotron

The cyclotron exploits the fact that the period of orbital revolution of a nonrelativistic charged particle in a fixed magnetic field is independent of the energy of the particle. This makes resonance acceleration by an alternating electric field possible without change of frequency. Because of the relativistic mass increase, fixed-frequency cyclotrons are limited as to maximum attainable energy. Several review articles have been published [Livingston (1, 6); Fremlin & Gooden (3); Pickavance (4); Rotblat (5)].

The principal advances in cyclotron design and construction during 1951 lie in the direction of increased energies and ion currents. At the Oak Ridge National Laboratory, considerable attention has been given to the use of very high dee voltages in order to push the output particle energy as far into the relativistic region as possible. The use of 2 kv. negative bias on the dee system permits very successful use of a grounded-grid, self-excited oscillator that gives 280 to 400 kilovolt dee-to-dee voltage. With this arrangement and an 86-in. magnet, protons have been accelerated to 20 Mev, which corresponds to almost twice the relativistic mass increase of any other cyclotron [Livingston (27)].

A high relativistic mass increase has also been obtained with the Argonne 60-in. cyclotron, constructed by the Collins Radio Company. This machine has produced 100 μamp. of external deflected deuterons at 24 Mev [Livingood (28)]. Deuterons have been accelerated to 25 Mev on an internal target of the 89-in. cyclotron at the Nobel Institute for Physics in Stockholm [Atterling & Lindström (29)]. A 60-in. cyclotron has recently been built at the University of Washington in Seattle. This is designed to produce 20 Mev deuterons, and has thus far yielded internal currents in excess of 100 μamp. [Donnelly *et al.* (30)].

Extremely high current at moderate voltage is the objective of an 18-in. cyclotron approaching completion at Brookhaven National Laboratory [Cottingham *et al.* (31)]. It is designed to produce an external beam of at least 1000 μamp., of protons with energy between 0.5 and 3 Mev, or deuterons with energy between 0.5 and 2 Mev. It is portable in the sense that components are packaged and interconnected in such a way as to facilitate disassembly at one location and reassembly at some other location. The high current implies high gas flow to the ion source, and hence an unusually high-speed pumping system.

SYNCHROCYCLOTRON

The relativistic mass increase destroys resonance in the cyclotron for sufficiently high energy. Resonance can be maintained without interfering with the focusing by the magnetic field, either by increasing the magnetic field strength or decreasing the frequency of the accelerating electric field in time as the particle gains energy. The first method is used in the electron synchrotron, the second in the synchrocyclotron, and both together are used in the proton synchrotron. In the 170-in. University of Chicago synchrocyclotron, for example, the frequency drops to 63 per cent of its intial value as protons are accelerated to their maximum energy of 450 Mev. Since particles are accelerated only during the sweeping time of the frequency, the duty cycle is much lower than that of a fixed-frequency cyclotron, and the average current is far less. There are several review articles on synchrocyclotrons that summarize developments up to 1951 [Livingston (1, 6); Fremlin & Gooden (3); Pickavance (4); Rotblat (5)].

A relatively small synchrocyclotron has recently been completed by Philips and installed in the Institute for Nuclear Studies at Amsterdam [Heyn (32)]. This machine has a 71-in. magnet and has produced 28 Mev deuterons with an average internal current of 20 μamp. While this energy is not outside the reach of a fixed-frequency cyclotron, the design is simplified and the operation made more reliable by using variable frequency. This is especially so in that a low dee voltage may be used, 15 kv. peak as compared with more than 100 kv. peak for fixed frequency. The relatively high beam current for this type of machine is attained by sweeping the frequency at a very high rate, 2000 times per second.

The yields of neutrons and other reaction products from an internal target in a synchrocyclotron will be affected by multiple traversals of the target by the beam. The controlling factors are beam spread in the target from multiple Coulomb scattering, and refocusing of the beam by the magnetic field. Theoretical and experimental studies have been made by Knox at Berkeley (33), and by Cassels, Dickson & Howlett at Harwell (34), and provide sufficient information to estimate the number of traversals to be expected in a wide variety of circumstances. This effect is more important here than with a fixed-frequency cyclotron because the spacing between successive turns of the ion orbit is much smaller because of the smaller dee voltage.

Since the most expensive part of a machine of this type is the magnet, various attempts are being made to economize on magnet iron without sacrifice of the product of maximum orbit radius and field strength, which determines the output particle energy. Careful theoretical and model studies on the Carnegie Institute of Technology 142-in. magnet have developed an economical design that produces the very high central field of over 20,000 gauss, and a maximum usable orbit that lies within 15 per cent of the gap dimension from the edge of the pole [Foss (35)]. For most other synchrocyclotrons, this 15 per cent figure is between 35 per cent and 60 per cent. A

different approach to the problem of magnet cost is being considered at the University of Birmingham, where design studies for an air-cored synchrocyclotron are being made [Riddiford (36)]. Here it is hoped to obtain a pulsed field of 270,000 gauss over an orbit 9.3 in. in diameter, and thus accelerate protons to an energy of 400 Mev. A machine of quite modest dimensions would result; the chief saving in cost would come from dispensing with magnet iron, since the power supply and other costs would be comparable with those for an iron-cored machine of similar proton energy output.

In the Berkeley 184-in. synchrocyclotron it was desired to be able to accelerate both protons and deuterons with a minimum of change-over time. Accordingly, an oscillator system was developed that provides the full 2.4 to 1 frequency ratio required to accelerate protons to 350 Mev and deuterons to 190 Mev, with a change-over time of about 5 min. [MacKenzie (37)]. This system has operated very successfully, and a similar oscillator arrangment is being incorporated in the University of Liverpool 156-in. synchrocyclotron now under construction [Moore (38)].

An interesting extractor for the ion beam has been proposed by Tuck & Teng (39) at the University of Chicago. This consists of static magnetic field perturbations placed azimuthally around the orbit of near-maximum radius, that increase the amplitude of the radial oscillations and suppress the vertical oscillations. These perturbations consist of an azimuthal region in which the magnetic field falls off faster than normal with increasing radius (peeler), and another region approximately 90° ahead of it in the direction of ion rotation in which the magnetic field increases with increasing radius (regenerator). With suitable design it is believed that the orbit radius can be made to increase as much as 1.5 in. in a single revolution; this is enough to clear the mouth of a magnetic channel which guides the ions out of the main field. A more quantitative analytical study that confirms these results has been published by Le Couteur (40).

Although the acceleration of heavier stripped ions is not new, it is interesting to note that a record for the energy of artificially accelerated particles has been set at the University of Chicago, where carbon nuclei have been accelerated to about 1250 Mev [Anderson (41)]. The energy per nucleon is of course substantially less than that of the 450 Mev protons obtained with the same machine.[2]

Betatron

The betatron and the electron synchrotron have many problems and features in common. The following comments on electron injection, beam-target interaction, beam extraction, and energy loss from radiation, apply for the most part to both types of machine. There are several recent review

[2] This record has since been broken at Brookhaven National Laboratory, where the cosmotron (proton synchrotron) has produced 2300 Mev protons.

articles on the betatron [Livingston (1); Fremlin & Gooden (3); Goward (5)].

Considerable attention has been directed toward understanding the injection process, since it is at this point that the greatest improvement in output beam current can be achieved. The problem is to see why the electrons do not strike the back of the injector on subsequent revolutions. Even if they miss on the first time around because they are oscillating about the instantaneous equilibrium orbit, they would be expected to return after several revolutions. There appears to be an empirical correlation between the presence of large magnetic field perturbations which come from injector currents, and the success with which electrons are trapped into orbits. Theoretical investigation shows that there is a resonance-damping effect that can convert the energy of orbital oscillation into kinetic energy of the electrons in so short a time that the oscillations are damped out by the time the electrons would have hit the injector [Barden (42)]. Experiments on the Case Institute of Technology 30 Mev betatron generally confirm this analysis [Gregg (43)]. This work points the way toward designing suitable field perturbations that will increase the efficiency of electron capture.

A recently proposed alternative scheme for injection consists in providing a means for continuously bending the equilibrium orbit away from the injector at a rapid rate during the injection time by magnetic or electric fields [Davis (44)]. It is believed that this can be done fast enough to cause a substantial fraction of the electrons to miss the injector the next time around when the usual oscillations are taken into account.

It is desirable for experiments in nuclear physics to have the energy of the electron beam as well-defined as possible when it strikes the target. This has been accomplished with considerable success with the University of Saskatchewan 22 Mev betatron by developing a circuit that integrates the time rate of change of the flux linking the electron orbit so as to provide a measure of the electron energy at all times; this circuit can then be set to expand the orbit so that it strikes the target at any prearranged electron energy [Katz *et al.* (45)]. This arrangement, suggested earlier at the University of Illinois, now provides 30-kv. energy control at Saskatchewan, and has made it possible to detect discontinuities in the activation curve for photoneutrons from oxygen [Montalbetti (46)].

For high yields of photon-induced radioactivities, the external γ-ray beam produced by the usual internal target does not have maximum effectiveness. In this case, a probe can be inserted into the circulating electron beam ahead of the target [Becker (47)]. By facing the material to be irradiated with a piece of material of high atomic number, about a hundredfold higher yield can be obtained.

A modification of the internal target to make it effectively thick has been suggested by McMillan (48). The spacing between successive turns in a betatron or synchrotron during final expansion is so small that the beam will not normally traverse a thick target. However, a thin fin of low atomic

number material, mounted at the edge of a thick target, will cause the electrons to lose a fairly definite amount of energy by ionization without being scattered appreciably. This will decrease the energy of the beam and cause it to strike the thick target the next time around. Such an arrangment would be useful for producing a wide-angle, high-intensity beam of x-rays. The radiated spectrum can be calculated by correcting the distribution of x-rays in energy and angle produced by a very thin target [Schiff (49)] for multiple scattering and ionization loss.

An important factor in the use of a betatron or synchrotron is the duty cycle, or the fraction of the time that the electron beam is striking the target. Various schemes have been proposed to shape the beam so as to increase the on-time above the several microseconds that are obtained without special effort. With the University of California 340-Mev synchrotron, the radio-frequency (rf) voltage is gradually decreased (instead of turned off abruptly) so that the radiation losses of those electrons that are most nearly in phase with the rf voltage are compensated, while those that have the largest phase oscillations become phase-unstable first and strike the target [Gauer & Nunan (50)], giving an x-ray pulse about 3000 μsec. long. Both long and very short pulses have been obtained with the University of Illinois 340 Mev betatron by displacing the equilibrium orbit in an appropriate manner by means of coils placed diametrically opposite to the target [Kerst (51)].

Recent attempts to extract the electron beam have been reported in connection with the General Electric 80 Mev synchrotron [Pollock, Hebb & Noble (52)], and the National Bureau of Standards 50 Mev betatron [Foote (53)]. The problem here is in a way the inverse of the injection problem, in that the beam must be made to miss the extractor for the several revolutions just before it is removed; on the other hand, the magnetic field is of course much greater than during injection. At the General Electric Company, the equilibrium orbit is expanded slowly to the point of instability, when the electrons spontaneously spiral outward into an electrostatic deflection channel; useful external electron beams have been obtained in this way. At the Bureau of Standards, an extractor has been built that will cancel the betatron field for a 2 μsec. interval over about 19° of the equilibrium orbit by means of a pulsed current through a wire network. This enables the electrons to escape, and it is believed that efficiencies approaching 100 per cent can be realized in this way. Both of these systems are developments of the earlier work on extraction schemes at the University of Illinois.

A question as to the validity of classical radiation theory for the calculation of the energy loss by radiation from electrons circulating in a betatron or synchrotron, was raised recently by Parzen (54). Subsequent examination of the mathematical analysis by Judd *et al.* (55), and of the wave-packet argument by Schiff (56), indicate that the classical theory should be valid for electron energies small in comparison with 10^9 Mev for a magnetic field of 10,000 gauss, or 10^8 Mev for a field of 100,000 gauss. This means that the usual classical calculation can be employed for all accelerators now contemplated.

In concluding this section, it is worth noting two European industrial developments in the betatron field. Brown, Boveri and Company have built a 31 Mev betatron for nuclear physics, medical, and radiographic applications [Wideröe *et al.* (57)]. An interesting feature of this machine is that electrons are accelerated in opposite directions during the two halves of the 50 c.p.s. alternating current excitation of the magnet. Philips is reported to be developing a light-weight, compact, air-cored betatron that operates at about 2500 c.p.s., and is intended to give x-rays in the 5 to 9 Mev range (58).

Electron Synchrotron

Most of the recent progress with electron synchrotrons has been covered in the preceding section, since the work discussed is closely related to similar work on betatrons. So far as additional new information is concerned, it seems worth reporting here only the current status of one of the large synchrotrons now under construction at the General Electric Company (59). The review articles listed at the beginning of the preceding section deal also with synchrotrons, as does the article by Thomas, Kraushaar & Halpern (7).

The General Electric synchrotron is an air-cored machine with a circular orbit 48 in. in diameter. It is currently planned to produce electrons of approximately 300 Mev energy by means of a peak magnetic field of 16,000 gauss. This field is to be produced by a half-sinusoid current (peak value 26,000 amp.) flowing in four water-cooled coils coaxial with the orbit, this being the best that can be done with the present power supply. The synchrotron itself has been designed so that with increased power input it should produce electrons with energies of approximately 1000 Mev. The limiting factors will then be the mechanical strength of the conductors and the energy loss by radiation. Thus far, a synchrotron beam of about 150 Mev energy has been produced.

Proton Synchrotron

The proton synchrotron differs from the electron synchrotron in that there is a large change in the speed of the particle during the acceleration. This means that if the economy of the ring-shaped magnet is to be retained (nearly constant orbit radius), the frequency of the rf voltage must be increased as the magnetic field is increased during acceleration. Since the energy loss by radiation is negligible for protons, this machine offers the best opportunity of any of the circular accelerators to obtain particle energies in the several thousand Mev range. Developments up to 1951 are described in recent review articles [Livingston (1, 6); Fremlin & Gooden (3)]; no significant events seem to have occurred since the latest of these (6) was prepared.[2]

Proton Linear Accelerator

The first high energy, proton, linear accelerator was constructed at the University of California in Berkeley shortly after the end of the war. Since

then, one other has been started, at the University of Minnesota. Recent review articles deal with both of these machines [Fry & Walkinshaw (2); Slater (8)], and a detailed description of the Berkeley machine has been published [Alvarez *et al.* (60)].

An interesting recent development with the Berkeley machine is its ability to operate without focusing grids. It has been shown in a very general way that phase stability (or focusing in the longitudinal direction) is incompatible with first-order transverse focusing in linear accelerators, unless a foil or grid is placed across the entrance to each drift tube [McMillan (61)]. Nevertheless, if the accelerator is short enough, it can be operated unstably so far as transverse focusing is concerned, and the loss of ions will not be too severe. Experiments with the Berkeley accelerator have shown that such a beam can be obtained that has roughly the magnitude of that obtainable with grids, although the criticality of adjustment is greatly increased [Panofsky (62)].

The Minnesota accelerator differs from the Berkeley machine in several respects [Williams (63)]. Instead of a single 40-ft. cavity with drift tubes, the Minnesota accelerator has three separate resonant cavities in series 20 ft., 40 ft., and 40 ft. long. These are driven at 200 Mc. by continuously pumped resnatrons that act as power amplifiers excited by a coherent source. Automatic volume and frequency controls, and the high-power rf coupling, present new problems in radio engineering that are being solved by joint efforts of the University and the Collins Radio Company.

Electron Linear Accelerator

When the linear accelerator is applied to production of high energy electrons, the small rest mass and consequent extreme relativistic behavior of the electrons lead to important advantages. The wave guide structure used for acceleration has conveniently small unit dimensions when microwave frequencies (about 3000 Mc.) are employed, and extremely high power sources are now available at these frequencies as an outcome of the klystron development program at Stanford University. Further, no transverse focusing arrangment need be used once the electrons have speeds close to that of light, in spite of the fundamental instability [McMillan (61)], since the relativistic mass increase permits the electron beam to spread only in proportion to the logarithm of the distance traveled down the accelerator. This effect may also be visualized from the coordinate system of the moving electron; for example, since the 220-ft. length of the Stanford 1000-Mev accelerator is Lorentz-contracted to about one foot, while the transverse dimensions of the aperture are not affected, it is easy to get electrons through without having them strike the sides. These factors, together with the virtually complete absence of energy loss by radiation, make the electron linear accelerator the only competitor to the proton synchrotron for the production of particle energies in the several thousand Mev range. Review articles on this type of machine have been published recently [Livingston (1); Fry & Walkinshaw

(2); Slater (8)], and a preliminary description of the Stanford accelerator has been given by Ginzton, Hansen & Kennedy (64).

Two linear accelerators have been constructed at the Microwave Laboratory of Stanford University, and a third is under construction. The first two operate at 6 Mev [Becker & Caswell (65)] and at 35 to 50 Mev [Post (66)], and are past the development stage. The third has produced 200 Mev electrons in microsecond pulses of 10^{11} electrons each, 60 times per sec., with 80 ft. of accelerator in operation. It is now undergoing extension to its final 220 ft. of length, and it is expected that increased power input will then bring the electron energy up to 1000 Mev. This accelerator is of the traveling-wave type, powered with klystrons that give over 10 Mw. peak of 3000 Mc. power, spaced every 10 feet along the wave guide. All klystrons are operated as power amplifiers and are driven by a single coherent source in pulses 1 to 2 μsec. long. A thorough analysis of the electromagnetic fields in the accelerator wave guide and of the electron orbits in these fields [Chu (67)] has among other things yielded information with which an effective buncher has been designed [Neal (68)]. This buncher collects the injected electrons into phases that are very close to the peaks of the rf cycle, and also provides intial focusing. The effect of random constructional errors in reducing the output electron energy has also been calculated [Schiff & Post (69); Post (66)].

Apart from work in the Atomic Energy Research Establishment at Harwell [Fry (70)], no other significant developments seem to have occurred since the latest review article (8) was prepared. In addition to the Harwell accelerators reported on earlier, a 45-Mev machine is now under construction, with a designed peak current of 100 m. amp. A Stanford-type klystron will feed into a 3 m. length that will add 35 Mev to the energy of electrons from a 10-Mev bunching section. Work has also gone forward on the design of dielectric-loaded wave guides for accelerator construction [Harvie (71)], as an alternative to the metal disk-loaded wave guide used at Stanford and most other places. Theoretical studies indicate that at 3000 Mc., the rf power efficiency can be doubled by the use of dielectric rather than metal iris disks. The ceramics considered have been mainly $MgTiO_3$ and TiO_2, of which the latter appears the more promising.

Other Types of Accelerators

In conclusion, mention may be made of some accelerators that do not fit into the nine types discussed above. At the Cavendish Laboratory of the University of Cambridge, an experimental continuously-pumped magnetron is being used to drive an accelerator that consists of a single cylindrical cavity [Wilkinson (72)]. The magnetron has been developed under sponsorship of the Ministry of Supply as part of a project for linear accelerator power sources. It produces several megawatts of 1200 Mc. power in 4 μsec. pulses at a rate of 5 or 10 per sec. Some electrons have been accelerated, and it is hoped that half an ampere peak of 2 Mev electrons will result.

Two electrostatic devices have recently been mentioned as showing considerable promise, although experimental work on both appears to be at an early stage. At Grenoble, Félici & Morel (73) have mounted two rotating variable condensers on a shaft, and used the change in capacity to produce a potential rise when the condensers are initially charged at low potential. Voltages of 200 kv. have been obtained, and a 1-Mv. machine is reported to be under construction. At Mexico City, Malpica (74) is developing an electrostatic direct current transformer. In this device, charge is placed by means of brushes on a number of rotating dielectric disks in parallel, and removed at nearly the same potential by brushes placed at different azimuthal positions on the disks. The discharging brushes can then be connected in series so as to multiply the input voltage. The dielectric disk serves to insulate the primary from the secondary brushes so that the latter can be connected in series while the former are connected in parallel.

The use of a traveling-wave helix for the acceleration of protons is now being seriously considered as a competitor for the proton linear accelerator at Associated Electrical Industries [Chick & Petrie (75)] and at the École Royale Militaire in Brussels [Ledrus, Dutrannois & Goens (76)]. The helix provides a means for reducing the phase velocity of an electromagnetic wave so that it can conveniently be kept in step with the accelerating protons. Focusing presents a serious problem in this type of machine, and the English workers suggest using for this purpose an electron beam that moves in the opposite direction to the proton beam. No experiments have been reported as yet.

LITERATURE CITED

A. Recent Review Articles

1. Livingston, M. S., in *Advances in Electronics*, **1**, 269–316 (Marton, L., Ed., Academic Press, Inc., New York, N. Y., 475 pp., 1948)
2. Fry, D. W., and Walkinshaw, W., *Repts. Progress Phys.*, **12**, 102–32 (1949)
3. Fremlin, J. H., and Gooden, J. S., *Repts. Progress Phys.*, **13**, 295–349 (1950)
4. Pickavance, T. G., in *Progress in Nuclear Physics*, **1**, 1–20 (Frisch, O. R., Ed., Academic Press, Inc., New York, N. Y., 224 pp., 1950); Fortescue, R. L., 21–36
5. Rotblat, J., *The Acceleration of Particles to High Energies*, 1–13 (Institute of Physics, London, England, 58 pp., 1950); Goward, F. K., 14–28; Shire, E. S., 29–40
6. Livingston, M. S., *Ann. Rev. Nuclear Sci.*, **1**, 157–74 (1952)
7. Thomas, J. E., Kraushaar, W. L., and Halpern, I., *Ann. Rev. Nuclear Sci.*, **1**, 175–98 (1952)
8. Slater, J. C., *Ann. Rev. Nuclear Sci.*, **1**, 199–206 (1952)

B. Recent Bibliographies

9. Thomas, E., Mittelman, P., and Goldsmith, H. H., *U. S. Atomic Energy Commission Document, BNL-L-101* (1948)
10. Cushman, B. E., *U. S. Atomic Energy Commission Document, UCRL-1238* (1951)

C. REFERENCES OF CURRENT INTEREST

11. Yenicay, F. E., *Nature*, **167**, 765 (1951)
12. Collie, C. H. (Personal communication)
13. Arnold, W. R., *Rev. Sci. Instruments*, **21**, 796–99 (1950)
14. Woodyard, J. R. (Personal communication)
15. Bergstralh, T. A., Dunning, K. L., Durand, E., Ellison, C. H., Howerton, H. K., and Slavin, W. (In press)
16. Forbes, S. G., Graves, E. R., and Little, R. N. (In press)
17. Alvarez, L. W., *Rev. Sci. Instruments*, **22**, 705–6 (1951)
18. Bennett, W. H., *U. S. Pat. 2,206,558* (July 2, 1940)
19. Willard, H. B. (Personal communication)
20. McKibben, J. L. (Personal communication)
21. Seagondollar, L. W. (Personal communication)
22. Kowarski, L. (Personal communication)
23. Blewett, J. P., *Phys. Rev.*, **81**, 305 (1951); (Personal communication)
24. Robinson, D. M., McIntosh, L. R., and Nygard, J. C., *Phys. Rev.*, **83**, 233 (1951); Robinson, D. M. (Personal communication)
25. McKibben, J. L., and Boyer, K., *Phys Rev.*, **82**, 315 (1951)
26. Morand, M., and Raskin, A., *Compt. rend.*, **209**, 297 (1939); Winand, L. (Personal communication)
27. Livingston, R. S. (Personal communication)
28. Livingood, J. J. (Personal communication)
29. Atterling, H., and Lindström, G., *Nature*, **169**, 432–34 (1952)
30. Donnelly, F. K., Engebretson, H. J., Henderson, J. E., Morgan, T. J., Schmidt, F. H., and Streib, J. F., *Phys. Rev.*, **85**, 767 (1952); Schmidt, F. H. (Personal communication)
31. Cottingham, J. G., Glasoe, G. W., Green, G. K., and Lasky, C., *U. S. Atomic Energy Commission Document, BNL Quart. Rept. on Accelerators* (July 1 to September 30, 1951)
32. Heyn, F., *Philips Technical Rev.*, **12**, 241–56, 349–64 (1951)
33. Knox, W. J., *Phys. Rev.*, **81**, 693–97 (1951)
34. Cassels, J. M., Dickson, J. M., and Howlett, J., *Proc. Phys. Soc.* (*London*), [B]**64**, 590–94 (1951)
35. Foss, M. H., *Carnegie Inst. Technol., NYO-911* (1951)
36. Riddiford, L., *Proc. Phys. Soc.* (*London*), [B]**64**, 218–24 (1951)
37. MacKenzie, K. R., *Rev. Sci. Instruments*, **22**, 302–9 (1951)
38. Moore, M. J. (Personal communication)
39. Tuck, J. L., and Teng, L. C., *Phys. Rev.*, **81**, 305 (1951); *Inst. Nuclear Studies, Univ. of Chicago. Synchrocyclotron Prog. Rept. III*, Chap. 8 (1950)
40. Le Couteur, K. J., *Proc. Phys. Soc.* (*London*), [B]**64**, 1073–84 (1951)
41. Anderson, H. L. (Personal communication)
42. Barden, S. E., *Proc. Phys. Soc.* (*London*), [B]**64**, 579–90 (1951)
43. Gregg, E. C., *Case Inst. Technol., 1082* (1951)
44. Davis, L., *Rev. Sci. Instruments*, **21**, 971–72 (1950)
45. Katz, L., McNamara, A. G., Forsyth, P. A., Haslam, R. N. H., and Johns, H. E., *Can. J. Research*, **28**, 113–19 (1950)
46. Montalbetti, R. (In press)
47. Becker, R. A., *Rev. Sci. Instruments*, **22**, 773–76 (1951)
48. McMillan, E. M., *Rev. Sci. Instruments*, **22**, 117 (1951)

49. Schiff, L. I., *Phys. Rev.*, **83,** 252–53 (1951)
50. Gauer, G., and Nunan, C., *U. S. Atomic Energy Commission Document, UCRL-714* (1950)
51. Kerst, D. W. (Personal communication)
52. Pollock, H. C., Hebb, M. H., and Noble, P. C., *General Electric Research Lab., RL-546* (1951)
53. Foote, R. S., *Nat. Bur. Standards, 1001* (1951)
54. Parzen, G., *Phys. Rev.*, **84,** 235–39 (1951)
55. Judd, D. L., Lepore, J. V., Ruderman, M., and Wolff, P., *Phys. Rev.* (In press)
56. Schiff, L. I., *Am. J. Phys.* (In press)
57. Wideröe, R., Waldvogel, P., von Arx, A., Joyet, G., Mauderli, W., Fritz-Niggli, H. and Wäffler, H., *Brown Boveri Mitteilungen*, **38,** 259–310 (1951)
58. *Office of Naval Research (London), ONRL-48-50* (April 20, 1950)
59. Lawson, J. L. (Personal communication)
60. Alvarez, L. W., Bradner, H., Gordon, H., Panofsky, W. K. H., Richman, C., and Woodyard, J. R., *U. S. Atomic Energy Commission Document, AECU-120* (1948)
61. McMillan, E. M., *Phys. Rev.*, **80,** 493 (1950)
62. Panofsky, W. K. H., *U. S. Atomic Energy Commission Document, UCRL-1216* (1951)
63. Williams, J. H. (Personal communication)
64. Ginzton, E. L., Hansen, W. W., and Kennedy, W. R., *Rev. Sci. Instruments*, **19,** 89–108 (1948)
65. Becker, G. E., and Caswell, D. A., *Rev. Sci. Instruments*, **22,** 402–5 (1951)
66. Post, R. F., *A 50 Mev Linear Electron Accelerator* (Doctoral thesis, Stanford University, Stanford, Calif., 1950)
67. Chu, E. L., *Stanford Univ. Microwave Lab. Rept., 140* (1951)
68. Neal, R. B., *Stanford Univ. Microwave Lab. Rept., 136* (1951)
69. Schiff, L. I., and Post, R. F., *Phys. Rev.*, **81,** 655 (1951)
70. Fry, D. W. (Personal communication)
71. Harvie, R. B. R. S., *Atomic Energy Research Establishment (British) EL/R 402* (1949)
72. Wilkinson, D. H. (Personal communication)
73. Félici, N. J., and Morel, R., in *Office of Naval Research (London), ONRL-61-50* (June 26, 1950)
74. Malpica, J. M., *Rev. Sci. Instruments*, **22,** 364–69 (1951)
75. Chick, D. R., and Petrie, D. P. R., *Nature*, **168,** 782–83 (1951)
76. Ledrus, R., Dutrannois, J., and Goens, J. (Personal communication)

NUCLEAR REACTIONS INDUCED BY HIGH ENERGY PARTICLES[1]

By David H. Templeton

Department of Chemistry and Radiation Laboratory, University of California, Berkeley, California

Since 1946 machines have been available which will accelerate charged particles to energies in excess of a 100 Mev. These high energy particles, when they strike the nuclei of a target, induce many kinds of nuclear transmutations not possible with particles of lower energy. The products resulting from, and the nature of, these transmutations have been studied by radiochemical methods in several laboratories, especially at Berkeley with the 184-in. synchrocyclotron.

Many studies also have been made of nuclear reactions ("stars") induced by high energy particles, especially from the cosmic rays, by means of nuclear research emulsions and cloud chambers. This work has been reviewed

TABLE I

Low Energy Reaction Types

Projectile	Reactions
neutron	(n, γ), $(n, 2n)$, (n, p), (n, α)
proton	(p, n), $(p, 2n)$, (p, α)
deuteron	(d, n), $(d, 2n)$, $(d, 3n)$, (d, p)
helium ion	(α, n), $(\alpha, 2n)$, $(\alpha, 3n)$

recently in considerable detail by Rochester & Rosser (1) and by Adams (2). The data published are concerned mostly with the numbers of charged particles emitted in single events and the distributions in charge, mass, energy, and angle of these particles. Relatively little is known about the numbers of neutrons emitted, the identity of the heavy residue, or, in many cases, even of the identities of the target nucleus and projectile. On the other hand, in the radiochemical method the identities of the target, projectile, and final residue can be known, but the states of aggregation and energies of the small fragments must be inferred. Thus, the two methods should be complementary. Unfortunately, no data of both kinds are yet available for strictly comparable conditions. However, many conclusions reached independently by the two methods are in agreement, and there is no point of conflict apparent in the results. This review is concerned principally with the radiochemical investigations.

Previous transmutations induced with low energy particles in most cases changed each nucleus by adding or removing three nucleons or less. Some of

[1] The survey of the literature pertaining to this review was concluded in April, 1952.

the more common reactions are listed in Table I. In this representation of a reaction, the first symbol within each pair of parentheses identifies the projectile, and the subsequent symbols list all products except the heavy residue. The fission of heavy nuclei is the one important exception to the above generalization; in fission each nucleus usually is split into two heavy fragments plus a few neutrons and there results the complicated mixture of isotopes called the fission products.

Spallation

When a high energy nucleon strikes a nucleus, it may be absorbed to form a very highly excited compound nucleus, More likely. it will collide with one or more nucleons and then escape with a considerable fraction of its original kinetic energy. It may or may not exchange its charge in this process. Thus, there results in a target a wide range of degrees of excitation of nuclei.

Most of these nuclei are excited to energies far in excess of the binding energies of individual nucleons. If no other process intervenes, nucleons or small groups of nucleons, such as α-particles or lithium nuclei, will escape until the residue is left in a relatively stable condition. Reactions fitting this description are described by the term "spallation." All of the reactions in Table I except the (n,γ) are examples of spallation. At energies of 100 Mev or more a dozen or so nucleons may escape, and many combinations of neutrons and protons may be important. Thus many nuclides are produced in a single bombardment, in contrast to the relatively simple situation for low-energy spallation. When the projectile is a deuteron or α-particle, one or more of its nucleons may interact with the target nucleus, but the result is qualitatively the same as that described above.

Spallation has been studied in several cases by the comparison of the yields of many radioactivities produced in a target of a pure element when irradiated with particles of a particular kind and energy. One observes, of course, only those radioactivities of suitable half-life. Some of these are "shielded" by stable or long-lived isobars so that their independent yields can be measured. In other cases, one measures the yield of a nuclide together with the yields of short-lived progenitors.

Throughout this work it has been found that the independent yields in a particular irradiation are reasonably smooth functions of the neutron number N and atomic number Z of the product. On this basis one frequently can estimate what part of the gross yield of an activity is to be assigned as the independent yield.

The results of Hopkins (3) for the irradiation of arsenic ($Z=33$) with 190-Mev deuterons are a case where independent yields have been measured in many cases and can be estimated reasonably well in others. These data are represented in Figure 1 as a contour map on a plot of N and Z of the products. Each contour represents a factor of ten in independent yield on an arbitrary scale. Circles represent nuclides whose yields were measured,

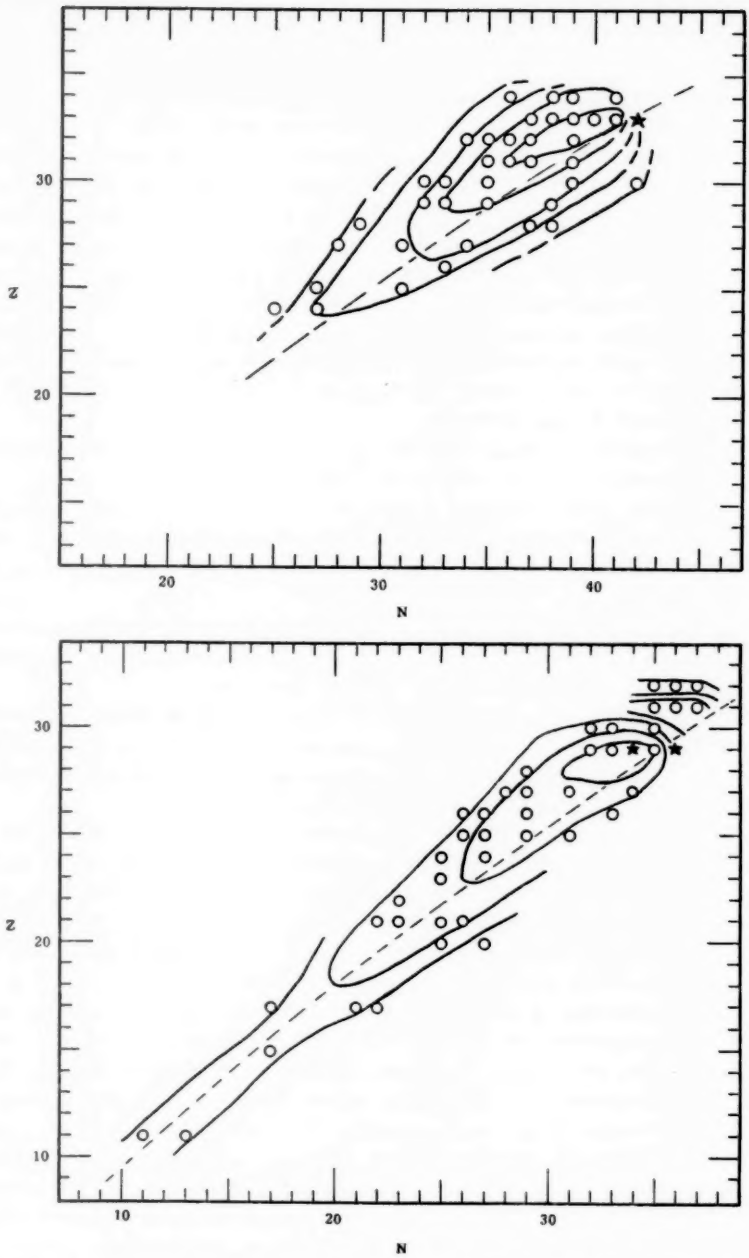

FIG. 1. (Upper) Yields of nuclides from arsenic plus 190-Mev deuterons, constructed from data of Hopkins (3).

FIG. 2. (Lower) Yields from copper plus 340-Mev protons, from data of Batzel, Miller & Seaborg (4).

and the dashed line approximates the center of the stable isotopes of each element. The star represents the target nucleus. If the stable isotopes are formed independently in amounts corresponding to these curves, they amount to about one-fourth of the total spallation yield in this case.

It is clear in this plot that the most probable reactions are those in which both neutrons and protons are ejected, in approximately the ratio two neutrons for each proton. The highest yields correspond to the ejection of three to seven nucleons. The reactions involving the emission of 20 or more nucleons are lower by a factor of about 1000 or more. The preponderance of reactions with relatively modest energy requirements is due in part to the absorption by the nucleus of only part of the available energy, as described above, and in part to the escape of fragments with energies far greater than that required to just surmount the nuclear potential barrier. More will be said later about the second effect.

Figure 2 shows a similar plot of the data of Batzel, Miller & Seaborg (4) for the spallation of copper ($Z=29$) with 340-Mev protons. The increased energy permits more extensive reactions, and the contours are elongated along the line of stable nuclides. Otherwise, the trends are much the same. The small yields of germanium and gallium indicated in the figure are explained by secondary reactions to be described in a later section of this review. In both these sets of data the most probable result of extensive spallation is a product very near the line of stable nuclides. Modes spallation tends to produce slightly neutron-deficient isotopes.

Zinc ($Z=30$) was irradiated with 340-Mev protons by Worthington (5). His yields of spallation products are represented in Figure 3. If one allows for the shift in target nuclides and the greater spread in their mass numbers, the curves match those for copper spallation quite well.

These experiments and others show that the character of spallation reactions depends very little on the identity of the target, except for certain regular trends with respect to atomic number. The most striking of these trends is the relatively greater difficulty of escape of protons or other charged fragments from the heavier nuclei because of the increased coulombic potential barrier. This effect is perceptible in the data of Lindner & Perlman (6) for the spallation of antimony ($Z=51$). Figure 4 is based on their data for 190-Mev deuterons. At bismuth ($Z=83$) the effect is so striking that the products which have been found are almost all neutron deficient. There are no extensive sets of relative yield values at hand for this region, because these products are largely radioactivities previously unknown and a considerable program of characterization of these nuclides was first required (7 to 12). Absolute counting of these radioactivities in many cases involves estimation of counting efficiencies for electron capture via complicated and unknown decay schemes. Much work of this sort remains to be done.

Nuclear reactions occurring at low energies (<40 Mev), are adequately explained in terms of Bohr's theory of the compound nucleus (13). A characteristic of such reactions is that the yield as a function of energy exhibits

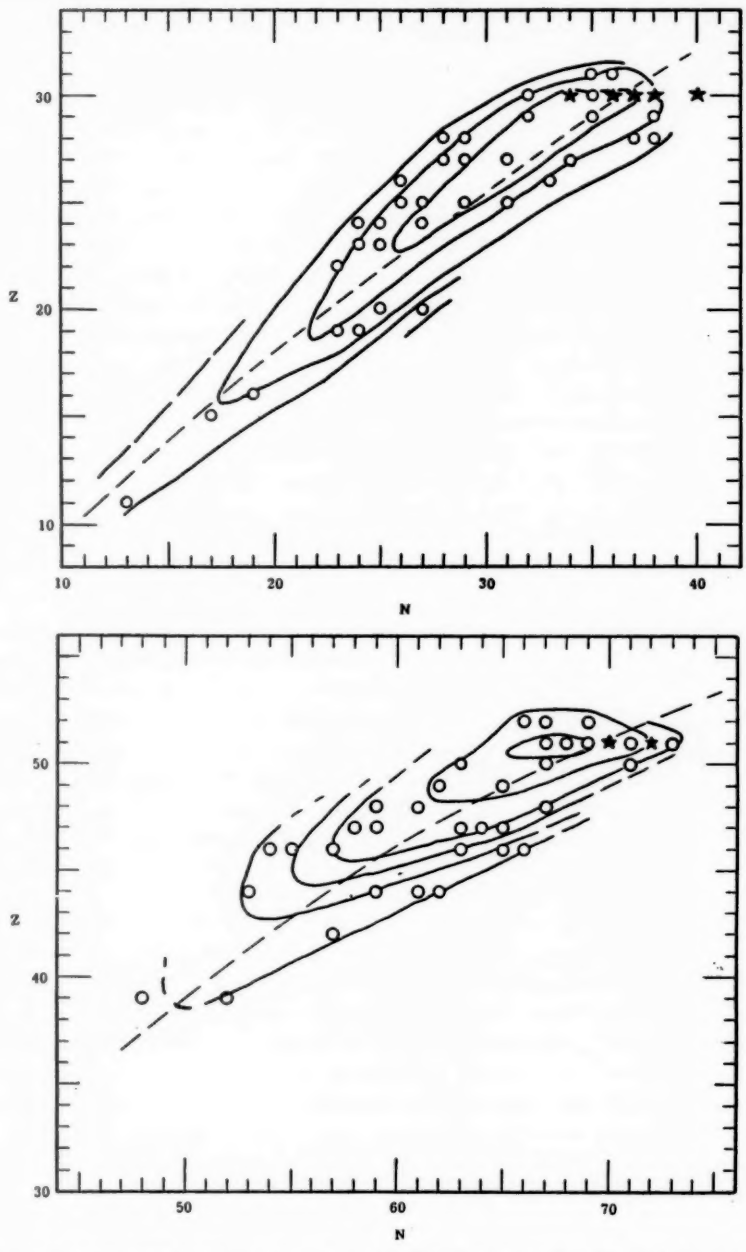

FIG. 3. (Upper) Yields from zinc plus 340-Mev protons, after Worthington (5).
FIG. 4. (Lower) Yields from antimony plus 190-Mev deuterons, from data of Lindner & Perlman (6).

a maximum within a few million electron volts of the threshold and then falls abruptly because of competition by reactions involving loss of additional particles. This behavior is exhibited by (p, xn) reactions up to very high energies. For example, Karraker (14) found a sharp maximum at 90 Mev for the yield of the reaction Bi^{209} (p, 8n)Po^{202}. Such reactions can take place only by capture of the incident proton or by charge exchange. The former mechanism accounts for the peak on yield, and the latter probably is principally responsible for the (much smaller) yield at higher energies. Certain other reactions which can take place without capture of the incident particle are seen to be much more probable in Figures 1 to 4. Typical excitation functions for reactions with such "hit-and-run" mechanisms increase monotonically with energy, or exhibit very broad maxima. Actual excitation curves frequently show combinations of both types of behavior; for example, the curve of Bartell & Softky (15) for $Mg^{24}(d, 2\alpha)F^{18}$ shows a very clear maximum at about 20 Mev for a compound nucleus mechanism, and a broad plateau above 100 Mev for the "hit-and-run" mechanism. Other examples have been published by Thornton & Senseman (16), Chupp & McMillan (17), Meadows & Holt (18, 19), Hintz (20), and Dickson & Randle (21).

Serber (22) has described these reactions in terms of interactions of the incident nucleons with individual nucleons of the target nucleus. He estimated for a 100-Mev nucleon an average energy transfer per collision of 25 Mev and a mean free path of 4×10^{-13} cm. Since the struck particles have a shorter mean free path than the incident one, they will usually distribute their energy to other nucleons through collisions, but it is possible that these struck nucleons can escape from the nucleus with little or no energy loss. The subsequent behavior of the excited nucleus is described by the evaporation model, with the excitation energy dissipated by boiling off particles each with kinetic energies of a few million electron volts. Numerical estimates of the probabilities of various events have been made for Serber's model by Goldberger (23) by a Monte Carlo method.

According to Batzel, Miller & Seaborg (4), the average energy loss for 340-Mev protons is about 70 Mev per collision in a copper nucleus, based on $n-p$ and $p-p$ scattering experiments (24, 25), and the mean free path is still about 4×10^{-13} cm. (26). This greater energy transfer is necessary to account for the much greater extent of spallation observed at the higher energy, for otherwise it would be unlikely that the maximum energy would be transferred in very many events. According to Serber's model (22), some incident particles should pass through the nucleus without any effect. For copper, the transparency makes the total reaction cross section calculated from the above data about 20 per cent less than the geometrical cross section of about one barn. The total cross section obtained by summation of the individual observed and estimated yields (4) is about 30 per cent less than the geometrical one. The agreement is probably as good as the accuracy of the yield estimations. This nuclear transparency is also evident in the total cross sections of the elements measured by attenuation of a beam of 90-Mev

neutrons by Cook, McMillan, Peterson & Sewell (27). There is no clear indication of nuclear transparency in the data for interaction mean free paths of the nucleonic and nuclear components of cosmic rays (1), but these data refer to spectra including particles of much higher energy and also are not in complete agreement with each other.

The clustering of the products along the line of stability, which is especially evident in Figures 2 and 3, is in disagreement with the spread to be expected if most of the particles leave by a random evaporation of neutrons and protons. Such clustering would result, however, if the particle most likely to be emitted at a particular time is strongly dependent on the relative binding energies of neutrons and protons at that instant. Thus, if several neutrons have been emitted, proton emission would be strongly favored, and vice versa. Another explanation is that a local "hot spot" is formed which largely evaporates before much energy is spread to other parts of the nucleus, so that the material lost is similar in composition to the original nucleus. A third mechanism which contributes to this effect and which may, indeed, explain it almost completely is the evaporation of deuterons, α-particles, and other small nuclei containing comparable numbers of neutrons and protons. It is known that such particles escape in significant number. In these cases of extreme reactions which are energetically possible only because of the economy resulting from the binding energy of composite particles, obviously, such particles are emitted in every event.

According to Page (28), 27 per cent of the charged particles from cosmic ray stars of more than six prongs are helium ions, which is in reasonable agreement with similar estimations of Addario & Tamburino (29, 30) and of Perkins (31). These stars presumably are disintegrations of silver and bromine nuclei in the nuclear research emulsion. Smaller stars have an even higher percentage of α-particles, as a result of contributions from carbon and oxygen in the emulsion. The extensive theoretical treatment by LeCouteur (32) of nuclear evaporation in terms of a Fermi gas model gives results in excellent agreement with these experimental results, as do the calculations of Yamaguchi (33). Crude statistical estimates by the author indicate that this many α-particles, together with lesser numbers of deuterons and tritons which are also emitted, are of the right order of magnitude to explain the clustering in the spallation yield curves. The idea of a hot spot with local evaporation has been advanced by Harding, Lattimore & Perkins (34, 35) in connection with very high energy events, but is considered unlikely by Fujimoto & Yamaguchi (36).

In drawing the contours of yield we have ignored certain irregularities which are not very important when one is considering factors of 10 in yield. Even-odd alternations in binding energy should result in correspondingly small alternations of yield. Somewhat larger fluctuations have been pointed out, however, and are cited as evidence for the preference for emission of α-particles. Fluctuations noted by Bonner & Orr (37) in the yields of Mn^{52} and Mn^{56} from a series of targets from chromium ($Z=24$) to strontium

($Z = 38$) were suggested to be due to this effect. Bartell, Helmholz, Softky & Stewart (38) and Batzel, Miller, & Seaborg (4) have made similar suggestions. However, these data perhaps are not sufficiently extensive to rule out other causes for the irregularities.

Other radiochemical studies of spallation yields from high-energy particles have been reported by Miller & Friedlander (39), Greenberg & Miller (40), and Knox (41). Pioneer work on spallation induced by high-energy photons has been done by Baldwin & Klaiber (42, 43, 44), and Perlman *et al.* (45 to 48). The most extensive sets of yield data for spallations of a single nuclide by photons are those of Sugarman & Peters (49) for bismuth with photon spectra of 48- and 86-Mev maximum energies. Spallation of as many as 10 nucleons was observed in the latter case. Relative yields for three tantalum activities produced from tungsten by photons of maximum energy 68 Mev have been reported by Moses & Martin (50).

Stars in nuclear research emulsions caused by particles accelerated artificially have been studied by Gardner & Peterson (51, 52), Bernardini, Booth & Lindenbaum (53), Titterton (54), Miller (55), Germain (56), and Fishman & Perry (57). The relation of these results to those for stars induced by cosmic rays were discussed by Bernardini, Cortini & Manfredini (58). Precise comparison with the radiochemical results described previously is impossible. One can say that the sharp decrease in frequency of stars as a function of number of prongs is in agreement with the decrease of spallation yield as a function of the number of particles removed. The facts that the highest spallation yields are removed from the target nucleus by no more than one charge and that the maxima in the star distributions occur at three prongs indicate either that the number of one and two prong stars is underestimated or that the light elements in the emulsion have enough effect to shift the maximum.

Direct mass spectrometric investigations of the spallation products would avoid the uncertainties of absolute counting and would extend the measurements to many stable and long-lived products. Present techniques of this kind seem to be not quite adequate for observation of the products from bombardments of reasonable duration, but it is hoped that such measurements may be possible in the future, either by improved technique or with bombardments of greater intensity and duration.

Fission

Perlman and co-workers (59) observed fission when elements of Z greater than 72 were irradiated with high-energy particles. This fission is evidenced by a group of products formed in considerable yield centered about a mass somewhat less than half that of the target nucleus, and separated from the region of spallation yields by a region of very low yields. The dividing line is not sharp, and in the case of uranium, at least, the spallation and fission product regions overlap (60). High-energy fission is more likely to be symmetrical than unsymmetrical, in contrast to the marked asymmetry of low-

energy fission. The distribution of yields from fission of bismuth has been studied in some detail by Goeckermann & Perlman (61). The distribution is much different from that resulting from fission induced by low energies, and the products of high-energy fission extend over a greater range of masses and to nuclides more deficient in neutrons. Goeckermann & Perlman have explained the observed yields from fission of bismuth by 190-Mev deuterons very well by a description of the fission mechanism. In simplified form, this mechanism is as follows: The compound nucleus (or excited nucleus, if the incident particle is not captured) undergoes spallation; because of the coulomb potential barrier, neutron emission is most likely. In a case where about 10 neutrons escape, the residual nucleus is sufficiently unstable toward fission that fission competes favorably with spallation. The fission must occur rapidly, allowing no time for a redistribution of the protons and neutrons, otherwise, further spallation dissipates the excitation energy. This mechanism explains the observed fact that the primary products have ratios of protons to neutrons approximately equal to that of Po^{200} and that the average mass of products is about 100 mass units. There is no generally accepted explanation for the symmetry of fast fission compared to the asymmetry of slow fission, though numerous explanations have been proposed (62, 63).

This fission of bismuth and neighboring elements was also demonstrated by ionization measurements of the fission recoil fragments by Kelly & Wiegand (64). Jungerman & Wright (65) showed that the ionization caused by these fission fragments corresponds reasonably well with that expected from the coulomb repulsion of the fragments. Yamaguchi (66) has given theoretical support to the idea that fission will be more probable than spallation after 12 neutrons have been lost from bismuth. Fission of bismuth by high energy photons is indicated by radiochemical identification of fission products by Sugarman (67).

It has been mentioned in the previous section that the extreme products of spallation may be formed only when composite particles, such as α-particles, are ejected, because the energy balance is unfavorable for removal of an equal number of individual protons and neutrons. By studying the yields of such products at reduced bombardment energies, Batzel & Seaborg (68) showed that some products are observed in copper, bromine, silver, and tin targets at bombardment energies too low even to be explained by α-particle emission. Such cases probably are most properly described by the term "fission." An example is:

$$Br^{79} + p \rightarrow Sc^{44} + P^{34} + 2n.$$

The yields of these reactions are very low under the conditions where such deductions are possible. These reactions are quite different, experimentally, from the fission of elements above tantalum in that the "fission" products are not clearly separated from the spallation products, and at the highest energies studied probably many products are produced by both mechanisms and indeed by all degrees of intermediate mechanisms.

Throughout this work it has been the rule that any reaction which is possible energetically takes place with some yield. Thus it is not surprising that the products from spallation and "fission" of an element like copper seem to extend continuously to the lightest elements (4, 40, 68 to 70). Experiments in the region of very low yields from carbon to phosphorus are plagued by effects of trace impurities in the targets which make the yields somewhat uncertain and which perhaps explain the discrepancies between some of the numerical results.

Secondary Reactions

A complication of the study of high-energy reactions is that the small fragments produced by spallation may have enough kinetic energy themselves to induce transmutations. The yields from these secondary reactions are small, but they seem to be quite common. They are distinguishable from primary reactions in those cases where the product has a charge or mass greater than is possible for a primary reaction. Bonner and co-workers (71) explained abnormal products in photon irradiated targets as due to secondary neutrons and protons. Deuterons on Bi^{209} produce At^{211} by the mechanism (72, 73)

$$Bi^{209} + d \rightarrow He^4 + \text{other products}$$
$$He^4 + Bi^{209} \rightarrow At^{211} + 2n.$$

Protons on lead produce the same astatine by the action of secondary lithium nuclei:

$$Pb^{208} + p \rightarrow Li^7 + \text{other products}$$
$$Li^7 + Pb^{208} \rightarrow At^{211} + 4n.$$

Marquez & Perlman (70) made an extensive study of such reactions. They concluded that to account for the observed yields, it is necessary to postulate that secondary α-particles and lithium nuclei escape with energies considerably greater than seems reasonable on the nuclear evaporation model. That individual neutrons or protons are ejected with very high energy can be explained by direct collisions of the incident particle, but nuclear theory is not adequate to explain how so much energy is suddenly transferred to six or seven nucleons in such a way that they escape as a lithium nucleus. Perkins (35) and Sörensen (74) have recently published evidence that, in cosmic ray stars, fragments with charges up to 10 units are emitted with energies in excess of those that would result from coulombic repulsion. They have suggested that some long-range nuclear force may be the explanation. Other examples of secondary reactions have been noted by Batzel, Miller & Seaborg (4) and are indicated in Figure 2, and by Wagner & Wiig (75).

LITERATURE CITED

1. Rochester, G. D., and Rosser, W. G. V., *Repts. Progress Phys.*, **14,** 227–87 (1951)
2. Adams, R. V., *Ann. Rev. Nuclear Sci.*, **1,** 107–36 (1952)
3. Hopkins, H. H., Jr., *Phys. Rev.*, **77,** 717–18 (1950)
4. Batzel, R. E., Miller, D. R., and Seaborg, G. T., *Phys. Rev.*, **84,** 671–83 (1951)
5. Worthington, W. J., Jr., *High Energy Spallation Products of Zinc*, 57 (Master of Science Thesis, Univ. of California, Berkeley, Calif., 58 pp., 1952)
6. Lindner, M., and Perlman, I., *Phys. Rev.*, **78,** 499–508 (1950)
7. Templeton, D. H., and Perlman, I., *Phys. Rev.*, **73,** 1211 (1948)
8. Neumann, H. M., and Perlman, I., *Phys. Rev.*, **78,** 191–98 (1950)
9. Karraker, D. G., and Templeton, D. H., *Phys. Rev.*, **81,** 510–16 (1951)
10. Barton, G. W., Ghiorso, A., and Perlman, I., *Phys. Rev.*, **82,** 13–19 (1951)
11. Karraker, D. G., Ghiorso, A., and Templeton, D. H., *Phys. Rev.*, **83,** 390–93 (1951)
12. Moon, J. H., and Thompson, A. L., *Phys. Rev.*, **83,** 892 (1951)
13. Bohr, N., *Nature*, **137,** 344–48 (1936)
14. Karraker, D. G., *U. S. Atomic Energy Commission Document, UCRL-1202* (1951)
15. Bartell, F. O., and Softky, S., *Phys. Rev.*, **84,** 463–65 (1951)
16. Thornton, R. L., and Senseman, R. W., *Phys. Rev.*, **72,** 872–73 (1947)
17. Chupp, W. W., and McMillan, E. M., *Phys. Rev.*, **72,** 873–74 (1947)
18. Meadows, J. W., and Holt, R. B., *Phys. Rev.*, **83,** 47–49 (1951)
19. Meadows, J. W., and Holt, R. B., *Phys. Rev.*, **83,** 1257 (1951)
20. Hintz, N. M., *Phys. Rev.*, **83,** 185–86 (1951)
21. Dickson, J. M., and Randle, T. C., *Proc. Phys. Soc.* (*London*), [A]**64,** 902–5 (1951)
22. Serber, R., *Phys. Rev.*, **72,** 1114–15 (1947)
23. Goldberger, M. L., *Phys. Rev.*, **74,** 1269–77 (1948)
24. Chamberlain, O., and Wiegand, C., *Phys. Rev.*, **79,** 81–85 (1950)
25. Kelly, E., Leith, C., Segrè, E., and Wiegand, C., *Phys. Rev.*, **79,** 96–98 (1950)
26. Fernbach, S. (Personal communication to G. T. Seaborg)
27. Cook, L. J., McMillan, E. M., Peterson, J. M., and Sewell, D. C., *Phys. Rev.*, **75,** 7–14 (1949)
28. Page, N., *Proc. Phys. Soc.* (*London*), [A]**63,** 250–58 (1950)
29. Addario, M. M., and Tamburino, S., *Phys. Rev.*, **80,** 749–50 (1950)
30. Addario, M. M., and Tamburino, S., *Nuovo Cim.*, **8,** 82–95 (1951)
31. Perkins, D. H., *Phil. Mag.*, **41,** 138–43 (1950)
32. LeCouteur, K. J., *Proc. Phys. Soc.* (*London*), [A]**63,** 259–82 (1950)
33. Yamaguchi, Y., *Progress Theoret. Phys.* (*Japan*), **5,** 142–43 (1950)
34. Harding, J. B., Lattimore, S., and Perkins, D. H., *Proc. Roy. Soc.* (*London*), [A]**196,** 325–43 (1949)
35. Perkins, D. H., *Proc. Roy. Soc.* (*London*), [A]**203,** 399–417 (1950)
36. Fujimoto, Y., and Yamaguchi, Y., *Prog. Theor. Phys.* (*Japan*), **5,** 76–81 (1950)
37. Bonner, N. A., and Orr, W. C., *Phys. Rev.*, **76,** 140–41 (1949)
38. Bartell, F. O., Helmholz, A. C., Softky, S. D., and Stewart, D. B., *Phys. Rev.*, **80,** 1006–10 (1950)
39. Miller, J. M., and Friedlander, G., *Phys. Rev.*, **84,** 589 (1951)
40. Greenberg, D. H., and Miller, J. M., *Phys. Rev.*, **84,** 845–46 (1951)
41. Knox, W. J., *Phys. Rev.*, **75,** 537–41 (1949)
42. Baldwin, G. C., and Klaiber, G. S., *Phys. Rev.*, **70,** 259–70 (1946)

43. Baldwin, G. C., and Klaiber, G. S., *Phys. Rev.*, **71**, 3–10 (1947)
44. Baldwin, G. C., and Klaiber, G. S., *Phys. Rev.*, **73**, 1156–63 (1948)
45. Perlman, M. L., and Friedlander, G., *Phys. Rev.*, **72**, 1272 (1947)
46. Perlman, M. L., and Friedlander, G., *Phys. Rev.*, **74**, 442–48 (1948)
47. Lawson, J. L., and Perlman, M. L., *Phys. Rev.*, **74**, 1190–91 (1948)
48. Perlman, M. L., *Phys. Rev.*, **75**, 988–89 (1949)
49. Sugarman, N., and Peters, R., *Phys. Rev.*, **81**, 951–2 (1951)
50. Moses, A. J., and Martin, D. S., *Phys. Rev.*, **84**, 366–7 (1951)
51. Gardner, E., and Peterson, V., *Phys. Rev.*, **75**, 364–69 (1949)
52. Gardner, E., *Phys. Rev.*, **75**, 379–82 (1949)
53. Bernardini, G., Booth, E. T., and Lindenbaum, S. J., *Phys. Rev.*, **80**, 905 (1950); **83**, 669–71 (1951)
54. Titterton, E. W., *Phil. Mag.*, **42**, 109–12 (1951)
55. Miller, J. F., *Phys. Rev.*, **83**, 1261–62 (1951)
56. Germain, L. S., *Phys. Rev.*, **82**, 596–97 (1951)
57. Fishman, H., and Perry, A. M., *Phys. Rev.*, **86**, 167–70 (1952)
58. Bernardini, G., Cortini, G., and Manfredini, A., *Phys. Rev.*, **79**, 952–63 (1950)
59. Perlman, I., Goeckermann, R. H., Templeton, D. H., and Howland, J. J., *Phys. Rev.*, **72**, 352 (1947)
60. O'Connor, P. R., and Seaborg, G. T., *Phys. Rev.*, **74**, 1189–90 (1948)
61. Goeckermann, R. H., and Perlman, I., *Phys. Rev.*, **76**, 628–37 (1949)
62. Seaborg, G. T., and Templeton, D. H., *Ann. Rev. Phys. Chem.*, **2**, 88 (1951)
63. Swiatecki, W. J., *Phys. Rev.*, **83**, 178–79 (1951)
64. Kelly, E. L., and Wiegand, C., *Phys. Rev.*, **73**, 1135–39 (1948)
65. Jungerman, J., and Wright, S. C., *Phys. Rev.*, **76**, 1112–16 (1949)
66. Yamaguchi, Y., *Progress Theoret. Phys. (Japan)*, **5**, 143–4 (1950)
67. Sugarman, N., *Phys. Rev.*, **79**, 532–3 (1950)
68. Batzel, R. E., and Seaborg, G. T., *Phys. Rev.*, **79**, 528 (1950)
69. Wright, S. C., *Phys. Rev.*, **79**, 838–45 (1950)
70. Marquez, L., and Perlman, I., *Phys. Rev.*, **81**, 953–57 (1951)
71. Bonner, N. A., Friedlander, G., Pepkowitz, L. P., and Perlman, M. L., *Phys. Rev.*, 511–20 (1947)
72. Templeton, D. H., *Artificial Radioactive Isotopes of Polonium, Bismuth, and Lead*, 43–47 (Doctoral thesis, Univ. of California, Berkeley, Calif., 53 pp., 1947)
73. Templeton, D. H., and Perlman, I., *Abstracts Am. Chem. Soc., 114th Meeting*, 55 (Portland, Ore., September 13–17, 1948)
74. Sörensen, S. O. C., *Phil. Mag.*, **42**, 188–201 (1951)
75. Wagner, G., and Wiig, E. O., *J. Am. Chem. Soc.*, **74**, 1101–3 (1952)

RECENT STUDIES OF PHOTONUCLEAR REACTIONS[1]

By Karl Strauch

Department of Physics, Harvard University, Cambridge, Massachusetts

INTRODUCTION

Following the first photodisintegrations of deuterium (1) and beryllium (2) with γ-rays emitted by naturally occurring radioactive elements, experimental and theoretical investigations of photonuclear reactions have progressed steadily. The recent development of artificial sources of high-energy x-rays such as betatrons and synchrotrons have resulted in a very much increased and broadened interest in this field, so that today a large number of groups are active in investigating the interaction of photons with nuclei. The year 1951 has been very fruitful both from an experimental and theoretical point of view in developing a basis for the understanding of the processes involved, although this basis is still quite incomplete and a large amount of future work is required. This report attempts to summarize some of these recent investigations and to examine the results with respect to the various models that have been proposed for the mechanism of photonuclear reactions. The term "photonuclear reactions" refers here to any photon initiated nuclear transformation in which either one or many γ-rays, neutrons, protons, or aggregates of nucleons are emitted. Thus photomeson production is not included, except where it appears to play a role in the mechanism of reactions under study. The photodisintegration of deuterium and helium is left out, since this topic more properly belongs to the subject of interaction of elementary particles.

Some of the more recent experiments are based on new methods developed to use to best advantage the type of photon source available. These methods will be reviewed first. The theoretical and experimental investigations usually fall into one of two photon energy regions: (*a*) the low-energy region which includes the main dipole photon absorption; (*b*) the high-energy region which extends beyond the meson production threshold. These two regions will be considered in turn. Since no general review article covering our subject has appeared so far, it was sometimes found necessary to briefly summarize some of the older work on which the more recent developments are based.

NEW TECHNIQUES FOR THE MEASUREMENT OF REACTION ENERGIES

Introduction

The majority of experiments concerned with photonuclear reactions are carried out with *bremsstrahlung* emitted by artificially accelerated electrons. The continuous energy distribution of this type of photon source requires

[1] The survey of the literature pertaining to this review was concluded in February, 1952.

the use of special techniques to measure the energy of the photons responsible for a given process and to obtain the corresponding cross section. Different methods for the energy determination have been developed recently the applicability of which depends on whether the maximum beam energy E_0 is of the order, or much larger than, the photon energy E_e effective in a reaction. At first glance such a division seems unnecessary, but synchrotrons designed for 300 Mev do not operate very efficiently below about 50 Mev, where many of the important reactions are found. In addition, the techniques available differ with respect to the number of bombardments which are required to determine the photon energies: in general, the larger the number of bombardments, the more detailed is the information obtained.

Multiple Bombardment Methods

These methods involve the measurement of the yield of the process under study as a function of the maximum beam energy E_0 and the irradiation dose as measured by a beam monitor. From these data a plot of the yield as a function of E_0 can be drawn; this is the yield or activity curve. The cross section as a function of energy can then be reconstructed from the yield curve, the *bremsstrahlung* spectrum, and the energy response of the monitor. Such calculations are quite laborious and the results depend on the detailed shape of the yield curve drawn through the experimental points.

Two methods have been suggested recently to deal with this computation. Johns *et al.* (3) use a "total spectrum" method which requires a gradual smoothing out of the cross section curve which, as pointed out by Katz & Cameron (4), introduces a certain amount of arbitrariness. These authors therefore propose a "photon difference" method (4) which, by the use of tabulated functions of the *bremsstrahlung* spectrum and the monitor response, allows a more rapid and less arbitrary calculation of the cross section.

Whatever the method of computation, small changes in the yield curve can introduce large variations in the calculated cross section. Each point of a yield curve can usually be obtained with 3 per cent accuracy in a reasonable time interval. When a curve is fitted through these points, the result involves a certain amount of arbitrariness which, although small, can seriously affect the cross section. This question has been carefully examined by Katz & Cameron (4), who suggest the use of the following criteria for the more usual type of yield curve: both the first and second derivatives must be smooth. Katz & Cameron have recomputed most of the cross section curves obtained by the Saskatchewan group, and in all cases except one [the reaction $C^{12}(\gamma, n)C^{11}$] find good agreement with the results that had been calculated by the older and less accurate total spectrum method [see Tables IV and V in reference (4)].

The precision obtainable in the cross section curves with these methods depends on: (*a*) The accuracy of the yield curve. This is mainly a question of time since it depends on the number and accuracy of the points taken. In addition the beam stability is involved, since small details can be smeared

out by a beam with fluctuating maximum energy. (*b*) The validity of the *bremsstrahlung* spectrum used in the calculations. The theoretical calculations of Schiff (5, 6) are usually used. (*c*) The validity of the assumed energy response of the monitor that measures the incident energy flux. The response of ionization measuring devices is usually calculated with the assumption that equilibrium between the primary photons and secondary electrons has been established. The effect of scattering must be taken into account. Such calculations become quite difficult at energies above 50 Mev; this is one of the reasons why, except for the early work of Baldwin & Klaiber (7) which proved unreliable, yield curves have not been converted into cross section curves when measured with beams of energy larger than 27 Mev and monitored by ionization chambers.

It is possible, however, to calibrate a beam monitor by measuring the photon flux with a pair spectrometer as first done by Lawson & Perlman (8) or by using the method of Blocker, Kenney & Panofsky (9). Such calibrations, done at various beam energies, would then experimentally determine the energy response of the beam monitor up to the maximum beam energy attainable.

Once the yield curve of a reaction has been accurately measured, it can be used to monitor the x-ray dosage in any bombardment. This method has been used extensively by Sagane (10), Terwilliger & Jones (11), and the Saskatchewan group because of its ease and simplicity. Newkirk (12) monitors the beam by alternately bombarding two samples with fixed and variable maximum beam energies.

Single or Few Bombardment Methods

The methods described in the previous section give detailed information on the energy dependence of the cross section of any photoprocess. A large number of bombardments are required, however, and the monitoring problem becomes more difficult as the energy of the photons involved increases. As a result, several other methods have been developed recently which involve very few irradiations and which do not require a measurement of the beam energy flux at various bombarding energies. The information given by these methods is not very detailed, however. It usually consists of some kind of average energy[2] for the photons responsible for a given process, the effective photon energy E_e. All three methods used so far obtain E_e by studying the electromagnetic interaction of the effective photons with various materials.

Koch, McElhinney & Cunningham (13) measured in the usual way the absorption co-efficient in lead and aluminum of the photons effective in the reactions $Cu^{63}(\gamma, n)$ and $C^{12}(\gamma, n)$ under conditions of good geometry with x-rays from a 50-Mev betatron. The monitor foils and absorbers were placed

[2] The kind of "average" obtained in each case depends on the energy dependence of the method.

TABLE I

(γ, n) REACTIONS*

Target	Product	Q (Mev)	E_{max} (Mev)	ΔE (Mev)	E_e (Mev)	σ_{max} (barns)	σ_{int}† (Mev-barns)	E_s (Mev)	Reference
C^{13}	C^{11}	18.7	22.9	2.8		.0131	.046	27	(4, 41)
					22.1			50	(13)
					23, 32		.086	50	(14)
					27		.090	320	(15)
N^{14}	N^{13}	10.5	24.2			.00284	.015	25	(17)
O^{18}	O^{15}	15.6	24.2			.0114	.031	25	(17)
Mg^{24}	Mg^{23}	16.2	19.4	5.8		.0098	.057	24	(48)
Al^{27}	Al^{26}	14.0	19.2	4.7		.0081	.045	24	(48)
P^{31}	P^{30}	12.4	19.5	6.5		.0167	.129	25	(4, 62)
Fe^{54}	Fe^{53}	13.8	18.7	6.3		.067	.48	24	(4, 40)
Ni^{58}	Ni^{57}	12.0	18.5	5.6		.054	.34	24	(4, 40)
Cu^{63}	Cu^{62}	10.9	17.5	6.0		.10	.60	22	(65)
			17.5	5.5		.10	.66	24	(61)
			18.1	6.1		.104	.66	26	(3, 4)
					17.2			50	(13)
					17.3, 21.0			50	(14)
							.77	50	(86)
					18		.76	320	(15)
Cu^{65}	Cu^{64}	10.7	18.6	7.0		.151	1.11	26	(3, 4)
					19		1.00	320	(15)
Zn^{64}	Zn^{63}	11.6	18.7	7.9		.124	.99	24	(4, 40)
					19		.69	320	(15)
Mo^{92}	Mo^{91*}		18.7			.145	.87	24	(87)
Mo^{92}	Mo^{91}		18.7			.030	.18	24	(87)
Ag^{107}	Ag^{106}				16			320	(15)
Ag^{109}	Ag^{108}	9.3	16.5	4.2		.32	1.65	22	(65)
Sb^{121}	Sb^{120}	9.3	14.8	4.8		.685	3.53	26	(3, 4)
Sb^{123}	Sb^{122}	9.3	14.8	4.8		.362	1.92	26	(3, 4)
Ta^{181}	Ta^{180}	8.0	13.9	4.6		>.080	>.47	26	(3, 4)
					19			320	(15)

* Reactions for which only the yield relative to another reaction has been measured are not listed.
† The cross section value is integrated to the maximum photon energy available.

far from the detector foils to minimize the effect of secondaries. Values of E_e were then obtained from the experimental and theoretical values of the total absorption coefficient. As can be seen in Table I, the results obtained by this method compare favorably with other measurements.

Marshall (14) used a similar but refined method to obtain values of E_e for the reactions $C^{12}(\gamma, n)$, $Cu^{63}(\gamma, n)$, and $Zn^{64}(\gamma, n)$. Again using good geometry, the absorption coefficient of the effective photons is measured in many elements of different atomic number Z. Since the cross section for nuclear pair production varies as Z^2, while the Compton and electronic pair production cross sections have a Z dependence, it is possible to separate the first absorption process from the other two. The absorption coefficient corresponding to each of the two groups of processes involved determines a value of E_e. The difference between these two values of E_e obtained for one reaction

TABLE II

(γ, p) REACTIONS

Target	Product*	Q (Mev)	E_{max} (Mev)	ΔE (Mev)	E_e (Mev)	σ_{max} (barns)	σ_{int} (Mev-barns)	E_e (Mev)	Reference
C	p	16.0	21.5	1.7		.034	.063	25	(46)
O^{18}	N^{17}	16.0	24			.038	.15	24	(18, 19)
Mg^{25}	Na^{25}	11.5	20.5	3.6		.0137	.056	24	(58)
			21.7	6.0		.0148	.10	24	(48)
Mg^{26}	Na^{25}	14.0	22.6	3.3		.0193	.085	24	(48)
Al^{27}	p	7.4	21.2	5.4		.022	.12	24	(46)
Co^{59}	p		21.5	5.7		.024	.14	24	(46)
Ni	p		18.7	5.4		.058	.32	24	(46)
Zn^{68}	Cu^{67}				24		.075	320	(15)
Nb	p		21.3	6.6		.018	.12	24	(46)
Rh	p		19			.005		20	(64)

* When the reaction has been measured by detecting the emitted proton, this is indicated by "p."

is a measure of the width of the resonance absorption, although difficult to measure and to interpret quantitatively. Marshall's results are summarized in Table I.

The absorption coefficient methods give the effective photon energy E_e with few bombardments and without special monitor. Since conditions of "good geometry" must be used to minimize the effect of secondaries, these methods become difficult to use when the x-ray beam energy E_0 is much larger than the photon energy E_e. Strauch (15) has developed the transition curve method for this case. Here absorption type curves are measured with lead under conditions where all the secondary radiation is detected. This means that monitor foils, absorbers, and detector foils are larger than the beam cross section and are placed as close together as possible. When the relative activity is plotted against thickness of absorber, a decrease resulting from the absorption of effective photons present in the original beam is observed at first. At larger absorber depths, the relative activity often increases above unity as a result of the production of effective photons by cascade processes. At very large depths multiplication becomes unimportant and an exponential decrease is finally observed. Eyges (16) has shown that the area under each transition curve or "track length" is the best measure of the photon energy E_e, and he gives theoretical results correlating these two quantities. The results obtained from transition curves are summarized in Tables I and II. Where comparison with similar results obtained by other methods is possible, the agreement is satisfactory.

LOW ENERGY REGION

INTRODUCTION

In the study of photonuclear reactions, the low energy region is best defined to include most of the resonance dipole absorption which results in

(γ, n) and (γ, p) reactions. This means that the upper limit for the energy of the photons effective in this region is about 30 Mev for light elements and 20 Mev for heavy nuclei. Since about one-half or more of the total photoabsorption of nonmesonic origin takes place below these limits, and since relatively many 24-Mev betatrons are in operation, more detailed information is available in the low energy region than at higher energies. As a result the general nature of the mechanisms for photon absorption are fairly well understood, and rapid progress is being made toward more quantitative descriptions.

As long as the wave length λ of the incident photons is much larger than the nuclear radius R, classical radiation theory should describe the nuclear photon absorption. Thus dipole absorption should be larger than quadrupole absorption by a factor of $(\lambda/R)^2$. However, for dipole absorption to occur, the nuclear center of mass must be displaced from the center of charge. The strong correlation between nucleons inside the nucleus (α-particle structure) makes such a separation difficult and suppresses the dipole photoeffect. As the photon energy increases beyond about 9 Mev for heavy nuclei and 17 Mev for light nuclei, it apparently becomes possible to excite nuclear vibrations which result in the displacement of the center of mass from the center of charge and thus give rise to dipole absorption.

Quadrupole Photon Absorption

In order to observe nuclear reactions initiated by photons absorbed by quadrupole interaction, a reaction must be chosen whose threshold is well below the energy region where dipole vibrations become dominant. The (γ, n) and (γ, p) reactions in certain light nuclei fulfill this criterion. Johns *et al.* (17) have carefully investigated the reaction $N^{14}(\gamma, n)N^{13}$ (see Fig. 1). The cross section rises rapidly above the threshold of 10.5 Mev to a value of about .3 millibarn, after which there is a slow decrease to 17 Mev. Beyond this point the cross section increases rapidly and steeply. It appears that the main processes involved above and below 17 Mev differ, and the magnitude of the cross section at low energies is of the order of that expected from quadrupole photon absorption. The slow decrease beyond the initial rise is probably due to (γ, pn) competition. The sudden increase of the cross section beyond 17 Mev is due to the beginning of dipole absorption. Similar evidence for quadrupole absorption has been obtained by Johns *et al.* (17) for the reaction $O^{16}(\gamma, n)O^{15}$ (see Fig. 1) and by Stephens, Halpern & Sher (18) and Montalbetti (19) for the reaction $O^{18}(\gamma, p)N^{17}$. It seems quite possible that the direct photoeffect contributes to the low-energy absorption. A study of the angular distribution of emitted particles might settle this question.

In a very beautiful piece of work, Haslam *et al.* (20) have recently found fine structure in the yield curve for the reaction $O^{16}(\gamma, n)O^{15}$ in the region of quadrupole absorption. This corresponds to the excitation of five previously unreported levels of O^{16}. Using this method, it should be possible to find new levels in other nuclei.

The (γ, α) process has a low enough threshold in most elements to be produced by photons absorbed by a quadrupole mechanism. As a result of experimental difficulties and the low cross sections involved, most of the work reported so far has been done in photographic plates. The related reactions $C^{12}(\gamma, \alpha)Be^{8}$ and $C^{12}(\gamma, 3\alpha)$ have been studied by several investigators (21 to 25) with Li γ-rays and betatron x-rays. Wilkins & Goward (23) show

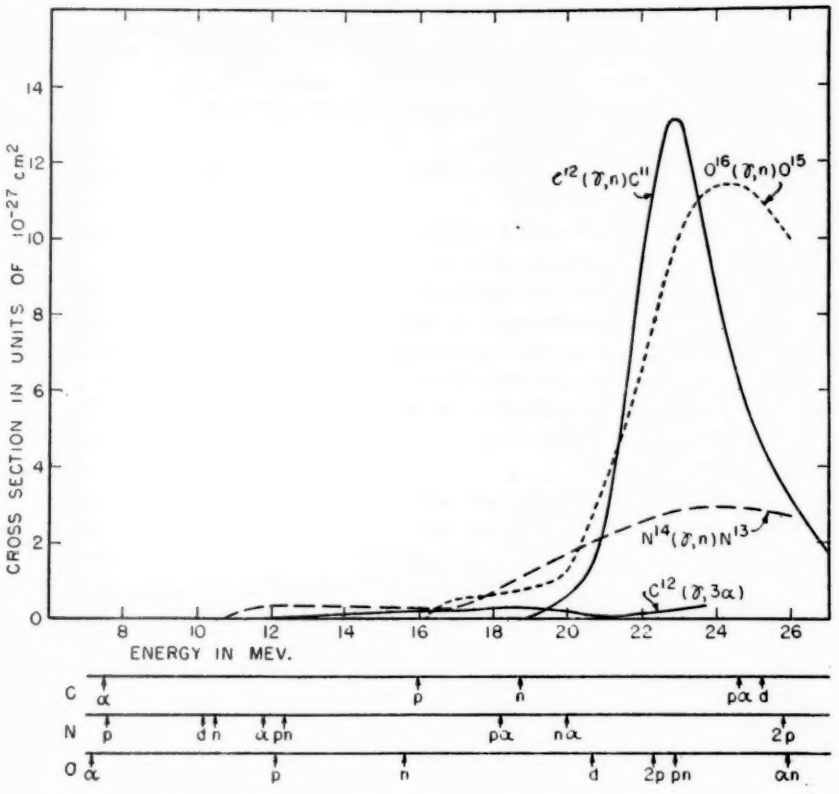
CROSS SECTION IN UNITS OF 10^{-27} cm^2
ENERGY IN MEV.
$C^{12}(\gamma,n)C^{11}$
$O^{16}(\gamma,n)O^{15}$
$N^{14}(\gamma,n)N^{13}$
$C^{12}(\gamma,3\alpha)$
C α p n pα d
N p d n α pn pα nα 2p
O α p n d 2p pn αn

FIG. 1. Cross section curves for several photoreactions in C, N, and O [as reported in references (4, 17, 23, 41)]. Thresholds for various x-ray induced reactions are also indicated.

that the cross section goes through a pronounced peak at about 19 Mev with a value of .24 millibarn, and rises again beyond 21 Mev to much larger values. The probable interpretation is similar to that given for the (γ, n) process in N, only here the decrease beyond the small quadrupole peak is due to (γ, n) competition. Telegdi (25) finds that the energy distribution of the α-particles produced by photons below 21 Mev is consistent with the idea of quadrupole absorption.

Dipole Resonance Absorption

The sudden and rapid rise at higher energies of the cross section curves discussed in the preceding section above the values expected for nuclear quadrupole absorption is the result of a different and much more powerful process for photon capture. The existence of such a mechanism first followed from the pioneer work of Perlman & Friedlander (26, 27) and of Lawson & Perlman (8) with the 100-Mev General Electric betatron. The larger magnitude and the resonance type of energy dependence of (γ, n) processes found by these workers could only be accounted for by a dipole absorption process.

Levinger & Bethe (28) have made a very general calculation of the expected integrated dipole cross section σ_{int} and find

$$\sigma_{int} = \int \sigma(E)dE = 0.060NZ/A(1 + .8x) \text{ Mev-barns}$$

where x is the fraction of the neutron proton force that has an exchange character. The nonexchange part of this expression is derived from electromagnetic sum rules and is independent of any nuclear model. The modification introduced by the exchange character of nuclear forces is probably valid for a large variety of nuclear potentials. Levinger & Bethe have also obtained expressions for various nuclear potentials of "the mean photon energy" for absorption by dipole processes. These results are again of a quite general character and do not depend on the mechanism by which dipole absorption can occur.

A simple mechanism responsible for the separation of the nuclear center of mass from the center of charge was first suggested by Bohr (29, 30) and later rediscovered by Goldhaber & Teller (31). The neutron and proton center of gravities are displaced with respect to each other, and this results in dipole oscillations of the neutron fluid against the proton fluid with fixed resonance frequencies. These vibrations are damped by internal friction, and the energy absorbed is dissipated into random motion of particles inside the nucleus. Thus considerations based on the statistical model should apply for the description of the decay of the excited nucleus.

The quantitative arguments of Goldhaber & Teller are based on a simplified model in which the solid neutron sphere moves against the solid proton sphere. The resonance frequency is determined by the magnitude of the restoring force, and the width depends on the internal friction. The frequency is estimated to be

$$\hbar\omega_0 = 40A^{-1/6} \text{ Mev}$$

and the result for the integrated cross section is similar to that of Bethe & Levinger with no exchange force.

The difference between the energy of the resonance dipole absorption and the mean energy of dipole absorption must be emphasized. The former refers to the energy at which a very particular type of dipole oscillation predominates. The latter gives an energy averaged over all possible modes of dipole photon absorption. There is thus no contradiction between the resonance

energy predicted by Goldhaber & Teller and the higher valued mean energy calculated by Levinger & Bethe. As will be seen below, the present evidence suggests that about one-half of the photon absorption takes place in the resonance region.

Steinwedel & Jensen (32) have used a model which at first glance requires fewer "reasonable" constants. The nuclear density is assumed to be constant during the dipole vibrations; that is, every local neutron density decrease is compensated by a corresponding proton density increase. Using considerations based on the hydrodynamics of two liquids in a sphere, the resonance frequency and integrated cross sections are given as:

$$\hbar\omega_0 = 60A^{-1/3} \text{ Mev and } \sigma_{\text{int}} = .0065A \text{ Mev-barns.}$$

These results involve the inertial mass of a nucleon inside a nucleus. Danos (33) has pointed out that this is not necessarily the same as the free mass, since neutrons and protons need only interchange meson fields to produce dipole oscillations, thus reducing the effective inertial mass. This effect will tend to increase the resonance frequency and the integrated cross section. If the effective mass is taken as one-half the free mass, then better agreement with the experimental results is obtained. Danos & Steinwedel (34) have also examined the influence on the results of these calculations of the perturbation of the coulomb energy during the vibration, and of the nonuniform distribution of protons in the original nucleus. The first effect is negligible, while the second decreases slightly the $A^{-1/3}$ dependence of the resonance frequency.

Since some of the constants involved in the Goldhaber-Teller and Steinwedel-Jensen calculations can only be estimated, an experimental proof should verify the A dependence of σ_{int} (identical in both calculations) and distinguish between the $A^{-1/6}$ and $A^{-1/3}$ dependence predicted for the peak absorption frequency.

Levinger & Bethe (28) have proposed an alternate mechanism for the narrow dipole absorption in which the breaking up of some subunit of the nucleus, such as an α-particle, is involved. This is suggested by the calculated size of the absorbing unit, which appears to be smaller than the nuclear radius. These authors suggest a connection between the resonance absorption around 20 Mev and the large γ-ray yield of the He^3 $(p, \gamma)He^4$ reaction in this region. However, no resonance level in He^4 has as yet been found (35). When the breakup of these α-particles (or any other nuclear subunit such as a deuteron) occurs near the nuclear surface, the probability for a proton to escape from the nucleus without further collision is large. Compared to the total number of emitted particles, the number of protons emitted in this way seems to be quite small in the region of resonance absorption, but becomes more important at higher energies as will be seen below.

The Nuclear Photoeffect

The smallest nuclear subunit that can interact with an incident photon is the neutron or proton. Courant (36) has investigated the theory of the low-energy photoeffect, and concludes that its magnitude is roughly of the

order of the (γ, p) cross sections measured by Hirzel & Wäffler (37) with Li γ-rays in the heavier elements. This suggestion of Courant seems to resolve the difficulty presented by the results of the Swiss group who found higher (γ, p) cross sections than expected from the statistical model. It should be noted that Schiff (38) had previously proposed another explanation for these results based on the photoexcitation of particular nuclear levels; as will be reported in more detail later, his model does not appear to predict the correct particle energy distribution.

The magnitude of the (γ, p) processes that can be explained by the nuclear photoeffect represents only a small fraction of total cross section for photon absorption, for in the elements under consideration the (γ, n) process is still two orders of magnitude more probable than the (γ, p) reaction (37). However, a small contribution by a direct photon-nucleon interaction in the region of dipole resonance absorption explains the results of Hirzel & Wäffler and the existence of a few high-energy anisotropic protons that are emitted by some of the heavier elements. This last point will be considered later.

The (γ, n) and (γ, p) Reactions

Many investigators have obtained yields and cross sections for a large number of (γ, n) and (γ, p) reactions. Their results are summarized in Tables I and II. Where detailed excitation curves have been measured, the peak energy E_{max}, the peak cross section σ_{max}, the width ΔE and the integrated cross section σ_{int} are listed. In some experiments only an effective energy E_e for the photons responsible for a given reaction are obtained. Finally, the reaction threshold Q (when available) and the maximum beam energy E_0 are given for each measurement.

Most of the reactions listed in Tables I and II were detected by the yield of the radioactive product nucleus. The corresponding reaction cross section curves do not then necessarily represent photon absorption cross section curves, since other reactions leading to stable isotopes are completely missed. Some of the proton resonance curves were obtained from yield measurements of the ejected particles; this leads to some doubt about the nature of the reaction involved since there is no way to distinguish between (γ, p), (γ, pn) or $(\gamma, 2p)$ processes. The first detection method thus gives a lower limit to the width of the resonance photon absorption; the reverse is true for the second method.

Some general conclusions can be drawn from the results summarized in Tables I and II: (*a*) All cross section curves that have been investigated to high enough energies exhibit a resonance behavior. That is, the cross section rises from the threshold to a peak value, after which it decreases rapidly. The shapes of the various curves are not all similar, but it is difficult to estimate how much of this variation is due to experimental uncertainties. (*b*) The width of the excitation curves (defined as the full width at one-half the maximum cross section) varies from 1.7 Mev to 7.9 Mev, with the large majority being close to 6 Mev. In addition to such relatively narrow resonances, there may, of course, be high-energy tails. (*c*) The energy at which the peak

cross section occurs decreases slowly with increasing mass number A. (*d*) The values of the peak cross section, integrated cross section, and relative yield for (γ, n) reactions increase rapidly with increasing A, while for (γ, p) processes they are fairly constant. (*e*) The energy E_{max} of cross section peaks lies on the average about 6 Mev above the reaction threshold Q. In particular, in those cases (N, Mg) where the difference $E_{max} - Q$ deviates appreciably from the average value, the value of E_{max} is not different from corresponding energies in neighboring isotopes.

Some of the better known reactions listed in Tables I and II will now be considered in some detail, especially with regard to the energy dependence of the photoabsorption. The resonance behavior of the observed reaction cross section curves can be caused by one or both of two factors: a resonance in the photon absorption, or a steady absorption with an undetected reaction competing increasingly with the process under study, thus causing a decrease in the observed yield.

Zinc.—These two possibilities are well illustrated by recent studies on the decay of the Zn^{64} nucleus when excited by different methods. The probability of nuclear capture of charged particles increases rapidly with increasing energy, below the coulomb barrier. However, as shown by Ghoshal (39), the reactions $Ni^{60}(\alpha, n)Zn^{63}$ and $Cu^{63}(p, n)Zn^{63}$ exhibit a strong resonance behavior with a width of 10.5 Mev. Here the decrease of the cross section beyond the peak can be completely explained by the increasing yield of the $(\alpha, 2n)$, (α, pn) and $(p, 2n)$, and (p, pn) processes. Katz *et al.* (4, 40) have studied the reaction $Zn^{64}(\gamma, n)Zn^{63}$ which passes through the same compound nucleus. They also find a resonance cross section curve with a width of 7.9 Mev. The smaller width found with x-ray excitation merely indicates that the probability of photon capture does not increase as rapidly with energy as that of charged particles. It is only because the (γ, n) cross section is twice as large as the sum of the (γ, pn) and $(\gamma, 2n)$ reactions, as shown by Strauch (15), that it can be concluded that the photon absorption cross section must decrease at or beyond the peak of the (γ, n) reaction. Unfortunately, only the effective energies for the $(\gamma, 2n)$ and (γ, pn) reactions are known. However, the fact that the differences between the effective energies and the relative yields of these photoreactions are the same as the corresponding quantities of the similar particle-induced reactions indicates that the photon absorption cross section does not drop too abruptly beyond the observed peak of the (γ, n) process. Thus, values of the peak energy and width of the cross section of this last reaction can be used only as a first approximation (really a lower limit) to the corresponding values of the photon absorption cross section curve.

Carbon, nitrogen, oxygen.—The (γ, n) excitation curves C, N, and O have been recently measured by the Saskatchewan group (4, 17, 41) (see Fig. 1). They are of particular interest not only because the low-energy quadrupole absorption is detectable, but because the dipole cross section peaks occur within 1.5 Mev of each other. This common behavior must be contrasted with the large differences in (γ, n) and higher order reaction thresholds, as

much as 8.2 Mev (see Table I). It thus appears that the mechanism for dipole photon absorption is relatively insensitive to the details of the nuclear structure, at least so far as its energy dependence is concerned. The small cross section value at the peak of the N curve compared to those of C and O is due to the large competition from the reaction $N^{14}(\gamma, pn)C^{12}$. Its low 12.4-Mev threshold is below the region of large photon absorption, while this is not the case for the corresponding reactions in C and O. Gaerttner & Yeater (42 to 45) using a gas filled cloud chamber have indeed found a much larger number of "flags" corresponding to (γ, pn) processes in N than in C and O.

The (γ, n) cross section curves shown in Figure 1 do not of course represent the photon absorption curves, although the similarity in peak energies suggests a strong correspondence as far as shape is concerned. That the (γ, p) reaction contributes about as much as the (γ, n) process to the total photon absorption has been shown by Gaerttner & Yeater (43, 44) for N and O, and by Halpern & Mann (46) for C. In this last investigation, a very narrow and high resonance cross section curve was found (Table II). This might be connected with the tight binding of the constituents of the C nucleus, but the result should probably be checked before any definite conclusions can be drawn.

From an analysis of the stars observed in their cloud chamber by Gaerttner & Yeater it is apparent that in the case of C and O the (γ, pn) and higher order reactions have too small a cross section to account for the decrease of the (γ, n) and (γ, p) yields at higher energies. This decrease must be the effect of a decreased absorption of photons.

Sagane (47) has recently presented evidence for the existence of a long tail in the cross section curves of the reactions $C^{12}(\gamma, n)C^{11}$ and $O^{16}(\gamma, n)O^{15}$. This could support the existence of the nuclear photoeffect which will be considered later.

Magnesium, aluminum.—The cross section curve for the photo proton yield from Al has been measured by Halpern & Mann (46), and Katz & Cameron (48) have obtained the excitation curve of the reaction $Al^{27}(\gamma, n)Al^{26}$. Both curves exhibit a strong resonance character, which is difficult to explain except by a resonance type of photon absorption, as shown in detail by the authors for these and similar reactions in Mg. As can be seen from Table II, the characteristic features of the (γ, p) cross section curves of Mg^{25}, Mg^{26} and Al^{27} are remarkably similar considering the large differences in threshold. This again suggests that the photon absorption process involved does not depend strongly on the individual nuclear structure.

Antimony, tantalum.—Eyges (49) has noticed a correlation between the maxima of the (γ, n) cross section curves of Cu^{65}, Ag^{109}, Sb^{121}, Sb^{123}, Ta^{181} and the thresholds of the corresponding $(\gamma, 2n)$ reactions. From this he concludes that the photon absorption cross section near the peaks is reasonably flat, and that at least part of the observed cross section decrease is produced by competition from the $(\gamma, 2n)$ reaction. Using the available (γ, n) excitation curves (3, 4) and the neutron yield measurements of Price & Kerst (50) and McDaniel, Walker & Stearns (51), Eyges has tried to reconstruct the photon

absorption curve for Sb and Ta. Heavy nuclei were chosen for this investigation since in light elements the (γ, pn) reaction can offer more competition than the $(\gamma, 2n)$ process as in Zn. The reconstructed photon absorption cross section curves have a definite resonance characteristic, with a width 2.5 Mev wider and a peak energy .5 Mev higher than the related (γ, n) excitation curves. This apparent close correspondence between the (γ, n) and photon absorption cross section curves in the heavy elements Sb and Ta is not necessarily expected for lighter nuclei since the photon absorption takes place at higher energies where higher order reactions are possible.

The following general conclusions can be drawn from a study of the features of the various (γ, n) and (γ, p) reactions summarized in Tables I and II, and studies of higher order reactions:

(*a*) The resonance behavior of many measured cross section curves cannot be explained by competition alone, but a resonance type of photon absorption seems to occur. The mechanism does not depend strongly on the individual nuclear structure, since peak reaction energies and particle thresholds do not appear to be related.

(*b*) The values for the cross section, resonance energy, and resonance width, obtained from a particular reaction, represent lower limits only to the corresponding characteristics of the photon absorption curve.[3] However, the peak energies obtained for the (γ, n) reaction in heavy elements and the proton yield measurements in light elements probably represent fair approximations to the peak photon absorption energy. The dependence of these values on the mass number A is about $A^{-1/4.5}$ which is intermediate between the predictions of Goldhaber & Teller (31) and Steinwedel & Jensen (32).

(*c*) When measured by *bremsstrahlung* with E_0 of 27 Mev or less, the integrated cross sections for the (γ, n) and (γ, p) reactions are much larger than expected from quadrupole photon absorption. They are smaller but of the same order of magnitude than the cross section for dipole photon absorption calculated by Levinger & Bethe (28) with a Serber-type, neutron-proton force.[4] For $A<30$, the (γ, p) cross section is often larger than that of the (γ, n) reaction, and for C and Al the sum of these two reactions contributes 50 per cent or less to the total dipole absorption. For $A>30$ the (γ, p) process becomes rapidly less important, with the (γ, n) reaction alone often contributing more than 50 per cent to the expected dipole photon absorption.

Neutron Yield Measurements

Price & Kerst (50) have measured the neutron yield of many elements with 18-Mev and 22-Mev x-ray beams. They find that above $Z=10$, the

[3] It would be worthwhile to measure the photo neutron yield as a function of E_0 using for beam monitor the product activity from the (γ, n) process in the element under investigation. This would provide a very sensitive measure of the contribution of higher order reactions to the region of resonance photon absorption.

[4] The reaction $Sb^{121}(\gamma, n)Sb^{120}$ is an exception; however, the decay scheme of the product nucleus is not well known (4).

yield increases as $Z^{2.7}$ and $Z^{2.1}$ in the 18-Mev and 22-Mev bombardments respectively. This more rapid increase with Z obtained at lower energy is expected if the frequency of the maximum absorption decreases with an increase in Z.

Cameron (52) has calculated the expected ratio of 18-Mev to 22-Mev yields, taking an average (γ, n) excitation curve and using the observed energy variation of the (γ, n) cross section peak with mass number A. A comparison of the results of this calculation with the measurements of Price & Kerst shows that above $Z=30$ there are more neutrons than can be accounted for by the (γ, n) reaction alone. Cameron estimates that for $E_0=22$ Mev the sum of the $(\gamma, 2n)$ and (γ, pn) integrated cross sections is of the order of 30 per cent of that of the (γ, n) process. Using the 22-Mev measurements below $Z=30$, and the 18-Mev yields above, Cameron has also calculated the expected (γ, n) cross sections as a function of Z. The result agrees quite well with the cross sections measured by activation methods.

McDaniel, Walker & Stearns (51) have obtained neutron yields using Li γ-rays. The general trend of their measurements is similar to that of the 22-Mev results of Price & Kerst except above $Z=74$ where the Li γ-rays produce a decreased yield. This can be understood if it is assumed that for high Z elements the peak photon absorption occurs below 17.6 Mev, that is below the energy of the strong Li line.

Since the Li γ-ray spectrum is well known (58) and consists of two lines only, it is possible to compare these measurements with the theoretical predictions. Using the statistical theory of the compound nucleus, Heidmann & Bethe (54) have calculated the number of neutrons emitted per Li quantum absorbed for many elements. The role of competing (γ, p) (γ, α) and $(\gamma, 2n)$ reactions was taken into account. From this and the measurements of McDaniel, Walker & Stearns (51), the cross section $\sigma(Z)$ for capture of Li γ-rays can be calculated as a function of the atomic number Z. Except for three light elements for which some doubt seems to exist about the experimental data, the following relation represents the data within 25 per cent:

$$\sigma(Z) = 2.4 \times 10^{-27} Z \text{ cm.}^2$$

This result cannot be directly compared to the predictions of the two models for dipole absorption since the resonance energy is a function of the mass number.

Danos (33) has used the model of Steinwedel & Jensen to calculate the absorption cross section $\sigma(Z)$ for the Li γ-rays. He found good agreement between his results and the measurements of McDaniel, Walker & Stearns when using a resonance absorption curve with a half width of 5 Mev, an $A^{-1/3}$ dependence, and assuming that one neutron is emitted per photon absorbed. This last assumption is quite inaccurate as shown by the work of Heidmann & Bethe (54). When this factor is taken into account, the good agreement of the Li γ-ray measurements and the assumed model disappears.

Strauch (55) has attempted to fit the data of McDaniel, Walker & Stearns (51) using (*a*) the results of Heidmann & Bethe (54) for the number

of neutrons emitted per photon absorbed, and (*b*) the predictions of the two models for dipole resonance absorption. This attempt is moderately successful with the Goldhaber-Teller model.

Even though there is some question whether the existing interpretations of the neutron yield experiments can distinguish between particular models, these measurements agree with the idea that photon absorption is of the resonance type in the energy region under investigation and that the corresponding cross section varies approximately as the mass number A.

Proton Yield Measurements

Mann & Halpern [(56) note cross section correction quoted in (46)] have measured the proton yield of 20 elements irradiated in a 25-Mev x-ray beam, and their results are compared with the 22-Mev data of Price & Kerst (50). The general features are similar to those obtained from studies of individual (γ, n) and (γ, p) reactions: below $Z = 20$ the proton yield is in general larger than the neutron yield, while the reverse is true in heavier elements.

The Decay of the Photoexcited Nucleus

From the (γ, n) and (γ, p) cross section curves and relative yield measurements, it seems possible to conclude that a resonance type of photon absorption must predominate and that it has a dipole character. To gain a more detailed picture of the nature of the absorption mechanism involved, it is valuable to study the decay of the excited nucleus, that is, the angular and energy distribution of emitted particles. Several such studies have been reported recently, and those carried out in the low-energy region will be considered in this section.

Light elements.—When x-ray beams are used as a photon source, possible details of the energy spectrum of emitted particles are easily washed out. This fact gives particular interest to the work of Wilkinson & Carver (57) who used Li γ-rays to bombard an A target. The gas was enclosed in a proportional counter, and the energy of emitted particles was obtained by pulse height analysis. The energy distribution of emitted charged particles has the following characteristics: (*a*) A large peak is present which is clearly of the type predicted by the statistical theory in that it occurs at a much lower energy than would be expected from the model of Schiff (38) or the direct photoeffect (36). Actually, its position at 2.2 Mev is even lower than expected from the coulomb barrier, but this type of discrepancy has been found even in particle-induced reactions. (*b*) Two small, high-energy peaks are found that correspond to direct transition to the ground state and first excited state of Cl^{39}. Wilkinson & Carver conclude that even these transitions are not produced by a direct photoeffect. Thus, this work indicates that the photoexcited A^{40} nucleus is primarily of the type described by the compound nucleus formalism.

Toms & Stephens (58) have measured by the photographic plate technique the angular and energy distribution of protons from normal Mg and enriched Mg^{25} when irradiated by x-rays from a 24-Mev betatron. This ele-

ment was chosen because Hirzel & Wäffler (37) had found a relatively large yield for the reaction $Mg^{25}(\gamma, p)Na^{24}$. The energy distribution of emitted protons is in very good agreement with that calculated from the statistical theory using the known level density of Na^{24}. Protons with energies both above and below 7 Mev are emitted symmetrically within an accuracy of about 15 per cent [this estimate is based on the standard deviations and scattering of points on Fig. 6 in reference (58)]. Thus, even in the case of a light element with a large (γ, p) yield the nucleus has its excitation uniformly distributed with subsequent evaporation of protons and neutrons. Similar conclusions had been reached previously by Diven & Almy (59) from their study of photoprotons from Al.

To study the photonuclear reactions in C, Gaerttner & Yeater (45) have observed the disintegrations produced in a methane-filled cloud chamber by 100-Mev x-rays. They report that the protons emitted in the (γ, p) reaction have an angular distribution represented by $1+3\sin^2\theta$, where θ is the angle between the emitted proton and the incident x-ray beam. This anisotropic distribution must be the result of low-energy photons since the high-energy photoeffect produces a forward peak (60). However, these cloud chamber results do not agree with the counter measurements of Levinthal & Silverman (60) who find an isotropic distribution for 10-Mev protons emitted by C irradiated with 322-Mev *bremsstrahlung*. This disagreement could be caused by the difference in beam energies used in the two investigations, but this does not appear too probable. Before any definite conclusions can be drawn for the decay of the excited C nucleus, the angular distribution of low-energy protons should be reinvestigated with x-rays below the meson threshold.

Medium weight and heavy elements.—The most complete study so far of disintegration products of an element has been carried out by Byerly & Stephens (61). Using photographic plates, these authors have measured energy and angular distributions of protons, deuterons, and α-particles and the energy distribution of neutrons emitted from copper targets irradiated by 24-Mev *bremsstrahlung*. Both neutron and proton energy distributions are in good agreement with the predictions of the statistical model except for an excess of high-energy particles. The Schiff energy level hypothesis does not seem to apply. The origin of the high-energy protons became clear when the angular distributions were obtained: protons with energies below 10 Mev are emitted isotropically, while the more energetic ones show a pronounced peak at 90°. This peak is expected from the direct photoeffect, but it represents only about 6 per cent of the total number of emitted protons. It is quite possible that some of the low-energy protons are also ejected by a similar process, but could not be differentiated from the much larger number of evaporation particles.

Byerly & Stephens also conclude that while the relative number of emitted neutrons, protons, and α-particles agree in general with calculations from the statistical model, the number of deuterons is much larger than expected. They suggest that an "internal pickup" process might be responsible,

in which an evaporated neutron or proton joins with an opposite nucleon just before or after leaving the nuclear well.[5]

The fact that an appreciable number of protons emitted from heavy nuclei had energies larger than expected from the statistical model and showed an angular asymmetry around 90° had already been shown by Curtis *et al.* (64) for a Rh target, and by Diven & Almy (65) with Ag. It is not surprising that it was not possible to observe a similar effect in the light elements. In heavy nuclei, the decay of an excited nucleus by proton evaporation is suppressed by the coulomb barrier. By comparison, the emission of the relatively high-energy protons by the direct photoeffect is much less inhibited. In addition, the level density of the light elements investigated does not appear to increase rapidly with energy. In this case, the statistical theory predicts a relatively high (γ, p) cross section and a large number of high-energy protons. This makes it difficult to observe protons not originating from a compound nucleus in the case of light elements and low-energy photons. As seen below, these difficulties disappear at higher energies.

It is not possible to say whether the importance of the nuclear photoeffect increases as the weight of the element increases, since the detection merely becomes easier as the number of evaporation protons decreases. This last effect is, of course, compensated by an increased neutron emission, so that for both light and heavy nuclei the direct photoeffect plays a small role in the low-energy region.

Neutron distributions.—This conclusion is supported by the few available measurements of neutron angular distributions. Relatively little work has been done with neutrons since it is so much more difficult to define neutron energies and there seems little reasons to suppose that their behavior is much different from that of protons. Price & Kerst (50), using a detector sensitive to low and high-energy neutrons (but probably emphasizing the low energies) with 19.7 -Mev x-rays, find an isotropic neutron distribution from Fe and Pb, and some deviations from D and Be. Terwilliger, Jones & Jarmie (66) employed a detector with similar characteristics, but used 320-Mev *bremsstrahlung*. They find neutron isotropy with Fe, Ni, and Cu targets, and very small 90° peaks from C and S. Poss (67) using $Al^{27}(n, p)Mg^{27}$ dectors with a 4.6-Mev threshold observed a peaked emission around 90° with Bi, Pb, and W targets placed in a 20-Mev x-ray beam. These experiments suggest that the emission process for neutrons, at least for those of low energy, is not much different from that for protons.

α-Particle distributions.—Byerly & Stephens (61) find that the energy distribution of α-particles emitted from a Cu target exposed to 24-Mev x-rays consists of a single peak and is of a shape consistent with the evaporation model.

The Saskatchewan group (68, 69) has investigated the energy distribution of α-particles emitted by Ag and Br in photographic emulsions. With 26.6-Mev *bremsstrahlung* two peaks are found, centered around 4 Mev and

[5] Katz & Cameron suggest a similar explanation for the large (γ, d) yield from S as quoted in references (62, 63).

8 Mev, respectively. The low energy α-particles are interpreted by Haslam *et al.* (69) to originate from the "threshold favored" $(\gamma, n\alpha)$ and $(\gamma, p\alpha)$ reactions, that is, to be emitted after the excited nucleus has decayed by photon and particle emission to a low-energy state where only photon or α-particle emission is possible. Apparently even low-energy α-particles can compete successfully, although a small fraction of the time only, with γ-ray emission. The second and high-energy peak is ascribed to normal evaporation processes resulting in (γ, α) and $(\gamma, \alpha n)$ reactions. These interpretations are supported by rough cross-section curves. The evidence indicates that α-particles can penetrate the potential barrier more easily than predicted from theory, a conclusion similar to that reached by Wilkinson & Carver (57) for photoprotons from A.

Summary

It appears that the most important photon absorption process in the low-energy region is of a dipole character and usually results in an excited nucleus which can be described with the statistical theory of the compound nucleus. The cross section for this absorption process appears to have a resonance type of energy dependence and does not depend strongly on the individual nuclear structure. It is as yet not possible to choose between the various mechanisms proposed for dipole absorption.

Photons are also absorbed by nuclei by quadrupole interaction and the direct photoeffect, but in the low-energy region the cross sections for these processes are much smaller than for the resonance absorption.

THE HIGH ENERGY REGION

Introduction

The high-energy region can be defined as starting where the resonance type of low-energy dipole photon absorption has decreased to a small fraction of its peak cross section. Although the number of investigations, both experimental and theoretical, concerned with this energy region is still relatively small, it appears that photonuclear reactions produced by high-energy photons fall into two groups depending on whether or not meson production plays a part in the initial interaction.

High Order Reactions

There are as yet few reactions initiated by high-energy photons and involving the emission of several particles for which detailed data is available. The measurements of Katz & Penfold (4, 62, 63) for the reaction $S^{32}(\gamma, np$ and/or $d)P^{30}$ indicate an integrated cross section four times smaller than for $S^{32}(\gamma,n)$ S^{31} which has been studied by Haslam, Cameron & Cook (70). Strauch (15) finds that for a Zn target the yields (and cross sections where measured) of various reactions with a maximum of five ejected nucleons decreases with the number of particles emitted. He also observed unidentified reactions produced in Pb and Bi by effective photons of 78 Mev. Sugarman & Peters (71) have studied the relative yield of several reactions in Bi with 86-

Mev and 48-Mev x-rays and also suggest that the yield decreases with increasing number of emitted particles. Similar conclusions can be drawn from the stars observed by Gaerttner & Yeater (42, 43, 44) in N and O with 100-Mev *bremsstrahlung*.

Since, on the average, the number of particles ejected increases with the energy of the photon responsible, these results suggest that the cross section for photoproduction of multiple reactions decreases with increasing energy in the region where mesonic effects are unimportant. However, these reactions should contribute appreciably to the total integrated cross section for photon absorption, especially in the light and medium elements, since the sum of (γ, n) and (γ, p) processes represent only about one-half of the total dipole cross section. In the case of Zn, Strauch (15) adding the contributions from eight reactions finds $\sigma_{\text{int}} \geqq 1.4$ Mev-barns. Eyges (49) gives estimates from yield and cross sections measurements of $\sigma_{\text{int}} \geqq 2.4$ Mev-barns for Sb and $\sigma_{\text{int}} \geqq 3.77$ Mev-barns for Ta. These cross sections are in excellent agreement with the calculations of Levinger & Bethe for a Serber-type neutron-proton exchange force. Gaerttner & Yeater give values of 0.6 Mev-barns for the integrated cross section of N and O which are higher than predicted by the theory. But their beam calibration appears to be too high by nearly a factor of two when their (γ, n) cross sections are compared to other measurements, and when this is taken into account the discrepancy disappears.

The higher order reactions thus explain the difference between the observed (γ, n) cross sections and the predictions of Levinger & Bethe (28) for dipole absorption in the few cases where enough experimental data is available. The average energy of photon absorption is especially sensitive to small, high-energy contributions, and it is thus satisfying that the 30-Mev estimate for Zn (15) is again in good agreement with the expected value (28). However, many more elements should be studied.

Too little information is available on the energy dependence of high-order reactions to make a worthwhile comparison with theoretical predictions of the mechanisms of the high-energy photonuclear interaction. The dipole vibration suggested by Bohr (29) and Goldhaber & Teller (31) to explain the low-energy resonance absorption should be accompanied by higher-order oscillations. Danos & Steinwedel (34) have examined these contributions using the model of Steinwedel & Jensen (32). Taking the fundamental vibration ω_0 as reference, they predict an additional 8 per cent and 2 per cent photon absorption due to quadrupole vibrations at 1.8 ω_0 and the first dipole harmonic at 2.86 ω_0, respectively. Still higher multipole interaction contributions are shown to be much smaller. Whether these resonances could be observed separately from the fundamental is doubtful since they should be quite broad because of the rapid increase of the nuclear level density with energy.

The dipole vibration model could thus explain the apparently decreasing photon absorption at higher energies. It does not predict the emission of high-energy anisotropic protons that has been observed. These must be produced

by the interaction of photons with a small subunit of the nucleus such as a deuteron. It this process occurs near the nuclear surface, the proton has a good chance to escape without further collisions. If it takes place in the interior, the probability is great that the proton will lose part or all of its energy by multiple collisions, resulting in the formation of an excited nucleus from which many particles are evaporated. It is quite possible that many of the high order reactions are the result of this type of photon capture.

When photons with energies above the meson threshold are used, it appears that many of the observed reactions are produced by photons captured by meson-connected mechanisms, as will be seen in the following sections.

Photo Stars

Stars produced by high-energy x-rays in photographic emulsions have been studied by Miller (72) and Kikuchi (73, 74). Miller finds a nearly constant cross section of 7.5×10^{27} cm.^{2} for the production of stars with three or more prongs for photon energies between 161 Mev and 322 Mev and suggests that at least some of these stars are associated with meson production. This can be seen directly in a few cases where π-mesons originate in the star. In addition, Mozley (75) has observed an $A^{-1/3}$ dependence of the yield per nucleon for photoproduction of π^+-mesons suggesting a surface effect for this process. Since the nucleus does not seem to appear opaque to high-energy photons, Miller suggests that stars could be produced by the emission and reabsorption of mesons inside the nucleus. The order of magnitude of the cross sections involved supports these views, since the star production cross section is comparable to A times the photomeson cross section of a nucleon. The results and conclusions of Kikuchi are similar.

Neutron Yield Measurements

The yield of neutrons has been measured as a function of Z with 320-Mev *bremsstrahlung* by Kerst & Price (76) and with 322-Mev x-rays by Terwilliger, Jones & Jarmie (66). The results of these two investigations agree well, except for a 27 per cent discrepancy in absolute cross section which is assumed to be due to beam energy and neutron source calibrations. The Z dependence above $Z = 30$ is similar to that found with 22-Mev *bremsstrahlung* by Price & Kerst (50). Below $Z = 30$ relatively more neutrons are emitted at high energies which is not surprising considering the Z dependence of the low-energy absorption resonance. The same jumps in neutron yields in adjoining light elements are observed in the low and high energy investigations.

Levinger & Bethe (77) have examined the results of these yield measurements for heavy elements and conclude that there is no discrepancy with their calculation of the integrated cross section for dipole photon absorption. Eyges (49) has compared the neutron yield expected from Sb and Ta according to his reconstructed photon absorption curves with the high energy measurements. He concludes that about 43 per cent of the neutrons observed with 320 Mev are not produced in the low-energy region.

This has been recently verified directly by Jones & Terwilliger (78). Using the $Cu^{63}(\gamma, n)Cu^{62}$ and $D(\gamma, p)p$ reactions to monitor the irradiation dose, these authors report an average neutron yield from nine elements which is 29 per cent higher with 320-Mev than with 160-Mev *bremsstrahlung*. The results of Kikuchi & Miller suggest that a large fraction of these neutrons are emitted from stars produced by virtual or real photomeson production.

If the Eyges estimate for the neutron yield from heavy elements above 22 Mev is taken seriously and is combined with the 160-Mev and 320-Mev yield measurements, the neutron yields of heavy elements irradiated with 22-, 160-, and 320-Mev x-rays are in the ratio 1.00:1.35:1.30. This result is consistent with a slowly decreasing nuclear photon absorption up to the meson threshold. However, the lead transition curve measured by Terwilliger, Jones & Jarmie (66) has been interpreted by Eyges (49) as indicating very little photon absorption between 22 Mev and 160 Mev. It is apparent that more work on the cross section and energy dependence of star formation, neutron and proton yields and reactions is needed before the magnitude of photon absorption in the high-energy region can be accurately estimated.

Photoprotons

The angular and energy distributions of protons observed with low-energy x-rays show only a small number of particles which have not originated in an evaporation process. This is not true in the high-energy region. Using a 195-Mev x-ray beam to minimize meson effects, Walker (79, 80) has studied the photoprotons emitted at 30°, 60°, 90°, and 135° from a C target. He gives the total nuclear cross section for protons with energies larger than 70 Mev and 90 Mev as $(2.3 \pm 1.6) \times 10^{-28}$ cm.^{2} and $(9 \pm 6 \times 10^{-29})$ cm.^{2} per unit Q. The high-energy protons ($E \geqq 70$ Mev) are emitted preferentially in the forward direction but still have an appreciable cross section at 135°. Walker also presents integral proton spectra which can be fitted approximately by an E^{-n} dependence where n varies from 5.7 to 4.9 as the emission angle increases.

Levinthal & Silverman (60) used the 322-Mev Berkeley synchrotron to study protons with energies from 10 Mev to 70 Mev emitted from several targets. Their results for the differential proton spectrum emitted from C, Cu, and Pb targets indicate a differential cross section of the form E^{-n} where n equals 1.7, 1.9, and 2.2 respectively; 10-Mev protons from Be, C, and Cu targets were found to be emitted isotropically, while 40-Mev protons show a distinct forward peak. The cross section per nucleus for the production of 40-Mev protons was found to be proportional to Z.

Keck (81) has made a similar study with the 300-Mev photon beam of the Cornell synchrotron and included in his measurements protons with energies larger than 70 Mev. He reports that the differential proton-energy spectrum from C and Cd is proportional to E^{-2} from 70 Mev to 130 Mev (in good agreement with Levinthal & Silverman) and to E^{-6} from 130 Mev on. He finds the yield per nucleus of 130-Mev protons to be proportional to Z. The angular distribution of protons from C is strongly peaked in the for-

ward direction, the anisotropy increasing at higher proton energies. Keck also reports an excitation curve for 105-Mev protons emitted at 90° from C which shows a steep rise in the 200-Mev region.

The results of Walker, Levinthal & Silverman and of Keck agree well in the energy regions in which they overlap, except for the absolute cross section values where the discrepancy is not much beyond the relatively large experimental uncertainties. As pointed out by these authors, their results for the angular distribution indicate that the photon interaction resulting in the production of high-energy protons must take place with a small nuclear subunit in order to transfer enough forward momentum to the ejected proton. This suggests a simple proton Compton effect. However, such a process cannot explain the relatively large number of high-energy protons emitted at large angles, and it so predicts too small a cross section. Levinthal & Silverman (10) overcome this difficulty by using a "one nucleon" model in which the proton inside the nucleus has the momentum distribution derived by Chew & Goldberger which includes an appreciable contribution from high-momentum components. The cross section calculated on the basis of this model agrees with the experimental results between 30 Mev and 70 Mev (60). However, it is difficult to see how the observed break in the differential energy spectrum observed by Keck around 130 Mev would follow from the "one-nucleon" model. No calculation of the expected angular distribution has been published as yet.

Levinger (82) has investigated a "two-particle" model in which the photon interacts with a deuteron subunit of the nucleus. He points out that a nucleon will have a high momentum inside the nucleus (which is required to explain the observations) if it is subject to strong forces by being close to another nucleon. In that case the product of a deuteron-type wave function and a wave function for the remainder of the nucleus should describe the correct nuclear model. Using these ideas, Levinger transforms the calculations of Schiff (83) and Marshall & Guth (84) for the photodisintegration of the deuteron to the laboratory system and modifies the results to take into account the presence of the deuteron inside a nucleus.

The deuteron model explains qualitatively the break in the differential spectrum observed by Keck around 130 Mev, since the proton is expected to carry away only about half the absorbed photon energy. However, the quantitative agreement with the measured angular and energy distributions is not satisfactory (81, 82). A possible explanation might lie in the observations of Benedict & Woodward (85) who find a larger cross section for the high-energy photodisintegration of the deuteron than predicted by the calculations used by Levinger. As mentioned by Keck, coincidence studies, e.g. between neutrons and protons, would be helpful in understanding the nature of the nuclear subunit involved. Finally it must be remembered that many of the protons observed wth 320 Mev *bremsstrahlung* could be the secondary result of a photon meson interaction as suggested by Kikuchi.

LITERATURE CITED

1. Chadwick, J., and Goldhaber, M., *Nature*, **134**, 237 (1934)
2. Szilard, L., and Chalmers, T. A., *Nature*, **134**, 494 (1934)
3. Johns, H. E., Katz, L., Douglas, R. A., and Haslam, R. N. H., *Phys. Rev.*, **80**, 1062 (1950)
4. Katz, L., and Cameron, A. G. W., *Can. J. Physics*, **29**, 518 (1951)
5. Schiff, L. I., *Phys. Rev.*, **70**, 87 (1946)
6. Schiff, L. I., *Phys. Rev.*, **83**, 252 (1951)
7. Baldwin, G. C., and Klaiber, G. S., *Phys. Rev*, **73**, 1156 (1948)
8. Lawson, J. L., and Perlman, M. L., *Phys. Rev.*, **74**, 1190 (1948)
9. Blocker, W., Kenney, R. W., and Panofsky, W. K. H., *Phys. Rev.*, **79**, 419 (1950)
10. Sagane, R., *Phys. Rev.*, **84**, 586 (1951)
11. Terwilliger, K. M., and Jones, L. W., *Phys. Rev.*, **85**, 689 (1952)
12. Newkirk, L. I., *Bull. Am. Phys. Soc.*, **26**, 19 (1951)
13. Koch, H. W., McElhinney, J., and Cunningham, J. A., *Phys. Rev.*, **81**, 318 (1951)
14. Marshall, L., *Phys. Rev.*, **83**, 345 (1951)
15. Strauch, K., *Phys. Rev.*, **81**, 973 (1951)
16. Eyges, L., *Phys. Rev.*, **81**, 981 (1951)
17. Johns, H. E., Horsley, R. J., Haslam, R. N. H., and Quinton, A., *Phys. Rev.*, **84**, 856 (1951)
18. Stephens, W. E., Halpern, J., and Sher, R., *Phys. Rev.*, **82**, 511 (1951)
19. Montalbetti, R. (Personal communication transmitted by L. Katz)
20. Haslam, R. N. H., Katz, L., Horsley, R. J., Cameron, A. G. W., and Montalbetti, R. (Presented at Meeting Am. Phys. Soc., Washington, D. C., 1952)
21. Goward, F. K., Telegdi, V. L., and Wilkins, J. J., *Proc. Phys. Soc.* (*London*), [A]**63**, 402 (1950)
22. Wilkins, J. J., and Goward, F. K., *Proc. Phys. Soc.* (*London*), [A]**63**, 1173 (1950)
23. Wilkins, J. J., and Goward, F. K., *Proc. Phys. Soc.* (*London*), [A]**64**, 201 (1951)
24. Telegdi, V. L., and Zunti, W., *Helv. Phys. Acta*, **23**, 751 (1950)
25. Telegdi, V. L., *Phys. Rev.*, **84**, 600 (1951)
26. Perlman, M. L., and Friedlander, G., *Phys. Rev.*, **74**, 442 (1948)
27. Perlman, M. L., *Phys. Rev.*, **75**, 988 (1949)
28. Levinger, J. S., and Bethe, H. A., *Phys. Rev.* **78**, 115 (1950)
29. Bohr, N., *Nature*, **141**, 326 (1938)
30. Bohr, N., *Nature*, **141**, 1096 (1938)
31. Goldhaber, M., and Teller, E., *Phys. Rev.*, **74**, 1046 (1948)
32. Steinwedel, H., and Jensen, J. H. D., *Z. Naturforsch.*, **6a**, 218 (1951)
33. Danos, M., *Z. Naturforsch.*, **6a**, 218 (1951)
34. Danos, M., and Steinwedel, H., *Z. Naturforsch.*, **6a**, 217 (1951)
35. Benveniste, J., and Cork, B., *Phys. Rev.*, **83**, 894 (1951)
36. Courant, E. D., *Phys. Rev.*, **82**, 703 (1951)
37. Hirzel, O., and Wäffler, H., *Helv. Phys. Acta*, **20**, 373 (1947)
38. Schiff, L. I., *Phys. Rev.*, **73**, 311 (1948)
39. Ghoshal, S. N., *Phys. Rev.*, **80**, 939 (1950)
40. Katz, L., Johns, H. E., Baker, R. G., Haslam, R. N. H., and Douglas, R. A., *Phys. Rev.*, **82**, 271 (1951)
41. Haslam, R. N. H., Johns, H. E., and Horsley, R. J., *Phys. Rev.*, **82**, 270 (1951)
42. Gaerttner, E. R., and Yeater, M. L., *Phys. Rev.*, **77**, 570 (1950)
43. Gaerttner, E. R., and Yeater, M. L., *Phys. Rev.*, **77**, 714 (1950)

44. Gaerttner, E. R., and Yeater, M. L., *Phys. Rev.*, **79,** 401 (1950)
45. Gaerttner, E. R., and Yeater, M. L., *Phys. Rev.*, **82,** 461 (1951)
46. Halpern, J., and Mann, A. K., *Phys. Rev.*, **83,** 370 (1951)
47. Sagane, R., *Phys. Rev.*, **84,** 587 (1951)
48. Katz, L., and Cameron, A. G. W., *Phys. Rev.*, **84,** 1115 (1951)
49. Eyges, L., *U. S. Atomic Energy Commission Document, UCRL-1581* (1951)
50. Price, G. A., and Kerst, P. W., *Phys. Rev.*, **77,** 806 (1950)
51. McDaniel, B. D., Walker, R. L., and Stearns, M. B., *Phys. Rev.*, **80,** 807 (1950)
52. Cameron, A. G. W., *Phys. Rev.*, **82,** 272 (1951)
53. Walker, R. L., and McDaniel, B. D., *Phys. Rev.*, **74,** 315 (1948)
54. Heidmann, J., and Bethe, H. A., *Phys. Rev.*, **84,** 274 (1951)
55. Strauch, K. *Phys. Rev.*, (In press)
56. Mann, A. K., and Halpern, J., *Phys. Rev.*, **82,** 733 (1951)
57. Wilkinson, D. H., and Carver, J. H., *Phys. Rev.*, **83,** 466 (1951)
58. Toms, M. E., and Stephens, W. E., *Phys. Rev.*, **82,** 709 (1951)
59. Diven, B. C., and Almy, G. M., *Phys. Rev.*, **80,** 407 (1950)
60. Levinthal, C., and Silverman, A., *Phys. Rev.*, **82,** 822 (1951)
61. Byerly, P. R., Jr., and Stephens, W. E., *Phys. Rev.*, **83,** 54 (1951)
62. Katz, L., and Penfold, A. S., *Phys. Rev.*, **81,** 815 (1951)
63. Katz, L., and Penfold, A. S., *Phys. Rev.*, **83,** 169 (1951)
64. Curtis, N. W., Hornbostel, J., Lee, D. W., and Salant, E. O., *Phys. Rev.*, **77,** 290 (1950)
65. Diven, B. C., and Almy, G. M., *Phys. Rev.*, **80,** 407 (1950)
66. Terwilliger, K. M., Jones, L. W., and Jarmie, W. N., *Phys. Rev.*, **82,** 820 (1951)
67. Poss, H. L., *Phys. Rev.*, **79,** 539 (1950)
68. Millar, C. H., and Cameron, A. G. W., *Phys. Rev.*, **78,** 78 (1950)
69. Haslam, R. N. H., Cameron, A. G. W., Cook, J. A., and Crosby, E. H., *Phys. Rev.* (In press)
70. Haslam, R. N. H., Summers-Gill, R. G., and Crosby, E. H. (Personal communication)
71. Sugarman, N., and Peters, R., *Phys. Rev.*, **81,** 951 (1951)
72. Miller, R. D., *Phys. Rev.*, **82,** 260 (1951)
73. Kikuchi, S., *Phys. Rev.*, **80,** 492 (1950)
74. Kikuchi, S., *Phys. Rev.*, **83,** 1255 (1951)
75. Mozley, R. F., *Phys. Rev.*, **80,** 493 (1950)
76. Kerst, D. W., and Price, G. A., *Phys. Rev.*, **79,** 725 (1950)
77. Levinger, J. S., and Bethe, H. A., *Phys. Rev.*, **85,** 577 (1952)
78. Jones, L. W., and Terwilliger, K. M., *U. S. Atomic Energy Commission Document, UCRL-1618* (1951)
79. Walker, D., *Phys. Rev.*, **81,** 634 (1951)
80. Walker, D., *Phys. Rev.*, **84,** 149 (1951)
81. Keck, J. C., *Phys. Rev.*, **85,** 410 (1952)
82. Levinger, J. S., *Phys. Rev.*, **84,** 43 (1951)
83. Schiff, L. I., *Phys. Rev.*, **78,** 733 (1950)
84. Marshall, J. F., and Guth, E., *Phys. Rev.*, **78,** 738 (1950)
85. Benedict, T. S., and Woodward, W. M., *Phys. Rev.*, **85,** 924 (1952)
86. Marshall, L., Rosenfeld, A. H., and Wright, S. C., *Phys. Rev.*, **83,** 305 (1951)
87. Montalbetti, R.. and Katz. I.., *Phys. Rev.*, **83,** 892 (1951)

ANGULAR CORRELATION OF NUCLEAR RADIATION[1]

By Hans Frauenfelder[2]

Swiss Federal Institute of Technology, Zurich, Switzerland

We wish in this review to give a short account of the theoretical and experimental work on angular correlation of successive nuclear radiation. We confine our paper to problems involving a well-defined intermediate nuclear state. Other topics, e.g., simultaneous emission of two or more particles, radiation from aligned nuclei, and angular distribution of nuclear reactions, will be omitted completely.

ANGULAR CORRELATION IN NUCLEAR PHYSICS[3]

One of the main problems of contemporary low energy nuclear physics is the determination of the properties of nuclear energy levels. We may characterize nuclear states by the following quantities: energy (E), total angular momentum (I), parity (π), magnetic moment (μ), electric quadrupole moment (Q), partial level widths, and total transition probability. All these properties are as well defined for excited levels as for stable and for unstable ground states; the experimental determination of the enumerated quantities is, however, very different for stable and for unstable states. Stable isotopes are usually available in weighable quantities. Their ground states can therefore be investigated with methods in which time and quantity of material necessary for a measurement play no decisive role. The techniques of determining the characteristic qualities of ground states have achieved a very high degree of precision, and the known material is rapidly growing.

For radioactive nuclei, and especially for short-lived excited nuclear states, most of these well known methods fail completely and new ways have to be developed. Easiest to determine is the energy difference to the ground state by means of the highly developed alpha-, beta-, and gamma-spectroscopy. The total transition probability can in most cases also be ascertained by following the radioactive decay over a suitable period or by measuring delayed coincidences. For a large number of radioactive nuclei, the mode of decay has already been established, and some indications regarding the partial level widths have thus been obtained. Mechanical moments (spins) and parities are much more difficult to determine, because at present in all but a few cases direct methods are inapplicable. Much work has therefore been devoted to the establishment of nuclear decay schemes, from which

[1] The survey of the literature pertaining to this review was concluded in April, 1952.

[2] Now at the University of Illinois, Urbana, Illinois.

[3] We use throughout this article the following notations: the "directional correlation" is the angular correlation for cases in which the detectors are insensitive to polarization. For "polarization correlation" measurements, one or both detectors must also be sensitive to the direction of polarization. The term "angular correlation" includes both cases.

spins and parities may be inferred. Magnetic and electric moments have completely escaped any determination except for the ground states of a few long-lived radioactive nuclei. But exactly the investigation of these two properties for excited levels could throw light on topics of current importance, e.g., the explanation of the magnetic and electric moments.

The assignment of spin and parity to different energy levels is based mainly on a careful measurement of the properties of the radiation and a comparison with the corresponding theories (e.g., 27, 35, 43, 44, 59, 70, 92, 101, 130, 135). A study of the cross section and of the angular distribution of nuclear reactions also yields valuable information, especially for light nuclei (e.g., 13, 28, 35).

In order to make the assignment of spin, parity, and radiation character unique, it is important to use as many different methods of approach as possible. The measurement of the angular correlation of successively emitted nuclear radiation, developed in recent years, provides an additional method and has therefore rapidly become a valuable tool in nuclear spectroscopy (e.g., 26, 35, 87). It is naturally confined to those decays in which at least two particles are emitted successively and is therefore applicable only to a restricted class of radioactive isotopes. But this limitation is compensated by the fact that the angular correlation technique may not only yield information about spin and parity of nuclear levels, but may provide additional data:

(*a*) If one of the rays of a cascade is composed of two different multipoles, both being consistent with the selection rules, the angular correlation may be very sensitive to the mixing ratio and the relative nuclear phase. A measurement of the angular correlation therefore allows an exact determination of the phase and the intensity ratio, even in cases where the admixture is very small (3, 77, 80).

(*b*) In a few cases, the lifetime of the intermediate nuclear level can be measured by means of delayed coincidences. If this lifetime lies between 10^{-8} sec. and 10^{-5} sec., the directional correlation can be influenced by an external magnetic field, and this influence can be measured. Such a measurement of the anisotropy as a function of the external field-strength allows the determination of the nuclear g-factor. The magnetic moment then follows immediately, if the spin of this level is also known (4, 5, 10, 11).

(*c*) The correlation between a β-particle and a subsequent γ-ray depends not only on the spins of the three states and the characters of both radiations, but also on the type of interaction involved in β-decay. Likewise, the directional correlation between a β-particle and the simultaneously emitted neutrino, measured as correlation between β-particle and recoil nucleus, depends on the type of interaction. Both experiments therefore permit in principle a decision among the different possible forms of interaction in β-decay (40, 52, 108, 118).

(*d*) If the lifetime of the intermediate nuclear state is longer than a certain lower limit, say 10^{-10} sec., there always exists the possibility that the magnetic and electric fields of the electron shell and the surroundings partial-

ly or completely destroy the angular correlation. These interactions, which make questionable to some extent all angular correlation measurements, allow as a natural compensation the investigation of the interaction between shell and nucleus and of the state of the shell after a radioactive decay (2, 9, 50, 58, 117).

As one can see from these considerations, angular correlation measurements open several new and promising fields of research. But the presence of these many possibilities provides evidence that the whole domain is extremely complicated and that many phenomena are not well understood today. Much work, especially on the experimental side, needs to be done before these problems are properly solved.

THEORY

Principles and Method of Calculation

Introduction.—The basic problem of all angular correlation calculations can be stated as follows: A nucleus decays from a first level A by emitting a radiation R_1 with direction $\boldsymbol{k}_1$ into the intermediate state B and from there through the emission of R_2, direction $\boldsymbol{k}_2$, into the final state C. We ask then for the relative probability $W(\theta)\mathrm{d}\Omega$ that the radiation R_2 is emitted at an angle θ with respect to the direction $\boldsymbol{k}_1$ of the radiation R_1 into the solid angle $\mathrm{d}\Omega$. This probability $W(\theta)$ may depend upon the nature and the properties of the radiations R_1 and R_2, upon the properties of the three nuclear levels A, B, C, and also upon the presence of magnetic and electric fields.

At first sight, the appearance of anisotropic correlation functions seems surprising, because the radiation from a single transition A→B with equally populated magnetic sublevels m_a is always isotropic. But just the observation of the first radiation R_1 in the specified direction $\boldsymbol{k}_1$ causes the sublevels m_b of the intermediate state B to be populated according to the different transition probabilities $m_a \rightarrow m_b$. The radiation R_2, corresponding to the sum of all transitions $m_b \rightarrow m_c$, then has a definite and in general anisotropic distribution with respect to the direction $\boldsymbol{k}_1$ of the first radiation R_1.

The problem, which has to be solved by angular correlation theory, is to give explicit formulae for the various possible cases in a form suitable for comparison with experimental results. In recent years this problem has been attacked by a considerable number of authors, and a satisfactory theory has been worked out for many cases. At present, one can dare say that in the field of angular correlation, theory is well in advance of experiment.

The description of the entire angular correlation theory lies outside the scope of this review. We present therefore only a short account of the main lines of development, together with a survey of those results which are essential for the application to the experimental work. For all detailed questions, we refer to the original papers or to a forthcoming review article by Rose & Biedenharn (103). Elementary introductions into the theory can be found in the article of Deutsch (35) or in a book on theoretical nuclear physics by Weisskopf & Blatt (131).

Hamilton's theory.—The first theoretical investigation of the directional correlation between successively emitted nuclear γ-rays was made by Pryce. His calculations have not been published, but some of his results are contained in a paper by Dunworth (37). In the same year, Hamilton gave independently the first complete treatment of the subject (63). We summarize here his main considerations, because they form the basis of almost all later calculations. We use, however, mostly the notation of Falkoff & Uhlenbeck (39).

Hamilton starts with a system consisting of a nucleus and a quantized radiation field. Applying second-order damping theory, he finds the following expression for the directional correlation $W(\theta)$ between the two γ-rays with directions $\boldsymbol{k}_1$ and $\boldsymbol{k}_2$:

$$W(\theta) = W(\boldsymbol{k}_1, \boldsymbol{k}_2) = S_1 S_2 \sum_{m_a, m_c} \left| \sum_{m_b} (\mathrm{A}_{m_a} | \, \mathrm{H}_1(\boldsymbol{k}_1) \, | \, \mathrm{B}_{m_b})(\mathrm{B}_{m_b} | \, \mathrm{H}_2(\boldsymbol{k}_2) \, | \, \mathrm{C}_{m_c}) \right|^2 . \quad 1.$$

A_{m_a}, B_{m_b}, C_{m_c} are the wave functions for the degenerate sublevels of initial, intermediate, and final nuclear state, which are characterized by their total angular momenta I_a, I_b, I_c, and their magnetic quantum numbers m_a, m_b, m_c. $H_i(\boldsymbol{k}_i)$ represents the interaction Hamiltonian for the emission of the particle i in the direction $\boldsymbol{k}_i$. The matrix elements $(\mathrm{A}_{m_a} | \, H \, | \, \mathrm{B}_{m_c})$ are the probability amplitudes for the various possible transitions between degenerate sublevels. S_1 and S_2 mean averaging over all nonmeasured radiation properties (e.g., spin, polarization), $\sum_{m_a, m_c}$ denotes the summation over the usually equally populated initial and final sublevels. It is to be noted that in Equation 1, and in all following formulae, uninteresting (i.e., angular independent) factors are discarded.

Equation 1 is not very suitable for evaluation, because the summation over the intermediate degenerate sublevels m_b has to be carried out before (rather than after) squaring. This therefore means that interference exists among the various possible transitions from a given initial to a given final state. This interference can be removed if the z-axis of quantization is taken along the direction of emission of one of the decay particles. Hamilton has proved this theorem, which greatly facilitates all explicit calculations, for the $\gamma-\gamma$-case. It was later shown by Lloyd (79), Spiers (113), and Tolhoek & de Groot (123) that the theorem holds for all particles, provided that the detectors are polarization-insensitive. An especially simple proof has been provided by Lippmann (78): If the first quantum is emitted along the axis of quantization, its magnetic quantum number and therefore also the magnetic quantum number of the intermediate nuclear state are constants of the motion and can, at least in principle, be measured. This naturally removes all interferences. Because Equation 1 is symmetrical with respect to the first and second radiation, this holds also if the second quantum is emitted along the axis of quantization.

Thus, with the direction $\boldsymbol{k}_1$ of the first quantum chosen to be the axis of quantization, Equation 1 becomes

$$W(\theta) = \sum_{m_b} \left\{ \sum_{m_a} [S_1 | (A_{m_a} | H_1(0) | B_{m_b})|^2] \sum_{m_c} [S_2 | (B_{m_b} | H_2(\theta) | C_{m_c})|^2] \right\}. \quad 2.$$

In this form, the physical interpretation of the summands occurring in Equation 2 can immediately be seen (39):

$$S_1 | (A_{m_a} | H_1(0) | B_{m_b})|^2 \equiv P_{m_a m_b}(0)$$

is the relative probability for the emission of the first γ-ray along the direction $\theta = 0$. A similar statement holds for the second factor in Equation 2. The directional correlation can therefore be written as

$$W(\theta) = \sum_{m_a m_b m_c} P_{m_a m_b}(0) P_{m_b m_c}(\theta). \quad 3.$$

The probabilities for each transition A→B and B→C now appear independently in Equation 3. One can therefore first study the structure of $P_{m_a m_b}(\theta)$ for a single transition and then proceed to the directional correlation.

The relative probability $P_{m_a m_b}(\theta)$ for the emission of a quantum, with total and z-component of angular momentum L and M_1 between the two sublevels (I_a, m_a), (I_b, m_b) of A and B in the direction θ with respect to the z-axis can be decomposed into two factors (cf. 39, 63, 133):

$$P_{m_a m_b}(\theta) = [C^{I_b m_b}_{I_a m_a LM}]^2 F_L^M(\theta) \quad 4.$$

$$I_a + L = I_b, \qquad m_a + M = m_b. \quad 5.$$

The first factor of Equation 4, $[C^{I_b m_b}_{I_a m_a LM}]^2$, gives the intensity for this particular transition and depends only upon the quantum numbers I_a, m_a, I_b, m_b, L, but not upon the nature of the radiation. The $C^{I_b m_b}_{I_a m_a LM}$ are directly the vector addition coefficients ("Wigner" or "Clebsch-Gordan" coefficients) for the vector addition 5 (cf. 30, 95, 133). In the notation of Condon & Shortley (30), they are given by $(I_a, L, m_a, M \mid I_a, L, I_b, m_b)$.

The second factor, $F_L{}^M(\theta)$, represents the angular distribution of this transition and depends entirely upon the nature of the radiation and its quantum numbers L and M.

Hamilton calculated the correlation of successive γ-rays, each having a definite value of the quantum number L (further referred to as pure γ-rays), by using the equations 3 and 4 and carrying out the necessary tedious summations. He showed that for radiations not higher than quadrupole, the angular correlation function 3 can be written as

$$W(\theta) = 1 + a_2 \cos^2\theta + a_4 \cos^4\theta \quad 6.$$

and gave explicit formulae for the coefficients a_2 and a_4 for dipole and quadrupole radiation.

Restrictions in Hamilton's theory.—Hamilton's work contains a number of essential restrictions. We will enumerate these restrictions and discuss their meaning and importance.

I. The intermediate nuclear state is assumed not to be disturbed by ex-

ternal fields (58, 63). A perturbation of the intermediate nuclear state can occur, e.g., through the interaction of the nuclear magnetic moment with the magnetic field of the electron shell or of the nuclear electric quadrupole moment with inhomogeneous electric fields. Condition I then implies that the precession of the nuclear spin, induced through such interactions, is negligible during the lifetime of the intermediate state, i.e., that the natural line-width of the intermediate nuclear state is much larger than the hyperfine splitting of that state. The magnetic quantum numbers m_b are then constants of the motion. From the theoretical standpoint, the fulfillment of this condition can easily be assumed. In most experimental cases, however, it is very difficult to decide whether the measured correlation function is really undisturbed or not.

II. The magnetic sublevels of the initial (and final) nuclear states are assumed to be uniformly populated. This condition is usually fulfilled in all double cascades (i.e., cascades consisting of two successive radiations). It may, however, be violated when the angular correlation of a double cascade is observed at very low temperatures under the influence of a strong external magnetic field (111), or when one measures three radiations in cascade (triple cascade) (21). In the first case, the different intitial sublevels have slightly different energies and are therefore populated according to a Boltzmann distribution. In the second case, the sublevels of the second nuclear state, forming the initial sublevels for the following double cascade, are populated according to the transition probabilities for the different components of the first transition.

III. The radiations R_1 and R_2 are assumed to be pure γ-rays. The dependence of the angular correlation function $W(\theta)$ upon the nature of the radiation is contained entirely in the expression $F_L{}^M(\theta)$ of formula 4. The extension of the theory to radiations other than γ-rays requires a knowledge of the corresponding functions $F_L{}^M(\theta)$. For particles with spin 0 (e.g., α-particles) and spin 1 (pure and mixed γ-rays), the $F_L{}^M(\theta)$ can be derived using classical theories (39, 77). For other radiations, e.g., β-particles and conversion electrons, an interaction Hamiltonian without classical analog enters explicitly into the calculation (40, 52, 102).

IV. Both detectors have to be polarization-insensitive, i.e., the angular correlation is averaged over the polarization of both γ-rays (directional correlation). This restriction allows removal of interferences between the two transitions by choosing as quantization axis the direction of emission of one particle. But if the polarization is also measured, instead of Equation 2, the more general formula 1 has to be used.

Generalization of the method.—One of Hamilton's main results was the explicit calculation of the coefficients a_2 and a_4, occurring in the directional correlation function $W(\theta)$, Equation 6, for pure dipole and quadrupole radiation. In order to find these coefficients, he had to carry out summations over the magnetic quantum numbers. This laborious task makes it cumbersome to extend the theory in its original form to higher multipoles. The further

development was therefore devoted not only to the removal of the restrictions I to IV, but also to the simplification of the theory. It is this second topic which we will consider here.

A first essential step was the extensive use of group theory. The application of this powerful tool seems natural in view of the symmetry properties of angular correlation problems. Some group theoretical theorems appeared in the first papers of Hamilton and Goertzel (58, 63), but the treatment of angular correlation, based entirely on group theory, comes from Yang (136) and Fierz (46). Yang proved general statements about the form of the directional correlation function $W(\theta)$. Fierz calculated the expressions for the angular correlation of γ-rays and conversion electrons, but could not give closed formulae.

The next improvement was made by Gardner (53) in his work on the correlation of conversion electrons. As said before, the calculation of the coefficients a_{2k} in the expansion

$$W(\theta) = 1 + \sum_{k=1}^{k_m} a_{2k} \cos^{2k} \theta \qquad 7.$$

involves summations which cannot be performed in closed form. Gardner showed that coefficients A_{2k} may be obtained in closed form if one uses in place of the expansion 7 a better suited one:

$$W(\theta) = 1 + \sum_{k=1}^{k_m} A_{2k} P_{2k}(\cos \theta). \qquad 8.$$

Here, the P_{2k} (cos θ) are the Legendre polynomials of degree $2k$. The coefficients A_{2k} involve the product of five Clebsch-Gordan coefficients C, summed over certain arguments. Now Racah had shown earlier (95) that the sums of products of three C's can all be evaluated using so-called Racah coefficients $W(abcd; ef)$. Using Racah's relation twice, Gardner could transform the coefficients A_{2k} into the following form:

$$A_{2k} = C^{2k0}_{L_{i0}L_{i0}} W(I_B I_A 2k L_1; L_1 I_B) C^{2k0}_{L_{20}L_{20}} W(I_B I_C 2k L_2; L_2 I_B) \qquad 9.$$

where all symbols have the usual meaning. It can be seen from this formula that the coefficients A_{2k} can be separated into two factors

$$A_{2k} = (\mathrm{AB})_{2k}(\mathrm{BC})_{2k}. \qquad 10.$$

Each of these factors depends upon only one of the transitions A→B, B→C. Tables of the functions C and W have been published (30, 67), so the coefficients A_{2k} can immediately be written down.

Gardner's formulae are restricted to the directional correlation of conversion electrons. Later work was devoted to the application to other radiations. As was shown especially by Lloyd (79, 82), Alder (9, 11), and Racah (96), it is advantageous to use suitable functions (in no case $\cos^{2k}\theta$) for the development of the angular correlation function. It is then possible to find closed expressions for the coefficients of this expansion, even for arbitrary nuclear particles and when multipole mixtures and polarizations are included.

For arbitrary particles, but pure and unpolarized radiation, the expansion 8 holds and the factors $(AB_{2k}$, $(BC)_{2k}$ can be written as

$$(AB)_{2k} = \left\{ \sum_M C^{2k0}_{LML-M}(-1)^M F_L^M(0) \right\} W(I_B I_A 2kL; LI_B). \qquad 11.$$

A general expression for the directional distribution function $F_L{}^M(\theta)$ has been given, e.g., by Falkoff & Uhlenbeck (39) [cf. also (11, 77, 82)].

Recently, Fano (42) introduced the density matrix into the theory in order to avoid the summations over the magnetic quantum numbers. This technique permits a generalization of Racah's algebra. Fano's method has yielded no new results, but is perhaps well suited to the investigation of the influence of extranuclear fields upon the angular correlations.

Angular Correlation Theory for a Free Nucleus

Notation.—It is the purpose of the following paragraphs to give the theoretical results, without numerical values, to the extent usually required by an experimental worker.

A double cascade between the states A, B, and C will be written as $A(R_1, L_1)B(R_2, L_2)C$. R_1 and R_2 denote the particles emitted in the first and second transitions, e.g., α, β, γ, e^-. L_1 and L_2 characterize these particles; e.g., for γ-rays, L_1 and L_2 are the multipole orders. A, B, and C are replaced by I_A, I_B, and I_C when the angular momenta are sufficient to characterize the nuclear states. The symbols R_1 and R_2 will be omitted if the emitted particles are otherwise specified.

For the description of the directional correlation function $W(\theta)$, we use in general the expansion into Legendre polynomials (formula 8), coefficients A_{2k}). Formulae for the conversion $A_{2k} \rightleftarrows a_{2k}$ have been given by Lloyd (83). A denotes always the anisotropy, defined by

$$A = [W(180°)/W(90°)] - 1. \qquad 12.$$

Directional correlation of $\gamma-\gamma$-cascades with pure radiations.—The coefficients a_{2k} for dipole and quadrupole radiation can be found in Hamilton's paper (63). Falkoff (41) gives numerical values for the coefficients a_{2k} for cascades $I_A(L_1)I_B(L_2)I_C$, with $I_C = 0$, $L_1 \leqq 7$, $L_2 \leqq 3$.

Numerical values for the coefficients A_{2k} for $L_1 \leqq 4$, $L_2 \leqq 6$, together with a general expression for A_{2k} have been published by Lloyd (83) for transitions where the γ-rays are emitted with the lowest angular momentum allowed by selection rules (cf. also 56).

Some general statements which are important for the application to experimental results can be taken from the different theoretical papers:

(*a*) The directional correlation function $W(\theta)$ depends only upon the multipole orders L_1, L_2 of the γ-rays and the angular momenta I_A, I_B, I_C of the three nuclear levels, but not upon their parities. It is therefore impossible to distinguish between electric and magnetic radiation of the same multipole order. This statement is immediately rendered plausible from a classical analogy: the transformation electric$\rightarrow$magnetic ($\boldsymbol{E} \rightarrow \boldsymbol{H}$, $\boldsymbol{H} \rightarrow -\boldsymbol{E}$) leaves the

Poynting vector and therefore the distribution of the radiated energy unaltered.

(*b*) The maximum value k_m in either the expression 7 or 8 is given by

$$k_m \leqq \text{Min}\,(L_1, L_2, I_B),\ k_m \text{ integer.} \qquad 13.$$

Therefore no correlation exists if $I_B = 0$ or $1/2$. $W(\theta)$ has the form $1 + A_2 P_2$ $(\cos\theta)$ if either $I_B = 1,\ 3/2$, or L_1 or $L_2 = 1$ (39, 58, 63, 135).

(*c*) Two pairs of transitions which are each other's inverses, i.e., $I_A(L_1)$-$I_B(L_2)I_C$ and $I_C(L_2)I_B(L_1)I_A$, have the same correlation function (63).

(*d*) The directional correlation is the same for both of the cascades

$$I - L_1(L_1)I(L_2)I + L_2 \quad \text{and} \quad I + L_1(L_1)I(L_2)I - L_2$$

and is furthermore independent of the value of I (82, 83).

The directional correlation theory has been extended by Biedenharn, Arfken & Rose (21) to triple cascades. These authors have also investigated the directional correlation between the γ-rays of the first and third transition in a triple cascade (one-three-correlation) (12).

$\gamma-\gamma$-Correlation with mixed transitions.—Parity and angular momentum selection rules permit in general the simultaneous emission of different magnetic and electric multipole radiations within the same transition. Recent theoretical estimates of Weisskopf (130, 131) indicate that in parity-favored transitions, where EL and $M(L+1)$-pole[4] are the lowest and next-lowest allowed multipoles, the magnetic radiation can always be neglected. In parity-unfavored transitions, where ML and $E(L+1)$-pole compete, most of the γ-rays are emitted as magnetic radiation. In certain cases, however, the contribution of the $E(L+1)$-pole radiation may be appreciable. Such a contribution has been experimentally observed for $M1+E2$ transitions, where two reasons can account for occurrence of a mixture: additional selection rules may make the $M1$ transition forbidden (14) or the $E2$ transition may be of the "cooperative" type [cf. (59)]. Such a mixed transition can be characterized by the ratio δ of the nuclear matrix elements for the emission of the two multipoles. The sign of the real quantity δ then gives the relative phase of both multipoles, its square δ^2 the intensity ratio of the $E(L+1)$ to the ML-pole radiation.

The first theory of the directional correlation for a cascade, in which only one transition is pure, was given by Ling & Falkoff (77). They assumed the first γ-ray to be pure dipole or pure quadrupole radiation, the second transition to be a mixture of $M1$ and $E2$-pole radiation and obtained expressions for the coefficients a_2 and a_4. These coefficients are functions of the intensity ratio $\delta^2(E2/M1)$, of an arbitrary nuclear phase (δ complex), and of I_A, I_B, I_C, L_1, and L_2. It turns out that the correlation function $W(\theta)$ of a mixture is not the weighted sum of the individual functions, because of the occurrence of interference terms. The anisotropy of a mixed cascade can be considerably greater than that of either one of the pure cascades and may even have the opposite sign [cf. Figure 2 of (3) and Figure 2 of (77)].

[4] We denote with $E\,L$ ($M\,L$) electric (magnetic) L-pole radiation.

Using Ling & Falkoff's expressions, the interpretation of an experimentally measured correlation involves considerable arbitrariness because of the arbitrary choice of the nuclear phase. Lloyd, however, showed that only the values 0° and 180° of the phase have physical significance, i.e., that the quantity δ is real (80). The theory of Ling & Falkoff, together with Lloyd's restriction, is now well suited for the interpretation of pure-mixed correlations involving radiations not higher than quadrupole.

Lloyd further extended the theory to cascades, in which both transitions are mixed (δ_1, δ_2) and in which higher multipole orders than $L=2$ can occur (82, 83). His formulae are, however, restricted to small mixing ratios, i.e., terms in δ_1^2 and δ_2^2 are neglected.

Directional correlation with α-particles.—The angular distribution functions $F_L{}^M(\theta)$ are especially simple for spinless particles (39); one expects therefore simple rules for the directional correlation. Lloyd (82, 83) and Rose, Biedenharn & Arfken (102) have in fact shown that the $\alpha-X$-correlation function can easily be obtained, if, e.g., the corresponding $\gamma-X$-correlation function is known (X denotes any particle).

We suppose the $\gamma-X$-correlation for the cascade $I_A(\gamma)I_B(X)I_C$ to be given by Equation 8. If now instead of the γ-ray an α-particle with definite angular momentum L_1 is emitted in the first transition (which involves a nuclear parity change of $(-1)^{I_A-I_B}$ if $I_A \neq I_B$ and (-1) if $I_A=I_B$), then the $\alpha-X$-directional correlation is

$$W(\theta) = 1 + \sum_{k=1}^{k_m} z_{2k}(L_1)A_{2k}P_{2k}(\cos\theta) \qquad 14.$$

with

$$z_{2k}(L) = \frac{2L(L+1)}{2L(L+1) - 2k(2k+1)}. \qquad 15.$$

If the α-particle is emitted in the second transition, the resulting formula is quite analogous [cf. for $\alpha-\gamma$-correlation also (122)].

Directional correlation involving conversion electrons.—The directional correlation of cascades in which one or both radiations are conversion electrons from s states (e.g., K-shell) has been dealt with in various approximations by several authors (46, 53, 54, 75). Only Rose, Biedenharn & Arfken (102) have given, however, the correct relativistic treatment, restricted to K electrons. We summarize here their main results:

(*a*) The internal conversion directional correlation ($e^- - \gamma$, $\gamma - e^-$, $e^- - e^-$) depends not only upon the spins of the three nuclear states and the angular momenta of the emitted radiations, but also upon the physical parameters Z, π, and k. Z is the nuclear charge, π and kmc^2 are parity and γ-ray energy of the converted radiation(s).

(*b*) The directional correlation between a conversion electron and any other radiation X can be obtained immediately if the corresponding correlation function with a γ-ray replacing the conversion electron is known. Suppose the $\gamma-X$-correlation for cascade $A(\gamma, L_1)B(X)C$ to be given by formula

8. Then we obtain the $e^- - X$-correlation simply by multiplying each coefficient A_{2k} of 8 by a parameter b_{2k}:

$$W_{e^- - X}(\theta) = 1 + \sum_{k=1}^{k_m} b_{2k}(e^-) A_{2k} P_{2k}(\cos\theta). \qquad 16.$$

If both transitions are converted (e_1^-, e_2^-), we start with formula 8 for the corresponding $\gamma-\gamma$-cascade and insert two parameters $b_{2k}(e_1^-)$ and $b_{2k}(e_2^-)$:

$$W_{e^- - e^-}(\theta) = 1 + \sum_{k=1}^{k_m} b_{2k}(e_1^-) b_{2k}(e_2^-) A_{2k} P_{2k}(\cos\theta). \qquad 17.$$

Rose, Biedenharn & Arfken have calculated the coefficients b_{2k} for K shell conversion for 12 values of Z in the range $10 \leqq Z \leqq 96$ and transition energies from 0.3 mc^2 to 5.0 mc^2 for five electric and five magnetic multipoles (102).

(*c*) Because of the close relationship of internal conversion with γ-directional correlation, the rule (*b*) of the section, *Directional correlation of $\gamma-\gamma$-cascades with pure radiations*, is valid also for conversion electrons. The same holds for the rules (*a*) and (*d*) of the same section under the assumption that the parameters Z, π, and k have the same values for corresponding radiations.

(*d*) If the γ-transition in an $e^- - \gamma$ or $\gamma - e^-$-cascade is mixed, formula 16 holds also, provided the coefficients $A_2 k$ have been calculated for the mixed $\gamma-\gamma$-cascade (cf. section on $\gamma-\gamma$-*Correlation with mixed transitions*).

(*e*) The case where the converted transition is mixed has not yet been calculated. Fierz (46) and Gardner (54) have noted that interference terms are absent when only K-electrons are considered and when a nonrelativistic treatment of internal conversion is justified. Gardner (55) has shown, however, that interference terms arise as soon as one of these two restrictions is violated.

(*f*) In the high energy limit, conversion electrons give the same correlation function as do the corresponding γ-rays. For small energies (and low Z) the correlation parameters b_{2k} tend for electric transitions toward threshold values, which are independent of Z and the energy k. The b_{2k} values for magnetic transitions on the other hand depend also in the nonrelativistic limit upon Z and k [cf. also (56)].

$\beta-\gamma$ Directional correlation.—The theory of the $\beta-\gamma$-directional correlation differs essentially from the cases described under the four preceding sections in that the choice of the interaction Hamiltonian remains as yet far from unique. It is well known that one has to consider in β-decay five different types of interaction (70) and every theory of $\beta-\gamma$-correlation has to be worked out for all these interactions.

Falkoff & Uhlenbeck (40) first developed a theory of $\beta-\gamma$-correlation, but assumed two important restrictions: a zero nuclear charge Z and only one nuclear matrix element responsible for the β-transition. Fuchs & Lennox (51, 52) later relaxed both restrictions and found results considerably differing from those of Falkoff & Uhlenbeck [cf. also (102) for an objection raised to the calculation of Fuchs].

The theoretical basis of the $\beta-\gamma$-correlation is therefore at present not completely developed, and we give here only a few general statements:

(*a*) The $\beta-\gamma$-directional correlation of a cascade $A(\beta)B(\gamma, L_2)C$ depends in general not only upon spin and parity of the two first and spin of the third nuclear state, multipole order L_2 of the γ-ray, and energy E of the β-particle, but also upon the β-interaction Hamiltonian, and upon specific properties of the nuclear wave functions in the states A and B.

(*b*) The $\beta-\gamma$-correlation for β-rays in the particular energy range E to $E+dE$ will be called the differential correlation $W(\theta, E)$. The integral directional correlation $W(\theta)$ will be observed if β-particles of all energies are detected. The differential correlation has in general its maximum anisotropy for the maximum β-energy E_{max} and always becomes isotropic for $E \rightarrow 0$.

(*c*) The correlation function $W(\theta, E)$ can be represented by the expansion 8. The highest term k_m is limited by the order of the spherical harmonic of the electron wave function (and by I_B and L_2). All allowed and a few additional matrix elements therefore cause isotropic distributions. If the shape of the energy spectrum is strictly identical with that of an allowed transition, $W(\theta, E)$ is also isotropic.

(*d*) For matrix elements giving rise to anisotropic correlations, there is a close connection between the behavior of the correlation and that of the correction factor $C(Z, E)$ by which an allowed spectrum has to be multiplied to give the desired forbidden distribution. For $C(Z, E) \approx C(Z)$, there results practically no directional correlation. On the other hand the correlation is large if $C(Z, E)$ is strongly dependent on E, but only slightly on Z. With $C(Z, E)$ depending equally on both parameters Z and E, the correlation is small, but does not completely vanish.

(*e*) The connection (*d*) holds as long as only one matrix element is present. When two or more matrix elements are nonvanishing, strongly anisotropic interference terms can occur and mask the connection between the directional correlation and the correction factor.

Polarization correlation.—The polarization correlation of successive γ-rays was first investigated by Falkoff (38), following a suggestion of Madansky. He found an expression for the relative polarization of two successive antiparallel quanta. (This polarization-polarization correlation is experimentally difficult to realize, because statistics will always be very poor.) Hamilton (64) calculated the correlation between the direction of one and the direction and polarization of the other quantum, for dipole and quadru pole radiation. Zinnes (137) extended the theory of the direction-polarization correlation to higher multipoles and included also mixed transitions.

We give here a short account of the main features of the direction-polarization correlation:

(*a*) In contradistinction to the directional correlation of successive γ-rays, the direction-polarization correlation provides a means of distinguishing between the electric and magnetic multipole character of the γ-transition and can therefore be used to investigate the relative parities of nuclear levels.

(*b*) All information concerning the polarization of a γ-ray can be expressed in terms of the intensities $J_\parallel$ and $J_\perp$ of the linear polarizations parallel and perpendicular to the plane defined by the two γ-rays. (In Hamilton's notation $J_\parallel = J_\theta$, $J_\perp = J_\theta$, and the direction of polarization is identified with the direction of the electric vector.)

(*c*) The direction-polarization correlation of pure γ-rays is simply related to the corresponding directional correlation. For dipole and quadrupole radiation, Hamilton (64) has found the connecting expressions. Formulae for γ-rays up to octopole have been given by Zinnes (137) [cf. also (84)].

(*d*) The ratio $J_\parallel/J_\perp (= J_\theta/J_\phi)$ is always unity at $\theta = 180°$ and takes on the maximum deviation from unity at $\theta = 90°$.

(*e*) The direction-polarization correlation of a cascade in which one transition is mixed is also related to the corresponding directional correlation. Combining the tables of Zinnes (137) and Ling & Falkoff (77) and using Lloyd's restriction (80), the direction-polarization correlation can be calculated.

The Influence of Extranuclear Fields on Angular Correlation

The basis of all statements made thus far is that the magnetic quantum numbers of the intermediate nuclear state are constants of the motion, i.e., that condition I of p. 5 is satisfied. In his very first paper, Hamilton pointed out the importance of this restriction (63). Goertzel (58) extended the directional correlation theory to take into account the effect of the atomic shell electrons and of external magnetic fields. Alder (9, 10, 11) generalized Goertzel's calculations and gave in addition particularly simple expressions for some special cases [cf. also (81)].

These theoretical papers all assume the shell to be in a stationary state and the atom to be free. In reality, these two important restrictions are justified only in very few cases. A removal of them, however, would require a complete treatment of the processes which occur in the shell after a radioactive decay and a detailed theory of the influence of the surroundings on the electron shell. Both are lacking at present, and instead of being able to calculate the exact state of the shell during the time the nucleus is in its intermediate level, we have to be satisfied with qualitative considerations.

The interaction between shell and nucleus in a free atom.—The following theoretical results are valid for free atoms with their electron shells in stationary states, and under the assumption that all individual nuclear cascades, regardless of their lifetime in the intermediate state, are observed [cf. (5)].

(*a*) The disturbance of the angular correlation by the electron shell is negligible if the radiation width of the intermediate nuclear level is much greater than the hyperfine-splitting (hfs) $\Delta\nu$ caused by the atomic electrons (58, 63). This condition is fulfilled if the lifetime T_B of the intermediate nuclear state satisfies the relation

$$T_B \ll T_{\text{crit.}}; \qquad T_{\text{crit.}} = (2\pi c \Delta\nu)^{-1}. \qquad 18.$$

Assuming for $\Delta\nu$ values between 0.01 cm.$^{-1}$ and 1 cm.$^{-1}$, one obtains upper limits to $T_{crit.}$ between 5×10^{-10} sec. and 5×10^{-12} sec. A comparison of these values with theoretical (130, 131) and empirical (59) lifetime formulae shows that almost all multipole radiations occurring in angular correlation measurements may be subject to perturbations.

(*b*) The directional correlation function in the presence of the field of the electron shell can be written as

$$W(\theta) = 1 + \sum_{k=1}^{k_m} G_{2k} A_{2k} P_{2k}(\cos\theta), \qquad 19.$$

where the whole influence of the shell is contained in the attenuation factor G_{2k} (9, 11). As can be seen from special cases, the attenuation becomes stronger with increasing index k and with decreasing spin I_B.

(*c*) For large values of $\Delta\nu\times T_B$, the attenuation factor G_{2k} tends toward a minimum value $G_{2k,\,min}$, which in general is different from zero. (If, however, the atoms are imbedded in a solid, the directional correlation may be entirely destroyed.)

(*d*) If the attenuation of the directional correlation is due to the action of the magnetic field of the electron shell, the undisturbed correlation function can be obtained by bringing the radioactive atoms in a strong magnetic field parallel to the direction of one of the measured quanta (58). The condition for the magnetic field H to be sufficiently strong to restore the directional correlation is given by

$$\mu H \gg h\Delta\nu, \qquad 20.$$

where μ is the magnetic moment of the electron shell level.

Atomic processes in solids after a radioactive decay (*Qualitative considerations*).—Consider, e.g., a $\gamma-\gamma$-cascade, $A(\gamma_1)B(\gamma_2)C$, between the nuclear states A, B and C, the lifetimes of the first two levels being T_A and T_B. The radioactive decay which initiates the cascade and leads to state A causes in general also the electron shell to be in an excited state; e.g., K-capture creates a hole in the K-shell, β^--decay causes the atom to be singly ionized. The nuclear recoil also can play an important role. After the initial event (e.g., K-capture, or β^--decay), shell and nucleus tend to reach their ground states; the nucleus by decaying through the $\gamma-\gamma$-cascade, the shell by setting free the excitation energy through successive emission of Auger electrons and X-rays (K-capture) or by capturing an electron (β^--decay).

The nuclear and the shell cascades run off after the initial event almost independently of each other. We are now interested in the state of the shell during the time the nucleus spends in level B. A knowledge of its properties, especially of the hyperfine splitting $\Delta\nu$ and the spin J, allows an estimation of the effect which the shell executes on the angular correlation.

We consider first the processes occurring in a free atom. After a β^--decay, the atom remains singly ionized (106). After a K-capture, the atom initially remains neutral. But because the de-excitation in general occurs not only

through the emission of x-rays, but also by Auger electrons, the atom may even become charged (31).

The disturbance of the angular correlation in a free atom therefore depends on how far the shell cascade has proceeded when the nucleus reaches the intermediate state B; i.e., it depends on T_A, T_B, and the different shell transition probabilities.

If the atom is imbedded in a solid, the whole picture is more complicated. An atom, ionized after a β^--decay, can capture an electron. The de-excitation in the outermost shell after a K-capture may be much faster than in the free atom because of radiationless transitions. Furthermore, the splitting of the atomic energy levels brought about by the crystalline electric field causes in many solids the orbital moment of the shell (and therefore also the magnetic field at the nucleus) to be considerably smaller than in a free atom [Quenching, cf. (1, 125)].

The field strengths, present at the nucleus in a free atom and in a solid, are in some cases known from investigations of optical hyperfine structure (71) and nuclear resonance absorption (22, 62, 94). We give in Table I some

TABLE I

TYPICAL FIELD STRENGTHS AT THE NUCLEUS

Source of the field	Field strength Approximate values	$T_{crit.}$ sec.	Literature
Electron shell	10^5–10^6 oersted	10^{-10}–10^{-11}	(71)
Inhomogeneous electric fields in crystals or molecules	10^{16}–10^{19} Volt/cm.^{2}	10^{-6}–10^{-9}	(124, 94)
Neighboring paramagnetic atoms (in solids or liquids)	10^4 oersted	10^{-8}	(62)
Neighboring nuclei (in solids or liquids)	1 oersted	10^{-4}	(22)

typical values. If the lifetime T_B of the intermediate nuclear state is of the same magnitude as $T_{crit.}$, a perturbation of the angular correlation is to be expected.

Atoms with vanishing magnetic moment in the ground state.—The electron shells of many nuclides with measurable $\gamma-\gamma$-cascades have in their ground state no magnetic moment [cf. Table I of (50)]. For all of these cascades, no disturbance is to be expected in the three following cases (T_s denotes the time the shell needs to return into its ground state after the initial exciting decay):

(*a*) $T_B \ll (2\pi c\Delta\nu)^{-1}$ (cf. p. 13), (*b*) the shell returns to its ground state before the probability of the nucleus to be in the intermediate state is appreciable ($T_s \ll T_A$) (this condition is sufficient only if the first γ-ray of the cascade causes no new excitation of the electron shell), (*c*) the time during

which the shell acts on the intermediate state is too short to have an effect $[T_s \ll (2\pi c\Delta\nu)^{-1}]$.

If the first particle of the cascade to be investigated also excites the electron shell (e.g., $\beta-\gamma$- or $e^-\gamma$-correlation), only the cases (*a*) and (*c*) allow undisturbed observations.

One way to find under favorable circumstances an influence of the electron shell on the angular correlation is to use a suitable radionuclide with sufficiently long lifetime T_B so that condition (*a*) is not fulfilled, and to imbed it in different media (50).

The radioactive atom imbedded carrier free in a suitable ionic crystal can act as an impurity center. Impurity centers in general have long decay times in the outermost shell ($T_s \gg 10^{-8}$ sec.), caused by the fact that the excited electron orbits have a great radial extension (15, 89). The matrix element for the transition from the excited to the ground state then is small, the lifetime therefore large (89).

If on the other hand the radioisotope is imbedded in a suitable metal, the time T_s may be very short, because the hole (created initially by the K-capture or β^--decay) can move in the full band. A crude calculation gives very short times $T_s (T_s < 10^{-12}$ sec.) so that probably our considerations have to include also the lifetime in the next inner shell (which can be longer).

The angular correlation of "ionic crystal" sources therefore may be disturbed, whereas measurements with "metal" sources yield in favorable cases the true correlation function.

The influence of external magnetic fields.—The influence of a constant external magnetic field, in the absence of any perturbation by the electron shell, can be calculated explicitly (10, 11). An external field H, applied perpendicular to the plane of the two registered quanta, induces in the directional correlation an attenuation and a phase shift [cf. also (81)]. Both can be observed, if each detector is sensitive to only one γ-ray:

$$W(\theta, H) = \text{Real part of } \left\{ \sum_{k=0}^{k_m} \frac{b_{2k}}{1 - i\,2k\omega T_B} e^{2ki\theta} \right\}, \qquad 21.$$

with

$$\omega = \mu H / I_B \hbar = g\mu_k H/\hbar \qquad 22.$$

($\hbar = h/2\pi$, $g = g$-factor of the intermediate nuclear level, $\mu_k =$ nuclear magneton).

If both detectors are equally sensitive to both γ-rays, the attenuation factor becomes real, the phase shift vanishes:

$$W(\theta, H) = \sum_{k=0}^{k_m} \frac{b_{2k}}{1 + (2k\omega T_B)^2} \cos 2k\theta. \qquad 23.$$

METHOD AND APPARATUS

General Remarks

Let us consider a radioactive source which emits in cascade the radiations R_1 and R_2. Two detectors, one fixed and one movable, subtend an angle θ at the source. Two radiations are recognized to belong to the same decay by means of a coincidence circuit. The directional correlation function $W(\theta)$ is then given, apart from corrections, by the number of coincidences recorded for different angles θ.

The idea of measuring the directional correlation is thus extremely simple. With the present experimental technique, crude results can be found for many $\gamma-\gamma$-cascades in a short time and without great precautions. But as soon as precision measurements or the extension to other than $\gamma-\gamma$-cascades are requested, problems grow difficult. Without going into details, we shall point out those problems and difficulties which arise in most directional correlation experiments. The extension to polarization correlation is in most cases obvious.

Angular correlation measurements have a weak point in common with all other coincidence measurements: statistical accuracy achievable in a certain time is limited entirely by the properties of the detectors and the coincidence circuit and cannot be indefinitely increased by increasing the source strength. A suitable choice of the radioactive source, of the detectors and of the coincidence circuit, and a careful evaluation of the data, taking into account all necessary corrections, are the preliminary conditions for successful investigations.

Experimental Problems

The radiation detector.—The radiation detectors have two purposes: to choose the radiation with the desired character and energy out of the variety of all emitted radiations and to count this radiation with a counting efficiency as high as possible. In many cases a simple counter, suitably chosen and with an adequate absorber in front, performs both tasks sufficiently well. But as soon as the decay scheme of the nucleus under investigation is complicated, more elaborate arrangements have to be used.

The first correlation measurements were done with G.M. counters (17, 24, 60, 69). G.M. counters are still in use, but real experimental progress was first made with the use of the scintillation counter, introduced by Kallmann and applied to angular correlation measurements by Deutsch & co-workers (25, 34).

The counting efficiencies of both types of counter are different for α-, β- and γ-rays. Both types of counter therefore act partially as radiation selectors, G.M. counter and scintillation counters with thin crystals prefer α- and β-rays, whereas scintillation counters with thick crystals and suitably thick absorbers in front discriminate against α- and β-rays.

The selection of electrons with a certain energy can be greatly improved

by using a magnetic spectrograph, which must be so constructed that no γ-rays strike the β-counter (110, 118). Scintillation spectrometers are appropriate for the selection, according to energy and particle type, of α- and β- as well as of γ-rays (32, 99).

As in usual coincidence work, a detector can be characterized by the counting efficiency $\epsilon(i)$ for the particle i, the solid angle Ω and, if necessary, additional data (e.g., absorption factors, dead time, time lag, momentum resolution).

The coincidence circuit.—Coincidence circuits and the problems involved in coincidence measurements have been described in so many papers (e.g., 27, 35, 37, 66, 110) that we omit here any discussion.

The radioactive source.—In any angular correlation measurement involving electrons, the state of the source is of the highest importance. Only if the source is uniform and very thin is the scattering of the electrons small enough that a correlation can be observed. Recently, it has been shown (2, 3, 50, 117) that the physical state of the source (e.g., source material, chemical compound, "crystal" sizes) also plays an important role and that the preparation of the source becomes a central problem even for measurements involving only γ-rays.

Thin sources can be prepared from chemical solutions, by electrolysis, or by evaporation in a vacuum. The first method has the disadvantage that considerable variations in thickness occur (74) so that the average thickness (measured in milligrams per square centimeter) may lead to erroneous conclusions. The evaporation technique (49, 109) yields the best sources, but cannot be applied in all cases.

Corrections

The variation of the coincidences with the position of the movable detector corresponds to the theoretical correlation function $W(\theta)$ only under the assumption of centered point sources, ideal point detectors, no scattering, and no disturbing radiations. In order to compare experimental and theoretical results, the experimental data have to be corrected for the various deviations from such an ideal arrangement. We have divided the corrections into four groups, A to D, according to their origin. Some of the most important corrections and operations for the evaluation of experimental results are summarized in Table III in the order in which they have to be applied.[5]

Radioactive properties.—A satisfactory interpretation of a measured angular correlation is possible only if the decay scheme of the radioactive isotope

[5] One method of evaluation, found in a number of papers, may result in serious mistakes: theoretical curves, corrected for the finite angular resolution of the detectors, are fitted exactly with the experimental value at the point $\theta=90°$. The experimental points for the other angles are then compared with the theoretical curves. The 90°-point thus gets infinite statistical weight. The correct procedure, however, is to use least square analysis and to fit all points (including $\theta=90°$) with their respective statistical weights.

is not too complicated and is well known. Usually, besides the investigated cascade, other radiations from the same or from other isotopes are also present. If these radiations are noncoincident, they increase the number N_{acc}^{c} of accidental coincidences, but do not change the anisotropy. But if they give rise to true coincidences, they considerably disturb the measurements and have therefore to be eliminated through the use of a radiation selector. If this is impossible, the single counts N_p and the coincidences N_p^c have to be subtracted in the evaluation.

Positrons, which in the sample give rise to annihilation radiation, always have to be considered as a serious source of errors. Because the two annihilation quanta are emitted in opposite directions (cf. 33), positrons appreciably raise the coincidence rate at $\theta = 180°$. If the annihilation radiation cannot be eliminated, an appropriate correction must be applied. The correction can be calculated if the fraction of positrons and the source thickness are well known. Otherwise, the correction has to be estimated by changing the solid angle of the counters in the 180° position and comparing the respective coincidence rates. If, e.g., the distance of both counters (supposed to have equal solid angles Ω) from the source are changed by the same amount, the "nuclear" coincidences vary in proportion to Ω^2, whereas the "annihilation" coincidences are proportional to Ω.

Positrons (of nuclear origin or resulting from hard γ-rays), which are annihilated not in the source, but in material near the counters, can give rise to spurious coincidences, whose elimination is analogous to that of coincidences created by scattered quanta.

The coincidence rate, defined as the ratio of the true coincidences to the true single counts in the movable detector (cf. formula 24 in Table III) is independent of the source strength and therefore does not need to be corrected for the radioactive decay of the source (35, 127).

The source strength has to be chosen so that the accidental (random, chance) coincidences do not outweigh the true coincidences. This gives an upper limit for the source strength, because the number of true coincidences rises linearly with the source strength, while the accidental coincidences rise with its square (35, 37).

Apparatus corrections.—The finite resolving time τ of the coincidence circuit always causes accidental coincidences. N_{acc}^{c} and therefore τ can be measured in the usual way: One separates the two detectors and uses two independent sources, preferably the same radioisotope as in the actual correlation experiment. The resolving time τ is then determined from the relationship $N_{acc}^{c} = 2\tau N_{m,1} N_{m,2}$, where $N_{m,1}$ and $N_{m,2}$ are the measured single counts in the two counters (37).

For most purposes, one makes the resolving time as small as possible, because one can then use strong sources. In special cases, however, the resolving time has to be greater than the lifetime T of the intermediate nuclear level [cf.(5)].

A resolving time τ comparable with the lifetime T of the intermediate

state gives rise to coincidence losses, which can be calculated if τ and T are known. A second source of coincidence losses arises with the apparatus itself [for example (66)]. These apparatus losses can be determined by measuring the coincidences of a very fast cascade (e.g., Ni^{60}) as a function of the resolving time τ.

Small changes in the efficiency of the movable detector which occur during a measurement are corrected for by using the coincidence rate $CR(\theta)$ for the calculation of $W(\theta)$. Fluctuations in the efficiency of the fixed detector can be taken into account by observing its single counts N_1 and by correcting the coincidence rate $CR(\theta)$ for any deviation of N_1 from the theoretical decay curve. [For very long-lived isotopes, this is simply done by dividing $CR(\theta)$ by N_1.] In addition, one should frequently change the position of the movable detector, an operation which is best done by an automatic device.

Geometrical problems.—If the source is slightly decentered, i.e., if the movable detector registers different single counts N_2 for different angles θ, the coincidences from an isotropic source vary as the single counts N_2. The decentering is therefore automatically corrected for, in a first approximation, if one uses in the denominator of the coincidence rate $CR(\theta)$ the single counts N_2 of the movable detector (127).

The finite size of the detectors and the source in general reduces the anisotropy ("smears out" the correlation function). Walter (127) and Frankel (47) have investigated the problem of finding the true correlation function from the measured coincidence rate. Walter takes into account not only the finite (but small) extension of the detectors, but also the finite (but small) extension of the source and different forms of source and detector. His calculations, restricted to correlation functions of the form $W(\theta) = 1 + a_2 \cos^2\theta$, can be generalized to functions with higher terms.[6] Frankel's formulae are restricted to centered point sources and circular counters, but

[6] Suppose the directional correlation to be given by

$$W(\theta) = 1 + a_2 \cos^2\theta + a_4 \cos^4\theta.$$

The measured coincidence rate $CR(\vartheta)$ then becomes:

$$\text{const. } CR(\vartheta) = 1 + a_2\left\{\cos^2\vartheta + \frac{\Omega^*}{6}(1 - 3\cos^2\vartheta) + \frac{1}{6}\left(\frac{L}{D}\right)^2 \cos\vartheta(1 - \cos\vartheta)\right\}$$
$$+ a_4\left\{\cos^4\vartheta + \Omega^*\cos^2\vartheta\left(1 - \frac{5}{3}\cos^2\vartheta\right) + \frac{1}{3}\left(\frac{L}{D}\right)^2 \cos^3\vartheta(1 - \cos\vartheta)\right\}$$
$$+ \text{terms of higher order in } \Omega^* \text{ and } \left(\frac{L}{D}\right)^2.$$

ϑ is the mean angle subtended at the source by the two detectors. The source, length L, is supposed to be linear and is placed centrally in the axis of rotation. D denotes the source-detector distance. Ω^* is related to the solid angle Ω (steradian) of the detectors by: $\Omega^* = \Omega$ for square detectors, $\Omega^* = (3/\pi)\Omega$ for circular detectors.

do not make any assumption as to the highest term in the expansion of the correlation function or the size of the counters.

The solid angles of the detectors, Ω_1 and Ω_2, which enter into all calculations, can be determined with a known activity. A measurement of the directional correlation of annihilation radiation gives the azimuthal "angular resolution" of the apparatus (26). It is not possible, however, to apply this result directly to the correction of an ordinary directional correlation experiment. The correct procedure consists in first calculating from the "angular resolution" the solid angle of the detectors (taking into account their actual form) and then applying the correction formulae.

Scattering.—Effects caused by scattering may completely mask any true correlation: (*a*) Scattering of the radiation to be investigated in the source or its neighborhood tends to reduce the anisotropy and to "smear out" the true correlation. (*b*) Scattering of any radiation in the counters or in the material near the counters can give rise to spurious coincidences. These in general are not isotropic and therefore simulate a correlation.

(*a*) Frankel (47) has given a general treatment of corrections which are due to scattering of electrons in the source and to finite solid detector angles, showing that a close formal similarity between both corrections exists. Walter (127) assumed that the scattering in the source corresponds approximately to an enlargement of the solid angle of the counters. He presents a nomogram which gives directly the most probable angle of deviation as a function of electron energy and source thickness [cf. also (65, 110)].

For low energy electrons, the scattering in the air between source and detector is sufficient to reduce considerably any correlation. Experiments with low energy electrons therefore are best carried out in a vacuum.

Investigations with γ-rays are not extremely sensitive to scattering in the source and its surrounding material. Nevertheless, an estimation of the effect is always necessary. In Table II, "critical" thicknesses z for aluminum are given for different γ-ray energies. For some other materials, the "critical" thickness can be calculated from: $z(\mathrm{Fe}) = 0.36\ z$, $z(\mathrm{Ag}) = z(\mathrm{Pb}) = 0.29\ z$,

TABLE II

CRITICAL SOURCE AND ABSORBER THICKNESSES*

γ-ray energy	0.2	0.6	1.25	Mev
"Critical" thickness z of material surrounding the source	0.5	0.85	1.4	mm. Al
Minimal front absorber	0.6	2.2	4	mm. Pb
Minimal side absorber	2	6.5	9.5	mm. Pb

* All data represent only approximate values.

$z(H_2O) = 2.36\ z$. Scattering in sources of less than "critical" thickness reduces the anisotropy by less than a factor of 0.98. The values have been calculated by Aeppli (5) under the assumption of a linear radioactive source, surrounded by scattering material (wall-thickness z) of cylindrical symmetry. For other arrangements, the values of z are not appreciably different; e.g., if the activity is distributed homogeneously over a "scattering cylinder" of radius r then $r = 1.18\ z$. For sources thicker than "critical," a suitable correction must be applied (5).

(*b*) Walter has enumerated the different ways in which spurious coincidences can occur (127). The following process yields the most important contribution: a γ-ray becomes registered in one counter by a Compton effect. The scattered quantum enters the second counter and thus may create a spurious coincidence. For the scattering angles necessary to strike the second counter, the scattered quanta fortunately always have considerably less energy than the primary γ-rays. This property allows a sufficient elimination of the spurious coincidences. One way to perform the elimination consists in shielding the side and front of the counters with lead. The primary quanta than have to go through one front absorber, whereas the scattered γ-rays have to penetrate two absorbers (26, 127). Table II contains data on front and side absorbers. These absorbers, applied to both counters, reduce any simulated anisotropy below 0.3 per cent. If high energy electrons are present, which would not be stopped by the absorbers of Table II, additional aluminum absorbers in front of the counters (and not around the source) have to be used.

A second possibility for eliminating spurious coincidences consists in the use of scintillation spectrometers as detectors (99). The detectors then register only pulses which are due to the primary quanta and discriminate against the smaller ones of the scattered quanta.

The best method of avoiding scattered γ-quanta and scattered electrons in experiments involving electrons is to select electrons of the desired energy by a suitable magnetic spectrometer (110, 118).

Even if an apparatus is seemingly well designed, the following tests are valuable (26, 127): (*a*) The counting rate for angles symmetrical with respect to 90° (e.g., 60° and 120°) should be equal. (*b*) The counting rate for $\theta = 90°$ should be the same whether or not an additional absorber, not disturbing the primary radiation, is inserted between the counters (127). (*c*) A source without coincidences (e.g., $\gamma-\gamma$:Fe^{59}) or with isotropic correlation ($\beta-\gamma$:Co^{60}) should give equal coincidence rates for all positions. A dangerous test at present, however, is the measurement of a source with "known" anisotropy. Unless any perturbation by the electron shell is excluded, and unless the decay scheme is absolutely certain, one should not assume a certain directional correlation to be a standard.

An additional effect has also to be considered. Scattering in the neighborhood of the scintillation crystals can increase the effective solid angle of the detectors. Aluminum around the crystals absorbs the photo- and Comp-

TABLE III

CORRECTIONS AND OPERATIONS INVOLVED IN THE EVALUATION OF DIRECTIONAL CORRELATION MEASUREMENTS

No.	Operation or correction	Literature
1	Calculation of the accidental coincidences, $N_{acc}^c = 2\tau N_{m,1} \cdot N_{m,2}$ (N_m, N_m^c measured single counts and coincidences).	(5, 35, 127)
2	Counting loss corrections: $N = N_m(1+\delta)$, $N^c = N_m^c(1+\delta^c)$.	(5)
3	Subtraction from corrected single counts N and coincidences N^c of	
	a) the background N_0 and N_0^c,	
	b) perturbing activities N_p and N_p^c,	(5)
	c) single counts N_s and coincidences N_s^c due to scattered particles.	(5, 127)
4	Calculation of the coincidence rate $CR'(\theta)$, with the single counts all referring to the movable detector: $CR'(\theta) = \frac{(N_m^c - N_{acc}^c)(1+\delta^c) - N_0^c - N_p^c - N_s^c}{N_m(1+\delta) - N_0 - N_p - N_s}$ 24.	(127)
5	Correction of the coincidence rate $CR'(\theta)$ for fluctuations in the efficiency of the fixed counter.	
6	Least square fitting of the corrected coincidence rate $CR(\theta)$ by a function $W(\theta)$ (of the form 7 or 8, taking into account	(127)
	a) the finite solid angle of the detectors	(47, 127)
	b) the finite size of the source	(127)
	c) the scattering in the source	(5, 47, 127)

ton-electrons (which are mainly responsible for this effect), without contributing appreciably to their production.

RESULTS AND DISCUSSION[7]

The following critical survey of the experiments done in recent years on angular correlation reveals the fact that only very few experiments allow a

[7] For references concerning decay schemes see "Nuclear data" (129). $\gamma-\gamma$-cascades are denoted by the isotope in which the cascade takes place, e.g., Ni^{60} and not Co^{60}. As in second section (Theory), the coefficients of the expansion 7 are designated by a_{2k}, those of expansion 8 (Legendre polynomials) by A_{2k}. All errors are mean statistical deviations.

complete, unique, and satisfactory interpretation. It is therefore important that further research yield more precise results, corrected for any deviation from ideal arrangement and investigated for a possible influence of the electron shell.

Angular correlation data can be interpreted only if no influence of the electron shell is present or if the amount of perturbation by the shell is known. Before discussing the results belonging to pure nuclear physics, we therefore report measurements which show the importance of perturbations by the electron shell.

The Influence of the Electron Shell on Directional Correlation

The $\gamma-\gamma$-cascade of Cd^{111}.—The first experimental demonstration of an influence of the electron shell was found by investigating the $\gamma-\gamma$-cascade of Cd^{111}. The mother substance, In^{111}, decays by K-capture into Cd^{111} and the whole decay scheme is well known (85). The first measurements of the directional correlation, with $InCl_3$-sources, gave anisotropies of $A=-0.07\pm0.04$ (23) and $A=-0.06\pm0.02$ (98).

In order to investigate the influence of the electron shell on the directional correlation of Cd^{111} ($T_B=1.2\times10^{-7}$ sec.), the Zürich group used the "double stream" evaporation technique (49) to imbed Cd^{111} in different solids [cf. p. 153 and (50)]. The main results of the measurements with such sources follows (2, 3).

The anisotropy of the Cd^{111}-cascade, with the source imbedded in ionic crystals, vanishes: $A=+0.004\pm0.01$. Cd^{111} imbedded in silver by a "double stream" evaporation onto a heated surface (3) shows a pronounced anisotropy: $A=-0.200\pm0.006$. Imbedding Cd^{111} in various other elements (Al, Fe, Se, Cd, In, Sn, Sb, Au) results in the previous value $A=-0.06\pm0.02$. Although these results are not inconsistent with the qualitative considerations on p. 153, no final explanation can be given at present for the different behavior of Ag and the other imbedding metals. These results were confirmed by Steffen (117) and by Deutsch & Kluyver (36).

Further tentative results.—A perturbation of the directional correlation by the electron shell seems also to be present in some other cascades:

Pd^{106}. The directional correlation function, first measured by Brady & Deutsch, shows a highly pronounced anisotropy [cf. also (19, 114)]. Both γ-rays are $E2$ (7, 88). No simple theoretical explanation of the correlation function is possible as yet, even when multipole mixtures are taken into account (76, 77). Other cascades, also present in the decay of Pd^{106}, cannot explain the discrepancy between the experimental and any theoretical data (72). The coefficients A_2 and A_4 of the measured directional correlation as well as the coefficients of the direction-polarization correlation (87) are half those to be expected for the cascade $0(E2)2(E2)0$. A perturbation by the electron shell would therefore explain the measured data. Efforts to alter the correlation have, however, thus far been fruitless (26, 117). A careful de-

termination of the coefficients A_2 and A_4 would perhaps throw some light on the problem, because in the case of a shell perturbation, the attenuation factor G_4 should be smaller than G_2 (cf. p. 142). Spiers has put forward the explanation that the measured cascade actually is a superposition of two cascades, only slightly different in energy (112).

Ni^{60}. The decay of $Co^{60}-Ni^{60}$ has been extensively studied, especially by Deutsch and co-workers, and it was shown that the directional and direction-polarization correlation of the $\gamma-\gamma$-cascade in Ni^{60} is consistent with the assignment $4(E2)2(E2)0$ (19, 26, 87, 99, 114). The theoretical value for the anisotropy then is $A=0.167$. Recent work of the Zürich group, however, finds the anisotropy to be somewhat smaller: $A_{exp.}=0.148\pm0.002$, and the correlation to be unchanged with different sources and under the influence of an external magnetic field (6). This value is no longer compatible with the above scheme. In view of the fact that no other spin and parity assignment appears possible it seems reasonable to believe that the discrepancy is caused by a perturbation by the shell. This explanation leads to an estimate of the lifetime T_B of the intermediate nuclear state: assuming a reasonable value of the hyperfine splitting and using the fact that the external magnetic field remains without influence (cf. formula 20), one gets $T_B \backsim 10^{-11}$ sec. This value is in essential agreement with the assignment $E2$ and the lifetime formula of Weisskopf (130). The fact that a perturbation is possible even for such short life-times calls for precaution in the interpretation of all angular correlation measurements. Before final conclusions can be drawn, the experiments of the Zürich group have to be confirmed.

Pb^{204}. The $\gamma-\gamma$-directional correlation of Pb^{204} ($T_B=4\times10^{-7}$ sec.) has been studied by the Brookhaven group (121). The possible theoretical values for the anisotropy are all greater than the experimental one ($A=0.22\pm0.05$). It is again possible that a perturbation is responsible for the discrepancy.

Rb^{86}, Sb^{122}. The values for the integral anisotropy of the Rb^{86} $\beta-\gamma$-correlation, taken from different papers, vary considerably: $A=+0.019\pm0.014$ (97), $A=+0.035\pm0.020$ (90), $A=0.057\pm0.010$ (120), $A=0.13(\pm0.01)$ (118). A similar discrepancy exists for Sb^{122} (97, 107).

Tm^{170}. The integral $\beta-\gamma$-directional correlation of Tm^{170} ($T_B=2.3\times10^{-9}$ sec.) has been measured by Novey (90): $A \backsim 0.25$. The anisotropy for the $\beta-e^-$-correlation (K-electrons) then should be $A' \backsim 0.045$ (102). Siegbahn, however, found an isotropic differential correlation between β-rays of $\backsim 700$ kev and the L-conversion electrons (110).

Th^{228} (Rd Th). The $\alpha-\gamma$-directional correlation of Th^{228}, investigated by Beling, Feld & Halpern (16), cannot be fitted under reasonable assumptions by any theoretical correlation function. The electron shell of the daughter atom, Ra^{224}, has no magnetic moment in its ground state. The α-decay and the nuclear recoil, however, may sufficiently excite the electron shell to provide a perturbation.

Angular Correlation of $\gamma-\gamma$-Cascades

Brady & Deutsch first demonstrated convincingly the value of directional correlation measurements in nuclear spectroscopy (24, 25, 26); Metzger & Deutsch showed that direction-polarization correlation gives additional information (34, 87). Since the performance of these pioneer experiments, a considerable number of related papers have appeared. Out of the 19 $\gamma-\gamma$-cascades investigated up to the present time, only three allow a unique and completely satisfactory interpretation (Hf^{177}, Xe^{131}, Cd^{111}). In seven cases, the results seem satisfactory, but additional experiments would be valuable (Mg^{24}, Ti^{46}, Ni^{60}, Ba^{134}, Ce^{140}, Nd^{144}, Pb^{208}). The remaining nine cascades do not allow at present any definite conclusions, because the correlation function cannot be explained (Pd^{106}, Pb^{204}), or the given interpretations provoke difficulties (Ar^{38}, Cu^{65}, Sr^{88}, Cd^{114}, Pt^{196}), or the decay is too complicated (Cd^{110}, Te^{124}).

A complete description of each cascade lies outside the scope of our paper, but we discuss several interesting cases and quote the literature for all of the others.

Unambiguous cases.—Directional correlation and conversion coefficients of the two γ-rays emitted in cascade by Hf^{177} have recently been measured by McGowan, Klema & Bell (86), and agree well with the assignment $\frac{5}{2}\,(E1)\,\frac{7}{2}\,(E2)\,\frac{3}{2}$ ($a_{2,\,\mathrm{exp.}} = -0.21 \pm 0.02 \rightarrow A_{2,\,\mathrm{exp.}} = -0.15 \pm 0.015$, $A_{2,\,\mathrm{theor.}} = -0.153$). The appearance of electric dipole radiation, however, contrasts with the shell model.

The decay scheme of $I^{131} \rightarrow Xe^{131}$ is well investigated and the intermediate state of the $\gamma-\gamma$-cascade in Xe^{131} has been shown to have spin 1/2 (126). This fact agrees with the result of Schiff, who found an isotropic directional correlation (104).

4−2−0-cascades.—Even-even nuclei (which in the ground state presumably have spin 0) are expected in many cases to have the spin values 2 and 4 in the first two excited levels and to possess the same parity in all three states (59). The lowest order multipole transition allowed by selection rules is then electric quadrupole radiation. The coefficients of the directional correlation function of the resulting cascade $4(E2)2(E2)0$ are: $A_2 = 0.1020$, $A_4 = 0.0091$ (or $a_2 = 1/8$, $a_4 = 1/24$, $A = 0.167$). The measured directional correlation functions of the following six cascades seem to be consistent with the assignment 4(2)2(2)0: Mg^{24} (19, 26, 29), Ti^{46} (26, 90), Ni^{60} (19, 26, 99, 114), Ba^{134} (19, 26, 99, 105), Ce^{140} (100), Pb^{208}(ThD) (93). In three cases (Ti^{46}, Ni^{60}, Ba^{134}), also the direction-polarization correlation has been investigated by Metzger & Deutsch (87) and shows [under the assumption of a cascade 4(2)2(2)0] both γ-rays to be electric quadrupole. Williams & Wiedenbeck (134) confirm the results of Metzger & Deutsch in the case of Ni^{60} (and Pd^{106}), but find no direction-polarization correlation in Ba^{134}. [Note, however, that the definition of the function $(N_{\parallel}/N_{\perp})$ in (34) and (134) differs from that in (87).]

The only nuclide whose decay scheme is uniquely determined by all

known measurements even when multipole mixtures are taken into account is Ni^{60}. But as we have pointed out on p. 153, recent measurements raise some doubts about the complete agreement between experimental and theoretical correlation functions even in the case of Ni^{60}. A careful redetermination of the correlation function for the various nuclides and measurements of as many additional properties as possible therefore seem desirable.

In the decay of Ba^{134} and Ce^{140}, more than two γ-rays are emitted in cascade and the measured "over-all" directional correlation is difficult to interpret. Robinson & Madansky (99, 100) therefore used an improved arrangement: a third scintillation counter detects β-particles of a certain energy interval. Only those $\gamma-\gamma$-cascades are measured which are related to the β-transition (threefold coincidences). Robinson & Madansky succeeded in measuring the directional correlation in Ba^{134} and Ce^{140}

Mixed transitions.—Ling & Falkoff (77) first showed that the directional correlation of Sr^{88} ($a_2 = -0.06$) (26), not explicable with pure γ-rays, could be fitted by assuming the first γ-ray of the cascade to be a mixture of $E2$ and $M1$. The decay of Sr^{88}, however, is not investigated well enough to decide if the assumption of a multipole mixture is necessary.

The investigation of the three isobars Ag^{111}, Cd^{111}, and In^{111} has made it possible to establish a complete decay scheme for Cd^{111} (85). For the γ-γ-cascade in Cd^{111}, following K-capture in In^{111}, there results the following unique assignment: $g_{7/2}$ $(M1)$ $d_{5/2}$ $(E2)$ $s_{1/2}$ (where the nuclear states are designated according to the single particle model for an odd neutron). The theoretical anisotropy for the directional correlation of the $\gamma-\gamma$-cascade then would be $A_{\text{theor.}} = -0.103$. This is in crude agreement with the first experimental determinations (23, 98), but disagrees markedly with the revised value, $A_{\text{exp.}} = -0.200 \pm 0.006$ (2, 3). Selection rules, however, allow the first γ-ray to be a mixture of $E2$ and $M1$. The measured directional correlation actually can be well fitted by assuming a mixture with intensity ratio $E2/M1 = 0.01 \pm 0.003$ and a relative nuclear phase $\delta = 180°$ (3). It can be seen from this result that very small admixtures considerably alter the directional correlation.

Additional references.—Data on directional correlation experiments not quoted hitherto can be found in the following papers: A^{38} (114), Cu^{65} (132), Cd^{110} (19), Cd^{114} (68, 115), Te^{124} (18, 118), Nd^{144} (8), Pt^{196} (116).

Directional Correlation of $\beta-\gamma$- and $\beta-e^-$-Cascades

The first reports on $\beta-\gamma$-directional correlation came from Garwin (57) and Grace, Allen & Halban (61). These authors found seven cases with isotropic, but no case with anisotropic correlation. As of now, 23 $\beta-\gamma$- and 4 $\beta-e^-$-cascades have been investigated, but only seven $\beta-\gamma$-cascades deviate from isotropy.

The $\beta-\gamma$-directional correlation depends upon more variables than, e.g., the $\gamma-\gamma$-correlation. This causes greater difficulties in the interpretation of experimental results, and one cannot in general expect to receive from

TABLE IV

CASCADES WITH ANISOTROPIC β-γ DIRECTIONAL CORRELATION

Nucleus	Betaspectrum		Anisotropy			Literature	
	log ft (45)	E_{max} (Mev)	Integral (Approximate values)	Differential		Integral	Differential
				E(mev)	$A(E)$		
K^{42}	7.44	2.04	−0.06	1.55	−0.065	(20)	(119)
As^{76}	8.35	2.5	+0.08	—	—	(127)	—
Rb^{86}	7.63	0.716	+0.13	0.5	+0.21	(90, 97, 120)	(118)
Sb^{122}	> 7.37	1.36	+0.07	1	+0.157	(97, 107)	(107)
Sb^{124}	10.35	2.37	−0.23	2.0	−0.4	(18, 32, 37)	(32, 118)
I^{128}	7.46	0.85	—	0.7	+0.21	—	(118, 119)
Tm^{170}	9.71	0.886	−0.26	—	—	(90, 91)	—

$\beta-\gamma$-directional correlation alone definite and unambiguous information. Nevertheless, it seems desirable to develop theory and experiment still further and to compare correlation data with information from β-spectroscopy in as many cases as possible.

Cascades with isotropic directional correlation.—The following cascades have been found to show no directional correlation:

$\beta-\gamma$: Na^{22} (118), Na^{24} (20, 57, 61), Sc^{46} (90), Mn^{56} (127), Co^{55} (118), Co^{56} (118), Co^{60} (20, 57, 61, 90, 118), Nb^{95} (120), Ru^{103} (57), Ru^{105} (57), Cd^{115} (57, 20), I^{124} (118), I^{131} (20), Cs^{134} (20, 118, 120), Ir^{192} (57), Au^{198} (57, 97, 120, 127).

$\beta-e^-$: Sn^{153}, Tm^{170}, Au^{199}, Pb^{212} (ThB) (110)

In almost all cases the isotropy seems explainable, because the β-transition is allowed or the β-spectrum has an allowed shape. In a few cases, however, the possibility of a perturbation by the electron shell cannot be excluded [Mn^{56}, Co^{56}, Cd^{115}, I^{124}, Cs^{134}, Ir^{192}, Tm^{170} ($\beta-e^-$)].

Cascades with anisotropic directional correlation.—The main data on those cascades which show an anisotropic $\beta-\gamma$-directional correlation are summarized in Table IV.

A tentative explanation for the shape of the differential correlation function has been proposed for Rb^{86} by Fuchs (52) and for Sb^{124} by Opechowski (32).

VARIOUS ADDITIONAL MEASUREMENTS

Directional correlation of $e^-\!-\!\gamma$ and $e^-\!-\!e^-$-cascades.—Measurements involving conversion electrons are in general difficult. Highly converted γ-rays usually have low energy and the scattering of the conversion electrons in the radioactive source can then "smear out" the correlation. Furthermore, a comparison between theory and experiment is possible only for K-electrons, because, as yet, no calculation of the directional correlation involving L-electrons is available.

The following isotopes have been investigated: $e^- - \gamma$: Mo^{93}, Hf^{181} (118); $e^- - e^-$: Hf^{181} (128), Hg^{197} (48, 127), but no comparison with theory is at present possible.

$\alpha - \gamma$-Directional correlation.—The $\alpha - \gamma$-directional correlation has been measured in two cases: Th^{228} (16) and Bi^{212} (73), but no definite conclusions can be drawn at present.

Determination of the g-factor of an excited nuclear level.—Brady & Deutsch (26) first pointed out that the nuclear g-factor of the intermediate state in a $\gamma - \gamma$-cascade can be determined by observing the effect of an external magnetic field on the directional correlation [cf. also (81)]. Such an experiment can be carried out only if the nucleus is not disturbed by the electron shell and if the lifetime of the intermediate nuclear state lies between 10^{-8} sec. and 10^{-5} sec. The lower limit, 10^{-8} sec., is set by the available magnetic field-strength (10^4–10^5 oersted). The upper limit, 10^{-5} sec., is determined by the circumstance that an optimum measurement of the attenuation requires a resolving time of the coincidence circuit which is comparable to, or longer than, the lifetime of the intermediate nuclear state (5). The number of accidental coincidences, however, is proportional to the resolving time and outweighs the true coincidences for lifetimes longer than 10^{-5} sec. The theory for the case of an external magnetic field perpendicular to the plane of the two registered γ-rays has been given by Alder [cf. p. 143 and (10, 11)].

The first determination of a g-factor, based on Alder's formulae, was carried out by the Zürich group with the $\gamma - \gamma$-cascade of Cd^{111} (4, 5). Cd^{111} is particularly well suited, because the lifetime T_B fulfills the necessary condition: $T_B = 1.23 \times 10^{-7}$ sec. The measurement of the directional correlation as a function of the applied magnetic field H in sources of maximum anisotropy and with equallly sensitive detectors determined the magnitude of g (cf. formula 23). The sign of g could be found by measuring the coincidence rate with $\theta = 135°$ for upward and for downward external magnetic field; the two γ-rays were differentiated by means of different absorbers in front of the two detectors. The final result, corrected for the finite resolving time of the coincidence circuit, is $g(Cd^{111}, \text{intermediate state}) = -(0.28 \pm 0.05)$ (5). The negative sign confirms the assignment $d_{5/2}$ to the intermediate nuclear state. The resulting magnetic moment, $\mu(d_{5/2}) = -(0.70 \pm 0.12)\ \mu_k$, differs only slightly from that of the ground state, $\mu(s_{1/2}) = -(0.59492 \pm 0.00008)\mu_k$.

This method of measuring g-factors of excited nuclear levels can be improved by using scintillation spectrometers as detectors. It is to be hoped that by this method the magnetic moments of a few other nuclear states can be determined in the future.

ACKNOWLEDGMENTS

I wish to express my appreciation to Professors P. Scherrer and V. F. Weisskopf for their continued interest and for many valuable discussions. I am deeply indebted to all my friends for their advice and helpful criticism:

Dr. M. R. Schafroth especially on the theoretical part and for numerous suggestions, Dr. A. S. Bishop for many useful discussions and his help in brushing up my English, Drs. M. Walter and H. Aeppli for invaluable advice concerning the experimental parts, and Dr. W. Känzig for his suggestions throughout the paper. Finally, I wish to thank all members of the "Zürich group" for their indefatigable work and their many discussions during the measurements.

LITERATURE CITED

1. Abragram, A., and Pryce, M. H. L., *Proc. Roy. Soc.* (*London*) [A]**205,** 135 (1951)
2. Aeppli, H., Bishop, A. S., Frauenfelder, H., Walter, M., and Zünti, W., *Phys. Rev.*, **82,** 550 (1951)
3. Aeppli, H., Frauenfelder, H., and Walter, M., *Helv. Phys. Acta*, **24,** 335 (1951)
4. Aeppli, H., Albers-Schönberg, H., Bishop, A. S., Frauenfelder, H., and Heer, E., *Phys. Rev.*, **84,** 370 (1951)
5. Aeppli, H., Albers-Schönberg, H., Frauenfelder, H., and Scherrer, P., *Helv. Phys. Acta*, **25,** 339 (1952)
6. Aeppli, H., Frauenfelder, H., Heer, E., and Ruetschi, R., *Phys. Rev.*, **87,** 379 (1952)
7. Alburger, D. E., *Phys. Rev.*, **85,** 734 (1952)
8. Alburger, D. E., and Kraushaar, J., *Phys. Rev.*, **86,** 633 (1952)
9. Alder, K., *Phys. Rev.*, **83,** 1266 (1951)
10. Alder, K., *Phys. Rev.*, **84,** 369 (1951)
11. Alder, K., *Helv. Phys. Acta*, **25,** 235 (1952)
12. Arfken, G. B., Biedenharn, L. C., and Rose, M. E., *U. S. Atomic Energy Commission Document ORNL 1103* (1952)
13. Arnold, W. R., *Phys. Rev.*, **80,** 34 (1950)
14. Austern, N., and Sachs, R. G., *Phys. Rev.*, **81,** 710 (1951)
15. Baltensberger, W., *Phys. Rev.*, **83,** 1055 (1951)
16. Beling, J. K., Feld, B. T., and Halpern, I., *Phys. Rev.*, **85,** 155 (1951)
17. Beringer, R., *Phys. Rev.*, **63,** 23 (1943)
18. Beyster, J. R., and Wiedenbeck, M. L., *Phys. Rev.*, **79,** 169 (1950)
19. Beyster, J. R., and Wiedenbeck, M. L., *Phys. Rev.*, **79,** 411 (1950)
20. Beyster, J. R., and Wiedenbeck, M. L., *Phys. Rev.*, **79,** 728 (1950)
21. Biedenharn, L. C., Arfken, G. B., and Rose, M. E., *Phys. Rev.*, **83,** 586 (1951)
22. Bloembergen, N., Purcell, E. M., and Pound, R. V., *Phys. Rev.*, **73,** 679 (1948)
23. Boehm, F., and Walter, M., *Helv. Phys. Acta*, **22,** 378 (1949)
24. Brady, E. L., and Deutsch, M., *Phys. Rev.*, **72,** 870 (1947)
25. Brady, E. L., and Deutsch, M., *Phys. Rev.*, **74,** 1541 (1948)
26. Brady, E. L., and Deutsch, M., *Phys. Rev.*, **78,** 558 (1950)
27. Cavanagh, P. E., *Progress Nuclear Phys.*, **1,** 140 (1950)
28. Chao, C. J., *Phys. Rev.*, **80,** 1035 (1950)
29. Charpak, G., and Suzor, F., *J. phys. radium*, **11,** 633 (1950)
30. Condon, E. U., and Shortleg, G. H., *Theory of Atomic Spectra* (Cambridge Univ. Press, London, England, 441 pp., 1951)
31. Cooper, E. P., *Phys. Rev.*, **61,** 1 (1942)
32. Darby, E. K., and Opechowski, W., *Phys. Rev.*, **83,** 676 (1951)
33. DeBenedetti, S., Cowan, C. E., and Konneker, W. R., and Primakoff, H., *Phys. Rev.*, **77,** 205 (1950)
34. Deutsch, M., and Metzger, F., *Phys. Rev.*, **74,** 1542 (1948)
35. Deutsch, M., *Rept. Phys. Soc. Progress Phys.*, **14,** 196 (1951)
36. Deutsch, M. (Personal communication)
37. Dunworth, J. W., *Rev. Sci. Instruments*, **11,** 167 (1940)
38. Falkoff, D. L., *Phys. Rev.*, **73,** 518 (1948)
39. Falkoff, D. L., and Uhlenbeck, G. E., *Phys. Rev.*, **79,** 323 (1950)
40. Falkoff, D. L., and Uhlenbeck, G. E., *Phys. Rev.*, **79,** 334 (1950)
41. Falkoff, D. L., *Phys. Rev.*, **82,** 98 (1951)

42. Fano, U., *Natl. Bur. Standards (U. S.), Rept. 1214* (1951)
43. Feenberg, E., and Trigg, G., *Revs. Modern Phys.*, **22,** 399 (1950)
44. Feenberg, E., *Ann. Rev. Nuclear Sci.*, **1,** 43 (1952)
45. Feingold, A. M., *Revs. Modern Phys.*, **23,** 10 (1951)
46. Fierz, M., *Helv. Phys. Acta*, **22,** 489 (1949)
47. Frankel, S., *Phys. Rev.*, **83,** 673 (1951)
48. Frauenfelder, H., Walter, M., and Zünti, W., *Phys. Rev.*, **77,** 557 (1950)
49. Frauenfelder, H., *Helv. Phys. Acta*, **23,** 347 (1950)
50. Frauenfelder, H., *Phys. Rev.*, **82,** 549 (1951)
51. Fuchs, M., and Lennox, E. S., *Phys. Rev.*, **79,** 221 (1950)
52. Fuchs, M., *The Effect of Nuclear Charge and Beta Interference on Beta-Gamma Angular Correlation* (Doctoral thesis, University of Michigan, 1951)
53. Gardner, J. W., *Proc. Phys. Soc. (London)*, [A]**62,** 763 (1949)
54. Gardner, J. W., *Proc. Phys. Soc. (London)*, [A]**64,** 238 (1951)
55. Gardner, J. W., *Proc. Phys. Soc. (London)*, [A]**64,** 1136 (1951)
56. Gardner, J. W., *Phys. Rev.*, **85,** 137 (1952)
57. Garwin, R. L., *Phys. Rev.*, **76,** 1876 (1949)
58. Goertzel, G., *Phys. Rev.*, **70,** 897 (1946)
59. Goldhaber, M., and Sunyar, A. W., *Phys. Rev.*, **83,** 906 (1951)
60. Good, W. M., *Phys. Rev.*, **70,** 978 (1946)
61. Grace, H. A., Allen, R. A., and Halban, H., *Nature*, **164,** 538 (1949)
62. Hahn, E. L., *Phys. Rev.*, **80,** 580 (1950)
63. Hamilton, D. R., *Phys. Rev.*, **58,** 122 (1940)
64. Hamilton, D. R., *Phys. Rev.*, **74,** 782 (1948)
65. Hamilton, D. R., and Gross, L., *Rev. Sci. Instruments*, **21,** 912 (1950)
66. Huber, O., Humbel, F., Schneider, H., and Shalit, A. de, *Helv. Phys. Acta*, **25,** 3 (1952)
67. Jahn, H. A., *Proc. Roy. Soc. (London)*, [A]**205,** 192 (1951)
68. Johns, M. W., Cox, C. D., and McMullen, C. C., *Bull. Am. Phys. Soc.*, **27**(1), 57 (1952)
69. Kikuchi, S., Watase, Y., and Itoh, J., *Z. Physik*, **119,** 185 (1942)
70. Konopinski, E., *Revs. Modern Phys.*, **15,** 209 (1943)
71. Kopfermann, H., *Kernmomente* (Akademische Verlagsgesellschaft, Leipzig, Germany, 270 pp., 1940)
72. Kraushaar, J. J., *Phys. Rev.*, **85,** 727 (1952)
73. Kulchitski, L. A., *Doklady Akad. Nauk. S.S.S.R.*, **73,** 1153 (1950)
74. Langer, L. M., Moffat, R. D., and Price, H. C., *Phys. Rev.*, **76,** 1725 (1949)
75. Ling, D. S. (Doctoral *thesis*, Univ. of Michigan, 1948)
76. Ling, D. S., and Falkoff, D. L., *Phys. Rev.*, **76,** 431 (1949)
77. Ling, D. S., and Falkoff, D. L., *Phys. Rev.*, **76,** 1639 (1949)
78. Lippmann, B. A., *Phys. Rev.*, **81,** 162 (1951)
79. Lloyd, S. P., *Phys. Rev.*, **80,** 118 (1950)
80. Lloyd, S. P., *Phys. Rev.*, **81,** 161 (1951)
81. Lloyd, S. P., *Phys. Rev.*, **82,** 277 (1951)
82. Lloyd, S. P., *The Angular Correlation of Successive Nuclear Radiations* (Doctoral thesis, Univ. of Illinois, 1951)
83. Lloyd, S. P., *Phys. Rev.*, **83,** 716 (1951)
84. MacDonald, J. E., and Falkoff, D. L., *Phys. Rev.*, **83,** 875 (1951)
85. McGinnis, C. L., *Phys. Rev.*, **81,** 734 (1951)

86. McGowan, F. K., Klema, E. D., and Bell, P. R., *Phys. Rev.*, **85**, 152 (1952)
87. Metzger, F., and Deutsch, M., *Phys. Rev.*, **78**, 551 (1950)
88. Metzger, F., *Phys. Rev.*, **79**, 398 (1950)
89. Mott, N. F., and Gurney, R. W., *Electronic Processes in Ionic Crystals* (The Clarendon Press, Oxford, England, 275 pp., 1940)
90. Novey, T. B., *Phys. Rev*, **78**, 66 (1950)
91. Novey, T. B., *Phys. Rev.*, **84**, 145 (1951)
92. Perlman, I., Ghiorso, A., and Seaborg, G. T., *Phys. Rev.*, **77**, 26 (1950)
93. Petch, H. E., and Johns, M. W., *Phys. Rev.*, **80**, 478 (1950)
94. Pound, R. V., *Phys. Rev.*, **79**, 685 (1950)
95. Racah, G., *Phys. Rev.*, **62**, 438 (1942)
96. Racah, G., *Phys. Rev.*, **84**, 910 (1951)
97. Ridgway, S. L., *Phys. Rev.*, **78**, 821 (1950)
98. Roberts, D. M., and Steffen, R. M., *Phys. Rev.*, **82**, 332 (1951)
99. Robinson, B. L., and Madansky, L., *Phys. Rev.*, **84**, 604 (1951)
100. Robinson, B. L., and Madansky, L., *Phys. Rev.*, **84**, 1067 (1951)
101. Rose, M. E., Goertzel, G., Spinrad, B. I., Harr, J., and Strong, P., *Phys. Rev.*, **83**, 79 (1951)
102. Rose, M. E., Biedenharn, L. C., and Arfken, G. B., *Phys. Rev.*, **85**, 5 (1952)
103. Rose, M. E., and Biedenharn, L. C., *Revs. Modern Phys.* (In press)
104. Schiff, D., *Phys. Rev.*, **85**, 727 (1952)
105. Schmidt, F. H., and Keister, G. L., *Phys. Rev.*, **86**, 632 (1952)
106. Schwartz, H. M., and Edwards, R. R., *J. Chem. Phys.*, **19**, 385 (1951)
107. Shaknov, I., *Phys. Rev.*, **82**, 833 (1951)
108. Sherwin, C. W., *Phys. Rev.*, **82**, 52 (1951)
109. Sherwin, C. W., *Rev. Sci. Instruments*, **22**, 339 (1951)
110. Siegbahn, K., *Arkiv Fysik*, **4**, 223 (1952)
111. Spiers, J. A., *Nature*, **161**, 807 (1948)
112. Spiers, J. A., *Phys. Rev.*, **78**, 75 (1950)
113. Spiers, J. A., *Phys. Rev.*, **80**, 491 (1950)
114. Steffen, R. M., *Phys. Rev.*, **80**, 115 (1951)
115. Steffen, R. M., *Phys. Rev.*, **83**, 166 (1951)
116. Steffen, R. M., and Roberts, D. M., *Phys. Rev.*, **83**, 222 (1951)
117. Steffen, R. M., *Bull. Am. Phys. Soc.*, **27**(1), 57 (1952)
118. Stevenson, D. T., and Deutsch, M., *Phys. Rev.*, **83**, 1202 (1951)
119. Stevenson, D. T., and Deutsch, M., *Phys. Rev.*, **84**, 1071 (1951)
120. Stump, R., and Frankel, S., *Phys. Rev.*, **79**, 243, (1950)
121. Sunyar, A. W., Alburger, D. E., Friedlander, G., Goldhaber, M., and Scharff-Goldhaber, G., *Phys. Rev.*, **79**, 181 (1950)
122. Thirion, J., *Compt. rend.*, **230**, 2090 (1950)
123. Tolhoek, H. A., and Groot, S. R. de, *Phys. Rev.*, **83**, 189 (1951)
124. Townes, C. H., *Phys. Rev.*, **71**, 909 (1947)
125. Van Vleck, J. H., *The Theory of Electric and Magnet Susceptibilities* (Oxford Univ. Press, London, England, 384 pp., 1932)
126. Verster, N. F., Nijgh, G. J., Lieshout, R. van, and Bakker, C. J., *Physica*, **17**, 637 (1951)
127. Walter, M., Huber, O., and Zünti, W., *Helv. Phys. Acta*, **23**, 697 (1950)
128. Ward, A. H., and Walker, D., *Nature*, **163**, 168 (1949)
129. Way, K., Wood, M., and Thew, K., *Natl. Bur. Standards, Circ. 499* (1950)

130. Weisskopf, V. F., *Phys. Rev.*, **83**, 1073 (1951)
131. Weisskopf, V. F., and Blatt, J., *Theoretical Nuclear Physics* (John Wiley & Sons, Inc., New York, N. Y. To be published, 1952)
132. Wiedling, T., and Carlsson, A., *Phys. Rev.*, **83**, 181 (1951)
133. Wigner, E., *Gruppentheorie und ihre Anwendung auf die Quantenmechanik der Atomspketren* (Friedrich Vieweg & Sohn, Braunschweig, Germany, 332 pp., 1931)
134. Williams, A. H., and Wiedenbeck, M. L., *Phys. Rev.*, **78**, 822 (1950)
135. Wu, C. S., *Revs. Modern Phys.*, **22**, 386 (1950)
136. Yang, C. N., *Phys. Rev.*, **74**, 764 (1948)
137. Zinnes, I., *Phys. Rev.*, **80**, 386 (1950)

SUBNUCLEAR PARTICLES[1]

By John S. Blair and Geoffrey F. Chew
Department of Physics, University of Illinois, Urbana, Illinois

INTRODUCTION

This chapter is to be concerned with the unstable[2] particles which appear to have a strong and intimate connection with nuclear matter and nuclear forces. An experimental characterization of these particles can be made by saying that they are produced copiously in nuclear events of sufficiently high energy and are strongly scattered and absorbed by nuclei. The most prominent of these "subnuclear" entities so far are the pions, but heavier objects, the τ-, V-, and κ-particles, have recently been discovered. From a phenomenological point of view, it is still possible to discuss all known properties of pions without reference to their heavier brothers (although a final theory will certainly have to handle the group as a whole), and an independent treatment of the pions is to be given here. Following this will be a review of the data on the τ-, V-, and κ-particles.

Deliberately omitted is any discussion of electrons, neutrinos, and muons, all of which do interact with nuclei and with each other but with a strength of interaction which is smaller by many orders of magnitude than the strength which characterizes the particles which we here choose to designate as "subnuclear."[3] For a review of the current knowledge about muons, Marshak's article (1) in the first volume of the *Annual Review of Nuclear Science* may be consulted. Relatively few new developments in this field have taken place in the past year.

PROPERTIES OF PIONS

There have been a number of important qualitative discoveries about pions in 1951, and quantitative knowledge has increased greatly. An attempt will be made here to summarize the best available information about all pion properties at present susceptible to experimental measurement. The organization of material is to be based on the property itself, rather than the type of measurement, so that a single experiment may be referred to at more than one point if it serves to measure more than one property. No special effort will be made to describe the original discovery or measurement of a particular property. The emphasis will be on what the authors believe to be the most accurate information available at the end of 1951.

[1] The survey of the literature pertaining to this review was concluded in March, 1952.

[2] The neutron is considered a stable particle, for the purposes of the discussion here.

[3] We are cautious about using the term "meson," which not only would include the muon but would not include the heavy V-particle, which is more massive than the proton.

The originators of important theoretical contributions will be mentioned when they are known, but it should be recognized that in these days of rapid and frequent communication many ideas have no well-defined source. Ideas of this kind which have received wide acceptance will be presented without any special attempt to give credit to authors. When references are given in such cases they will generally be to the *Physical Review*, as a matter of convenience.

The Masses of the Pions

There has been almost no improvement during 1951 in the available values of pion masses. The results which have the lowest quoted probable error are still those of Barkas, Smith & Gardner (2). They found by a photographic emulsion technique, $m_\pi{}^+ = 277.4 \pm 1.1$ and $m_\pi{}^- = 276.1 \pm 1.3$, in units of the electron mass. The completely independent measurement of $m_\pi{}^+$, which is based on the energetics of the reaction $p+p \rightarrow \pi^+ + d$, has been repeated by different investigators. The new number, given by Peterson *et al.* (3) is $m_\pi{}^+ = 279.0 \pm 1.5$, to be compared to Cartwright's (4) original figure of 275.1 ± 2.5. No attempt has been made to improve the $m_\pi{}^-$ value which is based on the energetics of the reaction, $\pi^- + p \rightarrow n + \gamma$. The old value of 275.2 ± 2.5, given by Panofsky *et al.* (5) still stands.

Also unchanged is the best value of 10.6 ± 2.0 for the $\pi^- - \pi^0$ mass difference. This was obtained by Panofsky *et al.*, (5) by observing the Doppler shift of the two γ-rays which result from the decay of a neutral pion ($\pi^0 \rightarrow 2\gamma$; see section, The Decay of the Pions), which in turn had been produced in the reaction $\pi^- + p \rightarrow \pi^0 + n$.

To summarize, it seems probable that the positive and negative pions have equal masses which are each 276 ± 2 times the electron mass, while the neutral meson is lighter than this by 11 ± 2 electron masses. The most obvious interpretation of the difference would be in terms of a self energy caused by interaction with the electromagnetic field. The order of magnitude and sign of the difference is certainly not inconsistent with such an explanation.

Spin and Parity of the Pions

By the end of 1951 it was established beyond any reasonable doubt that the pions have zero intrinsic angular momentum (spin), and an odd intrinsic parity. (We assume neutrons and protons both to have even intrinsic parity.) These properties are often summarized by saying that the pion field is pseudoscalar.

Briefly, the experimental demonstration of these properties has been as follows: The spin of the charged pion was determined by observing the reaction $\pi^+ + d \rightleftharpoons 2\ p$ in both directions and applying the principle of detailed balance. The ratio of backward and forward rates is then proportional to $(2s+1)$, if s is the pion spin. This method of spin measurement was pointed out by Cheston (6) and Marshak (7), and independently by Johnson (8).

The rate of the reaction, $p+p \rightarrow \pi^+ + d$, has been measured by several groups at Berkeley [Peterson *et al.* (3); Cartwright *et al.* (9); Whitehead & Richman (10)]. The reverse reaction, $\pi^+ + d \rightarrow 2p$, has been studied roughly by Clark, Roberts & Wilson (11) and more precisely by Durbin, Loar & Steinberger (12). Where cross-checking is possible between the different groups there is good agreement, and the spin of the charged pion is definitely determined by the experimental results to be zero.

The intrinsic parity of the charged pion is revealed by the non-radiative capture of negative pions in deuterium, i.e., the process, $\pi^- + d \rightarrow 2n$, observed by Panofsky *et al.* (5). If this capture takes place from a K-orbit (zero orbital angular momentum) of the pion around the deuteron then the total angular momentum of the initial system is simply the spin of the deuteron, one unit of $\hbar$, and the over-all parity is the intrinsic parity of the pion. Now because of the Pauli principle the only state of the final two-neutron system which can have total angular momentum $1\hbar$ is the $^3P_1$ state, which is of odd parity. Thus the charged pion must be of odd intrinsic parity, since the above process is observed to compete successfully with the process, $\pi^- + d \rightarrow 2n + \gamma$, for which there is no corresponding selection rule. The detailed calculation to show that the capture does not occur from a higher orbit than the K has been made by Brueckner, Serber & Watson (13).

It is plausible simply to assume that the neutral pion has the same spin and parity as the charged, but there is also direct evidence to substantiate this symmetry, at least with regard to the spin. The very existence of the decay process, $\pi^0 \rightarrow 2\gamma$, which was confirmed by Steinberger, Panofsky & Steller (14), shows the neutral pion to have integral spin; and selection rules for this process rule out the possibility of spin 1 [Yang (15)]. A spin of two units or higher cannot be ruled out on this basis but seems a priori unlikely.

A measurement of the relative polarization of the two decay photons from the neutral pion would determine the parity unambiguously [Yang (15)]. Lacking this direct test at present, there is still strongly suggestive evidence from the rates of such reactions as $\pi^- + p \rightarrow \pi^0 + n$ and $\gamma + p \rightarrow \pi^0 + p$ to support the assumption of odd parity for neutral as well as charged pions. These processes will be discussed below in connection with the interaction between pions and nucleons. It will be shown that only pion-nucleon couplings which correspond to opposite parities of the pion and nucleon fields can come reasonably close to explaining the experimental observations.

The Decay of the Pions

Unless captured by a nucleon, a charged pion will eventually decay into a muon of the same charge, with some kind of a light neutral particle emitted at the same time to absorb the recoil. The rate of this decay process has now been measured quite accurately for both positive and negative pions. The more accurate available figure applies to the positive pion, which will decay even after being stopped in dense material, and to which, therefore, fast electronics may be applied. The most recent published result is by Wiegand

(16), based on a technique developed by Chamberlain *et al.* (17) and independently by Kraushaar *et al.* (18). Wiegand gives for the mean life of the positive pion, $(2.58 \pm .13) \times 10^{-8}$ sec. With the same essential method but different apparatus, Jakobson, Schulz & Steinberger (19) found $(2.54 \pm .11) \times 10^{-8}$ sec.

The negative pion will be captured by nuclei if allowed to stop in dense material; so its decay must be studied in flight. The most accurate study has been made by Lederman *et al.* (20) who observed the decay of negative pions in crossing a cloud chamber. They found a mean life $(2.92 \pm .32) \times 10^{-8}$ sec. A direct comparison of the positive and negative mean lives by these same workers gave a ratio $\tau^-/\tau^+ = 1.01 \pm 0.1$. Thus, it seems probable that negative and positive pions have the same mean life, a result which is certainly to be expected.

The nature of the neutral recoil from the $\pi \rightarrow \mu$ decay is still unknown, but the measured value of the μ-meson range sets an upper limit to the mass of about 30 times the electron mass. There is evidence [see Marshak (1)] that the muon has half-odd integral spin; so the neutral recoil must also have half-odd integral spin, and in order to avoid introducing a new fundamental particle, it is generally assumed that the recoil is a neutrino, the same mysterious particle of spin $\frac{1}{2}\hbar$ which is invoked in order to understand the process of β-decay.

Of theoretical importance is the question of possible competing modes of decay of the pion which may have a longer lifetime than the $\pi \rightarrow \mu$ decay and are, therefore, difficult to detect experimentally. In particular, a mode in which an electron replaces the muon seems a priori not unlikely. However, a thorough search for the $\pi \rightarrow$ e decay carried out by Friedman & Rainwater (21) found only one possible event of this kind out of 1419 $\pi \rightarrow \mu$ decays. The one event may have been a $\mu \rightarrow$ e decay.

Recently a small number of anomalously short muon tracks from pion decays have been reported [e.g., Fry (22)]. These tracks are evidence for an alternative mode of decay, involving at least two neutral recoils, the most probable mode of this kind having one photon in addition to the usual one muon and one neutrino. A similar mode occurs in connection with β-decays, where it is called "inner bremsstrahlung" because one may interpret the photon emission as the inevitable radiation which accompanies the acceleration of charge as the electron is created [Knipp & Uhlenbeck (23)]. The order of magnitude of the number of short muon tracks observed so far is not in disagreement with such a "bremsstrahlung" hypothesis [Primakoff (24)].

The lifetime of the neutral pion against decay into two γ-rays is too short to be measured electronically, and so far the only measurements have been geometrical, based on the distance which the neutral pion travels from the time it is created in a nuclear event until it decays. The best of these measurements are by Kaplon, Peters & Ritson (25) who have used photographic emulsions to study the neutral pions from large cosmic ray stars. They find a lifetime of the order of 10^{-14} sec.

Granted that there exists a strong interaction between nucleons and neutral pions, the decay of the latter into a pair of γ-rays is not unexpected theoretically, since a pair of protons may be virtually formed and then decay into a pair of γ-rays. This process was first pointed out by Sakata & Tanikawa (26) and is represented schematically by the equation $\pi^0 \rightarrow p^+ + p^- \rightarrow 2\gamma$. Steinberger (27) has given a recipe for calculating in weak coupling approximation the rate of this process, a recipe which avoids divergences, and preserves gauge invariance. Recently Schwinger (28) has made formal improvements in the derivation of the recipe. The validity of these calculations is not clear, and the only reason they are taken at all seriously is that they actually predict the correct order of magnitude for the neutral pion lifetime, while attempts to guess the order of magnitude by dimensional arguments generally lead to much too short a value.

The Interaction Between Pions and Nucleons

Almost all attempts to understand the coupling between pions and nucleons have been based on the Yukawa assumption that the fundamental process consists of the emission and absorption of single pions by nucleons. This assumption arises by analogy with the coupling of the electromagnetic field to charged particles. In Maxwell's theory the field quantities appear linearly in the Hamiltonian terms representing the interaction with charges and currents. When the Maxwell theory is quantized, this linearity leads to the fundamental principle that the quanta of the electromagnetic field (photons) are emitted and absorbed one at a time by charged particles. Yukawa first conceived of the pions as the quanta of the nuclear force field, and it was natural to maintain the feature of linearity and thus of single pion emission and absorption.

It was expected at first that the main difference between photons and pions would be that pions have a nonzero rest mass. We have already seen another difference demonstrated: the photon has intrinsic angular momentum $1\hbar$ (the electromagnetic field is a vector field); the pion on the other hand has zero spin (a pseudoscalar field). Nevertheless most of the current thinking continues to assume a pion-nucleon coupling linear in the pion field, and we shall do so here, as a basis for discussion. It will appear that this assumption leads to an excellent qualitative understanding of many experiments, but one cannot be certain that nonlinear couplings, such as proposed by Schiff (29), would not give just as good agreement. The best argument in favor of a linear interaction is that its effects are simpler to calculate.

The nature of the interaction between pions and nucleons may be investigated by measurements of the energy levels of stationary states or by measurements of the rate and angular distribution of reactions. Just as in atomic physics, it should be possible to learn the most from simple systems, i.e., those involving a small number of particles. At the present time we have only a rough and qualitative theoretical interpretation of even the one- and two-nucleon systems; so it is too early to expect to understand experments involving the interaction of pions with complex nuclei. Of course, as Schiff (29)

points out, if nonlinear meson effects exist, they will be most prominent in complex nuclei where the meson field strengths are strongest. Many experiments with complex nuclei have been done, usually because single nucleons or deuterons are harder to handle in the laboratory, and it is an interesting theoretical exercise to assume linearity and try to relate the results of an experiment with a complex nucleus to the corresponding experiment with a single nucleon or deuteron. However, we are still too ignorant of complex nuclear wave functions to arrive at any definite conclusions from such a procedure.

By the end of 1951, at least rough studies had been made of the following four simple systems, each one with and without the addition of an electromagnetic field: (*a*) The single nucleon; (*b*) one nucleon and one meson; (*c*) two nucleons; (*d*) two nucleons and one meson. We shall consider these systems and the measurements made on them in the order given, which is the order of simplicity. We shall not consider any of the many experiments with complex nuclei, since up to now nothing definitive about the pion-nucleon coupling has been learned from these experiments.

The single nucleon.—It may seem strange that a single neutron or proton should be of interest in considering the pion-nucleon interaction. According to present day field theories there does indeed exist the concept of a bare nucleon, or "nucleor" which is completely free of mesons. However, such a bare nucleon is not a stationary state since there is always an interaction between the nucleor and the zero point fluctuations of any fields to which the nucleor may be coupled. The physically observed neutron or proton is an eigenstate of the total Hamiltonian, including all interactions, and, therefore, will contain components corresponding to the presence of one or more quanta of the fields to which the nucleors are coupled. These components are small for the electromagnetic quanta (photons) because of the small value of $e^2/\hbar c$ (1/137), but the strength of coupling between pion and nucleor fields (usually characterized by a constant, $g^2/\hbar c$) is at least one order of magnitude larger than this. It is to be expected, therefore, that the physically observed nucleon actually consists of a bare nucleon and one or more pions a substantial fraction of the time. We have rather firm convictions about some of the properties of a bare nucleon; so a study of the corresponding properties of a physical nucleon should yield information about the number and distribution of the attendant pions and thus about the pion-nucleor coupling.

Up to now no excited states (isobars) of the single nucleon have been detected which are stable against meson emission. The existence of such stable states should lead to inelastic nucleon-nucleon scattering whenever the relative kinetic energy in the center of mass system is greater than the energy of the excited state relative to the ground state. There still may be, of course, virtual isobars which are unstable against meson decay. Such states can be studied most naturally by reactions involving a free meson which are to be taken up in the next section. The lack of stable isobars is of great theoretical significance since it puts an upper limit on the strength of the

pion-nucleon coupling. In particular, the so-called strong coupling theory, first proposed by Wentzel (30), cannot be correct in its primitive form since it predicts an isobar in the neighborhood of 40 Mev excitation energy.[4]

We can also get useful information from another property of a single nucleon: the magnetic moment. Knowing the spin to be $\frac{1}{2}\hbar$, it is extremely plausible to assume that the Dirac equation applies to nucleors as well as to electrons and that, therefore, the magnetic moment of a bare proton is one nuclear magneton ($e\hbar/2Mc$) and the magnetic moment of a bare neutron is zero. The deviations of the actually observed proton and neutron magnetic moments from these "bare" values may be attributed, we hope, to the pion "clouds" surrounding the nucleors [Wick (31); Fröhlich & Heitler (32)].

It has already been shown that the pion has zero spin and an intrinsic parity opposite to that of the nucleor. Conservation of angular momentum and parity then requires that if a pion is emitted by a nucleor, it must be emitted into a P state. The parity requirement excludes the even orbital angular momentum quantum numbers ($l=0, 2, 4 \ldots$), and since the nucleor has spin $\frac{1}{2}$ both before and after emission of the pion, the latter can at most carry away one unit of angular momentum. This argument neglects the possible formation of nucleon pairs, a neglect which would be rigorously correct only if the mass of the nucleor were infinite. It remains a plausible approximation, however, for pions of kinetic energy well below the rest energy of a nucleon ($\sim$1 Bev); and since the latter seem to predominate (see below) we may expect to find the pions in the "cloud" surrounding the nucleor to be mainly in P states. (If the intrinsic parity of the pions were even, the above argument would lead to an S state distribution which of course would give no contribution to the magnetic moment. The very existence of the anomalous moments, therefore, is an indication that our parity assignment is correct.)

The magnetic moment caused by the circulation of a charged pion in a P state is roughly $e\hbar/2m_\pi c$,[5] so the expected order of magnitude of the anomalous magnetic moment can be estimated if we assume the number of pions in the cloud to be on the average no greater than one. For the proton, the circulating pion will be positive, with its orbital angular momentum parallel to the total angular momentum (the observed "spin"). Thus the proton moment should be greater than one nuclear magneton by an amount somewhat less than $e\hbar/2m_\pi c$ (roughly seven nuclear magnetons). For a neutron the circulating pion will be negative, with its orbital angular momentum still parallel to the total angular momentum, so by symmetry the anomalous neutron magnetic moment should be equal and opposite to that of the proton. Experimentally the anomalous proton moment is 1

[4] The strong coupling theory corresponds to the assumption that very many pions are, on the average, simultaneously present in the "cloud" surrounding the nucleor.

[5] This is a nonrelativistic argument, whereas actually the pions in the cloud are moving very fast. A correct treatment is not difficult and does not alter our conclusions.

(nuclear magnetons) and the neutron moment -1.9, substantiating our qualitative notions.

Quantitatively, however, the theory is very shaky. It is not possible to arrive at a finite probability for finding a single meson in the cloud, if the nucleor is treated as a point source of pions. As in many other problems of field theory, one encounters here an ultraviolet catastrophe resulting from the overwhelming statistical weight of short wave length pions. A cutoff can be introduced by allowing the nucleor to recoil [Case (33); Luttinger (34); Slotnick & Heitler (35); Drell (36); Borowitz & Kohn (37)], but this cannot be the whole story because this cutoff occurs at such small wave lengths that the contribution to the magnetic moment from the nucleor recoil becomes comparable to the contribution owing to the pions, and the symmetry between neutron and proton is completely spoiled.

It appears that a much more drastic cutoff procedure is required, such as is obtained by "spreading out" the nucleor over a finite region of space [Pauli (38)]. If this is done, sensible results can be obtained by suitably adjusting the "shape" of the nucleor, but it is doubtful whether at present such a procedure should be called a "theory." One can only say that the average wave length in the pion cloud seems to be considerably longer than a nucleor Compton wave length and the average number of pions present less than one. Even if a large average number of pions did not lead to an excessively large net magnetic moment, it would lead to equal and opposite total (not anomalous) moments for the neutron and proton, as shown explicity by Pauli & Dancoff (39).

In addition to producing an anomalous magnetic moment, the charged pion cloud also has detectable electrostatic properties, so that the anomalous electromagnetic interactions of a nucleon cannot completely be described in terms of a magnetic moment. There are additional terms which, for example, cause the neutron to be scattered by the coulomb field of an electron without flipping its spin. The actual existence of such terms has been indicated by experiments of Havens and co-workers (40) and Hughes *et al.* (41); but the electrostatic effects seem much smaller than one might expect on the basis of elementary theoretical reasoning. Fermi & Marshall (42) have emphasized that if the nucleon core is concentrated at the center of a pion cloud whose average radius is of the order of the pion Compton wave length, then the neutron should have a short range electrostatic potential associated with it which is many times as strong as is observed. In fact, Foldy (43) has shown that the entire observed neutron-electron scattering can be attributed to a relativistic (nucleon recoil) effect which has nothing to do with the separation of pionic and nucleonic charge. A simple but startling conclusion which might be drawn is that the charge of the nucleon "core" is distributed over approximately the same volume as is the pionic charge!

One nucleon and one pion.—At the present time two comparably simple types of reactions, involving one nucleon and one free pion, are amenable to experiment. The first is the type $\pi+N\rightarrow\pi+N$, where N represents a

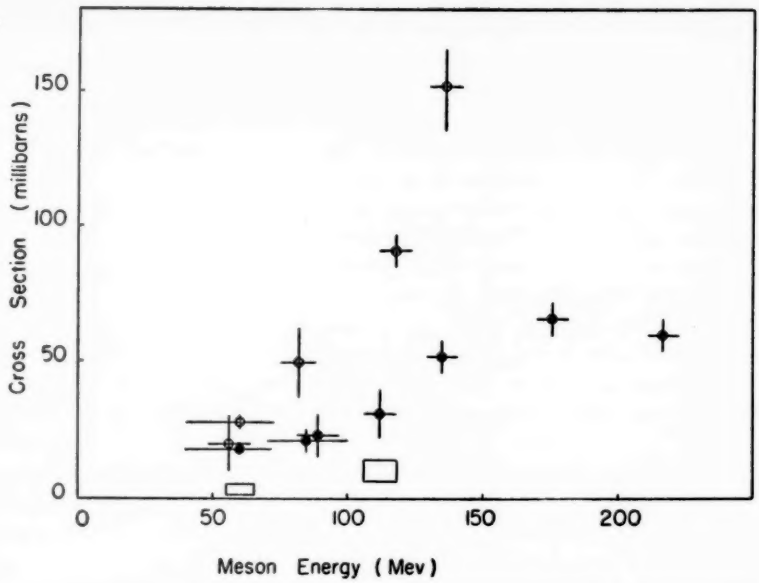

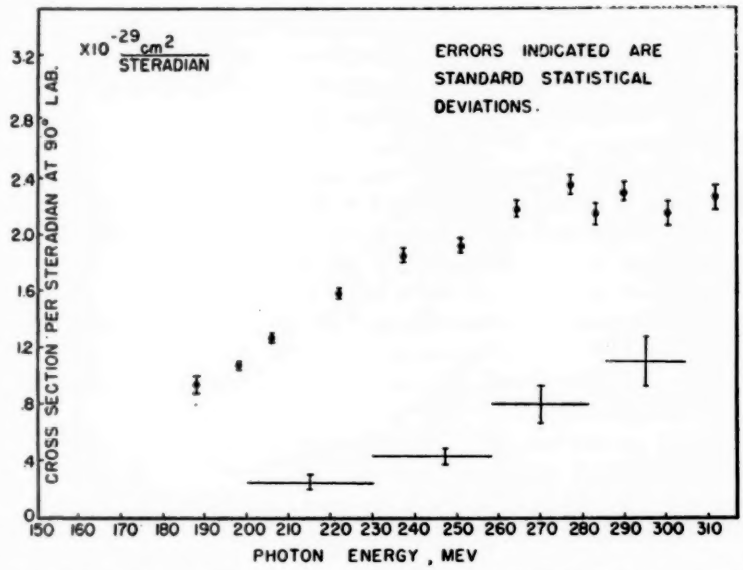

FIG. 1. (Upper) Total cross sections for scattering of pions by hydrogen as a function of pion energy in laboratory system. Circles denote positive pions, squares negative pions. The open rectangle at 60 Mev represents the total elastic negative cross section as measured by Shutt, Fowler, *et al.* (46). The open rectangle at 112 Mev is the total elastic negative cross section as inferred by the Chicago group from an observation at 90° to the beam.

FIG. 2. (Lower) Photoproduction cross section for pions emitted at 90° to the incident beam versus incident photon energy. The higher set of points represent positive pion, the lower crosses neutral pion production.

nucleon and π a pion. This is of course pion-nucleon scattering. The second type is $\gamma+N\rightleftharpoons\pi+N$, where the reaction going to the right is usually called photo-pion production and that to the left the radiative absorption of pions.

The most useful available data on pion-nucleon scattering are due to workers at Chicago [Anderson, *et al.* (44)] and at Columbia [Isaacs, Sachs & Steinberger (45)]. The latter group has measured the total cross section for negative pions on hydrogen at 60 and 85 Mev kinetic energy (in the lab system) and for positives at 60 Mev. The former group has covered the range from 90 to 217 Mev for negatives, and from 56 to 135 Mev for positives. The results are summarized in Figure 1. At one energy and one angle (112 Mev and 90° in the laboratory) it has been established at Chicago that the negative total cross section is divided between ordinary scattering ($\pi^-+p\rightarrow\pi^-+p$) and exchange scattering ($\pi^-+p\rightarrow\pi^0+n$) roughly in the ratio one to two.

The rapid initial increase of the cross sections with energy is immediately understandable in terms of our previous conclusion that the primary interaction between pions and nucleons is in P states. At low kinetic energies, in the absence of a resonance, a P-wave scattering cross section will increase in proportion to the square of the kinetic energy. The increase cannot go on indefinitely, of course, for the absolute upper limit of the cross section for scattering in a state of orbital angular momentum 1 is $4\pi(2l+1)\lambda\!\!\!^{-2}$ (where $\lambda\!\!\!^{-}$ is the relative wave length divided by 2π). For example, at 200 Mev laboratory kinetic energy the value of $\lambda\!\!\!^{-2}$ is approximately 7 millibarns, so that the absolute maximum (a 90° phase shift) for a pure P-wave cross section is $12\pi(7\text{ millibarns})=260$ millibarns. The positive pion cross section is already 150 millibarns at 135 Mev laboratory kinetic energy and, if the increase continues at the same rate as for the negative, it will be near 200 millibarns at 200 Mev. Thus the cross section, if it is a P-wave effect primarily, will have to turn over near 200 Mev and start down. It is obvious from the numbers already measured that between 100 and 200 Mev laboratory kinetic energies we are dealing with phase shifts approaching 90°; so, if we wish, we may speak of "resonance" scattering in this region. (The "resonance" is so broad that some people object to the use of the concept. The whole question is purely one of language and readers who feel so inclined should substitute the phrase "strong interaction" whenever the word "resonance" reappears.)

In order to discuss the ratios of positive to negative and ordinary to exchange scattering, it will be worth while first to review the hypothesis of charge independence, enunciated by Breit & Feenberg (47) and put into mathematical form by Kemmer (48) to include pions as well as nucleons.[6] According to this hypothesis the proton and the neutron have identical properties except for their interactions with the electromagnetic field. A similar statement also holds true for the positive, negative, and neutral pions. In

[6] Recently Watson (49) has called attention to the fact that Kemmer's mathematical formulation of the charge independence principle is unique.

the language of spectroscopy, one refers to the nucleon as a doublet in charge space (with two possible states, neutron or proton, which cannot be distinguished in the absence of an electromagnetic field) and to the pion as a triplet (positive, negative, and neutral). The charge degree of freedom is called the "isotopic spin," and one superposes the isotopic spins of the various particles in a system according to the vector model to form the total "isotopic angular momentum." It is possible to restate the principle of charge independence as the principle that the total isotopic angular momentum is a constant of the motion. It is true, of course, that one can never get away entirely from an electromagnetic field, for even in a vacuum the zero point field fluctuations may induce self energies and other effects. (The not quite equal masses of neutron and proton and of charged and neutral pions are presumably due to electromagnetic self energies.) However, because $e^2/\hbar c$ is small, electromagnetic effects will usually be small in comparison to the large effects from the pion-nucleon interaction. Such will not be the case, of course, in a reaction such as photo-meson production which depends for its very existence on the electromagnetic field; and in such reactions one cannot expect the conservation laws, which result from charge symmetry, to hold even approximately. They should hold quite well, however, in a reaction such as pion-proton scattering.

Heitler (50) has pointed out that if one accepts the principle of charge independence for the pion-nucleon system certain relationships between the rates of the reactions, $\pi^+ + p \rightarrow \pi^+ + p$, $\pi^- + p \rightarrow \pi^- + p$, and $\pi^- + p \rightarrow \pi^0 + n$, must exist. The only charge variable on which the scattering may depend is the total isotopic angular momentum, I, which in the pion-nucleon system may take on just two values, $I = \frac{1}{2}$ and $I = 3/2$ (the nucleon has isotopic spin $\frac{1}{2}$; the pion isotopic spin 1). Brueckner (51) recalled that in the strong coupling approximation, field theory predicts the lowest lying excited state (isobar) of pion-nucleon system to have an isotopic spin 3/2 and a total angular momentum 3/2 [Pauli & Dancoff (39)]; and he suggests that the scattering observations should be interpreted in terms of such a virtual state occurring at an energy of about 280 Mev. (This is 140 Mev relative kinetic energy, corresponding to a laboratory kinetic energy of 200 Mev.)

Whether or not the strong coupling approximation makes any sense at all, if one accepts simultaneously the principle of charge independence and the notion that there is a "resonance," it is plausible that the "resonance" might occur in one or the other of the two isotopic spin states, $I = \frac{1}{2}$ or $I = 3/2$, but not both. Thus, as pointed out by Fermi (44), it makes sense to see if the majority of the observed scattering in the energy region between 100 and 200 Mev lab kinetic energy can be ascribed to either the $I = \frac{1}{2}$ or the $I = 3/2$ state. A very simple calculation shows that with a proton target the ratio of the three cross sections

$$\sigma_{(+)\rightarrow(+)}/\sigma_{(-)\rightarrow(0)}/\sigma_{(-)\rightarrow(-)}$$

will be 0:1:2 for pure $I = \frac{1}{2}$ scattering and 9:2:1 for pure $I = 3/2$ scattering.

The agreement of the latter set of ratios with the Chicago total cross sections is startling, but preliminary measurements of angular distributions indicate that the $I=\frac{1}{2}$ states are not negligible.

Direct tests of the charge independence hypothesis are possible and are being attempted in several laboratories. A simple example of such a test is the comparison of the two reactions, $p+p\rightarrow\pi^{+}+d$ and $n+p\rightarrow\pi^{0}+d$. Yang (52) has pointed out that with charge independence the second of these two reactions must have half the rate and the same angular distribution as the first. Another example is the reaction $p+d\rightarrow\pi^{+}+d+n$, pointed out by Garwin (53), which with charge independence must have twice the cross section for the reaction, $p+d\rightarrow\pi^{0}+d+p$.

Let us consider next the available information on photo-pion production from protons. The reaction $\gamma+p\rightarrow\pi^{+}+n$ has been studied most thoroughly by Steinberger & Bishop (54). The cross section for pions emitted at 90° to the incident beam was observed to increase gradually with energy, as shown in Figure 2. The angular distribution has been measured for 255 Mev photons, but it will be seen that interpretation at such a high energy is difficult; so this aspect of the results will not be discussed here.

We may crudely visualize the photo-pion production process as resulting from the absorption of the incident photon by a charged pion in the cloud. If the pion were to escape without a secondary interaction with the nucleon core, the resulting energy and angular distribution would depend entirely on the current density distribution in the initial pion cloud. However, a secondary interaction with the nucleon core (a virtual "scattering") will certainly affect the result, and on the basis of the measured pion-proton scattering cross sections we must be prepared for significant secondary "scattering" whenever the emitted photo-pion has a kinetic energy greater than about 50 Mev. For lower energies, the measured scattering cross sections are sufficiently small in comparison with the dimensions of the cloud that neglect of secondary interactions in the photo-pion process may be reasonable. Confirmation of these qualitative ideas is given by the observed excitation function for neutral photo-pions. According to our picture, the most important mechanism for neutral photo-pion production is the secondary "exchange scattering" of a charged pion which has absorbed the photon. Since the scattering cross sections are strongly increasing functions of the energy, the neutral photo-pion excitation function should increase much more rapidly with energy than the charged does, but become very small near the threshold. This is exactly what has been observed both by Panofsky *et al.* (55) and by Silverman & Stearns (56). The experiment of the latter group is the more complete and shows a cross section for neutral pions emitted at 90° to the photon beam which increases steeply with photon energy, as shown in Figure 2.

The relatively copious production of neutral photo-pions at photon energies above 200 Mev shows that pion-nucleon scattering will have to be thoroughly understood before an analysis can be made in this energy region

of either the charged or the neutral photo-pion production. However, first attempts, based on the virtual isobaric state model, have already been published [Brueckner & Case (57); Fujimoto & Miyazawa (58); Brueckner & Watson (59)], while Drell (60) has applied the Bloch-Nordsieck technique. A phenomenological calculation has been made by Kaplon (61) who attempts to replace the effect of the secondary scattering by giving the bare nucleor an intrinsic magnetic moment equal to the static nucleon magnetic moment.

One fairly clean-cut theoretical statement can be made about the angular distribution of the neutral photo-pions, if they are due to a secondary scattering and if this scattering occurs, as we believe, predominantly in P states. The neutral pions must obviously, then, emerge in P states and their angular distribution can only be of the form, $A+B\cos^2\theta$ (in the center of mass system). Brueckner & Watson (59) point out, further, that if the scattering takes place predominantly in states of total angular momentum 3/2, the distribution will be of the form, $5-3\cos^2\theta$. Kaplon's model (61), on the other hand, predicts $1+\cos^2\theta$. Experimentally, the angular distribution of neutral photopions is still in doubt.

It should be possible, by charged photo-pion measurements very close to threshold, where the secondary scattering is small, to determine some features of the current distribution in the initial pion cloud. For example, the naive picture which has been employed here ascribes the current simply to the motion of the pions. It is very easy to show that, if this is the case, no pions can be emitted either forward or backward, while the excitation function near threshold will vary with the 3/2 power of the excess energy. Conventional field theory on the other hand [see Steinberger & Bishop (54) for references] leads to a strong additional current, concentrated on the nucleon core, which near threshold gives isotropic pion production with a 1/2 power energy excitation function. The confirmation or disproof of the existence of this strange anomalous current must await further experiments.

If one assumes no anomalous currents, the absolute value of the charged photo-pion cross section at the lowest energy (190 Mev photon energy, 23 Mev pion energy) measured by Steinberger & Bishop (54) may be used to give the density of moderate frequency pions in the cloud [Blair, Chew, Friedman & Salzman (62)]. When combined with the experimental value of the anomalous nucleon magnetic moment, this density leads to an estimate that the total probability for finding a charged pion in the cloud is about 30 per cent, while the average pion momentum is $\sim m_\pi c$. Note that this is just the order of magnitude of the pion momentum which is most strongly scattered by a nucleon.

The inverse of the photoproduction of charged pions is susceptible to experiment in the reaction $\pi^-+p\rightarrow\gamma+n$. So far, this reaction has only been studied for pions of zero energy [Panofsky *et al.* (5)], and no absolute value for the rate is known. What is known is that the reaction has a rate roughly the same as that of the competing reaction $\pi^-+p\rightarrow\pi^0+n$ (which is made

possible by the $\pi^- - \pi^0$ mass difference). This coincidence is not easily discussed in terms of our simple picture. The S state of the pion-nucleon system is involved in an essential manner and, until further data are available on the strength of the S-state interaction, no definite conclusions about the significance of the capture experiment are possible. A weak coupling calculation [e.g., Marshak, Tamor & Wightman (63)], in which the anomalous current mentioned above plays the crucial role, gives fair agreement with the experimental ratio.

Two nucleons.[7]—It is clear, in view of the difficulty of describing even the single nucleon, that we must be still very far from understanding the two-nucleon system; and beyond the most qualitative considerations, attempts to make a theory of the interaction between two nucleons in terms of the associated pion fields have been unsuccessful. This does not mean that Yukawa's original idea is incorrect, for most of the difficulty can be attributed to an excessive abundance of high frequency pions which is given by conventional field theory (point nucleons) and which leads to a theoretical prediction that the range of nuclear forces (resulting from the exchange of pions between the two individual clouds) should be of the order of a nucleon Compton wave length (2×10^{-14} cm.) rather than, as is actually observed, a pion Compton wave length (1.4×10^{-13} cm.). The observed range, of course, is a measure of the average radius of the pion clouds, confirming again that in the cloud the average pion wave length is relatively long. Also, the fact that nuclear forces are observed to couple the nucleonic spin with the orbital angular momentum (the deuteron has a quadrupole moment) confirms the anisotropy of the individual clouds; so the experimental observations on the two-nucleon system substantiate our notion that a cloud of "long" wave length P-wave pions is associated with each nucleon. These observations have so far, however, added very little to our quantitative knowledge of the pion-nucleon interaction.

In spite of the complexity of the two-nucleon system, it can give some information about the validity of the charge independence hypothesis. According to this hypothesis, the force (nonelectromagnetic) acting between two neutrons, two protons, or a neutron and a proton, should be the same in states of the same orbital angular momentum and spin. It has been shown that in the singlet S state at low energies (<10 Mev) the n–p and p–p forces are equivalent; but experiments at higher energies have not yet been analyzed in terms of the individual contributing states. Information about the n–n force is based on an analysis of the differences between light mirror nuclei, which shows that, except for electromagnetic effects, the n–n and p–p interactions are identical.

Extensive studies have been made of the two-nucleon system in the presence of an electromagnetic field; but as might be expected, nothing about the

[7] For references and background to the material mentioned so briefly in this section, see Blatt & Weisskopf (64).

pion-nucleon interaction has been deduced from the results that cannot be more directly deduced from experiments on the one pion-one nucleon system. For reasons of economy, therefore, these studies will not be discussed here.

Two nucleons and one pion.—Except for the existence of selection rules resulting largely from the Pauli principle, the combination of two nucleons and one pion would seem much too complicated to yield new information of a fundamental character. It has already been pointed out, of course, that the best demonstration of the odd, intrinsic parity of a pion rests on the reaction $\pi^-+d\rightarrow 2n$, and that an excellent test of the validity of the charge independence hypothesis could be made by comparison of the reactions $p+p\rightarrow \pi^++d$ and $n+p\rightarrow\pi^0+d$. The chief reason why the latter application works for example, is that the Pauli principle requires the deuteron to be a state of total isotopic spin zero, thus greatly simplifying the problem. It seems not unlikely that other applications based on the Pauli principle are yet to be discovered.

However, because the deuteron is an unusually loosely bound structure it may be considered in a certain approximation as simply a free neutron plus a free proton, and as such it offers two fundamental advantages in the study of the pion-nucleon interaction: (*a*) It is the closest approximation to a free neutron target which is available for experiment. (*b*) Coherent effects, resulting from the geometrical proximity of the neutron and proton, will be significant in certain reactions, so that not only the magnitude of the pion wave function, but also its phase, can be studied. The detailed study of pion-deuteron scattering now being carried out at Chicago and Columbia may well turn out to be an important source of fundamental information if the approximation of treating the neutron and proton as essentially free is justified. A preliminary study of the question of justification has been made by Chew & Wick (65) and by Segall (66).

It should be emphasized here that in the absorption or emission of a pion by a pair of nucleons, the interaction between the nucleons cannot be neglected, since without this interaction the reaction could not proceed. The discussion of emission and absorption processes, therefore, is on a much less firm basis than that of scattering, and except where selection rules can be applied the theoretical interpretation of experiments is very difficult. The most informative experimental study to date is by Durbin, Loar & Steinberger (12) who measured the rate and angular distribution of the reaction $\pi^++d\rightarrow 2p$ at laboratory pion kinetic energies running from 25 to 53 Mev. The angular distribution is strongly peaked at 0° and 180° in the center of mass system, a fact which can be qualitatively understood in terms of a strong P-wave pion-nucleon interaction [Chew, Goldberger, Steinberger & Yang (67)]; but the detailed shape of the angular distribution does not seem important in view of the complexity of the nucleon-nucleon interaction. The fact that the magnitude of the absorption cross section is observed to increase steeply with increasing meson kinetic energy may likewise not be important; but, with the indications of a P-wave "resonance" already discussed

for the pion-proton system, it is tempting to suppose that this rapid increase may indicate the approach to a "resonance" here.

It is not possible to measure the deuterium capture cross section for neutral pions because of their instability. However, the inverse reaction, $n+p\rightarrow\pi^0+d$, is possible, as well as the companion process, $p+p\rightarrow\pi^0+p+p$. The importance of the former reaction as a test for the charge independence hypothesis has already been mentioned. However, the currently available high energy neutron beams are inadequate; so direct data exists only for the latter reaction. The former must be approximated by using deuterons as targets. Hales, Hildebrand, Knable & Moyer (68) found the cross section for the production of neutral pions by 340 Mev protons incident on hydrogen to be less than that for protons incident on deuterium by a factor $.08\pm.07$, which implies that the reaction $p+p\rightarrow\pi^0+p+p$ is strongly inhibited with respect to the reaction $p+n\rightarrow\pi^0+d$. The probable explanation of this inhibition was pointed out by Brueckner & Watson (69): The experiment in question was carried out fairly close to threshold (22 Mev pion kinetic energy in the center of mass system), so that the relative angular momentum of the two nucleons in the final state must have been zero with an overwhelming probability. The Pauli principle then required that the two-proton system be a singlet, with $J=0$. Now we have seen that the strong pion-nucleon interaction occurs in P states; so one expects the bulk of the final states to have total $J=1$ and even over-all parity. But there are no such states in the initial proton-proton system, again because of the Pauli principle; so the much weaker S state interaction must be relied upon, and the reaction rate is greatly reduced.

The remaining reaction of the two nucleon-pion type about which something is known is photo-pion production in deuterium, $\gamma+d\rightarrow\pi^++2n$, or π^-+2p, or π^0+n+p. These processes are tractable theoretically in the same sense as is pion-deuteron scattering [Machida & Tamura (70); Morpurgo (71); Chew & Lewis (72); Feshbach & Lax (73)] but experimental studies are still in a preliminary stage. The most significant result so far is that to within about 10 per cent the rates of positive and negative pion production are equal [White *et al.* (74); Littauer & Walker (75)]. In the approximation in which the nucleon is considered infinitely heavy, this result is anticipated, from the same symmetry argument which predicts equal and opposite anomalous magnetic moments for neutron and proton.

Summary of information on the pion-nucleon interaction.—The experimental data available imply that the interaction between pions and nucleons is strong only in P states. The P wave interaction is not strong enough to produce a stable nucleonic isobar but it gives very large phase shifts (perhaps as large as 90°) for pion-nucleon scattering with relative kinetic energy in the range 100 to 150 Mev. All existing experiments are consistent with the picture that the pion field associated with a single nucleon (which is to be regarded as the "ground" state of the pion-nucleon system with isotopic spin $\frac{1}{2}$ and total angular momentum $\frac{1}{2}$) contains predominantly P-wave

components whose wave lengths are of the order of a pion Compton wave length (1.4×10^{-13} cm.). Indications are that less than, but of the order of, one pion is present in the cloud on the average.

Two grave difficulties have blocked attempts to make a field theory in analogy with quantum electrodynamics: (*a*) The coupling is too strong for a weak coupling approximation and too weak for a strong coupling approximation. (The solution for a case of intermediate coupling is extremely difficult to obtain.) (*b*) The only simple type of point coupling (the so-called pseudovector or gradient coupling), which has a chance of explaining the low frequency behavior of pions, predicts a catastrophic pion-nucleon interaction at high frequencies. A distributed type of coupling (nonlocal theory), which spreads the nucleor over a volume whose radius is a substantial fraction of the meson Compton wave length, might circumvent this difficulty [Pauli (38)], but theoretical work on this idea is still in the most primitive stage.

THE HEAVIER SUBNUCLEAR PARTICLES

In recent years several particles have been discovered in the cosmic radiation which are heavier than pions but which also seem to have strong nuclear interactions. The masses of these particles are too large to be produced by any of the presently operating accelerators, although some of the machines now being constructed may eventually be capable of generating them. At the moment the available information on the new particles is sketchy and in places very confusing. We shall discuss the various particles in the order of increasing confusion.

The Tau Mesons

The charged τ-mesons have been identified by their characteristic decay in nuclear emulsions. In cases observed to date, the singly charged τ-meson comes to rest, then decays into three other charged particles [Brown *et al.* (76); Harding (77); Fowler *et al.* (78); Hodgson (79)]. It is believed that only three secondaries result, since in all five cases the secondaries are coplanar.

In four instances it has been possible to measure some characteristics of the secondaries such as the angles between secondaries, range, grain density, and small angle scattering. Suitable combinations of these data have yielded values for the masses or ratios of masses of the secondaries which are consistent with the decay scheme

$$\tau \rightarrow 3\pi. \qquad 1.$$

As further support for this mode of decay, Brown *et al.* (76) have observed one slow secondary which was almost certainly a π^--meson since it produced a nuclear disintegration from which two protons were seen to emerge.

When it is assumed that all the secondaries are π-mesons, the total energy released is found to be unique within experimental error in the four measurable cases, and the τ-meson mass is thus found to equal 966 ± 10 electron masses. Independent estimates for the mass of two τ-mesons have been ob-

tained from measurements on the primary τ, and, while not very precise, these estimates are consistent with the value given above [Fowler *et al.* (78)].

The Bristol group has estimated that the lifetime of the τ-meson is not less than 10^{-9} sec. [Fowler *et al.* (78)].

Jacobsohn (80) has shown that the τ-meson must be pseudoscalar if: (*a*) the decay scheme into three pions is valid, (*b*) the pions themselves are pseudoscalar, and (*c*) two-particle decay into two pions or a pion and a photon is strictly forbidden. The last assumption is the only questionable one.

A neutral τ-meson has not yet been identified, but the lack of data should not be interpreted as evidence against its existence. The process by which a neutral τ-meson would decay might involve neutral secondaries and thus be extremely difficult to identify.

Neutral *V*-Particles

Neutral *V*-particles have been postulated to explain the anomalous forks which appear in cloud chamber photographs of penetrating showers. The forks consist of a pair of oppositely charged particles originating at a single point in the gas; in the majority of cases the angle between the tracks is less than 90°, and the tracks are close to minimum ionization.

Among the investigators in this field, there seems to be agreement on the following characteristics of the forks:

(*a*) The great majority of the forks cannot be explained by well-known mechanisms in nuclear physics and must be ascribed to the decay of a neutral particle into at least two charged secondaries.

(*b*) Measurements of ionization and momentum have revealed that some of the positive secondaries are protons [Armenteros *et al.* (81); Leighton *et al.* (82); Thompson, *et al.* (83, 84)].

(*c*) By similar measurements, a large fraction of negative secondaries appear to be mesons. Both Leighton and Armenteros and their associates have observed an apparent π–μ decay in the gas, suggesting that at least some of the negative secondaries are pions. Thompson's group at Indiana has reported one case where both negative and positive secondaries were slow; the negative appeared to be a meson, the positive a proton.

(*d*) Electronic secondaries seem unlikely since no radiative showers caused by the secondaries have originated in plates contained in the cloud chambers [Armenteros *et al.* (81); Seriff *et al.* (85)]. The absence of radiative showers has also been cited as evidence against neutral pion secondaries.

(*e*) Where high energy nuclear disintegrations and V^0 tracks have appeared simultaneously, the fork of the V^0 has usually been coplanar to the nuclear disintegration. This is a strong argument in favor of two-particle decay. Fretter & May (86) have reported the most evidence on this point and find 27 out of 35 instances of coplanarity. Supporting evidence comes from Seriff *et al.* (85), Armenteros *et al.* (81), and Deutschmann (87).

The apparent lack of coplanarity in some instances does not necessarily imply that there are also three-particle decays. It is possible to explain the apparent anomalies by supposing either that these V^0-particles had nothing to do with the observed nuclear disintegration and the true origins of the V^0's were outside the chamber, or that the V^0's were scattered before decay.

There is less agreement on the subject of positive meson secondaries than there has been on the above five topics. The Manchester group of Armenteros and co-workers feel that a considerable fraction of the positive secondaries are mesons; they find that 8 of 14 low momentum positives fail to show the heavy ionization characteristic of protons, thus implying that these more lightly ionizing secondaries have mass less than that of a proton.

On the other hand, in nine tracks reported by Leighton and co-workers only two positive secondaries could have meson mass while the other 7 positives were probably protons or particles with mass of the order 1000 m_e. Similarly Thompson records that only one of his four measured positive secondaries has a mass less than that of the proton.

In the face of these uncertainties, the creation of decay schemes to describe the disintegrations is still a speculative enterprise. From an analysis of the dynamics of the decay, the Manchester workers feel that it is possible to describe their observations in terms of the following two-particle processes which have roughly equal probability:

$$\begin{aligned} &(a) \quad V^0 \rightarrow p + \pi^- \\ &(b) \quad v^0 \rightarrow \pi^+ + \pi^-. \end{aligned} \qquad 2.$$

Using this scheme they obtain $Q_{V,v}$, the energy release in the rest system of the V^0, v^0-particles:

$$Q_V = 46 \text{ Mev} \qquad Q_v = 122 \text{ Mev}.$$

The individual data show considerable spread about these values, and it is stated that the experimental uncertainties are large. The Indiana group has described several events according to scheme (a) and finds that $Q \cong 35$ Mev with only about 5 Mev experimental error.

When Leighton and associates (82) analyze those forks which appear to contain protons according to scheme (a), they find a spread of individual Q values similar to those obtained by the Manchester group. One of their interpretations has been that there are two unique Q values for scheme (a) of the order 34 and 75 Mev.

At the present time the question of neutral V-particle decay can best be summarized: There is fair evidence for the decay of a neutral V by process (a) into a proton and a negative meson; decay into two mesons may also occur but the light positive secondary has not been convincingly identified.

The lifetime has been estimated by Seriff and associates and also by Deutschmann to be about 3 (10^{-10}) sec. from the distribution of decay points along the line of flight. Fretter & May believe that a lower limit of (10^{-10}) sec. can be placed on the lifetime.

CHARGED κ- AND V-PARTICLES

Nuclear emulsion and cloud chamber studies have revealed that other charged particle transmutations are possible besides the characteristic three body decay of charged τ-mesons. O'Ceallaigh (88) of the Bristol group has uncovered a breed of heavy charged particles in emulsions which he has christened "κ-mesons."[8] These κ-mesons have been characterized by their observed decay from rest into another singly charged particle and by a mass of the order of 1200 m_e. On the other hand, charged particles decaying in cloud chambers with about one-fifth the frequency of neutral V forks have been dubbed charged V-particles. The present data on these charged V decays allow only a few guesses to be made about the nature of the primaries and secondaries.

O'Ceallaigh's original two κ-mesons had the following properties: One particle (κ_1) of mass about 1300 m_e gave rise to a light particle with mass less than 400 m_e moving at minimum ionization. The other particle (κ_2) of mass 1125 m_e led to a μ-meson with 6 Mev kinetic energy, identified by its characteristic electron decay.

While it may be possible to classify some of the decay products from charged V-particles as muons, this cannot be true in all cases. For example, Bridge & Annis (89) have recorded a charged V-decay in which the secondary was strongly scattered in a lead plate quite unlike the expected behavior for a μ-meson. The masses of the charged V-particles have not been measured with the precision of the κ-mesons and mass estimates to date have depended on assumptions concerning the nature of the neutral secondaries [Armenteros *et al.* (90)].

An interesting case has been reported by Armenteros *et al.* (90) who observed an apparent double decay where a neutral V emerged from the original charged V disintegration; these workers believe that the neutral V decayed into two mesons.

CONCLUSION

It has been possible to discuss almost all phenomena involving pions without reference to the heavier particles which also interact strongly with nucleons; but it is of course true that a final theory must treat simultaneously all the particles mentioned in this article as well as others which are still undiscovered or unidentified. Considering the preliminary status of the experimental observations on the heavier particles, the successful construction of theory should probably not be expected for at least a few years. However, attempts are already being made along at least two distinct lines.

One line of attack starts with the notion of a fundamental length in the universe and seeks to set up a self-consistent mathematical formalism upon

[8] The term "κ-meson" as used in this article refers to a characteristic type of observation, not to a unique particle.

this premise. In one attempt of this kind, Darling (91) found that a discrete spectrum of particle masses was a natural consequence. A more empirical approach is being made by other workers, who seek to find simple patterns in the interactions and the masses of the various particles. A rather ambitious and moderately successful attempt in this direction was recently reported by Pais (92). It would be premature at the present time to discuss in detail any of these schemes.

LITERATURE CITED

1. Marshak, R. E., *Ann. Rev. Nuclear Sci.*, **1**, 1–42 (1952)
2. Barkas, W. H., Smith, F. M., and Gardner, E., *Phys. Rev.*, **82**, 102 (1951)
3. Peterson, V., Iloff, E., and Sherman, D., *Phys. Rev.*, **84**, 372 (1951)
4. Cartwright, W. F., *Phys. Rev.*, **82**, 460 (1951)
5. Panofsky, W. K. H., Aamodt, R. L., and Hadley, J., *Phys. Rev.*, **81**, 565 (1951)
6. Cheston, W. B., *Phys. Rev.*, **83**, 1118 (1951)
7. Marshak, R. E., *Phys. Rev.*, **82**, 313 (1951)
8. Johnson, M. H. (Personal communication)
9. Cartwright, W. F., Richman, C., Whitehead, M. N., and Wilcox, H. A., *Phys. Rev.*, **78**, 823 (1950); **81**, 652 (1951)
10. Whitehead, M. N., and Richman, C., *Phys. Rev.*, **83**, 855 (1951)
11. Clark, D. L., Roberts, A., and Wilson, R., *Phys. Rev.*, **83**, 649 (1951)
12. Durbin, R., Loar, H., and Steinberger, J., *Phys. Rev.*, **83**, 646; **84**, 581 (1951)
13. Brueckner, K., Serber, R., and Watson, K., *Phys. Rev.*, **81**, 575 (1951)
14. Steinberger, J., Panofsky, W. K. H., and Steller, J., *Phys. Rev.*, **78**, 802 (1950)
15. Yang, C. N., *Phys. Rev.*, **77**, 242 (1950)
16. Wiegand, C. E., *Phys. Rev.*, **83**, 1085 (1951)
17. Chamberlain, O., Mozley, R. F. Steinberger, J., and Wiegand, C., *Phys. Rev.*, **79**, 394 (1950)
18. Kraushaar, W. L., Thomas, J. E., and Henri, V. P., *Phys. Rev.*, **78**, 486 (1950)
19. Jakobson, M., Schulz, A., and Steinberger, J., *Phys. Rev.*, **81**, 894 (1951)
20. Lederman, L. M., Booth, E. T., Byfield, H., and Kessler, J., *Phys. Rev.*, **83**, 685 (1951); (personal communication)
21. Friedman, H. L., and Rainwater, J., *Phys. Rev.*, **84**, 684 (1951)
22. Fry, W. F., *Phys. Rev.*, **83**, 1268 (1951)
23. Knipp, J. K., and Uhlenbeck, G. E., *Physica*, **3**, 425 (1936)
24. Primakoff, H., *Phys. Rev.*, **84**, 1255 (1951)
25. Kaplon, M. F., Peters, B., and Ritson, D. M., *Phys. Rev.*, **85**, 900 (1952)
26. Sakata, S., and Tanikawa, Y., *Phys. Rev.*, **57**, 548 (1940)
27. Steinberger, J., *Phys. Rev.*, **76**, 1180 (1949)
28. Schwinger, J., *Phys. Rev.*, **82**, 664 (1951)
29. Schiff, L. I., *Phys. Rev.*, **84**, 10 (1951)
30. Wentzel, G., *Helv. Phys. Acta*, **13**, 269 (1940)
31. Wick, G. C., *Accad. Lincei*, **21**, 170 (1935)
32. Fröhlich, H., and Heitler, W., *Nature*, **141**, 37 (1938)
33. Case, K. M., *Phys. Rev.*, **76**, 1 (1949)
34. Luttinger, J. M., *Helv. Phys. Acta*, **21**, 483 (1948)
35. Slotnick, M., and Heitler, W., *Phys. Rev.*, **75**, 1645 (1949)
36. Drell, S. D., *Phys. Rev.*, **76**, 427 (1949)
37. Borowitz, S., and Kohn, W., *Phys. Rev.*, **76**, 818 (1949)
38. Pauli, W., *The Meson Theory of Nuclear Forces*, 11 (Interscience Publishers, Inc., New York, N. Y., 69 pp., 1946)
39. Pauli, W., and Dancoff, S. M., *Phys. Rev.*, **62**, 85 (1942)
40. Havens, W. W., Rainwater, L. J., and Rabi, I. I., *Phys. Rev.*, **82**, 345 (1951)
41. Hughes, D., Harvey, J. A., and Goldberg, M. D., 27(4), D6 (1952)
42. Fermi, E., and Marshall, L., *Phys. Rev.*, **72**, 1139 (1947)
43. Foldy, L. L., *Phys. Rev.*, **83**, 688 (1951)

44. Anderson, H. L., Fermi, E., Long, E. A., Martin, R., Nagle, D. E., Lundby, A., and Yodh, G. B., *Phys. Rev.*, **85**, 934 (1952)
45. Isaacs, P., Sachs, A., and Steinberger, J., *Phys. Rev.*, **85**, 803 (1951)
46. Shutt, R. P., Fowler, E. C., Miller, D. H., Thorndike, A. M., and Fowler, W. B., *Phys. Rev.*, **84**, 1247 (1951)
47. Breit, G., and Feenberg, E., *Phys. Rev.*, **50**, 850 (1936)
48. Kemmer, N., *Proc. Cambridge Phil. Soc.*, **34**, 354 (1938)
49. Watson, K., *Phys. Rev.*, **85**, 852 (1952)
50. Heitler, W., *Proc. Roy. Irish Acad.*, **51**, 33 (1947)
51. Brueckner, K. A., *Bull. Am. Phys. Soc.*, **27**(1), Y9 (1952)
52. Yang, C. N. (Personal communication)
53. Garwin, R. L., *Phys. Rev.*, **85**, 1045 (1952)
54. Steinberger, J., and Bishop, A. S., *Phys. Rev.*, **78**, 494 (1950); *Phys. Rev.*, **86**, 171 (1952)
55. Panofsky, W. K. H., Steinberger, J., and Steller, J., *Phys. Rev.*, **86**, 180 (1952)
56. Silverman, A., and Stearns, M., *Phys. Rev.*, **83**, 853 (1951)
57. Brueckner, K. A., and Case, K. M., *Phys. Rev.*, **83**, 1141 (1951)
58. Fujimoto, Y., and Miyazawa, H., *Progress Theoret. Phys. (Japan)*, **5**, 1052 (1950)
59. Brueckner, K. A., and Watson, K., *Phys. Rev.*, **86**, 923 (1952)
60. Drell, S. D., *Phys. Rev.*, **83**, 555 (1951)
61. Kaplon, M. F., *Phys. Rev.*, **83**, 712 (1951)
62. Blair, J. S., Chew, G. F., Friedman, M. H., and Salzman, F., *Phys. Rev.* (Personal communication)
63. Marshak, R. E., Tamor, S., and Wightman, A. S., *Phys. Rev.*, **80**, 765 (1950)
64. Blatt, J., and Weisskopf, V., *Nuclear Physics*, Chap. 2, p. 38 (John Wiley & Sons, Inc., New York, N. Y., 864 pp., 1952)
65. Chew, G. F., and Wick, G. C., *Phys. Rev.*, **85**, 636 (1952)
66. Segall, B., *Phys. Rev.*, **83**, 1247 (1951)
67. Chew, G. F., Goldberger, M. L., Steinberger, J., and Yang, C. N., *Phys. Rev.*, **84**, 581 (1951)
68. Hales, R. W., Hildebrand, R. H., Knable, N., and Moyer, B. J., *Phys. Rev.*, **85**, 373 (1952)
69. Brueckner, K. A., and Watson, K. A., *Phys. Rev.*, **83**, 1 (1951)
70. Machida, S., and Tamura, T., *Progress Theoret. Phys. (Japan)*, **6**, 572 (1951)
71. Morpurgo, G., *Nuovo cimento*, **8**, 552 (1951)
72. Chew, G. F., and Lewis, H. W., *Phys. Rev.*, **84**, 779 (1951)
73. Feshbach, H., and Lax, H. (Personal communication)
74. White, R. S., Jakobson, M. J., and Schulz, A. G., *Bull. Am. Phys. Soc.*, **26**(8), P3 (1951)
75. Littauer, R. M., and Walker, D., *Phys. Rev.*, **83**, 206 (1951); **82**, 746 (1951)
76. Brown, R., Camerini, U., Fowler, P. H., Muirhead, H., Powell, C. F., and Ritson, D. M., *Nature*, **163**, 82 (1949)
77. Harding, J. B., *Phil. Mag.*, **41**, 405 (1950)
78. Fowler, P. H., Menon, M. G. K., Powell, C. F., and Rochat, O., *Phil. Mag.*, **42**, 1040 (1951)
79. Hodgson, P. E., *Phil. Mag.*, **42**, 1060 (1951)
80. Jacobsohn, B. A., *Bull. Am. Phys. Soc.*, **27**(1), Y7 (1952)
81. Armenteros, R., Barker, K. H., Butler, C. C., and Cachon, A., *Phil. Mag.*, **42**, 1113 (1951)

82. Leighton, R. B., Wanlass, S D., and Alford, W. L., *Phys. Rev.*, **83,** 843 (1951)
83. Thompson, R. W., Cohn, H. O., and Flum, R. S., *Phys. Rev.*, **83,** 175 (1951)
84. Karzmark, C. J., Thompson, R. W., and Cohn, H. O., *Bull. Am. Phys. Soc.*, **27**(1), G9 (1952)
85. Seriff, A. J., Leighton, R. B., Hsiao, C., Cowan, E. W., and Anderson, C. D., *Phys. Rev.*, **78,** 290 (1950)
86. Fretter, W. B., and May, M. M., *Bull. Am. Phys. Soc.*, **26**(8), Q3 (1951)
87. Deutschmann, M., *Z. Naturforsch.*, **7a,** 142 (1952)
88. O'Ceallaigh, C., *Phil. Mag.*, **42,** 1032 (1951)
89. Bridge, H. S., and Annis, M., *Phys. Rev.*, **82,** 445 (1951)
90. Armenteros, R., Barker, K. H., Butler, C. C., Cachon, A., and Chapman, A. H., *Nature*, **167,** 501 (1951)
91. Darling, B. T., *Phys. Rev.*, **80,** 460 (1950)
92. Pais, A., *Phys. Rev.*, **86,** 663 (1952)

RADIATION EFFECTS IN SOLIDS[1]

By G. J. Dienes

Brookhaven National Laboratory, Upton, Long Island, New York

INTRODUCTION

High energy radiations may bring about extensive changes in the properties of solid substances. In particular, fast massive particles possess sufficient momentum to produce atomic displacements in solids. Wigner (1) first called attention to this effect, which is of considerable importance in the field of solid-state physics and reactor technology. Experimental verification came from the Radiation Chemistry Section of the Manhattan Project as reported by Burton (2, 3). In the last few years the study of the disordering of solids by radiation has become an important branch of the physics of crystal imperfections [See, for example, Seitz (4, 5)].

The fundamental theory of radiation effects centers around the laws of energy dissipation of a fast charged particle as it moves through a lattice. A major contribution to this field has been made by Bohr and his school (6). Their work has been mainly on the action of fast particles in gases, but many of the features are similar in solids. The present status of the theory for solids has been described in detail by Seitz (7). The whole field of the effects of radiation on materials has been critically reviewed by Slater, from a theoretical as well as experimental point of view, in a report written during the summer of 1949 and recently published as a declassified article (8). The purpose of the present paper is to summarize the progress of the last three years. It will be assumed that the reader is familiar with the major results described by Slater.

GENERAL SURVEY

Radiation effects are conveniently grouped into two quite distinct categories, namely, ionization effects and displacement effects. Ionization effects have been studied for many years (9 to 12) and it is not the purpose of this paper to review this extensive field. It must be appreciated, however, that it is impossible to produce atomic displacements either by fast neutrons or by fast charged particles without producing ionization. Theory shows (7, 8) that a large fraction of the energy of a fast charged particle is dissipated in ionization as the particle is slowed down. In a good conductor the ionization effects will disappear very quickly and will only contribute to the heating of the material. In an insulator, however, the electrons liberated by ionization may be trapped at various lattice imperfections resulting in more or less permanent changes in the substance. Similarly, in a molecular crystal ionization will bring about changes which are best described as chemical ones. For the purposes of the present paper emphasis will be placed on radiation effects

[1] The survey of the literature pertaining to this review was concluded in March, 1952.

resulting from displaced atoms. Ionization effects will be discussed briefly whenever they are of particular importance.

Theory of Displacement Production

On an atomic scale the production of displaced atoms may be described as follows. Consider first a fast neutron which will produce recoil atoms of a few hundreds of thousands of electron volts along its path. These recoil atoms which are fast charged particles, will in turn produce secondary recoils and so on. The fraction of energy dissipated in ionization decreases rapidly as the fast charged particle slows down and a large portion of the displacement damage is done at the end of the range although the integrated damage in the early part of the range is not negligible. The picture is essentially the same for fission fragments and for accelerated charged particles except for details of assigning the energy dissipated to ionization and to displacement effects. The number of displaced atoms may be calculated theoretically by essentially following the history of each particle, which is the procedure adopted by Seitz (7). The theory appears to be satisfactory within the regime of fast particles but much more needs to be done in the important range of intermediate energies (from a few hundred kv. down), which is the region of high displacement production. No significant contribution to the theory has been published since 1949.

The number of displacements produced by a fast particle depends significantly on what is called the "unit displacement energy," i.e., the energy required to knock an atom out of its position in the lattice. Seitz (7) has estimated this energy to be about 25 ev. This energy has been measured recently by Lark-Horovitz and co-workers (13) for germanium. They obtained a value of 31 ev for the unit displacement energy. This experiment, which will be discussed in more detail later, represents the most significant contribution to the problem of displacement production in the last few years.

A thermodynamic or statistical approach to damage production is also possible. The primary particle suddenly introduces a large amount of heat at a localized point in the lattice and a considerable region of material around the track of the fast charged particle will be heated to a high temperature. The region of excitation will rapidly expand accompanied by rapid fall of temperature. The result is a so-called "thermal spike," i.e., rapid heating and quenching of a small volume of the material. The basic idea of a thermal spike, namely that energy release takes place within a region of atomic dimensions, is not in disagreement with the atomic displacement picture, at least for substances of relatively high atomic weight. The primary recoils are essentially in the elastic collision range and lose their energy in travelling only a few lattice distances. The details of this picture, which are quite complex, are not completely worked out. Theoretical work by Brooks (14) indicates that, at least for metals, only a small fraction of the energy is transmitted to the lattice and a rather small additional activation is predicted for rate processes such as self-diffusion. In some cases, such as the disordering of

ordered alloys by irradiation, it appears profitable to invoke the thermal spike picture (15). It is not at all clear at present which theoretical picture will turn out to be the more profitable one.

Effect of Displaced Atoms on Physical Properties

It is clear that the properties of a solid may be drastically altered by displacing an appreciable fraction of its atoms. The changes will remain frozen in at all temperatures below the range of significant diffusion of the lattice disturbances. Various measurements and their interpretation are discussed later in this paper. For purposes of orientation, however, the more significant changes in physical properties are listed here. Electrical resistivity and hardness are significantly increased in metals. Crystal structure may be significantly altered as in disordering of ordered superlattice alloys. Further, it has been found that subsequent rate processes, such as reordering, are altered by prior irradiation. In semiconductors large changes are observed in electrical resistivity and other electromagnetic properties. As a matter of fact n-type germanium can be converted to p-type by nucleon bombardment. In insulators, in addition to ionization type of damage, physical property changes have been observed which are ascribable to displaced atoms. For example, pile irradiation of ionic crystals leads to large decrease in thermal conductivity. As a matter of fact, displacement damage in ionic compounds and ceramics appears to be considerably larger than in most metals (8). This is possibly associated with low annealing rates and the inability of most ceramics to flow plastically and thereby relieve large internal stresses. All of the above radiation effects can be removed (annealed) by appropriate heat treatment.

Pile bombardment may result in nuclear transmutations and bombardment with charged particles will leave a certain number of foreign particles in the sample. In both cases impurity atoms are left in the lattice which may have an appreciable effect on physical properties. The influence of fission fragments lodged in the material is expected to be very similar. Damage caused by impurity atoms is expected to be essentially impossible to anneal except at very high temperatures where a fraction of the impurity atoms may diffuse out of the lattice. Experience to date indicates that in most cases displacement damage far outweighs impurity damage, presumably because there are a large number of displaced atoms for every impurity atom.

It should be mentioned that both theory and experiment indicate that essentially the same type of damage is produced by neutron and accelerated particle bombardment. The reason for this is that, in both cases, the number of displaced atoms produced by secondaries, tertiaries, etc., is very large compared with that produced by the incident particle. Thus, the method of producing the initial recoil is unimportant. The choice is primarily one of experimental convenience. Excellent use has been made of cyclotron bombardment in the last few years, particularly by the groups at North American Aviation and Purdue University. A major advantage of this type of irradia-

tion is the low radioactivity level produced in the bombarded sample. As annealing studies have progressed, the importance of accurately controlled irradiations and low temperature studies has been appreciated and emphasized.

Basic Problems

The fundamental theory of radiation damage, discussed at the beginning of this section, gives an estimate of the number of displacements produced but tells us very little about the nature of the disturbance left behind in the lattice. The basic question of radiation effects in solids is this: What is the nature of the disturbances introduced in the lattice and what influence do they have on lattice properties? Two essential difficulties are immediately encountered when an answer is attempted: (*a*) we have only a vague picture of what these disturbances are or how many there are, and (*b*) our theories of physical properties of materials as influenced by atomic displacements are still very crude.

Most of the work of the last few years has been concerned with just these questions. The various models and analogies that have been used may be summarized as follows:

Interstitials and vacancies.—It is clear, on an atomic scale, that knocked-on atoms will leave vacant lattice sites behind and will finally come to rest in interstitial positions. This is a fundamentally attractive picture which is able to correlate many of the experimental results both on metals and semiconductors. These disturbances may, however, be highly localized in clusters along the track of the primary particle so that, in some cases at least, it may be more profitable to think about a disordering of the lattice akin to that produced by cold work or rapid local heating and quenching (thermal spike).

Cold work.—The analogy to cold work is based on the notion that the properties of crystals are a unique function of atomic positions regardless of how the atoms got there. In many cases this has been a fruitful notion and many of the radiation effects are similar to those produced by cold work. However, the analogy must break down if the nature of the disturbances introduced by cold work and by radiation is quite different. First of all, plastic deformation involves the motion and multiplication of dislocations while irradiation is not expected to introduce such an organized lattice disturbance. Some significant differences in behavior are, therefore, to be expected on this basis. Further, differences are also expected in the vacancy-interstitial type of disturbances left behind in the lattice as indicated by the following considerations. It is known from recent theoretical work by Seitz (5) that cold work very probably introduces vacancies. Interstitials may also be introduced by plastic deformation but it requires much higher energies to produce interstitials than vacancies, at least in metals (16, 17), so that one may expect the number of interstitials created by cold work to be rather small. No such restrictions apply, of course, to the production of interstitials by fast particle irradiation and one may expect corresponding differences in

the behavior of cold worked and irradiated materials. Indeed, significant differences in annealing behavior have been observed which may be explicable by such considerations. As a matter of fact, one may learn more from a critical study of the differences rather than the similarities of radiation effects and the effects of cold work.

Thermal spikes.—Rapid heating and quenching caused by the passage of a thermal spike may leave a portion of the lattice in a disordered state. In simple close packed solids a fraction of the atoms will be left in displaced positions after the cooling of a spike. The end result is, therefore, equivalent to a localized production of vacancies and possibly interstitials. The properties of such an agglomeration of disturbances are not well known, nor is it clear whether it is necessary to invoke this type of description which is more complex than a description in terms of simple interstitials and vacancies since the interaction among the disturbances must be taken into account. In alloys or compounds, the rapid heating and quenching of the material may promote local atomic exchanges and thereby leave the substance in an altered state even though most of the atoms have returned to lattice positions. The best known example is the disordering of ordered alloys by irradiation. The notion of thermal spikes has been useful in interpreting such phenomena.

A Systematic Breakdown of the Field of Radiation Effects in Solids

It is evident that a great deal of careful experimental and theoretical work will be required to elucidate the nature of radiation damage and to decide among the alternatives presented in the previous section. Most of the early work was primarily concerned with simple measurement of the changes in physical properties brought about by irradiation. Recently more powerful tools have been looked for. Some work has been done with x-rays but the use of x-ray and neutron diffraction studies has by no means been exhausted. The importance of rate studies, such as the annealing of lattice disturbances and the effect of prior irradiation on subsequent rate processes, has recently been emphasized by Dienes (18). A kinetic study essentially looks at the motion of lattice disturbances and consequently investigates the nature of the disturbance much more closely than can be done by measurement of the amount of damage alone.

Clearly this whole field of study could be systematized along several lines. If an over-all theory were available the results could be discussed within a proper theoretical framework. Since this is not the case, it is sensible to organize the material either according to types of solids or properties. The decision is necessarily somewhat arbitrary but it appears preferable to use the various types of substances as the primary breakdown.

It is convenient to construct a table, such as Table I, in which materials are listed along a column and the properties studied along a row. A rough over-all impression of the status of the field is obtained by inserting the per-

TABLE I

CURRENT STATUS OF RESEARCH ON RADIATION EFFECTS IN DIFFERENT MATERIALS
(AS OF FEBRUARY, 1952)

Properties Studied / Materials	Crystal Structure	Electrical	Mechanical	Thermal	Optical	Rate Processes	Magnetic	Chemical Structure	Surface Effects
Metals	15, 35, 36, 37, 38, 39, 40	18, 35, 41, 42, 43, 44, 45	35, 38, 46, 48, 48, 49, 50, 51, 52, 107			18, 53, 54, 55, 56, 57, 58, 59, 60, 61, 62, 63, 64, 106			50(?)
Semiconductors		65, 66, 67, 69, 70, 71, 72, 73, 74, 75, 76, 77, 78, 79, 80			68, 76, 81, 82, 83	72, 73, 74	67, 69, 71, 72, 73, 76		
Insulators				96, 97, 98	84, 85, 86, 87, 88, 89, 90, 91, 108	84, 85, 86, 87, 88, 89, 90, 91, 96, 97, 98	94, 95	92	93
Molecular Solids			102, 103, 104		104, 105			100, 101, 102, 103 104	

tinent references in the appropriate boxes. Essentially this organization will be followed in the text.

It has been pointed out that radiation effects are also of considerable interest in connection with several important questions of the theory of imperfect crystals. The writer feels that this general survey would not be complete without mentioning the fact that, in spite of some security restrictions, the interaction between general solid state research and the field of radiation effects has been a very healthy one. A number of fundamental studies have been stimulated directly or indirectly by the new problems and phenomena discovered in this new field. Perhaps it is proper to cite graphite as an example. A number of fundamental unclassified contributions have appeared in the literature, many of them undoubtedly stimulated by the need for a more thorough understanding of the basic properties of this substance, whose importance in reactor technology is well known. Electronic structure (19), electro-magnetic properties (20 to 26), mechanical properties (27, 28), properties of interstitial compounds (29, 30, 31), diffusion characteristics (32), crystal structure (33), and lattice vibrations (34) have been extensively studied in the last few years.

RADIATION EFFECTS IN DIFFERENT TYPES OF MATERIALS

In this section specific experiments and their interpretation will be discussed. The organization of the material follows essentially that of Table I.

Metals

Changes in crystal structure.—The copper-gold order-disorder alloys are the only systems exhibiting structural changes which have been extensively studied. Siegel (15) first called attention to the very large changes in resistivity obtained upon neutron bombardment in ordered samples of $AuCu_3$. On the basis of resistivity changes he concluded that the ordered structure was essentially destroyed by bombardment while a disordered sample showed practically no change. X-ray studies indicated that the superlattice lines had disappeared. Similar results were obtained by Martin and co-workers (35) on both $AuCu_3$ and AuCu. In this study the alloys were irradiated with the α-particle beam of the Berkeley 60-in. cyclotron and the effects of such irradiations on several physical properties were investigated. Changes in lattice parameters, illustrated in Figures 1 and 2 prove conclusively that the fast particle irradiation has disordered the originally ordered alloy. No change in lattice parameter was observed in bombarded samples which were initially disordered. The results for AuCu are particularly convincing. The ordered structure of this alloy is tetragonal while the disordered one is face-centered cubic. Figure 2 shows clearly the gradual transition from the tetragonal structure of ordered AuCu to the cubic phase corresponding to complete disorder. Figure 1 is interpreted similarly since $AuCu_3$ is known to expand as it transforms from order to disorder. The resistivity changes are in complete aggreement with the x-ray results. Recent experiments of Cook &

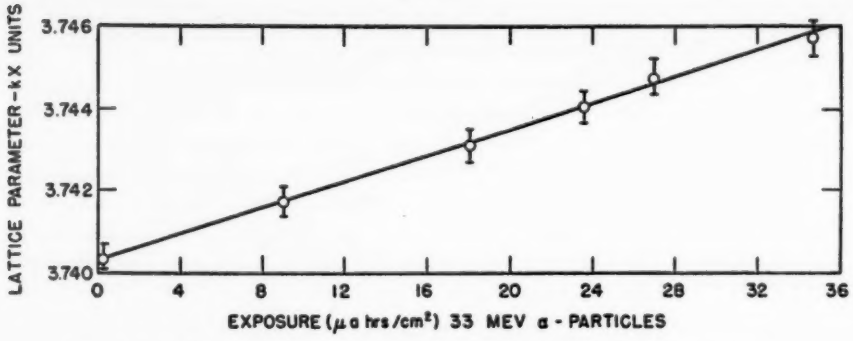

FIG. 1. Effect of α-particle bombardment on the lattice parameter of ordered Au Cu_3 (from reference 35).

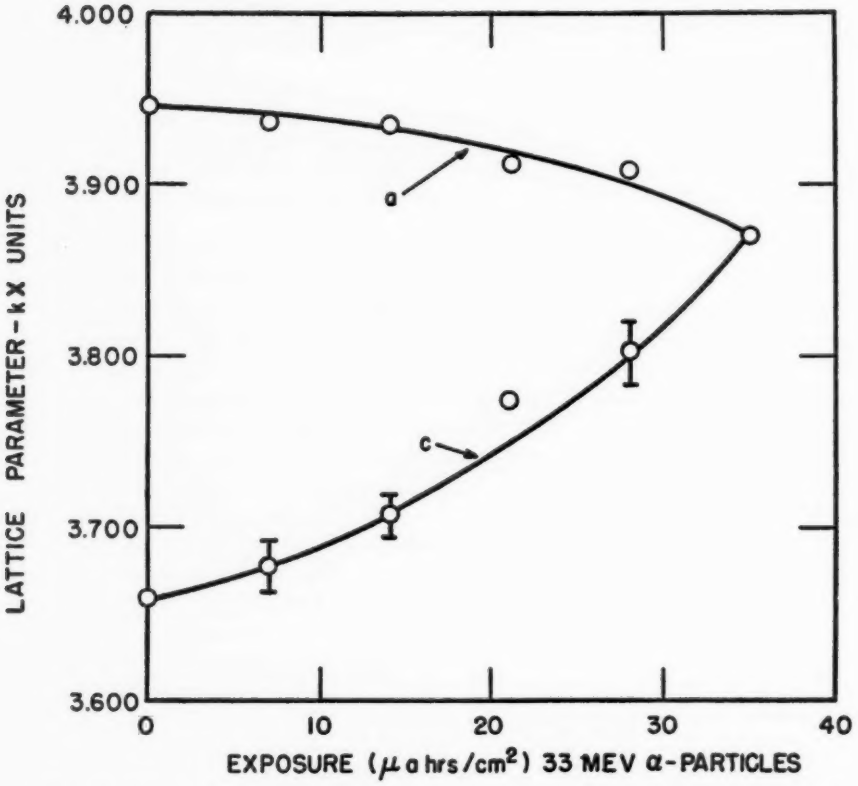

FIG. 2. Effect of α-particle bombardment on the lattice parameters of ordered AuCu (from reference 35); a and c are the tetragonal lattice parameters, and 1 KX unit is very nearly equal to 10^{-8} cm.

Cushing (36) on $AuCu_3$ exposed in the NRX reactor at Chalk River are also in agreement with the results described here.

Hardness measurements indicate (35), however, that irradiation does not leave the alloy in a state identical to that obtained by thermal disordering. For AuCu, for example, the hardness change (an increase) resulting from bombardment is in the opposite direction to the change expected for a disordering process. Similarly, both ordered and disordered samples of $AuCu_3$ increase in hardness as a result of irradiation. Kinetic studies have also shown that subsequent reordering rates are quite different in thermally disordered and radiation disordered alloys. These experiments will be discussed in detail under *Rate processes*. It may be mentioned at this point, however, that irradiation will probably change the local order in disordered as well as in ordered alloys.

Siegel (15) and Cook & Cushing (36) have interpreted the above results in terms of the thermal spike picture. Recent work by Martin (37) indicates that the results may also be described in terms of the number of displaced atoms although this question cannot be settled until the unit displacement energy has been measured for these alloys.

Order-disorder alloys are particularly suitable for radiation damage studies for two reasons: (*a*) physical property changes that result from displaced atoms may be observed even after the displaced atoms have returned to lattice sites since they are expected to return in a random manner and hence leave the degree of order altered; and (*b*) several properties of these alloys are very sensitive to the state of order of the material. Further study of these systems will undoubtedly be very profitable.[2]

Other metallic systems amenable to structural studies are precipitation-hardening alloys. The copper-beryllium system has been studied by Billington & Siegel (38), Martin and co-workers (35) and Murray & Taylor (39). Radiation hardening in solution annealed samples of this alloy is much greater than in pure copper. Resistivity increases are also quite large. In general, the more beryllium there is in solution the greater is the effect of irradiation. These findings suggest that segregation or preprecipitation nucleation processes occur during irradiation. The x-ray evidence, however, is not yet conclusive. Billington & Siegel (38) report further line broadening on samples whose lines are already broadened as the result of prior cold work or heat treatment. No line broadening was found in the other experiments discussed above. Murray & Taylor observed, however, a small shift in the 311-line corresponding to a lattice contraction. Guinier-Preston zones, which should detect the earliest stages of precipitation, have been looked for in

[2] Recently Williams & Nesbitt observed a decrease in the saturation magnetic moment of ordered $MnNi_3$ upon irradiation in the Brookhaven pile (111). This change is presumably attributable to disordering of the sample. Preliminary experiments at North American Aviation (112) on β-brass indicate that this alloy can also be disordered by irradiation at low temperature even though disorder cannot be frozen in by quenching.

complex and at its present stage of development its predictive usefulness is still very limited.

From a fundamental standpoint it is desirable to study the effect of radiation on those properties which are best understood, namely the elastic constants. In general, a bulk property is not expected to be changed appreciably by the displacement of a relatively small number of atoms. Recent theoretical work by Dienes (46) indicates, however, that the presence of interstitial atoms will result in appreciable increases in the elastic moduli, at least for close packed metallic lattices. In such substances the elastic constants are determined primarily by the repulsive interactions of the closed ion shells. This potential is of an exponential nature and varies extremely rapidly with interatomic distance. As the interaction distance is shortened, for example by creating an interstitial, the energy of the system increases sharply on the repulsive side of the potential curve. The creation of vacancies by removal of atoms results essentially in the destruction of some normal interactions. Thus, one expects the influence of the interstitials to outweigh heavily the effect of the vacancies. Detailed calculations confirm the above picture. Vacancies alone reduce the elastic moduli by essentially a bulk effect while interstitials increase appreciably the elastic moduli. In copper, for example, it is estimated that 1 per cent interstitials increase the elastic moduli by 5 to 7 per cent. It is concluded that the theoretically predicted effects should be easily observable in copper and that changes in elastic constants may serve, therefore, as a useful tool for distinguishing between interstitial atoms and lattice vacancies. This latter point is quite important, since, as indicated in the previous section, vacancies and interstitials are not distinguishable by changes in electrical resistivity. Preliminary experiments by Bowman & Tarpinian (47) indicate that Young's modulus of Cu increases by as much as 10 per cent upon heavy cyclotron irradiation. Much more work is required before the theory can be evaluated properly.

In contrast to bulk properties, some structure-sensitive mechanical properties are very drastically changed by irradiation. As indicated above, their interpretation, however, is much more difficult and intricate. Increase in hardness caused by irradiation appears to be a very general phenomenon in metals (35, 38). The work of Blewitt, Coltman & Sherrill (48) on single crystals of Cu shows very clearly that the major effect is on the critical shear stress. These investigators studied the stress-strain curves of irradiated and unirradiated crystals. The critical shear stress increased from 0.241 to 2.00 kg./mm.^{2} for a fast neutron flux of about 2×10^{18} nvt.[3] After appreciable plastic deformation the differences in the stress-strain curves essentially disappear as shown in Figure 4. The discontinuities at a shear strain of about 0.6 are due to an additional irradiation of about 2×10^{18} nvt. It is clear that after cold work the effect of irradiation is much smaller than for

[3] The number of neutrons per square centimeter incident on the sample is indicated by nvt; nv is the flux in neutrons per square centimenter per second, and t is the irradiation time.

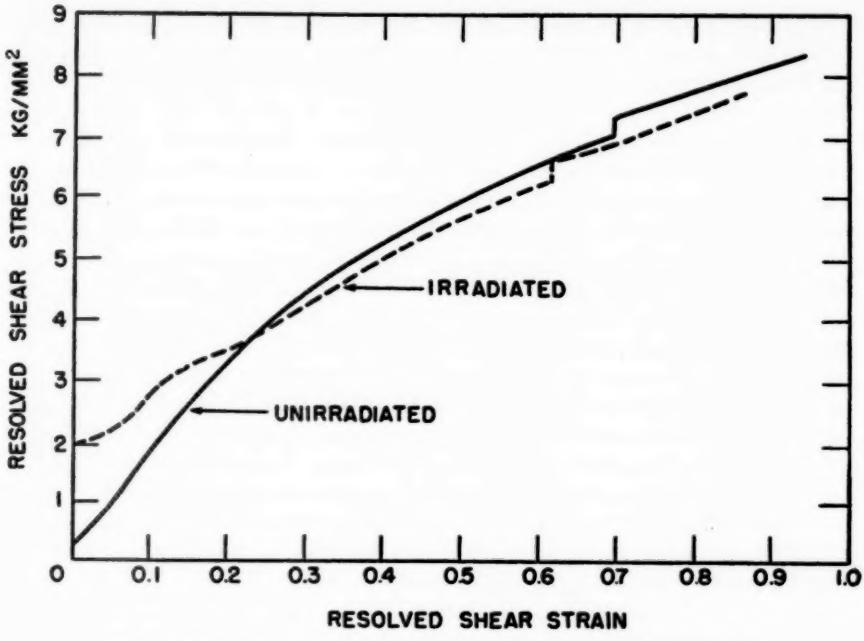

FIG. 4. Stress-strain curve of copper crystals (from reference 48).

annealed samples. It is also clear from Figure 4 that there is no one-to-one correspondence between cold work and radiation hardening. On the basis of the shape of the stress-strain curve of the irradiated specimen Blewitt and co-workers suggest that irradiation is somewhat similar to solid-solution hardening.[4] Vacancies and interstitials would act as impurity atoms and impede the motion of dislocations. The change in critical shear stress, however, is much larger than would be expected on the basis of this analogy. Simple interstitials and vacancies may not be able to account for these results and more complex disturbances may have to be postulated.[5]

A more detailed comparison of cold work and radiation effects will be

[4] In this connection Jamison & Blewitt (107) have recently presented some interesting new results. They have investigated the slip lines formed upon cold working irradiated and unirradiated single crystals of copper and observed pronounced differences in the two cases. The slip characteristics of the irradiated crystal were similar to those of α-brass.

[5] Recent and more detailed studies by Blewitt and co-workers (109) indicate that isolated vacancies and interstitials may explain the change in critical shear stress. Critical shear stress vs. bombardment curves indicate strong similarity to shear hardening by dissolved impurities. If comparison with the action of impurities in ionic crystals is valid then, from the data given by Schmid & Boas (110), one may conclude that a very small fraction of disturbances can lead to large changes in critical shear stress.

presented in the next section in connection with annealing studies. The subject of creep also belongs to *Rate processes* but since its importance is in connection with the mechanical stability of materials it will be discussed here.

It is very difficult to estimate theoretically the effect of radiation on creep rate (8, 49). One can argue that the imperfections introduced in the lattice should impede the motion of dislocations and thereby reduce the creep rate. On the other hand creep may be more rapid during irradiation since enough of the atoms may be kept stirred up by the irradiation to allow the stress to relax more rapidly. Experiments to date are not consistent. Andrade (50) measured the creep rate of cadmium under α-particle bombardment from polonium and found appreciable increase in the creep rate, particularly during the early stage of the creep process. Andrade's results may be explicable on the basis of surface effects. It is known that the creep rate of some metals is extremely sensitive to surface conditions (see, for example, reference 51). More recently, Witzig (52) found no change in the creep rate of copper while under deuteron bombardment. Witzig, however, used rather low rates of irradiation and his null results may not be valid at heavier exposures.

Creep experiments in the presence of radiation are very difficult to carry out primarily because creep is extremely temperature-sensitive and, therefore, very accurate temperature control is required. In this particular case in-pile experiments may be actually easier to carry out and fortunately a number such experiments are planned or are in progress.

Rate processes.—It has been mentioned in the GENERAL SURVEY that kinetic studies may serve as an important tool for investigating the nature of lattice disturbances more closely than is possible by simple measurement of changes in physical properties. Kinetic studies fall naturally into two groups, namely, measurements during irradiation and measurements designed to study the nature of "frozen-in" damage. Altered creep and diffusion rates are examples of the first class. The influence of crystalline damage caused by irradiation upon kinetic processes taking place in the crystal constitutes the second class. Annealing of the lattice disturbances themselves and changes in the ordering rates subsequent to irradiation of order-disorder alloys, for example, are representative phenomena of this second group.

The influence of irradiation on creep rates has already been discussed in the previous section. The effect of irradiation upon diffusion in expected to be in the direction of increasing the rate of diffusion. Thermal spikes, general stirring up of the lattice, or an increased number of vacancies all would lead to increase diffusion rates. It is difficult to predict theoretically whether the lifetime of the various lattice disturbances introduced by irradiation is long enough at the unusual diffusion temperatures to alter appreciably the diffusion rate. It is known that at sufficiently low temperatures vacancies may be preserved (53) but it may not be possible to investigate diffusion at low enough temperatures by the usual techniques. The first careful study of

self-diffusion in the presence of radiation was carried out by Martin, Johnson & Goeddel (54) using the standard sectioning technique. These investigators found that irradiation with 10 Mev protons from the Berkeley 60-inch cyclotron had no effect on self-diffusion in polycrystalline silver. Recently these experiments were extended to single crystals of silver in order to eliminate grain boundary effects and thereby be able to make comparisons at lower temperatures (55). Still no effect could be observed at about 550°C. These results may not be conclusive since the diffusion region is irradiated in a non-uniform manner in such a cyclotron experiment and a large fraction of the damage is done near the end of the range of the particle which is also the region of low isotope concentration. This is again an experiment which is better done in the pile although it is possible to carry out the experiment under conditions of uniform irradiation in the cyclotron or an electron accelerator. It has been suggested that a rotating hollow cylinder plated on the end and irradiated from the side may serve for this purpose (56).

It should not be concluded from the essentially negative results discussed above that radiation has no important effect on rate processes. On the contrary, lattice disturbances introduced by irradiation have a very important influence on rate processes taking place in the lattice. First of all, annealing of the lattice disturbances themsevles, i.e., healing of the material after irradiation, is an extremely important feature of solid-state irradiation phenomena. Techniques for studying annealing as a function of temperature and general methods of analyzing such data have been described by Parkins, Dienes & Brown (57). The activation energies for the various annealing processes can always be derived from isothermal annealing curves without specifying the relation between the measured physical property and the lattice disturbance being annealed. In rendering a kinetic interpretation, however, one is faced with one of the fundamental problems of solid-state physics, already mentioned in the GENERAL SURVEY, namely, the theory of physical properties of solids as a function of crystal imperfections. Nevertheless some very interesting and suggestive results have been obtained. The most detailed work of this kind has been done by Bowen and co-workers (18, 58, 59) on copper. These workers investigated the annealing of cold work and radiation damage using residual resistivity as the physical property sensitive to lattice disturbances. They showed that the lattice disturbances introduced by these means obey Mattheisen's rule and consequently the residual resistivity may be taken as proportional to the number of lattice disturbances present. A comparison of the annealing of cold work and radiation damage, based on some of their early data, was given by Dienes (18) and is illustrated in Figure 5. In this graph, the incremental change in residual resistivity per unit change in annealing temperature is plotted as a function of annealing temperature for a typical tempering experiment; i.e., the specimen was annealed for a specified period of time (2 min.) at each of the increasingly higher temperatures (25°C. apart). While full analysis of such curves is difficult (57), the results show very clearly that the annealing

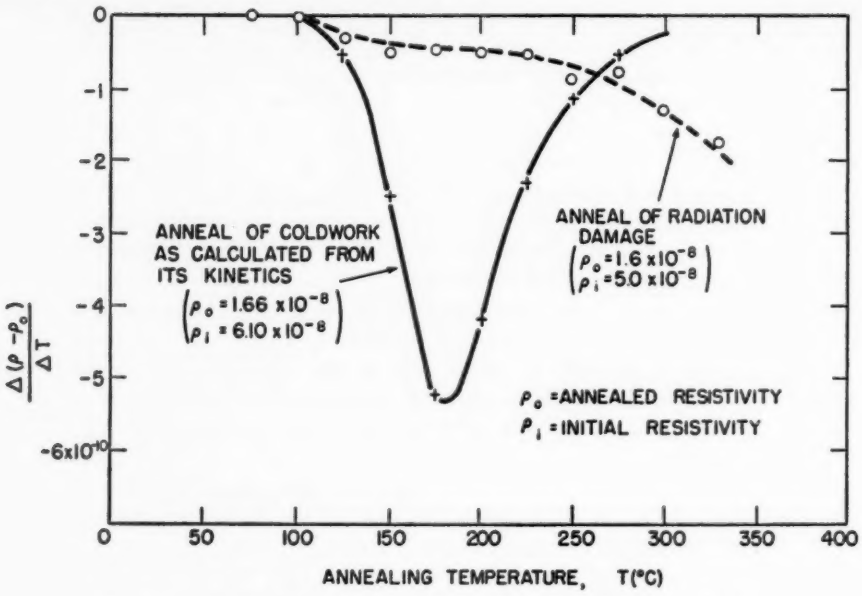

FIG. 5. Comparison of anneal of cold work and radiation damage in copper (from reference 18).

of cold work and radiation damage are quite different in character. The damage remaining in Cu at room temperature anneals out at a considerably higher temperature and probably over a wider temperature range than cold work. More recent results of the work of Bowen and co-workers may be summarized as follows:

(*a*) Copper, cold worked or irradiated at low temperature, exhibits large amounts of annealing starting at about −100°C. and extending up to near room temperature. For cold work these results are in agreement with the preliminary work of Molenar & Aarts (60) and Blewitt and co-workers (61). Similar results have been reported by Randolph (41) for radiation-damaged molydenum. In this respect a similarity between cold work and radiation effects has been demonstrated. While full kinetic studies have not yet been made, differential annealing curves of the type shown in Figure 5 indicate that also at low temperature the annealing characteristics of the two types of damage are quite different.

(*b*) Detailed kinetic studies for the annealing of cold work introduced at room temperature have been completed. In the 100°–250°C. range annealing can be represented as a process of single activation energy and as a reaction of high order. Comparable kinetic studies on radiation damage are not yet complete—the data so far confirm in its essentials the earlier results shown in Figure 5 (62).

(*c*) The data are not yet complete enough for sound interpretation and

it is not yet known whether a satisfactory interpretation can be based on the concept of simple interstitials and vacancies and their diffusion or diffusion and aggregation.

Investigations of this type are considered important and significant. Low temperature studies are to be emphasized. Further, it is important that annealing studies be carried out based on other physical property changes in addition to resistivity both for cold work and radiation effects.

Rate studies of the ordering of the order-disorder alloy AuCu have shown that this solid state reaction is considerably affected both by cold work and

TABLE II

EFFECT OF VARIOUS DISORDERING TREATMENTS ON THE KINETICS OF ORDERING IN THE ALLOY AuCu*

Treatment	Relative reaction rate for reordering at 250° C.†	Activation Temperature, E/k
Thermally disordered—rapidly quenched	1	13,940° K.
Ordered—disordered by α-particle cyclotron irradiation	2	13,365° K.
Ordered—disordered by cold work	3	6870° K. to 11,980° K.
Thermally disordered—rapidly quenched—cold worked	4	5950° K. to 10,700° K.
Thermally disordered—relatively slowly cooled	5	14,700° K.
Thermally disordered—rapidly quenched—irradiated	6	18,390° K.

* From reference (64).

† In order of decreasing rate, i.e. #1 of the series was observed to order most rapidly while #6 exhibited the lowest ordering rate at this temperature.

irradiation (18). This particular alloy was chosen for study because its ordering reaction appeared to be of a rather simple nature on the basis of earlier studies (63). Preliminary data reported by Dienes (18) indicated that the rate of ordering, subsequent to disordering by irradiation, was considerably higher than that following disordering by thermal means. These experiments were followed up by a much more detailed study by Stello (64), who considerably improved upon the earlier irradiation and cold working techniques. It was also found that the manner of thermal disordering, specifically the rate of quenching from above the transition temperature, had an appreciable influence on subsequent ordering rates. The present status of this study is summarized in Table II, where activation energies, and relative rates for order-

ing are given as affected by prior treatment of the samples. Attention is called to the following points:

(*a*) The activation energy for ordering is very closely the same for thermally disordered and radiation disordered samples although the reaction rates are changed considerably. The differences among these three samples may possibly be explained on the basis of the relative number of vacancies present, provided the ordering reaction may be thought of as catalyzed by the vacancies. Thermal creation and destruction of vacancies would be very slow at these temperatures but their random diffusion can bring about microscopic atomic exchanges.

(*b*) Disordering by cold work results in highly variable activation energies. One is probably dealing here with one or more complicating processes.

(*c*) Irradiation of a disordered specimen alters the subsequent reordering quite drastically—the rate is lowered and the activation energy is appreciably increased. The state of the sample is evidently quite different from that of either the cold worked or quenched ones. This last result is quite unexpected on the basis of (*a*) above and indicates that in addition to vacancies other disturbances (possibly interstitials) have been introduced. Further, irradiation may well change the short range order in disordered as well as in ordered alloys. This point has not yet been investigated.

These experiments prove conclusively that irradiation can influence very appreciably the course of solid-state reactions. Interpretation evidently will not be so easy as originally thought (18, 63). These phenomena are of sufficient importance, however, to warrant considerably more work and an extension to other order-disorder systems.[6]

Annealing studies of radiation effects and of the influence of irradiation on reaction rates are considered to be important tools in investigating the nature of radiation damage. Undoubtedly a great deal can be learned from critical comparisons with cold work and thermal treatment and the results are bound to be of interest in the general field of solid-state physics.

Semiconductors

Electrical properties.—The properties of semiconductors may be changed by heat treatment and by the introduction of impurities. One certainly expects that these substances will exhibit radiation effects produced by the passage of neutrons and charged particles. As a matter of fact, these materials are particularly sensitive to the action of nucleons because the number of car-

[6] In a very interesting recent article Blewitt & Coltman (106) argue that microscopic diffusion rates are appreciably increased by irradiation. They base this conclusion on measurements of the ordering rates of disordered $AuCu_3$ in the presence of a neutron flux. They find that the ordering rates are appreciably increased and interpret the results in terms of increased number of interstitials and vacancies. These results are in no way contradictory to the discussion given in this paper on AuCu. In view of the complex kinetic effects observed for AuCu, however, the writer feels that much detailed study is required for proper interpretation.

riers present in the semiconductor is so small that even short irradiations will lead to easily observable changes in the electrical properties of the material. Nucleon-bombarded, elementary semiconductors (Ge and Si) have been extensively studied in recent years mainly by groups at Purdue and Oak Ridge (65 to 73). An extensive account of this work has been published by Lark-Horovitz (72) and, consequently, the subject will be treated relatively briefly here.

New permanent semiconductors may be produced by bombardment via nuclear reactions. The nuclear reactions essentially produce small amounts of permanent impurities. Lattice disorder is produced at the same time but this can be annealed out at about 450°C. If the cross sections are known it can to predicted theoretically with good accuracy what the impurities and their effects will be. For example, primarily gallium and arsenic are produced by thermal neutrons in germanium. Since more gallium than arsenic is produced (by about a factor of 3), acceptors (Ga) will be more prevalent than donors (As) and a *p*-type germanium should be produced. Experiments on pure germanium fully confirmed the above predictions. Similar considerations apply to deuteron and α-particle bombardment—in germanium these particles usually lead to *n*-type material. In comparison with the displacement effects produced by nucleon bombardment, to be discussed below, the effect of impurities introduced by nuclear reactions is usually, although not always, negligible. (69, 73)

Most of the radiation effect studies to date have been carried out on germanium and silicon. Cyclotron irradiations using α-particles and deuterons as well as neutron irradiations in the Oak Ridge pile have been employed. The experimental findings are briefly as follows:

(*a*) Bombardment of *n*-type Ge results in a decrease of conductivity, initially at a uniform rate. On further irradiation a minimum is reached followed by an increase in the conductivity. Hall coefficient measurements prove that near the conductivity minimum the sample has been converted to a *p*-type semiconductor. A typical experimental curve is shown in Figure 6 (73). A *p-n* boundary can be produced in predetermined locations by a well defined beam of charged particles.

(*b*) Bombardment of a *p*-type Ge sample leads to a steady increase in conductivity, with the rate of increase decreasing monotonically. A typical experimental curve is shown in Figure 7 (73). Recently a decrease in conductivity had been observed in bombarded high conductivity *p*-type Ge (73). Thus, at high hole concentrations the introduction of donors is apparently of importance.

(*c*) At room temperature a large fraction of the radiation effect anneals out. Brattain & Pearson (74), working with α-particle irradiations from a polonium source, found that about 75 per cent of the carriers introduced by bombardment annealed out at room temperature. The annealing kinetics appeared to be of first order. Pile irradiations give essentially similar results (73) with some evidence pointing, however, to the presence of more complex annealing processes.

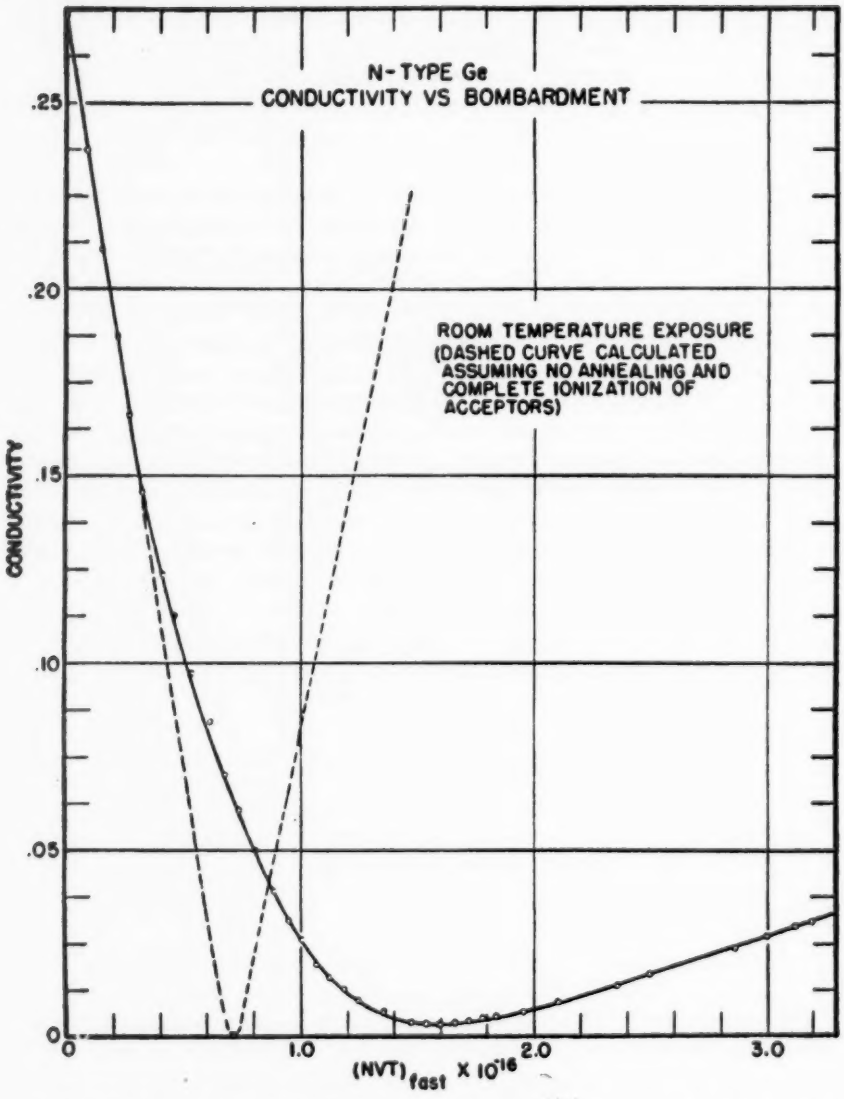

FIG. 6. Conductivity of *n*-type Ge versus integrated fast neutron flux bombarded at room temperature. The dashed line indicates the expected behavior in the absence of annealing, variation in mobility, and complete ionization in introduced acceptors (from reference 73).

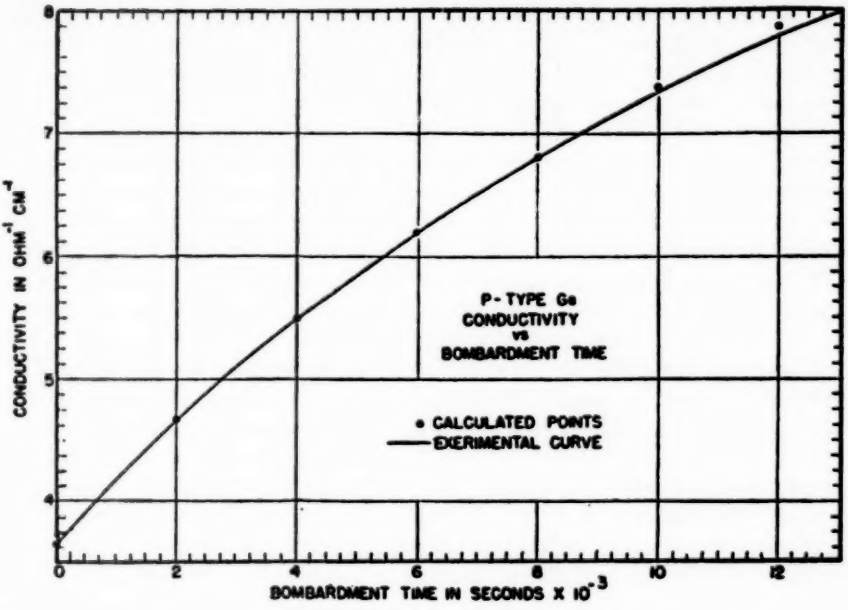

FIG. 7. Conductivity of p-type versus bombardment time, bombarded at room temperature (from reference 73).

(*d*) Radiation effects in silicon are quite different. Both n-type and p-type Si increase in resistance upon irradiation either with neutrons or deuterons. The increase in resistance of the p-type material is far greater than of the n-type sample.

(*e*) In both Ge and Si the radiation effects are completely removable by annealing the samples in vacuum at 450°C.

These experimental results have been interpreted on the basis of the production of vacant lattice sites and interstitial atoms by the irradiation. If one assumes that the vacancies and interstitials act like substitutions from the next columns of the period system, then vacancies produce empty acceptor states above the full band and interstitials produce donor states below the conduction band. If these were produced in the same way as in chemical substitution, and if they were equal in number, there would be no change in conductivity since they would cancel each other. In the case of chemical impurities, the ionization energies are so small that practically all donors and acceptors are ionized at room temperature. The ionization energies of irradiation defects, however, are distributed over a wide range of energies. In germanium only acceptors appear to be important; the donors presumably lie near the top of the filled band and are not effective in releasing electrons or trapping holes. In silicon both types of traps appear to be equally important.

The effects of bombardment on Ge may now be pictured as follows. As vacant acceptor states are introduced in *n*-type Ge they will trap electrons from the conduction band and from the original donors, thereby decreasing the conductivity. Both deep-lying and high-lying acceptors will be filled and the resistivity of an *n*-type sample will increase most rapidly during initial irradiation. As further acceptors are introduced, the low-lying vacant states states begin to act as acceptors leading to hole conduction. Thus, the material becomes *p*-type. Bombardment of a *p*-type sample leads to increased conductivity via augmenting the concentration of holes in the full band. This latter process is expected to be considerably less efficient than the initial electron removal since only sufficiently deep-lying vacant states can act as acceptors for electrons from the full band.

Quantitative considerations indicate that the above picture is correct in its essentials and is in approximate agreement with Seitz's theory (7) of displacement production. In the quantitative treatment it has been assumed that (*a*) annealing is negligible, (*b*) change in mobility may be neglected, (*c*) photo-effects are negligible, and (*d*) all the acceptor states lie far below the initially available donor levels so that each state produced will remove an electron from the conduction band. From the initial portion of the conductivity curve it can be deduced that the number of carriers introduced per incident neutron is three in an *n*-type material and 0.6 to 0.8, depending on the temperature, in a *p*-type material. Assuming a scattering cross section of 1×10^{-24} cm.^{2}, this corresponds, in an *n*-type material, to 81 traps per scattered neutrons. Application of the procedures worked out by Brown & James to this experiment gives 135 displaced atoms per scattered neutron (75). In view of the roughness of the calculations and the assumptions made, this agreement must be considered quite good.

Brattain & Pearson's (74) analysis of their experiments on α-particle-bombarded Ge leads to similar conclusions. These workers conclude that 78 conduction electrons are removed for each impinging α-particle during the initial bombardment of *n*-type Ge. Seitz's calculations for α-particles of somewhat lower energy give 59 displaced atoms per α-particle. Consequently, they suggest that one acceptor or electron trap is created for each displaced atom.

More recent theoretical work by James & Lark-Horovitz (76) indicated that a more detailed study of changes in the band structure is required for further understanding. They suggest that: (*a*) vacancies and interstitials may act as acceptors and donors for more than one electron, (*b*) the second ionization energy of the acceptors and donors, rather than the first, is critical for the behavior of bombarded material, and (*c*) at least part of the interstitial atoms are doubly ionized and part of the vacancies hold two electrons.

As already pointed out, the conductivity of both *p*-and *n*-type silicon decreases with bombardment and apparently approaches some limiting value. This behavior is explicable by postulating that both electron and hole traps are introduced near the center of the forbidden energy band. On the basis

of presently available data it is found that the initial rates of carrier removal per incident neutron, the value being about 5, are practically the same for both *p*- and *n*-type silicon (77). This would indicate that acceptors and donors are introduced in equal numbers. The analysis of James & Lark-Horovitz (76) suggests that the difference in behavior between bombarded Ge and Si may be understood on the basis of a much greater second hole ionization energy of silicon vacancies. They suggest that in Si most of the interstitials and vacancies will be singly ionized.

It has been assumed throughout that irradiation of these materials results in the production of single interstitials and vacancies. However, clusters of disorder may well be produced and the formation of clusters of vacancies and interstitials would affect considerably the quantitative aspects of the interpretation. Sufficiently detailed annealing studies have not yet been carried out to permit one to settle this point. Fortunately, much further work is planned at Purdue and at Oak Ridge both on the energy distribution of electron traps and the kinetics of annealing (73).

Some preliminary experiments have also been carried out on Cu_2O (77, 78). The resistivity of this material increases monotonically. The initial slope is not constant but appears to be approximately exponential. Hall coefficient measurements indicate that the ionization energy of the acceptors increases with bombardment. Hence the properties of bombarded Cu_2O appear to be more complex than those of Ge and Si.

The resistivity of a semiconductor is high enough so that some ionization effects should be observable. Transient phenomena, attributable to ionizing radiation, have been observed by Lark-Horovitz and co-workers (72). Germanium irradiated with electrons of energy below 0.7 Mev exhibits conductivity pulses and a decrease in resistance up to a factor of about 10. These pulses last about 10μsec. Further, natural as well as artificial *p-n* barriers act as crystal counters when exposed to ionizing radiation.

Theoretical work by Mills indicated (79) that, in addition to the transient effects discussed above, electron irradiation may produce displaced atoms provided the electrons are of high enough energy. This phenomenon can be used to measure the unit displacement energy. Early experiments (72), using changes in rectification characteristics as the sensitive physical property, proved that displaced atoms can indeed be produced by high energy electrons. More precise experiments have established the value of the unit displacement energy for Ge quite accurately (80). The experiment was carried out on *n*-type Ge which was bombarded with electrons of increasing energy while the total number of incident particles per bombardment was made constant. The change in conductivity was observed as a function of the energy of the incident particles. The curve shown in Figure 8 was obtained, which clearly shows a level portion indicating no change followed by a sharp decrease in conductivity. Extrapolation to the level portion indicates a threshold energy of about 0.65 Mev. A second experimental curve, which contained fewer points, dropped somewhat more sharply to 0.63 Mev. This

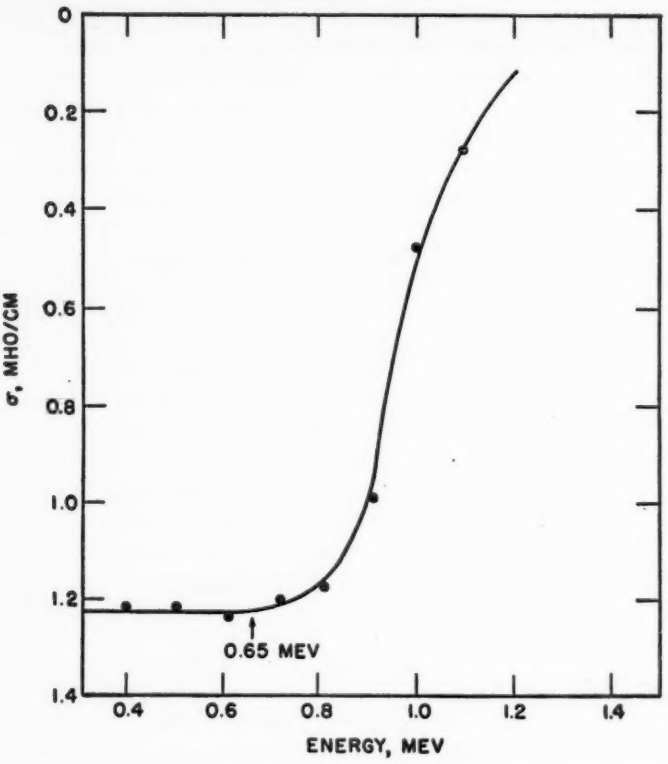

FIG. 8. Determination of the threshold for displacements by electron bombardment of *n*-type Ge. Extrapolation to level portion indicates a threshold of 0.63 Mev (from reference 80).

corresponds to a unit displacement energy of 31 ev, which is slightly higher than the value of 25 ev estimated by Seitz (7).

Optical properties.—Important changes in the infrared absorption characteristics of silicon upon bombardment have been observed (68, 81, 82, 83). The experimental observations may be summarized as follows: (*a*) Bombardment with neutrons and deuterons has similar effect and is the same for *n*-and *p*-type Si. (*b*) A new narrow absorption band has been observed at 1.75 μ. This band sharpens with decreasing temperature and its peak shifts toward shorter wave lengths as the temperature is lowered. (*c*) The longer wave length absorption is reduced to very small values. (*d*) The absorption edge shows an apparent shift toward longer wave lengths.

Fan (83) and James & Lark-Horovitz (76) interpret these results in the following manner. The reduction of long wave length absorption to very small values indicates strongly that this absorption is due to free carriers since bombardment results in a large reduction in carrier concentration.

The new absorption band at 1.75 μ is probably due to electron transitions between discrete energy levels in the energy gap. Excitations from hole traps to higher discrete levels or from lower discrete levels to electron traps or from both are probably responsible for this band.

Insulators

Optical properties.—It has already been shown in the case of semiconductors that as the electronic conductivity is decreased ionization effects become observable. These phenomena, which are not observable in metals, are transient in semiconductors but become more or less permanent in insulators. The effect of ionizing radiation on ionic crystals has been studied for many years and it is not the purpose of this paper to review this extensive field. It may be mentioned, however, that electrons trapped at various lattice imperfections result in various color centers and optical studies have given perhaps the most insight into the nature of these phenomena although important contributions have come from investigations of electrical properties. On the more practical side, the subject of crystal counters and dosimetry is an important part of this field.

Pringsheim and co-workers (84 to 87) have shown that neutron irradiation of alkali halides produces essentially the same sort of damage as is observed with ionizing radiation. Large differences in the stability of color centers have been observed depending on their temperature of production and on the type of radiation used (x-rays, electron bombardment, pile irradiation) to produce the color centers. Suggested explanations involve an intricate interpretation of the interaction of various types of color centers (88, 89, 90).

The coloration of glasses by high energy radiation exhibits some interesting features (91). So far mainly empirical rather than fundamental investigations have been reported. Coloration of these substances by high energy radiation is of considerable importance from the instrumentation standpoint. As to the mechanisms of coloration, lattice imperfections are not expected to play an important role since a glass is characterized by an absence of crystalline regularity and a condition of "imperfection" is hard to visualize. At least two other mechanisms are easily suggested: (*a*) trapping of electrons by an ion yielding a neutral atom and hence colloidal coloring, and (*b*) oxidation-reduction processes via exchange of electrons among various ions. Very little fundamental work has been done and some very interesting studies of solid-state reactions could be carried out on glass systems. In many respects these changes can be thought of as chemical reactions induced by high energy radiation. In this connection it should be mentioned that crystalline ionic crystals can be decomposed by irradiation. Allen & Ghormley (92) have found that irradiation of barium nitrate with an electron beam results in the liberation of oxygen and the production of nitrite ions. The mechanism of the process has not yet been elucidated.

A very interesting phenomenon has been observed by Koch (93) in con-

nection with glasses. It has been found that the bombardment of glass (both crown and flint) with krypton ions (of about 60 kev and at about 20μ amp./cm.^{2}) results in a permanent change in the surface such that the reflection of light from the surface is reduced and the transmission through the glass is increased. The bombarded surface is quite stable against strong acids, rubbing and annealing up to 400°C., but cannot withstand scraping with a knife. No appreciable increase in transmission could be observed with ions other than those of the inert gases. The reflection is evidently reduced by a surface layer, of thickness of the order of a quarter of a wave length, which has a small index of refraction at the surface. This phenomenon cannot be ascribed directly to the retained inert ions since their penetration is of the order of a tenth of a wave length. This observation is of considerable interest since it represents a clear case of a surface effect brought about by charged particle bombardment. The field of surface effects has been neglected entirely, unless Andrade's observations on creep are really attributable to surface effects (50), although it is clear that one should be able to alter surface properties drastically by fast charged particle irradiation.

Thermal properties.—It has been intimated in the previous section that ionization type of damage is perhaps the most important in insulators. It should not be concluded, however, that displaced atoms do not play an important role in these substances. On the contrary, large changes in thermal conductivity of ionic crystals have been observed which are undoubtedly due to the scattering of thermal waves (phonons) by lattice imperfections. Before the details of some of these experiments are given, it should also be mentioned that early preliminary studies of paramagnetic resonance in LiF (94, 95) indicate that neutron irradiation may produce somewhat different effects from electron bombardment.[7,8]

Berman (96, 97) and Klemens (98) have studied in some detail the low temperature thermal conductivity of quartz crystals irradiated in the Harwell pile. Extensive reduction in thermal conductivity upon irradiation is observed as illustrated in Figure 9. The temperature was kept below 100°C. during irradiation and curve 3 of Figure 9 shows that no noticeable annealing took place during irradiation, although this result does not assure one that a low temperature annealing state, analogous to that observed in the

[7] See also recent work of Westervelt (108) on sodium chloride. Some of the coloration phenomena produced by fast particle irradiation indicate that interstitial sodium atoms may have been produced.

[8] Very recent and as yet unpublished work of Smith & Turkevich on phosphors should also be mentioned (113). These investigators found very large changes in the properties of a copper activated zinc sulfide phosphor after very short periods of pile irradiation. Neutron bombardment resulted in marked decrease of luminescence efficiency, increase of decay rate, increased sensitivity to infrared quench, decreased growth of luminescence and striking changes in the glow curves. It appears that neutron bombardment produces deep electron traps which do not participate in the phosphorescence process and lose their electrons by nonradiative transition to the ground state.

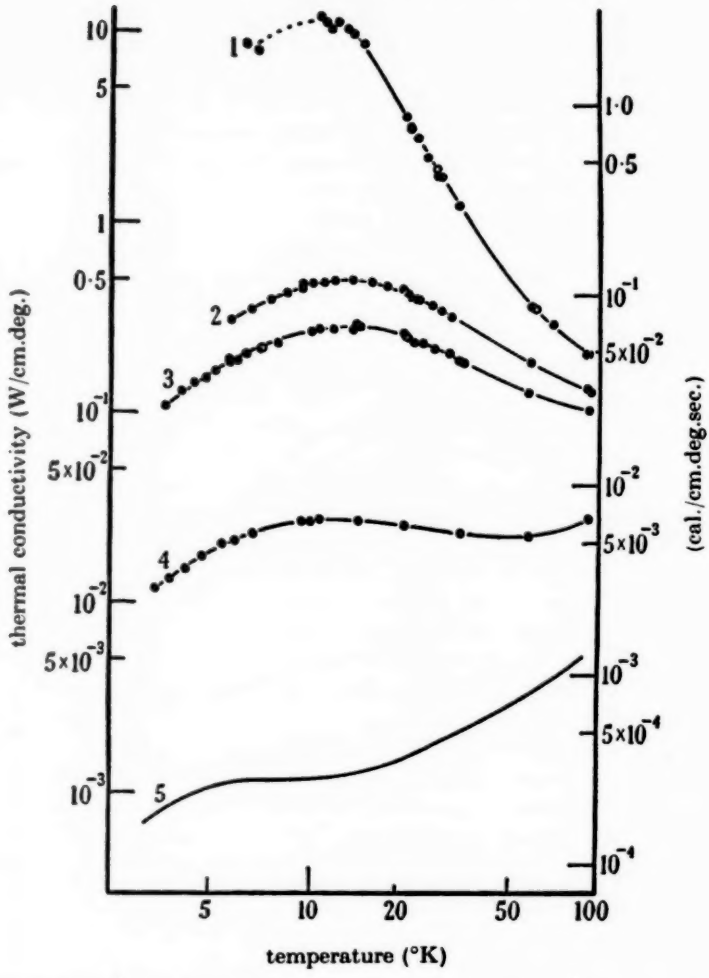

FIG. 9. Thermal conductivity of quartz crystal, irradiated quartz crystal, and quartz glass: (1) quartz crystal perpendicular to axis 5 mm. square cross section: • length measured 3.05 cm.: ○ length measured 2.15 cm (2) after first irradiation—1 unit (3) • after second irradiation—1.4 units; ○ after subsequent heating at 100°C. for three weeks (4) after third irradiation—16.5 units (5) quartz glass (from reference 97).

residual resistivity of copper (see section on Metals), may not exist. Annealing studies at elevated temperatures were also carried out and the results are shown in Figure 10.

To a first approximation the thermal resistance produced by the irradiation can be regarded as additive to the normal lattice resistance. This extra

resistance is a minimum at about 15°K. and increases roughly linearly with the temperature above 15°K. Below this temperature the extra resistance increases more rapidly than the inverse of the temperature. It is suggested (96, 98) that the extra resistance above 15°K. is to be attributed to the presence of single lattice defects. Below 15°K. the resistance appears to be of the nature of boundary resistance and may be caused by the presence of clusters of lattice defects.

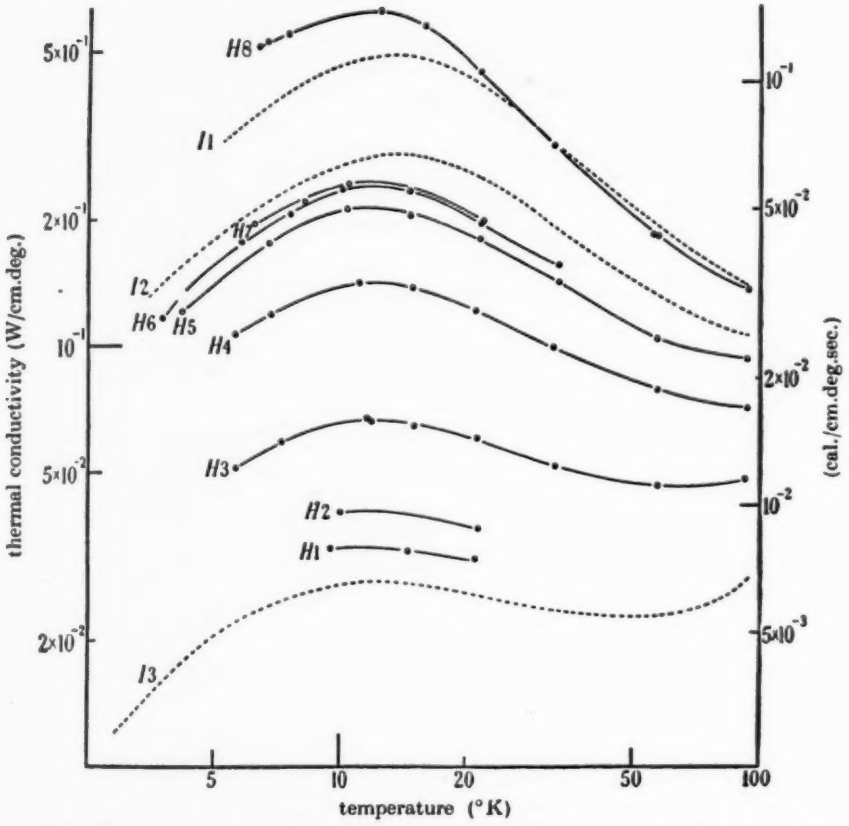

FIG. 10. Thermal conductivity of quartz crystal after successive periods of heating following the third irradiation (from reference 97).

11, 12, and 13, after first, second and third irradiations I_1, I_2, and I_3

	after heating at (°C.)	for (hr.)		after heating at (°C.)	for (hr.)
H1	300	8	H5	540	60
H2	400	6	H6	540	677
H3	510	6	H7	600	1
H4	565	6	H8	700	6

The annealing studies of Figure 10 indicate the following. After considerable anneal at high temperature the conductivity above 25°K./becomes essentially that of the least irradiated sample. Below 25°K. however, the conductivity of the annealed crystal is higher. This result indicates that the total number of defects is about the same in the two samples but that the density of the clusters of defects (which presumably account for the low temperature end of the curve) is less after the heat treatment. Heat treatment of an unirradiated crystal produced no change in conductivity between 10° and 25°K. nor were any unusual annealing effects observed in the irradiated crystals in going across the α-β-transition (573°C.).

There experiments are considered very significant in being the first detailed study of radiation damage by displaced atoms in an insulator. The above data are evidently reasonably well interpreted in terms of vacancies, interstitials, and possibly their clusters. Further work on this and similar systems would be very welcome.

Molecular Solids

The study of radiation effects in molecular compounds is essentially a part of the field of radiation chemistry. The primary effects will be the result of ionization with or without excitation and will be essentially the same for all types of high energy radiation. As stated before, it is not the purpose of this paper to review this extensive field, particularly since an excellent review by Burton (12) has been published recently. However, it is worthwhile to call attention to several studies which exhibit some features of interest to solid state.

Perhaps irradiation studies of ice will serve as a suitable first example. It is known that water undergoes dissociation under the action of radiation. The characteristics of this dissociation in ice are somewhat different from that in liquid water. (99, 100, 101). Gas formation in gas-free ice caused by α-rays occurs at a lower rate than in water. In the presence of oxygen the rate of H_2O_2 formation is lower than in water and is independent of temperature down to -190°C. At -180°C. no decomposition of ice is observed with x-rays and in the presence of oxygen the rate of H_2O_2 formation becomes negligible at -115°C. All the measurements in these investigations were made after the ice melted. It would be of interest to combine low temperature irradiations with low temperature measurements in an effort to look for trapped free radicals. Apparently no such studies have been made.

The resistance of high polymers to radiation has been studied, although primarily from an empirical point of view since these substances are of considerable practical importance in reactor technology. The currently available information has been summarized recently by Sisman & Bopp (102). Discoloration, brittleness, chemical decomposition, and many other changes may result from pile exposure of plastics. Sisman & Bopp (102) have been able to classify empirically a large number of plastic materials into 12 groups in order of decreasing radiation resistance. Mineral-filled phenolics appar-

ently withstand radiation best. Among the unfilled polymers polystyrene is outstanding. In both cases the well known stabilizing effect of benzene rings is apparent. At the other end of the scale, methyl methacrylate, halogenated polyethylenes, and cellulosics are extremely poor in radiation resistance.

More fundamental studies have been carried out by Davidson & Geib (103) on rubbers and by Dole (104) on polyethylene. Natural rubber has been found to increase in molecular weight while polyisobutylene is degraded. It is suggested that free radicals in natural rubber are able to initiate chain reactions involving the double bonds, and apparently the cross-linking achieved this way more than compensates for the broken chains. In polyisobutylene no chain reaction can be effected and the end result has to be a decrease in molecular weight.

Dole (104) chose polyethylene as the simplest high polymer for investigating radiation effects. Irradiations in the presence of both air and vacuum were carried out in the Argonne heavy water pile. The polyethylene used was in the form of sheet film. Chemical and infrared absorption analyses showed that considerable unsaturation occurred in the vacuum-irradiated samples. Oxidation was the major effect in the material irradiated in air. Stress-strain measurements showed that extensive changes in mechanical properties were brought about by the irradiation. Exposure in the presence of air decreased the tensile strength while irradiation in vacuum had very little influence on this property. In both cases, however, the ability to be cold-drawn has been lost entirely and the extensibility of the material had almost disappeared. Molecular weights and molecular weight distributions have not yet been measured nor have the electrical properties been investigated. Tentatively Dole suggests that the major chemical changes occur upon neutralization of the positive charge which is situated somewhere along the chain as a result of electron depletion by the irradiation. Free radicals are produced as a result of the split in the C—C bond leading to unsaturation and to oxidation in the presence of air. Possibly some cross-linking may also occur.

In connection with plastics, some very interesting observations on optical effects have been reported recently by Day, Schneider & Stein (105). These investigators found some striking color changes upon x-ray irradiation of polymethylmethacrylate samples containing various dyes. The x-ray irradiation resulted in the development of an absorption band at a wave length longer than the absorption band of the basic dye. At the same time the optical density in the original band of the dye decreased. The optical density of the new band depends on both dye and oxygen concentration in the material. Thermal annealing has also been observed although it is very slow at room temperature. These results are interpreted as the trapping of electrons by the dye, the proportion trapped depending on the competition for the electrons between the dye and other acceptors in the system. The phenomenon appears to be analogous to the formation of color centers in alkali halides. These materials may be useful for studying electron-capture processes in solids since one has some control over the number and nature of the electron acceptors.

LITERATURE CITED

1. Wigner, E. P. (See Ref. 2)
2. Burton, M., *J. Phys. & Colloid Chem.*, **51**, 611–25 (1947)
3. Burton, M., *Chem. Eng. News*, **26**, 1764–66 (1948)
4. Seitz, F., in *Imperfections in Nearly Perfect Crystals* (Nat. Research Council Symposium, Shockley, W., Ed., John Wiley & Sons, Inc., New York, N. Y., 490 pp., 1952)
5. Seitz, F., *Advances in Physics*, **1**, 43–90 (1952)
6. Bohr, N., *Kgl. Danske Videnskab. Selskab. Mat. -fys. Medd.* **18**, 8 (1948); see also Madsen, B. S., **23**, 8 (1945); Bohr, A., **24**, 19 (1948)
7. Seitz, F., *Discussions Faraday Soc.*, No. 5, 271–282 (1949)
8. Slater, J. C., *J. Applied Phys.*, **22**, 237–256 (1951)
9. Lind, S. C., *Chemical Effects of α-particles and Electrons*, (Chemical Catalogue Company, New York, N. Y., 252 pp., 1928)
10. Burton, M., and Rollefson, G. K., *Photochemistry* (Prentice-Hall, Inc., New York, N. Y., 1939)
11. Mott, N. F., and Gurney, R. W., *Electronic Processes in Ionic Crystals* (Oxford Univ. Press, London, England, 1940)
12. Burton, M., *Ann. Rev. Phys. Chem.*, **1**, 113–32 (1950)
13. Lark-Horovitz, K., *Nucleon Bombarded Semi-conductors, Reading Conference on Semi-conducting Materials* 47–78 (Butterworths Scientific Publications, London, England, 251 pp., 1951)
14. Brooks, H. (Personal communication, February, 1952)
15. Siegel, S., *Phys. Rev.*, **75**, 1823–24 (1949)
16. Huntington, H. B., and Seitz, F., *Phys. Rev.*, **61**, 315 (1942); **76**, 1728 (1949)
17. Huntington, H. B., *Phys. Rev.*, **61**, 325 (1942)
18. Dienes, G. J., *U. S. Atomic Energy Commission Document, TID-5013* (1951)
19. Wallace, P. R., *Phys. Rev.*, **71**, 622 (1947)
20. Bowen, D., *Phys. Rev.*, **76**, 1878 (1949)
21. Mrozowski, S., *Phys. Rev.*, **78**, 644 (1950); **85**, 609 (1952)
22. Eatherly, W. P., *Bull. Am. Phys. Soc.*, **26**(8), 20 (1951)
23. McClelland, J. D., and Donoghue, J. J., *Bull. Am. Phys. Soc.*, **26**(8), 20 (1951)
24. Loebner, E. E., *Bull. Am. Phys. Soc.*, **26**(2), 8 (1951); *Phys. Rev.*, **84**, 153 (1951)
25. Donoghue, J. J., and Eatherly, W. P., *Rev. Sci. Instruments*, **22**, 513 (1951)
26. Parkins, W. E., Dienes, G. J., and Brown, F. W., *J. Applied Phys.*, **22**, 1012 (1951)
27. Malmstrom, C., Keen, R., and Green, L., Jr., *J. Applied Phys.*, **22**, 593 (1951)
28. Mrozowski, S., *Bull. Am. Phys. Soc.*, **27**(1), 47 (1952)
29. Hennig, G., *U. S. Atomic Energy Commission Document, ANL-4579* (1951)
30. Hennig, G., *U. S. Atomic Energy Commission Document, ANL-4645* (1951)
31. Hennig, G., *J. Chem. Phys.*, **19**, 922 (1951)
32. Feldman, M., Goeddel, W., and Dienes, G. J., *U. S. Atomic Energy Commission Document, NAA-SR-167* (1952); *Bull. Am. Phys. Soc.*, **27**(1) 48 (1952)
33. Lukesh, J. S., *J. Chem. Phys.*, **19**, 383 (1951); *Phys. Rev.*, **80**, 226 (1950)
34. Gurney, R., *U. S. Atomic Energy Commission Document, AECD-3243* (1947)
35. Martin, A. B., Austerman, S. B., Eggleston, R. R., McGee, J. F., and Tarpinian, M., *Bull. Am. Phys. Soc.*, **25**(6), 21 (1950); see also unclassified portions of *U. S. Atomic Energy Commission Document, NAA-SR-75* (1951)
36. Cook, L. G., and Cushing, R. L. *The Effect of Fast Neutron Irradiation on Ordered Cu_3Au* (Paper presented at Chem. Inst. Canada Symposium in Ottawa, Canada, Jan. 28, 1952)

37. Martin, A. B. (Personal communication, February, 1952)
38. Billington, D. S., and Siegel, S., *Metal Progress*, **58**, 847–852 (1950)
39. Murray, G. T., and Taylor, W. E., *U. S. Atomic Energy Commission Document, TID-5017* (1951)
40. Taylor, W. E., and Murray, G. T. (Personal communication)
41. Randolph, B., *Bull. Am. Phys. Soc.*, **26**(6), 14 (1951)
42. Bowen, D., Eggleston, R. R., and Kropschot, R. H., *Bull. Am. Phys. Soc.*, **26**(5), 5 (1951)
43. Bowen, D., Eggleston, R. R., and Kropschot, R. H., *U. S. Atomic Energy Commission Document, NAA-SR-143* (1951)
44. Bowen, D., and Eggleston, R. R. (see Ref. 18)
45. Brooks, F. C., *U. S. Atomic Energy Commission Document, WAPD-33* (1951)
46. Dienes, G. J., *Phys. Rev.*, **86**, 228 (1952); see also unclassified *U. S. Atomic Energy Commission Documents, NAA-SR-80, -125, -144* (1951)
47. Bowman, F., and Tarpinian, M. (Personal communication February, 1952)
48. Blewitt, T. H., Coltman, R. R., and Sherrill, F. A., *U. S. Atomic Energy Commission Document, TID-5015; Bull. Am. Phys. Soc.*, **26**, No. 213 (1951)
49. Nabarro, F. R. N., *Conference on Strength of Solids*, 75 (The Physical Society, London, England, 1948)
50. Andrade, E. N. da C., *Nature*, **156**, 113 (1945)
51. Phillips, D. G., and Thompson, N., *Proc. Phys. Soc.* (*London*), [B]**63**, 839 (1950)
52. Witzig, W. F., *U. S. Atomic Energy Commission Document, WAPD-43* (1951)
53. Nowick, A. S., *Phys. Rev.*, **82**, 551 (1951)
54. Martin, A. B., Johnson, R. D., and Goeddel, W. V., *Bull. Am. Phys. Soc.*, **26**(5), 5 (1951)
55. Martin, A. B. (Personal communication, February, 1952)
56. Feldman, M., and Dienes, G. J., *U. S. Atomic Energy Commission Document, NAA-SR-Memo-22* (1951)
57. Parkins, W. E., Dienes, G. J., and Brown, F. W., *J. Applied Phys.*, **22**, 1012 (1951)
58. Bowen, D., Eggleston, R. R., and Kropschot, R. H., *Bull. Am. Phys. Soc.*, **26**(5), 5 (1951)
59. Bowen, D., Eggleston, R. R., and Kropschot, R. H., *Effects of Cold Work on the Residual Resistance of Metals, U. S. Atomic Energy Commission Document, NAA-SR-143;* (Paper presented at meeting of Am. Inst. Physics, Chicago, Ill., October, 1951)
60. Molenar, J., and Aarts, W. H., *Nature*, **166**, 690 (1950)
61. Blewitt, T. H., Taylor, W., and Coltman, R. R., *Bull. Am. Phys. Soc.*, **26**(2), 13 (1951); see also discussion by Seitz in Ref. 5
62. Bowen, D. (Personal communication, February, 1952)
63. Dienes, G. J., *J. Applied Phys.*, **22**, 1020 (1951)
64. Stello, P. G., *U. S. Atomic Energy Commission Document, NAA-SR-171* (In press)
65. Lark-Horovitz, K., Bleuler, E., Davis B. E., and Tendam, P. L., *Phys. Rev.*, **73**, 1256 (1948)
66. Davis, R. E., Johnson, W. E., Lark-Horovitz, K., and Siegel, S., *Phys. Rev.*, **74**, 1255 (1948)
67. Johnson, W. E., and Lark-Horovitz, K., *Phys. Rev.*, **76**, 442 (1949)
68. Lark-Horovitz, K. Becker, M., Davis, R. E., and Fan, H. Y., *Phys. Rev.*, **78**, 334 (1950)

69. Cleland, J., Lark-Horovitz, K., and Pigg, J. C., *Phys. Rev.*, **78**, 814 (1950)
70. Crawford, J. H., and Lark-Horovitz, K., *Phys. Rev.*, **78**, 815 (1950); **79**, 889 (1950)
71. Johnson, V. A., and Lark-Horovitz, K., *Phys. Rev.*, **79**, 176 (1950)
72. Lark-Horovitz, K., *Nucleon Bombarded Semi-Conductors, Reading Conference on Semi-Conducting Materials* 47–78 (Butterworths Scientific Publications, London, England, 281 pp., 1951)
73. Cleland, J. W., Crawford, J. H., Lark-Horovitz, K., Pigg, J. C., and Young, F. W., Jr., *Phys. Rev.*, **83**, 312 (1951); *Bull. Am. Phys. Soc.*, **26** (6) 34 (1951); *Phys. Rev.*, **84**, 961 (1951)
74. Brattain, W. H., and Pearson, G. L., *Phys. Rev.*, **80**, 846 (1950)
75. Evans, G. E. (Unpublished data); (see Ref. 72 and 73)
76. James, H. M., Lark-Horovitz, K., *U. S. Atomic Energy Commission Document, TID-5011; Z. physik. Chem.*, **198**, 107 (1951)
77. Cleland, J. W., Crawford, J. H., Lark-Horovitz, K., Pigg., J. C., and Young, F. W., Jr., *Atomic Energy Commission Document, TID, 5016* (1951)
78. Pigg, J. C., Cleland, J. W., Crawford, J. H., and Lark-Horovitz, K., *Bull. Am. Phys. Soc.*, **26**(2), 7 (1951)
79. Mills, M. M. (Personal communication to Lark-Horovitz, K.; see Ref. 72)
80. Klontz, E., and Lark-Horovitz, K., *U. S. Atomic Energy Commission Document, TID-5010* (1951)
81. Fan, H. Y., and Becker, M., *Infra-red Optical Properties of Silicon and Germanium, Reading Conference on Semi-Conducting Materials* 132–48 (Butterworths Scientific Publications, London, England, 281 pp., 1951)
82. Becker, M., Fan, H. Y., and Lark-Horovitz, K., *Bull. Am. Phys. Soc.*, **26**(6), 34 (1951)
83. Fan, H. Y., *Bull. Am. Phys. Soc.*, **26**(6), 34 (1951)
84. Pringsheim, P., and Yuster, P., *Phys. Rev.*, **78**, 293 (1950)
85. Casher, R., Pringsheim, P., and Yuster, P., *J. Chem. Phys.*, **18**, 887 (1950)
86. Casher, R., Pringsheim, P., and Yuster, P., *J. Chem. Phys.*, **18**, 1564 (1950)
87. Delbecq, E. J., Pringsheim, P., and Yuster, P., *J. Chem. Phys.*, **19**, 574 (1951)
88. Seitz, F., *Phys. Rev.*, **79**, 529 (1950); **80**, 239 (1950)
89. Pick, H., in *Fundamental Mechanisms of Photographic Sensitivity* 9–12 (Butterworths Scientific Publications, London, England, 347 pp., 1951)
90. Schneider, E. E., *Fundamental Mechanisms of Photographic Sensitivity* 13–23 (Butterworths Scientific Publications, London, England, 347 pp., 1951)
91. Monk, G. S., *U. S. Atomic Energy Commission Document, ANL-4536* (1950)
92. Allen, A. D., and Ghormley, J. A., *J. Chem. Phys.*, **15**, 208 (1947)
93. Koch, J., *Nature*, **164**, 19 (1949)
94. Hutchison, C. A., Jr., *Phys. Rev.*, **75**, 1769 (1949)
95. Tinkham, M., and Kip, A. F., *Phys. Rev.*, **83**, 657 (1951)
96. Berman, R., Klemons, P. G., Simon, F. E., and Fry, T. M., *Nature*, **166**, 864 (1950)
97. Berman, R., *Proc. Roy. Soc.* (*London*), [A]**208**, 90 (1951)
98. Klemens, P. G., *Proc. Roy. Soc.* (*London*), [A]**208**, 108 (1951)
99. Duane, W., and Scheuer, O., *Le Radium*, **10**, 33 (1913)
100. Bonet-Maury, P., and Lefort, M., *Compt. rend.*, **226**, 1445 (1948)
101. Gunther, P., and Holzapfel, L., *Z. physik. Chem.*, [B]**44**, 374 (1939)
102. Sisman, O., and Bopp, C. D., *U. S. Atomic Energy Commission Document, ORNL-928* (1951)

103. Davidson, W. L., and Geib, I. G., *J. Applied Phys.*, **19**, 427 (1948)
104. Dole, M., in Army Chemical Center Symposium on Chemistry and Physics of Radiation Dosimetry, 120–48 *U. S. Atomic Energy Commission Document, NP-3237* (1950)
105. Day, M. J., Schneider, E. E., and Stein, G., *Nature*, **168**, 644 (1951)
106. Blewitt, T. H., and Coltman, R., *Phys. Rev.*, **85**, 384 (1952)
107. Jamison, R. E., and Blewitt, T. H., *Bull. Am. Phys. Soc.*, **27**(2), 8 (1952)
108. Westervelt, D., *Bull. Am. Phys. Soc.*, **27**(2), 10 (1952)
109. Blewitt, T. H. (Personal communication, March, 1952)
110. Schmid, E., and Boas, W., *Plasticity of Crystals*, 236–37 (F. A. Hughes and Co., London, Eng., 353 pp., 1952)
111. Williams, H. J., and Nesbitt, E. A. (Personal communication, March, 1952)
112. Eggleston, R. R. (Personal communication, March, 1952)
113. Smith, A. W., and Turkevich, J. (Personal communication, March, 1952)

ISOTOPES[1]

By Jacob Bigeleisen

Chemistry Department, Brookhaven National Laboratory, Upton, Long Island, New York

Introduction

There is a considerable range of interests in researches connected with the fundamental properties of isotopes as well as with the uses of isotopes. Any review of the literature on isotopes must therefore be somewhat restrictive and will usually reflect the interests of the reviewer. This review covers the general field of the chemistry of isotopes, i.e., studies of the physical state and the chemical properties of matter which are affected by the nuclear mass. Knowledge of the abundances of isotopes and their masses is important to such studies and a review of the progress of these subjects is therefore included.

Mass Measurements

There has been considerable progress in the precise determination of nuclear masses. Li, Whaling, Fowler & Lauritsen (1) have compiled a table of masses for nuclides up to mass 20 based entirely on nuclear reaction data. The estimated uncertainties range from three to thirty micro mass units. There is very good agreement between this table of masses and the one of Ewald (2), which is derived from mass spectrographic determination of doublets. Ewald's compilation utilizes his determinations of some of the important doublets of the light elements, which were carried out with a resolution of 25,000 to 40,000. Ewald also measured some new doublets involving O^{17}, O^{18}, Ne^{20}, Ne^{22}, P^{31}, S^{34}, and Cl^{35}. Nier and his students have described a double focusing mass spectrometer which utilizes electrical recording (3), as well as measurements made with this instrument. Their later measurements, in which they have studied the effects of focusing and the kinetic energy of the ion fragments (4), give a value for the proton mass in substantial agreement with Li (1) and Ewald (2). There is still disagreement on the mass of C^{12} and the value of the doublet $C^{12}H^1_4$—O^{16} between Nier (4), Ogata & Matsuda (5), and Mattauch and Bieri (see ref. 4) on the one hand and Ewald (2), Bönisch (6), and Li (1) on the other. Nier has called attention to the need for additional measurements on this important doublet. The earlier masses reported from Nier's laboratory (7, 8) are in error in part because of the cycles chosen by them. Wapstra (9) has shown that Roberts' cycle (8) is

[1] This review covers the calendar year of 1951 and was prepared at the Brookhaven National Laboratory under the auspices of the United States Atomic Energy Commission. The coverage of foreign journals is incomplete as many issues of these were not available in this country at the time this review was prepared.

in agreement with other data if the value for the doublet $C^{12}H^{1}_{4}$—O^{16} is taken from nuclear reaction data.

Collins, Nier & Johnson (4) have measured a considerable number of new doublets in the region of mass 40 and find good agreement with other data such as nuclear reaction data, the Bohr-Wheeler formula, and the ratio of Cl^{35}/Cl^{37} obtained from microwave spectroscopy. There is a serious discrepancy for the Q value of the reaction $Ca^{43}(d, p)Ca^{44}$ as determined from nuclear reaction data and mass spectroscopic measurements.

Duckworth & Preston (10) have measured the packing fractions, by the doublet technique, of nuclides in the neighborhood of magic number nuclei. They find a minimum in the packing fraction at $_{28}Ni^{60}$, a break in the curve at $A = 90$, which may be at $_{40}Zr^{90}$, a change in the slope of the curve at $_{50}Sn^{120}$, and a break at $_{82}Pb^{208}$. The additional stability of all of these nuclides are predicted by the nuclear level scheme of M. G. Mayer (11) but not by those of Nordheim (12) or Feenberg (13).

In the past few years considerable effort has been devoted to increase the precision of mass measurements of medium and high atomic weight nuclides. Instruments which measure the time of flight of ions in a magnetic field or the cyclotron frequency are capable of a precision which is independent of the mass of the ion, in contrast to conventional spectrometers, where the precision decreases with increasing mass. Hays, Richards & Goudsmit (14) have achieved a precision of one to two millimass units in the measurement of some nuclides ranging from S^{32} to Xe^{134}. They have also given a detailed analysis of the factors limiting the precision of a time of flight spectrometer. Smith (15) has described a mass spectrometer with which he has measured the mass of S^{32} to one millimass unit and expects to increase the precision by a factor of ten with a larger instrument.

Isotopic Abundances

Graham *et al.* (16) have determined the absolute abundances of the germanium isotopes with an accuracy of 0.5 per cent and the relative abundances to 0.1 per cent. Six different ores were studied and all gave the same results except GeO_2 from zinc ores of the Joplin, Missouri district, which had the light isotopes favored. The intensities of the $GeCl^+$ and GeF_3^+ ions from $GeCl_4$ and GeF_4 respectively were measured. Their results are in good agreement with the previous measurements by Inghram (17) on Ge, and Hibbs (18) on GeF_4 and GeI_4, except for the ratio of Ge^{76}/Ge^{73} which Graham *et al.* find greater than unity. All of the mass spectrographic data lead to an atomic weight between 72.63 and 72.65, whereas the International Atomic Weight is given as 72.60.

Rakestraw, Rudd & Dole (19) have continued the work on the variation of O^{18} in the atmosphere. They have measured the isotopic composition of O_2 dissolved in the Pacific Ocean as a function of depth. They find a maximum in the O^{18} concentration and a minimum in the amount of dissolved O_2 at a depth of about 800 m. They suggest that the enrichment in O^{18} and the depletion in dissolved O_2 results from metabolism by marine vegetation, plank-

ton, bacteria, and other sea life and that O^{16} is metabolized faster (3 per cent) than O^{18}.

Milatz, Kluyver & Hardebol (20) have reported the determination of C^{13} by measurements on the 4.3 μ band of CO_2 in an instrument designed for the analysis of simple gaseous mixtures by infrared absorption. For samples containing one to ten per cent C^{13} an accuracy of 20 per cent in the C^{13} abundance has been obtained and an increase of a factor of ten in the accuracy is anticipated by the use of a double beam instrument. If the latter is achieved, the method could serve as an alternate for mass spectrometric analysis in many cases.

Isotope Separation

Several important works have appeared this year on the theory of isotope separation processes. The volume on the theory of isotope separation by Cohen (21) in the National Nuclear Energy Series has been published. This book presents a logical development of the theory of multistage separation processes with a small enrichment factor in each stage. The basis of the theory is the conservation of matter: The theory concerns itself with the productivity, enrichment, equilibrium time, hold up, and the control problem of both ideal and real cascades. There is a chapter on the fundamental equations of the centrifuge and a discussion of evaporative, concurrent, and countercurrent centrifuges. There is a discussion of the behavior of liquid-gas countercurrent chemical exchange columns in terms of the film transfer coefficients. Finally, there is a derivation of the equations of the Rayleigh distillation in one of the appendices. The book should prove valuable to all concerned with the combination of separative elements in a multistage operation.

Majumdar (22) has found an exact solution of the equations of the thermal diffusion column without the restriction of low concentration of one of the components. The theory gives good agreement with the experimental measurements of Clusius & Dickel (23) on the rate of approach to equilibrium of a column separating air into its constituents. Dickel (24) has derived the equations for the thermodynamic efficiency of isotope separation processes by the use of the methods of the thermodynamics of irreversible processes and applied them to the analysis of the thermal diffusion column. Here again good agreement is found with experiment.

Several papers have been published on isotope separation processes and equipment. Keim (25) has reviewed the past five years of production of enriched stable isotopes with the calutron, and his report lists the quantities and purities of enriched isotopes available from the Atomic Energy Commission from this operation. There is a report of a small plant that has been set up at the Scientific Research Institute in Tokyo (26) to produce ten per cent N^{15} by the exchange between NH_3 and NH_4^+. The engineering study by North & White (27) on the plate efficiency and the separation factor for the concentration of S^{34} by the sulfur dioxide-bisulfite ion exchange in packed towers has been mentioned in Stewart's review (28).

Klemm (29, 30) has continued his studies of isotope separation by electrical migration in molten salts. In one set of experiments the light isotopes of zinc were enriched by the electrolysis of molten zinc chloride in a cell which had solid lead chloride in the catholyte compartment. From these experiments the diffusion constant of Zn^{++} has been calculated. In another experiment Li^6 was enriched from 7.3 per cent to 16.1 per cent by electrical migration in molten lithium chloride.

At the National Bureau of Standards 99.8 per cent pure HD has been prepared (31) by the reaction of $LiAlH_4$ with D_2O and subsequent fractional distillation.

Isotope Effects on Phase Equilibria

In the past few years there has appeared a considerable addition to the literature on the thermal properties and vapor pressures of hydrogen, both as affected by isotopic substitution and equilibration with respect to the *ortho* and *para* states. Most of this work has been carried out at Los Alamos Scientific Laboratory, National Bureau of Standards, and the Ohio State University Cryogenic Laboratory. Workers in these laboratories have published seven papers this year on the subject. Grilly (32) has measured the vapor pressures of solid n-H_2, n-D_2 and n-T_2[2] and of the liquid forms of these substances up to 3 atm. He has also measured the densities of liquid T_2 between 20.6° and 29°K. (33) with an estimated accuracy of 0.2 per cent. At the Bureau of Standards (34) the vapor pressures of e-H_2, HD and e-D_2 have been measured from the triple points to the critical temperatures. Also the vapor pressures of a sample of n-D_2 was measured between 21° and 34°K. Dew points of mixtures of n-H_2, HD, and n-D_2 were measured between 17° and 20°K. Positive deviations, of the order of 3 ± 1.5 per cent, were found from the laws of ideal solution. These workers (35) have also measured P-V isotherms in the neighborhood of the critical temperatures of e-H_2, HD, and e-D_2. There is a pronounced difference in the shapes of the domes in the P-V diagrams for the hydrogen molecules and substances like CO_2. The Ohio State group have measured the thermal properties and vapor pressures of e-D_2 from 13.1° to 23.6°K. (36), the vapor pressures of n-D_2 between the boiling point and critical point (37), and have arrived at an empirical correlation of the freezing points, boiling points, and critical points of the isotopic n-H_2 molecules in terms of their molecular weights (38). They have also intercompared the vapor pressures in terms of these fixed points by the use of two constant vapor pressure equations and a Dühring chart. The procedure is completely empirical and, therefore, no theoretical significance can be attached to it.

Intercomparison of the vapor pressure data from these laboratories indicates some serious areas of disagreement. If the discrepancies are interpreted in terms of differences in temperatures, then one finds that data of Grilly (32) and of Hoge & Arnold (34) on n-D_2 agree to within ten millidegrees. The data of Kerr, Rifkin, Johnston & Clarke (36) on e-D_2 show a temperature

[2] The prefix n refers to material in equilibrium with respect to *ortho* and *para* species at 300°K., while the prefix e refers to material equilibrated at 20.4°K.

discrepancy which decreases from 0.11°K. at 19°K. to 0.05 °at 23.5°K. from those of Hoge & Arnold (34). The data of Friedman, White & Johnston (37) on n-D_2 show a temperature discrepancy of 0.11°K. from 23°–27°K. from those of Grilly (32). These discrepancies indicate that the Los Alamos temperature scale is in excellent agreement with that of the Bureau of Standards, while that of the Ohio State University Cryogenic Laboratory is lower by about 0.10°K. It is clear that additional work will be necessary to bring these temperature scales into closer agreement. It is difficult to estimate which scale is most closely correct.

The discrepancies between Grilly's vapor pressure data on n-T_2 from those calculated by Hammel (39) indicate the inadequacy of the semiempirical quantum corrections of de Boer (40) to the law of corresponding states.

Becker & Stehl (41) have intercompared the gas viscosities of e-$H_{2\ 298°K.}$ and e-$H_{2\ 77°K.}$ at 77°K. to test the theory of Halpern & Gwathmey (42). According to this theory, there should be a difference of 0.8 per cent between the viscosities of these gases because of a quantum correction to the collision cross section. Previous experiments by Harteck & Schmidt (43) found no effect as large as 0.1 per cent. The differential measurements of Becker & Stehl indicate a difference of $7.4 \pm 0.7 \times 10^{-2}$ per cent. The experiments are being continued to obtain more information about this difference.

New measurements confirm the suggestion that liquid He^3 is the stable form at 0°K. Osborne, Abraham & Weinstock (44) have determined the melting curve of He^3 between 1.02° and 1.51°K. by the blocked capillary technique. Extrapolation of the data to lower temperatures, where additional experimental work is being carried on, indicates no triple point down to 0°K.

Mazur & Prigogine (45) have applied the methods of the thermodynamics of irreversible processes to the hydrodynamics of solutions of He^3 in He^4. Their method is a general one, and if one applies the restriction of inhibition to momentum transfer, then one obtains the hydrodynamic equations of Gorter (46) directly. The theory gives good agreement with the experimental observations on the effect of He^3 on the fountain effect in He^4 (47, 48).

A monograph by Kirshenbaum (49) reviews the literature on the physical properties and analysis of D_2O. The book contains one chapter on physical properties, one on equilibrium constants for exchange reactions involving H_2O, HDO, and D_2O, three chapters on the analysis of heavy water by various means, and finally one chapter on the natural abundance of the isotopes of hydrogen and oxygen. Included in the compilation is a considerable body of experimental data accumulated at Columbia University under the Manhattan Project and released to the public in this monograph for the first time. The book is extremely detailed and the chapters dealing with the mass spectrometric analysis of the isotopes of hydrogen in the form of H_2 give complete diagrams of all parts of the spectrometers used at Columbia, many of which are now obsolete. In many respects the monograph is outdated by developments in this field since the end of the war. No data published after 1945 have been included. Nevertheless, the volume should prove

to be a useful compilation. The extensive discussion of the analysis of water for deuterium should prove helpful to the uninitiated, even though it is in many respects obsolete.

Schrader & Wirtz (50) have redetermined the relative densities of D_2O and H_2O between 20°–100°C. to 1/20,000. Their results are in substantial agreement with Kirshenbaum's compilation.

It has been known for some time that there is a hysteresis loop in the lambda transition in NH_4Cl (51) but none in the corresponding transition in ND_4Cl (52). Thomas & Staveley (53) have investigated the effect of particle size and deuterium substitution on the transition. Powders and crystals of NH_4Cl, NH_3DCl (prepared from NH_3 and DCl), ND_3HCl (prepared from ND_3 and HCl), and ND_4Cl were studied. The transition temperature was found to vary linearly with deuterium substitution and the hysteresis loop decreases with deuterium content. In the case of NH_4Cl an increase in the crystal size was found to increase the width of the hysteresis loop. Upon resublimation of the partially deuterated salts, the transition became more diffuse. This result may have come from an increase in the crystal size or a disproportionation of the partially deuterated salt to give a mixture of five salts. It is not certain whether the deuterium in the samples of the partially deuterated salts before resublimation were distributed in accord with the stoichiometric formulae or were in statistical equilibrium among the different NH_4^+ ions.

Some definitive experiments on the superconductivity of separated mercury and tin isotopes have been reported by Reynolds, Serin & Nesbitt (54) and by Maxwell (55) respectively. Both studies show that the critical temperature for superconductivity, T_c, varies inversely with the square root of the mass of the isotope. These results support the theories of Frohlich (56) and Bardeen (57), where superconductivity is attributed to an interaction of the conduction electrons with the lattice vibrations.

Isotope Effects in Chemical Equilibria

There is a limited number of molecules for which there are sufficient spectroscopic data to make a calculation of isotopic exchange equilibria with an accuracy of better than 1 per cent in the deviation from random distribution $(K/\sigma - 1)$. In many cases, even when the molecular parameters of the individual isotopic molecules are known, the anharmonicity coefficients are not, and they can introduce errors of this magnitude. Recently a sufficiently accurate potential function for N_2O was established (58, 59) to provide the basis for the calculation of the partition function ratios of the isotopic N_2O molecules and some exchange equilibria involving N_2O (59). McCrea (60) has carried out some calculations on N_2O which serve to illustrate the importance of the anharmonic and interaction terms in the potential function.

Stranks & Harris (61) have published a preliminary report of their measurements on the exchange equilibrium

$$Co(NH_3)_4C^{13}O_3^+ + C^{14}O_3^= = Co(NH_3)_4C^{14}O_3^+ + C^{12}O_3^= . \qquad 1.$$

At 25°C. the equilibrium constant is 0.886 at pH 9 and 0.892 at pH 10.

In a study of the exchange of hydrogen between D_2 and CH_4 catalyzed by nickel, Kemball (62) allowed some samples to come to equilibrium and measured the equilibrium constants for the reactions

$$CH_4 + CH_2D_2 = 2CH_3D \qquad 2.$$

$$CH_3D + CHD_3 = 2CH_2D_2 \qquad 3.$$

$$CH_2D_2 + CD_4 = 2CHD_3 \qquad 4.$$

in the neighborhood of 740°K. As one would expect a priori for isotopic disproportionation equilibria at high temperatures, the equilibrium constants are close to those predicted by classical statistics (random distribution). Kemball has also calculated the equilibrium constants from spectroscopic data and made an approximate correction for the anharmonicity by assuming that this correction is similar to that in water. The deviation of the experimental equilibrium constants from the calculated ones varies from 2 to 10 per cent. Part of this disagreement is due to the scatter in the experimental data.

Hunt & Taube (63) have carried out a very interesting study of the exchange of water between hydrated cations and the solvent. In the course of this investigation they have made some observations on fractionation processes involving water. Samples of solvent water were removed by distillation at 25°C. for analyses. In the distillation of 20 per cent of the water from pure water, they find $N_o/N_D = 1.005$, where N_o and N_D are the mole fractions of H_2O^{18} in the original sample and distillate respectively. From the theory of the Rayleigh distillation and the relative vapor pressures of H_2O^{18} and H_2O^{16} this ratio should be 1.007. The discrepancy may be ascribed to analytical errors and possibly entrainment in the distillation. In a similar experiment, where the solvent is 4.5 M in $NaClO_4$ and 1.45 M in $HClO_4$, this ratio became 1.009. The change is significant and in accord with theoretical expectations. The heavy isotope concentrates in the species with the strongest binding (64). For solutions containing Al^{+3}, Ga^{+3}, and Th^{+4} at high concentrations, this ratio varies between 1.010 and 1.016. The addition of these ions to water should improve the separation of O^{18} by the fractional distillation of water. Most of the work of Hunt & Taube deals with the slow exchange of $Cr(H_2O^{16})^{+3}$ with H_2O^{18} in the solvent. At equilibrium they find

$$Cr(H_2O^{16})^{+3} + H_2O^{18} = Cr(H_2O^{16})_5(H_2O^{18})^{+3} + H_2O^{16} \qquad 5.$$

$K_5 = 6(1.03)$. The larger fractionation factor in this case as compared with those mentioned above is consistent with the stronger binding of the first hydration sphere to Cr^{+3} and the slow exchange of this water with the bulk solution. All of the other ions exchange their water rapidly.

Becker & Vogell (65) have determined the relative solubilities of $HC^{12}N^{14}$, $HC^{13}N^{14}$, and $HC^{12}N^{15}$ in glacial acetic acid, where there is no polymerization. The relative solubilities of $HC^{13}N^{14}$ and $HC^{12}N^{15}$ as compared with $HC^{12}N^{14}$ were determined from the operation of a countercurrent distillation column of an undetermined number of theoretical plates at an unspecified tempera-

ture. Since the height of a plate is the same for $HC^{13}N^{14}$ and $HC^{12}N^{15}$, an analysis of the top and bottom of the column gives the ratio of the fractionation factors for these two isotopic species relative to $HC^{12}N^{14}$. If we consider the quantity $\epsilon = \alpha - 1$, where α is the relative solubility of one of the heavy HCN molecules compared with $HC^{12}N^{14}$, then Becker & Vogell find for the ratio $\epsilon(HC^{13}N^{14})/\epsilon(HC^{12}N^{15}) = 1.74 \pm 0.3$. Becker & Vogell have also determined the absolute value of $\epsilon(HC^{13}N^{14})$ by means of a Rayleigh distillation and find a value of $1.9 \pm 0.6 \times 10^{-3}$. The fact that the ratio $\epsilon(HC^{13}N^{14})/\epsilon(HC^{12}N^{15})$ differs from unity is indicative of the fact that the change in the vibration frequencies between the gas and solution plays a dominant role in the magnitude of the fractionation factor. If only the intramolecular forces were important, then the ratio $\epsilon(HC^{13}N^{14})/\epsilon(HC^{12}N^{15})$ would be identically unity. By making the assumption that the difference in each of the vibrational frequencies between any isotopic pair in the liquid is proportional to its difference in the gas phase, Becker & Vogell calculate 1.81 for the ratio $\epsilon(HC^{13}N^{14})/\epsilon(HC^{12}N^{15})$. This assumption is in accord with the Kirkwood theory for the effect of solvation on vibrational frequencies (66).

Urey and his associates (67, 68) have continued their investigation of paleotemperatures of marine life by the $CO_3^{=}$—H_2O temperature scale. This scale depends on the fact that there is a small, but measurable, temperature coefficient for the exchange equilibrium of O^{18} between $CaCO_3$ and H_2O. In one paper (68) they have set up a temperature scale by the analysis of $CaCO_3$ from marine animals which grew at known temperatures, which varied between 7.4° and 31°C. This temperature scale agrees with the one established previously (69) for inorganically precipitated $CaCO_3$. Measurements of the ratio of $C^{12}O^{16}O^{18}/C^{12}O_2^{16}$ can be made with a precision of 0.02 per cent, which corresponds to an error of ± 1°C. The errors in temperature determination are limited by other phenomena at present. For instance, variations in the O^{18} content of ocean waters amounting to 17 per cent have been found, which would correspond to a temperature variation on the $CO_3^{=}$—H_2O scale of 10°C. The O^{18} content of ocean waters varies linearly with salinity, a correspondence which seems plausible inasmuch as factors which tend to increase one also increase the other. An attempt is being made to develop the $PO_4^{=}$—H_2O thermometer, which has a different temperature coefficient from the $CO_3^{=}$—H_2O scale. If this is successful, then samples of $CO_3^{=}$ and $PO_4^{=}$ which were in equilibrium with the same water will suffice to determine the temperature and will eliminate the uncertainty in the composition of the water.

Since the temperature scale established from $CaCO_3$ of marine origin agrees with that determined by inorganically precipitated $CaCO_3$, it is safe to assume that O^{18} exchange equilibrium is achieved in marine growth. It has been found that large crystals of calcite, such as belemnite specimens, preserve the temperature record over long periods of time. In one experiment samples of $CaCO_3$ were ground from a belemnite shell as a function of the radius from the center. Seasonal variations in the growth of the animal were found and four winters and three summers could be identified. Furthermore, it was established that the animal died in the spring.

The growth temperatures of some belemnites, brachiopods, and oysters from the Upper Cretaceous of England, Denmark, and southeastern United States were determined. The results are entirely of geological interest and will not be discussed here.

Isotope Effects in Chemical Kinetics

During the past few years the tempo of activity in the determination of isotope effects on reaction rates has been constantly increasing as a result of improvements in experimental techniques, the wider distribution of enriched isotopes (stable and radioactive), and renewed theoretical interest in the problem. The carbon isotope effect in decarboxylation reactions has received particular attention.

The four papers published last year on carbon isotope effects have done a great deal to clarify our understanding of these effects. Previously, Yankwich & Calvin (70) had measured the C^{14} isotope effect in the decarboxylation of malonic acid at 150°C. and of brom-malonic acid at 115°C. Their reactions were carried to completion and they measured the relative rates of the following two processes:

$$CH_2(C^*OOH)(C^{13}OOH) \xrightarrow{k_4} C^{13}O_2 + CH_3C^*OOH$$

$$CH_2(C^*OOH)(C^{13}OOH) \xrightarrow{k_3} C^*O_2 + CH_3C^{13}OOH$$

It was pointed out by Bigeleisen (71) that the ratio k_4/k_3 can be calculated rather precisely from the theory of the relative rates of reaction of isotopic molecules (72) without any assumptions regarding either the normal molecules or the transition state. These calculations led to a value of 1.020 for k_4/k_3 where C^{13} is the label, and 1.038 where C^{14} is the label. Subsequent experiments by Bigeleisen & Friedman (73) on the decarboxylation of malonic acid containing one atom per cent C^{13} (natural abundance) gave a value of 1.020 for the ratio of k_4/k_3, in excellent agreement with theoretical predictions. These authors also measured the ratio of the rates of the reactions

$$CH_2(C^{13}OOH)(C^{13}OOH) \xrightarrow{k_1} C^{13}O_2 + CH_3C^{13}OOH$$

$$CH_2(C^{13}OOH)(C^{13}OOH) \xrightarrow{k_2} C^{13}O_2 + CH_3C^{13}OOH$$

They found $k_1/2k_2$ equal to 1.037 at 137°C. The theoretical calculation of this ratio, which requires a model, was in poor agreement with experiment. Subsequently Pitzer (74) proposed a model for the decarboxylation reaction which led to the values of 1.14 and 1.07 for C^{14} and C^{13} substitution respectively at 150°C. In Pitzer's model the ratio k_4/k_3 varies appreciably with temperature and is equal to $k_1/2k_2$.

Roe & Hellman (75) have repeated the experiments of Yankwich & Calvin on malonic acid with C^{14} at 153°C. They report a considerable scatter in their experimental data with a value of k_4/k_3 equal to $1.06 \pm .02$ from the average of their ten best runs.

Lindsay, Bourns & Thode (76) have repeated and extended the work of Bigeleisen & Friedman (73) on the C^{13} isotope effect in the decarboxylation of natural malonic acid. Their results are in quantitative agreement with those of the latter authors.[3] In addition they find the ratio k_4/k_3 independent of temperature, a condition which is just what had been predicted by Bigeleisen (71) and contrary to Pitzer's model. They also found that C^{13} is randomly distributed in natural malonic acid, as was assumed to be the case by Bigeleisen & Friedman.

Bothner-By & Bigeleisen (77) have measured the relative rates of decarboxylation of carboxyl-C^{12} and -C^{13} mesitoic acids at 61° and 92° and find the ratios $1.037 \pm .003$ and $1.032 \pm .001$ at these temperatures. They have also discussed the application of the theory of isotope effects in reaction kinetics to the decarboxylation reaction. Bigeleisen & Allen (78) have made a precise study of the relative rates of decarboxylation of 1-C^{12} and 1-C^{13} trichloracetate ions at 70°C. The 1-C^{12} ion was found to decompose 1.0338 $\pm .0007$ times as fast as the 1-C^{13} ion. These authors have also discussed the errors which arise in the determination of the relative rates of reaction of isotopic molecules. Neither of these two studies supports Pitzer's model.

Ropp, Weinberger & Neville (79) have measured the C^{14} isotope effect in the dehydration of formic acid by concentrated sulfuric acid. The ratio of the C^{12} to C^{14} reaction rates varies between $1.125 \pm .005$ at 0° and $1.094 \pm .006$ at 25°C. The relative rates are of the correct order of magnitude for this reaction. The temperature coefficient is somewhat larger than one would expect from theoretical calculations and may in part be due to an underestimate of the precision of the measurements.

Weigl, Warrington & Calvin (80) report that $C^{14}O_2$ is assimilated 0.83 times as rapidly as $C^{12}O_2$ in photosynthesis with barley shoots. The system is too complex to warrant further interpretation at this time.

Harris (81) has considered the general kinetics of isotopic exchange reactions. Where there is no isotopic specificity, the McKay first order law is obtained. In the general case the kinetics are those of a reversible chemical reaction. For the case where the tracer is present at low concentration, the kinetics are those of a first order reaction and the half-life is dependent on the equilibrium constant for the exchange reaction and is not given simply by McKay's law.

Jones (82) has made a very careful study of the relative rates of photochlorination of H_2 and HT. It is well known that the slow step in this reaction is the reaction of hydrogen molecules with chlorine atoms. HT can react with

[3] Lindsay, Bourns, and Thode report a value of $k_1/2k_3$ at 138° of 1.046. Subsequently Dr. J. G. Lindsay has communicated to this reviewer the results of a more extensive study of this ratio. The ratio was studied between 137° and 196°C., found to be independent of temperature, and equal to 1.036 ± 0.003.

chlorine atoms to give either HCl or TCl. In Jones' work the relative rates of the H_2 and the sum of the two HT reactions were measured. The ratio of the rate constants k_H/k_T was found to be

$$k_H/k_T = 1.35 \pm 0.03e^{552\pm7/RT}$$

Jones has compared this ratio with calculations based on the potential energy surface for this reaction constructed by Wheeler, Topley & Eyring (83). The theoretical calculations are in poor agreement with experiment. The sign of the temperature coefficient of the relative rates is incorrectly predicted and the calculated ratio of the frequency factors exceeds the experimental value considerably. Jones points out that the triangular complex suggested by Magee (84) may give better agreement with experiment.

Van Meersche (85) has reinvestigated and extended the measurements of Farkas & Farkas (85a) on thermal conversion of *para* hydrogen to *ortho* hydrogen and the exchange between H_2 and D_2. These reactions proceed by the reaction of atoms from the thermal dissociation with the molecule. The new results are in substantial agreement with those of Farkas and Farkas but the larger temperature range leads to a better value of the activation energy. In addition, Van Meersche has used a better value for the heat of dissociation of H_2 and as a result finds that the activation energy for the reaction between atom and molecule should be lowered from 7.6 to 7.2 kcal. A calculation is then made for the relative rates of some of the isotopic reactions of hydrogen atoms with hydrogen molecules. The agreement with the calculations of Hirschfelder, Eyring & Topley (86), and of Farkas & Wigner (87) is improved. There is a significant discrepancy in the reaction between deuterium atoms and molecules. Some of this discrepancy may in part be due to the heat of dissociation of D_2 used by Van Meersche, which does not agree too well with that of Woolley, Scott & Brickwedde (88).

Gilman, Dunn & Hammond (89) have found that ϕ_3SiD hydrolyzes six times as rapidly as ϕ_3SiH at room temperature. They attribute this large reverse effect to the displacement of a hydride ion in the silane and the formation of something similar to a hydrogen molecule in the transition state. The ratio of the partition function of HD and H_2 is not large enough to explain so large an effect and it is probable that water, which has a large ratio for the partition functions of HDO and H_2O, is involved in the transition state.

Duke & Pinkerton (90) have measured the relative rates of disproportionation of U^{+5} in light and heavy water. The rate is 1.7 times as fast in D_2O as in H_2O. The mechanism of the disproportionation reaction is believed to be

$$UO_2^+ + H^+ \overset{K}{\rightleftarrows} UOOH^{+2}$$

$$UO_2^+ + UOOH^{+2} \xrightarrow{k} UO_2^{+2} + UOOH^+$$

Duke & Pinkerton interpret the isotope effect as the result of the increased base strength of UO_2^+ toward deuterons as compared with protons. The ex-

planation seems quite plausible and is of the correct order of magnitude for such a process.

Post & Hiskey (91) have measured the deuterium overvoltage in solutions of DCl in D_2O on a mercury cathode as a function of temperature and current density. These data when combined with similar ones on the protium overvoltage give an electrolytic separation factor of protium from deuterium of 3.1 at 20°C., which is in excellent agreement with the direct experimental determinations of Horiuti & Okamoto (92a) and of Walton & Wolfenden (92b). This agreement supports theories which postulate that one particle is involved in the discharge process and rules out a slow step which involves the combination of two or more entities at the electrode.

Mason, Biddick & Boyd (93) have measured the effect of ultrasonic radiation on the electrolytic separation coefficient of deuterium from protium at a polished platinum cathode. The radiation was found to increase the separation factor and decrease its temperature coefficient. This has been interpreted in terms of inhibition of the exchange reaction between H_2 and HDO, which is believed to take place to some extent at the electrode. This back exchange decreases the separation factor and is presumably retarded by the removal of gases from the electrode surface by the ultrasonic radiation.

Bell & Caldin (94) have measured the rates of decomposition of nitramide and nitramide, containing 40 to 60 atom per cent deuterium, in anisole catalyzed by dimethylamine between 0° and 45°C. The study was undertaken to look for evidence of reaction by quantum mechanical leakage through the potential barrier. Such leakage is anticipated for a reaction where the rate-determining step is proton transfer. Leakage should manifest itself in a large increase in the frequency factor. No such effect was found and the difference in rates can be explained by a difference in activation energies of 1800 calories/mol. The experiments were unfortunately complicated by the fact that the nitramide was far from completely deuterated.

Taylor & Dibeler (95) have studied catalyzed and exchange reactions of H_2 and D_2 with olefins on nickel. The rate of the shift of the double bond in butene-1 is four times as rapid in the presence of H_2 as in the presence of D_2 at 60°C. This ratio drops to 2.5 at 130°C. Isomerization of *cis-* and *trans-*butene-2 proceeds at identical rates in the presence of H_2 and D_2. There is still insufficient information on these interesting but complex reactions to interpret these results.

Isotope Effects on Mass Spectra

Stevenson (96) has determined and discussed the mass spectra of the propanes and butanes containing one carbon atom enriched in C^{13}. From the spectra of the monoisotopic ions and the assumptions of no C^{13} isotope effects on the parent ions or in the rupture of C—H bond, it is possible to work out a mass spectrometric analytical method for $—C^{13}_0$, $—C^{13}_1$, and $—C^{13}_2$ in propanes and butanes. Isotope effects in the rupture of C—C bonds on electron impact are found and discussed qualitatively in terms of two effects to be

discussed below in connection with the mass spectra of the deuteroparaffins. It is interesting to note, as Stevenson points out, that the C_1 fragments from $C_3H_8^+$ and the C_1 and C_2 fragments from $i\text{-}C_4H_{10}^+$ are independent of the labeling in the original skeleton. The mass spectra of the isomeric C^{13}_1 compounds are identical in these fragments.

Stevenson & Wagner (97) have intercompared the mass spectra of all the C_1 to C_4 monodeuteroparaffins with the corresponding protium compounds. All the deuteroparaffins show isotope effects on bond rupture by electron impact. These are discussed in terms of two effects: (*a*) the application of the Franck-Condon principle to the transition from the ground state to an excited one which leads to ionization; (*b*) the relative dissociation probabilities of ions of the type ABA'^+ into AB^+ and $A'B^+$, where A and A' are isotopes of the same element. These two effects serve to explain the fact that the dissociation probability at D in CH_3D is lower than H in CH_4, after correction for a statistical factor of four, while the dissociation probability of H in CH_3D is higher than in CH_4. It is not possible to account for the entire mass spectra of the deuteroparaffins by the assignment of two parameters, one for the decrease in the dissociation probability of deuterium and the other for the increase in the dissociation probability of protium in the deuteroparaffin.

Lossing, Tickner & Bryce (98) have measured the difference in the ionization potentials of some protio- and deutero-paraffins. No difference is found between the pairs C_2H_2—C_2D_2 and C_2H_4—C_2D_4. The methanes show a linear increase in ionization potential on deuterium substitution, amounting to 0.18 volts between CD_4 and CH_4. From zero point energy considerations alone, this would require the force constants in CH_4^+ to be but one-fourth those in CH_4, an unreasonable requirement. The authors suggest that part of this difference might be explained in terms of the Franck-Condon principle. This difference in ionization potential limits the applicability of the method suggested by Stevenson & Wagner (99) for the analysis of mixtures of protio- and monodeutero-paraffins to successive pairs in the deutero-methane series (100). The method of Stevenson & Wagner utilizes low energy electrons so that only the parent ions are produced. The difference in ionization potentials, if small, as between successive pairs in the deutero-methane series, is negligible. When it amounts to 0.18 volts, errors are introduced. It appears that this limitation of the method of Stevenson & Wagner applies only to the methanes.

Dibeler & Bernstein (101) have intercompared the mass spectra of $CHCl_3$ and $CDCl_3$ obtained with 50 to 70 volt electrons. The C-H bond ruptures 3.0 times as frequently as the C-D bond. The ratio of HCl^+/DCl^+ from the two molecules is 1.6, while there is no effect of deuterium on the probability of rupture of C-Cl bonds.

Ploch & Walcher (102) have determined the yield of electrons by the impingement of positive ions (electron multiplier tubes) as a function of the mass of the positive ion. They have derived a correction formula to be applied to abundance determination of positive ions with electron multiplier tubes.

TABLE I

ISOTOPE SHIFTS IN MOLECULAR SPECTRA

Authors	Reference	Subject
Hillger & Strandberg	(109)	Theory of centrifugal distortion in the rotation of asymmetric top molecules. Application to HDS.
Weiss & Strandberg	(110)	Microwave inversion rotation spectra of the deutero-ammonias.
Nordman & Lipscomb	(111)	Theory of unit cell dimensions of LiH and LiD.
Lord & Nielsen	(112)	Infrared and Raman spectra of B_2H_6, $B_2{}^{10}H_6$, and $B_2{}^{10}D_6$.
Herzberg, Jones & Leitch	(113)	Photographic infrared spectrum of $CD_3C{\equiv}CH$.
Lohman, Reding & Hornig	(114)	Vibrations and crystal structure of H_2S and D_2S.
Lord & Ocampo	(115)	Raman spectrum of allene-d_4.
Hedberg & Badger	(116)	Infrared spectra and potential constants of HOCl and DOCl.
Crawford, Fletcher & Ramsay	(117)	Infrared spectra, structure, and force constants for CH_2N_2 and CD_2N_2.
Reding & Hornig	(118)	Vibrational spectra of solid NH_3 and ND_3.
Lancaster, Inskeep & Crawford	(119)	Infrared spectrum and assignments for $CH_2{=}CD_2$.
Cunningham, Boyd, Myers & Gwinn	(120)	Structure and dipole moments of 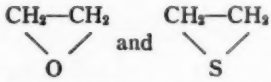 from the microwave spectra of the isotopic molecules.
Talley & Nielsen	(121)	Vibration-rotation spectrum of C_2D_2. Suggest possibility of measuring a vibration-rotation difference band in the microwave region.
Condon, McMurry & Thornton	(122)	Infrared and mass spectra of CH_3—$CD(OH)$—CH_3, CH_2—$CDCl$—CH_3, $CH_3CD_2CH_3$, and CH_3—$CD(CH_3)$—CH_3.
McMurry & Thornton	(123)	Infrared spectra and vibrational assignments of $CH_3CD_2CH_3$, $CD_3CH_2CD_3$, and $CD_3CD_2CD_3$.
Tiers	(124)	Analysis of *o*-, *m*-, and *p*- deuterotoluenes by infrared spectra.
Porter	(125)	Band spectrum of DNO_2 and identification of band spectrum of HNO_2.
Decius & Wilson	(126)	Sum rules for the vibrational spectra of isotopic molecules.
Fletcher & Arendale	(127)	Infrared spectra and vibrational assignments of parallel bands in CD_2CO and CHDCO.
Plyler & Gailar	(128)	Near infrared spectrum and structural parameters of C_2D_2.
Charette & Hemptinne	(129)	Infrared spectra and vibrational assignments of the deuteroethylenes.

Isotope Shifts in Atomic and Molecular Spectra

Fred, Tompkins, Brody & Hamermesh (103) have investigated the hyperfine structure of He^3I experimentally and theoretically. The observed structure conforms to a nuclear spin of one-half and a negative nuclear magnetic moment. The splitting of the ^3S terms are in good agreement with theory, while the splittings of the ^3P and ^3D terms indicate perturbations from neighboring fine structure levels. The isotope shifts from He^4 show deviations from those calculated by the Hughes-Eckart formula and are principally due to interactions between states.

The nuclear magnetic moment of Os^{189} has been found to be 0.6 ± 0.1 n.m.u. by means of hyperfine structure measurements (104). A preliminary report of the hyperfine structure of ErI (105) shows the presence of lines resulting from Er^{166}, Er^{168}, and Er^{170}. The absence of Er^{167} lines may be due to the large number of components of this isotope with nuclear spin 7/2. The shift between Er^{166} and Er^{168} is equal to that between Er^{168} and Er^{170}. The isotope shifts of U^{234} and U^{236} in the 4244 line of the arc spectrum of uranium have been measured (106). For the series U^{233}, U^{234}, U^{235}, U^{236}, and U^{238} the shift is strictly proportional to Δm.

Brix & Engler (107) have shown by a study of the hyperfine structure of GdI and EuI that the large isotope shifts found in the rare earths are not to be attributed to any peculiar property of the *f* electrons. Rather it results from the change in the nuclear volume after completion of the 82 neutron shell. By a study of the isotope shift in the CeII spectrum, Murakawa & Ross (108) have shown that the neutron number is more important than Z in determining the isotope shift in the spectra of the heavy elements.

In the field of molecular spectra and molecular structure, isotope shifts are valuable in the establishment of assignments of observed lines to transitions between energy states, the removal of certain degeneracies, and in the establishment of the potential energy function of the molecule. A detailed review of the progress in the use of isotopes in this field is a topic in itself. We shall record here in tabular form a brief abstract of the literature published in 1951.

LITERATURE CITED

1. Li, C. N., Whaling, W., Fowler, W. A., and Lauritsen, C. C., *Phys. Rev.*, **83**, 512 (1951)
2. Ewald, H., *Z. Naturforsch.*, **6a**, 293 (1951)
3. Nier, A. O., and Roberts, T. R., *Phys. Rev.*, **81**, 507 (1951)
4. Collins, T. L., Nier, A. O., and Johnson, W. H., Jr., *Phys. Rev.*, **84**, 717 (1951)
5. Ogata, K., and Matsuda, H., *Phys. Rev.*, **83**, 180 (1951)
6. Bönisch, A. (Doctoral thesis, Univ. of Vienna, Vienna, Austria, 1939)
7. Nier, A. O., *Phys. Rev.*, **81**, 624 (1951)
8. Roberts, T. R., *Phys. Rev.*, **81**, 624 (1951)
9. Wapstra, A. H., *Phys. Rev.*, **82**, 756 (1951)
10. Duckworth, H. E., and Preston, R. S., *Phys. Rev.*, **82**, 468 (1951)
11. Mayer, M. G., *Phys. Rev.*, **75**, 1969 (1949); **78**, 17 (1950)
12. Nordheim, L. W., *Phys. Rev.*, **75**, 1894 (1949)

13. Feenberg, E., and Hammack, K. C., *Phys. Rev.*, **75,** 1877 (1949)
14. Hays, E. E., Richards, P. I., and Goudsmit, S. A., *Phys. Rev.*, **84,** 824 (1951)
15. Smith, L. G., *Phys. Rev.*, **81,** 295 (1951); *Rev. Sci. Instruments*, **22,** 115 (1951)
16. Graham, R. P., Macnamara, J., Crocker, I. H., and MacFarlane, R. B., *Can. J. Chem.*, **29,** 89 (1951)
17. Inghram, M. G., Hayden, D. C., and Hess, R. J., Jr., *U. S. Atomic Energy Commission Document, ANL-4082* (1947)
18. Hibbs, R. F., Redmond, J. W., Gwinn, H. R., and Harman, W. D., *Phys. Rev.*, **75,** 533 (1949)
19. Rakestraw, N. M., Rudd, D. P., and Dole, M., *J. Am. Chem. Soc.*, **73,** 2976 (1951)
20. Milatz, J. M. W., Kluyver, J. C., and Hardebol, J., *J. Chem. Phys.*, **19,** 887 (1951)
21. Cohen, K., *The Theory of Isotope Separation as Applied to the Large-Scale Production of* U^{235} (McGraw-Hill Book Co., Inc., New York, N. Y., xviii+165 pp., 1951)
22. Majumdar, S. D., *Phys. Rev.*, **81,** 844 (1951)
23. Clusius, K., and Dickel, G., *Z. physik. Chem.*, [B]**44,** 397 (1939)
24. Dickel, G., *Z. physik. Chem.*, **197,** 197 (1951)
25. Keim, C. P., *Nucleonics*, **9**(2), 5 (1951)
26. Sugimoto, A., Nakane, R., and Watanabe, T., *Bull. Chem. Soc. Japan*, **24,** 153 (1951)
27. North, E. D., and White, R. R., *Ind. Eng. Chem.*, **43,** 2390 (1951)
28. Stewart, D. W., *Ann. Rev. Phys. Chem.*, **2,** 75 (1951)
29. Klemm, A., *Z. Naturforsch.*, **6a,** 489 (1951)
30. Klemm, A., Hintenberger, H., and Lunden, A., *Z. Naturforsch.*, **6a,** 512 (1951)
31. Fookson, A., Pomerantz, P., and Rich, E. H., *J. Research Natl. Bur. Standards*, **47,** 31 (1951)
32. Grilly, E. R., *J. Am. Chem. Soc.*, **73,** 843 (1951)
33. Grilly, E. R., *J. Am. Chem. Soc.*, **73,** 5307 (1951)
34. Hoge, H. J., and Arnold, R. D., *J. Research Natl. Bur. Standards*, **47,** 63 (1951)
35. Hoge, H. J., and Arnold, R. D., *J. Research Natl. Bur. Standards*, **47,** 75 (1951)
36. Kerr, E. C., Rifkin, E. B., Johnston, H. L., and Clarke, J. T., *J. Am. Chem. Soc.*, **73,** 282 (1951)
37. Friedman, A. S., White, D., and Johnston, H. L., *J. Am. Chem. Soc.*, **73,** 1310 (1951)
38. Friedman, A. S., White, D., and Johnston, H. L., *J. Chem. Phys.*, **19,** 126 (1951)
39. Hammel, E. F., *J. Chem. Phys.*, **18,** 228 (1950)
40. deBoer, J., *Physica*, **14,** 139 (1948)
41. Becker, E. W., and Stehl, O., *Naturwissenschaften*, **38,** 301 (1951)
42. Halpern, O., and Gwathmey, E., *Phys. Rev.*, **52,** 944 (1937)
43. Harteck, P., and Schmidt, H. W., *Z. physik. Chem.*, [B]**21,** 447 (1933)
44. Osborne, D. W., Abraham, B. M., and Weinstock, B., *Phys. Rev.*, **82,** 263 (1951)
45. Mazur, P., and Prigogine, I., *Physica*, **17,** 680 (1951)
46. Gorter, C. J., *Physica*, **15,** 523 (1949)
47. Daunt, J. G., Probst, H., and Johnston, H. L., *Phys. Rev.*, **73,** 638 (1948)
48. Taconis, K. W., Beenakker, J. J. M., and Dokoupil, Z., *Phys. Rev.*, **78,** 171 (1950)
49. Kirshenbaum, I., in *Physical Properties and Analysis of Heavy Water* (Urey, H. C., and Murphy, G. M., Eds., McGraw-Hill Book Co., Inc., New York, N. Y., xv+438 pp., 1951)

50. Schrader, R., and Wirtz, K., *Z. Naturforsch.*, **6a**, 220 (1951)
51. Smits, A., and MacGillavry, C. H., *Z. physik. Chem.*, [A]**166**, 97 (1933)
52. Smits, A., Muller, G. J., and Kröger, F. A., *Z. physik. Chem.*, [B]**38**, 177 (1937)
53. Thomas, D. G., and Staveley, L. A. K., *J. Chem. Soc.*, 1420 (1951)
54. Reynolds, C. A., Serin, B., and Nesbitt, L. B., *Phys. Rev.*, **84**, 691 (1951)
55. Maxwell, E., *Natl. Bur. Standards Rept. 1344* (1951)
56. Frohlich, H., *Phys. Rev.*, **79**, 845 (1950)
57. Bardeen, J., *Phys. Rev.*, **79**, 167 (1950)
58. Richardson, W. S., and Wilson, E. B., Jr., *J. Chem. Phys.*, **18**, 694 (1950)
59. Bigeleisen, J., and Friedman, L., *J. Chem. Phys.*, **18**, 1325 (1950)
60. McCrea, J. M., *J. Chem. Phys.*, **19**, 48 (1951)
61. Stranks, D. R., and Harris, G. M., *J. Chem. Phys.*, **19**, 257 (1951)
62. Kemball, C., *Proc. Roy. Soc.* (*London*), [A]**207**, 539 (1951)
63. Hunt, J. P., and Taube, H., *J. Chem. Phys.*, **19**, 602 (1951)
64. Bigeleisen, J., and Mayer, M. G., *J. Chem. Phys.*, **15**, 261 (1947)
65. Becker, E. W., and Vogell, W., *Z. Physik*, **130**, 129 (1951)
66. Herzberg, G., *Infra-Red and Raman Spectra of Polyatomic Molecules*, 534 (D. Van Nostrand Co., Inc., New York, N. Y., 1945)
67. Urey, H. C., Lowenstam, H., Epstein, S., and McKinney, C. R., *Bull. Geol. Soc. Am.*, **62**, 399 (1951)
68. Epstein, S., Buchsbaum, R., Lowenstam, H., and Urey, H. C., *Bull. Geol. Soc. Am.*, **62**, 417 (1951)
69. McCrea, J. M., *J. Chem. Phys.*, **18**, 849 (1950)
70. Yankwich, P. E., and Calvin, M., *J. Chem. Phys.*, **17**, 109 (1949)
71. Bigeleisen, J., *J. Chem. Phys.*, **17**, 425 (1949)
72. Bigeleisen, J., *J. Chem. Phys.*, **17**, 675 (1949)
73. Bigeleisen, J., and Friedman, L., *J. Chem. Phys.*, **17**, 998 (1949)
74. Pitzer, K. S., *J. Chem. Phys.*, **17**, 1341 (1949)
75. Roe, A., and Hellman, M., *J. Chem. Phys.*, **19**, 660 (1951)
76. Lindsay, J. G., Bourns, A. N., and Thode, H. G., *Can. J. Chem.*, **29**, 192 (1951)
77. Bothner-By, A. A., and Bigeleisen, J., *J. Chem. Phys.*, **19**, 755 (1951)
78. Bigeleisen, J., and Allen, T. L., *J. Chem. Phys.*, **19**, 760 (1951)
79. Ropp, G. A., Weinberger, A. J., Neville, O. K., *J. Am. Chem. Soc.*, **73**, 5573 (1951)
80. Weigl, J. W., Warrington, P. M., and Calvin, M., *J. Am. Chem. Soc.*, **73**, 5058 (1951)
81. Harris, G. M., *Trans. Faraday Soc.*, **47**, 716 (1951)
82. Jones, W. M., *J. Chem. Phys.*, **19**, 78 (1951)
83. Wheeler, A., Topley, B., and Eyring, H., *J. Chem. Phys.*, **4**, 178 (1936)
84. Magee, J. L., *J. Chem. Phys.*, **8**, 677 (1940)
85. Van Meersche, M., *Bull. soc. chim. Belges*, **60**, 99 (1951)
85a. Farkas, A., and Farkas, L., *Proc. Roy. Soc.* (*London*), [A]**152**, 124 (1935)
86. Hirschfelder, J. O., Eyring, H., and Topley, B., *J. Chem. Phys.*, **4**, 170 (1936)
87. Farkas, L., and Wigner, E. P., *Trans. Faraday Soc.*, **32**, 708 (1936)
88. Woolley, H. W., Scott, R. B., and Brickwedde, F. G., *J. Research Natl. Bur. Standards*, **41**, 379 (1948)
89. Gilman, H., Dunn, G. E., and Hammond, G. S., *J. Am. Chem. Soc.*, **73**, 4499 (1951)
90. Duke, F. R., and Pinkerton, R. C., *J. Am. Chem. Soc.*, **73**, 2361 (1951)
91. Post, B., and Hiskey, C. F., *J. Am. Chem. Soc.*, **73**, 161 (1951)
92a. Horiuti, J., and Okamoto, G., *Sci. Papers Inst. Phys. Chem. Research Tokyo*, **28**, 231 (1936)

92b. Walton, H. F., and Wolfenden, J. H., *Trans. Faraday Soc.*, **34**, 436 (1938)
93. Mason, D. F., Biddick, R. E., and Boyd, C. A., *J. Chem. Phys.*, **19**, 1551 (1951)
94. Bell, R. P., and Caldin, E. F., *Trans. Faraday Soc.*, **47**, 50 (1951)
95. Taylor, T. I., and Dibeler, V. H., *J. Phys. & Colloid Chem.*, **55**, 1036 (1951)
96. Stevenson, D. P., *J. Chem. Phys.*, **19**, 17 (1951)
97. Stevenson, D. P., and Wagner, C. D., *J. Chem. Phys.*, **19**, 11 (1951)
98. Lossing, F. P., Tickner, A. W., and Bryce, W. A., *J. Chem. Phys.*, **19**, 1254 (1951)
99. Stevenson, D. P., and Wagner, C. D., *J. Am. Chem. Soc.*, **72**, 5612 (1950)
100. Tickner, A. W., Bryce, W. A., and Lossing, F. P., *J. Am. Chem. Soc.*, **73**, 5001 (1951)
101. Dibeler, V. H., and Bernstein, R. B., *J. Chem. Phys.*, **19**, 404 (1951)
102. Ploch, W., and Walcher, W., *Rev. Sci. Instruments*, **22**, 1028 (1951)
103. Fred, M., Tompkins, F. S., Brody, J. K., and Hamermesh, M., *Phys. Rev.*, **82**, 406 (1951)
104. Suwa, S., *Phys. Rev.*, **83**, 1258 (1951)
105. Wilet, L., and Bradley, L. C., 3rd, *Phys. Rev.*, **84**, 1055 (1951)
106. Smith, D. D., Stukenbroeker, G. L., and McNally, J. R., Jr., *Phys. Rev.*, **84**, 383 (1951)
107. Brix, P., and Engler, H. D., *Naturwissenschaften*, **38**, 214 (1951)
108. Murakawa, K., and Ross, J. S., *Phys. Rev.*, **83**, 1272 (1951)
109. Hillger, R. E., and Strandberg, M. W. P., *Phys. Rev.*, **83**, 575 (1951)
110. Weiss, M. T., and Strandberg, M. W. P., *Phys. Rev.*, **83**, 567 (1951)
111. Nordman, C. E., and Lipscomb, W. N., *J. Chem. Phys.*, **19**, 1422 (1951)
112. Lord, R. C., and Nielsen, E., *J. Chem. Phys.*, **19**, 1 (1951)
113. Herzberg, G., Jones, A. V., and Leitch, L. C., *J. Chem. Phys.*, **19**, 136 (1951)
114. Lohman, J. B., Reding, F. P., and Hornig, D. F., *J. Chem. Phys.*, **19**, 252 (1951)
115. Lord, R. C., and Ocampo, J., *J. Chem. Phys.*, **19**, 260 (1951)
116. Hedberg, K., and Badger, R. M., *J. Chem. Phys.*, **19**, 508 (1951)
117. Crawford, B. L., Jr., Fletcher, W. H., and Ramsay, D. A., *J. Chem. Phys.*, **19**, 406 (1951)
118. Reding, F. P., and Hornig D. F., *J. Chem. Phys.*, **19**, 594 (1951)
119. Lancaster, J. E., Inskeep, R. G., and Crawford, B. L., Jr., *J. Chem. Phys.*, **19**, 661 (1951)
120. Cunningham, G. L., Jr., Boyd, A. W., Myers, R. J., and Gwinn, W. D., *J. Chem. Phys.*, **19**, 676 (1951)
121. Talley, R. M., and Nielsen, A. H., *J. Chem. Phys.*, **19**, 805 (1951)
122. Condon, F. E., McMurry, H. L., and Thornton, V., *J. Chem. Phys.*, **19**, 1010 (1951)
123. McMurry, H. L., and Thornton, V., *J. Chem. Phys.*, **19**, 1014 (1951)
124. Tiers, G. V. D., *J. Chem. Phys.*, **19**, 1072 (1951)
125. Porter, G., *J. Chem. Phys.*, **19**, 1278 (1951)
126. Decius, J. C., and Wilson, E. B., Jr., *J. Chem. Phys.*, **19**, 1409 (1951)
127. Fletcher, W. H., and Arendale, W. F., *J. Chem. Phys.*, **19**, 1431 (1951)
128. Plyler, E. K., and Gailar, N., *J. Research Natl. Bur. Standards*, **47**, 248 (1951)
129. Charette, J., and Hemptinne, M., de, *Acad. roy. Belg.*, **37**, 436 (1951)

NUCLEAR MOMENTS[1]

By Bernard T. Feld

Department of Physics and Research Laboratory of Electronics, Massachusetts Institute of Technology, Cambridge, Massachusetts

INTRODUCTION

In recent years, a vast amount of information has been accumulated concerning the static properties of nuclei. The techniques of optical spectroscopy, molecular and atomic beams, nuclear induction, and microwave spectroscopy have been applied to the measurement of nuclear spins, magnetic dipole, and electric quadrupole moments, primarily of the ground states of the stable nuclei; however, these techniques are being continuously expanded and improved, especially for the measurement of the properties of radioactive nuclei (1 to 5). Recent developments in these techniques were discussed by Ramsey in Volume I of this series (6).

One aspect of the above-mentioned techniques is the possibility of high precision in the measurement of nuclear moments (7 to 19). In the case of observations on the hydrogen isotopes, the deviations of the results from theoretical expectations have previously led to a re-examination of the theory and to the well-known revisions of quantum electrodynamics (20). It now appears that the theory is adequate for the interpretation of the best available measurements on the atomic spectra of the hydrogen isotopes (21 to 24).

For complex atoms, the interpretation of hyperfine structure measurements in terms of the nuclear moments is inherently relatively unprecise owing to the difficulty of obtaining accurate atomic wave functions (25). While magnetic dipole moments are alternatively obtainable through molecular beam and nuclear induction techniques, the most precise values of nuclear electric quadrupole moments still depend on atomic hyperfine structure determinations. Recent work by Sternheimer (26) on the electric shielding of the nucleus through polarization of the inner electron shells and by Koster (27) on the effects of configuration interactions on the atomic hyperfine structure lead to a better understanding of the uncertainties inherent in the measurement of nuclear electric quadrupole moments by atomic hyperfine structure and permit more accurate evaluations in many cases. The theory of molecular hyperfine structure has also received further attention (28, 29, 30), as has the theory of magnetic resonances in liquids and solids (28, 31 to 34); these investigations continue not only to lead to the more precise evaluation of nuclear moments but also to produce impor-

[1] This review is primarily, but not exclusively, a survey of work reported in 1951. It is, however, intended as a summary covering mainly the highlights, rather than as an exhaustive literature survey.

tant results for the understanding of certain aspects of the liquid and solid states.

However, the ground states of the stable nuclei constitute a rapidly diminishing fraction of the nuclear states about which meaningful information concerning the nuclear moments is now available. Most, but not all, of these data concern the spins (angular momenta) of the levels. Furthermore, the successes of the independent particle model of nuclei, in the form suggested by Mayer (35) and by Haxel, Jensen & Suess (36), in correlating and predicting the spins and moments of low-lying nuclear levels, has given a tremendous impetus to the field of nuclear spectroscopy and has led to a re-examination of the systematics of nuclear magnetic dipole and electric quadrupole moments. It is the purpose of this article to review briefly recent developments in the techniques of determining the moments (including the mechanical moment or spin) of nuclear levels and the understanding of the values of observed nuclear moments in terms of possible nuclear models.

TECHNIQUES FOR MEASURING THE MOMENTS OF UNSTABLE NUCLEAR STATES

The conventional techniques for measuring nuclear moments are applicable to the ground states of the stable nuclei, to relatively long-lived radioactive nuclei, and to some isomeric states, provided that the excited nuclei can be obtained in sufficient quantity (1 to 5). For all other nuclear levels, other means must be devised to determine the properties (spin, parity, moments). Such means do exist, and considerable progress has been made in their development and extension. As a result of the application of these techniques, a considerable amount of information has been accumulated concerning the properties of nuclear energy levels, especially for the lighter nuclei (37, 38, 39).

The measurements of the properties of relatively short-lived nuclear levels depend, perforce, on studies of the properties of the emitted radiations. In particular, means are available, under favorable circumstances, for determining the angular momentum and parity change carried off by the emitted radiation. When such a determination is possible, the spin and pairty of the emitting state is determined, provided that the spin and parity of the final state is known. Thus, in the final analysis, the determination of the spin and parity of an excited state depends on a previous knowledge of the properties of a stable state, which properties must be determined by conventional techniques. The aspect of the emitted radiation which is most directly associated with the change in angular momentum and parity is its angular distribution (with respect to some physically meaningful direction). Other aspects from which pertinent conclusions can be drawn are the lifetime and the interaction with the atomic electrons.

The Angular Distribution of Nuclear Decay Products

The techniques for measuring the properties of nuclear energy levels by means of "angular correlation" experiments have recently been summarized by Deutsch (40). For the purposes of this survey, we distinguish (quite arbitrarily) three general methods.

Radiation from polarized nuclei.—The polarization of nuclei is equivalent to establishing an unequal distribution of nuclei in the normally equally populated magnetic substates. A number of experimental possibilities for achieving this end have been suggested and discussed by various authors (41 to 46). Some of these involve the actual alignment of nuclear spins in an external magnetic field or in the previously aligned atomic fields (sometimes referred to as "dipolarization"); others depend on interactions which are proportional to m^2 (the square of the magnetic quantum number), e.g., the nuclear electric quadrupole interaction (hence, the term "quadrupolarization"). All of these require very low temperatures, $<1°$ K., and some require very strong magnetic fields to achieve even a small degree of polarization.

Given a system of polarized radioactive nuclei, the intensity of the emitted radiation will, in general, depend on the angle of emission with respect to the direction of polarization. The angular distribution is a function of the angular momentum, spin, and parity change carried away by the radiation (as well as, of course, the degree of polarization). The theory of the angular dependence has been developed by Spiers (47, 48) and others (49, 50).

The experimental achievement of an appreciable degree of nuclear polarization has proved to be an exceedingly difficult task. However, successes have recently been reported by groups at Oxford (51, 52) and at Leiden (53, 54) in observing deviations from isotropy in the γ-radiation from Co^{60}, aligned by the method of Bleaney (45). Assuming the decay scheme and spin ($I=5$) suggested by Deutsch & Scharff-Goldhaber (55), these experimenters infer the magnetic moment $|\mu| \approx 3$ nuclear magnetons for Co^{60}.

Angular distributions in nuclear reactions.—In nuclear reactions, the direction of the incident particle (or radiation) provides a natural axis with respect to which the reaction products may be asymmetrically distributed. In order for the distribution to deviate from spherical symmetry, it is necessary that both the incident particle and the reaction products carry angular momenta greater than $\hbar/2$. A simple and well-known example is the photodisintegration of the deuteron (56). For photon energies not too far above the reaction threshold, two processes are predominant. One, the photoelectric disintegration, corresponds to the absorption of an electric dipole ($l=1$) γ-ray, with the subsequent conversion of the ground, $^3S_1$-state of the deuteron into a free neutron and proton in a ^3P-state. (The selection rule for electric dipole absorption is $\Delta L = \pm 1$, $\Delta S = 0$.) The angular distribution, in the center

of mass co-ordinate system, of the emitted neutron and proton is thus $\sin^2\theta$ with respect to the direction of the incident γ-ray. This distribution also follows from a classical argument, since the electromagnetic radiation acts on the instantaneous dipole moment of the deuteron through the electric vector, which is perpendicular to the direction of propagation of the photon. The second process is magnetic dipole absorption, which corresponds to the "flipping" of one of the nuclear spins with respect to that of the second ($\Delta L=0$, $\Delta S=\pm 1$), and consequently, converts the ${}^3S_1$ ground state to a ${}^1S_0$-state. The angular distribution for this reaction is accordingly spherically symmetrical in the center of mass system. Such simple reactions, which do not involve the formation of a compound nucleus, are observed mainly in the light elements. Their angular distributions have been used to identify the spins and parities of many of the levels of the light nuclei (37, 57).[2]

For most nuclear reactions, however, it is necessary to take into account the formation of a compound nucleus in which, especially for reactions involving heavy nuclei, the energy levels may be closely spaced as compared to the energy spread in the incident beam. Here we may distinguish two extreme cases. In the first, we may consider the compound nucleus energy levels so closely spaced as to constitute a continuum, with a statistical distribution of level spins and parities. In this case the angular distribution of the reaction products is obtained as a sum over all possible absorption and decay processes. When, however, the final (product nucleus) state is discreet, the observed angular distribution can yield the properties of this state, as shown by Hauser and associates (58) for the case of inelastic scattering of neutrons by intermediate and heavy nuclei. The second case, which is easier to interpret, is that in which a single level (resonance) of the compound nucleus is involved. In this case, knowledge of the properties of the initial and final states and a measurement of the angular distribution of the reaction products yield the spin and parity of the compound nucleus level in question (59, 60).

It is worth noting at this point that a simple measurement of the peak total cross section of a compound nucleus resonance reaction can, itself, yield the spin of the compound nucleus level, since (58)

$$\sigma_{\text{peak}} = 4\pi\lambda\!\!\!^{-2}(2J+1)/(2S+1)(2I+1) \qquad 1.$$

where J is the spin of the compound nucleus level, S is the spin of the bombarding particle, I is the spin of the target nucleus, and $\lambda\!\!\!^{-}$ is the Dirac wave length of the bombarding particle.

Of special interest among nuclear reactions, for the purpose of measuring nuclear spins, are the (d, p) and (d, n) "stripping" reactions. These do not involve the formation of a compound nucleus but rather the "capture" of one of the deuteron constituents directly into a level of the product nucleus. The product nucleus is frequently left in either the ground state or in one of its low-lying levels, with the uncaptured particle carrying off the reaction energy. Thus, the emerging protons or neutrons have a line spectrum of

[2] The references to experiments cited in this section are illustrative examples among many recent investigations.

energies. Each energy group has a distinct angular distribution, with one or more strong forward maxima and minima.

Butler (61) has developed a theory of the deuteron stripping reaction, in terms of which the angular distribution of the stripped particles can be used to determine the orbital angular momentum imparted to the nucleus by the capture of the other member. If the spin and parity of the target nucleus is known, such a measurement then determines the parity and limits the possible spin values of the product nucleus level involved. The theory has proved to be applicable over a wide range of target nuclei and deuteron energies (62 to 67).

Angular correlations between successive nuclear radiations.—Another means of specifying the orientation of a nucleus (the value or distribution of the azimuthal quantum number, m) is provided when a nucleus undergoes successive decays. In this case, the successive radiations will be correlated in their directions of emission, the form of the correlation depending on the angular momenta and parities of the levels involved in the cascade as well as on the nature of the particles emitted.

The theory of the angular correlation was first developed by Hamilton (68) for the case of successive emission of two γ-rays. It has been extended by many authors (69 to 77) to cover other radiation correlations, including β-γ (74, 77), internal conversion electron-γ (70, 73), α-γ, etc. (72, 74, 77). A simple physical picture of the type of effect which might be expected has been given by Moon (78) for the case of successive electric dipole γ-ray emission between levels of spins 0-1-0: Let the first γ-ray be emitted along the z-axis. The emission of the γ-ray imparts angular momentum one to the nucleus, which angular momentum must be orientated in the plane perpendicular to the z-axis, say along the x-axis. The emission of the second γ-ray must be such as to remove this unit of angular momentum, i.e., anywhere in the y-z plane, all angles having equal probability. Since the choice of the x-axis, as the direction of the angular momentum of the intermediate state was arbitrary, the angular correlation will be obtained by rotating the distribution of the second γ-ray (any direction in the y-z plane) about the z-axis. This leads to an angular correlation which is most probable along the $\pm z$-direction, and least probable in the x-y plane, i.e., $1+\cos^2\theta$, where θ is the angle between the two γ-rays.

The general case of level spins J-J'-J'' and higher multipole radiation is, unfortunately, not susceptible to such simple physical arguments. Its calculation proceeds along relatively straightforward quantum-mechanical lines provided that the azimuthal quantum numbers are all taken with respect to the direction of emission of the first quantum (Hamilton's theorem) (68, 79, 80). Under the conditions most frequently encountered in nuclei, the angular correlation can be expressed in the form (40, 81)

$$W(\theta) = \sum_{i=0}^{0} a_i \cos^{2i}\theta = \sum_k b_k P_k(\cos\theta) \qquad 2.$$

with $I = L, L', J'$, whichever is the smallest. (L and L' are the orbital angular

momenta of the successive radiations; J' the spin of the intermediate state.) There are, however, cases where odd powers of $\cos\theta$ are required, due to interference effects when a given level can decay by two or more modes (74, 75).

Since the first conclusive γ-γ angular correlation measurements by Brady & Deutsch (82), the technique has been widely applied to many radioactive nuclei. While most of the observations are interpretable in terms of the theory, some cases are demonstrably not. Many of these anomalies can be understood as resulting from a partial or complete destruction of the angular correlation resulting from reorientation (or loss of memory) in the intermediate state. Such reorientation will occur, for instance, if the lifetime of the intermediate state is long as compared to the period of precession of the nucleus in the magnetic field of the atomic electrons, or molecule, or crystal[3] (69, 83, 84, 85). As suggested by several authors (83, 86, 87), this effect can be used to measure the magnetic moment of the intermediate state, by observing the change (partial destruction) of the angular correlation resulting from the application of an external magnetic field. Such a measurement has been carried out successfully by Aeppli and co-workers (88) on Cd^{111}; they obtained, for the magnetic moment of the 247-kev level ($I=5/2$), $\mu=-0.85\pm0.22$ nuclear magnetons.

In the case of angular correlations involving γ-radiation, the parities of the levels cannot be determined because of the ambiguity between electric and magnetic transitions; i.e., the same angular momentum change can be achieved by an electric or magnetic multipole γ-ray with opposite change in parity. In order to remove this ambiguity, it is necessary to make some other measurement(s) on the γ-radiation. One such possibility is to observe the direction of polarization of one of the γ-rays with respect to the direction of emission of the other (89, 90). This method has been applied by Metzger & Deutsch (91).

Among the other possible angular correlation measurements, we shall mention further only the α-γ correlation. This type of correlation, if observable, is perhaps the easiest to interpret, since the α-particle possesses no intrinsic angular momentum. Hence, the transition via α-particle emission, between states $J\rightarrow J'$, is accomplished by the emission of an α-particle with $L=|J-J'|$, $\Delta m=0$, $\Delta\text{parity}=(-1)^L$. The α-γ angular correlations have been used to identify the 482-kev level of Li^7, excited in the $B^{10}(n,\alpha)$ reaction (92, 93, 94), to assign spins and parities to the states in the resonant reaction $F^{19}(p)Ne^{20*}(\alpha)O^{16*}(\gamma)O^{16}$ (95), and to study the levels of ThX involved in the natural α-decay of RdTh (96, 97).

β-Ray Spectroscopy

Investigations of the properties of β-ray spectra have led to considerable information concerning nuclear energy levels. When the β-rays are accom-

[3] The nuclear precession time is measured by the reciprocal of the frequency of the hyperfine structure splitting.

panied or followed by other radiation, the angular correlation between the radiations can be studied as discussed above. The theory of β-γ angular correlations has been developed by Falkoff & Uhlenbeck (74) and applied by a number of investigators; the reader is referred to the recent work of Stevenson & Deutsch (98) for references to and discussion of this type of investigation. Another type of correlation is between the β-rays and the simultaneously emitted neutrinos (99, 100). Since the neutrino has so far eluded direct observation, such investigations have resorted to the observation of the correlation between the β-rays and the recoiling nuclei (101, 102). Finally, an angular correlation has recently been observed between the β-particles and the associated continuous electromagnetic radiation (103).

The use of the characteristics of β-ray spectra to investigate the properties of nuclear energy levels is complicated by the fact that the form of the interaction between nucleons and the electron-neutrino field is still in question, if indeed it is possible to make a unique choice between the possible forms (104). However, despite the present uncertainty in the form of the interaction (and, consequently, in the selection rules) it has been possible to connect the β-ray characteristics with the change in angular momentum and parity. The following two general procedures are available.

Comparative half-lives or ft values.—The original theory of Fermi (105) and its extensions and modifications (104) predict a connection between the half life for β-decay, t, the maximum β-ray energy W_0, and the change of angular momentum and parity involved in the decay. This connection is usually expressed through the ft value, or comparative half life,

$$ft = \frac{2\pi^3(2I_i + 1) \ln 2}{G^2 \cdot \sum |(k|M|i)|^2} \qquad 3.$$

where t is the half life, I_i is the spin of the parent nucleus, G the Fermi constant, a measure of the strength of the interaction, and $(k|M|i)$ the matrix element for the β-transition, which must be summed over the magnetic substates. The factor $f = f(Z, W_0)$ can be computed from the theory (104, 106).

The selection rules come into operation through the matrix element which, according to the theory, can take on a series of decreasing values, depending on the angular momentum and parity change. These values are expected to decrease by more or less discreet steps, so that the various β-disintegrations should fall into groups. The group corresponding to the smallest ft value (largest matrix element) is called "allowed"; the next larger ft group is "first forbidden," then "second forbidden," etc. The selection rules are determined by the type of interaction and fall into two groups, the Fermi (105) and the Gamow-Teller (107) selection rules. The two schemes are compared in Table I (104).

Recent compilations and interpretations of ft values (106, 108) show the expected behavior only to a limited extent. There is a group of allowed transitions with $ft < 10^4$. (These are mostly transitions between image nuclei and are sometimes referred to as "super-allowed.") The grouping of $ft > 10^4$ transitions is not nearly so convincing, but appears to be separable into allowed

TABLE I

SELECTION RULES IN β-DECAY

	Fermi		Gamow-Teller	
	ΔJ	parity change?	ΔJ	parity change?
allowed	0	no	$0, \pm 1$(no $0 \rightarrow 0$)	no
first forbidden	$0, \pm 1$(no $0 \rightarrow 0$)	yes	0	yes
			$0, \pm 1$(no $0 \rightarrow 0$)	yes
			$0, \pm 1, \pm 2$(no $0 \rightarrow 0, 1 \leftrightarrow 0, 1/2 \rightarrow 1/2$)	yes
second forbidden	$\pm 1, \pm 2$(no $1 \leftrightarrow 0$)	no	± 2	no
	± 1	no	$\pm 2, \pm 3$(no $0 \leftrightarrow 2$)	no
			$0 \rightarrow 0$	no

unfavored, first forbidden, etc. The shading of groups into each other is perhaps not unreasonable, since the matrix element may be expected to fluctuate from nucleus to nucleus. On the basis of present observations (e.g., $He^6 \rightarrow Li^6$, $\Delta J = 1$, no parity change, allowed transition with $ft \sim 10^2$–10^3) the Gamow-Teller selection rules seem to be preferred.

The shapes of β-ray spectra.—The most useful way of exhibiting the shape of a β-ray spectrum is by plotting a certain function of the momentum and β-ray intensity versus energy. This is known as a "Kurie plot" or "Fermi plot" (104, 109). When plotted in this fashion, allowed spectra fall on a straight line, with an intercept on the energy axis corresponding to the value of W_0. However, certain forbidden spectra are expected to deviate significantly from a straight line; the form of the deviation is characteristic of the interaction (104).

Up to 1949, all spectra, for which the measurements were demonstrably reliable,[4] exhibited straight line Kurie plots, with the exception of RaE (110, 111). However, following the demonstration, by Langer & Price (112), of the forbidden shape of the β-ray spectrum from Y^{91}, many forbidden shapes have been and continue to be found. Most of the forbidden spectral shapes seem to favor interactions leading to the Gamow-Teller selection rules. For a summary of progress in this field, the reader is referred to an excellent review by Wu (113).

THE PROPERTIES OF ISOMERIC TRANSITIONS

When the spin of an excited nuclear state differs by a relatively large number of units (say $\geqq 3$) from those of the lower levels and when its excitation energy is relatively low (say 500 kev), the lifetime of the state may be

[4] Apparent deviations from a straight line at the low-energy end of the spectrum may be due to the finite source thickness (113).

relatively long (say $\gtrsim 10^{-1}$ sec.). Such states[5] are known as "isomeric states" or simply as "isomers." In particular, isomeric states of nuclei with stable ground states decay by γ-ray emission. In such isomeric transitions, an appreciable fraction of the γ-rays may be "internally converted"; i.e., a monoenergetic electron is emitted from the atomic K^-, L^-, or M^- shell, followed by x-rays characteristic of the decaying element. Both the lifetime and the internal conversion probabilities of the decay γ-ray are (for a given energy) primarily determined by the change in angular momentum and parity associated with the transition. These changes determine the multipole order of the emitted γ-ray and are usually designated according to the classification shown in Table II.

TABLE II

CLASSIFICATION OF ISOMERIC TRANSITIONS

designation	*E*1	*M*1	*E*2	*M*2	*E*3	*M*3	*E*4	*M*4	*E*5
$\lvert\Delta J\rvert$	1	1	2	2	3	3	4	4	5
parity change?	yes	no	no	yes	yes	no	no	yes	yes
multipole order	1	2		3		4		5	

It has been recognized for some time (e.g., 114, 115) that a log-log plot of the mean life versus decay energy for all the known isomers tends to separate into a number of straight lines. The disintegrations corresponding to the different lines have been associated with the different types of transitions, designated in Table II as *E*2, *M*2, *E*3, etc., with the lifetime increasing (for a given decay energy) with increasing multipole order.

The other approach, that of observing the "conversion coefficients," has also been used to classify isomers (114, 115). This method, however, suffers not only from a greater experimental difficulty but also from uncertainty as to the accuracy of the theory. In any event, the two methods of classifying isomeric transitions have been, until this past year, very frequently in conflict.

However, the identification of nuclear isomers is now on relatively firm footing, in large measure as a result of clarification and codification by Goldhaber & Sunyar (116). They have, with the help of nuclear shell theory (see the next section), established empirical lifetime versus energy relationships for isomeric transitions. These may be summarized as follows: For $\lvert\Delta J\rvert > 3$, the lifetime of an isomer is essentially determined by the spin change rather than by the multipole order or parity change. The lifetimes for magnetic transitions agree with the predictions of the theory of Weisskopf (117). The electric transitions are somewhat slower than predicted, except

[5] Obviously, the classification of a state as an isomer is a function of the ability of the observer to detect a delay in its decay.

for $E2$, which are sufficiently rapid so that they frequently compete with $M1$.

The same authors have established empirical curves for the K/L conversion ratios which can be used, in place of the less accurate theoretical curves (118, 119), to aid in the identification of isomeric transitions.

THE INDEPENDENT PARTICLE MODEL AND NUCLEAR MOMENTS

Nuclear Shell Structure

The independent particle model of nuclei, while by no means a new idea (120, 121) has, in the past few years, had a phenomenal revival. According to this model (sometimes referred to as the quasi-atomic model) each nucleon can be regarded as moving in a central field, which is the average of its interaction with all the other nucleons in the nucleus. The nucleons occupy the various energy levels according to the Pauli prinicple (i.e., no two neutrons or protons can occupy the same state). Thus, the nuclear ground states may be expected to exhibit a shell structure with the completing of the various shells resulting in particularly stable nuclei (analogous to the noble gases in the atomic case). While it was the observation of the phenomenon of closed shells, dubbed "magic numbers" in the nuclear case, at 20, 28, 50, 82, or 126 nucleons which led to the revival of the independent particle model, these particular numbers could not be accounted for in a satisfactory fashion until the introduction by Mayer (35) and by Haxel, Jensen, & Suess (36), of the assumption of a strong spin-orbit coupling for the individual nucleons. Figure 1 shows, schematically and not to scale, the order of nuclear energy levels according to various assumptions concerning the shape of the nuclear potential.

The closest correspondence with observation is obtained on the assumption of a "square well with rounded edges" (122) together with a spin-orbit coupling which increases with the orbital angular momentum. It should be pointed out that no really satisfactory theoretical basis has yet been established, either for the independent particle model per se or for the assumption of a strong spin-orbit coupling (123, 124). Nevertheless, the experimental evidence for the model is by now so overwhelming and its usefulness in understanding and correlating the properties of the low-lying nuclear energy levels so convincingly demonstrated that it no longer seems necessary to make a very strong case for its empirical validity. In fact, assuming the independent particle model, it is difficult to understand why its effects appear to persist even in the range of relatively high excitation energies (125).

The shell model as outlined above is not only successful in explaining the magic numbers but it can also account for the angular momenta and parities of the ground states and low-lying excited states of almost all nuclei. In order to accomplish this it is necessary to adopt certain rules concerning the coupling of more than one particle in an incomplete shell. In essence, these rules state that an even number of nucleons couple to give $J=0$ and even parity, while on odd number of nucleons, each with angular momentum j, in an incomplete shell couple to a total angular momentum $J=j$, with the same parity as the individual nucleon states. Actually, these rules can be

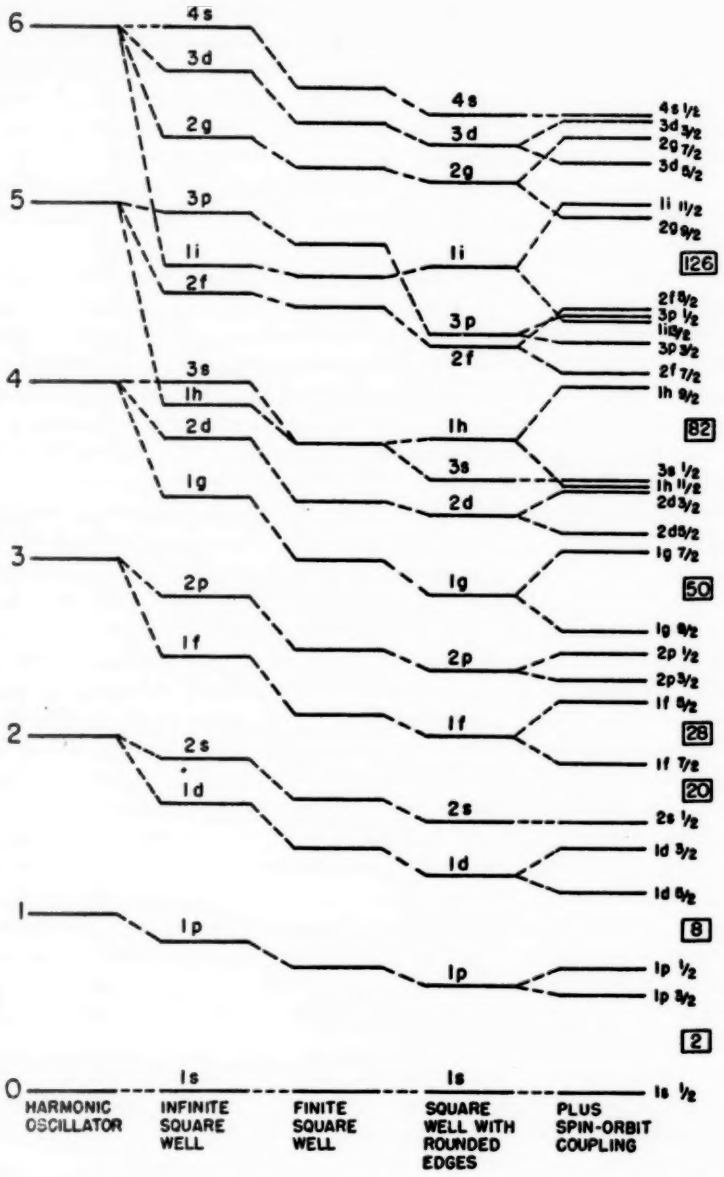

FIG. 1. Order of energy levels on the independent particle model of nuclei under various assumptions concerning the shape of the nuclear potential and including the effects of spin-orbit coupling. The energy is not to scale, nor should the exact order of the levels within a given shell be taken too seriously.

shown to follow from the assumption of a δ-function, spin-independent interaction between the nucleons (35), but they also hold on the assumption of a finite range, spin-independent interaction, provided that the range is not too large (126, 127). Nevertheless, there are a few exceptions, all of which follow the subsidiary rule that an odd number of nucleons of angular momentum j can sometimes couple to a state $J=j-1$, with the parity of the individual nucleons. The question of the coupling of odd neutrons and protons (in the odd-odd nuclei) is somewhat more complex and will be discussed in a following section.

The order of filling of levels within a shell frequently departs from the scheme depicted in Figure 1. The first and somewhat trivial reason is that the exact order of levels depends on the shape and size of the nuclear potential which may show fluctuations from element to element. The same reason can account for differences between the filling of neutron and proton shells. A more important effect is due to the "pairing energy," i.e., the energy gained by having two nucleons in the same subshell, which increases rapidly with increasing orbital angular momentum (35). This has the effect that the states of higher angular momentum tend to be filled in pairs so that the ground states of odd-even nuclei prefer the lower j-values, when they are available. The pairing effect accounts for the fact that there is no known odd-even nuclear ground state of $J>9/2$ despite the fact that the 50–82 and 82–126 shells contain $h_{11/2}$ and $i_{13/2}$ subshells, respectively. These states are, however, found among the low-lying levels in the appropriate regions of the periodic table.

The close proximity (in energy) of levels with a large difference in j-values accounts for the "islands of isomerism" which occur in the regions of the periodic table just before the number of odd neutrons or protons reaches a magic number (128, 129), e.g., at the end of the 28–50 shell where the $p_{1/2}$ and $g_{9/2}$ levels are adjacent. The properties of these isomers now appear to be essentially understood (116). In the case of the even-even nuclei, the empirical evidence is that the first excited state is almost invariably a state of $J=2$, even parity.

The shell model has also contributed a great deal to the clarification and classification of β-decay transitions (130, 131, 132). For disintegrations involving odd-odd nuclei, however, further assumptions are required concerning the scheme of coupling of the odd nucleons (131); this question will be considered in a following section.

The usefulness of the independent particle model with strong spin-orbit coupling for the light nuclei is much more questionable. This problem has recently received considerable attention, especially in its application to the properties of the mirror nuclei (57, 133 to 137).

Nuclear Moments

Ever since the observation by Schmidt (138), that the measured magnetic dipole moments of the odd-proton or odd-neutron nuclei agree very well with the predictions of an extreme single particle model, there has been much speculation concerning both the reasons for the agreement and for

the deviations from the "Schmidt limits"[6] (139). Further accumulation of data (140, 141) has served not only to confirm the observation of Schmidt but also to clarify the nature of the deviations. Thus, all the moments of the odd-nucleon nuclei (with the exceptions of H^3 and He^3) fall between the Schmidt limits, along two curves which are roughly parallel to the Schmidt curves (140). If the state of the odd particle is assumed to be that indicated by the Schmidt curve to which it lies closest, the states so determined are in almost universal agreement with the expectations of the independent particle model with spin-orbit coupling. Taking this model seriously, then, the problem becomes one of explaining the deviations of the nuclear moments from the Schmidt curves.

One solution is not to take the independent particle model so seriously. Thus, following Davidson (142), one can assume that the nuclear ground state wave function is a mixture of the appropriate single particle wave function and a many-particle wave function corresponding to the same J, but with L differing by one unit.[7] The magnetic moment of such a state will lie between the appropriate Schmidt limit and the opposite Margenau-Wigner limit (139); it may be made to agree with the measured value by the appropriate choice of the percentage admixture of many-particle state. This scheme, as well as some other suggestions (143, 144), appears to offer a useful means for predicting some of the unmeasured nuclear moments.

In the following sections we consider two suggestions which have recently been developed to account for the deviations of the nuclear moments from the predictions of the strict independent particle model. Both of these have the virtue (from our point of view) that they start from the shell model and offer simple physical mechanisms (which are more or less calculable) for its modification.

The asymmetric core hypothesis.—A survey of nuclear electric quadrupole moments shows two striking features: First, there is a strong correlation, both in sign and in magnitude, between nuclear quadrupole moments and nuclear shell structure (145, 146). Second, many quadrupole moments are very much (order of magnitude) larger than could be accounted for by a single nucleon. (Odd-neutron nuclei also possess electric quadrupole moments.)

[6] The Schmidt limits are the moments of a single neutron or proton with spin $s = 1/2$, orbital quantum number l, and total angular momentum quantum number j. They are: (*a*) for a proton

$$\mu = \mu_p + j - 1/2, \text{ for } j = l + 1/2$$
$$\mu = (j + 3/2 - \mu_p)j/(j + 1), \text{ for } j = l - 1/2$$

(*b*) for a neutron

$$\mu = \mu_n, \text{ for } j = l + 1/2$$
$$\mu = -\mu_n j/(j + 1), \text{ for } j = l - 1/2.$$

It is assumed in the above that the g-factors for orbital motion are 1 and 0 for the proton and neutron, respectively. The moments of the free proton and neutron are:

$$\mu_p = +2.793$$
$$\mu_n = -1.913 \text{ nuclear magnetons.}$$

[7] Parity can still be a good quantum number, since the parity of a many-particle wave function need not be that corresponding to the L-value.

These facts suggest that another mechanism, in addition to the independent particle, must come into play in such a way as to cause the nuclear core to participate in the asymmetrical charge distribution which leads to an electric quadrupole moment.

Such a mechanism has been suggested by Rainwater (147) and explored by a number of investigators (148 to 153). Essentially, the mechanism is the polarization of the nuclear core by the asymmetrically distributed odd particle, an effect which appears to be energetically preferred (to a spherical core). The existence of asymmetric core nuclei had been considered for some time, not only in connection with the large quadrupole moments, but also to account for certain anomalies in the spectroscopic isotope shifts (154, 155). Kopfermann (156) has recently summarized the arguments in its favor. One of his most convincing arguments is derived from a consideration of the moments of isotopic pairs which differ by two neutrons and which have the same spin (e.g., $Cl^{35,37}$, $Cu^{63,65}$, $Ga^{69,71}$, $Br^{79,81}$, $Eu^{151,153}$). If a linear relationship is assumed to hold between the magnetic dipole and electric quadrupole moments of each pair, then extrapolation to zero quadrupole moment (i.e., no core asymmetry) yields, within the experimental uncertainties, a value of the magnetic moment which is identical with the Schmidt limit predicted by the shell model.

Bohr (151) has explored the consequences of such an asymmetric core model for the nuclear spins and magnetic moments. He has considered the motion of a nucleon in an approximately fixed field produced by an asymmetric core with rotational and vibrational degrees of freedom, leaning heavily on the analogy with the structure of symmetric top molecules. Under reasonable assumptions as to the coupling between the nucleon and the core (at least for a single nucleon outside of or a single hole in a closed shell) the model predicts $J=j$ for the nuclear spin. The moment depends on the coupling assumed. In general Bohr obtains better agreement with observed moments than is obtained with the Schmidt curves.[8]

Quenching of the nucleon moments in nuclear matter.—An entirely different explanation of the deviations from the Schmidt limits has been suggested by Bloch (157), by De-Shalit (158), and by Miyazawa (159). According to their approach the magnetic moments of nuclear ground states can be computed according to the strict independent particle shell model with, however, the modification that the anomalous magnetic moments of nucleons are partially quenched in nuclear matter. Thus, the magnetic moments are given by the Schmidt limits with

$$1 < \mu_p < \mu_p^f$$
$$0 > \mu_n > \mu_n^f$$

where μ_p^f and μ_n^f are the moments of the free nucleons.[6]

[8] The model of Bohr provides, in a certain sense, a specific method for supplying an admixture of many-particle state to the nuclear ground state wave function, a procedure which was attempted by Davidson (142) in a much more general fashion. The consequences for the nuclear moments and asymmetries are, however, very different in these two models.

In the language of meson theory, the anomalous magnetic moments of the nucleons arise from the virtual emission and readsorption of mesons. On the basis of such a model, Miyazawa (159) pointed out that the anomalous moments should, at least partially, be quenched in nuclear matter since the Pauli principle forbids the emission of mesons which give rise to recoiling nucleons whose momenta correspond to states already filled by other nucleons. The computation of this effect is, however, subject to the uncertainties inherent in current meson theories (which cannot even successfully predict the values of the anomalous magnetic moments of free nucleons); hence, the result of Miyazawa's calculations, which predict a very appreciable quenching of the anomalous moments, should not be taken as more than a qualitative indication of the effect.

Villars & Weisskopf (160) have adopted a phenomenological approach to this problem, in which they derive the properties of the fundamental nucleon-nucleon interaction from low-energy data. Their computation of the quenching effect is closely connected with computations of the "exchange magnetic moments" in nuclei (161 to 166). They find a very small quenching effect, which is not nearly enough to account for the deviations from the Schmidt limits.[9]

It appears reasonable that a quenching effect should exist although it may be much smaller than required to account for the observed moments. However, it is clear that this conclusion does not eliminate the asymmetric core model from consideration; the electric quadrupole moments and other effects still require explanation. Rather, it seems at the present writing that a combination of the two models may account for all of the anomalies observed in the behavior of the nuclear moments.

The hyperfine structure anomaly.—From the preceding discussion, we may conclude that it is possible, by the introduction of physically reasonable modifications of the independent particle model, to account for the deviations of nuclear magnetic moments from the Schmidt limits. In order to distinguish between the various models on the basis of magnetic effects, it is necessary to observe some other phenomenon which depends on the details of the model. Such a phenomenon is the hyperfine structure anomaly which, as pointed out by Kopfermann (167) and by Bitter (168), depends on the spacial distribution of the nuclear magnetic dipole in the nucleus. The theory of the hyperfine structure anomaly has been developed by Bohr & Weisskopf (169) and elaborated by Bohr (152). Its application to the available data is discussed by Eisinger, Bederson & Feld (170).

The hyperfine structure anomaly arises from the fact that the atomic hyperfine structure splitting $\Delta\nu$ deviates, in general, from the value it would have if the nucleus were a point magnetic dipole, i.e., $\Delta\nu=\Delta\nu_{pt}(1+\epsilon)$. Since $\Delta\nu_{pt}$ depends on the electron wave functions, it is in general not possible to determine ϵ by a measurement of $\Delta\nu$ on a single isotope. However, $\Delta\nu_{pt}\propto(2J$

[9] It should be noted that effects of the type which lead to quenching may also alter the orbital g-factors; i.e., change that of the proton from the value 1, and give the neutron an orbital g-factor. However, these effects are expected to be considerably smaller than the quenching of the spin moments.

$+1)g$, where J is the nuclear spin and $g \equiv \mu/J$. Hence, for two isotopes of the same element (and assuming the same electron wave functions for both isotopes)

$$\frac{\Delta\nu_1}{\Delta\nu_2} = \frac{(2J_1+1)}{(2J_2+1)} \frac{g_1}{g_2}(1+\Delta). \qquad 4.$$

$\Delta \cong \epsilon_1 - \epsilon_2$, which can be obtained from independent measurements of the ratio of the $\Delta\nu$'s and of the g's, is the hyperfine structure anomaly.

The difference in the ϵ's between two isotopes arises from differences in the spin and orbital contributions to the magnetic moments. The values of the ϵ's can be computed for the various models (152, 169, 170). The predictions are compared with the experimental values in Table III (from 170). In addition, a small anomaly for $Li^{6,7}$ ($\sim$0.01 per cent) is probably due to electronic and nuclear structure effects in these light nuclei, and an anomaly for the $Tl^{203,205}$ isotopes (0.01 to 0.02 per cent) can be explained on the basis of a change in the nuclear radii (173, 174).

TABLE III

COMPARISON BETWEEN OBSERVED AND COMPUTED VALUES OF THE HYPERFINE STRUCTURE ANOMALY

Nuclei	Δ (percent)				References
	Experiment	Model 1	Model 2	Model 3	
K^{39}-K^{40}	0.466 ±0.019	0.52	0.54	0.43	(170)
K^{41}-K^{39}	0.266 ±0.010	0.36	0.36	0.23	(152, 170, 171)
Rb^{86}-Rb^{87}	0.3501 ±0.0006	0.33	0.34	0.26	(152, 170, 172)

Model 1. Quenched moment with $\Delta\mu_l = 0$; $\Delta\mu_s'$ from the experimental moments.
Model 2. Model of Feenberg and Davidson (142).
Model 3. Asymmetric core model of Bohr (152).

On the basis of Table III it is impossible to choose between the various models. The asymmetric core model is definitely better for the K-isotopes and worse for the Rb-isotopes. It is somewhat surprising that models 1 and 2 agree so well in their predictions, although this may be fortuitous for these nuclei. The general conclusion has been drawn, however (170),

that the available data on the hfs anomalies give strong support to nuclear models which are, in their essential features, based on the independent particle model with spin-orbit coupling.

Some comments on the odd-odd nuclei.—The coupling of two or more nucleons in the same shell has been discussed in a previous section, where rules have been given for the order of the low-lying nuclear levels in a *jj*-coupling scheme. These rules seem to be fairly well substantiated, at least for nuclei

TABLE IV

SPINS AND MAGNETIC MOMENTS OF ODD-ODD NUCLEI

Nucleus	Z	N	J	μ	Proton State	Neutron State	J (Nordheim)	J (Kurath)	μ (Calc.)	References
H^2	1	1	1	0.8574	$(1s_{1/2})^1$	$(1s_{1/2})^1$	1	0 or 1	0.88	(141)
Li^6	3	3	1	0.8219	$(1p_{3/2})^1$	$(1p_{3/2})^1$	>0	0 or 3	0.63	(141, 177)
B^{10}	5	5	3	1.800	$(1p_{3/2})^{-1}$	$(1p_{3/2})^{-1}$	>0	0 or 3	1.88	(141, 177)
N^{14}	7	7	1	0.4037	$(1p_{1/2})^1$	$(1p_{1/2})^1$	1	0 or 1	0.37	(141, 177)
Na^{22}	11	11	3	1.746	$(1d_{5/2})^3D_{3/2}$ $(1d_{5/2})^3d_{5/2}$	$(1d_{5/2})^3D_{3/2}$ $(1d_{5/2})^3d_{5/2}$	>0 >0	— 0 or 5	1.73 1.73	(141, 177)
Na^{24}	11	13	4	(−)1.7	$(1d_{5/2})^3D_{3/2}$ $(1d_{5/2})^3d_{5/2}$	$(1d_{5/2})^{-1}$ $(1d_{5/2})^{-1}$	— >0	— 4	0.96 2.30	(2, 178)
Cl^{36}	17	19	2		$(1d_{3/2})^1$	$(1d_{3/2})^{-1}$	>0	2	0.85	(141)
K^{40}	19	21	4	−1.298	$(1d_{3/2})^{-1}$	$(1f_{7/2})^1$	2	4	−1.68	(170, 177)
K^{42}	19	23	2	−1.14	$(1d_{3/2})^{-1}$ $(1d_{3/2})^{-1}$	$(1f_{7/2})^3f_{7/2}$ $(1f_{7/2})^3F_{5/2}$	2 —	4 —	−1.72 −0.99	(178)
Rb^{86}	37	49	2	−1.69	$(1f_{5/2})^{-1}$	$(1g_{9/2})^{-1}$	2	2 or 7	−2.13	(3, 178)
Cs^{134}	55	79	4	2.95	$1g_{7/2}$	$(2d_{3/2})^{-1}$	>2	(4)	2.18	(178)
Lu^{176}	71	105	≤ 7	3.8	$1g_{7/2}$	$1h_{9/2}$	>1	—	—	(131, 141)

with $A > 50$ (126, 127, 175). The problem of the coupling of odd-neutrons and odd-protons is, however, still under investigation.

Nordheim (131), on the basis of empirical evidence mainly from β-decay schemes, suggests the following rules:

(1) The individual configurations of neutrons and protons in odd-odd nuclei are the same as in odd-A nuclei with the same number of nucleons in the odd particle group.

(2) If the odd neutron and proton groups belong to different Schmidt groups, then their resultant spins will subtract.

(3) If the odd neutron and proton groups belong to the same Schmidt group, their spins will couple to a larger than minimum resultant.

Kurath (176), on the basis of a spin-independent δ-function interaction between the odd nucleons, has obtained these rules for $1p$, $1d$, and $1f$ nucleons: (a) for $(j_1)^1(j_2)^1 n-p$, $J=|j_1-j_2|$; (b) for $(j_1)^1(j_2)^{-1}n-p$, $J=j_1+j_2-1$. For a finite range interaction, $J=j_1+j_2$ for rule (a) becomes more likely, while rule (b) probably remains unchanged.

The available data on the spins and magnetic moments (in nuclear magnetons) of the odd-odd nuclei are collected in Table IV. Also shown are the neutron and proton configurations expected on the basis of shell theory (columns 6 and 7), the predictions of Nordheim (column 8) and Kurath (column 9) for the nuclear spin, and the expected magnetic moment (column 10), computed on the basis of a strict independent particle model with jj-coupling and assuming the measured spin and the proton and neutron states given in columns 6 and 7. It should be noted that, resulting from quenching, modifications of the nucleon moments have a tendency to cancel for the odd proton and neutron, especially if they are in similar states (177), so that deviations from the predictions should be somewhat smaller than for nuclei with odd-A.

On the whole, the agreement on the moments is not too unsatisfactory, except for the possible case of Na^{24}. (It is interesting to note, parenthetically, that the assumption of a $d_{3/2}$ proton state and $d_{5/2}$ neutron state, in contradiction with our shell model, yields $\mu=-1.79$ for Na^{24}.) As far as the spins are concerned, however, it would be premature to assert that we have a successful recipe for jj-coupling in the odd-odd nuclei.

LITERATURE CITED

1. Tomkins, F. S., Fred, M., and Meggers, W. F., *Phys. Rev.*, **84**, 168 (1951)
2. Smith, K. F., *Nature*, **167**, 942 (1951)
3. Bellamy, E. H., *Nature*, **168**, 556 (1951)
4. Walchli, H., Livingston, R., and Hebert, G., *Phys. Rev.*, **82**, 97 (1951)
5. Johnson, C. M., Gordy, W., and Livingston, R., *Phys. Rev.*, **83**, 1249 (1951)
6. Ramsey, N., *Ann. Rev. Nuclear Sci.*, **1**, 97 (1952)
7. Jeffries, C. D., *Phys. Rev.*, **81**, 1040 (1951)
8. Gardner, J. H., *Phys. Rev.*, **83**, 996 (1951)
9. Ramsey, N. F., and Silsbee, H. B., *Phys. Rev.*, **84**, 506 (1951)
10. Kolsky, H. G., Phipps, T. E., Jr., Ramsey, N. F., and Silsbee, H. B., *Phys. Rev.*, **81**, 1061 (1951)

11. Smoller, B., Yasaitis, E., and Anderson, H. L., *Phys. Rev.*, **81,** 896 (1951)
12. Logan, R. A., and Kusch, P., *Phys. Rev.*, **81,** 280 (1951)
13. Jaccarino, V., and King, J. G., *Phys. Rev.*, **83,** 471 (1951)
14. Geschwind, S., Gunther-Mohr, R., and Townes, C. H., *Phys. Rev.*, **81,** 288 (1951)
15. Livingston, R., *Phys. Rev.*, **82,** 289 (1951)
16. Loomis, C. C., and Strandberg, M. W. P., *Phys. Rev.*, **81,** 798 (1951)
17. Proctor, W. G., and Yu, F. C., *Phys. Rev.*, **81,** 20 (1951)
18. Sheriff, R. E., and Williams, D., *Phys. Rev.*, **82,** 651 (1951)
19. Dharmatti, S. S., and Weaver, H. E., Jr., *Phys. Rev.*, **84,** 843 (1951)
20. Weisskopf, V. F., *Revs. Modern Phys.*, **21,** 305 (1949)
21. Kroll, N. M., and Pollock, F., *Phys. Rev.*, **84,** 594 (1951)
22. Karplus, R., Klein, A., and Schwinger, J., *Phys. Rev.*, **84,** 597 (1951)
23. Low, F. E., and Salpeter, E. E., *Phys. Rev.*, **83,** 478 (1951)
24. Adams, E. N., 3rd, *Phys. Rev.*, **81,** 1 (1951)
25. Davis, L., Jr., Feld, B. T., Zabel, C., and Zacharias, J. R., *Phys. Rev.*, **76,** 1076 (1949)
26. Sternheimer, R., *Phys. Rev.*, **84,** 244 (1951); **86,** 316 (1952)
27. Koster, G. F., *Phys. Rev.*, **86,** 148 (1952)
28. Ramsey, N. F., *Phys. Rev.*, **83,** 540 (1951); **86,** 243 (1952)
29. Nierenberg, W. A., *Phys. Rev.*, **82,** 932 (1951)
30. Gutowsky, H. S., *Phys. Rev.*, **84,** 589 (1951)
31. Dickinson, W. C., *Phys. Rev.*, **81,** 717 (1951)
32. Gutowsky, H. S., and McCall, D. W., *Phys. Rev.*, **82,** 748 (1951)
33. Gutowsky, H. S., *Phys. Rev.*, **83,** 1073 (1951)
34. Petch, H. E., Smellie, D. W., and Volkoff, G. M., *Phys. Rev.*, **84,** 602 (1951)
35. Mayer, M. G., *Phys. Rev.*, **74,** 235 (1948); **75,** 1969 (1949); **78,** 16, 22 (1950)
36. Haxel, O., Jensen, J. H. D., and Suess, H. E., *Phys. Rev.*, **75,** 1766 (1949); *Z. Physik*, **128,** 301 (1950)
37. Hornyak, W. F., Lauritsen, T., Morrison, P., and Fowler, W. A., *Revs. Modern Phys.*, **22,** 291 (1950)
38. Alberger, D. E., and Hafner, E. M., *Revs. Modern Phys.*, **22,** 373 (1950)
39. Mitchell, A. C. G., *Revs. Modern Phys.*, **22,** 36 (1950)
40. Deutsch, M., *Repts. Progress Phys.*, **14,** 196 (1951)
41. Simon, F. E., *Le Magnetisme* (Presented at Conférence à Strasbourg, France, (1939)
42. Gorter, C. J., *Physica*, **14,** 504 (1948)
43. Rose, M. E., *Phys. Rev.*, **75,** 213 (1949)
44. Pound, R. V., *Phys. Rev.*, **76,** 1410 (1949); **79,** 685 (1950)
45. Bleaney, B., *Proc. Phys. Soc.* (*London*), [A]**64,** 315 (1951); *Phil. Mag.*, **42,** 441 (1951)
46. Simon, A., Rose, M. E., and Jauch, J. M., *Phys. Rev.*, **84,** 1155 (1951)
47. Spiers, J. A., *Nature*, **161,** 807 (1948); *Phys. Rev.*, **78,** 75 (1950)
48. Blin-Stoyle, R. J., and Spiers, J. A., *Phys. Rev.*, **82,** 969 (1951)
49. Tolhoek, H. A., and deGroot, S. R., *Physica*, **17,** 81 (1951)
50. Steenberg, N. R., *Phys. Rev.*, **84,** 1051 (1951)
51. Daniels, J. M., Grace, M. A., and Robinson, F. N. H., *Nature*, **168,** 780 (1951)
52. Bleany, B., Daniels, J. M., Grace, M. A., Halban, H., Kurti, N., and Robinson, F. N. H., *Phys. Rev.*, **85,** 688 (1952)
53. Gorter, C. J., Poppema, O. J., Steenland, M. J., and Beun, J. A., *Physica*, **17,** 1050 (1951)

54. Gorter, C. J., Talhoek, H. A., Poppema, O. J., Steenland, M. J., and Beun, J. A., *Physica*, **18**, 135 (1952)
55. Deutsch, M., and Scharff-Goldhaber, G., *Phys. Rev.*, **83**, 1059 (1951)
56. Bethe, H. A., and Bacher, R. F., *Revs. Modern Phys.*, **8**, 82 (1936)
57. Brown, A. B., Snyder, C. W., Fowler, W. A., and Lauritsen, C. C., *Phys. Rev.*, **82**, 159 (1951)
58. Hauser, W., *Phys. Rev.*, **87**, 366 (1952); see also Feld, B. T., Feshbach, H., Goldberger, M. L., Goldstein, W., and Weisskopf, V. F., *U. S. Atomic Energy Commission Document, NYO-636* (1951)
59. Blatt, J. M., and Biedenharn, L. C., *Phys. Rev.*, **82**, 123 (1951)
60. Baldinger, E., Huber, P., and Proctor, W. G., *Phys. Rev.*, **84**, 1058 (1951)
61. Butler, S. T., *Phys. Rev.*, **80**, 1095 (1950); *Proc. Roy. Soc.* (London), [A]**208**, 559 (1951)
62. Burrows, H. B., Gibson, W. M., and Rotblat, J., *Phys. Rev.*, **80**, 1095 (1950)
63. Holt, J. R., and Young, C. T., *Proc. Phys. Soc.* (*London*), **63**, 833 (1950)
64. Sun, K. H., Harris, D., Pacjak, F. A., Jennings, B., Allen, A. J., and Nachaj, J. F., *Phys. Rev.*, **82**, 266 (1951)
65. Falk, C. E., *Phys. Rev.*, **83**, 499 (1951)
66. Schecter, L., *Phys. Rev.*, **83**, 695 (1951)
67. Butler, S. T., and Symonds, J. L., *Phys. Rev.*, **83**, 858 (1951)
68. Hamilton, D. R., *Phys. Rev.*, **58**, 122 (1940)
69. Goertzel, G., *Phys. Rev.*, **70**, 897 (1946)
70. Berestetski, V. B., *J. Phys.* (*U.S.S.R.*), **18**, 1057 (1948)
71. Ling, D. S., Jr., and Falkoff, D. L., *Phys. Rev.*, **76**, 1639 (1949)
72. Devons, S., *Proc. Phys. Soc.* (*London*), **62**, 580 (1949)
73. Gardner, J. W., *Proc. Phys. Soc.* (*London*), **62**, 763 (1949)
74. Falkoff, D. L., and Uhlenbeck, G. E., *Phys. Rev.*, **79**, 323, 334 (1950)
75. Lloyd, S. P., *Phys. Rev.*, **81**, 161 (1951)
76. Falkoff, D. L., *Phys. Rev.*, **82**, 98 (1951)
77. Racah, G., *Phys. Rev.*, **84**, 910 (1951)
78. Moon, P. B., *Artificial Radioactivity*, 97 (Cambridge University Press, Cambridge, England, 99 pp., 1949)
79. Lippmann, B. A., *Phys. Rev.*, **81**, 162 (1951)
80. Talhoek, H. A., and de Groot, S. R., *Phys. Rev.*, **83**, 189 (1951)
81. Yang, C. N., *Phys. Rev.*, **74**, 764 (1948)
82. Brady, E. L., and Deutsch, M., *Phys. Rev.*, **78**, 558 (1950)
83. Lloyd, S. P., *Phys. Rev.*, **82**, 277 (1951)
84. Frauenfelder, H., *Phys. Rev.*, **82**, 549 (1951)
85. Aeppli, H., Bishop, A. S., Frauenfelder, H., Walter, M., and Zünti, W., *Phys. Rev.*, **82**, 550 (1951)
86. Sunyar, A. W., Alberger, D., Friedlander, G., Goldhaber, M., and Scharff-Goldhaber, G., *Phys. Rev.*, **79**, 181 (1950)
87. Alder, K., *Phys. Rev.*, **84**, 369 (1951); **83**, 1266 (1951)
88. Aeppli, H., Albers-Schönberg, H., Bishop, A. S., Frauenfelder, H., and Heer, E., *Phys. Rev.*, **84**, 370 (1951)
89. Falkoff, D. L., *Phys. Rev.*, **73**, 518 (1948)
90. Hamilton, D. R., *Phys. Rev.*, **74**, 782 (1948)
91. Metzger, F., and Deutsch, M., *Phys. Rev.*, **78**, 537 (1950)
92. Feld, B. T., *Phys. Rev.*, **75**, 1618 (1949)

93. Devons, S., and Lindsey, G. R., *Nature*, **164**, 539 (1949)
94. Rose, B., and Wilson, A. R. W., *Phys. Rev.*, **78**, 68 (1950)
95. Arnold, W. R., *Phys. Rev.*, **79**, 170 (1950)
96. Kulchitzki, L. A., Latychev, G. A., and Buliginski, D. G., *Doklady Acad. Nauk. S.S.S.R.*, **64**, 57 (1949)
97. Beling, J. K., Feld, B. T., and Halpern, I., *Phys. Rev.*, **84**, 155 (1951)
98. Stevenson, D. T., and Deutsch, M., *Phys. Rev.*, **84**, 1071 (1951)
99. Hamilton, D. R., *Phys. Rev.*, **71**, 456 (1947)
100. Greuling, E., and Meeks, M. L., *Phys. Rev.*, **82**, 531 (1951)
101. Sherwin, C. W., *Phys. Rev.*, **73**, 216, 1173 (1948); **75**, 1799 (1949)
102. Allen, J. S., Paneth, H. R., and Morrish, A. H., *Phys. Rev.*, **75**, 570 (1949)
103. Madansky, L., Lipps, F., Bolgiano, P., and Berlin, T. H., *Phys. Rev.*, **84**, 596 (1951)
104. Konopinski, E. J., *Revs. Modern Phys.*, **15**, 209 (1943)
105. Fermi, E., *Z. Physik*, **88**, 161 (1934)
106. Feenberg, E., and Trigg, G., *Revs. Modern Phys.*, **22**, 399 (1950)
107. Gamow, G., and Teller, E., *Phys. Rev.*, **49**, 895 (1936)
108. Feingold, A. M., *Revs. Modern Phys.*, **23**, 10 (1951)
109. Kurie, F. N. D., Richardson, J. R., and Paxton, H. C., *Phys. Rev.*, **49**, 368 (1936)
110. Flammersfeld, A., *Z. Physik*, **112**, 727 (1939)
111. Neary, G. J., *Proc. Roy. Soc.* (*London*), [A]**175**, 71 (1940)
112. Langer, L. M., and Price, H. C., Jr., *Phys. Rev.*, **75**, 1109 (1949)
113. Wu, C.-S., *Revs. Modern Phys.*, **22**, 386 (1950)
114. Dancoff, S. M., and Morrison, P., *Phys. Rev.*, **55**, 122 (1939)
115. Axel, P., and Dancoff, S. M., *Phys. Rev.*, **76**, 892 (1949)
116. Goldhaber, M., and Sunyar, A. W., *Phys. Rev.*, **83**, 906 (1951)
117. Weisskopf, V. F., *Phys. Rev.*, **83**, 1073 (1951)
118. Hebb, M. H., and Nelson, E., *Phys. Rev.*, **58**, 486 (1940)
119. Tralli, N., and Lowen, I. S., *Phys. Rev.*, **76**, 1541 (1949)
120. Elsasser, W., *J. phys. radium*, **4**, 549 (1933); **5**, 389, 625 (1934)
121. Dancoff, S. M., *Phys. Rev.*, **58**, 326 (1940)
122. Malenka, B. J., *Phys. Rev.*, **86**, 68 (1952)
123. Weisskopf, V. F., *Science*, **113**, 101 (1951)
124. Keilson, J., *Phys. Rev.*, **82**, 759 (1951)
125. Barschall, H. H., *Phys. Rev.*, **86**, 431 (1952)
126. Kurath, D., *Phys. Rev.*, **80**, 98 (1950)
127. Talmi, I., *Phys. Rev.*, **82**, 101 (1951)
128. Feenberg, E., and Hammack, K. C., *Phys. Rev.*, **75**, 1877 (1949)
129. Nordheim, L. W., *Phys. Rev.*, **75**, 1894 (1949)
130. Mayer, M. G., Moszkowski, S. A., and Nordheim, L. W., *Revs. Modern Phys.*, **23**, 315 (1951)
131. Nordheim, L. W., *Revs. Modern Phys.*, **23**, 322 (1951)
132. Taketani, M., Nakamura, S., Umezawa, M., Ono, K., and Yamaguchi, Y., *Phys. Rev.*, **82**, 441 (1951)
133. Adair, R. K., *Phys. Rev.*, **82**, 750 (1951)
134. Hummel, H. H., and Inglis, D. R., *Phys. Rev.*, **81**, 910 (1951)
135. Inglis, D. R., *Phys. Rev.*, **82**, 181 (1951)
136. Mottelson, B. R., *Phys. Rev.*, **82**, 287 (1951)
137. Koester, L. J., Jackson, H. L., and Adair, R. K., *Phys. Rev.*, **83**, 1250 (1951)

138. Schmidt, T., *Z. Physik*, **106**, 358 (1937)
139. Margenau, H., and Wigner, E. P., *Phys. Rev.*, **58**, 103 (1940)
140. Goldsmith, H. H., and Inglis, D. R., *The Properties of Atomic Nuclei*, I (Information and Publications Division, Brookhaven National Laboratory, Upton, New York, 5 pp., 1948)
141. Mack, J. E., *Revs. Modern Phys.*, **22**, 64 (1950)
142. Davidson, J. P., *Phys. Rev.*, **85**, 432 (1952)
143. Schawlow, A. L., and Townes, C. H., *Phys. Rev.*, **82**, 268 (1951)
144. Mizushima, M., and Umezawa, M., *Phys. Rev.*, **83**, 463 (1951)
145. Gordy, W., *Phys. Rev.*, **76**, 139 (1949)
146. Townes, C. H., Foley, H. M., and Low, W., *Phys. Rev.*, **76**, 1415 (1949)
147. Rainwater, J., *Phys. Rev.*, **79**, 432 (1950)
148. Foldy, L. L., and Milford, F. J., *Phys. Rev.*, **80**, 751 (1950)
149. Feenberg, E., and Hammack, K. C., *Phys. Rev.*, **81**, 285 (1951)
150. Gallone, S., and Salvetti, C., *Phys. Rev.*, **82**, 551 (1951); **84**, 1064 (1951)
151. Bohr, A., *Phys. Rev.*, **81**, 134 (1951)
152. Bohr, A., *Phys. Rev.*, **81**, 331 (1951)
153. Bohr, A., *Kgl. Danske Videnskab. Selskab. Mat.-fys. Medd.*, **26**, 14 (1952)
154. Brix, P., and Kopfermann, H., *Z. Physik*, **126**, 344 (1949)
155. Breit, G., Arfken, G. B., and Clendenin, W. W., *Phys. Rev.*, **78**, 390 (1950)
156. Kopfermann, H., *Naturwissenschaften*, **38**, 29 (1951)
157. Bloch, F., *Phys. Rev.*, **83**, 839 (1951)
158. De-Shalit, A., *Helv. Phys. Acta*, **24**, 296 (1951)
159. Miyazawa, H., *Prog. Theoret. Phys.* (Japan), **6**, 263 (1951)
160. Villars, F., and Weisskopf, V. F. (Personal communication)
161. Sachs, R. G., *Phys. Rev.*, **74**, 433 (1948); **75**, 1605 (1949)
162. Osborn, R. K., and Foldy, L. L., *Phys. Rev.*, **79**, 795 (1950)
163. Spruch, L., *Phys. Rev.*, **80**, 372 (1950)
164. Austern, N., and Sachs, R. G., *Phys. Rev.*, **81**, 710 (1951)
165. Kynch, G. J., *Phys. Rev.*, **81**, 1060 (1951)
166. Sachs, R. G., and Ross, M., *Phys. Rev.*, **84**, 379 (1951)
167. Kopfermann, H., *Kernmomente*, 17 (Akademische Verlagsgesellschaft, M.B.H., Leipzig, Germany, 270 pp., 1940)
168. Bitter, F., *Phys. Rev.*, **76**, 150 (1949)
169. Bohr, A., and Weisskopf, V. F., *Phys. Rev.*, **77**, 94 (1950)
170. Eisinger, J. T., Bederson, B., and Feld, B. T., *Phys. Rev.*, **86**, 73 (1952)
171. Ochs, S. A., Logan, R. A., and Kusch, P., *Phys. Rev.*, **78**, 184 (1950)
172. Ochs, S. A., and Kusch, P., *Phys. Rev.*, **85**, 145 (1952)
173. Berman, A. (Personal communication)
174. Crawford, M. F., and Schawlow, A. L., *Phys. Rev.*, **76**, 1310 (1949)
175. Flowers, B. H., *Phys. Rev.*, **86**, 254 (1952); *Proc. Roy. Soc.* (*London*), [A]**212**, 248 (1952)
176. Kurath, D., *Phys. Rev.*, **87**, 218a (1952)
177. Talmi, I., *Phys. Rev.*, **83**, 1248 (1951)
178. Smith, K. F., and Bellamy, E. H. (Personal communication)

THE EXPERIMENTAL CLARIFICATION OF THE THEORY OF β-DECAY[1]

By E. J. Konopinski and L. M. Langer

Physics Department, Indiana University, Bloomington, Indiana

INTRODUCTION

Fermi advanced his successful theory of β-decay in 1934. It has since then undergone development in which two general directions may be discerned. One has been a broadening of the scope of the theory, the other a narrowing of its initial ambiguities.

The Fermi type of interaction was invented expressly for nucleonic β-processes but now promises to apply to all known processes involving the direct interaction of four fermions (spin 1/2 particles). The known fermions are: the electron ($e^{\pm}$), the neutrino (ν), and antineutrino ($\bar{\nu}$), the nucleon (N or P) and the μ-meson or muon ($\mu^{\pm}$). The direct interactions among these for which evidence exists are listed in Table I. This review is primarily concerned with the β-processes only. The relation of the others to β-decay is briefly summarized in the section on the *Universal Fermi interaction.*

TABLE I

The Fermi-Type Processes

β-emission	$\begin{cases} N \rightarrow P + e^- + \bar{\nu} \\ P \rightarrow N + e^+ + \nu \end{cases}$
Orbital capture:	$P + e^+ \rightarrow N + \nu$
μ-decay:	$\mu^+ \rightarrow e^+ + 2\nu$
μ-capture:	$P + \mu^- \rightarrow N + \nu$

The other direction of development has been toward a progressive experimental clarification. Fermi provided criteria for a β-coupling which are not quite sufficient to give it a unique form. An arbitrary linear combination of five interaction forms (symbolized by S, V, T, A, and P) is consistent with the a priori provisions of the Fermi theory. The experimental effort has been to reduce this arbitrariness. As we shall interpret the evidence here, the correct law must be what is known as an STP combination. This remains for the present a phenomenological result. No principle has been suggested so far (cf. THE A PRIORI THEORETICAL BASIS) which escapes contradiction by the experiments as interpreted here.

The nature of the neutrino.—Another ambiguity besides its unspecific form has been inherent in the Fermi theory. This has to do with the character of the neutrino. The evidence that it is massless, at least within $\sim$1 kev (1), needs no review here. [Moffat & Langer (1) set an upper limit of 250 v. for

[1] The survey of the literature pertaining to this review was concluded in April, 1952.

the neutrino mass by a direct magnetic spectrometer measurement of the spectrum.] However, there still remains the question as to whether the antineutrino ($\bar{\nu}$) is distinguishable from the neutrino (ν), or whether $\bar{\nu} \equiv \nu$. The β-theory can be almost equivalently formulated for either case. The distinguishable antineutrino may be conceived as a "hole" in the sense used for positrons. This follows if Dirac's conventional equation of the electron is applied to neutrinos, after putting $e=m=0$. If, instead, the neutrino is described by a modified equation due to Majorana, no antiparticle exists and the same type of neutrino is emitted in both negatron and positron decay.

The most direct way to decide the point is to see whether nucleons make discriminations in capturing neutrinos. Unfortunately, the extreme rarity of the capture, in any case, has so far put it beyond practical observability. Furry (2) pointed out a somewhat more feasible method: measuring the half-life of double β-decay. There exist nuclei which become more stable structures if two of their neutrons are replaced by protons. If two Dirac antineutrinos must be emitted in such a transformation, a half life $\gtrsim 10^{20}$ years is expected (3, 4) for a kinetic energy release of $\sim$2 Mev. The transformation is much speeded up if a Majorana neutrino is emitted by one neutron and captured by the other, so that no neutrinos result and only two negatrons are ejected. The expected half life is then of the order 10^{12} years (4).

Several experiments have been performed (5 to 8) in which the double β-decay should probably have been detected if the Majorana neutrino were the existing one. These failed to prove existence of the double β-decay and Winter (8) set a lower limit of $\sim 10^{18}$ years on the half life. A positive result[2] was reported by Inghram & Reynolds (9): $\sim 10^{21}$ years. This depended on identifying Xe^{130}, in minerals containing Te^{130}, as the product of double β-decay. The 10^{21}-year half life is quite compatible with the emission of two Dirac antineutrinos, as was shown by Primakoff (4) when he introduced the latest values for the constants involved. The evidence seems to be definitely in favor of the Dirac distinguishable antineutrino picture as the correct one.

The chief remaining ambiguity which besets applications of Fermi's theory is not intrinsic to it but is a consequence of the incomplete knowledge concerning nuclear structure. A large number of inconsistencies, once considered difficulties for the β-theory, have since been traced to erroneous presumptions about the nuclear states from which the β-energy is drawn. The decay of nuclei of $A=4n+2$ nucleons is the outstanding example (cf. THE FAVORED TRANSITIONS).

The recent development of the shell model for nuclear states has helped enormously in the interpretation of the various cases of β-decay. The latter have in turn aided considerably in settling various difficulties with the shell model. Detailed exposition of this work is omitted since it is primarily con-

[2] An earlier report by Fireman (10) of the double β-decay of Sn^{124}, with a half life $\sim 10^{16}$ years, has failed to be confirmed by check experiments (6). It was this work that inspired the later activity in this field.

cerned with the problem of nuclear structure rather than with the theory of β-decay. However, frequent references to results from the shell model will be necessary.

The detailed formalism of the Fermi theory has been reviewed too often to warrant undue repetition here (11 to 14). Only enough will be presented to make the reading of the following self-contained for the particular points under discussion. The section on THE A PRIORI THEORETICAL BASIS introduces the forms S, V, T, A, and P which the Fermi theory can be given, together with a review of the principles which have been offered as guides to a particular combination.

The section, SELECTION RULES FOR β-TRANSITIONS, recapitulates the first consequences which serve to make distinctions between the various forms. These are the selection rules for the spin and parity changes in a transition: principally the so-called Fermi selection rules and the Gamow-Teller selection rules. Then the section, ALLOWED β-DECAY, presents formulas which can be compared directly with the experimental data.

The experiments may be ordered according to the degree of detail at which one aims.

(*a*) The least differentiated information is perhaps given by the half-life measurements. These become significant when coupled with the determination of the nature of the particles involved and the total energy release. An important function is to help distinguish the "forbidden transitions" of every degree. They are roughly those transitions with a decay rate distinctly slower than the maximum characteristic of a given energy release.

(*b*) More detail is involved when a given initial nucleus has several alternative modes of disintegration. Frequently this is due to the availability of several final nuclear states. Generally, one is interested only in distinguishing among the transitions so that each can be treated as an individual one.

The alternative disintegrations of a nucleus by positron emission and orbital electron capture can be quite important. Unfortunately, there frequently exists uncertainty as to whether capture without positron emission, leading to excited states, is not superposed in any given case. Of course, corresponding γ-rays should be observed but there is frequent doubt about their identification. The chance for such complications is great because orbital capture requires less energy by $2mc^2$ than does positron emission and consequently more energy is left for possible excitations. This situation is aggravated if the positron emission is forbidden.

(*c*) Measurements of the distribution-in-energy, i.e., the spectrum, of the electrons in β-emission differentiates the transitions further. The spectra are chiefly governed by the gross statistical sharing of energy between electron and neutrino, but deviations from the statistical form, particularly in forbidden transitions, are an important source of information.

(*d*) In rare cases, it has been possible to examine β-processes in even greater detail: by measurements on the nuclear recoils. The correlation be-

tween the recoil direction and the momentum vector of the electron can be particularly informative. Unfortunately, such experiments are extremely difficult and the results so far are amenable to too wide a range of interpretations. One of the greatest difficulties is the preparation of sources which will not seriously perturb the recoil direction before it is observed. So far, one can definitely say that such experiments have proved that a neutrino must provide part of the recoil which is observed (15).

It is chiefly the data on the half lives (*a*) and the spectra (*c*) which will be relied upon here to clarify the various theoretical ambiguities. The results of these clarifications are summarized at the end of this paper.

THE A PRIORI THEORETICAL BASIS

The basic Fermi assumptions.—Let Ψ, Φ, ψ, ϕ be the wave functions (field amplitudes) of the four fermions participating in a Fermi type of interaction. Then, Fermi's simple assumption for the interaction energy density may be represented schematically as

$$H = G(\Psi^*\Phi\psi^*\phi). \qquad 1.$$

The "Fermi constant" G measures the strength of the interaction. It is, in principle, to be evaluated from just one case of a transition induced by H whose rate is measured with sufficient precision. The expression 1 emphasizes the chief assumption: the quadri-linear dependence on the four field amplitudes involved, all to be evaluated at the same point of space. The Ψ^*, ψ^* are field amplitudes for the created particles whereas Φ, ϕ represent the absorbed particles. All the interactions (see Table I) can be regarded as the absorption of two particles and the creation of two others. The emission of an antiparticle is here viewed as the absorption of a particle from the filled negative energy states of the vacuum. It must be emphasized that equation 1 is a purely schematic expression with subsidiary formal detail omitted for the sake of simplicity.

In the example of negatron emission by a neutron, ψ^* and ϕ may describe the electron and the antineutrino. Then Φ and Ψ^* describe the neutron and proton states of the nucleon, respectively. If this nucleon is part of a nucleus which makes the energy available by a transition from a nuclear state U_i to a state U_f then Φ and Ψ are factors in the formation of these states. The consequent transition matrix element is, schematically:

$$\langle f|\, H|\, i\rangle = G\int (U_f^* U_i)(\psi^*\phi). \qquad 2.$$

The integration covers the configuration space of the nuclear states. The rate of transitions will be proportional to $|\langle f|H|i\rangle|^2$, as will be seen in equation 7.

The schematic expressions introduced are an adequate basis for the discussion of the ambiguities left by Fermi's essential assumptions, and already mentioned in the INTRODUCTION. They arise from the circumstance that the field amplitudes ψ, ϕ, Ψ, Φ are not mere numbers at a point in space-

time. The corresponding field quanta have spin 1/2 and so "internal" degrees of freedom remain to be described. This is done by attributing four components to each field amplitude. The values of such components (e.g., $\psi_1, \psi_2, \psi_3, \psi_4$) will depend on the space-time co-ordinate system used, in a way characteristic of the Dirac spinor (or half-vector). Such a product as $\psi_i^*\phi_j$ which might be inserted into equation 1 or 2 becomes, in a new co-ordinate system, where the components are ψ_i', ϕ_j', a bilinear combination like

$$\Sigma C_{kl}\psi_k'^*\phi_l' \equiv (\psi')^*C\phi'. \qquad 3.$$

The latter is merely the equivalent matrix notation, with C having as elements whatever constants C_{kl} are appropriate to the co-ordinate transformation. It is obvious that with four independent components to choose from for each factor, there are 16 independent ways in which $\psi_i^*\phi_j$, or bilinear combinations like equation 3, can be formed. Thus, Fermi's recipe is far from specific.

The arbitrariness is partially reduced when one requires that the interaction be independent of the space-time co-ordinates used (i.e., H is to be an ordinary scalar). An exhaustive enumeration of the possibilities for equation 1 to fulfill this requirement can be obtained as follows. One classifies them according to the behavior under space-time transformations of the 16 independent bilinear combinations like equation 3. It does not matter which pair of fermions is considered for this purpose.

(S): One bilinear combination like equation 3 does not change in value when the components in different co-ordinate systems are inserted. This is the scalar combination symbolized by $\psi^*\beta\phi$, in matrix notation.

(V): Four more are related to each other exactly like the components of a four-vector. Its three space components are symbolized by the ordinary vector $\psi^*\alpha\phi$ and the "time" component is: $i\psi^*\phi$. We have here an analogon to the electromagnetic potential four-vector.

(T): Six further bilinear combinations form an antisymmetric tensor, analogous in formal properties to the electromagnetic field tensor. The three components analogous to the magnetic field form the axial vector, $\psi^*\beta\sigma\phi$, proportional to the Dirac spin operator σ. Analogous to the electric field is the polar vector symbolized by $\psi^*\beta\alpha\phi$.

(A): Four of the remaining five independent combinations constitute a "pseudo" four-vector. That means that the "space" components form an axial vector, $\psi^*\sigma\phi$, again proportional to spin. The fourth component has the symbol $i\psi^*\gamma_5\phi$.

(P): The final independent combination is a pseudo-scalar, $\psi^*\beta\gamma_5\phi$, analogous to the scalar product of an axial vector with a velocity, say. Thus, the 16 initial possibilities fall into five groups within which the combinations are no longer independent, but related by space-time transformations.

To make the interaction energy density H the required scalar, the products $(\Psi^*\Phi)$ must be made appropriately complementary to the products $(\psi^*\phi)$ enumerated above. Appropriate scalars would then be:

$$H_S = G_S\rho_S = G_S(\Psi^*\beta\Phi)(\psi^*\beta\phi) \qquad 4S.$$

$$H_V = G_V\rho_V = G_V\{(\Psi^*\Phi)(\psi^*\phi) - (\Psi^*\alpha\Phi)\cdot(\psi^*\alpha\phi)\} \qquad 4V.$$

$$H_T = G_T\rho_T = G_T\{(\Psi^*\beta\sigma\Phi)\cdot(\psi^*\beta\sigma\phi) + (\Psi^*\beta\alpha\Phi)\cdot(\psi^*\beta\alpha\phi)\} \qquad 4T.$$

$$H_A = G_A\rho_A = G_A\{(\Psi^*\sigma\Phi)\cdot(\psi^*\sigma\phi) - (\Psi^*\gamma_5\Phi)(\psi^*\gamma_5\phi)\} \qquad 4A.$$

$$H_P = G_P\rho_P = G_P(\Psi^*\beta\gamma_5\Phi)(\psi^*\beta\gamma_5\phi) \qquad 4P.$$

The interaction densities ρ as defined by these equations will be convenient later. The sum of all these expressions, with arbitrary G's, is an equally good choice of scalar for the interaction energy density:

$$H = \sum_K G_K\rho_K \qquad 5.$$

with $K = S$, V, T, A, or P. This is the most general[3] form the Fermi interaction can be given. Any additional criterion which might be used for the interaction must yield a result expressible in the form 5 with special values for the G's.

The Critchfield-Wigner hypothesis.—Critchfield & Wigner (21) offered an additional criterion which leads to a unique form of the law expressible as

$$H_{CW} = G(\rho_S - \rho_A - \rho_P). \qquad 6.$$

This emerges when H is required to be antisymmetric in the interchange of any pair of the four fermions involved. It has the attractive feature that it puts all four fermions on the same footing. Perhaps, however, the requirement of indistinguishability during Fermi interaction of all four of the fermions is not quite compelling; it may be that new, as yet unknown variables will be needed for the complete description, and these might spoil symmetries among the variables considered so far. Nevertheless, it is obviously worthwhile to seek experimental evidence as to the validity of the Critchfield-Wigner principle. It will be seen that the present interpretation of the data contradicts it.

The Tolhoek-de Groot hypothesis.—Another possible criterion for reducing the arbitrariness of the Fermi interaction was suggested by Tolhoek & de Groot (22). They regard the electromagnetic effects of the nucleons on the electrons as irrelevant for the Fermi interaction proper and so require that, aside from electromagnetic effects, positron and negatron emissions

[3] Yang & Tiomno (16) and Gamba (17) showed that greater generality is conceivable. One can define different "types" of Dirac spinors, according to their behavior under inversion transformations. Such distinctions are comparable to the one between ordinary polar and axial vectors. The "type" of spinor by which each kind of fermion is described is unknown. With different choices of "type" available, the number of possible ways to express the Fermi interaction is doubled. It turns out, however, that the five newly added choices become physically identical with the five original ones if the neutrino mass is zero. The great interest of the new generalizations lies in the possibility they give of forbidding conceivable Fermi-type processes which are never observed, through suitable choices of "type" for each fermion. Further work along these lines (18, 19, 20) can be greatly simplified if the nonexistence of Majorana neutrinos (cf. INTRODUCTION) can be regarded as proved.

should be indistinguishable in physically equivalent situations (i.e., when the initial and final nuclear states for the two processes are interchanged). However, they find that the general interaction 5 leads to results which are then impermissibly different (at least in experiments which detect the polarization of the electron). This can be avoided in either of two ways:[4] (*a*) by putting $G_V = G_T = 0$, in which case the interaction density would be an arbitrary linear combination of ρ_S, ρ_A, ρ_P; (*b*) by putting $G_S = G_A = G_P = 0$, leaving an arbitrary linear combination of the polar vector and tensor interactions, ρ_V and ρ_T. One sees that the criterion applied here is not sufficiently restrictive to yield a unique form, but it does eliminate some possibilities. One also sees that the more restrictive Critchfield-Wigner principle is compatible with the Tolhoek-de Groot requirements since it offers a combination of ρ_S, ρ_A, ρ_P, although a unique one.

There is one consideration which disturbs the plausibility of the Tolhoek-de Groot argument and which is recognized by the authors themselves. The neutron and proton may well have differences of nonelectromagnetic origin, e.g., their mass difference; these may well make them less equivalent in Fermi interactions than is presumed and certainly less so than are the light particles and their antiparticles. It will be seen that like the Critchfield-Wigner principle, the Tolhoek-de Groot hypothesis is contradicted by the evidence.

Universal Fermi interaction.—One might expect a priori conditions on the β-coupling to follow upon accepting the hypothesis of a universal Fermi interaction for all fermions, such as mentioned in the INTRODUCTION. The fulfillment of this expectation is not quite straightforward.

The idea of a universal Fermi interaction seems to have originated with Klein's pointing out that the measured rate of the processes listed in Table I are all consistent with the same interaction strength (G) for each (25). Recent evaluations (19) put the G to be associated with μ-decay within 3 per cent of the value for β-decay. The μ-capture rate is known only roughly but again has an interaction strength which is not inconsistent with the others in view of the uncertainties. These coincidences are remarkable, particularly because of the heretofore unique position of the β-interaction strength among physical orders of magnitude :$G \approx 10^{-49}$ erg/cm.[3] (see THE FAVORED TRANSITIONS). The hypothesis that all the processes of Table I obey the same law of interaction follows quite naturally.

An immediate implication of the hypothesis is that Fermi-type transformations should occur among whatever four fermions one chooses, subject

[4] The results given here follow when all the G's are taken to be real. Trigg & Feenberg (23) pointed out that they might be complex. However, Tolhoek & de Groot (22) show that the constants must be taken real to retain the invariance to "charge-conjugacy" which characterizes Dirac's theory of the electron. Biedenharn & Rose (24) support that conclusion on somewhat different grounds. These consist of a demand for invariance under time reversal when the time reversal transformation of a spinor is defined in a less arbitrary manner than is usual.

only to conservation laws. An example is $P \rightarrow e^- + 2e^+$, which, however, is never observed, like many others which are now implied. It becomes necessary to call upon new kinds of conservation laws, i.e., invariance under new kinds of transformations. Hence, the importance of the new distinctions of "type" among fermions mentioned in footnote 3.

Now, the identification of the β-interaction with the meson interactions fails to impose conditions on it which can be regarded as a priori. There are choices to be made for the muon interaction forms just as there are for the β-decay. One has at best the addition of a wider field of data, now including muon phenomena, from which to draw phenomenological conclusions. Moreover, questions arise about the transcription of the law in applying it to phenomena involving different particles. One cannot be sure which particles play the equivalent roles when comparing the different processes. Actually, this problem is much ameliorated (19) by the fact that a given form is merely a linear combination of the forms obtained with a different correspondence of the particles, as is clear from the discussion above.

Since the study of μ-decay at present yields only partial, phenomenological conclusions about the interaction law, it seems wisest to restrict oneself to β-phenomena in coming to conclusions about the β-coupling. There is then a minimum of presumption. It will be seen in the following sections that the β-decay data can be sufficient for the phenomenological derivation of the unique law.

SELECTION RULES FOR β-TRANSITIONS

The consequences of the Fermi interaction which can be directly compared with experimental data are obtained as rates of transition or decay constants:

$$d\lambda = (2\pi/\hbar)\left| <f| H| i> \right|^2 (dn/dW_0) \qquad 7.$$

processes/sec. from a given initial nucleus; $<f|H|i>$ is the transition matrix element schematized in equation 2; dn/dW_0 stands for the number of final states per unit range of the energy release, W_0. In the most detailed experiments, the final states are characterized by an electron momentum $\boldsymbol{p}$ with energy W, and a neutrino momentum $\boldsymbol{q}$ with energy $cq = W_0 - W$, so that:

$$\frac{dn}{dW_0} = \frac{d\boldsymbol{p}}{h^3} \cdot \frac{d\boldsymbol{q}}{h^3} \cdot \frac{1}{dW_0} = \frac{p^2 dp d\omega_e}{(2\pi\hbar)^3} \cdot \frac{q^2 d\omega_\nu}{(2\pi\hbar)^3 c} \qquad 8.$$

which is the famous "statistical factor" referred to in (*c*) in the INTRODUCTION. For orbital electron capture, the electron's state is discrete and the electron part of the statistical factor does not appear. The continuous states have obviously been presumed normalized to one per unit volume in equation 8.

For the (anti)neutrino state ϕ which enters $<f|H|i>$, one may put the plane wave

$$\phi = u_\nu e^{\mp i\mathbf{q}\cdot\mathbf{r}/\hbar} \qquad 9.$$

since it is practically unperturbed; u_ν is Dirac's four-component amplitude which depends on the spin in the state. The electron wave ψ will be distorted by the coulomb field of the nucleus but it may be Fourier-analyzed into plane waves as well. In consequence, the product represented as $(\psi^*\phi)$ in equation 2 will bring into $<f|H|i>$ terms proportional to

$$(\psi^*\phi) \sim e^{-i(\mathbf{p}+\mathbf{q})\cdot\mathbf{r}/\hbar}. \qquad 10.$$

This factor plays a role like that of the so-called retardation factor in electromagnetic radiation. In the latter situation, one expands the exponential into a power series in order to obtain the various multipole orders. This is justified here also if the source size or nuclear radius $R \ll \hbar/|\mathbf{p}+\mathbf{q}| = \lambda\!\!\!^{-}$. Corresponding to the multipole orders of radiation, we speak here of "allowed," "once-forbidden," "twice-forbidden," etc., β-transitions. The physical interpretation of each is that the electron-neutrino pair is emitted with successively larger numbers of quanta of orbital angular momentum. Because of the centrifugal force associated with orbital angular momenta, the corresponding electron-neutrino waves have smaller amplitudes at the nucleus and are excited with smaller intensity, in the higher orders, by the factor $(R/\lambda\!\!\!^{-})^2$. Such an analysis is well justified for β-decay since the wave lengths concerned are at least of the order $\lambda\!\!\!^{-}_0 = \hbar/mc \approx 3.9(10)^{-11}$ cm. $\gg R(<10^{-12}$ cm).

The preceding discussion shows that after the expansion into multipole orders of equation 9, equation 2 becomes:

$$<f|H|i> = G\left[\int (U_f^* U_i) \mp (i/\hbar)(\mathbf{p}+\mathbf{q})\cdot\int \mathbf{r}(U_f^* U_i) + \cdots\right]. \qquad 11.$$

This is a simplified, schematic version such as was indicated in equation 2. It is enough to show, however, that the matrix element $<f|H|i>$ can be expressed as a series of matrix elements of the type

$$\int U_f^* \Omega U_i \equiv \int \Omega \qquad 12.$$

with some operators Ω which are independent of the electron and neutrino variables. According to equation 11, an Ω will have as factors components of the position vector $\mathbf{r}$ in various powers. Further, one must remember that $(U_f^* U_i)$ in equation 11 was meant to stand for products of nucleon states such as are exhibited in the expressions for the interaction density, ρ, of equation 4. Thus, the operators $\mathbf{\sigma}$, $\boldsymbol{\alpha}$, or γ_5 may also appear as factors in Ω (the operator β can often be used in its nonrelativistic approximation, $\beta \approx -1$, for nucleons). A partial list of operators which arise in this way is given in Table II. The spatial covariance of the theory enables the expression of each Ω as an ordinary tensor of some order.

It is apparent that Table II does not order the nuclear matrix elements $\int\Omega$ into allowed and forbidden classes strictly according to the description given above, i.e., according to the power of r appearing in Ω. A generalization due

TABLE II*

SELECTION RULES

Order	Nuclear Matrix Element $\int\Omega$	Occurring for Interaction Type	Selection Rules on Nuclear Spin, I
Allowed (no parity change)	$\int 1$ (or $\int\beta$)	S, V	$\Delta I=0$
	$\int\boldsymbol{\sigma}$ (or $\int\beta\boldsymbol{\sigma}$)	T, A	$\Delta I=0, \pm1$ (not $0\to0$)
Once Forbidden (parity change)	$\int\gamma_5$ (or $\int\beta\gamma_5$)	P, A	$\Delta I=0$
	$\int\boldsymbol{r}$	S, V	$\Delta I=0, \pm1$ (not $0\to0$)
	$\int\boldsymbol{\alpha}$	V, T	
	$\int\boldsymbol{\sigma}\times\boldsymbol{r}$	T, A	
	$\int\boldsymbol{\sigma}\cdot\boldsymbol{r}$	T, A	$\Delta I=0$
	$S_{ij}=\int\sigma_i x_j+\sigma_j x_i-\frac{2}{3}\boldsymbol{\sigma}\cdot\boldsymbol{r}\delta_{ij}$	T, A	$\Delta I=0, \pm1, \pm2$ (not $0\to0$, $\frac{1}{2}\to\frac{1}{2}$, $0\leftrightarrow1$)
Twice Forbidden (no parity change)	$\int\gamma_5\boldsymbol{r}$	P, A	$\Delta I=0, \pm1$ (not $0\to0$)
	$R_{ij}=\int x_i x_j-\frac{1}{3}r^2\delta_{ij}$	S, V	$\Delta I=0, \pm1, \pm2$ (not $0\to0$, $\frac{1}{2}\to\frac{1}{2}$, $0\leftrightarrow1$)
	$A_{ij}=\int\alpha_i x_j+\alpha_j x_i-\frac{2}{3}\boldsymbol{\alpha}\cdot\boldsymbol{r}\delta_{ij}$	V, T	
	$T_{ij}=\int[\boldsymbol{\sigma}\times\boldsymbol{r}]_i x_j+[\boldsymbol{\sigma}\times\boldsymbol{r}]_j x_i$	T, A	
	$\int\boldsymbol{\alpha}\cdot\boldsymbol{r}$	V, T	$\Delta I=0$
	$\int\boldsymbol{\alpha}\times\boldsymbol{r}$	V, T	$\Delta I=0, \pm1$ (not $0\to0$)
	$S_{ijk}=\int\sigma_i x_j x_k-\cdots$	T, A	$\Delta I=0, \pm1, \pm2, \pm3$ (not $0\to0$, $\frac{1}{2}\to\frac{1}{2}$, $\frac{1}{2}\leftrightarrow\frac{3}{2}$, $1\to1$, $0\leftrightarrow1$, $0\leftrightarrow2$)

* Actually, the operator enters all the matrix elements arising from the S, T, and P interactions. It is ignored to permit contraction of the Table. It has no effect on selection rules, but may affect sizes which are treated as unknown here anyway.

to relativistic effects is necessary. A loosely analogous generalization for electromagnetic radiation is the inclusion of magnetic multipoles. Here, the extra relativistic corrections appear as the second terms in the interaction densities ρ_V, ρ_T and ρ_A only, equation 4. These terms are smaller than "allowed terms" because they are of order v/c where v is the nucleonic velocity. (The operator $-c\boldsymbol{\alpha}$ is itself the velocity operator in Dirac theory. It produces products $\Psi^*\boldsymbol{\alpha}\Phi$ in which "large" components of Ψ are always multiplied with "small" components of Φ, and vice versa. The operation γ_5 also mixes large and small components and is therefore of order v/c. On the other hand $\boldsymbol{\sigma}\hbar/2$ is the spin operator of Dirac theory and so $\sigma\approx1$.)

The conservation of angular momentum is formally insured by the orthogonality of any final state U_f which does not match in angular momentum the state ΩU_i which is generated from U_i by the β-coupling as represented by Ω. The Ω operation determines what angular momentum is taken by the electron-neutrino pair in processes calculated from $\int\Omega$. In the case $\Omega=1$, which occurs if the β-coupling includes S(calar) or V(ector) interactions, $\int U_f^* U_i$ vanishes unless the nuclear spins I of U_i and U_f are the same. Further U_f cannot be even if U_i is odd, and vice versa. The consequent selection rules which must be obeyed if $\int 1$ is to contribute are: $\Delta I=0$ with no parity change. For once-forbidden transitions, $\int \boldsymbol{r}$ may occur. The selection rules under which $\int U_f^* \boldsymbol{r} U_i$ will make a nonvanishing contribution are familiar from ordinary radiation theory in which $\int \boldsymbol{r}$ is just the electric dipolar displacement. They are: $\Delta I=0, \pm 1$ but not $I_i=0 \rightarrow I_f=0$ because $\boldsymbol{\Delta I}$ is a vector of unit magnitude. Moreover, $\boldsymbol{r}$ is an odd function so U_i and U_f must have opposite parity. Now, it is actually the formal ordinary vector character of $\boldsymbol{r}$ which is essential to the selection rules; the connection of total angular momentum conservation and invariance to spatial rotations is well known. Thus $\int \boldsymbol{\alpha}$ requires the same selection rules as $\int \boldsymbol{r}$. The vector $\boldsymbol{\sigma}$ differs formally from $\boldsymbol{r}$ in being an axial rather than polar four-vector, consequently, for $\int \boldsymbol{\sigma}$ not to vanish: $\Delta I=0, \pm 1$ but not $0 \rightarrow 0$ and the parity must not change. All the selection rules of Table II result from similar considerations. They make plain the full basis on which the ordering into allowed and forbidden transitions is properly made. It is to be noted that the selection rules on parity alternate in the successive degrees of forbiddenness.

Of the selection rules listed in Table II, those characteristic of the S and V interactions, in each order, are known as Fermi selection rules. The rules characteristic of the T and A interactions are called Gamow-Teller selection rules. It will be noted that the spin changes permitted by the Gamow-Teller rules, in each order, exceed by one unit those permitted by Fermi rules. This may be ascribed to the fact that the T and A types of interaction couple the electron-neutrino spin directly to the nucleonic spin, as the presence of the spin operator $\boldsymbol{\sigma}$ in ρ_T and ρ_A indicates.

ALLOWED β-DECAY

The Theoretical Results

From an empirical standpoint, allowed decays are exhibited by the nuclei with the shortest observed half lives t for a given energy release W_0 (after corrections for coulomb effects). Theoretically, one expects the shortest half lives to occur when the nuclear spin I changes by no more than one unit and the parity does not change at all.[5] The only nuclear matrix elements which contribute appreciably to allowed decay are then expected to be $\int 1$ and $\int \boldsymbol{\sigma}$, according to Table II. Their relative importance depends on the relative sizes of $G_{S,V}$ and $G_{T,A}$. (Read $G_{S,V}$ as G_S or G_V.)

[5] See THE FORBIDDEN TRANSITIONS for evidence that the shortest half lives which could be obtained from the P(seudo scalar) interaction, therefore requiring a parity change, are long as compared to those now assigned to the allowed class.

The decay constants, equation 7, which follow from the general β-coupling, equation 5, must be integrated over those variables which are not observed in a given type of experiment, to be comparable with the corresponding experimental data. Experiments in which the nuclear recoil is observed, class (*d*) in the INTRODUCTION, requires the least such integration but, as previously indicated, we shall here confine ourselves to the experiments on spectra (*c*) and the lifetimes (*a*). To obtain the spectra, we count all the β-emissions $d\lambda(W)$ in which the electron emerges with energy W in the range $dW = c^2 p dp/W$. Energy conservation limits the neutrino energy to the value $cq = W_0 - W$. Then

$$d\lambda(W) = (2\pi^3\hbar^7 c^3)^{-1} \cdot F(\pm Z, W) \cdot q^2 p dW \cdot \left\{ \left| \int 1 \right|^2 [G_S^2 + G_V^2 \mp (2\gamma/W) G_S G_V] + \left| \int \boldsymbol{\sigma} \right|^2 [G_T^2 + G_A^2 \mp (2\gamma/W) G_T G_A] \right\}. \tag{13.}$$

Here $|\int \boldsymbol{\sigma}|^2 \equiv |\int \sigma_x|^2 + |\int \sigma_y|^2 + |\int \sigma_z|^2$.

$F(\pm Z, W)$ is the "coulomb factor" (28, 29) which reduces to unity if the effect of the charge Ze of the final nucleus on the electron is neglected. As might be expected, $F(\pm Z, W) = |\psi_e(R)|^2$ simply, if $\psi_e(R)$ is the electron wave amplitude in a coulomb field, normalized to 1 at infinity and evaluated at the nuclear radius, R. $F(-Z, W)$ applies to negatron emission and gives greater relative weight to slow electrons in consequence of their retardation by the coulomb attraction. $F(+Z, W)$ applies to positrons and makes slow ones relatively fewer. $\mp\gamma = \mp mc^2(1-\alpha^2 Z^2)^{1/2}$ with $\alpha = e^2/\hbar c$ apply to positron and negatron emission respectively.

It is customary to compare equation 13 with experimental spectra by plotting $[N(W)/pWF]^{1/2}$ against W, where $N(W)$ is the number of electrons observed per unit energy range. Of course, $N(W) \sim d\lambda/dW$ is expected. If one neglects the terms $2\gamma/W$ in equation 13, then the theory predicts the proportionality:

$$[N(W)/pWF]^{1/2} \sim cq = W_0 - W. \tag{14.}$$

Thus the plot should yield a straight line coming down to an intercept at $W = W_0$. Such a diagram is variously referred to as either a "Kurie," "*KRP*," or "Fermi" plot.

The terms $\sim 2\gamma/W$ in equation 13 are known as "Fierz interference" terms (30). As one can see, they are expected to exist only if the β-coupling involves both the S and V forms or both T and A. Further, their existence would spoil the conclusion (equation 14) as to the linearity of the Kurie plot. Actually, as will be seen in the discussion of THE ALLOWED SPECTRA in this section, the best measurements yield plots which are very closely linear. One then concludes that $G_S G_V = G_T G_A = 0$, i.e., not both the S and V nor both the T and A interactions can form part of the β-coupling.[6] This is a result

[6] Further evidence is given by measurements of the K-capture to positron-emission

which would follow from either the Critchfield-Wigner or the Tolhoek-de Groot criteria discussed in the section on THE A PRIORI THEORETICAL BASIS. Of course, the Fierz interference is likewise eliminated if the β-coupling has a single one of any of the forms S, V, T, A, and P alone.

After elimination of the Fierz interference, the expression (equation 13) for the spectrum is greatly simplified. Putting $G_{T,A}=G$ and $K=G_{S,V}/G$ one has:

$$d\lambda/dW = (2\pi^3\hbar^7c^3)^{-1}\cdot q^2pWF\cdot G^2\left\{\left|\int \mathfrak{d}\right|^2+K^2\left|\int 1\right|^2\right\}. \qquad 15.$$

Now equation 14 is exactly valid.

The completely integrated decay constant, λ, is the inverse of the mean-life of the decay:

$$\lambda = \ln 2/t = (2\pi^3)^{-1}(mc^2/\hbar)\left[mc^2(\hbar/mc)^3\right]^{-2}$$
$$\cdot f(\pm Z, W_0)\cdot G^2\left\{\left|\int \mathfrak{d}\right|^2+K^2\left|\int 1\right|^2\right\}. \qquad 16.$$

Here, f is a dimensionless function (28, 31) resulting from the integration over the spectrum (equation 15):

$$f = (mc^2)^{-5}\int_{mc^2}^{W_0} F(\pm Z, W_0)(W_0 - W)^2(W^2 - m^2c^4)^{1/2}W\,dW. \qquad 17.$$

One sees from equation 16 that one should expect

$$ft = (\text{universal constants})/\left\{\left|\int 1\right|^2+K^2\left|\int \mathfrak{d}\right|^2\right\}. \qquad 18.$$

Now, a given nuclear matrix element, $\int 1$ or $\int\sigma_k$, should be expected to be of order unity for allowed transitions since the $U_{i,f}$ of equation 12 are normalized wave functions. Thus, the "ft-value" (equation 18), sometimes known as the "comparative half life," should be the same for all allowed transitions, aside from fluctuations in $\int 1$ and $\int \mathfrak{d}$, which are presumed moderate. The constancy of comparative half lives for a given type of transitions is a highly sensitive test. The factors f and t individually vary by factors as great as 10^9 for known allowed transitions. Thus a variation of even a factor 100 in ft can be regarded as constancy to one part in 10^7!

The Data on Half Lives

To distinguish which are actually allowed transitions among the many cases of β-emission, one may proceed in either of two ways. First, we present an empirical approach. Here, one picks out the shortest half lives after due allowances for the energy release and the coulomb effect peculiar to each case. This is done by examining the comparative half life, ft, as evaluated from equation 17 and the observed half life t (in seconds). After the shortest ft

ratio. The unambiguous measurements invariably give good agreement with the theory only if the Fierz interference is eliminated. For conditions under which ambiguity may arise see statement (*b*) in the INTRODUCTION.

values are isolated, one can check whether the allowed selection rules are indeed obeyed in each case.

Next will be considered all the cases in which the spin changes by no more than one unit and the parity not at all, according to current knowledge concerning the nuclear states. It will then be seen whether the corresponding *ft* values are as uniformly low as is expected for allowed transitions. This approach leads to the discovery of the "*l*-forbidden" transitions.

Perhaps the most helpful compilation of observed *ft* values was made recently by Mayer, Moszkowski & Nordheim (32). These authors use the data to support their assignments of nuclear parities and spins from the shell model. The most up-to-date and complete compilation of *ft* values is perhaps that of Feingold (33).

Normal allowed transitions.—The empirical approach first uncovers a group of light nuclei with $\log 1_0 ft = 2.7$ to 3.7 as the shortest-lived. This, however, is an exceptional, homogeneous group, known as the "favored" transitions, and will receive separate attention in the section, THE FAVORED TRANSITIONS.

The shortest lived nuclei spread out over the periodic table, the "normal" allowed transitions, have $\log ft = 4$ to 5.8. The spin and parity assignments are most reliably known for the cases of odd A. According to Mayer & Moszkowski, about 12 of the latter undergo no spin or parity change; about 25 have $\Delta I = \pm 1$ and no parity change. This seems to make a form which yields Gamow-Teller rules (T or A) indispensable, at least for part of the β-interaction. Such a conclusion is supported by the less certain evidence of the even-A cases. About 20 of these are predicted by Nordheim to have spin-changes of one unit and no parity change.

The cases of $\log ft = 4$ to 5.8 which do not obey allowed selection rules are very few and perhaps understandable. They are Hg^{205}, Pb^{209}, and RaE'' (Tl^{206}), to be discussed as once-forbidden transitions in the section on THE FORBIDDEN TRANSITIONS.

One should notice that, in general, no correlation is found between the comparative half life, *ft*, and the assignment of $\Delta I = 0$ or of $|\Delta I| = 1$, to the transitions. One might expect $\Delta I = 0$ transitions to be shorter-lived because they receive help from the fact that for these $\int 1$ in equation 17 does not vanish, whereas $\int 1 = 0$ when $|\Delta I| = 1$ (see Table II). However, the presence of $\int 1$ should only make a difference of perhaps a factor two to the half life. Such a contribution is easily lost in comparing nuclei with $\log ft$ ranging from 4 to 5.8.

l-Forbidden transitions.—Now we consider all the β-transitions which are quite definitely expected to obey the allowed selection rules, at least of the looser Gamow-Teller type. Above were presented about 57 cases with $\log ft = 4$ to 5.8 which is thus established as the range of lifetimes to be expected for allowed transitions. The fluctuations within this range must, in the present state of knowledge concerning nuclear structure, be accepted as "accidental." Even nuclear states of equal angular momentum and parity cannot

be expected to overlap on each other prefectly. Many variables are needed to describe a structure of A nucleons completely. One cannot expect complete coincidence among all of them in the two states involved just because the states as a whole have the same parity and total spin. Even one particle states may have unlike radial distributions together with coincident angular distributions.

There are, however, several cases in which the deviations of the ft-values from the norm are too great, and too systematically directed toward longevity, to be dismissed as accidental fluctuations. There are five odd-A nuclei, expected to obey the allowed selection rules, yet having $\log ft = 6$ to 7. Even more strikingly, also four such cases with even A have $\log ft = 7$ to 9. Among the latter are the famous examples of C^{14} and P^{32}.

The C^{14} decay has a particularly well-established spin change since the parent was measured to have zero spin while the daughter, N^{14}, was measured to have unit spin. To both parent and daughter are attributed even parity by the shell model and that model is particularly reliable for predictions of parity. The evidence from the C^{14} spectrum (see below) supports these assignments. The information on P^{32} and the other seven cases mentioned is not as complete, but there is little doubt that we deal here with nine cases of transitions obeying allowed selection rules yet having up to 1000 times the lifetimes expected.

The gross failure, in these cases, of the parent and product states to be matched to each other by the β-coupling, in spite of the transition's obeying the allowed selection rules, points to a near-orthogonality of these states. That would be adequately describable only in terms of an additional selection rule, involving an additional "good" quantum number. In atomic spectroscopy, such an additional quantum number is furnished by a separately conserved orbital angular momentum. It has always been difficult to conceive of undisturbed orbital motions in nuclei, but the success of the shell model appears to imply the approximate validity of just such a picture. One is then led to suppose that two nuclear states connected by a β-transition may have different orbital angular momenta even with equal total spins. The β-coupling cannot change the orbital angular momenta in the allowed approximation. The consequence is the existence of much slowed down transitions obeying allowed selection rules on total spin. Such transitions are called l-forbidden.

Nordheim was the first to point out that the evidence for the l-forbidden transitions exists. He showed that the shell model fairly straightforwardly predicts different orbitals ($\Delta l = 2$, since parity is conserved) for parent and product in the cases of odd A mentioned above. The comparable shell model predictions for even-A nuclei required the formulation of special rules governing the coupling of two nucleons in a given shell. The C^{14} decay is predicted to go from an S_0 state to a D_1 state. The P^{32} decay presumably goes from D to S_0. Four of the odd-A cases connect $f_{5/2}$ and $p_{3/2}$ states. All the others of the nine cases can be similarly understood.

The data also seem to show that the orbits are frequently perturbed enough so that substantial deviations from the orthogonality of normally different orbitals can occur. In several cases, literal acceptance of the shell model assignments leads one to expect l-forbiddenness, yet the half life is not protracted as in the nine cases above. This may be the situation in $O^{19}(d_{3/2}\rightarrow s_{1/2}$ yet $\log ft=5.5$ only), $Cu^{61}(p_{3/2}\rightarrow f_{5/2}$ and 5.9), $Cu^{64}(D_1\rightarrow S_0$ and 5, 5.4), $Ga^{68}(D_1\rightarrow S_0$ and 5.1). Thus, the selection rule on the orbital angular momentum has a decided effect in 9 of 14 cases in which its operation might be expected. Its variable decisiveness is also exhibited in the rather wide range of the "accidental fluctuations" ($\log ft=6$ to 9) in the nine cases for which it seemed necessary to invoke this additional rule.

The Allowed Spectra[7]

It is most cautious to examine separately the measured spectra of favored, l-forbidden, and normal allowed transitions. Actually, all these categories are expected to yield spectra of the same, "allowed," shape. There is only a small chance that deviations might become detectable in l-forbidden transitions with $\log ft\rightarrow 12$, the value characteristic of twice-forbidden transitions (cf. THE FORBIDDEN TRANSITIONS). In that extreme, some of the "twice-forbidden" nuclear matrix elements of Table II may have magnitudes comparable to those of the "allowed" matrix elements, $\int 1$ and $\int \vec{\sigma}$. The twice-forbidden contributions generally depend on the energy in a way different from that characteristic of allowed transitions (cf. THE FORBIDDEN TRANSITIONS).

As early as 1939, Lawson & Cork (34) obtained an impressive confirmation of the theory by showing that the spectrum of In^{114}, a normal allowed transition, yielded a straight line Fermi plot over a large part of the energy distribution.

Early work in general showed excesses of electrons at low energies. Tyler's measurements on Cu^{64} (35) showed that at least some of the distortions are to be attributed to scattering in the finite thickness of the source. Great improvements in decreasing the average thicknesses of sources at first showed a persistence of low energy distortions (36). This was finally proved to be due to unexpectedly large nonuniformities (37, 38, 39). The end-result was that Cu^{64} yields straight-line Fermi plots to very low energies; the thinner and more uniform the source, the lower the energy to which the linearity persists. This is true for both the negatron and positron emissions. For the lowest energy positrons, even the small screening effects due to the outer electrons of the atom may become detectable and must be corrected for (37, 40, 41), in calculating $F(Z, W)$.

S^{35} is a good example of a normal allowed spectrum which has been measured with extreme care. It again yields a straight line Fermi plot (42 to 45).

[7] For a review of the intricate history of spectrum measurements see the article by Wu (86).

The spectra of many other normal allowed transitions have been determined with varying degrees of definitiveness.[8] In no case is there now genuine experimental disagreement with the allowed shape, i.e., one yielding a straight line Fermi plot.

The spectra of several favored transitions have also been well measured. In accordance with expectations, all have the predicted allowed shapes. The decay of the neutron (46), H^3 (1), He^6 (47), and N^{13} (48, 49) are examples.

The findings for the l-forbidden transitions are again that they yield the allowed spectrum shape, as expected. Cu^{64}, mentioned above, may be l-forbidden (32). Early measurements on P^{32} yielded distorted spectra, since shown to be due to impurity (50). The best measurements yield straight line Fermi plots (51, 52).

The l-forbidden transition with the longest known comparative half life, C^{14} which has $\log ft = 9.0$, is also the only one which shows slight indications of departure from the allowed shape. Cook, Langer & Price (42) reported such deviations and their work has been confirmed by Warshaw (53). The experimenters concerned regard the deviations as being too small to be completely unquestionable. Since the C^{14} rate of decay is still 1000 times as great as for ordinary twice-forbidden transitions, any deviations are expected to be very small.

A conclusion one draws from the fact that the allowed spectra in general yield straight-line Fermi plots, is that there can be no Fierz interference, of the kind discussed in THE THEORETICAL RESULTS. The existence of the latter requires that a factor $(1+a/W)$ appear in the spectrum, with the constant, a, depending on the unknown interaction strengths G_K. This would lead to a systematic deviation from linearity of the Fermi plots for which there is no evidence. One would expect such a deviation to be most apparent in high energy spectra, e.g. B^{12}($W_0 = 13.9$ Mev) and He^6(3.55 Mev). Measurements (47, 49) in these cases are considerable achievements because of the correspondingly short half lives. The main B^{12} spectrum unfortunately has superposed on it a 6 Mev spectrum yielding an excited final state. Between 6 and 13.9 Mev, however, there is no sign of deviation from a linear Fermi plot, although the Fierz interference contribution should produce a variation of 25 per cent. In He^6, linearity is displayed over the more than 85 per cent of the spectrum which could be well measured. The Fierz interference, if present, should make the slope vary by a factor $\sim(1+1.5a)$ over the measured range. An actual variation greater than 5 per cent would be inconsistent with the measured points. Thus the limit $a \lesssim 0.04$ is provided for the Fierz interference that can be present. Since, moreover, the experimental variation of the slope is unsystematic, rather than regular, as the Fierz interference requires, one must at present assume $a = 0$, hence $G_S G_V = G_S G_T = 0$ (see THE THEORETICAL RESULTS).

[8] Many spectrum measurements have as objectives the determination of decay schemes rather than the checking of the theory of the spectrum shape.

THE FAVORED TRANSITIONS

The supermultiplet theory.—The favored or super-allowed transitions are those identified empirically in the section, ALLOWED β-DECAY, as having exceptionally short half lives: log $ft = 2.9$ to 3.7. There are 27 cases in this range, all listed in Table III. None has more than $A = 43$ nucleons. All but 6 have for parent and product the mirror or Wigner isobars, characterized by $N - Z = \pm 1$. ($N = A - Z$ is the number of neutrons.) The other six cases

TABLE III

THE FAVORED TRANSITIONS

Iosbars	States	$\lvert\int\mathfrak{G}\rvert^2$	$\log_{10} ft$	Ref.
	Mirrors			
$n^1 \rightarrow H^1$	$s_{1/2} \rightarrow s_{1/2}$	3	3.1	(46)
$H^3 \rightarrow He^3$	$s_{1/2} \rightarrow s_{1/2}$	3	3.05	(1)
$Be^7 \rightarrow Li^7$	$p_{3/2} \rightarrow p_{3/2}$	5/3	3.36	
$\rightarrow Li^{7*}$	$\rightarrow p_{1/2}$	4/3	3.56	(63)
$C^{11} \rightarrow B^{11}$	$p_{3/2} \rightarrow p_{3/2}$	5/3	3.62	
$N^{13} \rightarrow C^{13}$	$p_{1/2} \rightarrow p_{1/2}$	1/3	3.67	
$O^{15} \rightarrow N^{15}$	$p_{1/2} \rightarrow p_{1/2}$	1/3	3.57	
$F^{17} \rightarrow O^{17}$	$d_{5/2} \rightarrow d_{5/2}$	7/5	3.36	
$Ne^{19} \rightarrow F^{19}$	$s_{1/2} \rightarrow s_{1/2}$	3	3.29	
$Na^{21} \rightarrow Ne^{21}$	$D_{3/2} \rightarrow D_{3/2}$	3/5	3.58	
$Mg^{23} \rightarrow Na^{23}$	$D_{3/2} \rightarrow D_{3/2}$	3/5	3.67	(64)
$Al^{25} \rightarrow Mg^{25}$	$d_{5/2} \rightarrow d_{5/2}$	7/5	3.47	
$Si^{27} \rightarrow Al^{27}$	$d_{5/2} \rightarrow d_{5/2}$	7/5	3.57	(64)
$P^{29} \rightarrow Si^{29}$	$s_{1/2} \rightarrow s_{1/2}$	3	3.57	
or	$d_{3/2} \rightarrow d_{3/2}$	3/5		
$S^{31} \rightarrow P^{31}$	$s_{1/2} \rightarrow s_{1/2}$	3	3.63	(64)
$C^{33} \rightarrow S^{33}$	$d_{3/2} \rightarrow d_{3/2}$	3/5	3.54	(64)
$A^{35} \rightarrow Cl^{35}$	$d_{3/2} \rightarrow d_{3/2}$	3/5	3.51	
$K^{37} \rightarrow A^{37}$	$d_{3/2} \rightarrow d_{3/2}$	3/5	3.43	(64)
$Ca^{39} \rightarrow K^{39}$	$d_{3/2} \rightarrow d_{3/2}$	3/5	3.6	(64)
$Sc^{41} \rightarrow Ca^{41}$	$f_{7/2} \rightarrow f_{7/2}$	9/7	3.4	
$Ti^{43} \rightarrow Sc^{43}$	$f_{7/2} \rightarrow f_{7/2}$	9/7	3.4	
	Triads			
$He^6 \rightarrow Li^6$	$^1S_0 \rightarrow {}^3S_A$	6	2.92	(47)†
$C^{10} \rightarrow B^{10*}$	$^1S_0 \rightarrow {}^3S_1$	6	3.30	
$\rightarrow B^{10**}$	$\rightarrow {}^1S_0$	0	3.7	(61)
$O^{14} \rightarrow N^{14*}$	$^1S_0 \rightarrow {}^1S_0$	0	3.5	
$F^{18} \rightarrow O^{18}$	$^3S_1 \rightarrow {}^1S_0$	2	3.57	
$Al^{26} \rightarrow Mg^{2(*?)}$	$^3S_1 \rightarrow {}^1S_0 {}^1S_0(?)$	(2)	3.34	

† A late and important development has been the finding by Dewan *et al.* (101) that the old value (47) of He^6 end-point energy, and consequently the old *ft*-value ($10^{2.75}$ sec.), is too low. The new endpoint is 3.55 ± 0.03 Mev, with the *ft*-value as used here. See the section on *Quantitative results*.

are all members of isobaric triads, having two nucleons over a core of even $N=Z$.

The understanding of the favored transitions is primarily a problem in nuclear structure rather than β-theory. However, the simplest nuclear structures are involved here and one naturally depends on these for the most precise determinations of the interaction strengths (the G_K's of equation 5) fundamental to the β-theory.

The fact that the favored transitions have the shortest observed half lives implies that they are the only ones which give about full values to the nuclear matrix elements $\int 1$ and $\int \beta$ of equation 18. One must explain why this occurs so exceptionally and apparently only for mirror transitions and in the triads. Just this much can be roughly understood on the basis of rather simple considerations.

One first makes use of the well-known "charge-independence" of the specifically nuclear forces. In an approximation which neglects any other forces, neutrons and protons may be substituted for each other, as in β-transitions, without changing the nuclear state. This would give the perfect overlapping of initial and final states needed to give the matrix elements full value and thus make the transition favored. The question is then whether the lowest states of the isobars connected by the β-transition will actually assume identical configurations just because the symmetrical forces by themselves permit them to do so. As long as the substitution of protons and neutrons for each other is supposed to make negligible differences one does expect this, except for the limitations imposed by the Pauli principle. The latter permits only two neutrons and two protons at a given "position" in the configuration. One may then expect first the formation of a saturated, inert core out of a maximum even number of neutrons matched by an equal number of protons. If, then, outside this core, neither of the isobars connected by a β-transition has more than two like nucleons, then both isobars may have their extra nucleons at the same "position" without conflicting with the Pauli principle. Only then can one expect favored transitions to be possible, on the basis of the crude picture we are here led to adopt.

The only isobaric pairs having no more than two like nucleons extra to an even $N=Z$ core are obviously: the $A=4n+1$ mirrors, with just one extra nucleon; the $A=4n+3$ mirrors with three extra nucleons but only two alike; the $A=4n+2$ members of triads, having just two extra nucleons. These then should have the only favored transitions, if our crude picture is sufficiently correct.

As contrast, an even $N=Z$ nucleus ($A=4n$) must have as a partner in a β-process an isobar with three like nucleons. The B^{12} and N^{12} transitions are examples; both have $\log ft=4.2$ (which may not be considered enough larger than the favored values to be entirely satisfactory). The nuclei O^{19}, Ne^{23}, Na^{25}, Si^{31}, and S^{35} each have three neutrons outside the core; for them $\log ft=5.6$, 5.0, 4.8, 5.9, and 5.0, respectively, and thus fairly substantially unfavored. No favored transitions are found for $A>43$ presumably because mirrors and triads cease to occur as A increases. This is a well-known effect

of the accumulating coulomb repulsion between protons, which leaves only nuclei with $N>Z+1$ stable enough to be isobars in β-processes.

Wigner's beautiful theory of supermultiplets (54) constitutes a way of refining our crude considerations. He finds it unnecessary to limit the considerations to so special a picture; e.g., he has no need to refer to our vague "position" in the spatial configuration. He obtains our results simply from postulating the approximate charge-independence and also spin-independence of the nuclear forces. These are the sources of the degeneracy characteristic of a supermultiplet of states. A supermultiplet belongs to a structure of A nucleons and various substates of the supermultiplet may refer to different nuclei, characterized by different $N-Z$ values for the given $A=N+Z$. Wigner, as to be expected, finds that all nuclei differing just by $4n$ nucleons have the same system of supermultiplets. This corresponds to our use of a core.

Our analogue for at least the lowest supermultiplet of a system was the vague "position" in the nuclear configuration. Where we said it is possible for two isobars to have identical configurations, Wigner describes it as a belonging of both normal states to the same supermultiplet. Unfavored transitions are those connecting different supermultiplets. This is, in effect, a new selection rule, additional to the rules governing total spin and parity. Such a new rule might have been expected. With the symmetrical forces presumed in the supermultiplet theory, nuclear states may have new types of symmetries. These are in addition to the orientational symmetries accompanying the possession of definite angular momentum and parity. Hence, there are new ways for two states to be orthogonal to each other, a result usually embodied in a selection rule. Violation of the new rule does not entirely destroy a transition because the symmetry of the forces in neutrons and protons is perturbed at least by the electromagnetic differences between these particles.

The results which were presented above as consequences of our initially described crude picture have all been justified by the supermultiplet theory. The latter has thus given a satisfying account of the fact that all favored transitions are between mirrors or in triads; it satisfactorily excludes favored transitions for any other type of nuclei. However, the complete situation is not so simple. There also exist transitions in the triads which are actually forbidden; worse, there seems to be at least one case (P^{30}) which is allowed but unfavored.

The existence of forbidden transitions in the triads is not necessarily inconsistent with the supermultiplet theory. They can be accounted for when one considers the role of orbital angular momenta, which has been ignored so far. A state in a given supermultiplet might have a spatial dependence characterized by a definite total orbital momentum L, or even definite individual orbital momenta for each nucleon. In our initial crude picture, this would correspond to letting the vague term "position in the spatial configuration" mean a spatial distribution characteristic of a more or less definite

orbital momentum. Because we used the requirement that only two like nucleons can occupy such a "position," it would seem that we demand a more localized distribution for it than is characteristic of a definite orbital. However, the refined theory of Wigner shows that the results we quoted are consistent with definite orbital momenta since it derives them by merely requiring certain limitations on the spin states for any supermultiplet.

The lowest supermultiplet of a triad limits the spin states thus: the two extra nucleons must be antiparallel if they are alike, as in the end-members of each triad; the unlike nucleons of the middle isobar may be in any mixture of $S=0$ and $S=1$ spin states. For the spatial dependence one may take individual nucleon orbitals as suggested by the shell model. Whatever these are, one expects a $^1S_0$ resultant for the end-members of each triad since all such are even-even nuclei. On the other hand, the middle isobar may well have a resultant with a near-maximum total angular momentum (Nordheim's rule, which is empirical rather than characteristic of the shell model). Thus, for all but the lowest individual orbitals, transitions between the middle isobar and the $^1S_0$ end-members can be forbidden.

In Li^6, the two extra nucleons are presumably in $p_{3/2}$ orbits. They combine to a $I=1$ state, according to measurements. Since the transition from He^6 ($^1S_0$) is highly favored ($ft=10^{2.9}$ sec.), one must presume a resultant $^3S_1$ state for Li^6.

B^{10} also has its two extra nucleons in $p_{3/2}$ orbits according to the shell model. Here they yield the maximum resultant $I=3$, according to measurements. As is now to be expected, the $Be^{10}\rightarrow B^{10}$ transition is highly forbidden ($\log ft=13.7$). C^{10} undergoes two favored transitions instead because it finds two excited states of B^{10} energetically available. These excited states are very likely $^1S_0$ and $^3S_1$ substates of the supermultiplet to which the Be^{10} and C^{10} ground states also belong. A fuller discussion is given in the section on *Quantitative results*.

The two extra nucleons of N^{14} are assigned $p_{1/2}$ orbitals. $^3D_1$ is the maximum resultant and is consistent with the measurement of $I=1$. Hence, the "l-forbidden" transition from $C^{14}(^1S_0)$ already mentioned in THE DATA ON HALF LIVES. O^{14} undergoes a favored transition to an excited N^{14*}. Evidence discussed in the section on *Quantitative results* indicates a $^1S_0$ character for the N^{14*}.

Two $s_{1/2}$ orbitals are combined in F^{18}. Thus its favored transition is to be expected if the F^{18} resultant is taken to be $^3S_1$.

$I=3$ is measured for Na^{22}. (The shell model assigns $d_{5/2}$ orbitals to the last nucleons.) The forbidden lifetime ($\log ft=14.0$) is thus accounted for.

Al^{26} is expected to have a high spin for much the same reasons as Na^{22}. Its favored transition is usually explained as going to excited Mg^{26*}. There seems to be no wholly unquestionable data on this point.

P^{30} seems to present the one difficulty for the supermultiplet theory, which is not readily explainable. Its extra nucleons are assigned $s_{1/2}$ orbits. The result should be a favored $^3S_1\rightarrow{}^1S_0$ transition. Nevertheless, $\log ft=4.7$,

a lifetime about 10 times too long. (There is a possibility that the extra nucleons occupy $d_{3/2}$ orbits and then couple to a resultant yielding an "*l*-forbidden" transition.)

The Cl^{34} and K^{38} transitions to the respective S^{34} and A^{38} ground states should be forbidden for the same reasons as for Na^{22}. This is confirmed by the fact that both transitions go to excited final states instead.

The shell model.—The shell model gives the best account of the nuclear structures anywhere in the periodic table and thus deserves examination as to its power to explain the exceptional character of the favored transitions. It appears that such an explanation must be alternative to the supermultiplet theory. An important proviso for the shell model is that spin-orbit coupling is dominant and this is on the whole inconsistent with the older theory since the latter finds it essential to assume the nucleonic spins to be separately conserved in the majority of cases.

It is possible for the shell model to distinguish between two kinds of allowed transitions. Transitions which require the transforming nucleon to change its orbit or those which require two nucleons to change quantum numbers might be considered unfavored (55). Transitions requiring neither may be the favored ones. These criteria predict favored transitions for the triads and the mirrors quite readily. When $N \approx Z$, as in these cases, the orbitals assigned to the transforming nucleon are usually the same in its neutron and proton states. The shell model explanation runs into difficulties largely because it predicts, on the above criteria, many more favored transitions than are observed.

S^{35} has $\log ft = 5.2$ and is thus an unfavored transition. Yet the transforming nucleon should be $d_{3/2}$ in both parent and product and so a favored transition instead is expected by shell model criteria. Ne^{23} and Na^{25}, having $\log ft = 4.9$ and 5.0, respectively, keep the transforming nucleon in the $d_{5/2}$ orbital nevertheless.

Transitions in which only $f_{7/2}$ nucleons are involved occur for Ca^{45}, $Sc^{43,47,49}$, Ti^{45}, and V^{47}. Their respective $\log ft$ values are: 6.0, 4.8+, 5.6+, 5.5, 4.7+, and 4.7+. The half lives seem definitely unfavored, yet the shell model criteria would predict favored transitions. More examples of these kinds are available.

The failure of the shell model to distinguish the favored transitions sharply may indicate that it applies to light nuclei only insofar as it does not conflict with the supermultiplet theory. Shell effects may persist but may not always be decisive. Such a conclusion is perhaps not completely unacceptable since the effects of the shell model are most noticeable in heavier nuclei and perhaps large cores are essential for decisive results.

Quantitative results.—A final calculation of a total allowed decay constant requires the evaluation of the matrix elements $\int 1$ and $\int \vec{\sigma}$. The latter requires a knowledge of the nuclear states involved. The most detail that is currently known about practically any nuclear state is its predominant orbital char-

acter. If one takes a pair of orbitals to be, respectively, complete descriptions of the initial and final states, then the calculation of $\int 1$ and $\int \sigma$ is straightforward. In doing this, one presumes that all degrees of freedom left undescribed by the simple orbital are also left unaffected by the transition. This is the chief condition for the matrix elements to take on maximal values. Accordingly, the transitions are being treated as favored and the method applies only to such.

The orbitals assigned to the mirrors and triads are listed in Table III. Most of the product nucleus spins have been measured, as indicated by bold-faced type for the subscripts denoting total angular momentum. The corresponding orbital characters are those judged to be dominant on the basis of measured magnetic moments. This is just the procedure used to construct shell models. The latter enable interpolations for the cases in which no measurements exist.

The information is most nearly complete for the mirrors. As one sees in Table III, the initial and final states are assigned the same characters. This seems fairly obviously justified for the dominant characters, aside from the fact that it conforms to the shell model. The arguments for assigning a $p_{1/2}$ orbital to Li^{7*} (an excited state) have been most recently reviewed by Inglis (56).

The values of $\left|\int \sigma\right|^2$ calculated (54) with the above assumptions are also listed in Table III. If $I_{i,f}$ are the initial and final total nuclear spins, and $l = I \pm \frac{1}{2}$ is the orbital quantum number:

$$\left|\int \sigma\right|^2 = (I+1)/I \qquad \text{for} \quad I_f = I_i = +\tfrac{1}{2} \tag{19a.}$$

$$\left|\int \sigma\right|^2 = I/(I+1) \qquad \text{for} \quad I_f = I_i = l - \tfrac{1}{2} \tag{19b.}$$

$$\left|\int \sigma\right|^2 = (2I_f+1)/(I_f+1) \qquad \text{for} \quad I_f = I_i - 1 = -\tfrac{1}{2} \tag{19c.}$$

$$\left|\int \sigma\right|^2 = (2I_f+1)/I_f \qquad \text{for} \quad I_f = I_i + 1 = l + \tfrac{1}{2} \tag{19d.}$$

Of course, $\left|\int 1\right|^2 = 1$ for $\Delta I = 0$ and vanishes when $I_f \neq I_i$.

The assignments of resultant orbitals to members of triads are more ambiguous than for the mirrors. They were presented in the discussion of the *Supermultiplext theory*. All the even-even nuclei are assigned $^1S_0$ orbitals. As a result, one expects favored transitions only between S-states. Thus one needs only the following:

$$S_0 \rightarrow S_0 \qquad \left|\int \sigma\right|^2 = 0 \qquad \left|\int 1\right|^2 = 2 \tag{20a.}$$

$$S_0 \rightarrow S_1 \qquad \left|\int \sigma\right|^2 = 6 \qquad \left|\int 1\right|^2 = 0 \tag{20b.}$$

$$S_1 \rightarrow S \qquad \left|\int \sigma\right|^2 = 2 \qquad \left|\int 1\right|^2 = 0. \tag{20c.}$$

These are based on the same normalizations of the interaction forms as equations 19.

With the above results, absolute values for favored half-lives can be calculated from equation 16:

$$ft = 5.57(10)^{-20}G^{-2}\left[\left|\int \sigma\right|^2 + K^2\left|\int 1\right|^2\right]^{-1} \text{ sec.} \qquad 21.$$

if G is expressed in units of $mc^2(\hbar/mc)^3 = 4.73(10)^{-38}$ erg cm.^{3}. $G = G_{T,A}$ and $K = G_{S,V}/G_{T,A}$ must first be evaluated (from at least two accurately known decays).

Only neutron decay involves no nuclear structure and so has exact values for the nuclear matrix elements: $\left|\int \vec{\sigma}\right|^2 + K^2\left|\int 1\right|^2 = 3 + K^2$. Unfortunately, measuring its half life is extremely difficult. The greatest precision was achieved by Robson (46), whose measurements lead to $\log ft = 3.1 \pm 0.1$. This is consistent with H^3, which also has $\left|\int \vec{\sigma}\right|^2 + K^2\left|\int 1\right|^2 = 3 + K^2$ on the basis discussed above (1): $\log ft = 3.05 \pm 0.05$. Detailed consideration of the H^3 and He^3 states indicates that the above evaluation of the matrix elements is not as much in error as that estimated here for the comparative half life measurements. Thus, one concludes that

$$G^2(3 + K^2) = 5.57(10)^{-20}/(1120 \pm 130) = (5.0 \pm 0.6)10^{-23}. \qquad 22a.$$

The best separate evaluation of G and K requires considering a case in which the proportions of $\left|\int \vec{\sigma}\right|^2$ and $\left|\int 1\right|^2$ are substantially different than for the neutron and H^3. At the same time, the evaluations of the nuclear matrix elements are probably most trustworthy for very light nuclei. He^6 is perhaps the most nearly ideal case since its expected $^1S_0 \rightarrow {}^3S_1$ transition has $\left|\int 1\right|^2 = 0$. Moreover, it is found to have such a short comparative half life ($\log ft = 2.92 \pm 0.03$), that about the full value $\left|\int \vec{\sigma}\right|^2 = 6$ is needed to reconcile it with other cases. It yields:

$$6G^2 = 5.57(10)^{-20}/(830 \pm 50) = (6.7 \pm 0.4)10^{-23} \qquad 22b.$$

and with equation 22a:

$$K^2(H^3, He^6) = G_{S,V}^2/G^2 = 1.4(0.7 \text{ to } 2.4)$$
$$G(He^6) = (3.3 \pm 0.2)10^{-12} \equiv (1.6 \pm 0.05)10^{-49} \text{ erg cm.}^3.$$

It should be noted that the value of G is relative to the normalization used in equations 19 and 20. The comparison of n, H^3, and He^6 shows these decays to be consistent with about equal sizes of $G_{S,V}$ and $G_{T,A}$. A comparable amount of pseudoscalar interaction (P) is still admissible, since it has no effect in allowed transitions.

Moszkowski (58) has also used the Be^7 decays for an evaluation of K. The $p_{3/2} \rightarrow p_{3/2}$ transition between ground states releases a neutrino of energy 0.863 ± 0.003 Mev. The $p_{3/2} \rightarrow p_{1/2}$ transitions to the excited state release 0.383 ± 0.002 Mev, and represent (12 ± 1) per cent of all the transitions. Now K-capture in light nuclei is quite accurately proportional to the square

of the neutrino energy, so that the ratio of the intensities of the two transitions here is given by:

$$\frac{88 \pm 1}{12 \mp 1} = \frac{(K^2 + 5/3)}{4/3}\left(\frac{.863 \pm .003}{.383 \pm .002}\right)^2 \qquad 22c.$$

which yields

$$K^2(\mathrm{Be}^7) = 0.3 \pm 0.2.$$

K-capture is extremely sensitive ($\sim Z^3$) to screening effects but these cancel in the ratio employed here. The error quoted here may be considerably underestimated because the values of the matrix elements used can scarcely be exact. Trigg (59) has attempted to evaluate the error of using pure orbitals for the states from the deviation of the magnetic moment of Li^7. His work demonstrates that an additional uncertainty of $\sim$60 per cent in K^2 may well be expected. One cannot consider Be^7 to yield conclusive evidence for $K<1$.

More positive evidence that the S or V interactions must form a part of the β-coupling comes from the decays of C^{10} and O^{14}.

Sherr, Muether & White (60) showed that O^{14} decays to an excited state N^{14*} which has just the energy to be expected if the state differs from the C^{14} and O^{14} ground states in no other respect than its having one proton more or less, respectively. $N^{14*}-C^{14}+n-p$ and $C^{14}-N^{14*}+n-p$, where each symbol stands for the appropriate mass-energy, are respectively equal to the differences of the coulomb repulsion energy to be expected in each case. The margin of error is of the order of 5 per cent. Since C^{14} and O^{14} are assigned $^1S_0$ orbitals, one concludes that the N^{14*} state must also be treated as $^1S_0$. Thus $\left|\int \mathfrak{G}\right|^2=0$ for the transition, and the favored half life can only be accounted for by admitting the presence of S or V interactions in the β-coupling.

The measured half life and energy release for O^{14} yield $\log ft=3.5\pm0.2$. Using $G(\mathrm{He}^6)$, found above, one can estimate the value of $K^2=G_{S,V}^2/G^2$ which can account for the O^{14} lifetime:

$$K^2(\mathrm{O}^{14}) = 0.8\ (0.5 \text{ to } 1.3).$$

An even stronger case for the existence of favored $^1S_0\rightarrow{}^1S_0$ transitions is provided by $C^{10}\rightarrow B^{10**}$, discovered by Sherr & Gerhart (61). The same arguments which led to assigning a $^1S_0$ character to N^{14*} also works for B^{10**}. In addition, the chance that B^{10**} is a $^3S_1$ state instead is practically eliminated by the simultaneous existence of the higher energy $C^{10}\rightarrow B^{10*}$ transition. This one is also favored and consequently must be $^1S_0\rightarrow{}^3S_1$.

For $C^{10}\rightarrow B^{10**}$, $\log ft=3.7\pm0.25$. The value of K^2 derivable from this is:

$$K^2(\mathrm{C}^{10}) \approx 0.5(0.3 \text{ to } 1).$$

Like the $K(O^{14})$ figure, this is based on a comparison with He^6. That is probably more meaningful than even direct comparison with the second C^{10} transition. The $^3S_1$ state of the latter may easily have suffered more dilution due to the complexity of the $A=10$ structure than the $^1S_0$ state.

It is interesting to note that Li^6 has also been found (62) to have an

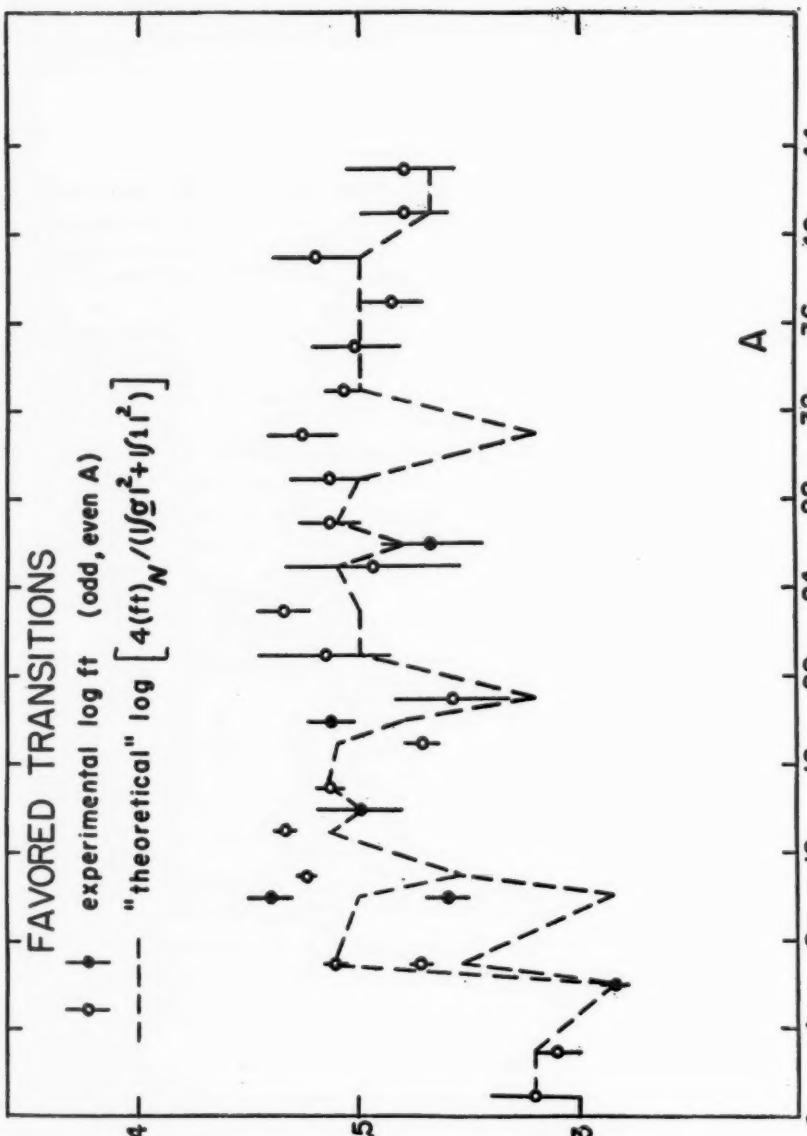

FIG. 1. Comparative half lives of the favored transitions Log_{10} *ft* versus *A*, the mass number.

excited state which is presumably $^1S_0$, on the same grounds as B^{10**} and N^{14*}. No conclusive evidence exists that He^6 decays to this Li^{6*} and indeed the β-energy would be so low that an easily observable competition with the ground state transition cannot be expected. The value of the discovery for β-theory lies in the fact that it provides an additional argument that the He^6 ground state must have $I=0$. The latter assumption has always been important in the evidence for the necessity of Gamow-Teller selection rules (and so for A or T interaction as part of the β-coupling).

Finally, we consider the consistency of the comparative half lives (equation 21) of all the favored transitions together. A rapid means of scanning the behavior as a whole is provided by Figure 1. The points are experimental log ft values, plotted against the mass number A. A "theoretical" histogram (dashed line) is also plotted for comparison. The "theoretical" values are those to be expected with $ft \sim [|\int \mathbf{\sigma}|^2 + |\int 1|^2]^{-1}$ normalized to the neutron or, equivalently, to He^6. Thus $K = G_{S,V}/G_{T,A} = 1$ is being presumed. This value of K produces about as good a general agreement as can be obtained, with the values of the matrix elements described above. $K=0$ yields a definitely poorer comparison, leading to much wider "theoretical" fluctuations (up to log $ft \approx 4$). The fact that some improvement here follows from assuming $K>0$ appears to have been first pointed out by Feenberg (55), and, independently, by Moszkowski (58).

Figure 1 demonstrates that there is some concurrence between the variations in the measured ft-values and the expectations based on the evaluations of the matrix elements presented above. For example, the comparatively low ft-values for the neutron, H^3, He^6, and Ne^{19} tend to agree with the expectations. The near-uniformity of most of the other values at log $ft \approx 3.5$ is also fairly well borne out. Perhaps the most glaring discrepancy is the high ft-value of S^{31} for what is presumed to be an $s_{1/2} \rightarrow s_{1/2}$ transition.

Attempts to obtain more detailed evaluations of the nuclear matrix elements have been made by Wigner (55) and by Trigg (59). Wigner considered nuclear states which would arise from jj-coupling, in conformity with the indications of the shell model. He showed that on this basis the short half life of He^6 would be difficult to understand; moreover, no markedly improved agreement is obtained for the other nuclei. Trigg makes the assumption that the nuclear states with $L = I \pm \frac{1}{2}$ have admixture of $L' = I \mp \frac{1}{2}$. The L' orbitals must be understood as resultants from the coupling of at least three particles. Trigg determined the amounts of admixture from the deviations of the measured magnetic moments. The straightforward application of this procedure did not produce a striking improvement. However, uncertainty of the experimental values is great enough so that adjustments to perfect agreement is possible. These attempts have great value, at least because they show that the degree of disagreement shown in Fig. 1 should not be surprising.

THE FORBIDDEN TRANSITIONS

"Unique" Forbidden Transitions

In an n-times forbidden transition, according to the classifications used in Table II:

$|\Delta I| \leqq n$ with Fermi selection rules (i.e. S or V interaction)
$|\Delta I| \leqq n+1$ with Gamow/Teller selection rules (i.e. T or A interaction)
$|\Delta I| \leqq n-1$ with P(pseudo-scalar) interaction.

It develops that $|\Delta I| = n+1$ transitions possess distinctive properties which are beautifully confirmed by experiments. The mere occurrence of transitions with such properties will prove that the T or A interactions form at least part of the β-coupling. Among the characteristics is the fact that only a single one of the many nuclear matrix elements $\int\Omega$ such as listed in Table II, has an appreciable value in any given case. This circumstance makes predictions and interpretations particularly unambiguous and is responsible for the name "unique" attached to these $|\Delta I| = n+1$ transitions.

The extra unit of angular momentum which the light particles carry off in the "unique" transitions does not reduce the transition probability to a size characteristic of the $(n+1)$-times forbidden transitions because this extra unit comes from a direct coupling of spins characteristic of the T or A interactions. If the extra unit must be carried off in the form of orbital angular momentum, as under Fermi rules, then the probability is indeed reduced to the $(n+1)$-times forbidden magnitude; n units of orbital angular momentum are accompanied by centrifugal repulsion which introduces the small factor r^n into the transition amplitude. The extra unit characteristic of Gamow-Teller rules introduces the factor $\boldsymbol{\delta}$, of unit magnitude.

Formally, the operator Ω, in the matrix element $\int\Omega$, must be a tensor of rank $(n+1)$ to permit $|\Delta I| = n+1$, as reviewed in the section, SELECTION RULES FOR β-TRANSITIONS. For the "unique" transitions, this tensor must be formed from $\boldsymbol{\delta}$, and n identical "moment arm" vectors $\boldsymbol{r}$ as factors. Only one such tensor can be formed for a given n and so only a single matrix element $\int\Omega$ need be considered in each order. For $n=1$, $\Omega \equiv S_{ij}$ and for $n=2$, $\Omega \equiv S_{ijk}$, according to Table II. Hence we denote the matrix element $\int\Omega$ characterizing "unique" n-times forbidden transitions by $\int\Omega = S_n$. The normalization is left arbitrary.

The appearance of the moment arm vectors $\boldsymbol{r}$ in S_n is a consequence of the multipole expansion of the electron-neutrino wave, $\exp -i(\boldsymbol{p}+\boldsymbol{q})\cdot\boldsymbol{r}/\hbar$, as in equation 11. The nth term yields a transition probability proportional to the square of $|\boldsymbol{p}+\boldsymbol{q}|^n$. Averaged over all directions of the electron and neutrino momenta, $\boldsymbol{p}$ and $\boldsymbol{q}$:

$$<|\boldsymbol{p}+\boldsymbol{q}|^{2n}> = \sum_{\nu=1}^{n} \frac{(2n+1)!}{(2\nu+1)!(2n-2\nu+1)!} p^{2\nu} q^{2(n-\nu)} = a_n(W). \qquad 23.$$

The spectra of "unique" transitions will be altered from the allowed shape

(equation 15) by just this "shape factor," $a_n(W)$. In place of equation 15, one now has:

$$d\lambda/dW \sim G^2|\ S_n|^2 F(\pm Z, W) q^2 pW \cdot a_n(W) \qquad 24.$$

aside from a numerical factor which depends on just how S_n is normalized. Of course, $K = G_{S,V}/G_{T,A}$ should not appear in this expression.

The spectrum (equation 24) is subject to further correction for coulomb effects than is embodied in $F(\pm Z, W)$, which is the factor used for allowed spectra. The further corrections are relatively unimportant except for the low energy fraction with $p < mc$. This much insensitivity to the coulomb force contrasts with most types of forbidden spectra (see below). Precise expressions for the coulomb effect are given by Konopinski & Uhlenbeck (65) and Greuling (66); their use is illustrated by Osoba (67) and Jensen, Laslett & Zaffarano (68).

Although the existence of the distinctive $|\Delta I| = n+1$ spectra was predicted (65) as early as 1941, none were reported as observed until 1949. A search for an example by Langer & Price (69) ended in the discovery of the Y^{91} case. This transition was expected to have $\Delta I = 2$ and a parity change from shell model considerations. Its spectrum was found to deviate distinctly from the allowed shape as shown by the nonlinearity of the conventional Kurie plot (see Fig. 2). When this plot is appropriately corrected by multiplying with $a_1^{-1/2}$, with

$$a_1 = p^2 + q^2 = c^{-2}[(W^2 - m^2c^4) + (W_0 - W)^2] \qquad 24a.$$

according to equation 23, then the excellent linearity exhibited in Figure 2 was achieved. Almost simultaneously, a similar spectrum was reported by Peacock & Mitchell (70) for the transition of Cs^{137} to an excited state of Ba^{137}. These cases presented the first deviations from the statistical, "allowed" shape which conformed to the theory. They also constituted the first proof requiring no knowledge of nuclear spins that the T or A interactions must form part of the β-coupling.

Many more examples were found in rapid succession. Mayer, Moszkowski & Nordheim (32) list some 25 transitions which are expected to have $|\Delta I| = 2$ with parity change, on the basis of the shell model. The spectra of 17 of these have now been definitely measured and all such depart from the allowed shape according to the form factor a_1, as expected. The shell assignments thus confirmed are for: Cl^{38}, A^{41}, K^{42}, As^{76}, Kr^{85}, Rb^{86}, Sr^{89}, Sr^{90}, Sr^{91} (71), Y^{90}, Y^{91}, Y^{92} (72), Sn^{123m}, Cs^{137}, Pr^{142}, Tm^{170}, and Tl^{204}. Not given in the above list but belonging to it are the spectra of: A^{39}, As^{74}, and Sn^{125m}. Several even-A cases plainly exhibit the shape characteristic of the same class of transitions, but the shell model does not straightforwardly predict $|\Delta I| = 2$, with parity change, for them. These are As^{72} (73), Rb^{88} (74), Sb^{122} (75), Sb^{124} (76), and I^{124} (77). Most of the latter cases require further study before definitive conclusions can be drawn. The shell model predictions for even-A nuclei are hazardous in these cases. On the other hand, a few of the measured spectra are complex and some end in excited states.

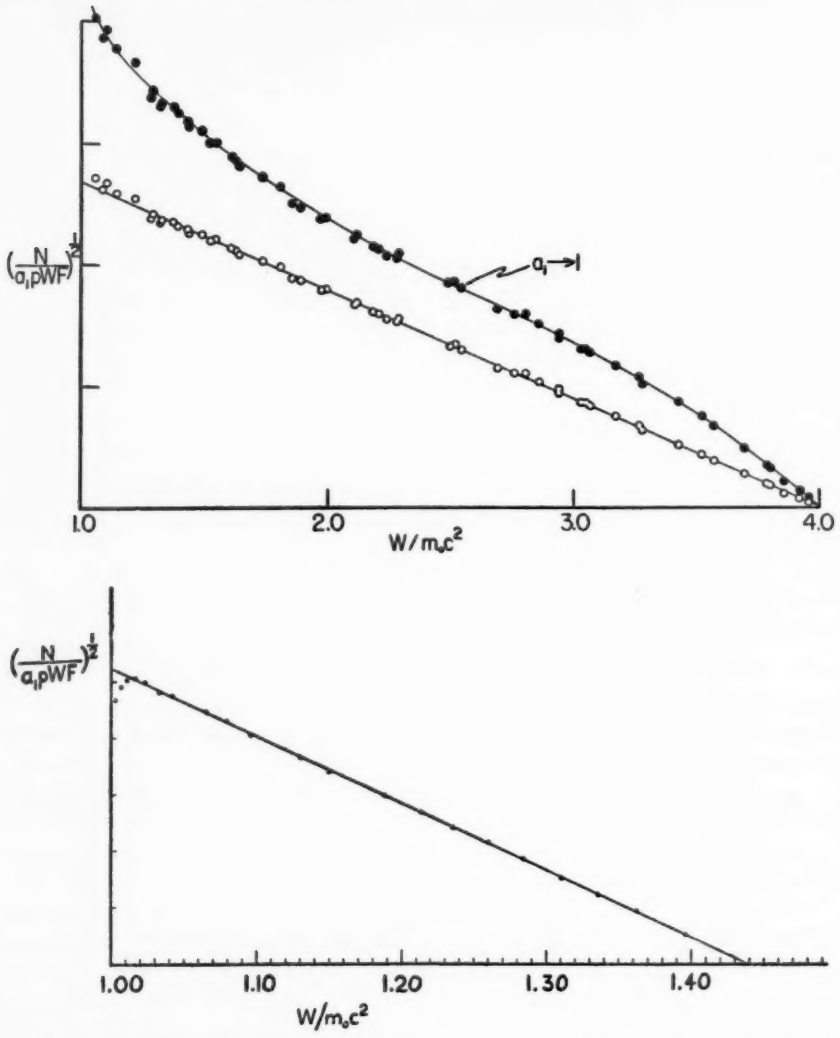

FIG. 2. (above) The unique once-forbidden spectrum of Y^{91}; a_1 is replaced by 1 for the conventional Fermi plot, which should be linear if the experimental shape is allowed; $a_1 = p^2 + q^2$ linearizes the data, as shown.

FIG. 3. (Below) Fermi plot of the Pm^{147} spectrum.

All the cases mentioned so far have the shape $\sim a_1$ expected with $|\Delta I| = 2$. It is interesting to note their characteristic measured *ft*-values: $\log ft = 7.3$ to 10.1. A wider range of variation than for normal allowed transitions is to be expected. Actually, since $f(W_0, Z)$ of equation 17 was obtained by integration over the allowed spectrum, *ft* should not be expected to be independent of the

energy release W_0 for transitions with the spectrum of equation 24. Rather for the "unique" transitions, $ft \sim$ spectrum average of $[a_n(W)]^{-1}$. A fair approximation (78) is $ft \sim (W_0^2-1)^{-1}$ for the case $n=1$. Now the measured values of $\log (W_0^2-1)ft$ should be more nearly constant. They are found to vary from 9.4 to 10.5, a 50 times narrower range of corrected half lives than was found above. Only Sb^{124}, with $\log (W_0^2-1)\, ft=11.5$, lies outside the range quoted here. This may be due (79) to a higher $\Delta l(=3)$ than in the other cases (all except one have $\Delta l=1$) but Tm^{170}, with $\Delta l=3$ also, has only $\log (W_0^2-1)\, ft=10.4$.

The "unique" forbidden transitions with $n>1$ are of course much fewer. All decay so slowly that accurate measurements are extremely difficult. However the spectra of $Be^{10}(\Delta I=-3, \log ft=13.7)$ and $K^{40}(\Delta I=-4, \log ft=17.6)$ were well measured. As expected theoretically, the Kurie plot for Be^{10} becomes linear (80 to 83) when the shape factor

$$a_2 = p^4 + q^4 + (10/3)p^2q^2$$

is taken into account. Similarly, the measured K^{40} spectrum (84 to 87) exhibits the shape factor

$$a_3 = p^6 + q^6 + 7p^2q^2(p^2 + q^2).$$

Thus, the theory has been found to work satisfactorily for "unique" once-, twice-, and three-times forbidden transitions.

Other Forbidden Transitions

Predictions for forbidden transitions in general are hampered by lack of knowledge concerning the nuclear matrix elements $\int\Omega$ of Table II, much more seriously than for allowed transitions or unique forbidden transitions. Several different $\int\Omega$ may be involved in a given transition, even if the interaction were settled as a single one of the forms S, V, T, A, or P. The several matrix elements may each be accompanied by its characteristic β-spectrum. Consequently, the observed spectrum is a resultant depending on the ratios of unknown matrix elements. Since these ratios are constant over a spectrum, one can at least see if any reasonable values exist which can make the theory fit the experimental spectra.

The same ambiguity of course did not affect the allowed spectra, even though two different matrix elements, $\int 1$ and $\int \vec{\sigma}$, may be contributing. That was because both of these possible allowed matrix elements led to the same spectrum shape. There was a similar lack of ambiguity for the unique forbidden spectra because there only one nuclear matrix element contributed to any given case.

The decay constant per unit electron energy range can always be put in the form:

$$d\lambda/dW = (G^2/2\pi^3\hbar^7c^3)F(\pm Z, W)q^2pW \cdot C_n \qquad 25.$$

as compared to equation 15, $n=0, 1, 2 \cdots$ refers to allowed, once-forbidden, twice-forbidden, $\cdots$ transitions. $G=G_T$ or G_A depending on which of the two forms T or A is included in the β-coupling.

It was seen that for allowed transitions $C_0=|\int \mathfrak{G}|^2+K^2|\int 1|^2$, which is a constant as regards dependence on the electron energy. $K=G_S/G$ or G_V/G, as before. Whenever C_n is energy-independent, equation 25 will yield a β-spectrum with the allowed shape.

For unique forbidden transitions, C_n depends on the electron energy: $C_n=|S_n|^2 a_n(W)$ of formula 23. Thus, in general, C_n is a shape factor by which a forbidden spectrum differs from the allowed shape. In what follows, unique forbidden transitions are omitted, since they have already been discussed. Henceforth, the designation "n-times forbidden" will refer only to transitions with $\Delta I=n$ or $n-1$, the cases with $\Delta I=n+1$ being the unique-forbidden ones.

Once-Forbidden Transitions

Half lives.—Mayer, Moszkowski & Nordheim have compiled lists of transitions which can be best brought into consistency with the shell model if they are assigned to the once-forbidden class, i.e., are attributed a parity change and $|\Delta I|=0$ or 1. It is then found that the range log $ft=6$ to 8 is characteristic of these cases. No distinction between $\Delta I=0$ and $|\Delta I|=1$ cases is to be found in this comparison of the comparative half lives.

The compilers bring out the remarkable fact that all interground (or -metastable) state transitions for $Z>60$ should be expected to have the parity change. This is because, in the $Z>60$ nuclei, the last neutron and the last proton fall into shells of opposite parity.

One consequence is that transitions to ground states are frequently outcompeted by allowed transitions to excited states, i.e., whenever suitable ones are energetically available. The lists referred to above are limited to ground state transitions because the shell model is considered most reliable then.

The odd-A nuclei in the Mayer-Moszkowski list include some 12 cases of $s_{1/2}\rightarrow p_{1/2}$ transitions. There are in the list about seven other odd-A isobars expected to have $\Delta I=0$. About 13 cases are listed as having $|\Delta I|=1$.

Nordheim's even-A list contains some ambiguous cases, as is to be expected when one must consider the coupling of two nucleons to determine the character of a state. Rb^{88} and Pr^{142} are tentatively given as $\Delta I=0$ transitions, but their spectra have been observed to have the unique-forbidden shape (see "Unique" Forbidden Transitions) so that the assignment $|\Delta I|=2$ becomes more plausible. This leaves N^{16}, Kr^{88}, Xe^{138}, Ce^{144}, Pr^{144}, RaE″(Tl^{206}), and perhaps RaE, in the list. All these probably undergo $0^+\leftrightarrow 0^-$ transitions.

The first information to be gained from the "parity-forbidden" transitions follows from the fact that, with only three exceptions, all have log $ft>6$. This is to be compared to log $ft=4$ to 5.8 which characterizes the allowed transitions (see ALLOWED β-DECAY). The longer half lives now met are significant particularly because the pseudo-scalar (P) part of the

β-coupling makes its largest contribution when $\Delta I=0$ with parity change. One concludes that the P interaction has no greater part in the β-coupling than the T or A interactions, in the sense that G_P is not of greater order of magnitude than $G_{T,A}$. It actually leads to smaller maximum transition probabilities because of the intrinsic misfit of the nuclear states of opposite parity. This general argument is necessarily rough and perhaps $0 \leqq G_P/G_{T,A} \lesssim 3$ are limits consistent with it. One is tempted to argue that G_P is smaller because the $\Delta I=0$ transition show no greater probability than $|\Delta I|=1$ transitions in spite of having the help of both the P and T (or A) interactions. This, however, would require the detection of a variation by a factor 10 in a set of empirical comparative half lives which exhibit variations by a factor 100.

The three exceptions mentioned in the preceding paragraph are Hg^{205}, Pb^{209}, and RaE″. Although shell model assignments putting them into the allowed class seem out of the question, nevertheless their respective log ft $=5.4$, 5.6, and 5.5 only. It is suggestive that, in each of these cases, the transforming nucleon, in both its neutron and proton states, is the first nucleon or first "hole" in a closed shell ("magic numbers" 82 and 126). This occurs only in the three cases here and also in RaE, which will be discussed below. Thus, it may be that there is a special "favoring" of the transitions, analogous to the favoring in the mirrors and triads (cf. THE FAVORED TRANSITIONS).

Normal spectra.—The next data concerning the once-forbidden transitions which should be considered are the measured spectra. Most of these are partially obscured by concurrent transitions. Among the few exceptions are Pr^{143}, Pm^{147}, Er^{169}, and W^{185}. All of these have rather low maximum energies and so not to much room is left for excited final states.

In many cases, a fair portion of the main spectrum is free of superpositions: Zr^{97}, Cd^{115}, Ba^{140}, La^{141}, Ce^{141}, Pr^{144}, and W^{187}. All these end in a ground state and so are most reliably classified once-forbidden. Na^{24}, Ga^{66}, and Mo^{99} end in excited states. They are usually classified once-forbidden only on the basis that their ft-values fall into the range log $ft=6$ to 8. This can be questioned, since l-forbidden transitions (cf. ALLOWED β-DECAY) may also fall into this range. The Rb^{86} and Au^{198} transitions to excited final states are superficially like cases; however, their assignment to the once-forbidden class is more plausible.

A striking fact emerges from an examination of the spectra mentioned in the last two paragraphs. They all have the same shape as allowed spectra, within the accuracy of the measurements. In some cases this accuracy is very high. The Pm^{147} measurement is an example (44); its Kurie plot is accurately linear from its end-point of 230 kev down to 8 kev (see Fig. 3). La^{141} has about the highest energy release (2.43 Mev) of the fairly well measured and most reliably classified once-forbidden spectra. It yields a straight line Kurie plot down to $\sim$0.91 Mev, where the superpositions of concurrent transitions begin (88).

There is just one spectrum,[9] that of RaE, which may be once-forbidden and does not have the allowed shape. It will be discussed below.

It is clear that the main task of the theory of once-forbidden spectra is to show that their allowed shape should prevail in most cases. The shape factor C_1 of equation 26 below must normally be energy-independent. The general theoretical expressions for C_1 containing arbitrary combinations of the S, V, T, A, and P interaction forms, are inordinately lengthy. The terms arising from each of the five interactions individually can be found in the Konopinski-Uhlenbeck paper (65).[10] Terms due to interference among the five forms have been calculated only recently, by Smith (92) and by Pursey (93). For the discussion here, a description of the salient features will suffice. According to the section on ALLOWED β-DECAY, only the following combinations need be considered: *STP* or *SAP* or *VTP* or *VAP*.

The spectra will be resultants of contributions accompanying each of the "once-forbidden" matrix elements of Table II. For convenience of discussion, these may be separated into two types: the "velocity" matrix elements, $\int\boldsymbol{\alpha}$ and $\int\gamma_5$; the "moment" matrix elements $\int\boldsymbol{r}$, $\int\boldsymbol{\sigma}\cdot\boldsymbol{r}$, $\int\boldsymbol{\sigma}\times\boldsymbol{r}$ and S_{ij}. The first type plays the role of relativistic corrections to the "allowed" matrix elements $\int 1$ and $\int\boldsymbol{\sigma}$, being of the order of the nucleon velocity v/c. Like the latter, the $\int\boldsymbol{\alpha}$ and $\int\gamma_5$ contribute energy-independent terms to C_n unless interference occurs (like the Fierz interference in allowed spectra). The partial expression for C_1 arising from the "velocity" matrix element is:

$$C_1(\boldsymbol{\alpha},\gamma_5) = [G_T^2 + G_V^2 + 2mc^2G_VG_T/W]\left|\int\boldsymbol{\alpha}\right|^2 + [G_A^2 + G_P^2 + 2mc^2G_AG_P/W]\left|\int\gamma_5\right|^2. \qquad 26.$$

[9] Kondaiah (89) suggests that the Ru^{103} transition to an excited final state be classed as once-forbidden although it has log $ft=5.6$, in the allowed range. This is because he finds the spectrum to deviate from the allowed shape for energies below 0.1 Mev, in a direction opposite to that which could be caused by too thick a source. Mei, Huddleston, and Mitchell (90) find only the deviation due to a thick source, below 0.06 Mev. However, it is possible that in the latter measurement the thick source obscured the effect found by Kondaiah. The latter effect could be fitted with the interference terms of C_1 (91), but this would contradict several other measured spectra, e.g., Pm^{147}, which has an almost identical endpoint. The latter spectrum has been measured under ideal conditions (44) and moreover is definitely once-forbidden [$d_{5/2}\rightarrow f_{7/2}$ (32) with log $ft=7.6$]. The Ru^{103} deviation also cannot be explained in the same way as RaE because such an explanation requires a greater comparative half life than normal. For the present, one must await a renewed check of the measurement and of its Kurie plot.

[10] Because the five interaction forms are there considered as alternatives, the largest P contribution is referred to as "allowed." When combinations of the five forms are admitted, as here, the P contribution must be considered "once-forbidden" (see Table II), particularly when its small size is noted (see preceding paragraphs).

Some of the G's vanish, depending on which of the combinations STP, SAP, VTP, or VAP represents the β-coupling correctly.

One can see that to obtain an energy independent shape factor from equation 26, the VT and AP interferences must be avoided.[11] This interference may be called of the "Fierz type" since it is exactly like the SV or TA interference in the allowed spectra. Here, however, there are further contributions still to be considered.

The "moment" matrix elements are characterized by the presence of the "moment arm" $\mathbf{r}$, in the integrals over the nuclear states. Its presence is accompanied by the energy-dependent factor $\mathbf{p}+\mathbf{q}$, as one learns from the multipole expansion (equation 11) and also from the experience with the unique forbidden transitions ($\sim\Sigma|S_{ij}|^2$) discussed above. The latter experience leads one to expect terms in $C_1 \sim a_1 = p^2+q^2$, as in formula 24a. Such terms indeed occur but they are usually overwhelmed in size by further terms due to the coulomb effect on the electrons, except for just the contributions $\sim\Sigma|S_{ij}|^2$. It was pointed out in the section "UNIQUE" FORBIDDEN TRANSITIONS that the coulomb effect on the latter is moderate.

The importance of the coulomb effect on transitions resulting from the "moment" matrix elements is due to the peculiar character of the relativistic coulomb wave functions. When these are derived for an idealized point charge then they are singular at the point of the charge. Thus their modification for the actual, though small, spread of the charge on the nucleus is quite essential. Fermi originally introduced the procedure of allowing for the nonpoint charge character of the nucleus by using the values of the idealized coulomb wave functions at the nuclear radius, R, rather than at $r=0$. The validity of this procedure for most spectra (in contrast to half lives) has been checked by Rose & Holmes (95) in greatest detail [cf. Good (96)]. For these investigations, reasonable assumptions about the distribution of nuclear charge were adopted, then a comparison with the Fermi procedure was carried out. The conclusion is that the latter procedure is sufficiently accurate for most spectra. Only the lowest energy portions of spectra from high Z nuclei need special care (e.g., RaE, below).

[11] Critchfield (21) argues that the interferences in equation 26 do not come into play despite simultaneous operation of the AP (or VT) interactions. He expects the A and P contributions to lead to different final nuclear states only, because the latter are eigenfunctions of the time-reversal operator. Closer examination seems to show that this argument does not hold. The mathematical mechanism by which the orthogonality of time-reversal eigenstates would operate here is by the vanishing of expressions like (R^*I+RI^*) when R is a "real" operator and I a pure imaginary one, in the sense used by Wigner. However, such operators actually occur here as $i(R^*I-RI^*)$ instead, as to be expected when one starts from a formalism having proper invariance to time-reversal. Longmire & Messiah (94) derived the full consequences of the time-reversal invariance in this connection when they showed that each matrix (e.g., I or R) is a single parameter quantity, i.e., real or imaginary, but not complex.

The main terms provided in C_1 by the coulomb effects just discussed are proportional to $(Ze^2/Rmc^2)^2$. They are usually the dominant terms, essentially because the coulomb "barrier" energy, Ze^2/R, is usually substantially larger than the characteristic β-energy releases (a few mc^2). Thus, for La^{141}, one of the most energetic β-emitters listed above, $Ze^2/R \approx 10$ Mev whereas the maximum electron energy is 2.43 Mev. For most of the other measured spectra quoted above, the coulomb factor is much more dominant (perhaps the best measured case, Pm^{147}, has $Ze^2/R \approx 11$ Mev and the end point energy only 0.23 Mev). Consequently, we write C_1 in an approximation keeping only the dominant coulomb terms:

$$C_1 \approx (\alpha Z/2R)^2 \left\{ (G_T^2 + G_A^2) \left(\left| \int \boldsymbol{\sigma} \cdot \boldsymbol{r} \right|^2 + \left| \int \boldsymbol{\sigma} \times \boldsymbol{r} \right|^2 \right) + (G_S^2 + G_V^2) \left| \int \boldsymbol{r} \right|^2 \right.$$
$$\left. - \left[i \left(\int \boldsymbol{r} \right)^* \cdot \left(\int \boldsymbol{\sigma} \times \boldsymbol{r} \right) + c.c. \right] [G_S G_T + G_V G_A + (G_S G_A + G_V G_T)/W] \right\} \quad 27.$$

Again, not all the G's are nonvanishing and, further, only interferences produce dependence on the electron energy in these largest terms.

The usual once-forbidden spectrum has $Ze^2/R \gg mc^2$ and will have a shape factor which is the sum of terms from equations 26 and 27. One cannot neglect the terms of equation 26 just because the large factor $(Ze^2/Rmc^2)^2$ is not evident there; the matrix elements $\int \boldsymbol{\alpha}$ and $\int \gamma_5$ should be expected to be larger than the "moment" matrix elements. Pursey (93) makes the estimate $\int \boldsymbol{\alpha} \approx i(\alpha Z/R) \int \boldsymbol{r}$ from a reasonable, although special, model of the nucleus. A similar ratio can be derived for the magnitudes of $\int \gamma_5$ and $\int \boldsymbol{\sigma} \cdot \boldsymbol{r}$. The conclusion is that the terms of both equation 26 and equation 27 make up most of the shape factor for the usual, "normal" once-forbidden spectrum.

The last statement provides a basis for evaluating the evidence that the normal once-forbidden spectrum has the allowed shape. This evidence requires the elimination of the energy-sensitive interferences resulting from combination of the interactions V and T, that resulting from S and A, and also that resulting from A and P. The last of these comes into play only for $\Delta I = 0$ transitions, but several of the allowed spectrum shapes have been yielded in cases of $\Delta I = 0$. Thus, there appears to be left, for the explanation of all β-phenomena discussed so far, only the triplet of interactions STP or the doublet VA. The doublet VP is discarded not for reasons of Fierz-type interference but because it has already been shown that T or A are necessary constituents of the β-coupling. Only the latter can yield Gamow-Teller selection rules and the "unique" type of spectra.

Abnormal spectra.—It is clear from the foregoing that in exceptional cases, a once-forbidden spectrum differing from the allowed shape may appear. One way is for the electron energy to be high enough to challenge the dominance of the coulomb energy, Ze^2/R. A likely candidate is N^{16} with its 10.3-Mev energy release, as against $Ze^2/R \approx 2.6$ Mev. The spectrum has not yet been measured. Actually, small deviations from the allowed shape, for the reason now considered, should occur in some of the spectra already meas-

ured. Their detection requires higher accuracy than has been obtained so far, however. The present method of making a Kurie plot of the experimental points would lead one to draw a straight line through them even if the deviations being considered are present. This is not only because the departures are small but also because they have a certain amount of symmetry relative to a mean energy (most of the terms are symmetrical in p and q). In the latter respect, the deviations now discussed differ from the "Fierz type" arising from the interferences discussed above.

Still another way in which a once-forbidden spectrum may acquire a substantial deviation from the allowed shape in particular cases is through an "accidental" cancellation of the large energy-independent terms against each other, thus giving prominence to small energy-sensitive terms. This is essentially what happens in the Petschek-Marshak treatment (97) of the RaE spectrum.

RaE provided the earliest known case of deviation from the allowed shape and was initially explained as twice-forbidden (65). The advent of the shell model made it appear that RaE undergoes a parity change and thus should be classified as once-forbidden. Its spectrum does not have a unique forbidden shape and so must have $\Delta I=0$ or -1. Both possibilities were considered by Petschek & Marshak. They concluded that $\Delta I=0$ must be presumed because the observed spectrum shape can be derived only with the help of a P interaction in combination with T. The daughter nucleus is even-even, hence the spin change is $0^-\rightarrow 0^+$ and the S interaction cannot contribute (see Table II).

The nuclear matrix elements which contribute to $0^-\rightarrow 0^+$ transitions are $\int \boldsymbol{\sigma}\cdot\boldsymbol{r}$, from the T interaction, and $\int \gamma_5$, from the P interaction, according to Table II. The shape factor which yields the RaE spectrum was found by using the real (94) ratio

$$\Gamma = -(G_P/G_T)\left[i\int \gamma_5 \Big/ \int \boldsymbol{\sigma}\cdot\boldsymbol{r}\right]$$

as a free parameter. How correction with the shape factor obtained with $\Gamma=12.8$ transforms a conventional Kurie plot into a linear one is shown in Figure 4.

The value found here for Γ, 12.8, is not unreasonable. $G_P=G_T$ may be supposed, in view of the emphasis on the combination $H=G(\rho_S+\rho_P+\rho_T)$ for μ-decay (cf. THE A PRIORI THEORETICAL BASIS). As has been mentioned above, one may estimate the matrix element $\int \gamma_5$ to be of the order of $i(\alpha Z/R)\int \boldsymbol{\sigma}\cdot\boldsymbol{r}$. Since $\alpha Z/R\approx 26$, literal acceptance of the crude estimate leads to $\Gamma\approx 26$. Agreement within a factor of two here is better than one can expect.

The treatment of RaE may be regarded as unsatisfying because of its somewhat *ad hoc* character. However, the RaE spectrum has long been the only example of its kind. This makes less implausible the assertion that its energy dependence is the result of the accidental cancellation of large terms.

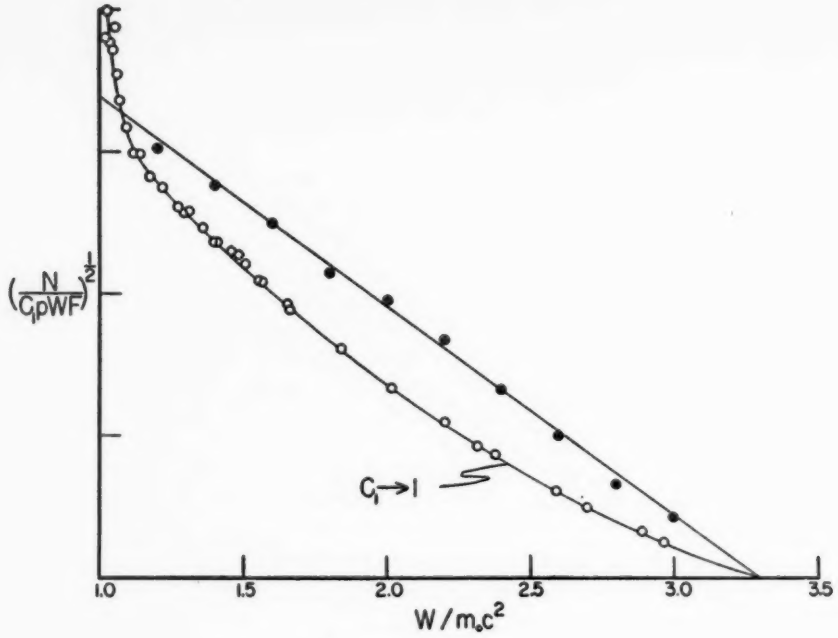

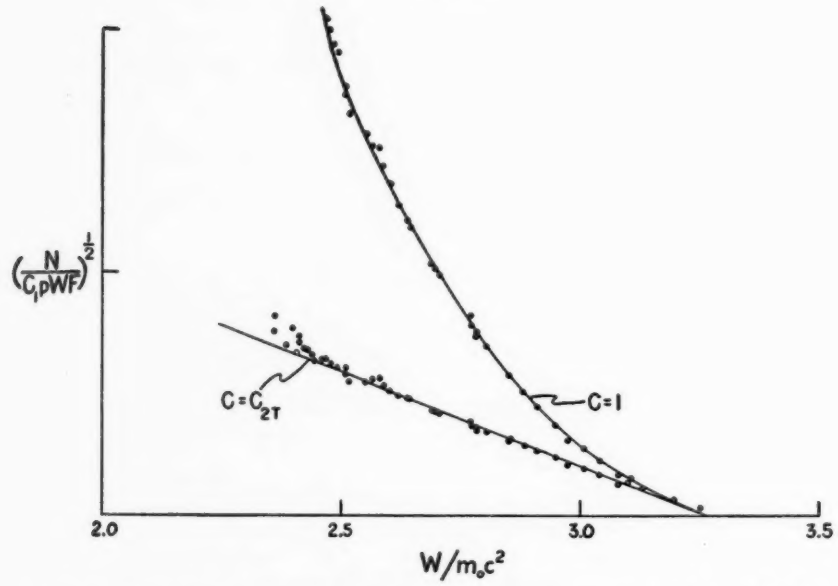

FIG. 4. (Above) Fermi plot of RaE spectrum. Conventional plot ($C_1 \rightarrow 1$) fails to linearize the data. C_1 as calculated by Petschek & Marshak (97) produces the linearization shown.

FIG. 5. (Below) Twice-forbidden spectrum of Cs^{137}. The conventional plot ($C=1$) is linearized by $C=C_{2T}$ (see text).

Moreover, we can offer qualitative corroboration from the evidence of its comparative half life.

RaE has $\log ft = 8.0$. In its decay, an eighty-third proton transforms into a one hundred twenty-seventh neutron. This puts it into the same class of transitions as Hg^{205}, Pb^{209}, and RaE'' discussed above. The latter all have $\log ft \approx 5.5$. Thus, the RaE transition is comparatively slow, and this may well be the result of the cancellations of large terms needed to explain its spectrum. The relative size of the large and small terms in question is about $(Ze^2/Rmc^2)^2 \approx 700 \approx 10^{2.8}$ approximately, enough to account for the discrepancy in ft values.

It should be noted that the case of RaE provides the only experimental data which require the presence of P interaction in the β-coupling. The previous evidence required the presence of only S and T interactions, for example, although a comparable admixture of P interaction was not inconsistent with it. Furthermore, the previous evidence has also been consistent with a VA combination, not containing P at all. This must now be discarded.

Twice-Forbidden Transitions

Mayer, Moszkowski & Nordheim (32) list just four transitions as twice-forbidden ($|\Delta I| = 2$ and no change in parity): Cl^{36}, Tc^{99}, Cs^{135}, and Cs^{137}. Actually, both the initial and final spins in the two Cs transitions have been measured; the spins of Cl^{36} and Ru^{99} are also measured. Since, further, the shell model is particularly unambiguous in its predictions of parity, all the cases here are classified with unusual reliability.

The four cases have comparative half lives in the range $\log ft = 12.2$ to 13.5. These are somewhat longer than follows from the simple ratio $(R/\lambda\!\!\!^{-})^2 \approx 4.10^{-4}$ which the once-forbidden half lives might be expected to bear to them. There are weight factors in the "highly convergent multipole expansion" (equation 11) which might easily be responsible. However, quantitative comparison seems to be rendered almost meaningless by lack of knowledge concerning nuclear matrix elements.

The spectra of all but Cs^{135} have been measured, and as is expected from any form of the theory (below), all deviate substantially from the allowed shape. This is illustrated for Cs^{137} (98) in Figure 5. The conventional Kurie plot of the data yields the curve shown [below 2.5 mc^2, the unique forbidden transition (70) to an excited state occurs]. The straight line is achieved when a shape factor, C_2, now to be discussed, is introduced. Cl^{36} (75, 99) and Tc^{99} (75, 100) behave in a like manner.

It will suffice to present the approximate shape factor which follows from the T interaction for $|\Delta I| = 2$:

$$\hbar^2 C_{2T} = \sum |T_{ij}|^2 (\alpha Z/2R)^2 (p^2 + 4q^2) + \sum |A_{ij}|^2 (p^2 + q^2) - \sum (T_{ij} A_{ij}^* + c.c.)(\alpha Z/2R)(p^2 + 2q^2) \qquad 28.$$

valid if $Ze^2/R \gg W_0$ and $\alpha Z \ll 1$. The matrix elements T_{ij}, A_{ij} are shown in Table II. The way in which the various types of terms arise is much the

same as was discussed for the once-forbidden transitions. Terms are kept in equation 28 which allow for the possibility that the unknown ratio A_{ij}/T_{ij} may be as large as $\alpha Z/R$.

When the ratio A_{ij}/T_{ij} is used as a real (94) parameter, equation 28 proves to fit the Cl^{36}, Tc^{99}, and Cs^{137} spectra remarkably well. The values found for the ratio are $A_{ij}/T_{ij}=4.25$, 2.57 and 7.65, respectively. The result for Cs^{137} is as shown in Figure 5.

It must now be mentioned that the V interaction can account for the present findings equally well. There is, in the approximation given in equation 28, merely a replacement of T_{ij} by R_{ij} of Table II. Thus, any combination of T and V might appear to serve equally well. However, the VT interference (92) produces terms of the same type as in equation 28 with the further factor: W^{-1}. This is again the Fierz interference kind of phenomenon. The necessity of its elimination is not as clear-cut here as for the once-forbidden spectra.

The equal ability of the V or the T interactions to explain the twice-forbidden spectra means that the latter do not exclude the VA combination as an alternative to STP. The VA interference (92) is not of the Fierz type ($\sim W^{-1}$) and merely adds, to the results for V, terms of a type already present with V alone. Thus the only evidence in favor of STP as against VA remains the singular RaE spectrum, as discussed in the preceding subsection.

One is thus finally left only with arbitrary combinations of the STP interactions. Admixtures of S and P to T will not alter the present explanation of the twice-forbidden spectra. The S interaction again merely adds terms of exactly the same kind as are already included in equation 28 except that T_{ij} is replaced by R_{ij} in the terms from the S interaction. Thus the spectra are fitted in the same way except that the ratio A_{ij}/T_{ij} may be altered and supplemented by the ratio R_{ij}/T_{ij}. The P interaction does not contribute at all to twice forbidden transitions because it requires $|\Delta I|<2$, and then the transition would be allowed instead.

SUMMARY

This review demonstrates that it is possible to arrive at a unique law of β-decay, consistent with Fermi's essential criteria, from data on β-decay. Fermi's work left the law open to construction out of arbitrary amounts of five types of interaction: S, V, T, A, and P. The data shows that the correct β-coupling must be a combination of S, T, and P, in proportions for which there is only a rough measure so far. Not only are these the only components which the β-interaction may contain but each of the three is necessary.

The comparable probabilities of allowed transitions with $\Delta I=0$ and 1, together with the existence of the "unique" spectra, showed that the T or A forms are necessary parts of the β-coupling.

The short life of $^1S_0 \rightarrow {}^1S_0$ transitions in C^{10} and O^{14} provides the main evidence that S or V are also necessary parts of the β-interaction law. This fact has some support from the trend of half lives among favored transitions.

The spectrum of RaE is the only datum requiring the presence of P interaction. It also requires the presence of T, but for this it has support from the evidence of other spectra, once the presence of P is granted. This excessive reliance on the singular RaE spectrum is supported by the comparison of RaE half life with that of similar nuclei, which confirms the interpretation of the spectrum.

The chief information gained from spectra other than RaE and the "unique" spectra, is that the Fierz-type of interference is absent. Its absence in allowed spectra forbids combining S and V or T and A. That, alone, narrows the alternatives to STP, SAP, VTP, and VAP. Next, the like absence of Fierz-type interference in once- and twice-forbidden spectra eliminates SA, AP, and VT combinations. Hence, from such arguments alone, one is left with only STP, or VP, or VA. Then VP must be discarded because it does not yield Gamow-Teller selection rules. However, STP is favored over VA only by the evidence of RaE.

The conclusions contradict both the Critchfield-Wigner and the Tolhoek-de Groot a priori "principles."

The present data are too inaccurate to give the proportions of S, T, and P quantitatively. The ratio $K=G_S/G_T$ is most nearly measured by the various favored transitions discussed in THE FAVORED TRANSITIONS. It seems that $K=1\pm0.5$ conforms roughly to that data. The half-lives of $\Delta I=0$, once-forbidden, decays and the fitting of the RaE spectrum appear to be roughly consistent with $G_P\approx G_T$.

LITERATURE CITED

1. (a) Curran, S. C., Angus, J., and Cockroft, A. L., *Phil. Mag.*, **50**, 53 (1949); (b) Hanna, G., C. and Pontecorvo, B., *Phys. Rev.*, **75**, 983 (1949); (c) Hamilton, D. R., Alford, W. P., and Gross, L., *Bull. Am. Phys. Soc.*, **26**, 24 (1951); (d) Langer, L. M., and Moffat, R. D., *Phys. Rev.* (In press)
2. Furry, W. H., *Phys. Rev.*, **54**, 56 (1937)
3. Goeppert-Mayer, M., *Phys. Rev.*, **48**, 512 (1935)
4. Primakoff, H., *Phys. Rev.*, **85**, 888 (1952)
5. Lawson, J. L., *Phys. Rev.*, **81**, 299 (1951)
6. Kalkstein, M., and Libby, W. F., *Phys. Rev.*, **85**, 368 (1952)
7. Levine, C. A., Ghiorso, A., and Seaborg, G. T., *Phys. Rev.*, **77**, 296 (1950)
8. Winter, R. G., *Carnegie Inst. Technology Rept.* (1951)
9. Inghram, M. G., and Reynolds, J. H., *Phys. Rev.*, **78**, 822 (1950)
10. Fireman, E. L., *Phys. Rev.*, **75**, 323 (1949)
11. Bethe, H. A., and Bacher, R., *Revs. Modern Phys.*, **8**, 82 (1936)
12. Konopinski, E. J., *Revs. Modern Phys.*, **15**, 209 (1943)
13. Skyrme, T., *Progress in Nuclear Physics* 115–39 (Frisch, O., Ed., Academic Press, Inc., New York, N. Y., 224 pp., 1950)
14. Preston, M. A., *Natl. Research Council Can. Ann. Rept. No. TL-29* (1950)
15. Crane, H. R., *Revs. Modern Phys.*, **20**, 278 (1948)
16. Yang, C., and Tiomno, J., *Phys. Rev.*, **79**, 495 (1950)
17. Gamba, A., *Nuovo Cimento*, **7**, 919 (1950)
18. Caianello, E. R., *Nuovo Cimento*, **8**, 749 (1952)
19. MacCallum, C., and Wightman, A., *Princeton Univ. Rept. No. 7* (1951)
20. Michel, L., *Proc. Phys. Soc.* (*London*), [A]**63**, 514 (1950)
21. Critchfield, C. L., *Phys. Rev.*, **63**, 417 (1943)
22. Tolhoek, H. A., and de Groot, S. R., *Phys. Rev.*, **84**, 150 (1951); *Physica*, **16**, 456 (1950)
23. Trigg, G. L., and Feenberg, E., *Phys. Rev.*, **82**, 982 (1951)
24. Biedenharn, L. C., and Rose, M. E., *Phys. Rev.*, **83**, 459 (1951)
25. Klein, O., *Nature*, **161**, 897 (1948)
26. Sagane, R., Gardner, W. L., and Hubbard, H. W., *Phys. Rev.*, **82**, 557 (1951)
27. Tiomno, J., and Wheeler, J. A., *Revs. Modern Phys.*, **21**, 144 (1949)
28. (a) Moszkowski, S. A., *Rept. Inst. Nuclear Studies, Univ. Chicago* (1950); *Phys. Rev.*, **82**, 35 (1951); (b) Bleuler, E., and Zünti, W., *Helv. Phys. Acta*, **19**, 375 (1946)
29. Feister, I., *Phys. Rev.*, **78**, 375 (1950)
30. Fierz, M., *Z. Physik*, **104**, 553 (1937)
31. Feenberg, E., and Trigg, G. L., *Revs. Modern Phys.*, **22**, 399 (1950)
32. Mayer, M. G., Moszkowski, S. A., and Nordheim, L. W., *Revs. Modern Phys.*, **23**, 315 (1951)
33. Feingold, A., *Revs. Modern Phys.*, **23**, 10 (1952)
34. Lawson, J. L., and Cork, J. M., *Phys. Rev.*, **57**, 982 (1940)
35. Tyler, A., *Phys. Rev.*, **56**, 125 (1939)
36. Backus, J., *Phys. Rev.*, **68**, 59 (1945); Cook, C. S., and Langer, L. M., *Phys. Rev.*, **73**, 601 (1948)
37. Wu, C. S., and Albert, R. D., *Phys. Rev.*, **75**, 315, 1107 (1949)
38. Langer, L. M., Moffat, R. D., and Price, H. C., Jr., *Phys. Rev.*, **76**, 1725 (1949)
39. Owen, G. E., and Cook, C. S., *Phys. Rev.*, **76**, 1726 (1949)

40. Rose, M. E., *Phys. Rev.*, **49**, 727 (1936)
41. Longmire, C. L., and Brown, H., *Phys. Rev.*, **75**, 264, 1102 (1949); Reitz, J. R., *Phys. Rev.*, **77**, 10 (1950)
42. Cook, C. S., Langer, L. M., and Price, H. C., Jr., *Phys. Rev.*, **74**, 548 (1948)
43. Albert, R. D., and Wu, C. S., *Phys. Rev.*, **75**, 847 (1949)
44. Langer, L. M., Motz, J. W., and Price, H. C., Jr., *Phys. Rev.*, **77**, 798 (1950)
45. Gross, L., and Hamilton, D. R., *Phys. Rev.*, **78**, 318 (1950)
46. Robson, J. M., *Phys. Rev.*, **83**, 349 (1951)
47. Perez-Mendez, V., and Brown, H., *Phys. Rev.*, **77**, 404 (1950)
48. Cook, C. S., Langer, L. M., Price, H. C., Jr., and Sampson, M. B., *Phys. Rev.*, **74**, 502 (1948)
49. Hornyak, W. F., and Lauritsen, T., *Phys. Rev.*, **77**, 160 (1950)
50. Sheline, R. K., Holtzman, R. B., and Fan, C.-Y., *Phys. Rev.*, **83**, 919 (1951)
51. Langer, L. M., and Price, H. C., Jr., *Phys. Rev.*, **76**, 641 (1949)
52. Agnew, H. M., *Phys. Rev.*, **77**, 655 (1950)
53. Warshaw, S. D., *Phys. Rev.*, **80**, 111 (1951)
54. Wigner, E., *Phys. Rev.*, **51**, 106 (1947); **56**, 519 (1939)
55. Wigner, E. (Lecture Notes, Univ. of Wisconsin, 1950)
56. Inglis, D. R., *Phys. Rev.*, **81**, 914 (1951)
57. Perez-Mendez, V., and Lindenfeld, P., *Phys. Rev.*, **80**, 1097 (1950)
58. Moszkowski, S. A., *Phys. Rev.*, **82**, 118 (1951)
59. Trigg, G. (Personal communication)
60. Sherr, R., Muether, H. R., and White, M. G., *Phys. Rev.*, **75**, 282 (1949)
61. Sherr, R., and Gerhart, J., *Phys. Rev.*, **86**, 619 (1952)
62. Harris, W. M., *Phys. Rev.*, **84**, 1249 (1951)
63. Turner, C., *U. S. Atomic Energy Commission Document, AECU-432* (Unpublished, 1942)
64. Boley, F. I., and Zaffarano, D. J., *Phys. Rev.*, **84**, 1059 (1951)
65. Konopinski, E. J., and Uhlenbeck, G. E., *Phys. Rev.*, **60**, 308 (1941)
66. Greuling, E., *Phys. Rev.*, **61**, 568 (1942)
67. Osoba, J. S., *Phys. Rev.*, **76**, 345 (1949)
68. Jensen, E. N., Laslett, L. J., and Zaffarano, D. J., *Phys. Rev.*, **80**, 862 (1950)
69. Langer, L. M., and Price, H. C., Jr., *Phys. Rev.*, **75**, 1109 (1949); **76**, 641 (1949)
70. Peacock, C. L., and Mitchell, A. C. G., *Phys. Rev.*, **75**, 1273 (1949)
71. Ames, D. P., Langer, L. M., and Sorensen, B. (Unpublished data)
72. Ames, D. P., and Bunker, M. E. (Unpublished data)
73. Mei, J. Y., Mitchell, A. C. G., and Huddleston, C. M., *Phys. Rev.*, **79**, 19 (1950)
74. Bunker, M. E., Langer, L. M., and Moffat, R. D., *Phys. Rev.*, **81**, 30 (1951)
75. Wu, C. S. (Presented at Intern. Conf. Nuclear Phys., Univ. of Chicago, Chicago, Ill., 1951)
76. Langer, L. M., Moffat, R. D., and Price, H. C., Jr., *Phys. Rev.*, **79**, 808 (1950)
77. Mitchell, A. C. G., Mei, J. Y., Maienschein, F. C., and Peacock, C. L., *Phys. Rev.*, **76**, 1450 (1949)
78. Shull, F. B., and Feenberg, E., *Phys. Rev.*, **75**, 1768 (1949); Taketani, M., Nakamura, S., Umezawa, M., Ono, K., and Yamaguchi, Y., *Phys. Rev.*, **82**, 441 (1951); Davidson, J. P., Jr., *Phys. Rev.*, **82**, 48 (1951)
79. Langer, L. M., *Phys. Rev.*, **84**, 1059 (1951); Nakamura, S., Umezawa, M., and Takebe, H., *Phys. Rev.*, **83**, 1273 (1951)
80. Feldman, L., and Wu, C. S., *Phys. Rev.*, **78**, 318 (1950)

81. Fulbright, H. W., and Milton, J. C. D., *Phys. Rev.*, **76**, 1271 (1949)
82. Alburger, D. E., Hughes, D. J., and Eggler, C., *Phys. Rev.*, **78**, 318 (1950)
83. Bell, P. R., and Cassidy, J. M., *Phys. Rev.*, **77**, 301 (1950)
84. Bell, P. R., Weaver, B., and Cassidy, J. M., *Phys. Rev.*, **77**, 399 (1950)
85. Alburger, D. E., *Phys. Rev.*, **79**, 236 (1950)
86. Wu, C. S., *Revs. Modern Phys.*, **22**, 386 (1950)
87. Good, M. L., *Phys. Rev.*, **83**, 1054 (1951)
88. Duffield, R. B., and Langer, L. M., *Phys. Rev.*, **84**, 1065 (1951)
89. Kondaiah, E., *Manne Siegbahn*, 411–485 (Inst. of Phys., Stockholm, Sweden, 845 pp., 1951)
90. Mitchell, A. C. G. (Personal communication)
91. Mahmoud, H. (Unpublished data)
92. Smith, A. M., *Phys. Rev.*, **82**, 955 (1951)
93. Pursey, D., *Phil. Mag.*, **42**, 1193 (1951)
94. Longmire, C. L., and Messiah, A. M. L., *Phys. Rev.*, **83**, 464 (1951)
95. Rose, M. E., and Holmes, D. K., *Phys. Rev.*, **83**, 190 (1951)
96. Good, R., *On the Theory of Forbidden Transitions* (Doctoral thesis, University of Michigan, Ann Arbor, Mich., 80 pp., 1951)
97. Petschek, A. G., and Marshak, R. E., *Phys. Rev.*, **85**, 698 (1952)
98. Langer, L. M., and Moffat, R. D., *Phys. Rev.*, **82**, 635 (1951)
99. Fulbright, H. W., and Milton, J. C. D., *Phys. Rev.*, **82**, 274 (1951)
100. (a) Taimuty, S. I., *Phys. Rev.*, **81**, 461 (1951); (b) Nakamura, S., Umezawa, M., and Takebe, H., *Phys. Rev.*, **83**, 1273 (1951); (c) Wu, C. S., and Feldman, L., *Phys. Rev.*, **82**, 332 (1951); (d) Wagner, F., Jr., and Freedman, M. S., *Bull. Am. Phys. Soc.*, **27**, 50 (1952)
101. Dewan, J. T., Pepper, T. P., Allen, K. W., and Almqvist, E., *Phys. Rev.*, **86**, 416 (1952); Wu, C. S., Rustad, B. M., Perez-Mendez, V., and Lidofsky, L., *Phys. Rev.*, **87**, 1140 (1952)

β-DECAY ENERGETICS[1]

By Charles D. Coryell

Department of Chemistry and Laboratory for Nuclear Science and Engineering, Massachusetts Institute of Technology, Cambridge, Massachusetts

Introduction

This review is concerned with the correlation of the total disintegration energy emitted in β-processes with the composition of the nucleus undergoing decay. It will be seen that a general systematization is fairly satisfactory even though finer details of the nuclear quantum states are overlooked. The correlations give information about the energy effects of nuclear shell structure, and they are useful in predicting the decay properties of imperfectly known or unknown nuclear species.

The commonest form of radioactive transformation is the general process of β-decay, whereby a neutron in the nucleus is transformed into a proton in the nucleus, with the creation of a negative β-particle (negatron) and a neutrino, or conversely, a proton is transformed into a neutron by capture of an orbital electron with the creation of a neutrino. A process alternative to orbital electron capture is the creation of a positive electron (positron β^+) and neutrino.

The energetics of these processes can be related to the atomic masses M of the original nuclide with nuclear charge Z and mass number A and of the daughter nuclide. In negatron decay, the sum of the energies of the β-particle and the neutrino[2] is the maximum energy E_{β^-} displayed in the β-energy spectrum, given as:

$$E_{\beta^-} = M(Z, A) - M(Z + 1, A). \qquad 1.$$

In the electron capture the energy release E_K is:

$$E_K = M(Z, A) - M(Z - 1, A) \qquad 2.$$

but the value is very difficult to determine by direct observation of the radiations. In contrast with these two complementary β-processes, positron emission has an energy threshold of $2m_0c^2 = 1.02$ Mev. The maximum energy E_{β^+} displayed in the β^+ energy spectrum is thus:

$$E_{\beta^+} = M(Z, A) - M(Z - 1, A) - 2m_0c^2. \qquad 3.$$

Considerable success has been achieved in relating the probability (or the half life) of negatron and positron processes with the energies E_{β^-} and E_{β^+} and the quantum states of the initial and product nuclei. These correla-

[1] The survey of the literature pertaining to this review was concluded in May, 1952.

[2] In accord with present evidence (1), it is assumed that the rest mass of the neutrino is zero.

tions are usually expressed through the *ft* product, a comparative half life, the function *f* from Fermi theory of β-decay making correction for nuclear charge and energy of the transition. The *ft* product is then used for detailed treatment of quantum properties of the system. A review of β-decay theory is given in this book by Konopinski & Langer (1). Analysis of large bodies of experimental data are given by Mayer, Moszkowski & Nordheim (2) for odd-A species and by Nordheim (3) for even-A species.

Nucleons can be designated by quantum numbers analogous to those for atoms with an orbital quantum number l, total angular momentum quantum number (spin) j, and parity $+$ or $-$. The l values 0, 1, 2, 3, $\cdots$ are designated by the letters s, p, d, f, $\cdots$. Almost all odd-A nuclei have quantum numbers deriving from those of the one odd nucleon (single particle model) as shown by Mayer (4, 5) and Haxel, Jensen & Suess (6, 7). All known nuclei with even numbers of protons Z and neutrons N have zero spin. Analysis of the experimental data (1, 2, 3) shows distinctions among classes of β-transitions with respect to change in orbital Δl, change in spin Δj, and change in parity as no or yes.

Because of the sensitive dependence of transition probability on specific quantum states, as outlined briefly above, it occurs very frequently that β-transitions lead to one or more excited states of the product species, with one or more γ-rays being emitted in the subsequent de-excitation of each excited state. The inclusion of appreciable γ-energy in the decay process depends on the chances that excited levels of favored transition probability have energy values in the proper region with respect to the energy of the parent nucleus. There is, however, little departure from regularity in the energy sequence of ground states of sets of nuclei in a given region of nuclear composition, except in sets that are broken by the closure of a nuclear shell. Thus, a high degree of regularity for correlations is found on considering the total energy of negatron decay Q^β, including the energy E_γ of rays in cascade with the β-ray and the excitation energy E_m of the metastable state of the daughter nucleus, if it occurs:

$$Q^\beta = E_\beta + E_\gamma + E_m. \qquad 4.$$

Since many practical applications of radioactivity are concerned with ground states, there is added reason for giving attention to the total decay energy.[3]

Definitions corresponding to equation 4 are set up for the total decay energies Q^K and $E_d^{\beta^+}$ in electron capture and in positron emission. It will be useful in the rest of this paper to refer only to these total decay energies. It will also be useful to invert these two processes and treat electron capture of

[3] While it is certainly true that sets of transitions between given quantum states, e.g., $d_{3/2} \rightarrow p_{1/2}$, would show high regularity in a given region of nuclear composition, information on most of the many such sets is fragmentary and is restricted to very small regions of composition. Similar relations among the energy levels for isomeric states, such as the sets for $s_{1/2}$, $d_{3/2}$, and $h_{11/2}$ for the odd-A nuclei recorded by Hill (8) are interesting.

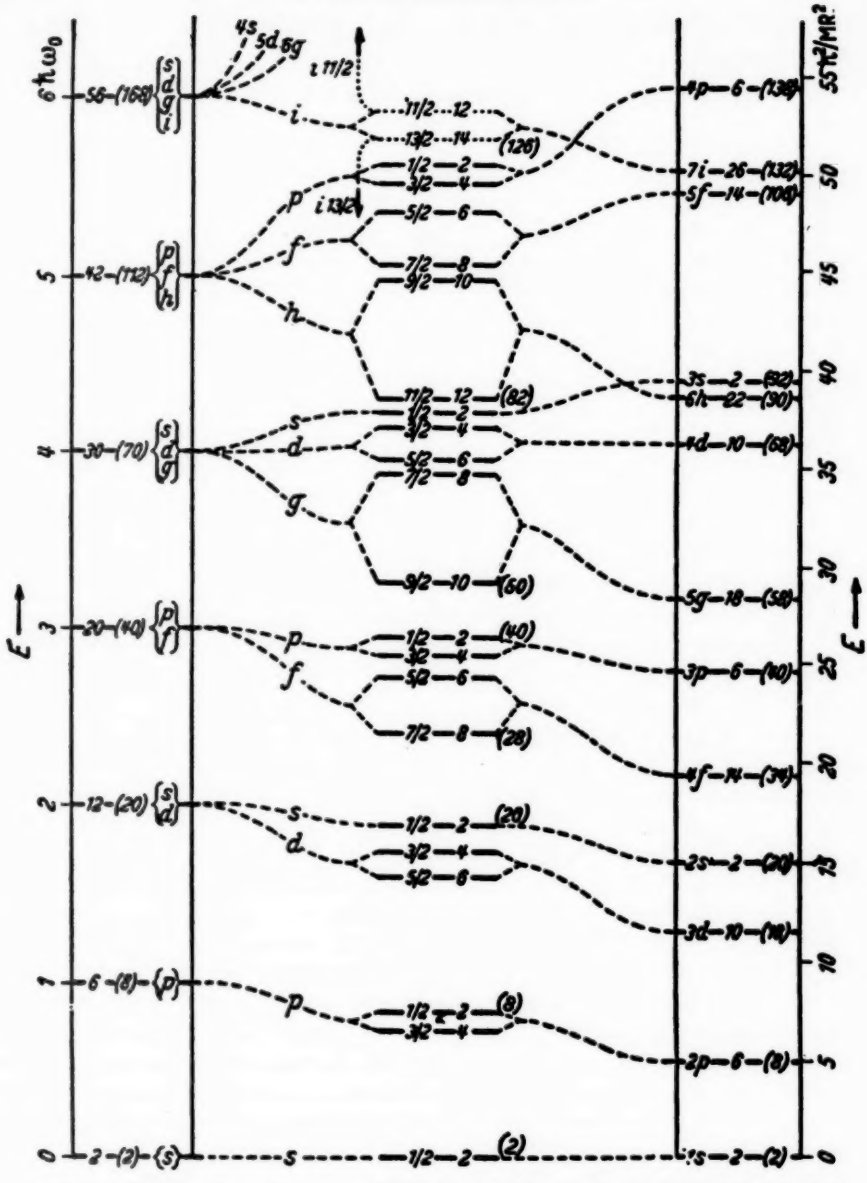

FIG. 1. Schematic nuclear term diagram. Left side, parabolic potential well; right side, square potential well; middle, level pattern expected for real nuclei, with strong spin-orbit coupling. Taken from (7). Note that the orbital nomenclature at the right is that of electronic orbitals rather than the more widely accepted one based on radial nodes plus one; the latter are used in the text, so that $2p$ becomes $1p$, $3d$ becomes $1d$, $4f$ becomes $1f$, etc.

the nuclide $(Z+1, A)$ as negatron decay of the nuclide (Z, A) with negative decay energy:

$$Q^{\beta}(Z, A) = -Q^{K}(Z+1, A) = -E^{\beta^+}(Z+1, A) - 1.02 \text{ Mev.} \quad 5.$$

Shells in the nucleus.—In the next section, there is given a review of the statistical treatment of nuclear stability that has been developed over the last 15 years, which gives a fair representation of β-decay energetics. There will be frequent consideration, however, of perturbations due to nuclear shell structure. As pointed out and detailed by Mayer (4, 5) and Haxel, Jensen & Suess (6, 7) the order of addition of protons or neutrons to a nucleus is that shown in the middle of Figure 1, intermediate between that expected for a parabolic potential well (harmonic oscillator; left side) or a square potential well (right side). The protons or neutrons (each of spin $\frac{1}{2}$) separately fill the levels, joining in pairs as far as possible. An odd proton or neutron exhibits strong spin-orbit coupling such that the state with $j=l+\frac{1}{2}$ is considerably more stable than that with $j=l-\frac{1}{2}$. The half-integers in Figure 1 indicate j values, the simple integers give subshell populations, and the numbers in parentheses give cumulative number of nucleons through the subshell. As in filling the electronic quotas of an atom, a shell occurs when there is a pronounced gap in the energy sequence. For small nucleon numbers, such gaps occur at 2, 8, and 20 with the filling of the orbitals $1s$, $1p$, and $1d+2s$. After this point, all shell closures occur at the breaks due to spin-orbit coupling at the numbers 28, 50, 82, and 126 corresponding to completion of the orbitals $1f_{7/2}$, $1g_{9/2}$, $1h_{11/2}$, and $1i_{13/2}$.

The quantum numbers of a nucleus with odd-A are almost always identical with those of the odd nucleon, as neutron and proton pairs make no contribution. The quantum numbers of all known nuclei of even-Z even-N nuclei (even-A) are zero. Those of odd-Z odd-N nuclei (also even-A) are derived from those of the odd proton and odd neutron by rules formulated by Nordheim (3). In a given shell sequence such as 28 to 50, there is only small energy difference between the orbitals $f_{5/2}$, $p_{3/2}$, $p_{1/2}$, and $g_{9/2}$. Levels of very high l tend to fill in pairs, putting the odd nucleon in an adjacent low-l orbital. Isomerism is common in the last half of each shell sequence because of the low isomeric transition probability for large change in j and l, e.g., from excited $g_{9/2}$ to ground state $p_{1/2}$.

It will be seen that discontinuities occur in β-energetics on crossing a shell edge and these provide the best available information on the energy gap in shell closure. Conversely, careful analysis of β-decay data may cast light on subshell effects, as might be expected for the spin-orbit split at the end of $2d_{5/2}$ (64 nucleons) or $2f_{7/2}$ (100 nucleons). There is also the possibility that breaks occur at the conclusion of $4f_{5/2}$ (34 nucleons) or $2p_{1/2}$ (40 nucleons). There is some evidence for the first two of these, but none yet apparent for the last two.

The Statistical Model and the Parabolic Energy Surfaces

The liquid-drop model.—The general features of the stability pattern of nuclides and therefore of the factors controlling the energetics of β-decay can be formulated from a simplified liquid-drop model that has been built up over the last two decades, beginning with a parabolic equation for β-energetics (9). The general utility of this model is great, and it seems useful to retain its main features for the present treatment of nuclear energetics, adding correction terms for the shell effects. Some of the historical origins of the liquid drop formulation are given by Bethe & Bacher (10), Bohr and Wheeler (11), and Kohman (12).

The nucleus is considered to be an incompressible sphere of nucleons, of radius $R=r_0A^{1/3}$. The energy of the nucleus has a stabilizing volume-interaction term from saturation forces, proportional to the number of nucleons A, with correction by a surface term for surface unsaturation, proportional to $A^{2/3}$. The stability pattern of light nuclei shows that neutron-proton forces exceed neutron-neutron or proton-proton forces, these being equivalent except for coulombic effects. The energy correction for the departure of the composition from symmetry in neutrons and protons can be expressed as a symmetry term proportional to $(A/2-Z)^2/A$. Coulombic repulsion adds another term, computed classically as $3Z^2e^2/5R$. A final correction is made for the instability resulting from unpaired spin of an odd proton or neutron, to give a noncontinuous term called the pairing term, to be discussed later. The mass of a nuclide (Z, A) is given thus as the mass of the free constituents, Z hydrogen atoms of mass M_H (to include the electrons as well as the protons)[4] and $A-Z$ neutrons of mass M_n:

$$M(Z, A) = M_HZ + M_n(A - Z) - a_1A + a_2A^{2/3} + \frac{a_3}{A}\left(\frac{A}{2} - Z\right)^2 + \frac{3}{5}\frac{(Ze)^2}{r_0A^{1/3}} + \text{pairing term} \qquad 6.$$

where the various terms on the right have been identified above. This statistical equation is only considered valid if the number of nucleons exceeds about 40.

The pairing term may be considered to arise from the fact that nucleons of a given kind show strong interaction in pairs, but a proton should not interact appreciably with a neutron in a different quantum state. If the pairing energy for two protons is 2π, the unpaired proton in an odd-Z nucleus will introduce an instability term of π compared to the paired protons; corresponding to the neutron pairing energy of 2ν, the unpaired neutron in an odd-N nucleus will contribute an instability term ν. Until recently, it was assumed that the two spin terms, π and ν, were essentially equivalent for a

[4] The binding energy of the electron in the hydrogen atom is ignored. The binding energies of the electrons in the heavier nuclides is included with the nuclear binding energies.

given small range of mass number, and either was taken as the term δ. The last term in equation 6 was expressed[5] as:

$$\text{pairing or spin term} = \begin{Bmatrix} \pi + \nu \cong 2\delta (A \text{ even, } Z \text{ and } N \text{ odd}) \\ \pi \cong \delta \ (A \text{ odd, } Z \text{ odd, and } N \text{ even}) \\ \nu \cong \delta \ (A \text{ odd, } Z \text{ even, and } N \text{ odd}) \\ 0 \quad (A \text{ even, } Z \text{ and } N \text{ even}) \end{Bmatrix} \qquad 7.$$

The parabolic energy surface.—It will be seen that equation 6 is, apart from the spin term, quadratic in Z, corresponding at constant A to parabolic dependence of $M(Z, A)$ on Z. Defining Z_A as the hypothetical charge of maximum stability for given A, the parabolic dependence is:

$$M(Z, A) = M(Z_A, A) + \frac{B_A}{2}(Z - Z_A)^2 + \text{spin term} \qquad 8.$$

where B_A is the curvature of the parabola, a function of A, and $M(Z_A, A)$ is the effective mass for the charge Z_A.

Setting the differential $(\partial M/\partial Z)_A$ of equation 6 equal to zero at $Z = Z_A$ and using a star on Z_A to show that it is restricted specifically to equation 6, it is found that:

$$Z_A^* = \frac{(M_n - M_H + a_3)A}{2a_2 + 6e^2A^{2/3}/5r_0} \qquad 9.$$

and comparing the coefficients of equations 6 and 8 with similar usage of the star, it is found that

$$B_A^* = \frac{1}{A}(2a_2 + 6e^2A^{2/3}/5r_0 = (M_n - M_H + a_3)/Z_A^* \qquad 10.$$

Equation 8 emphasizes the parabolic character in isobaric sequences of the nuclear energy surface. We shall have occasion to rely on this dependence regardless of the generality of equation 6. The spin terms of equation 7 show that the energy surface is split into four different levels according to evenness and oddness of Z and A. For even-A species, the two surfaces differ in energy by an amount which can be called δ_A approximately equal[6] to $\pi + \nu$. The total energy of β-decay can be established by substituting equation 8 for the ground states of nuclides (Z, A) and $(Z+1, A)$ into equation 1:

$$Q^\beta = B_A(Z_A - Z - 0.5) \mp \delta_A \quad (A\text{-even}) \qquad 11.$$

where the minus sign is valid for even-Z and the plus sign for odd-Z. The corresponding surfaces for odd-A species differ in energy by $\pi - \nu$, and the total energy of β-decay is given as:

$$Q^\beta = B_A(Z_A - Z - 0.5) \mp (\pi - \nu) \quad (A\text{-odd})^5 \qquad 12.$$

[5] Note added in galley proof: It is not feasible to determine the values of π and ν separately, but the difference $\pi - \nu$ occurs regularly in the β-energetics of odd-A nuclides. The author regrets not having accepted a recommendation of T. P. Kohman to use the symbol ϵ_A for this difference, as δ_A is used for the approximate sum. The pairing term is called the spin term in the remainder of this review.

with the same correlation of sign with evenness of Z. In many regions of mass number, $\pi - \nu$ is close to zero as assumed in the pre-1948 studies.

The occurrence of stable nuclides.—It is found experimentally that δ_A is comparable with B_A, with maximum value above $1.5B_A$. Under these conditions, no odd-Z odd-A species is stable to β-decay,[6] but there may be two or even three stable even-Z isobars. In principle, one of the two or two of the three will be unstable with respect to double β-decay, but this process is expected to be very highly forbidden (1) and has not yet been recognized experimentally[7] (13). The odd-Z nuclides lying between two stable even-Z isobars are unstable with respect to decay by both negatron emission and electron capture, and these processes will be competitive (e.g., K^{40}) and indeed, positron emission is generally permitted too (e.g., Cu^{64}).

The condition for stability of an odd-A nuclide of even charge Z is satisfied if:

$$-0.5 - (\pi - \nu)/B_A < Z_A - Z < 0.5 + (\pi - \nu)/B_A \qquad 13.$$

with reversed sign on the $\pi - \nu$ term for odd Z. Assuming that $\pi - \nu$ is negligible removes the restriction that Z be even and leads to the consequence that a stable nuclide occurs for only one Z value which lies within 0.5 charge unit of Z_A, a result of general significance.

Equation 12 cannot explain the occurrence of two stable odd-A isobars differing by one charge unit, except for the unlikely possibility that the neutrino has a finite rest mass[2] greater than the difference in mass of the two. The instability of one of such a pair is predicted (Mattauch's rule). Two such cases in nature have not yet been resolved: (Cd, In)^{113} probably[8] and (Sb, Te)^{123}, presumably because of low disintegration energy and very long half life of the unstable members.

The parameters for equation 6.—It is apparent that a satisfactory correlation of β-decay is obtained within the framework of the liquid-drop model by the evaluation of Z_A, B_A, π, and ν as a function of A. Parameters for equation 6 or its equivalent have been evaluated by a number of workers (10, 16 to 20) with closely similar numerical results. For convenience, discussion will be centered principally around the set of solutions given by Fermi (17), because of the very extensive computations made from these by Metropolis & Reitwiesner (21). Fermi used 1945 experimental values of 1.00812 for M_H and 1.00893 for M_n. He also took the parameter r_0 as an experimental quantity evaluated as 1.48×10^{-13} cm. from α-decay half lives and the energetics of decay of the mirror nuclides ($Z - N = \pm 1$). The sym-

[6] For the very light nuclei $_1H^2$, $_3Li^6$, $_5B^{16}$, and $_7N^{14}$ the condition $Z = N$ overrides the spin effect; these nuclei are much lighter than the range of validity of equation 6. Radioactivity has not yet been identified for the species $_{23}V^{50}$ recently discovered in low abundance in natural vanadium, but it seems certain that it occurs, especially in view of the mass data of Johnson (12a).

[7] Ingraham & Reynolds (14a) estimate from the isotope abundance of Xe^{130} in an old tellurium ore that the half-life of the Te^{130} for double β-decay is $\sim 1 \times 10^{24}$ years.

[8] It has been reported by Cohen (14) that In^{113} may decay by L-capture, but the evidence is weak in the presence of the more recently recognized β-decay of In^{115}.

metry parameter a_3 was then evaluated by trial fit to give by equation 9 a curve for Z_A^* as a function of A passing as well as possible within 0.5 charge unit of the Z values of all known β-stable odd-A nuclides. The value he chose was 0.083 A.M.U. = 77.2 Mev. The reliability of this value is shown graphically in Figure 2, where the solid line is based on this parameter.

The Fermi value of a_3 seems to be a very good choice, within the framework of equation 6 and its corollary equation 13, for covering the whole mass-number region from 40 to 240. The success of this parametric fit is taken as substantiation of the general usefulness of the statistical treatment embodied in equation 6. It will be noticed that there is a general tendency for the fit to be poorer in the region of shell-crossing, indicated in Figure 2 by arrows; the experimental data tend to depart from the Fermi line to follow the shell-lines. The specific nature of these departures points to the desirability of making shell corrections to the statistical formulation.

From current values of decay data, Fermi (17) also evaluated $\delta_A = 2\delta$ as $0.072/A^{3/4}$ A.M.U. or $67/A^{3/4}$ Mev, without explicit justification. This treatment is less satisfactory as the dependence of δ_A on A does not lend itself to simple functional representation, but it is best expressed graphically as shown later.

Difficulties with absolute masses.—It may be pointed out that Fermi (17) also evaluated the parameters a_1 and a_2 from currently accepted absolute masses, obtaining the values 0.01504 A.M.U. and 0.014 A.M.U. respectively. The whole set of Fermi parameters was used by Metropolis & Reitwiesner (21) to give computed masses for up to 48 Z values for each A from 1 to 260. There is now evidence that these computed masses show gross systematic departures from the observed masses, as for instance those reported by Duckworth and colleagues (22). Quantitative difficulties with the equation have been discussed by Stern (23), Harvey (24), and Merat (25), the latter cutting the discrepancies about twofold by lowering a_2 to 0.01335 and using the new value (26) for the neutron mass, $M_n = 1.008982$. Wapstra (27) assesses the departures from the computed masses for $A < 65$.

Part of the weakness of the broad-range mass fit based on equation 6 is due to cumulative effects of shell closure, i.e., systematically low binding energies in the first half of shell sequence, followed by high values in the last half, with downward discontinuities of 1 to 2 Mev at shell edges. A fairly radical modification of the parameters may be necessary to handle this, as for instance proposed by Collins, Nier & Johnson (28) for the parameters of the Wigner general mass equation (29) to account for the mass data in the region $30 < A < 70$, or it may even be necessary to overhaul the whole treatment.

Local solutions for Z_A and B_A.—The simple solution of the problem of dealing with β-decay is to seek local solutions for Z_A, B_A, and δ_A based on data in the immediate mass region, as done by Bohr & Wheeler (11). Feenberg (18) has made the most detailed study of these parameters, with regard to the general validity of equation 6 and the corrections to it for the effects

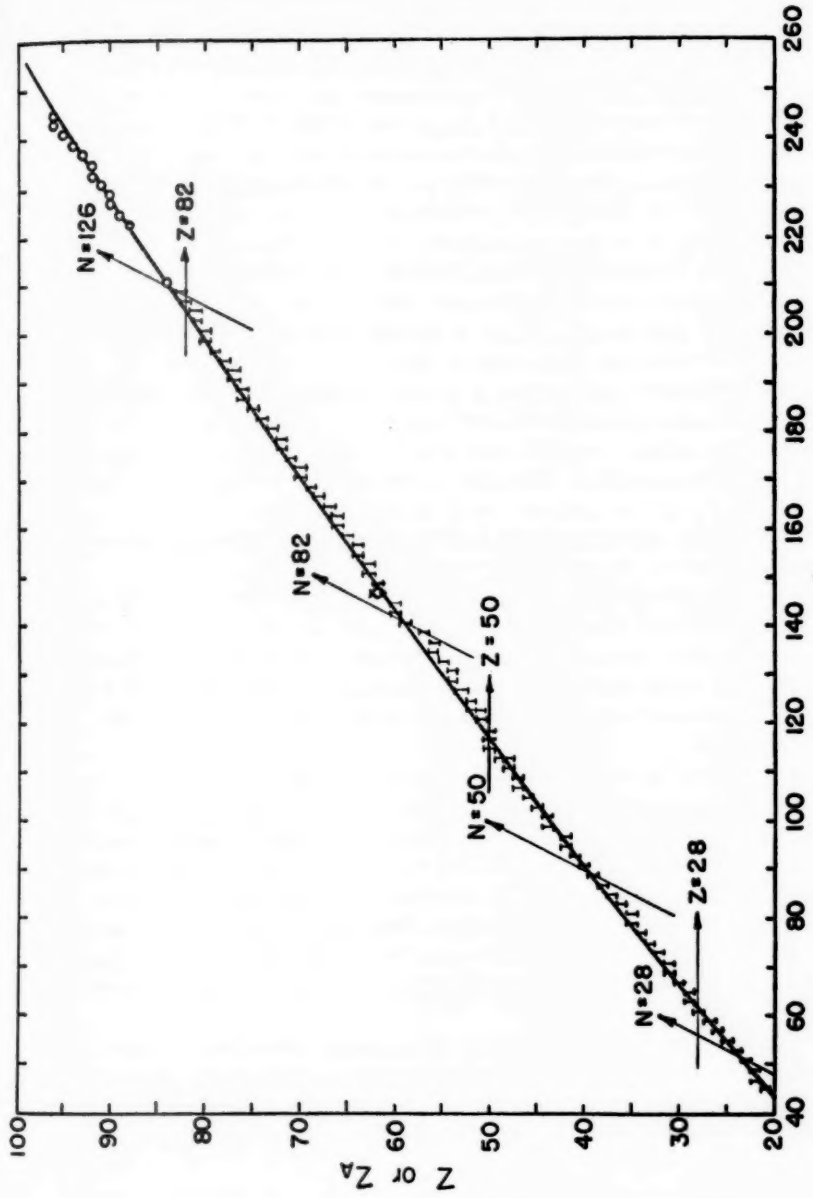

FIG. 2. Test of the statistical equation. The solid line is the Fermi curve (17) for Z_A^* based on 0.083 for the parameter a; vertical lines, stable odd-A nuclides; circles, β-stable odd-A α-emitters; arrows, proton and neutron shell numbers.

of change in volume of the nucleus under electrostatic force with deficiency in binding energy associated with the surface term and the symmetry term (large departure from the state $N=Z$). He also used details of the experimental values of the packing fraction in evaluating the parameters.

The local solutions for Z_A can be determined adequately by the requirements that the curve cut within 0.5 charge unit of the Z of all stable odd-A nuclides. A function with numerous contortions is obtained, but as would be indicated by Figure 2, one which does not depart greatly from the sweep given by equation 15. Remarkable concordance occurs among the solutions of Z_A as a function of A that are given by Bohr & Wheeler (11), Way (30), Joliot-Curie (31), Feenberg (18), and Kohman (12). Kohman used the existence of stable even-A isobars as auxiliary information.

The effect of shell closure on Z_A is discussed by Aten (32) in terms of stabilization of nuclei for about four nucleon numbers on either side of a shell number. Wapstra (33) makes a specific suggestion for the stabilizing corrections for shell closure that should be added to equation 6. He proposed empirically the terms: $-a[(Z-S_p)^2/w^2+1]^{-1}$ where S_p is a proton-shell number, with corresponding terms for neutron-shell numbers. The a value chosen was about 6 Mev and the width w about 3.5. Such corrections provide for a rounded zigzag in the Z_A curve giving qualitative approximation to the departures[9] of the smoothed "experimental" Z_A curve from the statistical function of equation 9. It is established (34, 35), however, from β-decay data that shell closure introduces real discontinuities in the Z_A function, not taken into account by the earlier workers. The ingenious Wapstra correction term would have difficulties in quantitative treatment of β-decay energies across a shell edge. The correction term should be more nearly triangular.

Local values of B_A have been derived by Bohr & Wheeler (11) and Feenberg (18). In the former study, a treatment analogous to equation 10 was used with local solution for Z_A. In the latter study, the B_A values are computed from an idealized packing fraction curve embodying a fairly complex treatment of the existence of stable nuclides and their masses. There is no evidence of an appreciable shell effect on these values, which are plotted in Figure 3. The function B_A^*, based on equation 10 with the Fermi parameters is given as the curve *FF*. The locally established values (11, 18) are given as circles.

The lines *AA* and *BB* of Figure 3 represent solutions for B_A based exclusively on decay data (34, 35). Using decay energies largely from one compilation (36), Brightsen (34) evaluated B_A and Z_A by equation 12 for odd-A nuclides of $N<50$ in the mass region 73 to 87. He considers the B_A values

[9] It is interesting to record the maxima and minima of the differences between the smoothed "experimental" Z_A values and the Fermi Z_A^* values at the corresponding mass numbers: +0.4 at 60, −0.5 at 80, +0.5 at 100, −1.1 at 132, ∼0 at 150, −0.6 at 160 rising to −0.2 at 200.

given as line AA to be reliable to about 7 per cent. An analogous treatment (35) including only even-Z odd-A nuclides above $Z=82$ and $N=86$ based on the Stern compilation (37) of masses of heavy nuclides gave the value 1.16 ± 0.16 Mev for B_A (line BB in Fig. 3), with no evidence of dependence on A in the region 209 to 243. It seems adequate for most work to take the

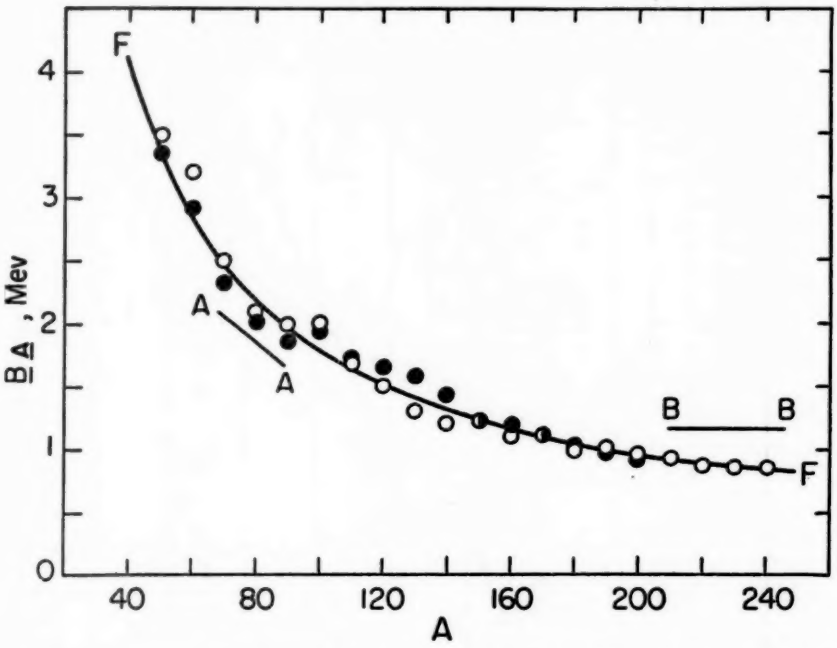

FIG. 3. Comparison of some B_A values: line FF based on Fermi parameters (17); lines AA and BB, local solutions from decay data (34, 35); ○ Bohr-Wheeler values (11); ● Feenberg values (18).

Fermi B_A* values from Figure 3, although the situation needs some clarification.

SHELL-REGULATED DISCONTINUITIES IN Z_A AND $\pi-\nu$

Discontinuities in decay energies at shell edges.—It has been foreseen that discontinuities in nucleon binding energies would be reflected in β-energetics, but the expression of the effect has only been formulated recently (34, 35, 38). If β-decay is represented in terms of evaporation of a neutron with energy effect $-B^n(Z, A)$, decay of the free neutron with energy release $M_n-M_H=0.78$ Mev, and condensation of the proton with energy release $B^p(Z, A)$, the total energy effect to be correlated with the parabolic treatment is:

$$Q^\beta = B^p(Z, A) - B^n(Z, A) + 0.78 = B_A(Z_A - Z - 0.5) \qquad 14.$$

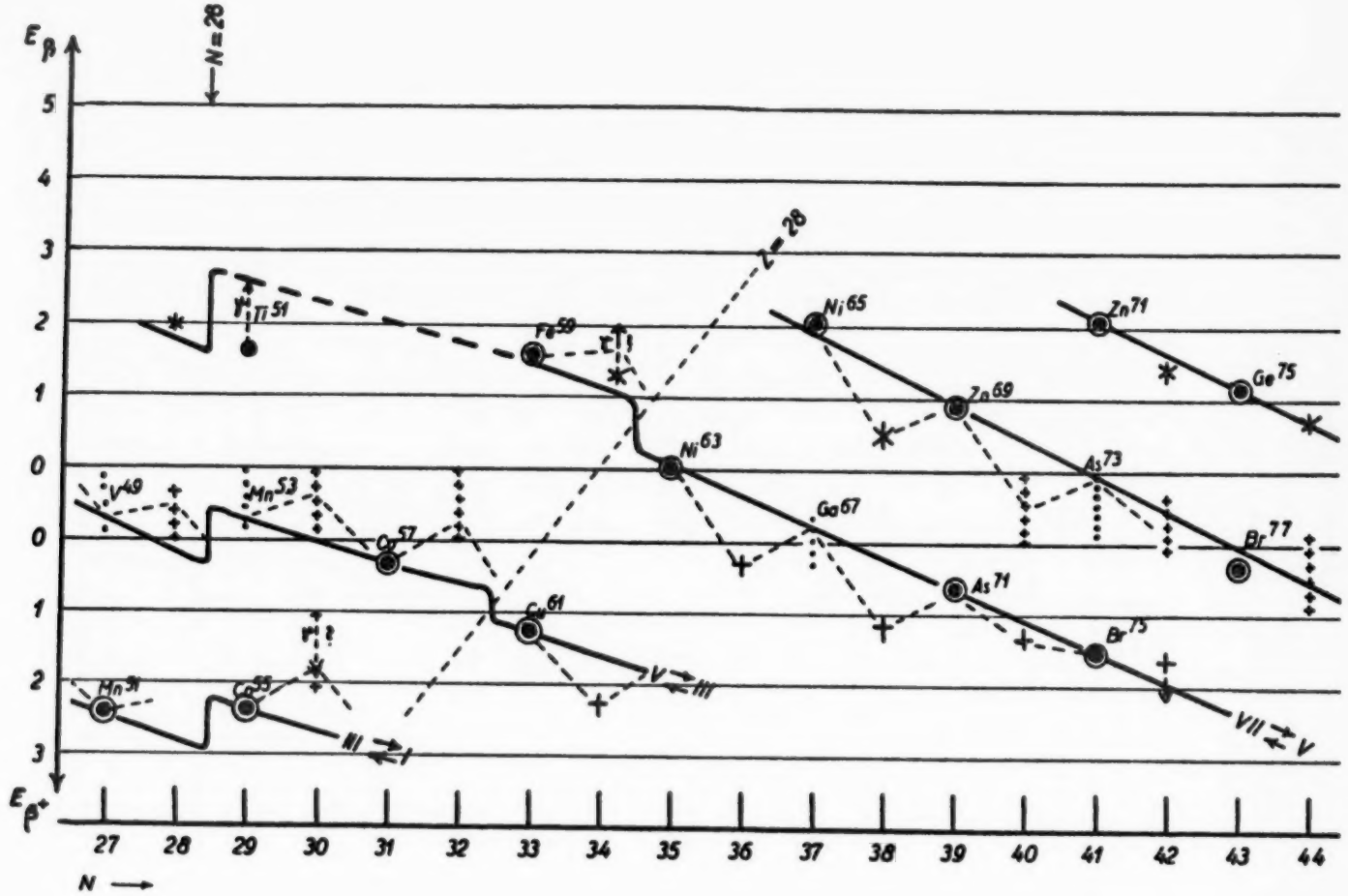
E_β
N=28
Z=28
5
4
3
2
1
0
0
1
2
3
E_{β^+}
Ti^{51}
Fe^{59}
Ni^{65}
Zn^{71}
Ge^{75}
Zn^{69}
Ni^{63}
As^{73}
V^{49}
Mn^{53}
Co^{57}
Ga^{67}
Br^{77}
As^{71}
Co^{61}
Br^{75}
Mn^{51}
Cr^{55}
V → III
III → I
VII → V
27 28 29 30 31 32 33 34 35 36 37 38 39 40 41 42 43 44
N →

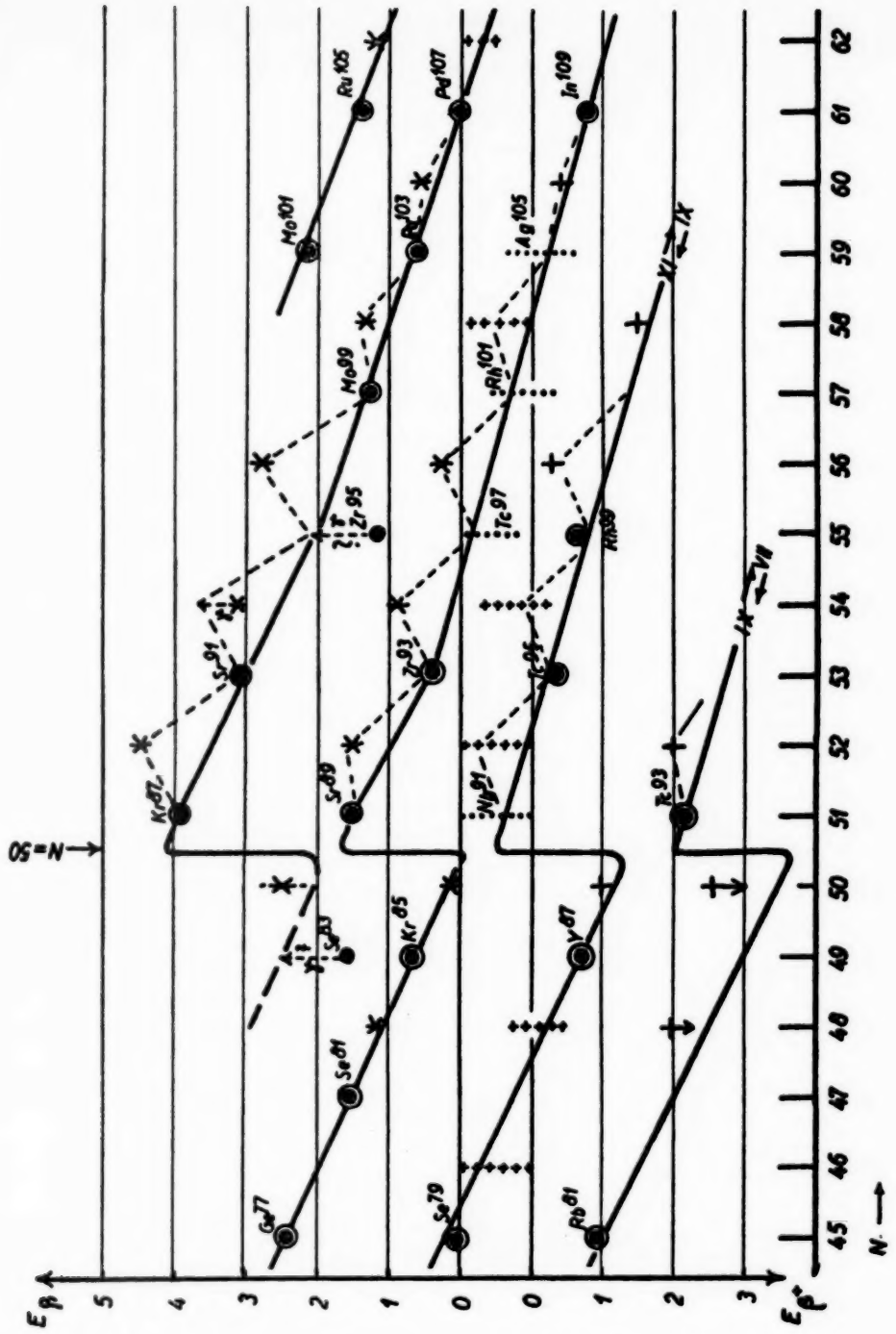

FIG. 4. Isodiapheric decay energies. Suess-Jensen plot of decay energies for sequences of constant I, identified in Roman numerals; ⊙, neutron rich member of even Z; * and +, neutron rich member of odd Z. Taken from Suess & Jensen (38).

where the right hand term is taken from equation 12 ignoring the $\pi-\nu$ effect and taking odd-A nuclides for convenience.

In traversing a mass-number sequence that crosses a neutron shell closure, B^n suffers a downward discontinuity, ΔB^n of 1 to 2 Mev, which must be reflected by a discontinuity in the right hand term of equation 14. Practically none of this is represented in B_A, as seen in Figure 3. The main effect, then, is an upward discontinuity ΔZ_A in Z_A of such magnitude that $B_A\Delta Z_A=\Delta B^n$. A similar argument shows that $-B_A\Delta Z_A\cong\Delta B^p$ when a proton shell-closure occurs in a sequence, causing a downward discontinuity in Z_A.

There has been some uncertainty in the behavior of B^n just before and just after shell closure. The detailed analysis of Harvey (24) gives B^n for a number of nuclides with N values near 50 and near 126. These binding energies show large fluctuation with evenness of N and trends with Z for given N. These perturbations can largely be removed by subtracting the neutron binding energies computed (21) from equation 6 with the Fermi parameters. Harvey (24) has done this and has plotted the difference in Figure 8 of his paper. This plot provides reasonable evidence, especially at the 126 shell, that the trend in B^n corrected for pairing and charge is not greatly changed on crossing the shell edge. The change in the slope $\partial B^n/\partial N$ thus corrected, will be taken up in equation 14 by a difference in the Z_A slope $\partial Z_A/\partial A$. It is to be expected that B^p will show very similar behavior in sequences crossing a proton shell closure. The important point to be recognized is that the shell effect in binding energy and in decay energy is not apparent on comparison with neighboring nuclides unless the shell edge is crossed.

Suess & Jensen (38, 39) have developed an informative correlation of decay energies with nuclear composition in a plot of the decay energies in sequences of isodiapheres (nuclides with constant neutron excess $I=N-Z$). A section of their plot is shown in Figure 4, taken from their graphical treatment (38) extending from $A=1$ to $A=215$ based on the data compiled by Way and co-workers (40). In negatron decay, I increases by two. Various I sequences are identified by Roman numbers for I values of the parent and daughter. The β-decay energy (ordinate) of successive members of the sequence decreases with increasing N numbers shown as abscissa, until the decay reverses direction as electron capture (generally of uncertain decay energy indicated by a long ordinate spread) and ultimately decay by positron emission occurs. The energy scale is represented as Q^β and $E_d^{\beta+}$ in Mev separated by the 1.02-Mev threshold for positron decay. The chemical symbols identify the species undergoing decay designating members with odd-N (even-Z) on the neutron-rich side. The curves are fitted to these points.

The most striking feature of Figure 4 is the general regularity of the slopes and spacing of successive lines, which gives strong support to the parabolic picture. The second is the dramatic discontinuity in the curves for the shell crossings. The offsets give directly ΔB^p and ΔB^n, and they support

the conclusions given above about the nature of the shell effects. The third is the discrepancy occurring in some regions between even-Z points (circles) and odd-Z points (crosses), pointing to appearance and disappearance of appreciable $\pi-\nu$ effects.

Difference in spin terms for odd protons and neutrons, $\pi-\nu$.—Before further analyses are made of the Z_A function, it is now necessary to handle the difference in pairing energy of protons and neutrons, identified since equation 7 as the $\pi-\nu$ effect.[5] The first reference to this in experimental material is by Glueckauf (41) who analyzed β-decay energies for mass numbers 219, 221, 233, and 239. He found a systematic odd-even effect amounting to a stabilization of even Z by 0.2 Mev compared to odd Z. Kowarski (42) showed that this type of explanation is required to explain the absence of stable isotopes of technetium and promethium. Suess (43) analyzed the situation quantitatively for these missing elements, showing that the odd-Z points in the isodiapheric sequences just above $N=50$ and $N=82$ lie about 0.7 Mev above the even-Z points. This offset, which is apparent also in Figure 4, corresponds by equation 12 to $2(\pi-\nu)$ for these regions. Kohman (44) has independently come to the same conclusion. An analysis (35) of the data for nuclides with $A>208$ shows that this effect persists for all six odd elements after the $Z=82$ and $N=126$ shells, from astatine through americium, with the $\pi-\nu$ value of 0.16 ± 0.05 Mev independent of Z. The plot of Suess & Jensen (38) shows that it fades out with rhodium or silver following the $N=50$ shell (Fig. 4), and that it is not apparent after promethium following the $N=82$ shell. Consideration of the charge statistics of odd-A nuclei (44, 45) would suggest that the effect is not omnipresent, and indeed that it has the opposite sign near $A=37$ and $A=67$. Suess & Jensen indicate tentatively (38) that $\pi-\nu$ is first apparent as a positive term for $20<Z<28$, that it is negative just above $Z=28$, positive for a few elements above $N=50$ and $N=82$, and also positive just before $Z=50$ (indium), and negative for antimony ($Z=51$) compared to tin and tellurium.

The $\pi-\nu$ effect is readily seen by plotting odd-A decay energies against N or A for isodiapheric sequences (38), as displayed in Figure 4. The odd-Z β-emitters exhibit a decay energy differing by $2(\pi-\nu)$ from the interpolated values for their even-Z neighbors. A second method of analysis involves plotting the odd-A decay energies for the isotopes of a series of elements against N or A (46). The decay data fall on parallel lines, as predicted by equation 12, but the lines for the odd-Z elements are not spaced evenly between those for even-Z elements if $\pi-\nu$ is not zero, the departure from equal spacing being $2(\pi-\nu)$. Another method of analysis (35, 45) is to define an effective Z_A^e or Z_A^o for even-Z or odd-Z elements, respectively, by ignoring $\pi-\nu$ in equation 12. These differ from the true Z_A by $-(\pi-\nu)/B_A$ and $+(\pi-\nu)/B_A$, respectively. This method is of low sensitivity if B_A is large.

The presently available numerical results for $\pi-\nu$ in different regions of nuclides are given in Table I, based on the analyses of two sets of workers

(35, 38) using principally the decay data of Way and co-workers (40). The first set of workers (35) only took into account decay data with fairly well established decay schemes to obtain the most reliable set of decay energies. It should be stated that the $\pi-\nu$ effects in Table I are for convenience listed for odd-Z elements in reference to their even-Z neighbors, although both odd-Z and even-Z decay energies are influenced by the effect (equation 12). Bold-face values are considered more reliable in this review.

TABLE I

ANALYSIS OF EXPERIMENTAL β-DECAY DATA FOR $\pi-\nu$ EFFECT (ϵ_A*)

Nuclide Region	$\pi-\nu$ (Mev) $=\epsilon_A$	Reference	Comments
$Z<20$	-0.7	(45)	Difference between Z_A^e and Z_A^0
$Z>20$, $N<28$	$+0.3$	(38)	Three points
	~ 0	(35)	$Z_A^e=Z_A^o$, five points
$Z<28$, $N>28$	$\sim+0.4$	(38)	No explicit data
	no effect	(35)	No evidence, two points
$Z>28$, $N<50$	Cu, Ga: -0.4	(38)	Four points; effect small for As
	Cu, Ga: **-0.3**; As, Br, Rb: **-0.1**	(35)	Two sets of four points
$Z<50$, $N>50$	Rb, Y, Nb, Tc: **$+0.4$**	(38)	Seven points; corroborated by (35) assume Rh**$+0.2$**, rest **zero**
$_{49}$In	$+0.5$ (38); small	(35)	Three points ($In^{115, 117, 119}$)
$Z>50$, $N<82$	Sb -0.4, rest zero	(38)	Sb^{127} $Q^{\beta-}$ 1.1 (38) or 1.9 (35)
	no effect	(35)	
$Z>50$, $N>82$	La, Pr, Pm **$+0.35$**	(38)	Four points; corroborated by (35) assume Eu 0.2 rest zero
$63<Z<82$, $N<126$	no effect	(38)	
$Z>82$, $N>126$	$+0.1$ (41); **$+0.16$**	(35)	Effect holds from Bi through Am.

* The $\pi-\nu$ effect is cited here conventionally in connection with the decay of an odd-Z element with respect to its even-Z neighbors; it also is associated with the adjacent even-Z elements. Compare also footnote 5.

There is no significant $\pi-\nu$ effect apparent in the region $155<A<208$, although good data are rare. After the almost coincident closure of the $Z=82$ and $N=126$ shells, the effect of 0.16 Mev occurs, persisting constantly through $Z=95$ rather than fading out as previous ones do.

Suess & Jensen (38) used their observations of the occurrence of the $\pi-\nu$ effect to propose a rule: "Each time a nucleon number crosses the magic number 28, 50, or 82, the pairing energy of this type of nucleon is smaller than that of the other type." They ascribe this to the drop in pairing energy

on going at high orbital moment from parallel spin-orbit coupling to antiparallel coupling. In this regard the 20-shell is different, as it is followed by the parallel spin-orbit coupling of the $f_{7/2}$ orbit. The analysis of this review in Table I negates this rule for the Z-shells 20, 50, and 82 (perhaps overridden by the $N=126$ shell effect), and the $N=28$ shell. Kohman (44) has examined several possible quantum mechanical explanations of the effect without accounting for the magnitude of the effect.

The typical course of Z_A and its discontinuities.—The prediction of Z_A is a matter of great interest in the correlation of β-decay energetics. Considerable clarification was introduced by the discovery[10] of Brightsen (34) of the shell-regulated discontinuities in the Z_A-A curve. The mode of attack used by Coryell, Brightsen & Pappas (35) can be described by a modification of equation 12 for odd-A nuclides:

$$Z_A^e = Z_A - (\pi - \nu)/B_A = Q^{\beta}/B_A + Z + 0.5 \qquad 15.$$

for Z even, with a corresponding equation for Z_A^o with reversed sign of the $(\pi-\nu)$ term. A careful analysis was made of Q^{β^-} values (36, 37, 40) for species of reasonably reliable decay scheme, using also *ft* analyses (2) for corroboration. The data for even-Z elements were treated by equation 15 to establish Z_A^e values, and the data for odd-Z elements were treated similarly to establish $\pi-\nu$ from the $Z_A^e-Z_A^o$ difference, the results of this analysis having already been presented in Table I. The values of B_A were taken from an adaptation of equation 10 using Fermi's value of 78.0 Mev for $M_n-M_H+a_3$ and a trial value of Z_A based on the existence of stable odd-A nuclides of the same shell-type in the neighborhood. The Z_A values from the various decay data are plotted against A together with vertical lines for stable odd-A nuclides of length $1.0\pm2(\pi-\nu)/B_A$ centered at the Z value of the stable nuclide.

A typical example of such a plot is given in Figure 5. The decay data on the figure are identified by element symbol, those below the curve being for β^--decay of even-Z elements, and those above the curve for odd-Z elements. Electron-capture decay data are distinguished as squares. The mass number is apparent from the abscissa. The stable nuclides are identifiable from ordinate Z and abscissa A. Data applying to the various shell regions are distinguished by filled or open symbols. In Figure 5 are included all reliable data from $A=115$ to $A=150$. In this sequence, two shell edges are crossed: $Z=50$ and $N=82$. The region of pronounced $\pi-\nu$ effect above $N=82$ is displayed [$\pi-\nu=0.35$ Mev, $(\pi-\nu)/B_A=0.27$], the points corrected for $\pi-\nu$ effect having crosses superimposed.

As may be seen, it is quite important to treat separately the various shell regions. Having done this, it is found that there is practically a unique solution for a smooth Z_A curve of small downwards concavity to pass among the

[10] This discovery is probably implicit in the independent analyses of Suess & Jensen (38, 43) of β-energetics.

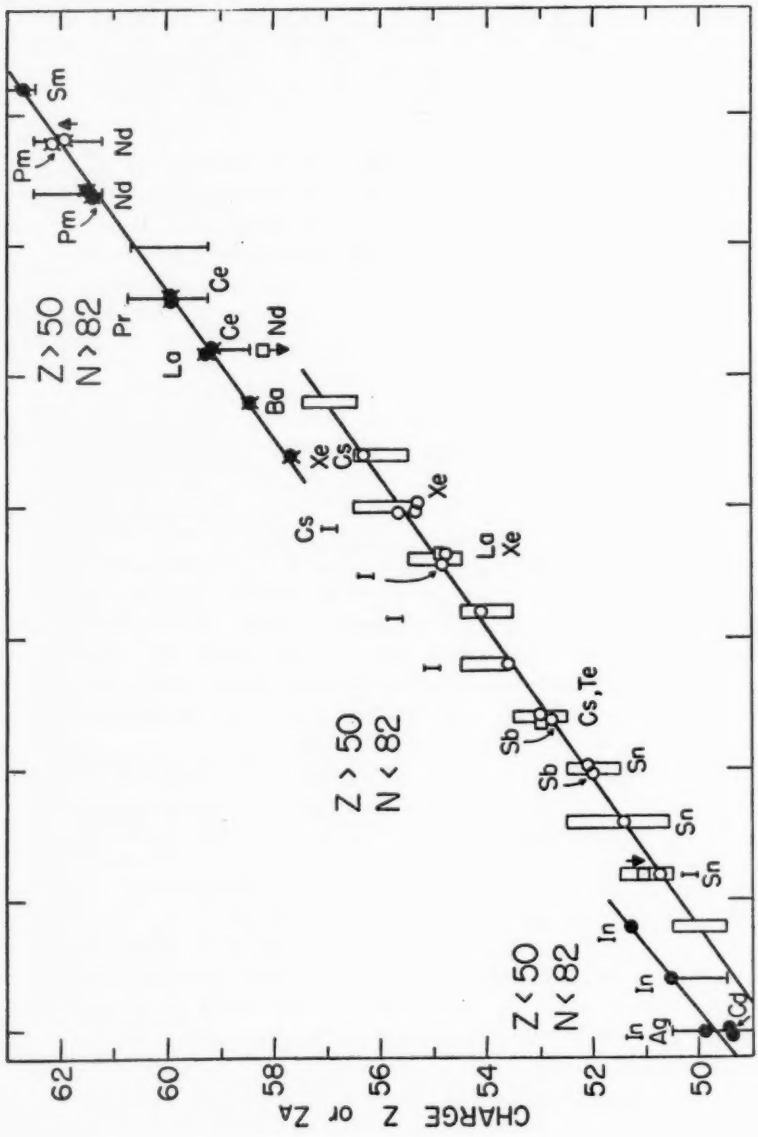

FIG. 5. Analysis for Z_A as function of A. I or □, stable odd-A nuclides; ●, ○, Z_A from β^--decay; □, Z_A from positron emission. Odd-Z β^- decay identified by element symbol above the curves, even-Z by element symbol below the curves.

points and cross all the lines for the stable odd-A nuclides. Indeed, it was found in the extended analysis (35) of the whole system of nuclides that Z_A is essentially linear with A in all shell sections. This observation simplifies the treatment.

The Z_A line for the first section ($Z<50$, $N>50$) is supported by data as far back as $A=87$, and by data without $\pi-\nu$ correction as far back as $A=107$. The line has the slope $\partial Z_A/\partial A=0.397$, only slightly greater than that given by the Fermi parameters in equation 15. It predicts that Cd^{113} is unstable[8] to β-decay by 0.6 Mev. The data for In^{115}, In^{117}, and In^{119} show an average departure from the curve of about 0.1 Z unit, precluding the irregularity reported previously (38), cf. Table I, for the element unless the course of the curve is altered significantly.

The Z_A line for the next section ($Z>50$, $69<N<82$) correlates the experimental data quite well. The lack of systematic segregation of even-Z data from odd-Z data shows that the $\pi-\nu$ effect is negligible in this region. The line is set lower than those at either end, and its slope is 0.350. The low course of the line permits tin to be the only element with three stable odd-A isotopes. The line also indicates that Sb^{123} and Te^{123} have almost exactly equal stability and thus gives no evidence as to which should be radioactive. The drop in Z_A at $Z=50$, measured at $A=118$ (the average mass number for partition of stable isotopes between the two curves) is 1.2 charge units. Taking B_A as 1.55 Mev, the energy gap or ΔB^p in proton binding at $Z=50$ is $-B_A\Delta Z_A=1.86$ Mev.

Immediately following $N=82$, there is a pronounced $\pi-\nu$ effect, which was taken as 0.35 Mev, corresponding to $Z_A-Z_A^e=0.27$. With the corresponding correction for odd-Z elements, again it is seen that a linear Z_A curve is in good accord with the data. The slope of the selected Z_A line is 0.357, slightly lower than the Fermi slope. The discontinuity in the line from that for the previous section, measured at $A=140$, is 1.40 charge units. Taking B_A as 1.34 Mev, the energy gap or ΔB^n in neutron binding at $N=82$ is $B_A\Delta Z_A=1.8_8$ Mev.

Elements with no stable odd-A isotopes.—The upward extension of the Z_A curve for the middle section in Figure 5 would provide for the stability of Ce^{141} and Ce^{143} if the $N=82$ shell did not intervene. As the result of the upward Z_A offset at a neutron shell-edge, cerium ($Z=58$) becomes one of the four elements with no β-stable odd-A isotopes. This effect happens because of the combination of the offset and the fact that the middle Z_A curve reaches 58.0 at $A=141.7$, where N is already above 82. Thus $^{81}_{58}Ce^{139}$ is unstable to electron capture and $^{83}_{58}Ce^{141}$ must be referred to the new high-Z_A curve, corresponding to appreciable β-decay energy. This discrimination against the odd-A isotopes of an element does not happen so decisively at the other neutron shell edges, but it does make A^{39} unstable.

More interesting is the fact that the $\pi-\nu$ effect and the course of the

third section of the Z_A curve in Figure 5 co-operate to eliminate stable isotopes for promethium ($Z=61$). The two necessary conditions for such an event, as occurs also for technetium ($Z=43$), are that $(\pi-\nu)/B_A$ exceed $0.5-\partial Z_A/\partial A$ and that Z_A reach the odd charge close to an even mass number. In Figure 5, the $\pi-\nu$ effect is taken care of by lengthening or shortening the lines for the stable nuclides by $(\pi-\nu)/B_A$ and adding $\pm(\pi-\nu)$ to the decay energies. The Z_A curve is thus seen to be in complete agreement with the data, corroborating the absence of stable isotopes of promethium and suggesting comparable small decay energy for 2.7-year Pm^{147} and for Pm^{145}, reported by Butement (47) to undergo electron capture with a half life of $\sim$30 years.

The analogous treatment is equally satisfactory for technetium since Z_A reaches 43.0 at $A=98.2$ with a slope of 0.397, and $(\pi-\nu)/B_A$ is 0.22. It also explains (45) the instability of A^{37}, since Z_A reaches 18.0 at $A=38.4$ with a slope of 0.45, and $(\pi-\nu)/B_A$ is -0.16. According to Seaborg and coworkers (48), astatine ($Z=85$) may fall in the same class due to the experimental close equality of masses of At^{215} and Rn^{215}. The situation is a tight one here, since Z_A reaches 85.0 at 214.1 with a slope of 0.354, but $(\pi-\nu)/B_A$ is only 0.14 ± 0.03.

Complete analysis of Z_A behavior.—Coryell, Brightsen & Pappas (35) have carried out analyses to establish Z_A as function of A from mass 31 through mass 245. Their results are given in Table II, segregated in the different proton and neutron shells described in the first column. The third column gives Z_A values for convenient mass-numbers given in the second column. The dependence of Z_A on A is taken as linear in these ranges. The third column gives the value of B_A used in the derivation of the Z_A points from decay data; except for the last three shell groups it is taken as $78.0/Z_A$ Mev. The numerical $\pi-\nu$ values in bold-face in Table I have been incorporated into the computations. The fifth column gives the slopes of the Z_A lines $\partial Z_A/\partial A$.

All of the data for the shell groups described in Table II are not known with equal certainty. The data for the first two ($Z<20$) show bad scatter for few data, and there are also only a few experimental points for the next to the last group ($Z>82$, $N<126$). Reliable decay data are also rare for the mass-numbers 150 to 200. The high B_A value of 1.16 ± 0.15 found for the last group ($Z>82$, $N>126$) shows the uncertainty that may exist in other areas. Because of this (compare Fig. 3), B_A is taken as 1.1 Mev for $180<A<210$. The B_A values are probably reliable to only 10 per cent, but the effect on Z_A is small because of the requirements of continuity and of agreement with the occurrence of stability of odd-A nuclides. The data for mass numbers 41 to 115 and 209 to 243 are about as good as those shown in Figure 5 (115 to 150), probably reliable to ±0.1 charge unit.

Search for evidence of subshell effects.—It is interesting to consider the

TABLE II

THE SECTIONS OF THE Z_A FUNCTION AND ASSUMED B_A VALUES (35)

Shell Groups	A	Z_A	B_A	$\partial Z/\partial A$
$Z<20$, $N<20$	30	14.2_5	5.4_7	0.45
	38	17.8_5	4.3_7	
$Z<20$, $N>20$	36	17.1	4.5_0	0.45
	42	19.8	3.9_5	
$Z<28$, $N<28$	40	18.5_5	4.2_0	0.43_5
	54	24.2	3.2_3	
$Z<28$, $N>28$	52	24.1	3.2_4	0.42_4
	63	28.7	2.7_2	
$Z>28$, $N<40$	60	27.1	2.8_8	0.40_3
	74	32.7_5	2.3_8	
$Z<40$, $N<50$	74	32.7_5	2.3_8	0.38_4
	90	38.9	2.0_1	
$Z<50$, $N>50$	86	38.2	2.0_4	0.39_7
	120	51.7	1.5_1	
$Z>50$, $N<82$	120	50.4	1.5_5	0.35_0
	140	57.4	1.3_6	
$Z<64$, $N>82$	136	57.4	1.3_8	0.35_7
	156	64.5	1.2_1	
$Z>64$, $N<106$	156	64.0	1.2_2	0.37
	180	72.8	1.0_7	
$Z<82$, $N<126$	180	73.3_5	1.16*	0.33
	205	81.5		
$Z>82$, $N<126$	200	79.2	1.16*	0.32
	210	82.4		
$Z>82$, $N>126$	210	83.5_5	1.16†	0.35_4
	245	95.9		

* Assumed for consistency with the last section.

† Local solution for B_A.

effect on the Z_A curves of the shell numbers, and to look for possible effects of subshell numbers suggested by Figure 1. Scatter of the few decay data and uncertainties in B_A made it difficult to evaluate (35) the effects of the shell numbers $N=20$ and $Z=20$. The first appears to correspond to an energy offset of ~0.7 Mev and the second ~1.6 Mev. Fairly good evidence was obtained for the offsets at $N=28$ and $Z=28$ although only five decay energies were trusted (35) between these shell edges. The other shell numbers 50, 82, and for neutrons, 126, show up very clearly.

Special attention was given to the data in search of evidence for offsets at Z or $N=34$ (completion of the $1f_{5/2}$ subshell), with negative results. The same attention was paid to Z or $N=40$ (completion of the $2p_{1/2}$ subshell) also with negative results for an offset. The slope of the Z_A curve seems to fall slightly, however, near $N=40$, as indicated in Table II. This may be an arbitrary interpretation of a general small downwards concavity otherwise overlooked. Attention was also given to Z or $N=64$ (completion of the $2d_{5/2}$ subshell); no effect was apparent for 64 neutrons, but the existence of two stable gadolinium isotopes after the two for samarium and europium is taken as evidence for a fall of Z_A by 0.5 for $Z=64$. The corresponding energy effect is 0.6 Mev. A break might be expected at $N=100$, corresponding to closure of the $2f_{7/2}$ subshell. The existence of the stable isotopes ${}_{70}\mathrm{Yb}^{171}$ and ${}_{70}\mathrm{Yb}^{173}$ with 101 and 103 neutrons argues against this, as does the stability of ${}_{72}\mathrm{Hf}^{177}$ and ${}^{72}\mathrm{Hf}^{179}$. The Z_A curve has, however, to have a rise in position and fall in slope in this region, which was accommodated by making a break near $N=106$ (perhaps the closure of the $2f_{5/2}$ subshell). The break is an upward offset of $\sim$0.5 charge units of $\sim$0.5 Mev, and the slope falls about 10 per cent. The last subshell break might be expected at $N=148$, corresponding to the completion of $2g_{9/2}$ after $1i_{11/2}$, but the fragmentary β-decay data in the high mass region do not give evidence of this, nor do the α-decay data (37, 48, 49).

Other workers have accumulated evidence on subshell effects. Duckworth (22) reported cusps in the mass defect curves for nuclei "magic" both in numbers of neutrons and protons. From these data he ascribes special stability (binding energy gap due to subshell closure) to the numbers 34, 40, and 58. Suess & Jensen (38) find that the slopes of their isodiapheric decay-energy curves (Fig. 4) become flatter at $Z=20$ and $Z=40$, and that they steepen at $Z=28$ and $Z=74$, little effect being apparent at $Z=50$. They ascribe these effects to irregularities in the nuclear volume not accounted for in the statistical model. Suess (50) and Brightsen (51) looked for shell influences on isotropic and cosmic abundances. Feather (52) also used isodiapheric analysis of β-decay energies to search for "magic number" effects near $A=210$.

The energetics of shell effects.—It is interesting to compare the energy offsets for the shell numbers as deduced by several sets of workers. The data are collected in Table III. The first column distinguishes the shell edge. The second gives the ΔZ_A values (35) corresponding to the data in Table II. The third gives $B_A|\Delta Z_A|$ which is the discontinuity in decay energy in crossing the shell edge, and by equation 14, the discontinuity ΔB^p or ΔB^n in proton or neutron binding, corrected for composition of the nucleus. The next three columns give the absolute value ΔQ^β of the decay energy offset in isodiapheric sequences, which can be interpreted in the same way as the data in column 3. The first set (column 4) is taken from curves in an unpublished

report of Suess (39), referring only to even-Z nuclides. The set in the fifth column is taken from the curves of Suess & Jensen (38) for even-Z nuclides, part of which are given in Figure 4, and the set in the sixth column is the corresponding one referring to the reviewer's general interpretation of the Suess-Jensen data (38) for odd-Z nuclides. There is evidence that they systematically minimized the offsets at proton shell numbers. They also give (38, p. 581) a list of energy offsets from the same curves that are consistently lower for no apparent reason: 0.6 Mev for the three proton shell effects, and

TABLE III

COMPARISON OF DISCONTINUITIES IN Z_A AND IN DECAY ENERGIES AT SHELL EDGES

Shell Edge	ΔZ_A (35)	$B_A\lvert\Delta Z_A\rvert$ (35)	ΔQ^β (39)	(Z-even) (38)	ΔQ^β (Z-odd) (38)	ΔB^n (24)	Rough Average
$Z=$ 20	∼−0.4	∼1.6	1.1	∼0.8	∼0.2	—	1.1
28	∼−0.4	∼1.1	1.0_5	∼0.6	>1.4	—	1.1
50	−1.2	1.9	1.3	∼0.7	>1.3	—	1.5
82	∼−0.7	∼0.8	—	—	—	—	(1.5)
$N=$ 20	∼+0.16	∼0.7	1.1	1.3	∼1.3	—	1.1
28	∼0.3	1.0	1.1	0.9	∼0.9	—	1.0
50	0.9	1.8	1.5	2.0	∼2.8	2.2	1.9
82	1.4	1.9	1.2	1.9	∼2.6	—	1.8
126	∼1.0	∼1.1	—	—	—	2.2	(1.8)
$Z=$ 64*	∼−0.5	∼0.6					
$N=$106*	∼0.5	∼0.5					

* Subshells rather arbitrarily introduced (35).

1, 0.7, 0.8, and 1.8 for the four neutron shell effects, respectively. In the seventh column are given the values for ΔB^n corrected by the statistical computations (21) for charge and spin effects, taken by the reviewer from Harvey's Figure 8 (24). These data should be comparable with the others from decay.

It should be noted that the average of columns 5 and 6 should be used to compare with column 3 or 7 because the $\pi-\nu$ effect operates on even-Z nuclides as well as odd-Z ones, and columns 3 and 7 are corrected for spin effects. Comparison of column 4 with column 5 indicates the latitude in treatment of the isodiapheric decay sequences. The differences come largely from differences in slopes according to the weighting of experimental data.

It should also be pointed out that Suess (39) used a statistical parameter corresponding to $a_3 = 69.5$ Mev (10 per cent below Fermi), which tends to regularize the slopes of various curves and to give them a reasonable curvature from the effect of $\partial B_A/\partial A$ on decay in the isodiapheric sequences. The data in the third column are poor for $Z = 20$ and $N = 20$, being more sensitive to the differences in shell offsets. The same is true for $Z = 82$ and $N = 126$ because the offsets occur close together in the nuclide system and tend to neutralize each other. Feather (52) concludes that the neutralization is complete. It is probably for this reason that the discovery of shell offsets in β-decay was not made much earlier.

The comparisons of Table II indicate that the evaluation of energy offsets at the shell edges is still in a rather unsatisfactory state. This is more surprising since the majority of the data have been taken from the same compilation (40), but it shows how unreliable much of the data is and how much freedom remains in interpolation and extrapolation. The last column in Table III gives a rough average of the values in the five previous columns. The high value from Harvey for $N = 126$ is used to obtain a value for $Z = 82$ consistent with the difference in the $Z = 82$ and $N = 126$ values of $B_A|\Delta Z_A|$.

The δ_A Effect and Even-A Nuclides

The treatment of even-A nuclides is formally the same as that for odd-A nuclides, with the large positive term δ_A taking the place of the small term $\pi - \nu$ of variable intrinsic sign in equation 12. Since the δ_A term is so prominent, attention was first given to odd-A nuclides to establish Z_A and B_A as a function of A. Two principal methods are now available to establish δ_A, one depending on establishing limits from the existence of stable even-A nuclides, and the other on the quantitative interpretation of β-decay energies for even-A nuclides.

The first method was used by Bohr & Wheeler (11), taking accessory information for heavy nuclides from decay energies. It was used with detailed exposition by Feenberg (18). Kohman (12) also used this principle to obtain from the occurrence of stable even-A nuclides secondary lines of stability separated by $\pm\delta_A/B_A + 0.5$ from his smoothed Z_A curve. The requirements for stability of any even-A nuclide with respect to β-decay or electron capture are:

$$\begin{aligned} \delta_A/B_A &> |Z_A - Z| - 0.5 \quad (Z, A) \text{ stable} \\ \delta_A/B_A &< |Z_A - Z| - 0.5 \quad (Z, A) \text{ unstable} \end{aligned} \qquad 16.$$

Above mass 90, B_A has become small enough (< 2.0 Mev) for the data to give fairly informative limits on δ_A/B_A. The term δ_A/B_A must lie above 1.50 in regions where triple stable isobars are found and below 1.50 in regions where single stable isobars are found; in addition, Z_A must be close to an even number for either of these special types of isobarism to occur.

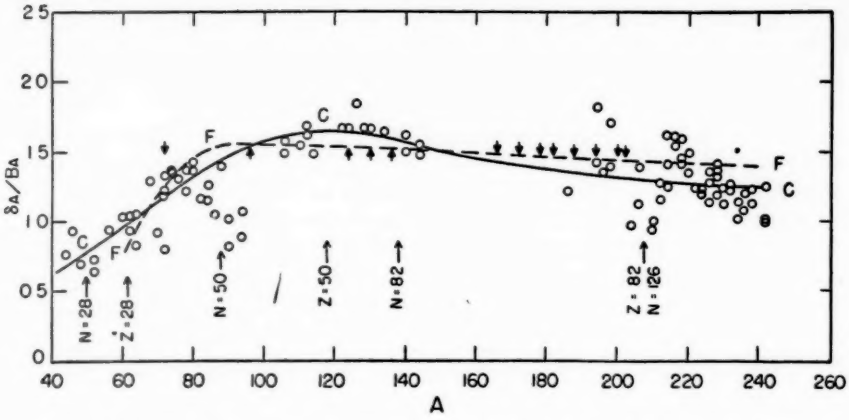

FIG. 6. Analysis of even-A decay data for δ_A/B_A. Line *FF*, Feenberg analysis (18) from occurrence of stable nuclides; Line *CC*, Coryell analysis (53): arrows up, occurrence of triple stable isobars; arrows down, occurrence of single stable isobars; proton and neutron shell numbers are noted.

In the neighborhood of a shell edge, however, the Z_A offsets may lead to the occurrence of only one stable nuclide for given A (e.g., Ce^{140}, Fig. 5). Supposing a stable even-A nuclide has a shell number S_n of neutrons. The nuclide $(Z-2, A)$ has S_n+2 neutrons corresponding to control of decay by the higher Z_A line for β-decay and the nuclide $(Z+2, A)$ has S_n-2 neutrons corresponding to the lower Z_A line. If Z were somewhat less than Z_A of the upper Z_A line, the nuclide $(Z-2, A)$ would be unstable to β decay, and if Z were also somewhat more than Z_A of the lower line, the nuclide $(Z+2, A)$ would be unstable to electron capture. This situation appears to prevail for $Cr^{52}(24, \mathit{28})$, $Sr^{88}(38, \mathit{50})$, $Zr^{90}(40, \mathit{50})$ and $Ce^{140}(58, \mathit{82})$, where proton and neutron numbers are given in parentheses with shell numbers italicized. A corresponding argument holds for stable even-A nuclides with S_p protons and the proper relation of Z to the Z_A lines, probably as exemplified by $Ni^{60}(\mathit{28}, 32)$, $Ni^{62}(\mathit{28}, 34)$, and $Sn^{118}(\mathit{50}, 68)$.

The second method becomes more instructive as more reliable β-decay data become available, and the utility of δ_A in predicting decay data will be apparent from the reliability of its determination. It is based on equation 11:

$$\mp \delta_A/B_A = Q^\beta/B_A + Z + 0.5 - Z_A. \qquad 17.$$

Numerical values for δ_A.—An extensive treatment by equation 11 has been given (53) for the data in the standard compilations (36, 37, 40) using the Fermi B_A up to mass 170 and the value 1.16 Mev beyond, as calibrated in the heavy mass region (35). The computed δ_A/B_A values for decays that seemed to be reasonably well known are plotted in Figure 6 against A extend-

ing from 40 to 242. There is considerable scatter among the data, the worst being for the low points near $N=50$ and near $Z=82$ and $N=126$. Gross perturbations are not apparent at $Z=50$ or $N=82$. Translated to energy terms, the scatter of the 22 points in the region $40<A<80$ corresponds to an average deviation of 0.32 Mev from the solid curve *CC* through the data, and the scatter in the 37 points in the region $210<A<240$ corresponds to an average deviation of 0.16 Mev from the same curve.

The solid line *CC* in Figure 6 is that drawn by Coryell (53) through the data. The broken line *FF* is that given by Feenberg (18), based on the occurrence or nonoccurrence of stable nuclides and the β^- and β^+ decay data for Cu^{64} and As^{74}. The solid black arrows pointing upwards represent the four cases of triple stable isobars, and the nine solid black arrows pointing downwards represent the cases of only one stable isobar, other than the cases related previously to shell edges. These arrows put limits on the crossing of the ordinate 1.50. It is clear that δ_A/B_A lies above 1.50 only in the region $\sim 90<A<\sim 150$. There is an unfortunate gap in the decay data from $144<A<186$, but it seems that δ_A/B_A should fall far enough below 1.50 after $A=144$ to prevent difficulties with isobarism. More data will be required to give reliability to the curve in this region. It may be noted that curve *CC* has no conflict with the data on stable nuclides that curve *FF* does not also have. It is proper, then, to judge it on the fit to the numerous energies, few of which were available when Feenberg carried out his analysis.

While all the decay data in Figure 6 may not be fully reliable, enough of them are to prove that δ_A is erratic and that it may be shell influenced. Analyses by Way (46) of data on proton and neutron binding energies just above Pb^{208}(*82, 126*) show also that unpaired protons or neutrons unexpectedly interact with their opposites or with a few pairs of their opposites in a way that would lower δ_A.

Various authors use different B_A values to compute δ_A. The different sets for rounded A values are collected in Table IV. The second column gives the values from the approximate formula given by Fermi (17), namely $\delta_A=2\delta=67/A^{3/4}$ Mev. The third column gives the values of Bohr & Wheeler (11), the numbers in parentheses being interpolations. The fourth column is based on values of δ_A/B_A taken from Feeenberg's Figure 5 (18) and computed to δ_A with his B_A values ($2\alpha/A$ mmu in his nomenclature, with α from his Table VI). The fifth column is based on the solid curve in Figure 6 with the B_A values presented in Table II.

The data in the last column are close to those in the third in the early part of the table and slightly above those in the fourth in the later part of the table. There is no question but that the power term of column 2 gives a poor representation of the situation. It is also clear that there is some flexibility in fitting the data. It may be that δ_A is too capricious a function of nuclear structure to be properly treated in this manner. The uncertainty or

TABLE IV

COMPARISON OF VARIOUS δ_A VALUES REPORTED

A	δ_A IN MEV			
	Fermi (17)	Bohr-Wheeler (11)	Feenberg (18)	Coryell (53)
40	4.22	—	—	2.5
60	3.20	$2._8$	1.9_3	2.7
75	2.63	$(2._7)$	2.8_8	2.8_4
100	2.11	$2._6$	3.0_3	2.8_4
125	1.79	$(2._0)$	2.0_8	2.4_5
150	1.56	$1._5$	1.8_3	1.8_6
175	1.38	(1.2_5)	1.5_5	1.6_2
200	1.25	$1._1$	1.3_4	1.5_3
225	1.15	(1.0_5)	—	1.4_7

indefiniteness in δ_A may add 0.2 to 0.4 Mev uncertainty to predicted decay energies of even-A nuclides.

PRACTICAL APPLICATIONS

Many workers are interested in a bold prediction of the total β-decay energy Q^β of unknown nuclides, or in a check evaluation of the parameters presented here. The procedure recommended by the reviewer for even-A nuclides is to apply equation 11 taking Z_A from Table II, B_A from Table II or Figure 3, and δ_A from Table IV. The procedure recommended for odd-A nuclides is to apply equation 12 with the same source for Z_A and B_A values, taking $\pi-\nu=\epsilon_A$ from Table I. Negative β-decay energy of species (Z, A) corresponds to electron capture with positive Q^K for the species $(Z+1, A)$.

Seventeen odd-A nuclides of reliably known decay energies (40) were taken over the region from S^{35} to Eu^{155}, with equal distribution for even and odd Z. The average deviation of the predicted decay energies from the observed was 0.40 Mev. Discarding the values for S^{35}, Ca^{45}, V^{51}, and Eu^{155}, the average deviation falls to 0.16 Mev. Similar good agreement is found for calculations in the region of the heavy nuclides. The parameters need improvement below $A=60$, and in the region $150<A<208$. The precision of prediction for even-A nuclides is covered in Figure 6 and its discussion; it is of the order of ± 0.50 Mev.

ACKNOWLEDGEMENTS

This work was carried out with assistance from the United States Atomic Energy Commission. The author wishes to acknowledge stimulating support

received for it when he was a guest in the laboratories of Dr. Roderick W. Spence of the Los Alamos Scientific Laboratory. He also has a great debt to Dr. Katharine Way, Mr. Ronald A. Brightsen, Prof. Truman P. Kohman, Dr. Alexis C. Pappas and Dr. Hans E. Suess. Technical assistance from Miss Charleen Perkins, Mrs. Grace Rowe, and Mr. Parviz Merat is appreciated.

LITERATURE CITED

1. Konopinski, E. J., and Langer, L. M., *Ann. Rev. Nuclear Sci.*, **2**, 261 (1953)
2. Mayer, M. G., Moszkowski, S. A., and Nordheim, L. P., *Revs. Modern Phys.*, **23**, 315 (1951); see also, Goldhaber, M., and Hill, R. D., *Revs. Modern Phys.* (In press)
3. Nordheim, L. P., *Revs. Modern Phys.*, **23**, 322 (1951)
4. Mayer, M. G., *Phys. Rev.*, 1969 (1949)
5. Mayer, M. G., *Phys. Rev.*, **78**, 16, 22 (1950)
6. Haxel, O., Jensen, J. H. D., and Suess, H. E., *Phys. Rev.*, **75**, 1766 (1949)
7. Haxel, O., Jensen, J. H. D., and Suess, H. E., *Z. Physik.*, **128**, 295 (1950)
8. Hill, R. D., *Phys. Rev.*, **79**, 1021 (1950)
9. Heisenberg, W., *Z. Physik.*, **78**, 156 (1932); Gamow, G., *Z. Physik.*, **89**, 592 (1934)
10. Bethe, H. A., and Bacher, R. F., *Revs. Modern Phys.*, **8**, 82 (1936)
11. Bohr, N., and Wheeler, J. A., *Phys. Rev.*, **56**, 426 (1939).
12. Kohman, T. P., *Phys. Rev.*, **73**, 16 (1948)

12a. Johnson, W. H., Jr., *Phys. Rev.*, **87**, 166 (1952)

13. Fireman, E. L., and Schwarzer, D., *Phys. Rev.*, **86**, 451 (1952); McCarthy, J. A., *Phys. Rev.*, **87**, 194 (1952); see also, McCarthy, J. A., *Phys. Rev.*, (In press)
14. Cohen, S. G., *Nature*, **167**, 779 (1951)

14a. Ingraham, M. G., and Reynolds, J. H., *Phys. Rev.*, **78**, 822 (1950)

15. Martell, E. A., and Libby, W. F., *Phys. Rev.*, **80**, 977 (1950)
16. Mattauch, J., and Flügge, S., *Nuclear Physics Tables and Introduction to Nuclear Physics* (Verlag Julius Springer, Berlin, Germany, 1942; Interscience Publishers, Inc., New York, N. Y., 173 pp., 1946)
17. Fermi, E., *U. S. Atomic Energy Commission Document*, LADC-255 (1946); *Lecture Series on Nuclear Physics*, notes by Halpern, I. (1946); *Nuclear Physics*, notes by Orear, J., Rosenfeld, A. H., and Schluter, R. A., (Univ. of Chicago Press, Chicago, Ill., 249 pp., 1949)
18. Feenberg, E., *Revs. Modern Phys.*, **19**, 329 (1947)
19. Rosenfeld, L., *Nuclear Forces*, I (Interscience Publishers, Inc., New York, N. Y., 181 pp., 1948)
20. Pryce, M. H. L., *Proc. Phys. Soc.* (*London*), [A]**63**, 692 (1950); Green, A. E. S., *Phys. Rev.*, **83**, 1248 (1951); Green, A. E. S., Engler, N., and Marinucci, N. J., *Phys. Rev.*, **86**, 609 (1952)
21. Metropolis, N., and Reitwiesner, G., *U. S. Atomic Energy Commission Document*, NP-1980 (1950)
22. Duckworth, H. E., and Preston, R. S., *Phys. Rev.*, **82**, 468 (1951); Duckworth, H. E., Kegley, C. L., Olson, J. M., and Stanford, G. S., *Phys. Rev.*, **83**, 1114 (1951)
23. Stern, M., *Revs. Modern Phys.*, **21**, 39 (1949)
24. Harvey, J. A., *Phys. Rev.*, **81**, 353 (1951)
25. Merat, P. *Revision of the Fermi Values of the Exchange and Surface Coefficients of the Semi-empirical Mass Formula*, (Bachelor of Science thesis in Physics, Massachusetts Institute of Technology, 1952)
26. Li, C. W., Whaling, W., Fowler, W. A., and Lauritsen, C. C., *Phys. Rev.*, **83**, 512 (1951)
27. Wapstra, A. H., *Phys. Rev.*, **84**, 838 (1951)
28. Collins, T. L., Nier, A. O., and Johnson, W. H., Jr., *Phys. Rev.*, **86**, 408 (1952)
29. Wigner, E., *Phys. Rev.*, **51**, 947 (1937); *University of Pennsylvania Bicentennial*

Conference on Nuclear Physics, (Univ. Pennsylvania Press, Philadelphia, Pa., 1941)
30. Way, K., Manhattan Project Report, CP-2497 (1944)
31. Joliot-Curie, I., *J. phys. radium*, [8]**6**, 209 (1945)
32. Aten, A. H. W., Jr., *Science*, **110**, 260 (1949)
33. Wapstra, A. H., *Physica*, **18**, 83 (1952)
34. Brightsen, R. A., *The Liquid Drop Model and Nuclear Shell Structure: B. Radioactive Isotopes of Arsenic in Fission*, (Master of Science thesis, Massachusetts Institute of Technology, Cambridge, Mass., 1950)
35. Coryell, C. D., Brightsen, R. A., and Pappas, A. C., *Phys. Rev.*, **85**, 732 (1952); *Nucleonics* (in press)
36. *Radiochemical Studies: The Fission Products*, Natl. Nuclear Energy Ser., Appendix C, Div. IV, **9** (Coryell, C. D., and Sugarman, N., Eds., McGraw-Hill Book Co., Inc., New York, N. Y., 2089 pp., 1951)
37. Stern, M., *U. S. Atomic Energy Commission Document, UCRL-1728* (1952)
38. Suess, H. E., and Jensen, J. H. D., *Arkiv Fysik*, **3**, 577 (1951)
39. Suess, H. E., *Rept. Inst. Nuclear Studies Univ. Chicago Empirical Systematics of Nuclear Binding Energies* (9 pp., February, 1951)
40. Way, K., Fano, L., Scott, M. R., and Thew, K., *Nuclear Data:* Way, K., Wood, M., and Thew, K., *Natl. Bur. Standards* (*U. S.*) *Circ. 499*, Suppl. 1 (1950–51); Way, K., Fuller, G., Wood, M., Thew, K., and Jurgens, A., *Natl. Bur. Standards* (*U. S.*) *Circ. 499*, Suppl. 2 (1950–51); Way, K., and Fuller, G., Suppl. 3, (1952); see also, Mattauch, J., and Flammersfeld, A., in *Landolt-Börnstein: Zahlenwerte und Funktionen*, I, Chapt. 5, 70–181 (Eucken, A., Ed., Springer Verlag, Berlin, Germany, 1952)
41. Glueckauf, E., *Proc. Phys. Soc.* (*London*), **61**, 21 (1948)
42. Kowarski, L., *Phys. Rev.*, **78**, 477 (1950)
43. Suess, H. E., *Phys. Rev.*, **81**, 1071 (1951)
44. Kohman, T. P., *Phys. Rev.*, **85**, 530 (1952)
45. Coryell, C. D., and Suess, H. E., *Phys. Rev.*, **86**, 609 (1952)
46. Way, K. (Personal communication); Way, K., and Wood, M., *Phys. Rev.*, **86**, 608 (1952)
47. Butement, F. D. S., *Nature*, **167**, 400 (1951)
48. Seaborg, G. T. (Personal communication)
49. Perlman, I., Ghiorso, A., and Seaborg, G. T., *Phys. Rev.*, **77**, 26 (1950)
50. Suess, H. E., *Experientia*, **5**, 266 (1949); see also, Suess, H. E. and Jensen, J. H. D., in *Landolt-Börnstein: Zahlenwerte und Funktionen*, **3**, 56–58 (Eucken, A., Ed., Springer Verlag, Berlin, Germany, 1952)
51. Brightsen, R. A., *Nucleonics*, **6**, 4: 14 (1950)
52. Feather, N., *Phil. Mag.*, [7] **43**, 133 (1953); *Proc. Roy. Soc. Edinburgh*, [A]**63**, 242 (1952)
53. Coryell, C. D., *Nucleonics* (In press)

ORIGIN AND PROPAGATION OF COSMIC RAYS[1]

By Ludwig Biermann

Max Planck Institut für Physik, Göttingen, Germany

Only with the present knowledge of the nature and the properties of the primary cosmic radiation, has it become possible to arrive at detailed theories of its origin. According to the region of the universe believed to be the main place of origin of that radiation which hits the earth, these theories may be divided into three classes: solar theories, galactic theories, universal theories. It is evident that the mode of propagation of cosmic rays is very important for discriminating between these possibilities. That the propagation is affected greatly by large scale magnetic fields, is demonstrated clearly by the geomagnetic effects on the intensity of cosmic radiation. Hence the question of cosmic magnetic fields is intimately connected with that of the place of origin of cosmic radiation. On the other hand, in order to understand the existence of cosmic radiation, it no longer seems to be necessary to assume a new law of nature or special events at the time of the origin of the universe. This holds specifically for the acceleration of charged particles up to cosmic ray energies. The solar events observed by Forbush and Ehmert leave hardly any doubt that violent eruptions on the sun are sometimes accompanied by the emission of cosmic rays; it appears possible to account theoretically for these observations. Thus there is probably no longer a need for a theory of cosmic rays outside the realm of ordinary physics and astrophysics.

Properties of Primary Radiation

In this section the properties of the primary cosmic radiation are reviewed in relation to their importance for the main topic of this article. No attempt will be made to give a full account of the observations; for this we may refer to the recent articles of Peters & Elliot (1) and to the forthcoming new edition of Heisenberg (2), *Kosmische Strahlung*.

Energy and mass spectrum.—It has been known for a long time that the energy spectrum of cosmic radiation for energies higher than a certain limit is, generally speaking, of the type of a power spectrum with negative exponent; that is, that $d(\log N(>E))/d(\log E)$ is $<O$ and a slowly varying function of E, where the intensity $N(>E)$ is the number of primary particles with energy $\geqq E$ per cm.^{2} per sec. per steradian, [so that $N(>E)$ gives the integral spectrum]. It is certainly not $\sim E$, as it would have to be for a spectrum of exponential type. The lower limit referred to is, according to the more recent observations, to be discussed presently, near 1 Bev for singly charged particles.

[1] The survey of the literature pertaining to this review was concluded in April, 1952.

The primary radiation contains at most 1 or 2 per cent negative electrons, or possibly none at all, and not more than 10 per cent or 15 per cent positive particles heavier than protons. The following discussion of the energy spectrum refers (unless otherwise stated) to the primary protons.

In the energy range below 15 Bev the energy spectrum is found with the help of the Störmer-Vallarta theory of geomagnetic effects. We reproduce Figure 1 from a recent paper by Kaplon, Peters *et al.* (3). The abscissa is the logarithm of the kinetic energy per nucleon (Bev). The ordinate is the vertical intensity (cm.$^{-2}$ sec.$^{-1}$ steradian^{-1}). It is seen that the slope in the range 2 to 15 Bev corresponds to an exponent of (pc/e) of ≈ 1.1, which gives $N(>E) \sim E^{-0.9}$, whereas below 2 Bev $N(>E)$ increases slowly and apparently tends towards a limiting value. It must be remarked, however, that the value of $N(>E)$ at high geomagnetic latitudes is not so well known observationally as that at middle or low latitudes. Furthermore the geomagnetic field may be modified outside the earth to some extent by interplanetary fields and by the corpuscular emission of the sun. Both circumstances may be expected to affect the low energy part of the energy spectrum relatively more than the high energy part. Hence the exact form of the function $N(>E)$ cannot be regarded as sufficiently well known below $E \approx 1$ Bev.

For higher energies the observations of Hilberry (4) made 12 years ago, which refer chiefly to energies of order 10^{13}–10^{16} ev, point to an exponent of -1.75. Whether $d \log N(>E)/d \log E$ is a monotonic function of E (as is usually assumed) or varies to some extent, is not known with any degree of certainty. The same holds for the still higher energies up to 10^{18} ev, which, perhaps, are possessed only by nuclei of high atomic number.

Kaplon, Peters *et al.* (3) have proposed spectra of the form $N(>E) \sim (1+E)^{-n}$ both for the proton component and the heavier nuclei for which the energy per nucleon (measured in Bev) is taken as abscissa. For the protons alone Winckler's (5) measurements lead to approximately $N(>E) = 0.4/(1+E)^{1.07}$, where, on account of imperfect elimination of secondaries, n may be slightly higher and the numerical factor correspondingly lower. For all the heavier components (He, CNO group, $Z \geqq 10$) the authors find independently for the exponent n the value 1.35, which differs only slightly from the value of n for protons in the same energy range. For the group with $Z \geqq 10$ this law is supported and extended to 50 Bev /nucleon using other methods. Regarding the energy spectrum of heavy nuclei there is some disagreement with unpublished results of Dainton, Fowler *et al.* (6a), who find a somewhat higher value of n [see Kaplon *et al.* (3)]

Chemical composition of primary cosmic radiation.—Our present knowledge on this is due to the observations of tracks of cosmic ray particles in special photographic emulsions exposed in high altitudes. There are several methods to find the charge Z and the energy. If Z^2 is large enough there are produced many δ-rays, i.e., knock-on electrons along the track, the number of which per unit length of track depends only on Z^2 and on the velocity; for relativistic particles with $Z \geqq 6$ the number of δ-rays is, for tracks of normal

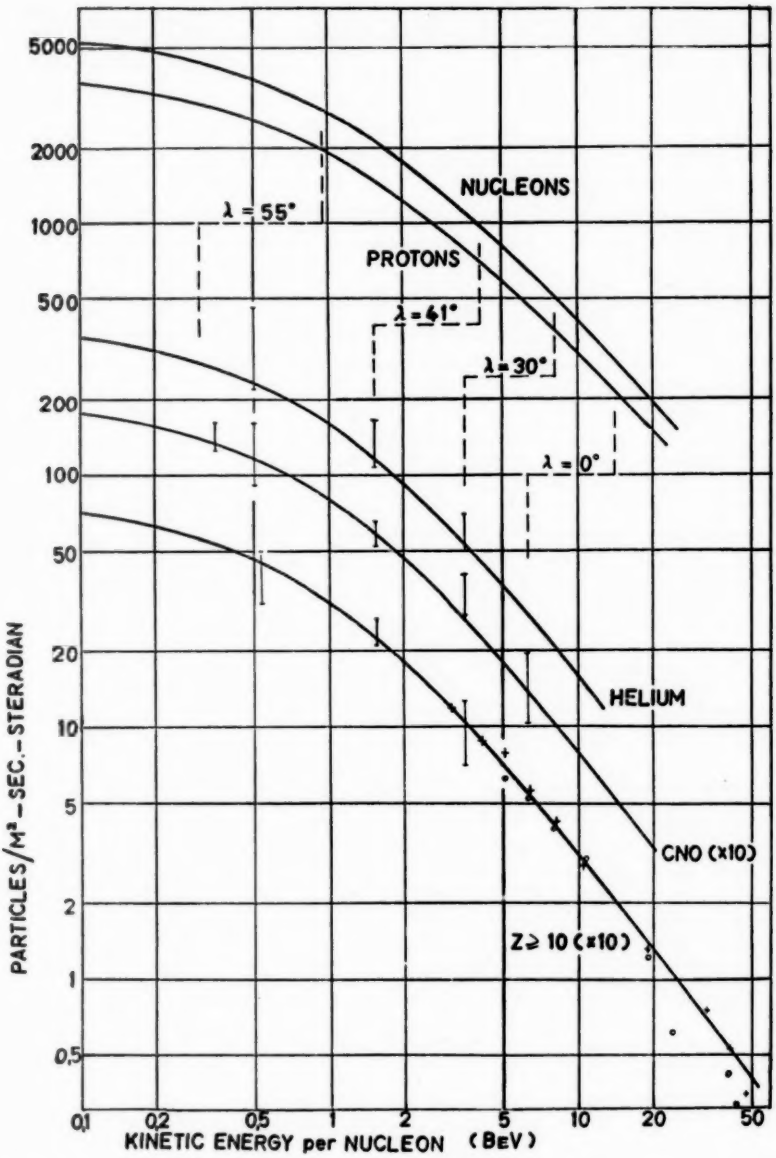

FIG. 1. Energy spectra. The limiting energies for vertical incidence corresponding to some geomagnetic latitudes are indicated by broken lines (3). The parts of the curves referring to energies below the limiting energy for 55° were extrapolated (see text)

length, sufficient to give a reliable determination of Z. The same holds for nonrelativistic particles, if the track ends in the plate. The specific ionization also depends on Z^2 and the velocity, but the grain density gives directly the energy loss only within certain limits. In sensitive plates saturation is already reached in tracks of relativistic particles with $Z \geqq 3$; therefore Bradt and Peters used stacks of plates in which sensitive and less sensitive plates are placed alternately. As a further method, the opening angle of α-particles evaporated after collisions with atoms of the photographic emulsions may be used for the determination of the energy of an incident relativistic particle. Finally, measurements of the mean scattering angle $\bar{\alpha}$ have been performed, especially by the Bristol group of observers. We reproduce Figure 2 from a paper by Dainton *et al.* (6). Later measurements by the same authors based on the tracks of many hundreds of particles fully confirm those of the paper just quoted (6a).

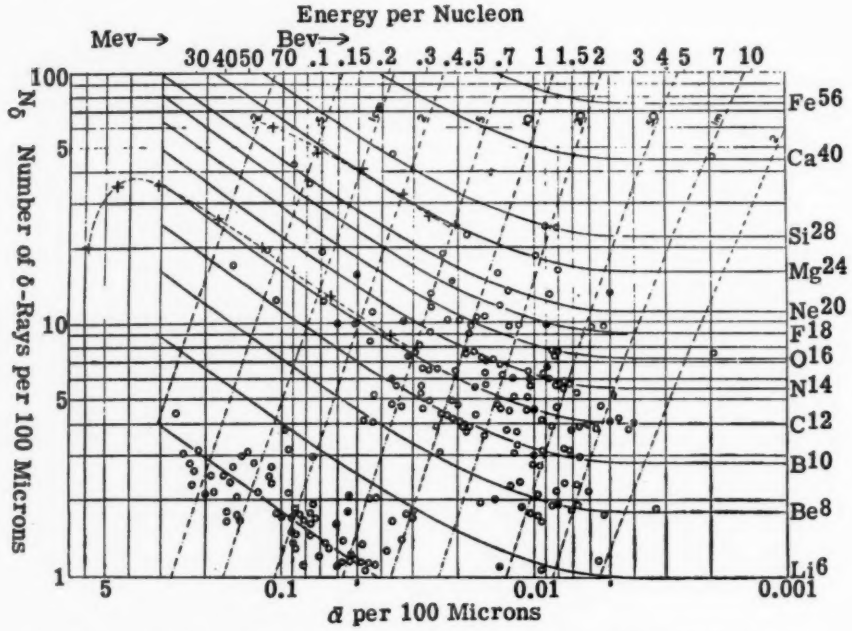

FIG. 2. Relation between $N\zeta$ and $\bar{\alpha}$ (100μ) for the tracks of 230 particles. Observations on tracks found in a systematic survey of 40 cc. of emulsion are shown thus: —○. Measurements on two tracks which terminate in the emulsion after travelling over 4 cm. in a single plate are shown thus—+---+. The full lines represent lines of constant charge, while the dashed lines are lines of constant range. An energy scale is included at the top of the figure (6).

We give now a table compiled from Tables 4 and 5 of Peters' recent review (for the last line see below), giving the vertical intensity of primary particles

at the top of the atmosphere (particles m^{-2} sec.$^{-1}$ steradian^{-1}, ϕ geomagnetic latitude).

TABLE I

VERTICAL DISTRIBUTION OF PRIMARY PARTICLES AT THE TOP OF THE ATMOSPHERE WITH DEPENDENCE ON CHARGE, Ze AND GEOMAGNETIC LATITUDE ϕ

ϕ	$Z=2$	3	4, 5	6 to 9	$\geqq 10$	
30°	60 ± 10	.	0.4	3.4 ± 0.5	1.0 ± 0.3	
41°	140 ± 30	.	.	5.8 ± 0.7	2.5 ± 0.5	According to
51°	340 ± 120	.	.	12.0 ± 3.0	3.5 ± 0.7	Peters (3)
55°	280	.	.	15.0 ± 1.5	4.5 ± 1.0	
55°		5	10 ± 1	12.0 ± 1.0	4.2 ± 0.6	According to Dainton (6a)

There seems to be no independent determination of the proton flux; this can be found at present only by subtracting the flux of particles with $Z \geqq 2$ from the total flux (section *Energy and mass spectrum*). Thus there are about ten times as many protons as heavier particles of equal energy per nucleon; at each given geomagnetic latitude however the ratio of number of protons to the number of particles with $Z \geqq 2$ is somewhat smaller (≈ 6 or 7) owing to the smaller value of m/e of the protons, which results in their being more easily deflected in the earth's magnetic field. The ratio 10:1 for protons to heavier particles seems to hold at least up to energies of some 10^{12} ev (3a).

Nuclei of charge 3 to 5 were found in large numbers by Dainton, Fowler & Kent (6, 6a) in latitude 55°. Their results, based on scattering angle measurement as well as on all the other methods mentioned before, are given in the last line of Table I. For nuclei $Z \geqq 6$ they are in reasonable agreement with the results given by Peters.

The question whether or not Li, Be, B nuclei are present in comparatively large numbers in the primary cosmic radiation, is—as will appear later—of great importance to the theories of its origin. In view of the large proportion of such nuclei among those with $Z \geqq 2$ found by Dainton and co-workers it does not appear possible to regard them as secondaries of heavier particles produced by collisions with molecules of the highest strata of our atmosphere but not recognized as such. Hence there does not seem to be any escape from the conclusion that this primary component at least at latitude 55°, is definitely present.

It may be remarked, incidentally, that the discovery of energetic heavy nuclei has practically ruled out the possibility that cosmic radiation is due to elementary acts (7).

Finally, one must examine the usual hypothesis that only completely ionized nuclei enter the earth's magnetic field from outside. Incompletely

ionized nuclei would be able to penetrate to lower geomagnetic latitudes than bare nuclei of the same energy. The observational material bearing on this question has been discussed by Peters (1), who concludes that, very probably, only bare nuclei enter the magnetic field of the earth. A partly ionized atom would lose its electrons after traversing $\gtrsim 10^{-2}$ gm./cm.^{2} with a velocity of the order of c.

Semiregular variations in time.—Most of the variations with time of the cosmic ray intensity can be shown to be simply produced by changes of the physical state of the atmosphere or of even more remote surroundings of the earth. This also holds probably for the changes connected with the ultraviolet radiation and the corpuscular emission of the sun, indicated by the variations of the geomagnetic field (2).

Apart from the sudden increases produced by eruptions on the sun, which are to be discussed in the next section, there remains only one type of variation relevant for the theory of the origin of cosmic rays, and that is the variation with sidereal time. It has sometimes been proposed that certain changes connected with solar time or with solar activity are directly produced by a solar component of cosmic radiation, but so far no definite proof appears to have been given.

From the beginning of cosmic ray research, observers have tried to find out whether or not there is a variation of cosmic ray intensity with sidereal time. Such a variation, if present, would give an indication of the degree of accuracy to which the cosmic radiation is isotropic, that is, how large the net flux of cosmic radiation is compared with its intensity outside the geomagnetic field; the direction of the flux would indicate from which parts of the universe it comes. That this problem is considerably complicated by the deflection of cosmic rays in cosmic magnetic fields was realized only in recent years. Only when there are no such fields is it possible to draw direct conclusions. One such effect discussed by Compton & Getting (8) has actually been assumed to exist for some time. If cosmic radiation were isotropic, everywhere in the universe, and if there were no cosmic magnetic fields, a slight variation with sidereal time would still result from the rotation of our galaxy, by means of which the sun is moving at a velocity of about 270 km./sec. in the direction of the constellation Cygnus. Thereby the intensity of cosmic radiation coming from this direction should be greater. The amplitude of this regular variation would be ≈ 0.2 per cent with a maximum at sidereal time 20^h40^m, in the case of no geomagnetic field; the effect of the field should be to advance the maximum by ≈ 7 hr. according to an investigation by Vallarta, Graef & Kusaka (9), who have taken $d \log N(>2)/d \log N$ to be equal to -2.

The most reliable observations discussed up to 1950 show that if there is any variation with sidereal time its amplitude is at most a fraction of 0.1 per cent. One major difficulty is that observations at one station alone are in general not sufficient to estabish the reality of the effect sought for, because of the impossibility of distinguishing a true sidereal time variation from a solar time variation modified by seasonal effects. For this it is necessary to com-

bine observations on both hemispheres of the earth or to use observations at equatorial stations. An investigation along these lines has just been carried out by Elliot & Dolbear (10), who relied largely on the observations of Forbush & Lange (11) with shielded ionizations chambers. According to the findings of these authors there is a sidereal time variation, but with an amplitude of only ≈ 0.2 per cent (that is, one tenth of that predicted by Compton & Getting (8) and Vallarta *et al.* (9) and with a maximum at about 5^h local sidereal time, which differs by about 8 hr. from the time calculated by Vallarta and co-workers for particles coming from other galaxies.

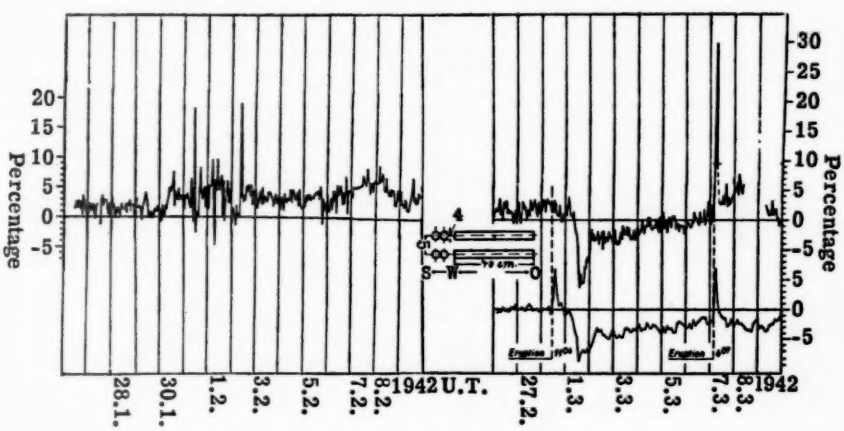

FIG. 3. Observations in February and March, 1942, by Ehmert (upper curve) and Forbush [Ehmert (13a)].

Sudden increases.—It was an old suspicion of workers in this field that sometimes the intensity of cosmic radiation increased considerably when the sun showed unusual activity. The first reliable observations of such effects were secured, however, only after a number of continuously working stations had been established, and the intensity of cosmic radiation recorded over long periods. The first modern net of such stations, working with ionization chambers shielded by 12 cm. Pb, was established by the Carnegie Institution of Washington (12) (Forbush *et al.*, beginning in 1935/36). The first station working with a counter telescope seems to have been that of Ehmert (13) at Friedrichshafen (in operation since 1940). At the present time about 20 such stations are in operation. Some of them record the intensity of the neutron component, as was first done by Adams (14) in Manchester.

In the 16 years elapsed since 1936 there have occurred four such increases, which have been observed at least three different stations. We reproduce here the following diagrams, which seem sufficient to show the essential features of the phenomenon: Observations by Ehmert (13, 13a) in Friedrichshafen (January 27 to February 9 and February 26 to March 9) and by For-

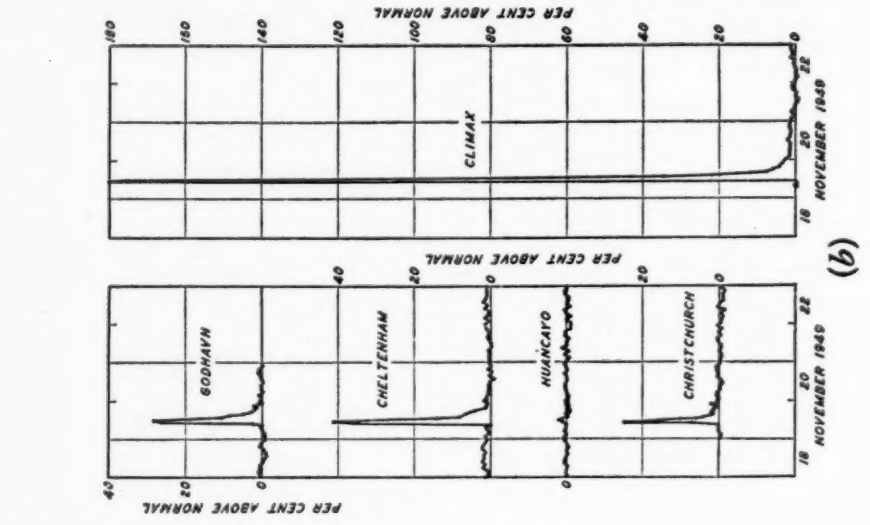
PER CENT ABOVE NORMAL
CLIMAX
NOVEMBER 1949
(b)
GODHAVN
CHELTENHAM
HUANCAYO
CHRISTCHURCH

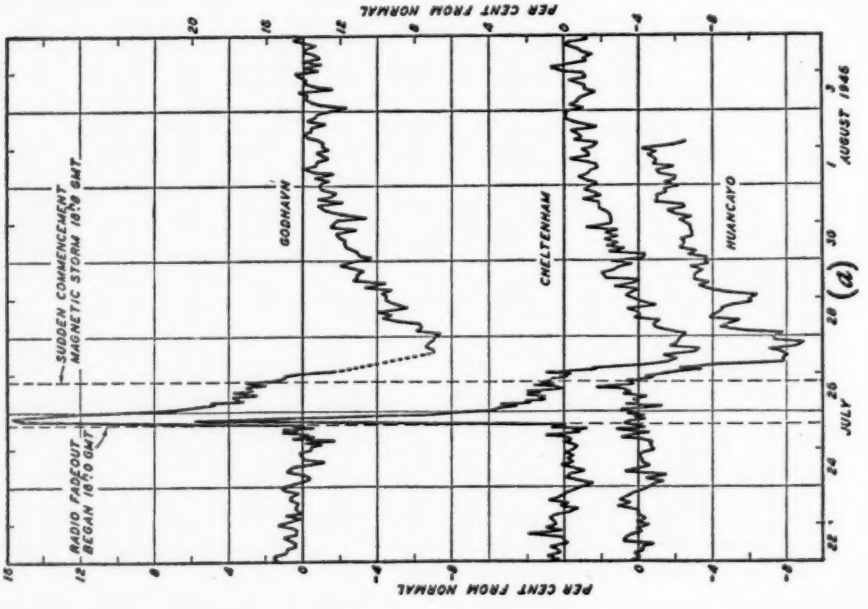
PER CENT FROM NORMAL
SUDDEN COMMENCEMENT MAGNETIC STORM 18h0 GMT
RADIO FADEOUT BEGAN 18h0 GMT
GODHAVN
CHELTENHAM
HUANCAYO
JULY
AUGUST 1946
(a)

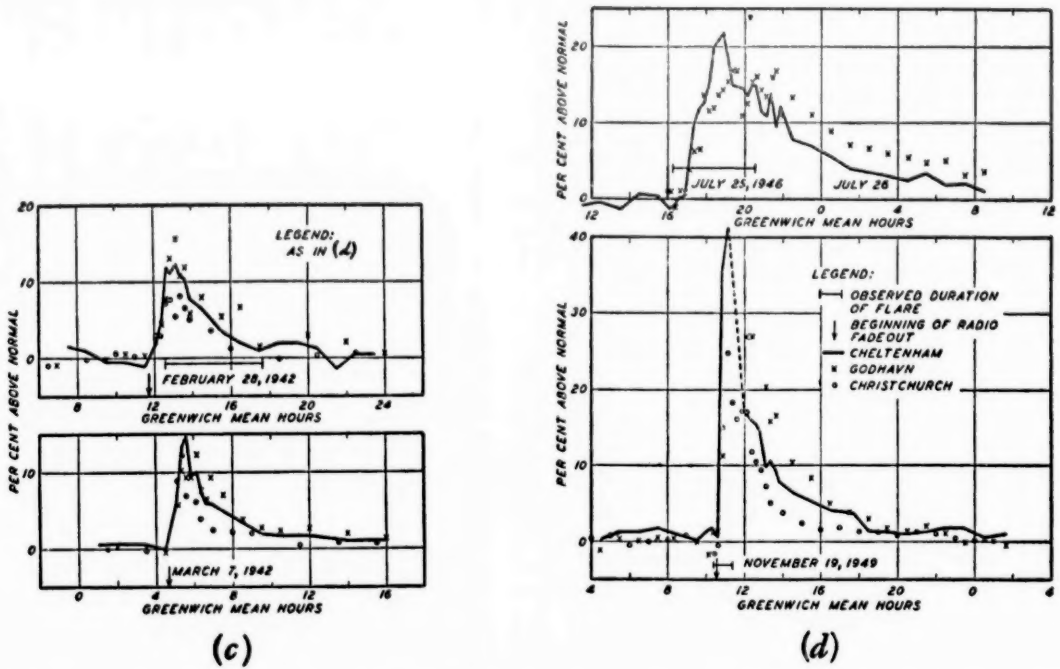

FIG. 4. Observations in 1942, 1946, and 1949 by Forbush and co-workers (12a): (*a*) increase of cosmic-ray intensity, July 25, 1946; (*b*) increase of cosmic-ray intensity, November 19, 1949; (*c*) increases in cosmic-ray intensity during two solar flares, for different stations; (d) increases in cosmic-ray intensity during two solar flares, for different stations.

bush in Cheltenham (February 26 to March 9, 1942); observations by Forbush and co-workers on five stations on November 19, 1949; observations by Adams (14) in Manchester on the same date. A further increase took place July 25, 1946.

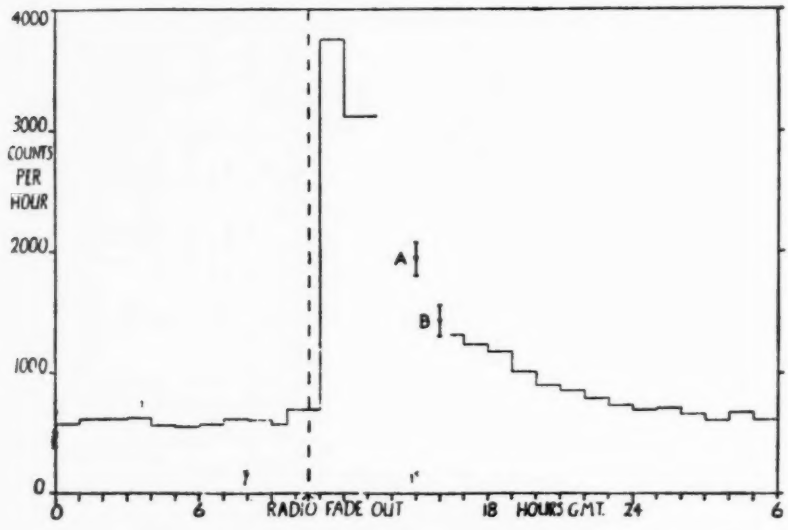

FIG. 5. Observations of the neutron component of cosmic radiation, November 19, 1949, by Adams (14).

In every case the increase took place very suddenly, i.e., in 1 or 2 hr. At sea level its relative amount at the middle or high latitude stations was of order 10 to 30 per cent, while, at Climax (at the height of 3500 m.) the increase was about five times as great on Nov. 19, 1949—observations were not made there until after 1946. But in Huancayo (3500 m., on the geomagnetic equator) on no occasion was an increase observed. The intensity of the neutron component increased on November 19, 1949, by a factor $\sim$6 and only reached again its normal value a long time after sunset (see Figure 5). On February 28, 1942, no increase was observed at the stations in Europe; also on the other dates there were marked differences between widely separated stations.

In every case there was a radio fade out (indicating an outburst of ultraviolet radiation from the sun), immediately before the cosmic radiation intensity started to increase. This fade out was caused, doubtlessly, by a violent chromospheric eruption near an active sunspot group. Furthermore observations with radio telescopes during the events of 1946 and 1949 revealed that the radio emission from the sun (not observed in 1942) increased by some power of 10. Sometimes there was a delay of up to one hour between the solar

phenomena and the variation of cosmic ray intensity, somewhat different at different localities (see the crosses representing Godhavn, Figure 4, c and d), which was, however, not clearly dependent on local solar time. When the active sun spot group as near the central meridian of the sun, as on February 28, 1942, and on July 25, 1946, a magnetic storm followed about 24^h later, which indicated a strong corpuscular emission observable only when the emitting center on the sun is favorably located relative to the earth.

From these facts the following conclusions can be drawn. During the events just described charged particles must have been accelerated to energies of some Bev per nucleon. The alternative of an indirect effect of solar wave radiation acting on the earth's atmosphere or on the geomagnetic field seems to be definitely ruled out by the large relative increases observed on November 19, 1949, in the charged component at Climax and in the neutron component at Manchester. The maximum energies cannot have greatly exceeded ≈ 10 Bev, since an increase has never been observed in Huancayo, where the limiting energy for protons arriving from the west is 10.2 Bev, according to the Störmer-Vallarta theory. Furthermore, the very high relative increase in Climax (at 3500 m.) points to a radiation of smaller average energy per particle than possessed by the normal cosmic radiation. Also the increase of the neutron component still noticeable after sunset indicates the same energy region, since protons of a few Bev are more likely to produce neutrons than mesons (15). Whether or not primary neutrons from the sun may be partly responsible for the daytime effect will be discussed later.

That in every case the increase of cosmic ray intensity has been observed in Godhavn (geomagnetic latitude 80° N.), is not so easily explained as it might seem at first. If the solar particles, say protons of some Bev, start near the celestial equator, both the equatorial as well as the polar regions of the earth are forbidden to them. This was pointed out by A. Schlüter (16), who extended Störmer's previous calculations. Godhavn, for instance, should be reached by protons starting on the celestial equator only if they have momenta below 10^8 ev/c or above 5×10^{10}ev/c. A distance of 10° or 20° from the celestial equator does not change these figures materially. Furthermore, protons of a few Bev should, in middle latitudes, arrive preferentially a few hours before noon. Since these predictions are not substantiated by the observations of 1946 and 1949, it must be concluded, that the "cosmic" ray particles of solar origin (if this inconsistency of nomenclature will be permitted) do not come directly from the sun to the earth, but travel at first to great distances from the plane of the ecliptic. The most natural (though not inevitable) explanation of this seems to be that in interplanetary space magnetic fields also exist—similar perhaps to the interstellar fields to be discussed later—, which deflect the particles of solar origin in such a way that their original starting point loses its significance.

Ehmert [(13, 13a), see Fig. 3], Clay (17), and occasionally other observers have rather often found relatively small increases which have not been

verified by observers at other stations. Although on general grounds one would expect such occurrences, their reality cannot yet be regarded as established beyond doubt.

One figure important for the theory of cosmic rays is the average production of "cosmic" rays by the sun. Ehmert (13) estimated it (1948) to be 0.1 per cent of the total intensity of cosmic radiation. Taking into consideration, however, the more recent observations, which indicate a relative intensity increase of order 10^1 or 10^2 outside the geomagnetic field, it appears that Ehmert's figure should be corrected probably by a factor of order 10. The big increases occurring on the average once in $\approx 10^8$ sec. are found to contribute alone almost ≈ 1 per cent of the total intensity of cosmic radiation. This estimate, of course, is still subject to some uncertainty.

Origin of Cosmic Rays

General survey.—The chief facts to be explained are: (*a*) the absence of a Compton-Getting effect and the smallness of the flux to intensity ratio of cosmic radiation ($\approx 10^{-4}$), (*b*) the energy density itself, which amounts to $\approx 10^{-12}$ erg/cm.^{3} and thereby approximately equals that of thermal radiation in interstellar space, (*c*) the acceleration processes observed on the sun, (*d*) the energy spectrum, (*e*) the mass spectrum of cosmic radiation and its relation to the cosmic abundance of the elements, (*f*) the absence of electrons from the primary radiation.

The nonexistence of the Compton-Getting effect (see *Semiregular variations in time*) still leaves open the possibility that the bulk of cosmic radiation arriving on the earth originates on other galaxies, but is deflected and scattered in the galaxy in such a way that the anisotropy caused by the rotation of our galaxy is completely blurred. Since there are independent astrophysical reasons for believing in the existence of extended magnetic fields in the galaxy, the hypothesis of a scattering of cosmic rays in the galaxy is not in itself improbable in any way. But the energy density of the thermal radiation of extragalactic origin ($\approx 10^{-14}$ erg/cm.^{3}) is very much smaller than that of cosmic radiation. This fact together with the observed degree of isotropy of cosmic radiation makes any theory of an extragalactic origin now appear very improbable. Hence we shall restrict the following discussions to the theory of galactic origin and to the "solar" theory, according to which the cosmic radiation observed on the earth was generated originally on the sun. It must be mentioned, however, that recent work of Biermann & Bagge (18) is related to the hypothesis of extragalactic origin; in another paper (19), it is tentatively suggested that there is a connection between the expansion of the universe and Fermi's mechanism described in section *Energy spectrum and mass spectrum.*

Both types of theories have in common the assumption that cosmic magnetic fields keep the cosmic ray particles trapped in such a way that they are deflected and scattered very often before they lose their energy in col-

lisions with other nuclei. Thus the observed degree of isotropy is explained without difficulty. Also it is easily seen that the energy density of cosmic radiation is considerably increased by this storage; in order to regard cosmic radiation as a phenomenon stationary in time, it is sufficient to assume that a very small part of the total energy output of the stars is used for the production of cosmic rays. The differences which have up to now appeared in these theories refer to the details rather than to the fundamental assumption. According to all these theories the original acceleration of the charged particles takes place in electromagnetic fields near stars, and perhaps chiefly during events of the kind observed by Forbush and by Ehmert. The theory of these events is therefore an important topic. It will even turn out that, in any case, the bulk of the energy of cosmic radiation is due to such processes.

Regarding the energy spectrum, within the frame of the "galactic" theory the interesting possibility arises that the further accelerations of cosmic ray particles, which must take place during the scattering processes already mentioned before, may play a significant role. Astrophysical evidence on the state of motion of interstellar matter does not seem to be in favor of this hypothesis, but probably it would be premature to consider the case as settled. The alternative is that the energy spectrum is essentially set up already during the primary acceleration. In both cases it must be assumed that our sun produces cosmic radiation at a rate which is far below the average in the galaxy, just as is the case, according to recent observations, for other types of nonthermal emissions, as, for instance, those in the radio frequency range.

The theory of the mass spectrum depends in a critical way on the evidence regarding the Li, Be, B nuclei in the primary radiation. The observations reported above (with the possible exception of those made at 30° latitude) fit well into the galactic theory, but here, too, some reservation of judgment seems to be indicated. This holds similarly for the absence of electrons in the primary radiation.

Cosmic magnetic fields.—Only recently has it been realized that magnetic fields are present probably everywhere in the universe where there is ionized fluid matter in motion. That this is so is based mainly on theoretical considerations, which must now be explained. We shall treat only the case of ionized gaseous matter; the analogous considerations referring to the origin of the earth's magnetic field have been worked out by W. Elsasser (20).

An ionized gas is called a plasma if the electric space charges are so small that all displacement currents and convective electric currents arising from mass motions, as well as the mechanical forces resulting from the action of the electric fields on these space charges, can be neglected. It can easily be shown that this condition usually is fulfilled in cosmic application. Furthermore, we shall give explicit equations only for the case of a completely

and singly ionized gas, for example, ionized hydrogen. The more general case of partial ionization can be treated in the same way, but the equations become rather more complicated.

An essential difficulty of the theory of rarefied ionized gases is the fact that the definition of the electric conductivity (σ) is no longer trivial as soon as magnetic fields are present. The formulation given here has been proposed by A. Schlüter (21); σ[sec.$^{-1}$] signifies the conductivity which is connected with the electron density (N) and the collision frequency (γ) in the ordinary way ($\sigma = e^2N/\gamma m_e$). It turns out that in some important cases in which the current density j[e.s.u.] may be regarded as known (e.g. those under consideration in this section), the Joule losses are still given by $(j)^2/\sigma$, even when the magnetic field associated with j compels the electrons to follow approximately close spirals around the magnetic lines of force. In such cases "impressed" electric forces (22) $\boldsymbol{E}^i$ usually appear, which may compensate part of the ordinary electric force $\boldsymbol{E}$ or of $\boldsymbol{E}^v \equiv \boldsymbol{E} + (v/c) \times \boldsymbol{H}$, the value of the electric force measured by an observer moving with the mass velocity $\boldsymbol{v}$. The field $\boldsymbol{E}^i$ summarizes the effects of the nonelectric forces on the diffusion of the electrons in terms of an equivalent electric field.

The dynamical behaviour of the plasma is then described by the following system of equations: (ρ signifies the total mass density, m_i and m_e the mass of an ion or electron, respectively, p_i and p_e their partial pressures, $\boldsymbol{g}$ the gravitational acceleration, $\boldsymbol{f}_i$ and $\boldsymbol{f}_e$ the net sums of all nonelectromagnetic forces on an ion or electron)

$$\rho(d\boldsymbol{v}/dt - \boldsymbol{g}) = -\operatorname{grad} p + (j/c) \times \boldsymbol{H} \cdots d(\boldsymbol{v})dt = \partial \boldsymbol{v}/\partial t + (\boldsymbol{v} \operatorname{grad})\boldsymbol{v} \qquad 1.$$

$$\begin{aligned} \boldsymbol{j} &= \sigma(\boldsymbol{E}^v + \boldsymbol{E}^i) \cdots e\boldsymbol{E}^i = (m_i f_i - m_e f_e)/(m_i + m_e) \\ &= (-m_i \operatorname{grad} p_i + m_e \operatorname{grad} p_e)/\rho + (m_i - m_e)(d\boldsymbol{v}/dt - \boldsymbol{g}) \end{aligned} \qquad 2.$$

$$\operatorname{curl} \boldsymbol{H} = 4\pi(j/c) \qquad 3.$$

$$\mathrm{D}\boldsymbol{H}/\mathrm{D}t \equiv \partial \boldsymbol{H}/\partial t - \operatorname{curl}[\boldsymbol{v} \times \boldsymbol{H}] = c \operatorname{curl} \boldsymbol{E}^i - c \operatorname{curl}(j/\sigma). \qquad 4.$$

The first equation determines the mass motion for vanishing viscosity, the second one the current density; the second form given for $\boldsymbol{E}^i$ holds in case that only pressure gradients, gravitation, and inertial forces contribute to the $\boldsymbol{f}$'s. These two equations, which follow from a momentum balance for both constituents, are implicitly contained in the treatise of Chapman & Cowling (23). The fourth equation is the law of induction; the operator $\mathrm{D}/\mathrm{D}t$ expresses the change of the flux through a boundary moving with the fluid. Finally, div $\boldsymbol{E}$ would be connected in the usual way with the space charges, which, however, under the assumed plasma conditions are too small to be important.

Equation 1 clarifies further the meaning of $\boldsymbol{E}^i$; it is that electromotive force, which in the absence of Joule losses causes the generation or annihilation of magnetic flux (23a). If, on the other hand, there are only such forces that curl $\boldsymbol{E}^i = 0$, it is the ordinary electric conductivity σ which determines

the time scale of the free decay of a given magnetic field. For a field of cross section Q it is order of magnitude $Q\sigma/c^2$.

This fact is of very great importance for the theory of cosmic magnetic fields, as was at first seen by Alfvén in 1937 (24). Since in interstellar gas σ is everywhere of the order of 10^{10} to 10^{12} e.s.u., even a field with a cross section of only (1 light year)$^2 = 10^{36}$ cm.^{2} decays in a time which is very large compared with the age of the universe. Therefore, once present, cosmic magnetic fields practically cannot lose their energy by Joule losses. Similarly, in the interior of a star a large scale magnetic field decays only in a time comparable with its age, as shown in detail by an investigation of Cowling (25).

This argument still leaves open the order of magnitude of the magnetic fields to be expected in interstellar gas. Here another consideration, in its first form also pointed out by Alfvén (26), is helpful. If there are irregular motions, say of turbulent character, as actually are observed in interstellar gas, then equation 3 may be interpreted by saying that the magnetic lines of force are frozen into the moving matter. As long as the magnetic field strength is small, the magnetic lines of force will be in general stretched out; to see this, it is perhaps appropriate to consider a closed bundle of magnetic lines of force, that is, a field of toroidal shape. Hence work will be done against the magnetic stresses and kinetic energy will become magnetic energy, at least as long as there is no appreciable change of the state of motion caused by the magnetic field. A little consideration shows that this may be expected to set in as soon as the densities of both forms of energy have become comparable. For this it is useful to eliminate $(\boldsymbol{j}/c)$ in equation 1 by means of equation 3.

The resulting equation contains both $\boldsymbol{v}$ and $\boldsymbol{H}$ in nonlinear terms of similar structure. For a general survey, a transformation of the equations 1 to 3, worked out by Elsasser (27), is very appropriate. For this purpose, $\boldsymbol{g}=0$, incompressibility, $\nabla\sigma=0$, and curl $\boldsymbol{E}'=0$ are assumed, and the viscosity term $\boldsymbol{v}\cdot\nabla^2\boldsymbol{v}$ is, in this case, included in 1. Putting $(1/4\pi\rho)=\lambda$ and $(c^2/4\pi\sigma)=\nu_m$, we find

$$\partial(\boldsymbol{v}+\sqrt{\lambda}\boldsymbol{H})/\partial t + [(\boldsymbol{v}-\sqrt{\lambda}\boldsymbol{H})\,\mathrm{grad}](\boldsymbol{v}+\sqrt{\lambda}\boldsymbol{H}) = -\,\mathrm{grad}\,q + \nabla^2[\nu_1(\boldsymbol{v}+\sqrt{\lambda}\boldsymbol{H}) + \nu_2(\boldsymbol{v}-\sqrt{\lambda}\boldsymbol{H})] \quad 5.$$

$$\partial(\boldsymbol{v}-\sqrt{\lambda}\boldsymbol{H})/\partial t + [(\boldsymbol{v}+\sqrt{\lambda}\boldsymbol{H})\,\mathrm{grad}](\boldsymbol{v}-\sqrt{\lambda}\boldsymbol{H}) = -\,\mathrm{grad}\,q + \nabla^2[\nu_1(\boldsymbol{v}-\sqrt{\lambda}\boldsymbol{H}) + \nu_2(\boldsymbol{v}+\sqrt{\lambda}\boldsymbol{H})] \quad 6.$$

where $\nu_{1,2}=\nu\pm\nu_m \approx \nu$ and $q=p/\rho+\lambda H^2/2$. It is seen that the equations are symmetrical with respect to the sum and the difference of $\boldsymbol{v}$ and $\sqrt{\lambda}\boldsymbol{H}$, and analogous to the ordinary Navier-Stokes equations.

Hence, according to the present ideas on the nature of turbulence (28) it may be said, that—in view of the smallness of the dissipative terms containing ν_1 and ν_2—a gaseous system obeying the equations 5 and 6 may be regarded as one with an infinite number of degrees of freedom, connected with each other by the nonlinear terms. If energy is put into the system, it will be expected under these conditions that the energy is distributed

among all degrees of freedom; in analogy to the case of ordinary turbulence, a more general kind of turbulence will result, the properties of which have to be investigated.

There is a twofold difference between the conditions considered here and those prevailing in nonconducting liquids. Firstly ν_m is very small compared with ν in interstellar space; this entails that the dissipation of energy will proceed only by ordinary viscosity. Furthermore the magnetic fields arising by the action of the impressed force (equation 2), or brought into interstellar space by corpuscular emission from stars, will be weak; energy is fed into the system practically only as mechanical energy. Hence in statistical equilibrium there will be in the average no net flow of energy from the field of mass motion (taken as a whole) to the magnetic field, or vice versa.

As long as there are only weak initial magnetic fields in the turbulent fluid, there will be a flow of kinetic energy into the magnetic field. The intensity of this flow may be found from the equation first derived by Batchelor (29)

$$\tfrac{1}{2}d(H^2)/dt = \boldsymbol{H}((\boldsymbol{H}\nabla)\boldsymbol{v}) = H^2(\partial v_H/\partial x_H) \qquad 7.$$

where the suffix H denotes a component in the direction of $\boldsymbol{H}$. That this expression is >0, as long as the $\boldsymbol{v}$ field is that of ordinary turbulence, may be seen by comparing with the analogous equation holding for (curl $\boldsymbol{v}$)^2. If the tensor field $\partial v_i/\partial x_k$ can be assumed to change randomlike after each time interval $\Delta x/\Delta v$, the increase of H^2 with time may be found to be exponential also from probability considerations (30). The stretching out of the magnetic lines of force depends only on the symmetric part of the velocity gradient tensor $\partial v_i/\partial x_k$, a purely rotational field producing no change of H^2

Regarding the nature of the final stationary state to be expected under these conditions, two different answers suggest themselves. The velocity spectrum of turbulence is contained essentially between two values, the greater of which is determined by the energy supply ϵ[erg/gm. sec.] and the dimension L_M of the mass. It measures the total kinetic energy of turbulent motion, which is of the order of $(\epsilon L_M)^{2/3}$. The lower limit v_*, on the other hand, and the corresponding length L_* are determined by the viscosity ν and by ϵ, such that $v_* L_*$ is (roughly) of the order of ν and v_*^4 of the order of $\epsilon\nu$. The general considerations outlined before would seem to make likely a final strength of $\boldsymbol{H}$ corresponding to the density of the total kinetic energy of turbulence. In this case the state of motion would be such that on the whole no further energy is fed into the magnetic field by stretching out the magnetic lines of force, while the dissipation by turbulent and ordinary viscosity goes on. But, from the formula 7 the fact emphasized first by Batchelor emerges that the large wave number components of the velocity field give the largest contribution to dH^2/dt, as long as $\boldsymbol{v}$ is not yet appreciably changed by the growing magnetic field; for all wave numbers $1/L$, the corresponding turbulent velocity v_L is of the order of $(\epsilon L)^{1/3}$, according to

the statistical theory of turbulence. This fact may be regarded as pointing to $H^2 \approx 4\pi\rho v^2$ in a stationary state.

Batchelor (29) and Chandrasekhar (31) have assumed the second alternative as likely to represent actual conditions, mainly for the reason just given, and on account of the analogy between curl $\boldsymbol{v}$ and $\boldsymbol{H}$ mentioned before, the latter author has worked out the mathematical theory in great detail, giving particular attention to the behaviour of certain invariants. Both authors assume curl $\boldsymbol{E}^i = 0$ and small scale initial magnetic fields; the initial increase of $\boldsymbol{H}$ with time is determined by equation 7.

The former alternative, originally proposed by Alfvén and by Fermi (32), was considered by Schlüter & Biermann (30) under the following aspect. For the interstellar gas it is assumed that the turbulence is maintained somehow by the differential rotation of the galaxy in accordance with the results of von Weizsäcker (33), or by this method plus corpuscular emission of stars. Every order of turbulence L gives rise to an impressed force $\boldsymbol{E}^i$ corresponding to this order, and hence after each time interval L/v_L to a magnetic field of order $(cm_i/e)\ (v_L/L)$ gauss. There are therefore initial magnetic fields associated with every wave number. It has been considered by the authors, in accordance with the general picture outlined before, that the action of the turbulence of an order L is to amplify H^2 with a time scale of order L/v_L, as long as the turbulence of this order is not affected by the growing magnetic field. Thus the large contribution to dH^2/dt of the high wave number components means that equality of turbulent and magnetic energy is first reached in the highest wave numbers, near $1/L_*$ and then gradually in those corresponding to larger values of L. With the simplifying assumption suggested by equation 7 that this increase is exponential, with the time scale L/v_L, and using numerical values as observed in interstellar gas, it is found that at the present time H^2 should correspond to $v_L \approx 10^6$ cm./sec., with L of the order of (roughly) 10^{21} cm. or 10^3 light years. The resulting value of H is of the order of some 10^{-6} gauss. If this picture is correct, the final stationary state would not yet be reached.

Critically it should be said, perhaps, that the argument has not yet been given with the same rigor as has been reached in the statistical theory of isotropic turbulence of viscous incompressible fluids without magnetic fields.

A further point to be mentioned is this. If, as seems probable, at an earlier time there has been still more violent turbulence in interstellar gas than is observed now, then even stronger magnetic fields would be expected than according to the arguments as given, and these fields should still exist now. Also, there is a definite possibility, alluded to already, that even now magnetic fields are transported into interstellar space from the surface of stars by corpuscular emission. As far as these arguments go, the field strengths discussed before should rather be considered as lower limits.

It may be said, therefore, that there is fair reason to expect interstellar

magnetic fields of the order of some 10^{-6} gauss or more. The same may be assumed for the interplanetary space. There is so far no conclusive observational evidence on these points. The observations of interstellar polarization (34) would fit the arguments given here best, if the interpretation of Davis & Greenstein (35) should prove to be correct—in contrast to the ferromagnetic theory (36). Regarding the question of interplanetary fields, the reader is referred to the evidence discussed in *Sudden increases.*

Propagation of cosmic rays.—If the existence of cosmic magnetic fields is granted, it is not difficult to explain the isotropic distribution of cosmic radiation on the basis of Liouville's theorem and the ergodic hypothesis, if several conditions are fulfilled. First, in order to guarantee a stationary state, the magnetic field must be able to resist the pressure of cosmic radiation. That is, the energy densities of both must be comparable, or that of the magnetic field must be greater. Hence, in view of the observed intensity of cosmic radiation, H must be at least of the order of some 10^{-6} gauss. If the theoretical considerations of the last section are generally correct, this is just the order to be expected in interstellar space, whereas in interplanetary space somewhat higher values of H are indicated by the observations discussed in *Sudden increases.* This value of H also ensures, as a second condition, sufficient for the validity of the explanation of the isotropic distribution given here, that at least in interstellar space the radii of the Larmor circles are small compared with the range over which inhomogenities of the magnetic field are to be expected. With $pc = 10^{10}$ ev and $H = 10^{-5.5}$ gauss a Larmor radius of 10^{13} cm. ($\frac{2}{3}$ of the distance earth-sun) is found; for 10^{16} ev and unit charge the value is 10^{19} cm. or 10 light years. From this it may be concluded, following a perturbation method devised by Alfvén (24), that a cosmic ray particle spirals round a magnetic line of force in such a way that the centre of its Larmor circle drifts away from the said line of force very slowly. The velocity of this drift is small compared with c in the same proportion (regarding order of magnitude), as the Larmor radius is small compared with the range, over which $\boldsymbol{H}$ is just noticeably inhomogeneous. Hence it must be concluded, that the cosmic ray particles, except for those of very high energy, follow very closely the magnetic lines of force throughout interstellar space. This entails that they leave the galaxy practically only where the magnetic lines of force pass into intergalactic space, as tends to be the case in places of uncompensated overpressure of cosmic radiation.

According to our picture the magnetic lines of force will be bent in a way more or less analogous to the streamlines of the turbulent interstellar gas. In order to arrive at a quantitative estimate of whether or not the observed degree of anisotropy is adequately explained, one may also use the conceptions of the theory of the propagation of light quanta in a diffusing medium. This has been done by Unsöld (37), who found that the observations can be understood even if the equivalent of the free path is very large provided, as seems likely, the "reflectivity" of the galactic boundary may be assumed to be very nearly equal to one.

If a cosmic ray particle is moving into a region of higher intensity of $\boldsymbol{H}$, it may be reflected under certain conditions. It may be shown, e.g., by the method of Alfvén already referred to that the magnetic moment of the particle produced by its spiralling motion is equal to $E_\perp/H$, ($E_\perp$ being the energy corresponding to that component of the motion which is perpendicular to $\boldsymbol{H}$). This magnetic moment remains constant if $\boldsymbol{H}$ varies with time or from place to place. Since $E_\perp$ cannot become larger than the total kinetic energy E, a particle for which $E_\perp$ is not $\ll E$, must be reflected from a region where $\boldsymbol{H}$ is too high. This phenomenon as such has already been known for a long time in Störmer's aurora theory, where surfaces reflecting charged particles exist in the dipolar field of the earth and, indeed, at definite positions which depend on the total kinetic energy of the particles.

The factor by which the energy density of cosmic radiation is increased by storage under these conditions is most easily evaluated if there is no escape at all into the intergalactic space. In this case one may simply compare the average time which a light quantum spends inside the boundaries of the galaxy with the mean life time of a cosmic ray particle. The resulting storage factor is of the order of 10^4. By the method indicated before it is possible to estimate the error caused by the assumption that there is no loss to intergalactic space. Leaving apart the possibility of local "holes" (for cosmic ray particles) in the boundary of the galaxy, it can be seen that the regular loss—limited by the drift perpendicular to $\boldsymbol{H}$, referred to before—can be presumed to be very small. Thus it may be said that the picture is at least consistent.

Richtmyer & Teller (7) have advanced the hypothesis that a magnetic field surrounding the sun, but filling a volume much larger than that enclosing the planetary orbits, is responsible both for making isotropic and for storing "cosmic" radiation, which according to this theory really would be of solar origin. If one tries to make quantitative estimates of the properties of this field, serious difficulties arise. From the approximately known solar output of cosmic ray particles and their lifetime of (at most) 10^7 years, their total energy present at any time may be found, and from their energy density (again 10^{-12} erg/cm.^{3}), the volume. Its order of magnitude turns out to be $\approx 10^{16}$ cm. (37). This is too small to prevent the escape of particles of high energy, since the Larmor radius of a particle with 10^{14} ev per unit charge is larger than this. Furthermore it is rather difficult to see how a magnetic field with the necessary strength could be maintained over this volume without getting mixed with interstellar fields. Hence the hypothesis of Richtmyer & Teller, though not disproven, seems to encounter difficulties more serious than those encountered by the galactic hypothesis.

Primary acceleration.—It is an old hypothesis that cosmic ray particles are charged particles accelerated to very high energies in cosmic electric fields. If these fields were to be due to space charges, the primary process of acceleration would be analogous to that producing lightning, and the enormous potential differences observed in the terrestrial atmosphere would seem to make such a theory very promising. Unfortunately the lowest layer

of our atmosphere is a rather exceptional region in the universe, as far as regards its electric conductivity; only its extremely small value permits large potential differences to be built up. In interstellar space and on the stars the conductivity is high, from 10^{9}–10^{13} e.s.u. in the former up to 10^{18} e.s.u. in the sun's center. No mechanism has so far been devised by which such potential differences might arise in interstellar space or on the surface of stars.

The remaining possibility is that the electric fields in question arise by induction, in connection with local changes of the magnetic field strength. The first to suggest a mechanism of this sort was Swann (38), who was followed by Alfvén (24, 26) and a number of others. We shall discuss some models, which seem to be relevant in connection with the effects observed by Forbush (12, 12a) and Ehmert (13, 13a). The tacit assumption of most of the earlier work on this problem is that the conductivity is vanishingly small. Then the difficulty is only to find conditions such that the magnetic fields, the changes of which give rise to the electric force, do not prevent the charged particles from following the electric lines of force. One such possibility, proposed by Swann and followed in some detail by Riddiford & Butler (39), is to assume a value of $\dot{H}$ according to observations (0.01 to 0.3 gauss/sec.), and to give attention to those time intervals during which H is very small; then the curling up of the particle does not yet interfere too much with the accelerations. If a magnetic field is assumed, which is homogeneous in a certain region (part of a sunspot) and which increases linearly with time, the path of a charged particle (charge Ze) and its energy E at any time may be given explicitly. For a particle with rest mass m_0 starting at $t=0$ at a distance r_0 from the axis of symmetry of the field with the small initial velocity u_0, it is found that

$$E = \pi^{-1/2}\Gamma(3/4)(m_0c)^{1/4}(\dot{H}ez)^{3/4}r_0t^{1/2} \text{ erg.}$$

Relativistic energies ($E \approx 10^{-2.8}$ erg for protons) are reached, with $\dot{H}=10^{-0.5}$, $r_0=10^{9.3}$ cm. at $t=10^{-2.8}$ sec. During this time interval the Larmor frequency, given by eH/mc, attains the value of about $10^{+0.7}$ sec.$^{-1}$. It is easily seen that, so far, the curling around the magnetic lines of force is of no influence. The electric force is of the order of $(\dot{H}/c)\cdot r_0$ or some volt/cm., and its line integral over the distance r_0 is of the order of 10^{10} ev. This is the energy resulting as long as no complicated path is described. But the formula given above shows that with $t \approx 10^{4}$ sec. (the highest value permitted by the assumption on $\dot{H}$), an energy of $10^{12.2}$ ev is attained. This additional gain is achieved during the further path of the particle, which, while circling around the magnetic lines of force, drifts towards the axis of symmetry.

This result is of interest because it shows in detail how under special conditions considerably higher energies may be reached than would be expected on first consideration. But the further discussion given in the quoted paper also reveals that for values of the dimensionless parameter $\dot{H}et_0^2 m_0c \gg 1$ (where t_0, the injection time, defines the value of H at the beginning of the

acceleration, the previous results holding for $t_0=0$) the resulting energy is $\approx m_0c(r_0/2t_0)\ (t/t_0)^{1/2}$ provided that $u_0 \ll r_0/2t_0$; otherwise $r_0/2t_0$ has to be replaced by $\sqrt{2}u_0$. It should be noticed that this last expression is independent of $\dot{H}$. For $t_0=2$ sec. the value of the parameter (with $\dot{H}/c=10^{-11}$) is 10^4 for protons. This is the limit at which energies of order 10^9 ev are still reached. For electrons the limiting value of t_0 is much smaller, for heavier ions somewhat higher, according to their state of ionization.

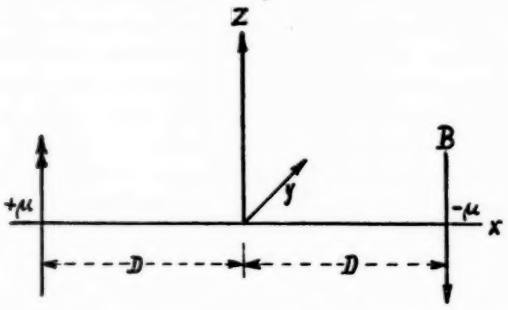

FIG. 6. Model for the acceleration of charged particles (see text).

Another possibility is that several magnetic fields are superposed in such a way that the induced electric forces do not vanish in regions of $\boldsymbol{H}=0$(18, 40). As a model we may think of two magnetic dipoles (sunspots) of equal moment (μ), but opposite direction, separated by some distance $2D$. Then $\boldsymbol{H}$ vanishes on a line (say the y-axis of a Cartesian coordinate system), perpendicular to both the direction of μ and to the line joining the dipoles, and intersecting the latter in the middle ($y=0$). Now suppose both dipoles approach each other with the velocity v. Then it is easily seen that on the said line (the y-axis) a parallel electric force arises of amount $(v/c)H'$, where H' is the magnetic force produced by one of the dipoles in the absence of the other. A charged particle starting on this line will be accelerated along the line and will never deviate. The final energy is found to be (with y_0 the initial coordinate of the particle),

$$E = \frac{Ze\mu}{D^2}\,\frac{v}{c}\left(1 - \frac{y_0/D}{\sqrt{1 + y_0^2/D^2}}\right),$$

which for $y_0 \ll D$ reduces to

$$E = (v/c)(Ze\mu/D^2).$$

For a comparison with our previous expression, $eZ(\dot{H}/c)r_0^2$, we observe that $\mu/D^3=H'(y_0=0)$ and that D/v gives the time scale of the variation of H. Thus both are seen to be identical apart from a factor of order 1. An acceleration needs a time approximately given by $(c/v)\ (m_0c/ZeH')$. In this model the restriction to low values of H' means in effect a restriction to the immediate neighborhood of the y-axis. Since electrons are more easily deflected than ions, at least in the energy range in which the ions get energies

of the order of their rest energy (the deflection per unit path length from the original direction being $\sim 1/m\dot{y}$ in this energy range), the electrons have again a considerable handicap when compared with the ions under otherwise equal conditions. Likewise the protons have also a definite, although much smaller, handicap, in comparison with the heavier ions.

The models discussed so far show that, through the changes of the magnetic intensity actually observed in sunspots, electric forces may arise which are sufficient to accelerate charged particles to cosmic ray energies. Of course, ideal conditions approaching those assumed in the models will rarely be realized; but also under actual conditions, especially above complex active sunspot groups, it should be expected that there will arise, in regions where $H=0$, a nonvanishing electric force (as in the last model) or, where $H \neq 0$, at least a finite component along H.

Some further difficulties disregarded in the discussion as given so far result from the fact that the electric conductivity may short-circuit the generator. The mechanism is such that all charged particles present in the region considered are accelerated; but as their velocities become comparable with that of light, the concept of conductivity loses its meaning. Owing to the plasma properties of the medium, local changes of H must be accompanied by mass motions, the velocity of which may now be denoted by v. Since E must be small for a comoving observer, an observer at rest must always find E to be $\approx (v/c)H$. The first equation of Maxwell leads, since $j' \approx eNc$, to (41)

$$4\pi N \leq H/(eL)$$

where L is a length such that H/L is of order of curl H. If L is chosen in such a way, that $e\,E\,L \approx W$, the kinetic energy (say 10^{-2} erg or 6.10^{9} ev), we find, using the given relation for E,

$$4\pi N \lesssim (H^2/W)(v/c).$$

Thus only the fraction v/c of $H^2/4$ will be converted into cosmic ray energy. From this equation it follows that the particle density must be extremely low if cosmic ray energies are to be attained; with $v/c \approx 10^{-3}$ and $H^2 \approx 10^{4\pm 2}$ it follows $N \approx 10^{3\pm 2}\text{cm.}^{-3}$ for $W = 10^{-2}$. The geometry of the region in question is therefore of great importance. If the length W/eE is assumed independent of L, the condition for N can be fulfilled without extreme assumptions since L may be comparatively small. This fact as well as the interconnection of local changes of H with mass motions have led to the hypothesis that there is a close relation between ordinary solar corpuscular emission and cosmic ray production (42). Kiepenheuer (43) has proposed as a model a narrow column of ionized gas which takes with it a magnetic field with H perpendicular to the long axis, its direction of motion; Schlüter (41) gives reasons for believing that the column itself can probably only be considered as a long-lived structure if there are magnetic fields holding it together, such as are connected with an electric current along its axis. If such a column is suddenly cut off from its solar source by a disturbance (say a

chromospheric eruption), an electric field will be induced parallel to the axis with all the characteristics discussed before. A detailed discussion of this model with the equations of plasma physics will have to wait for a theory of the origin of the solar corpuscular emissions.

Menzel & Salisbury (44) have advanced the hypothesis that the acceleration of the charged particles is due to electromagnetic radiation from the sun of very low frequency, of the order of a few cycles per sec. This hypothesis has been worked out in some detail by E. M. McMillan (45). In a plane wave of wavelength $\lambda \approx 10^{10}$ cm. with a field strength of 1–10 volt/cm. (such that $eE\lambda/2\pi$ is a small multiple k of the rest mass) the particle describes a path in the plane fixed by the direction of propagation of the wave (x direction) and that of the electric force (y direction). This path consists of a number of identical S-shaped pieces, with a displacement of order of $k^2\lambda$ along x and $k\lambda$ along y in each cycle, and with a mean velocity of progression in the x direction of order $c/(1+(2/k^2))$. The kinetic energy is oscillatory reaching a maximum value of order $k^2m_0c^2$ in the middle of each cycle, but returning to zero at the end.

The attempt to specify the conditions under which electromagnetic radiation of this frequency can exist and be propagated leads to great difficulties. Since the refractive index of the region in question should be real, much smaller electron densities are required than exist even in the HI regions of interstellar space. Hence such waves could probably exist only temporarily in limited regions, of extent, say, of a few wave lengths. They might be generated at the surface of the solar corona by a magnetic disturbance after a solar flare. It appears, however, that the conditions required by this theory are rather extreme.

Finally the possibility will be discussed that part of the neutrons observed on November 19, 1949, came directly from the sun (46). If the considerations put forward in this section are generally correct, it is to be expected that in the acceleration process a fraction of the accelerated charged particles will return to the solar surface. There they will be stopped by encounters with nuclei of the deeper layers of the solar atmosphere, in which secondary neutrons are generated. It is not yet possible to give a definite figure for the number of neutrons to be expected and for the probability that such a neutron will escape from the sun and reach the earth before its decay; but the discussion in the quoted paper shows that the effect might be of interest in connection with regular or sudden variations of the intensity of the neutron component of cosmic radiation.

Energy spectrum and mass spectrum.—Whereas the mechanism of the primary acceleration of cosmic ray particles appears to be understood in its essentials, the same cannot yet be said of the energy spectrum because this latter may be affected to a considerable extent by secondary processes. Two of these have been suggested which will be examined in turn.

The first one, suggested by Fermi (32), is based on the conceptions of interstellar magnetic fields outlined in the section *Cosmic magnetic fields.*

If cosmic ray particles move in these fields they are sometimes reflected from regions of high magnetic intensity. Also, when the particle changes its general direction by a large angle, while spiraling closely about a curved magnetic line of force, a reflection may be said to occur. In both cases the energy of the particle remains constant if the interstellar matter and the magnetic field "frozen" in it are at rest. But if the interstellar clouds and the magnetic fields are in motion themselves, an exchange of energy occurs. In the case of opposite direction of motion, resulting in a head-on collision between the cosmic ray particle and the magnetic cloud, the particle will gain energy. On the other hand, if the original directions of motion are parallel, that is, in the case of an overtaking collision, it will lose energy to the cloud, which for this argument may be considered to be a reflecting moving body of infinite mass. The average result of many collisions, however, will not be zero—as is clear already on general grounds—but a net gain will result, which is a small multiple of $(v/c)^2(E+m_0c^2)$, where v is the mean velocity of the clouds and E the kinetic energy of the particle. If collisions are frequent enough, the net gain will exceed the average energy loss by ionization of interstellar matter, which is $\approx 4.5\times 10^6$ ev per gm./cm^2 of interstellar matter, corresponding to $\approx 10^{24}$ cm. $= 10^6$ light years length of path, for kinetic energies of the order of 1 Bev or more, but which is much higher for smaller values of E. Hence for particles of high energy the ionization loss may be neglected; but it determines the lower limit of E ("injection energy"), below which the mechanism will not work.

For his numerical estimates Fermi uses the value v/c (designated by B) $= 10^{-4}$. Furthermore one collision per year is assumed. These values will be commented upon afterwards. They give the injection energy $E_i \approx 0.2$ Bev, since $B^2 \cdot 1.2$ Bev $= 12$ ev is about equal to the ionization loss per one light year for particles of this energy.

The energy spectrum of cosmic radiation is under these conditions determined on the one hand by the steady gain of energy with time of every cosmic ray particle, on the other hand by the probability of being eliminated by a nuclear collision. So far we consider only cosmic ray protons. The energy as a function of time (t) builds up according to the formula

$$E(t) + m_0c^2 = (E_0 + m_0c^2) \exp (B^2t/\tau),$$

where τ is the average time between two collisions. On the other hand the probable distribution according to age will be $N(t)dt \sim (dt/t_1)\exp(-t/t_1)$, under stationary conditions, where t_1 is the mean life time (60 million years) of a cosmic ray particle, as fixed by nuclear encounters and the average density of interstellar matter (assumed as 10^{-24} gm./cm.^{3}). By means of the relation between age and energy the distribution according to age, for E_0 assumed $\ll m_0c^2$, may be written as

$$N(E)dE \sim (dE + m_0c^2)^{-1-\tau/(t_1B^2)}$$

Hence the energy spectrum turns out to be of the type of an inverse power

law. With the values of the parameters given before, the exponent becomes about three, that is, nearly Hilberry's (4) value (Section *Energy and mass spectrum*). If B^2 has been overestimated, as seems likely on astrophysical grounds (see below), the exponent must be larger. This would mean that the collisions with interstellar clouds do not change the original energy appreciably. Also the injection energy becomes much higher, ≈ 6 Bev for $B^2 = 10^{-9}$, as is easily verified.

For protons the possibility of regeneration processes has to be taken into account. If a proton hits another proton in such a way that after the collision each has more than the injection energy, both protons will gain additional energy by encounters with interstellar clouds. If this process were effective, a very different energy spectrum would result for protons than for heavier particles, considerably handicapping the latter in comparison with the protons. These expectations, however, have not been borne out by observation.

The picture given so far may be refined by taking into account the probable distribution in space of the sources of primary particles. This has been done by Chang-Yun Fan (47), who found that with Fermi's value of B and τ the energy spectrum in the low energy region may be explained if it is assumed that most sources of primary cosmic radiation are situated near the center of the galaxy.

For heavy nuclei the minimum injection energy is about $0.2Z^2/A \approx 0.1Z$ Bev per nucleon (with Fermi's values of B^2 and τ). Also for this reason these nuclei would be handicapped compared to protons. Only particles injected with higher energies gain additional energy in the way considered by Fermi, whereas the others lose energy both continuously by ionization and discontinuously by nuclear encounters. This latter process, however, is very important as a source of cosmic secondaries. Whether or not it really takes place may be checked by looking for the cosmically rare elements Li, Be, B. Nuclei of these species are not to be expected among those originally accelerated owing to their very small cosmic abundance. If they are found in primary cosmic radiation, one must conclude that these nuclei are break-up products from heavier ones; under stationary conditions in interstellar space about as many Li, Be, B-nuclei are to be expected as heavier nuclei, since the probability of their formation in an encounter of a heavier cosmic ray particle with an interstellar nucleon is fairly high ($\approx 1/2$). Furthermore, large relative numbers of secondary protons and α-particles are to be expected, namely, about 10^2 and 10^1, respectively, per heavy nucleon ($Z \geqq 6$) according to an estimate by Bradt & Peters (48). The observations, as summarized in section *Energy and mass spectrum* are in accordance with this expectation [with the possible exception of the observations by Peters (3) at low latitudes referred to previously]. Furthermore they tend to show that a considerable fraction of the protons and α-particles of the cosmic radiation are actually cosmic secondaries; but there is no need to assume that this is the case for all protons and α-particles.

The cosmic abundance of the elements with $Z \geqq 11$, $Z = 10$, $9 \geqq Z > 6$, and helium, referred to hydrogen as unit, is, according to Unsöld (49), approximately $10^{-3.6}$, $10^{-3.0}$, $10^{-2.7}$ and $10^{-0.8}$. (According to Brown (50) all figures should be slightly lowered, by $\approx 10^{-0.2}$, the figure for $Z = 10$ being more uncertain than the others.) In primary cosmic radiation all elements with $Z > 2$ are relatively somewhat more abundant than otherwise in the universe. The figures given in the section *Energy and mass spectrum* can only be understood if there is a certain preference for heavier elements in the primary acceleration mechanism; a theoretical reason for this was suggested under the heading, *Primary acceleration.*

It should be remarked that the theory of a storage of cosmic radiation in cosmic magnetic fields demands that there be a more or less perfect fragmentation equilibrium between the heavier nuclei, and that Li, Be, B nuclei be present much in excess of their cosmic abundance.

The energy spectrum to be expected for such cosmic secondaries is more or less the same as that for the true primaries; since most of the collisions will be with interstellar hydrogen or helium nuclei, the energy per nucleon will not be greatly diminished.

We turn now to the astrophysical evidence on the values of B and τ. B may be estimated from the radial velocities derived from interstellar absorption lines in the spectra of distant stars, known chiefly from the work at the Victoria and Mount Wilson observatories (51). From this a mean square velocity of about 6 or 7 km./sec. may be derived according to Jentsch & Unsöld (52); more recent work of Schlüter & Stumpff (53) points to even smaller values for the common, rather opaque, clouds. These values refer to large distances, of the order of some hundred parsecs. According to the statistical theory of turbulence still smaller values should be expected for distances of the order of one light year. This result may be checked by comparing the density gradient of interstellar "smoke" (grains), which is approximately perpendicular to the plane of the milky way, with the known value of the acceleration towards this plane, as has been done by Unsöld. The result (6.3 km./sec.) is in agreement with the previous one; but it is an upper limit insofar as part of the gravitational attraction might be balanced by the pressure of cosmic radiation and by the force exerted by the magnetic fields on the ionized matter.

Hence there seems to be little doubt that B^2 is considerably smaller than has been assumed by Fermi (32). Furthermore the general resemblance of the energy spectrum of the protons with that of the heavier nuclei, for which contitions are still more unfavorable secondary acceleration, makes it unlikely that the processes affecting these spectra differ much from one another. It appears, therefore, that Fermi's process, though probably operative, does not determine the form of the spectrum. This must rather be ascribed chiefly to the primary mechanism. That this is not improbable in itself was pointed out by Unsöld (37), who remarked that the energy spectrum of cosmic radiation should reflect in a rough way the spectrum

of the disturbances on the stars' surfaces, which might be of a turbulent character.

At this point a difficulty appears, which must now be discussed. It has been pointed out already that, in order to keep up stationary conditions, the stars should produce, besides their thermal radiation, an additional fraction, of the order of 10^{-4}, in the form of cosmic radiation (this fraction would not be greatly different with Fermi's mechanism really operative). Now the sun emits, as we saw, on the average only about 10^{-10} of its energy in the form of cosmic radiation; if, however, we center our attention on the emitting part of the sun's surface during a particular outburst, this fraction probably becomes $\gtrapprox 10^{-3}$. Hence, if a considerable percentage of the stars are generally as active on great parts of their surfaces as is the sun during events of the kind of those considered in the section *Sudden increases*, this discrepancy would be explained.

Unsöld (37), has emphasized that the sun is just as inactive compared with a part of the members of our galaxy in regard to the emission in the radio frequency range ($\approx 10^8$ sec.$^{-1}$). In a radio telescope the brightness of the milky way and that of the sun are roughly comparable, notwithstanding the fact that they differ in the frequency range of thermal radiation by a factor of the order of 10^8. If one makes the tentative assumption that the radio emission indicates the order of magnitude of the amount of nonthermal emissions—a hypothesis which is supported by the resemblance of the spectrum of the solar radio emission during outbursts with the normal radio frequency spectrum of the milky way—one arrives just at the correct order of magnitude for the emission of cosmic radiation.

On the other hand, it must be said that there is so far no convincing evidence regarding the nature of the sources of galactic radio emission. There are observations tending to show that they are not all of the same nature.

Finally, the significance of the absence of electrons from primary cosmic radiation must be discussed. The recent work of Donahue (54) on this question shows that the processes usually thought of in this connection, e.g., energy loss by emission of long wave radiation in magnetic fields, or by collisions with light quanta, are not sufficient to explain the absence of electrons, at least not in the galactic theory. Within the scheme of the solar theory, the sun's thermal radiation would in effect eliminate the electrons. But from the point of view of the galactic theory one is forced to conclude that the electrons are strongly handicapped already in the process of primary acceleration, as in case of the lighter nuclei. In this connection reference must be made again to the considerations presented under *Primary accelerations*.

In conclusion, we may ask to what extent the observational facts enumerated in the *General Survey* are explained. The isotropy of cosmic radiation and the energy storage by some powers of ten are natural consequences of the presence of cosmic magnetic fields, the existence of which now seems

probable on theoretical grounds and is indicated, though no yet proven, by some observations. The amount of the energy density of cosmic radiation demands a very small production rate of the stars in general, in the frame of the galactic theory. One form of this production seems to be operative in the solar flare effects described under *Sudden increases*, the theory of which (*Primary acceleration*) has probably been worked out as far as permitted by the present astrophysical knowledge. Concerning the energy spectrum, the mass spectrum, and the absence of electrons from the primary radiation it can only be said that they seem to fit into the frame of the theory. But they provide no genuine test for the theory apart from the presence of the cosmically rare Li, Be, and B nuclei. Their presence can probably only result from a storage in cosmic magnetic fields.

On the whole it may be said, perhaps, that the hypothesis of a stellar origin of cosmic radiation, coupled with that of interstellar magnetic fields which prevent the cosmic ray particles from escaping into intergalactic space, seems to fit most easily the observed facts known at the present time. Further evidence may, however, either prove it definitely to be correct or show that it has to be replaced by a better hypothesis.

The assistance of Dr. Ferrell in the final drafting of the English text is gratefully acknowledged. I am indebted to Mr. Dainton for the permission to quote from his paper (6a) before publication.

LITERATURE CITED

1. Wilson, J. G., *Progress in Cosmic Ray Physics* (North-Holland Publ. Comp. Amsterdam, Netherlands, 557 pp., 1952)
2. Heisenberg, W., *Kosmische Strahlung* (Springer Verlag, Göttingen, Germany, 1952)
3. Kaplon, M. F., Peters, B., Reynolds, H. L., and Ritson, D. M., *Phys. Rev.*, **85,** 295 (1952)

3a. Kaplon, M. F., Ritson, D. M., and Woodruff, E. P., *Phys. Rev.*, **85,** 933 (1952)

4. Hilberry, N., *Phys. Rev.*, **60,** 1 (1941)
5. Winckler, J. J., Stroud, W. G., and Shanley, T. J. B., *Phys. Rev.*, **79,** 656 (1950)
6. Dainton, A. D., Fowler, P. H., and Kent, D. W., *Phil. Mag.*, **42,** 317 (1951)

6a. Dainton, A. D., Fowler, P. H., and Kent, D. W., *Phil. Mag.*, **43,** 729 (1952)

7. Richtmyer, R. D., and Teller, E., *Phys. Rev.*, **75,** 1729 (1949)
8. Compton, A. H., and Getting, I. A., *Phys. Rev.*, **47,** 817 (1935)
9. Vallarta, M. S., Graef, C., and Kusaka, S., *Phys. Rev.*, **55,** 1 (1939)
10. Elliot, H., and Dolbear, D. W. N., *Proc. Phys. Soc.*, [A]**63,** 137 (1950); *J. Atmos. Terr. Phys.*, **1,** 205 (1951)
11. Forbush, S. E., and Lange, I., *Carnegie Inst., Wash. Pub.*, 175 (1948)
12. Forbush, S. E., *Phys. Rev.*, **70,** 771 (1946)

12a. Forbush, S. E., Stinchcomb, T. B., and Schein, B., *Phys. Rev.*, **79,** 501 (1950)

13. Ehmert, A., *Naturwissenschaften*, **28,** 28 (1940)

13a. Ehmert, A., *Z. Naturforsch.*, **3a,** 264 (1948)

14. Adams, N., *Phil. Mag.*, **41,** 503 (1950)
15. Adams, N., and Braddick, H. J. J., *Phil. Mag.*, **41,** 505 (1950)
16. Schlüter, A., *Z. Naturforsch.*, **6a,** 613 (1951)
17. Clay, J., *Proc. Koninkl. Nederland. Akad. Wetenschap.*, **52,** 906, 923 (1949)
18. Biermann, L., and Bagge, E., *Z. Naturforsch.*, **4a,** 303 (1949)
19. Bagge, E., *Z. Physik*, **128,** 939 (1950)
20. Elsasser, W. M., *Phys. Rev.*, **69,** 106 (1946); *Phys. Rev.*, **70,** 202 (1946); *Phys. Rev.*, **72,** 821 (1947); *Rev. Mod. Phys.*, **22,** 1 (1950); see also Lüst, R., Trefftz, E., and Schlüter, A., *Z. angew. Math. Mech.* (In press)
21. Schlüter, A., *Z. Naturforsch.*, **5a,** 72 (1950)
22. Abraham, M., and Becker, R., *Classical Electricity and Magnetism* (Blackie, to appear 1953)
23. Chapman, S., and Cowling, T. G., *The Mathematical Theory of Nonuniform Gases* (Cambridge Univ. Press, London, England, 402 pp., 1939)

23a. Biermann, L. with an appendix by Schlüter, A., *Z. Naturforsch.*, **5a,** 65 (1950)

24. Alfvén, H., *Z. Physik*, **107,** 579 (1937)
25. Cowling, T. G., *Monthly Notices Roy. Astron. Soc.*, **105,** 166 (1945)
26. Alfvén, H., *Cosmical Electrodynamics* (Oxford University Press, London, England, 637 pp., 1950)
27. Elsasser, W. M., *Phys. Rev.*, **79,** 183 (1950)
28. Heisenberg, W., *Proc. Roy. Soc.*, **195,** 402 (1948)
29. Batchelor, G. K., *Proc. Roy. Soc.*, [A]**201,** 405 (1950)
30. Schlüter, A., and Biermann, L., *Z. Naturforsch.*, **5a,** 237 (1950)

30a. Biermann, L., and Schlüter, A., *Phys. Rev.*, **82,** 863 (1951)

31. Chandrasekhar, S., *Proc. Roy. Soc.*, [A]**204,** 435 (1950)
    Chandrasekhar, S., *Proc. Roy. Soc.*, [A]**207,** 301 (1951)
32. Fermi, E., *Phys. Rev.*, **75,** 1169 (1949)

33. v. Weizsäcker, C. F., *Astrophys. J.*, **114**, 165 (1951)
34. Hiltner, W. A., *Astrophys. J.*, **114**, 241 (1951)
35. Davis, L., and Greenstein, J. L., *Astrophys. J.*, **114**, 206 (1951)
36. Spitzer, L., Jr., and Tukey, J. W., *Astrophys. J.*, **114**, 187 (1951)
37. Unsöld, A., *Phys. Rev.*, **82**, 857 (1951)
38. Swann, W. F. G., *Phys. Rev.*, **43**, 217 (1933)
39. Riddiford, L., and Butler, T., *Phil. Mag.*, **43**, 447 (1952)
40. Bagge, E., and Biermann, L., *Naturwissenschaften*, **35**, 120 (1948)
41. Schlüter, A., *Z. Naturforsch.*, **7a**, 136 (1952)
42. Alfvén, H., *Phys. Rev.*, 1732 (1949)
43. Kiepenheuer, K. O., *Phys. Rev.*, **78**, 809 (1950)
44. Menzel, D. H., and Salisbury, W. W., *Nucleonics*, **2**, 67 (1946)
45. McMillan, E. M., *Phys. Rev.*, **79**, 498 (1950)
46. Biermann, L., Haxel, O., and Schlüter, A., *Z. Naturforsch.*, **6a**, 47 (1951)
47. Fan, C.-Y., *Phys. Rev.*, **82**, 211 (1951)
48. Bradt, H. L., and Peters, B., *Phys. Rev.*, **77**, 54 (1950)
49. Unsöld, A., *Z. Astrophys.*, **21**, 1 (1941); *Z. Astrophys.*, **24**, 323 (1948)
50. Brown, H., *Rev. Mod. Phys.*, **21**, 625 (1949)
51. Beals, L. S., *Monthly Notices Roy. Astron. Soc.*, **9a**, 661 (1936)
52. Jentsch, C., and Unsöld, A., *Z. Phys.*, **125**, 370 (1948)
53. Schlüter, A., and Stumpff, P., *Mitteilungen Astronomischen Gesellschaft*, 23 (1950)
54. Donahue, T. M., Feenberg, E., and Primakoff, H., *Phys. Rev.*, **84**, 972 (1951); *Phys. Rev.*, **73**, 449 (1948)

ADVANCES IN NUCLEON-NUCLEON SCATTERING EXPERIMENTS AND THEIR THEORETICAL CONSEQUENCES[1]

By G. Breit and R. L. Gluckstern
Yale University,[2] New Haven, Connecticut

INTRODUCTION

The large volume of work on scattering makes it impossible to do justice to all parts of the subject within the space limitations of the present paper. The major advances in 1951 and adjoining years appear to be a consolidation of knowledge of high energy nucleon-nucleon scattering in the region from 100 to 300 Mev and considerable improvement in the precision of measurements in the low energy region of a few Mev bombarding energy. Advances in theory have been principally along the lines of more comprehensive treatments of low energy material and some as yet speculative attempts to explain the simplicity of experimental results at high energies.

Symbols and Notation

E, E_{Mev}	energy of the bombarding particle, in Mev
$\Lambda = 2\pi\lambda\!\!\!^{-} = 2\pi/k$	wave length of relative motion
Θ, θ	scattering angle in the laboratory and center of mass systems respectively
σ, σ_S	cross section, scattering cross section
σ_θ, $\sigma(\theta)$, σ_Ω	differential cross section in the system of the center of mass
σ_m, σ_e	photomagnetic and photoelectric deuteron disintegration cross sections respectively
L, $\boldsymbol{L}$	orbital angular momentum
K_0, K_1, K_2	nuclear phase shift for $L=0$, 1, 2
ϵ	binding energy of the deuteron
${}^3a$, ${}^1a$	triplet, singlet Fermi intercepts (scattering lengths)
$V(r)$, $J(r)$	interaction potential
$\boldsymbol{\sigma}$	spin matrix vector times 2 (Pauli's $\boldsymbol{\sigma}$)
$\boldsymbol{\tau}$	isotopic spin matrix vector times 2
$S_{12}=\dfrac{3(\boldsymbol{\sigma}_1\cdot\boldsymbol{r})(\boldsymbol{\sigma}_2\cdot\boldsymbol{r})}{r^2}-(\boldsymbol{\sigma}_1\cdot\boldsymbol{\sigma}_2)$	tensor interaction
${}^3V$ odd, even	triplet potential for odd and even parity states respectively

[1] The survey of the literature pertaining to this review was concluded in April, 1952.

[2] Assisted by the joint program of the Office of Naval Research and the United States Atomic Energy Commission.

$\Upsilon(x)=e^{-x}/x$	Yukawa type well function
V_{ot}, V_{os}	triplet and singlet well depths respectively
r_t, r_s	triplet and singlet well ranges respectively
V_t	tensor well depth
P_M	Majorana space exchange operator
$\boldsymbol{S}$	total spin vector
ϕ_2	spin orbit coupling parameter of Case & Pais (23)
$\mathfrak{F}$	nucleon-nucleon radial wave function
m	electron mass
f	f-function of BCP (52)

HIGH ENERGY SCATTERING

Scattering Experiments

The striking features of high energy proton-proton scattering are: (*a*) approximate constancy of the observed cross section per unit solid angle in the center of mass system as the scattering angle is varied; (*b*) approximate constancy of the cross section as the energy is varied; (*c*) comparatively large value of σ which is too large to be explained by ^1S scattering. The situation is reviewed in detail in a paper by Chamberlain, Segrè & Wiegand (1) which gives an up-to-date account of experimental results on p-p scattering, the more relevant n-p scattering data and discusses comparison of experiment with theory. The source of protons is the external beam of the Berkeley 184-in. cyclotron. General layout of the experiment is shown in Figure 1. The collimator for the proton beam is seen in Figure 2. Other characteristics of the apparatus and method are:

Incident beam: 5×10^5 to 5×10^7 protons/sec.

Incident beam measurement: Ionization chamber, calibrated at $E=345$ Mev by means of a Faraday cup and used with current integrator circuit.

Targets: Polyethylene: [$(CH_2)_n$, 283 mg. cm.$^{-2}$] or liquid hydrogen. Latter used especially for small θ. Hydrogen content by chemical analysis in polyethylene = 14.44 by weight (14.37 by chemical formula).

Counting: Stilbene crystals in coincidence (method II), singly (method I). Method I was used for small θ.

Energy control: Lithium absorbers (cyclotron beam energy 345 Mev, reduced energies were 118, 120, 164, 247, 250 Mev).

Elimination of stray coincidences: Special experiments with carbon targets.

Accidental coincidences background: $\sim$10 per cent of true counts.

The results support earlier conclusions regarding the approximate independence of the scattering cross section in the center of mass system on the scattering angle and also regarding the approximate independence of the cross section on energy.

Sources of error considered explicitly in the Chamberlain, Segrè & Wiegand paper (1) are: (*a*) statistics of counts; (*b*) error in solid angle caused by

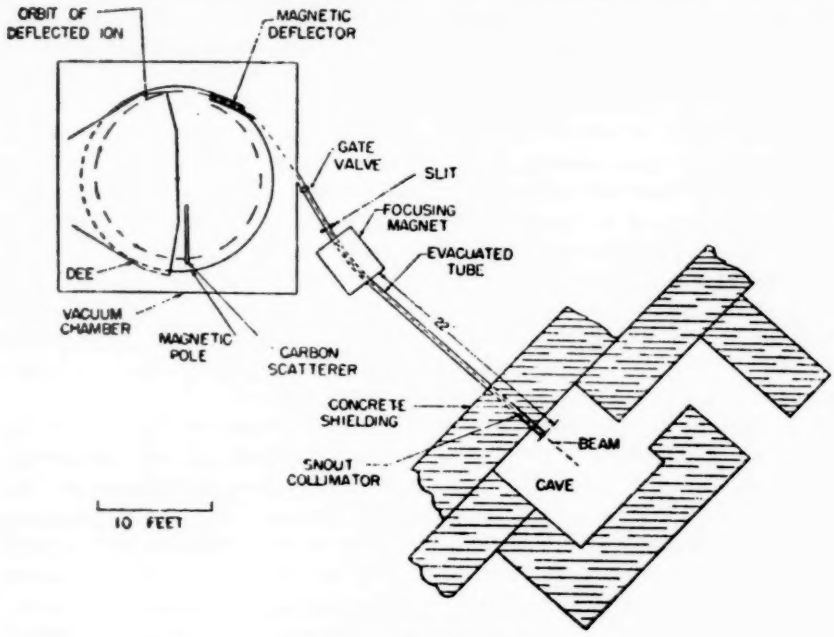

$$\sigma(\Phi) = H/(n\Omega N).$$

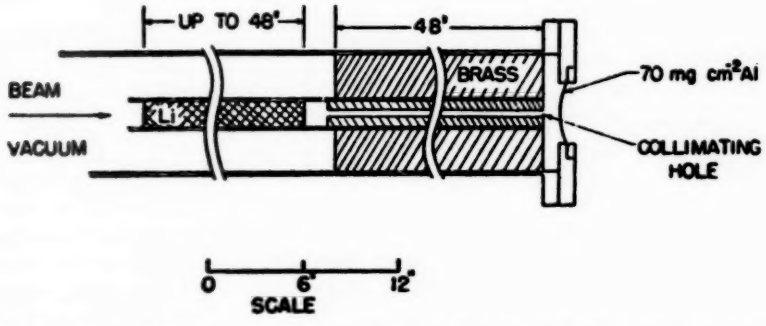

FIG. 1. (Above) Schematic diagram of the cyclotron, deflecting magnet, and collimator in the experiments of Chamberlain, Segrè & Wiegand (1).

FIG. 2. (Below) Collimator for proton beam used by Chamberlain, Segrè & Wiegand (1). Position of lithium absorbers occasionally used to reduce the energy of the beam is seen in this figure.

uncertainty of about 2 mm. in the depth to which the detecting crystal is penetrated before the scattered proton is counted; (*c*) possibility that the whole front of the detecting crystal is not uniformly sensitive; (*d*) consideration of systematic differences between results obtained by means of crystal

counters and older results obtained in the same laboratory by means of gas counters; and (*e*) errors arising in operation of the coincidence counter arrangements involving purely instrumental criteria of obtaining reasonably flat plateaus as the height of the scattering apparatus is varied with respect to the counters, as well as the existence of a good plateau for variation of photomultiplier tube voltage. Tests indicated that no appreciable error arose from item (*c*), detector uniformity. With respect to item (*d*), it was believed by Chamberlain, *et al.* that scattering of protons from the walls of the gas counters is responsible for the discrepancy and that the crystal counters are reliable. In addition to considering the above sources of error, a check was made regarding the correctness of the relativistic refinement of the 90° angle between scattered and recoil protons. This check served also as a test of the monoergic nature of the incident beam. The original paper contains a fuller account of the experimental procedure and precautions.

The results at 345 Mev bombarding energy are shown in Figure 3. There are two sets of points in this figure, the circles referring to measurements with polyethylene targets by the coincidence method, the crosses to the liquid hydrogen target by the single counter method. The latter is presumably the less accurate except at the smaller angles. It is impractical therefore to use one set of measurements as an accurate check of the other. At an angle of $\sim 10°$ the single counts method gave a marked and unexplained rise in σ_s. The geometry being less favorable for accuracy at such angles than at larger ones, the approximate agreement of the two methods for $30° < \theta < 50°$ is hardly relevant as a criterion in forming an opinion regarding the rise. A larger than estimated angular spread of the primary beam and a larger than estimated component of low energy protons would both tend to produce too large scattering at small angles.

In evaluating experiments in the 100–350 Mev range it is perhaps advisable to exercise more caution than in the "low energy" from .2–15 Mev. The instrumentation is relatively new and experience in its use is still limited. The large size of the equipment makes changes difficult. It is common experience that sources of error are difficult to locate unless the experimenter is free to change the arrangement and the dimensions of component parts of his apparatus and to check the resulting changes in his results against the theory of the experiment. Such changes require more thought and planning in the high energy region.

The correction for background caused by the scattering from carbon in polyethylene has been carefully considered by Segrè *et al.* (1). A superficial study of the work might leave one in doubt regarding the adequacy of these corrections. The special circumstance is that Segrè and co-workers have found that protons are knocked out of Li^7 at 345 Mev, mostly at 85° with respect to the incident direction as though they were free. There are similar knock out protons [Segrè (93)[3]] from carbon (2). If the angle between the

[3] In response to question by G. Breit regarding possible similar effect in carbon.

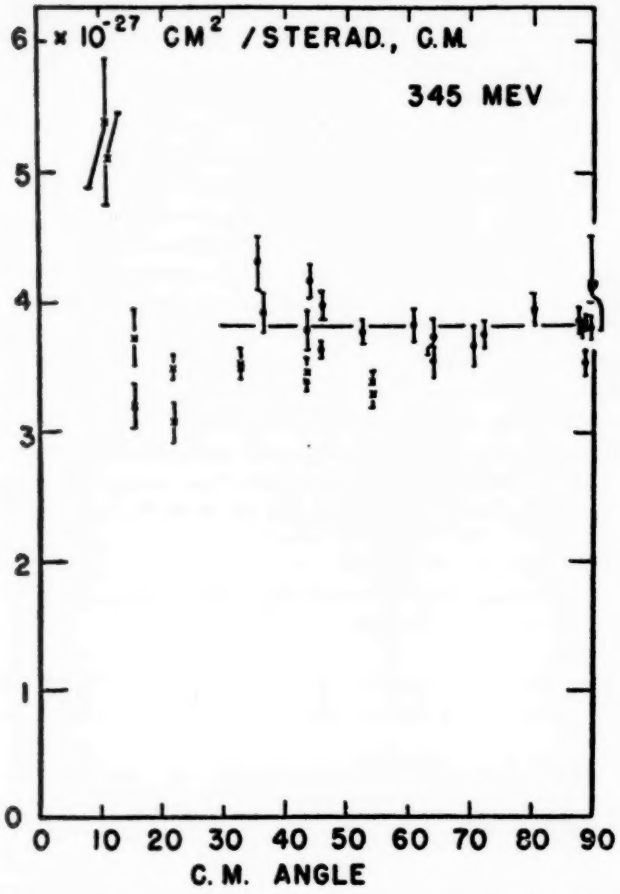

FIG. 3. Differential cross section in center of mass system for p-p scattering at 345 Mev obtained by Chamberlain, Segrè & Wiegand (1). Standard deviations derived from counting statistics are shown as errors. The scattering angle is shown in degrees. Crosses and square at 90°: liquid hydrogen target, single counter method. Circles: CH_2 target, coincidence method.

scattered and knock out protons were exactly the same as for free protons there would be doubt about the adequacy of the background corrections. In this case coincidences would not distinguish between the protons scattered from hydrogen and those from carbon. The authors have ascertained,[4] however, that the knock out protons are distributed in a cone with a half-value breadth of ~22° from the mean direction. This width they ascribe to the momentum distribution of protons in the carbon nucleus. The effect

[4] Emilio Segrè and Owen Chamberlain (personal communication).

of the width is to reduce the number of coincidence counts caused by a scattered proton and its partner knock out proton to a negligible fraction of the number of coincidence counts from hydrogen. The correction for background coincidence counts from carbon is made, therefore, on the basis of these counts being accidental. They arise mainly from accidental coincidences of protons coming from different carbon nuclei. Their number has been ascertained by substituting a carbon target for polyethylene and subtracting .6 of the carbon target coincidences from the polyethylene coincidences. The number .6 is arrived at by employing an experimentally observed ratio of 5:1 of single counts from carbon and hydrogen and the ratio of solid angles subtended by the two crystals. The reasoning is presented in detail in the section on "Targets" of the original paper (1). The procedure was tested by comparing results at different beam intensities.

Observations by other investigators made in other laboratories give approximately the same results as those obtained in the pioneer experiments of the Berkeley group. The numbers quoted above show, however, some of the inherent difficulties of the problem. It is encouraging to know, therefore, that new experiments are being planned at Berkeley and elsewhere; it is

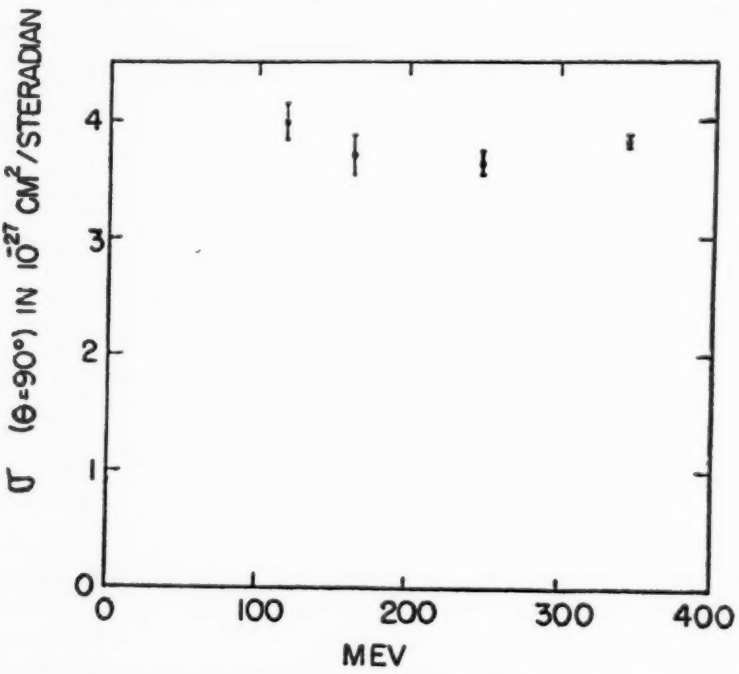

FIG. 4. Differential scattering cross section for $\theta = 90°$ as a function of incident proton energy according to Chamberlain, Segrè & Wiegand (1). Units: σ in 10^{-27}cm²/steradian, E in Mev. Limits of error are indicated in terms of standard deviations derived from counting statistics.

important to make sure that unavoidable experimental inaccuracies have not masked nonuniformities in angular distribution.

The results at 345 Mev are shown here in Figure 3. If the single counter measurements are taken by themselves, they show a drop from about 4.1 millibarns/steradian at $\theta = 90°$ to perhaps 3.5 millibarns/steradian at 20° and again a rise to about 5 millibarns/steradian at 11.3°. If one wishes to, one can read some angular variations in the data obtained by the coincidence method. The dashed horizontal line represents the authors' judgment regarding the proper interpretation of their data. The consistency of the position of the points with respect to the dashed line is not such, however, as to exclude the possibility of 10 or 20 per cent deviations from constancy of σ_θ for values of θ between 15° and 90°.

In Figure 4 is reproduced the Berkeley information regarding σ_θ at $\theta = 90°$. In Figure 5 are shown n-p results at $E = 40$, 90, 260 Mev together with theoretical curves of Christian & Hart (3). In a more recent paper Segrè (2) gives a revised version of the data presented here in Figure 5. (These data are plotted in Figure 5 of his paper and a collection of total cross section measurements is found in Table II, page 89 of his paper.) It will be noted that the three graphs of Segrè's paper are drawn through the experimental points and that they do not show a marked fore and aft asymmetry. At 90 Mev it would be difficult, however, to pass a curve through the experimental points without having ~10 or 20 per cent more scattering per unit solid angle at 180° than at 0°.

There is a striking difference in the character of the p-p and n-p results. The latter show a marked minimum at $\theta = 90°$ and σ_θ is not even approximately constant.

The work of Birge, Kruse & Ramsey (4) with the Harvard cyclotron was done at $E = 75$ and 105 Mev. The internal cyclotron beam was used. The work is similar to that of Chamberlain, Segrè & Wiegand (1) in general plan but differs with respect to (*a*) covering the angular range from $\theta = 40°$ to 90° only, in contrast to the larger range from $\theta = 15°$ to 90° at Berkeley, (*b*) employment of a low counting rate which made the number of accidental coincidences usually ~1/100 and occasionally ~1/10 of the true coincidences, (*c*) establishment of flat plateaus for curves showing (coincidence rate/defining counter rate) versus monitor amplifier (*i.e.*, second counter amplifier) gain, (d) employment of delayed coincidence rate as a measure of the number of accidental counts, a method which has advantages in eliminating accidental fluctuations of beam intensity in the comparison of counting conditions with background runs, (*e*) anthracene rather than stilbene crystal counters.

It is stated by the Harvard workers that the proton energy was measured to be 75 Mev with a 7 Mev half width at 35 in. from the cyclotron center and 105 Mev with an 8.5 Mev half width at 40 in. A probe between the cyclotron pole pieces in the positions just mentioned determined the energy of the protons. The shape of the energy distribution curve is not given and

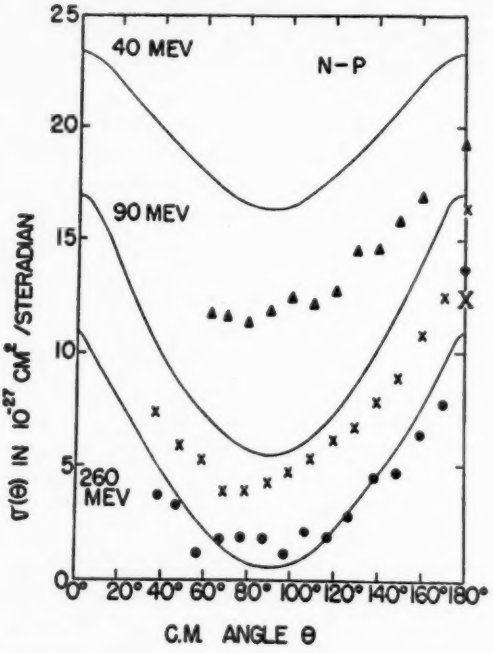

FIG. 5. Comparison of n-p scattering with calculations of Christian and Hart as in Fig. 12 of Chamberlain, Segrè & Wiegand (1). Points are plotted from measurements of Hadley, Kelley, Leith, Segrè, Wiegand and York (1949) and of Kelly, Leith, Leith, Segrè & Wiegand (1950). The large X has been communicated privately by R. H. Fox to CSW. Estimated uncertainty of experimental values is ~20 per cent. Potentials used in calculations of Christian & Hart (3):

$$V_{\text{singlet}} = (-35.3 \text{ Mev})(\tfrac{1}{2} + \tfrac{1}{2}P_M)\,\Upsilon(r/r_0)$$

$$V_{\text{triplet}} = \{(-25.3 \text{ Mev})(\tfrac{1}{2} + \tfrac{1}{2}P_M) + (-48.2 \text{ Mev})(0.37 + 0.63P_M)S_{12}\}\,\Upsilon(r/r_0);$$

where

P_M = Majorana (space exchange) operator;

$$S_{12} = \frac{3(\sigma_1 \cdot r)(\sigma_2 \cdot r)}{r^2} - (\sigma_1 \cdot \sigma_2); \quad r_0 = 1.35 \times 10^{-13} \text{ cm}.$$

the degree of masking of the angular distribution arising from the wings of the energy distribution curve is not obvious. The measured cross section is practically a constant for $40° < \theta < 90°$ and has the values 6.6 millibarns/steradian and 5.4 millibarns/steradian at 75 Mev and 105 Mev respectively. The absolute values depend on the knowledge of the cross section of $C^{12}(p, pn)C^{11}$ reaction which must depend in turn on the measurement of the primary beam intensity. Detail concerning this does not seem to be available.

The experimental results show deviations from an angle-independent σ_θ at $\theta = 40°$, 50°, and 80° for $E = 75$ Mev and for $\theta = 50°$ and 80° at $E = 105$ Mev.

At 75 Mev the deviations at 40° and 50° are appreciably greater than the statistical errors recorded by Birge *et al.* in their Figure 5. The other deviations are barely on the limit of the statistical error. The latter is of the order of .1 millibarn/steradian. One of the deviations is of the order of .4 millibarn/steradian. The values of σ_θ at 105 Mev are about 1.6 millibarns/steradian higher than expected from the Berkeley measurements. The Harvard workers point to their procedure in measuring the primary beam current as a possible reason for the discrepancy and hope to obtain a more definite answer regarding absolute values in experiments with an external beam. As in the Berkeley work a literal interpretation of angular distributions within the limits of statistical error would be risky; similarly the conclusion that indications of lack of constancy of σ_θ under variations of θ and lying outside the statistical error of σ_θ are unreal are perhaps also unjustifiable. The horizontal dotted lines used by both groups as a schematic representation of the dependence of σ_θ on θ are perhaps an oversimplification.

A thorough description of an experiment at $E=240$ Mev has been given recently by Oxley & Schamberger (5). The work was done in the internal beam of the Rochester synchrocyclotron. The characteristic features of this work are as follows. Primary beam current measurement was made by observing the β-activity of C^{11} produced in $C^{12}(p, pn)C^{11}$ as in the Harvard work. The C^{11} cross section was obtained from the measurements of Aamodt, Peterson & Phillips (6). An independent partial check was obtained by measuring the p-p cross section employing the C^{11} method both for the primary beam and the scattered proton measurements. The fact that the authors check their own value appears significant in view of their disagreement with Berkeley regarding the absolute value. The primary beam energy was computed to be 243 Mev from orbit dimensions and was measured as (235 ± 10) Mev by absorption in Cu. The primary beam energy spread was measured photographically to be <20 Mev at half maximum. Estimates regarding probable absence of low energy protons have been made on the basis of effects on angle of scattered and recoil protons and of deflection in the cyclotron magnetic field. The coincidences to singles ratio was about 3/100. The counting rate in the singles channels was about 3000 to 20,000/minute. A correction was made of $\sim$2.6 per cent for the loss of coincidences on account of a single pulse prior to the coincidence having paralyzed the discriminator univibrator. The procedure followed in determining the activity of C^{11} and the information available on target composition and recoil losses of C^{11} are gone into. Similarly the effect of the orbit oscillations in the cyclotron in producing a fine structure of the beam pulses has been considered in relation to the choice of counter resolving time. The effect of orienting the anthracene crystal in the beam of scattered protons has been analyzed and tested experimentally. The difference in the effect of the carbon background on the high and low angle sides of the coincidence peak has been taken into account by taking their mean.

The result of this work is $\sigma_\theta = (4.97 \pm .43)$ millibarns/steradian based on $\theta = 26.8°, 27.5°, 39.4°, 48.6°, 49.2°, 69.1°, 70°, 79°, 90°$. These values are used to give six points on the graph representing final results. Combined statistical and geometrical errors are considered to give an uncertainty of 3.5 to 5.5 per cent in relative values for different θ. Additionally, an uncertainty of 8.4 per cent is believed to exist on account of the employment of C^{11} for primary beam current measurements. The result is 29 per cent higher than that of the Berkeley group at the same energy. The discrepancy appears to be higher than the combined uncertainties of 8.8 and 8.6 per cent assigned to their results by the Berkeley and Rochester groups. The cross section is independent of angle within the relative error ($\sim$4.5 per cent).

The conclusions of Oxley & Schamberger (5) are checked in all essential respects by the work of O. A. Towler, Jr. (7), who employed a magnetic deflection method following a suggestion of Oxley's. The primary beam is measured by means of the $C^{12}(p, pn)C^{11}$ reaction employing (49 ± 3) millibarns for the cross section at 240 Mev. The protons are scattered by polyethylene targets with thicknesses ranging from 7.1 to .71 mg./cm.^{2}; for scattering through the largest angles polystyrene, $(CH)_n$, targets, .3 mg./cm.^{2}, were used in addition to the polyethylene. The target was exposed to the internal beam of the cyclotron and the scattered protons were observed in a photographic emulsion. Tracks formed by scattered protons were examined in the microscope regarding correctness of expected entrance direction, which was computed from a knowledge of the magnetic field of the cyclotron and the consequent possibility of computing the helical path of the scattered proton. Scattering from carbon nuclei was determined by substituting targets of nearly pure graphite for the polyethylene and polystyrene targets. The graphite targets were 17 mg./cm.^{2} for the higher energy scattered protons and 6 mg./cm.^{2} thick for scattered protons with energies of 15 to 30 Mev. Scattering from hydrogen was then found by subtraction.

The work of Towler (7) is likely to prove significant for the following reasons. (*a*) It provides a check on counter measurements by an independent procedure. (*b*) The observations are made on the low energy partner of the scattered-recoil pair providing an interesting variation in experimental procedure. (*c*) Observations on polyethylene have been checked with polystyrene targets, providing a valuable check on the procedure used in subtracting the carbon background. (*d*) In absolute value the results agree more closely with the observations of Oxley & Schamberger (5) and of Birge, Kruse & Ramsey (4) than of the Berkeley workers. (*e*) They corroborate the existence of a large rise in σ at small angles which is evident in the curves of Chamberlain, Segrè, & Wiegand (1). Towler's results give a practically constant σ_θ for θ between 13.0° and 71.9° with a mean value of $(4.66 \pm .39)$ millibarns/steradian; at $\theta = 8.7°$ the value of σ suddenly rises to (15.6 ± 1.6) millibarns/steradian. This rise is of a magnitude which admits an explanation in terms of Coulomb scattering and its interference with specific nuclear scattering. It

may be hoped that this circumstance will be of help in determining the presence of waves with $L>0$ with the aid of the Coulomb wave as a reference standard.

Proton-proton scattering experiments at $E=146$ Mev have been reported on by J. M. Cassels (8). These were performed in the external beam of the 110-in. Harwell cyclotron. Except for the smallest scattering angle (25°) the Wilson-Creutz coincidence technique (9) was used for counting scattered protons. The incident beam was monitored by an ionization chamber and an integrating D.C. amplifier. Two methods were used to calibrate the monitor. In the first a naphthalene crystal was exposed to the beam and the current was determined from the measured C^{11} activity and the known cross section for its production. In the second a photographic plate was exposed to the beam and the number of proton tracks was counted. The two methods checked each other. Cassels' results show a practically angle-independent $\sigma_\theta=(4.86\pm.25)$ millibarns/steradian at five scattering angles between $\theta=35°$ and 90°. At $\theta=25°$ his value of σ_θ is about 5.5 millibarns/steradian. He considers this point on his curve as less reliable than the others, since only one counter was used and the background correction was consequently difficult to make. It is noteworthy that the Berkeley value of σ_θ for larger scattering angles of $\sim$3.9 millibarns/steradian is lower than Cassels' value by roughly the same fractional amount as it differs from the Rochester and Harvard values. It may also be of interest that the photographic plate method of calibrating the primary beam monitor gave a slightly higher value (4.90 $\pm$.28) millibarns/steradian than the mean value (4.86$\pm$.25) millibarns/steradian.

A consideration of the above experiments indicates agreement among observers regarding the main features: approximate independence on angle for the larger scattering angles and approximate independence on energy. There is also some agreement regarding the existence of a rise in σ_θ at small θ, notably between the Berkeley and Rochester observers. Cassels' observation at 25° points in the same direction, but in his opinion this observation should be used with caution.

TABLE I

INTERACTIONS FOR SYMMETRICAL, CHARGED AND NEUTRAL THEORIES

Type Number	Form of Potential	Name
(I)	$V=\frac{1}{3}(\tau_1\cdot\tau_2)\{J_0(r)+J_1(r)(\sigma_1\cdot\sigma_2)+J_2(r)S_{12}\}$	Symmetrical
(II)	$V=\frac{1}{2}[1+(\tau_1\cdot\tau_2)]\{J_0(r)+J_1(r)(\sigma_1\cdot\sigma_2)+J_2(r)S_{12}\}$	Charged (Exchange)
(III)	$V=-\frac{1}{2}\{J_0(r)+J_1(r)(\sigma_1\cdot\sigma_2)+J_2(r)S_{12}\}$	Neutral (Ordinary)

Interpretation of Scattering Experiments

The features of high energy scattering occupying the center of interest are sufficiently different from those of the low energy region to justify a separate discussion. The presentation will be facilitated by a brief review of some of the older work.

A classification of types of interactions has been introduced by Rarita & Schwinger (10) and is frequently used in the literature. The original terminology has been suggested by forms of meson theories giving rise to the interactions.

The entries in parentheses in the last column of Table II are names introduced subsequently by Camac & Bethe (11) and by Wu & Ashkin (12), the latter in connection with *n-d* scattering. Denoting values of V for triplet and singlet states by ${}^3V$ and ${}^1V$ respectively and designating parity of the state by means of a subscript the following relations hold.

TABLE II

Relations between Interactions on Symmetrical, Charged and Neutral Theories

Interaction Type Number	Relations	Interaction Type
I	${}^3V_{\text{odd}} = -\frac{1}{3}{}^3V_{\text{even}}$	Symmetrical
I	${}^1V_{\text{odd}} = -3{}^1V_{\text{even}}$	
II	${}^3V_{\text{odd}} = -{}^3V_{\text{even}}$	Charged (Exchange)
II	${}^1V_{\text{odd}} = -{}^1V_{\text{even}}$	
III	${}^3V_{\text{odd}} = {}^3V_{\text{even}}$	Neutral (Ordinary)
III	${}^1V_{\text{odd}} = {}^1V_{\text{even}}$	

Expressing the potential for even L as

$$V_{\text{even}} = -\{1 - \tfrac{1}{2}g + \tfrac{1}{2}g(\sigma_1 \cdot \sigma_2) + \bar{\gamma}S_{12}\}J(r),$$

one has

$${}^3V_{\text{even}} = -(1 + \bar{\gamma}S_{12})J(r), \qquad {}^1V_{\text{even}} = -(1 - 2g)J(r)$$

and in terms of these the ${}^3V_{\text{odd}}$, ${}^1V_{\text{odd}}$ are obtainable from Table II. Camac & Bethe (11) have calculated the angular distribution of 20, 30, 40, and 80 Mev neutrons scattered by protons for a square well interaction employing well widths of 2.0 and 2.8×10^{-13} cm. for symmetric, exchange, and ordinary forces. Exchange and symmetric potentials give a maximum σ_s at 180° which is larger than the maximum at 0° scattering angle. The value of σ_s at the maximum is sensitive to the assumed range of force. In their calculation of phase shifts they find a convenient continued fraction for cot $(k\alpha + \delta)$ where α is the width of the square well and δ is the phase shift. The Camac-Bethe calculation does not consider the tensor force. Ashkin & Wu (13) consider

the effect of the tensor force and calculate neutron-proton as well as proton-proton scattering for incident energies from 100 to 200 Mev. The general features of the n-p results are similar to those of Camac & Bethe (11). In both investigations a similarity shows up between exchange and symmetric forces and a marked difference from ordinary forces regarding the sense of direction of asymmetry of scattering. Ordinary forces favor forward scattering. Considerable detail can be found in this paper regarding the forms of coupling between states with the same total but different orbital angular momenta and regarding the magnitude of error introduced by substituting the first Born approximation for the exact calculation. The total n-p scattering cross section on the symmetrical model is .129 barn at $E=100$ Mev, .090 barn at 200 Mev, compared to the experimental value of McMillan and coworkers (14) of $(.083 \pm .004)$ barn. Aside from this discrepancy the exchange and the symmetric theories give $\sigma(180°)/\sigma(90°) \sim 10$ while the experimental value is three. Ordinary forces give an angular distribution which is relatively too strongly forward. The experimental distribution is approximately symmetric about 90° suggesting the form

$$V = \tfrac{1}{2}(1 + P_M)J(r, \vartheta_1, \vartheta_2)$$

for the interaction potential. Here P_M is the Majorana exchange operator. This interaction was first proposed by Serber and is referred to as the even or Serber interaction. For it, odd orbital angular momenta do not give rise to scattering except for interference terms with even L.

Barker (15) and Chew & Goldberger (16) have made calculations closely related to Camac & Bethe's (11) with similar results. Eisenstein & Rohrlich (17) have made a number of calculations which favored the symmetrical interaction in preference to the other two. In another investigation Rohrlich & Eisenstein (18) give a more complete account of the effect of the tensor force showing that with the symmetrical theory an increase of scattering at 90° results from the use of the tensor force and that at 100 Mev with the symmetrical theory the tensor force increases σ_s (total) for a square well and decreases it for a Yukawa well. In order to approach agreement with experiment at 90 Mev they invoke a reduced range of the tensor force and postulate relativistic corrections of the order of 5 to 10 per cent. On the other hand an enlarged rather than a reduced range of the tensor force is apparently indicated by low energy data. In an earlier investigation Massey, Burhop & Hu (19) have also come to the conclusion that a simultaneous fit to the angular distribution and the total cross section for n-p scattering is difficult or impossible. More systematic investigations have been published by Hu & Massey (20) and by Burhop & Yadav (21) but these also do not succeed in accounting for the experimental results. The Yukawa potential well shape and the symmetrical theory are favored somewhat as in the work of Rohrlich & Eisenstein (18).

Data for $E>100$ Mev together with data for lower energies have been discussed theoretically by Christian & Hart (3), Christian & Noyes (22),

Case & Pais (23) and by Jastrow (24). Christian & Hart analyze n-p data from $E=40$ to 90 Mev on the basis of the $\frac{1}{2}(1+P_M)$ exchange potential. Their work falls outside the somewhat arbitrary Rarita-Schwinger classification of potentials according to relationship to form of meson theory. Their results are as follows. (*a*) Assuming the potential to have the same radial dependence in all states the value of a in $\frac{1}{2}(1-a+aP_M)$ is probably between .50 and .60. (*b*) A long-tailed potential is called for by the presence of phase shifts at high L at 40 Mev, with square and gauss potentials less probable than the exponential and Yukawa potentials. The latter two are acceptable within experimental uncertainties. (*c*) The angular distribution fit is improved by the inclusion of a tensor interaction which may be allowed to have a larger range than that of the central force.

Christian & Noyes (22) attempt to account for p-p scattering at 32 and at 340 Mev and n-p scattering at 40, 90, 280 Mev by means of static potentials. They claim that it is not possible to do so without giving up the assumption of charge symmetry in interactions between nucleons. This conclusion has been disagreed with by Case & Pais (23). The other conclusions of Christian & Noyes are as follows. (*a*) Data on p-p scattering at 32 Mev can be explained by two combinations of tensor and central force for both of which the tensor potential has a singularity at $r=0$ either of the type $1/r$ or $1/r^2$. The central potential is not long-tailed. The best fit is with a singlet square well of range 2.6×10^{-13} cm. and a tensor potential $V_t\Upsilon(r/R)$, $V_t=\pm23$ Mev, $R=1.25\times10^{-13}$ cm. or else the same square well and a tensor potential $V_t\Upsilon(r/R)/(r/R)$ with $V_t=\pm18$ Mev, $R=1.6\times10^{-13}$ cm. (*b*) The fit to 340 Mev is attained only by means of the latter type of singular tensor interaction. (*c*) The best p-p fit attributes about 1/3 of the scattering at 32 Mev to the tensor force. (*d*) A general argument, based on analogy to hard sphere scattering, is developed, according to which the region from $r=0$ to $.5\times10^{-13}$ cm. must be brought into play in order to explain $p-p$ scattering at 340 Mev. This argument serves as the justification for the employment of singular tensor potentials.

Case & Pais (23) arrive at a conclusion regarding charge independence of nuclear forces which is the opposite of that reached by Christian & Noyes (22). There is no proof of the impossibility of preserving this simplifying assumption in Christian & Noyes' paper, the argument being mainly one of plausibility on simultaneous inspection of p-p and n-p data. There is agreement between the two views regarding the fact that p-p data require emphasis on short distance interactions, but in effect Case & Pais (23) point out that the states present in p-p scattering could conceivably be more sensitive to whatever happens at short distances than the states $({}^3S, {}^1P, \cdots)$, which are present only in n-p scattering. Since among these ${}^3S$ has a large statistical weight and is the most important at 30 Mev, the presence of $({}^1S, {}^3P, \cdots)$ states in n-p scattering is only of secondary importance. The additional interaction considered by Case & Pais is represented by an addition to the potential energy of amount

$$V(r)(\boldsymbol{L}\cdot(\boldsymbol{s}_1+\boldsymbol{s}_2))$$

where $\boldsymbol{L}$ is the relative orbital angular momentum vector. For p-p scattering they use no additional interaction in triplet states and explain the rise in cross section toward 90° as the effect of three unequal phase shifts for ${}^3P_{0,1,2}$. These are in the ratios

$${}^3K_1^{(2)}:{}^3K_1^{(1)}:{}^3K_1^{(0)} = 1:(-1):(-2)$$

where the multiplicity is indicated on the left, L as a subscript, and the total angular momentum on the upper right. For 30 Mev they find ${}^3K_1^{(2)}\cong 3.7°$. The sign of this phase shift corresponds to attraction between the protons and fits the direction desired in the considerations of shell formation in heavy nuclei (25, 26). By means of the first Born approximation Case & Pais (23) show that terms in $\boldsymbol{L}\cdot\boldsymbol{S}$ have the property of raising 90° scattering and that the main features of p-p scattering at 350 Mev are not in contradiction with an interaction composed of an even part and a term in $\boldsymbol{L}\cdot\boldsymbol{S}$. A best fit is not presented by them because qualitative considerations show that the results are sensitive to the shape and range of the factor ϕ_2 which multiplies $\boldsymbol{L}\cdot\boldsymbol{S}$. Two general features of the 350 Mev results are considered by them. In the first place the ratio of 90° scattering cross sections at 350 and 30 Mev has to be accounted for. The singlet scattering at 350 Mev is small, $\sim$.2 millibarn, so they have to explain practically the whole experimental value of $\sim$4 millibarns on the basis of the term in $\boldsymbol{L}\cdot\boldsymbol{S}$. This ratio is very sensitive to assumed changes in radial dependence of ϕ_2. Secondly the flatness of the σ_Ω, θ curve has to be explained. Here they find an even more striking sensitivity to radial dependence of ϕ_2 obtaining the values of $\sigma(30°)/\sigma(90°)$ given in Table III.

TABLE III

VALUES OF $\sigma(30°)/\sigma(90°)$ AT 350 MEV p-p SCATTERING FOR DIFFERENT SHAPES OF FACTOR MULTIPLYING $\boldsymbol{L}\cdot\boldsymbol{S}$

Exponential	Yukawa	$r^{-2}\exp(-r/r_0)$	$\frac{Cd\Upsilon(x)}{xdx}$	Square well
930	40	4.7	1.6	.42

They expect that for $d\Upsilon/xdx$ there will be approximate energy independence of $\sigma(90°)$. Later observations are at least not in disagreement with this expectation.

Case & Pais (23) also have been able to produce reasonable arguments to the effect that new bound states of the deuteron will not be produced. Their arguments for considering n-p scattering as being not in disagreement with the theoretical view proposed is mainly that the contribution to 90° scattering caused by the $\boldsymbol{L}\cdot\boldsymbol{S}$ terms is estimated to be about four times as large in the p-p case as in the n-p. From p-p data they estimate therefore that

$\sigma_{LS}{}^{n-p}(90°)$ is $\sim$1 millibarn at $E=260$ Mev and this amount appears to be reconcilable with experiment.

Case & Pais (23) also considered the interference of p and s waves. Since the p phase shifts are small the first order effects cancel and they obtain a contribution having spherical symmetry in the center of mass system. A note in proof states that Christian has pointed out that the interference with d waves does not give rise to a spherically symmetric contribution to n-p scattering. Case & Pais find that this interference gives rise to an asymmetry in the n-p scattering which has a direction opposite to that observed and that the sign of ϕ_2 has to be changed so that the connection with "shell theory" is lost. Similarly there is difficulty in making a simultaneous fit to the 30 and 350 Mev data.

The reviewers nevertheless believe that the Case-Pais case is not finished, since many additional modifications have not been considered and since an interaction between spins and orbits must exist. Even apart from the possibility of tensor forces contributing appreciably (27) to the j-j coupling conditions in heavy nuclei, the energy with which the nucleons collide is so different from that encountered in an average heavy nucleus that there need not be a direct connection of sign in the two cases, different inter-nucleon distances assuming different relative importance. An explanation along the lines of Case & Pais (23) is only a schematized way of taking into account couplings of the type

$$\boldsymbol{A}_1 \cdot \boldsymbol{\sigma}_1 + \boldsymbol{A}_2 \cdot \boldsymbol{\sigma}_2$$

where $\boldsymbol{A}_1$, $\boldsymbol{A}_2$ are orbital matrix vectors. With such an interaction energy the possibilities of sign reversal are more natural than with the specialized form considered by Case & Pais.

Another way of preserving charge independence has been found by Jastrow (28), who points out that one can explain the main features of high energy scattering in terms of a potential with a repulsive core. The possibility of a repulsive core has been advocated from the viewpoint of saturation of nuclear forces by Kramers & Bethe (94). High energy p-p scattering appears now to give an indication of its existence but curiously only for interactions in singlet states and definitely not with the same radius of repulsive core in triplet states. In the final fit the triplet core radius is in fact taken to be zero.

Jastrow's considerations are carried out for a potential of the form:

Singlet	*Triplet*
$V = \infty, (r < r_0)$	$V = \{a + (1-a)P_M$
$V = V_{0s}\dfrac{1+P_M}{2}\exp\left(-\dfrac{r-r_0}{r_s}\right), (r > r_0)$	$+ [b + (1-b)P_M]\bar{\gamma}S_{12}\}V_{0t}\exp(-r/r_t)$

One of his better fits corresponds to

$r_0 = .60 \times 10^{-13}$ cm.	$V_{0s} = 375$ Mev
$r_s = .40 \times 10^{-13}$ cm.	$V_{0t} = 69$ Mev
$r_t = .75 \times 10^{-13}$ cm.	$\bar{\gamma} = 1.84$
$a = .50$	$b = .30$

The action of the repulsive core at 340 Mev for p-p scattering is principally that the ^1S phase shift becomes negative on account of the strong penetration of the s wave to the core. On the other hand the ^1D wave is positive, since the d wave does not penetrate to small distances so readily and is mainly exposed to the attractive part of the potential outside the core. There results a rise of σ at $\theta = 90°$ and a dip at $\sim 40°$. The tensor triplet interaction contributes enough in the region of the dip so that a flat σ, θ curve results.

In the region of $E = 30$ Mev the main problem is that of accounting for a rise in σ_Ω from ~ 12 millibarns at $\theta = 20°$ to ~ 15 millibarns at $\theta = 90°$. A large ^1D wave is a disadvantage in explaining such a rise because a positive ^1D wave shift gives, with a positive ^1S wave shift, a negative interference term for σ. At this energy the repulsive core diminishes the expected ^1D phase shift because the exponential potential used has a smaller range constant and a larger depth constant than it would have without the repulsive core. This circumstance results from fitting low energy data in the following manner. In making low energy fits one has to reproduce the same value of $r\partial\mathfrak{F}/\mathfrak{F}\partial r$ and of $\partial(\partial\mathfrak{F}/\mathfrak{F}\partial r)/\partial E$ at some value of E close to $E = 0$. The first requirement is equivalent to the reproduction of the scattering length, the second is often spoken of as the adjustment of the effective range. It is simpler, however, to look at the matter directly. Since $\partial(\partial\mathfrak{F}/\mathfrak{F}\partial r)/\partial E$ is of the form of a positive constant multiplied by $-\mathfrak{F}^{-2}\int_0^r \mathfrak{F}^2 dr$, the comparison of the $\partial/\partial E$ quantity for the same value of r with core and without shows that the effect of the core is opposite to that of concentrating the attractive region at small distances. The effect of the core is thus similar to an increase in the range parameter. The matter appears even more simply in terms of percentage changes of the effective kinetic energy. On account of the core the adjustment to scattering length requires the employment of more attraction at larger distances. The percentage change of the effective kinetic energy by changing E becomes therefore small in the attractive region and E has little effect on $\partial\mathfrak{F}/\mathfrak{F}\partial r$. On the other hand, attraction concentrated at small distances when compared with the "core plus attractive potential" at the same r leaves a region of r in which the percentage change of effective kinetic energy is large for the same change in E so that $\partial\mathfrak{F}/\mathfrak{F}\partial r$ is sensitive to energy.

On account of the necessity of fitting low energy data, the core requires a reduction in the range constant and consequently a diminution in the tail with a consequent decrease of phase shifts with larger L. The undesirable effect of the s-d interference is accordingly decreased, the d phase shift having dropped in Jastrow's calculations from 1.2° to .6°. The s-wave phase

shift at 30 Mev is also decreased by the introduction of the core and the average decrease in σ is compensated by the tensor interaction. These changes give an excellent fit to the angular distribution at $E=30$ Mev, the Coulomb scattering playing an important part. Pure Coulomb scattering at $\theta=20°$, $\Theta=10°$, $E=30$ Mev gives $\sigma\sim6.1$ millibarns/steradian. The observed value is ~12 millibarns/steradian.

A reader of Jastrow's paper can easily form the impression that the Coulomb wave has been neglected at all energies. Such a neglect would not be justifiable at 30 Mev and has not been made.

Increasing the core radius has the effect of decreasing the 90° cross section at 340 Mev and consequently a decrease in tensor strength is called for bringing with it a less complete filling of the dip in the σ, θ plot close to 50°. The two opposing requirements interfere with the reproduction of the experimental scattering isotropy.

The ^1S phase shift goes through 0 at $E\cong150$ Mev and $\sigma(90°)$ is consequently expected to have a minimum at about this energy. The Harvard, Rochester, Harwell data are at least not in disagreement with this expectation.

Agreement with n-p data as secured in Jastrow's work appears via the Christian-Hart (3) fit. The triplet interaction is assumed to have no repulsive core. The statistical weight 1/4 makes the states which are most important in Jastrow's p-p fit have secondary importance for n-p scattering. The fits are on the whole better at 90 and 240 Mev than at 40 Mev. The ratio $\sigma(\pi)/\sigma(\pi/2)$ is 1.55 experimentally and 1.3 theoretically for 40 Mev. There is an appreciable scatter of the experimental points collected in Jastrow's Figure 6 but the impression produced is that of a disagreement.

The possibility of a repulsive interaction in triplet states has been considered by Parzen & Schiff (29) and by Olsson (30). Parzen & Schiff have found that an excessive density of heavy nuclei may be expected as a result of a repulsive core in triplet states. Olsson calculated the consequences of the hard core model for n-p scattering between 38 and 140 Mev. He obtained agreement with experiment at low energies and was able to reproduce the experimental σ approximately at 90 Mev employing the symmetric interaction. At the high energies, however, the calculated values were about three times the observed. Olsson expresses doubt regarding the likelihood of strong spin dependence of the repulsive interaction.

The following general comments regarding the repulsive core hypothesis appear appropriate. (*a*) The introduction of the core has the effect of decreasing the range parameter of the singlet interaction. Jastrow's calculations are carried out for the exponential potential and consequences for the apparent meson mass are not directly obvious. An estimate shows (31),[5] however, that the meson mass needed to reproduce the attractive region of the corresponding Yukawa potential corresponds to $\mu\sim450\ m$. The validity of

[5] More detailed calculations of Hull & Herschman (31a) confirm this result.

the meson theory of nuclear forces comes less into question for the representation of the tail of the potential energy curve and the disagreement with the observed mass of the π-meson is therefore more significant with the repulsive core than without it. (*b*) As has been brought out by Jastrow (28), the smallness of the core radius interferes somewhat with the direct use of the repulsive core for saturation of forces in heavy nuclei. (*c*) The range of the tensor force is not likely to be the same as that of the central interaction. Appreciable differences are indicated by the work of Guindon (32), Broyles & Hull (33), Pease & Feshbach (34), Feshbach & Schwinger (35). (*d*) There is so far no evidence from meson phenomena which indicates the existence of a meson of much higher mass which can be held responsible for a very short range repulsion.

The above comments are largely critical. On the positive side of the argument one has the following considerations. (*a*) The convenient principle of charge symmetry can be kept as a result of introducing the hard core for singlet states. (*b*) There is an appealing connection with saturation of nuclear forces. (*c*) Fits to experiment can perhaps be improved by combining the repulsive core with interactions of the $\boldsymbol{A}_1 \cdot \boldsymbol{\sigma}_1 + \boldsymbol{A}_2 \cdot \boldsymbol{\sigma}_2$ type. The presence of such interactions is indicated by *j-j* coupling in heavy nuclei. There is the possibility, however, that strong coupling of $\boldsymbol{L}$ to $\boldsymbol{S}$ is a many-nucleon phenomenon.

The angular isotropy at high energies suggests either a superposition of phase shifts or else a radical departure from the low energy condition. A possibility of the latter type has been recently suggested (31, 36), the question having been raised as to whether protons have isomers. The formation of an isomer of one of the protons in the final state can be helpful in accounting for the facts provided it can be produced from states other than ^1S of the incident wave. Conservation of angular momentum and of parity are both satisfied if the isomer is odd and has spin 1/2 since then the $^3P_1$ state of the incident wave can produce a ^3S state. In order to maintain this explanation it would be necessary to suppose that transitions to an isomeric state are very improbable except in high energy collisions. Towler's (7) results and their agreement with the findings of Segrè *et al.* (2) regarding the maximum at low energies make the isomeric state explanation less attractive. Together with the Berkeley measurements they suggest that the Coulomb field interference with specific nuclear scattering is at least partly responsible for the apparent isotropy.

LOW ENERGY SCATTERING

Nuclear Force Parameters

The main purpose of the low energy (0 to 20 Mev) scattering experiments is the same as that of all *p-p* and *p-n* scattering work, viz., to ascertain the origin of the force between nucleons. In the present state of the subject one is apparently still far from the ultimate goal and the low energy scatter-

ing experiments have an additional practical value in furnishing a phenomenologic approach to the two-nucleon problem which is of value in studies of the structure of the lighter nuclei. The interpretation of low energy scattering experiments is closely connected with the knowledge of a few other nuclear force parameters and some of the progress in this related field will therefore be incidentally mentioned.

Binding energy of the deuteron.—The term "binding energy" will be used so as to give a negative quantity for a stable nucleus. Bell & Elliott (37) have obtained an improved value

$$\epsilon = -(2.230 \pm .007) \text{ Mev.}$$

by measuring the γ-ray energy for $n(p, \gamma)d$. From the threshold of $H^2(\gamma, n)H^1$ standardizing on 1.882 $(1 \pm .001)$ Mev for the $Li^7(p, n)Be^7$ threshold (38), Mobley & Laubenstein (39) obtained

$$\epsilon = -(2.226 \pm .003) \text{ Mev.}$$

A check is obtained by Salpeter (40) from the Q value (41) of $H^3(p, n)He^3$ and from the mass spectroscopic mass difference (42) between the deuteron and the hydrogen molecule. These lead to

$$\epsilon = -(2.224 \pm .006) \text{ Mev.}$$

Proton scattering of thermal neutrons.—In terms of the Fermi intercepts (scattering lengths) of $r \times$radial function the determinations are (43)

$$2(3\,{}^3a/4 + {}^1a/4) = (3.78 \pm .02) \times 10^{-13} \text{ cm.}$$

for the coherent amplitude and (44)

$$\pi[3({}^3a)^2 + ({}^1a)^2] = (20.36 \pm .10) \times 10^{-24} \text{ cm.}^2$$

for the scattering cross section of epithermal neutrons. Here $a > 0$ for a small attraction between the particles so that a has the same sign as the small positive phase shift to which it is related. The above values give

$${}^3a = -5.378(1 \pm .0038) \times 10^{-13} \text{ cm.}$$

$${}^1a = -23.69(1 \pm .0022) \times 10^{-13} \text{ cm.}$$

which differ slightly but not significantly from those used by Salpeter (40).

Photomagnetic capture.—Bishop, Halban, Shaw & Wilson (45) have measured the ratio of the photoelectric and photomagnetic deuteron cross sections. The theoretical angular distributions then enabled the determination of

$$\sigma_m/\sigma_e = .61 \pm .04.$$

The most recent measurement of the photomagnetic capture cross section for thermal neutrons is that of Whitehouse & Graham (46), who determined the ratio of the capture cross section of boron to that of hydrogen as 2270 ± 30 at an energy of (1/40) ev. The corresponding value of the capture cross sec-

tion for hydrogen according to Feshbach & Schwinger (35) is

$$\sigma^{\text{cap}} \text{ (photomagnetic)} = (.310 \pm .02) \times 10^{-24} \text{ cm.}^2$$

as obtained originally by Bethe & Longmire (47) from σ_B/σ_H and Fermi & Marshall's (48) result $\sigma_B = (707 \pm 7)$ barns. According to Bishop *et al.* (49) the error of this determination may be underestimated.

Photoelectric and photomagnetic disintegration.—Bishop *et al.* (49) have made precision measurements of the photodisintegration of the deuteron. Following Hulthén (50) Bishop *et al.* (49) also calculated the theoretically expected results and found general agreement with experiment. It is felt by some, however, that emphasis on a meson theory is premature for low energy γ-rays.

Data on Low Energy Proton-Proton Scattering

Yovits *et al.* (51) have summarized information on low and intermediate energy p-p scattering up to August 1951. Their fits to experiment are reproduced here in Figure 6. The data used are mentioned in the figure caption. The fits referred to in the figure may be described in terms of the expansion

$$f = f^{(0)} + f^{(1)}E_{\text{Mev}} + f^{(2)}E_{\text{Mev}}^2 + \cdots$$

where f is the function of Breit, Condon & Present (52)

$$f = [2\pi/(e^{2\pi\eta} - 1)] \cot K_0 - 2 \ln \eta + (q_0/\eta),$$

with

$$q_0/(2\eta) = 2\gamma - 1 + R.P.[\Gamma'(i\eta)/\Gamma(i\eta)] = \gamma - \frac{1}{1+\eta^2} + \sum_{s=2}^{\infty} \frac{\eta^2}{s(s^2+\eta^2)},$$

$$\gamma = 0.5772\cdots = \text{Euler's constant},$$

$$\eta = ZZ'e^2/\hbar v, \qquad 1/\eta^2 = 40.01E_{\text{Mev}}.$$

This function has an immediate simple significance in terms of the logarithmic derivative of the radial wave function and is related as follows to the functions introduced later

$$K = \tfrac{1}{2}f + 1 - 2\gamma = \tfrac{1}{2}f = 0.15443,$$
$$f_{\text{Bethe}} = f + 2 - 2\gamma = f + 0.84557.$$

Here K is the function used by Jackson & Blatt (53) in their most comprehensive report on p-p scattering and f_{Bethe} is the function used by Bethe (54). The fits in the figure correspond to values in Table IV.

The values used in the least-squares fits are confined to the energy range 0.25 to 3.53 Mev. The fit of experiment to theory for the Yukawa potential is shown in Figure 7. The quantity y in this figure is

$$y = (C'a'^2)^{-1/2}$$

where the Yukawa potential is written as

$$-C'\Upsilon(r/a')$$

TABLE IV

f-FUNCTION FITS FOR EXPERIMENTAL PROTON-PROTON SCATTERING DATA

Type of Potential Well	Type of Fit	$f^{(0)}$	$f^{(1)}$	$f^{(2)}$
Meson	Quadratic*	$7.788 \pm .009$	0.952 ± 0.005	-0.00948
Exponential	Quadratic†	7.810	0.922	-0.0015
Square well	Quadratic†	7.825	0.899	0.0048
None	Quadratic	7.785	0.956	-0.0104
None	Linear‡	7.811	0.917	0

* Mean of internal and mixed criteria used for relative weight assignment.

† These fits have not been made as accurately as the fit for the Meson well.

‡ In this and in the preceding fit an ordinary least-squares fit is made.

and C' is in mc^2, a' in e^2/mc^2. The "best" potentials of Figure 6 are given in Table V. Probable errors indicated in Table V have a nominal significance only. The fits to data made by Yovits *et al.* (51) presuppose a pure s wave scattering anomaly. Some quantities useful in such work are tabulated by them.

TABLE V

POTENTIAL FOR "BEST" FITS TO PROTON-PROTON SCATTERING DATA

Depth Constant	Range Constant	Potential	Potential Type
$C=(93\pm1)mc^2$	$a=(0.412\pm0.002)(e^2/mc^2)$	$-C\mathcal{Y}(r/a)$	Yukawa
$B=214mc^2$	$b'=0.251\ e^2/mc^2$	$-Be^{-r/b'}$	Exponential
$D=12.60$ Mev	$r_0=0.919\ e^2/mc^2$	$-D-(e^2/r)$, $(r<r_0)$ 0, $(r>r_0)$	Square well with suppression of Coulomb field
$D=13.50$ Mev	$r_0=0.919\ e^2/mc^2$	$-D$, $(r<r_0)$ 0, $(r>r_0)$	Square well

See opposite page for figures.

FIG. 6. (Above) *Lower curve:* Plot of f versus E for best fits with experimental points as designated, using scales on right and lower margins. *Upper curves:* Plot of f versus E for best fits as labeled with experimental points having the following designations: HKPP—Herb, Kerst, Parkinson & Plain (56); BFLSW—Blair, Freier, Lampi, Sleator & Williams (79); R—Rouvina (80); MP—May & Powell (81); M—Meagher (82); Ma—Mather (83); ZK—Zimmerman & Kreuger (84); WC—Wilson & Creutz (9); W—Wilson (85); RW—Faris & Wright (86); WLRWS—Wilson, Lofgren, Richardson, Wright & Shankland (87); C—Cork (88); PF—Panofsky & Fillmore (89). The scales on the left and upper margins are used with the upper curves.

FIG. 7. (Below) Theoretical values of f—$(7.7941+0.9643E)$ for $a^1=0.41$ and 0.415 with y_1, y_2, y_3 having the values 0.2514372, 0.2511965, 0.2509653, respectively, vs. E, together with the least-squares fit to data, and experimental points as designated.

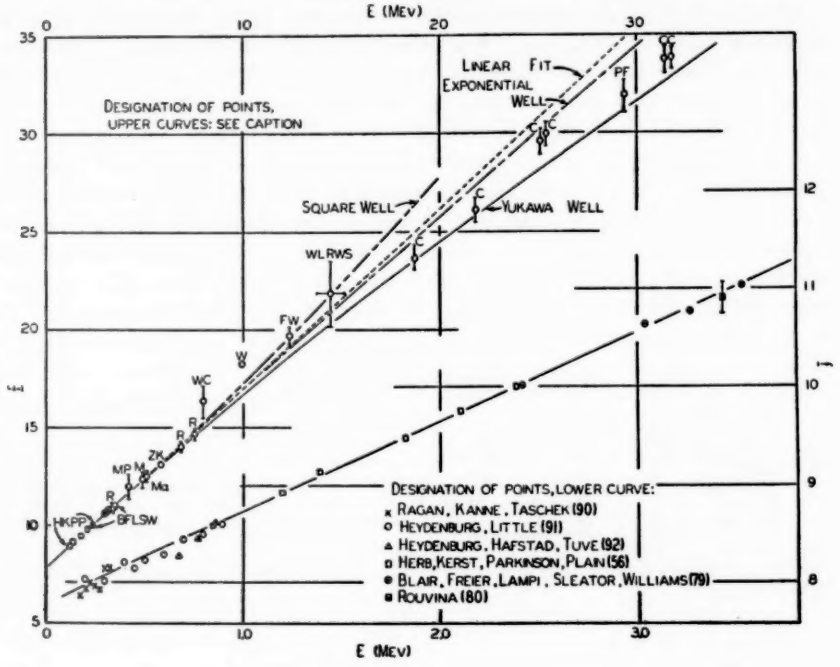
E (MEV)
LINEAR FIT
EXPONENTIAL WELL
DESIGNATION OF POINTS, UPPER CURVES: SEE CAPTION
SQUARE WELL
YUKAWA WELL
WLRWS
FW
WC
MP
ZK
BFLSW
HKPP
DESIGNATION OF POINTS, LOWER CURVE:
x RAGAN, KANNE, TASCHEK (90)
o HEYDENBURG, LITTLE (91)
△ HEYDENBURG, HAFSTAD, TUVE (92)
□ HERB, KERST, PARKINSON, PLAIN (56)
● BLAIR, FREIER, LAMPI, SLEATOR, WILLIAMS (79)
■ ROUVINA (80)
E (MEV)

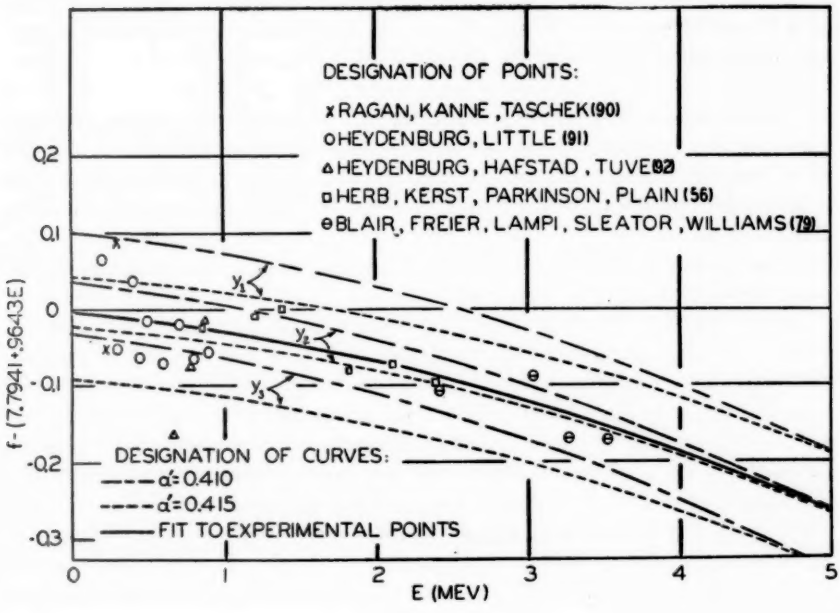
DESIGNATION OF POINTS:
x RAGAN, KANNE, TASCHEK (90)
o HEYDENBURG, LITTLE (91)
△ HEYDENBURG, HAFSTAD, TUVE (92)
□ HERB, KERST, PARKINSON, PLAIN (56)
⊖ BLAIR, FREIER, LAMPI, SLEATOR, WILLIAMS (79)
f-(7.7941+.9643E)
DESIGNATION OF CURVES:
α'=0.410
α'=0.415
FIT TO EXPERIMENTAL POINTS
E (MEV)

The most accurate measurements to date have been obtained by Worthington, Findley & McGruer (55) at the University of Wisconsin. This work was done under the supervision of Professor R. G. Herb and the benefit of previous experience (56) has been available to the group. The apparatus is in some respects an enlarged version of that used previously. Several essential new features have been incorporated and it is believed that these have resulted not only in an improvement regarding apparent consistency of data at different angles and energies but also in the elimination of systematic errors. The availability of higher energies and the exceptionally high energy resolution made possible by the large electrostatic analyzer (57) may be expected to make the new Wisconsin data especially reliable.

A vertical section of the scattering chamber is shown in Figure 8 (Figure

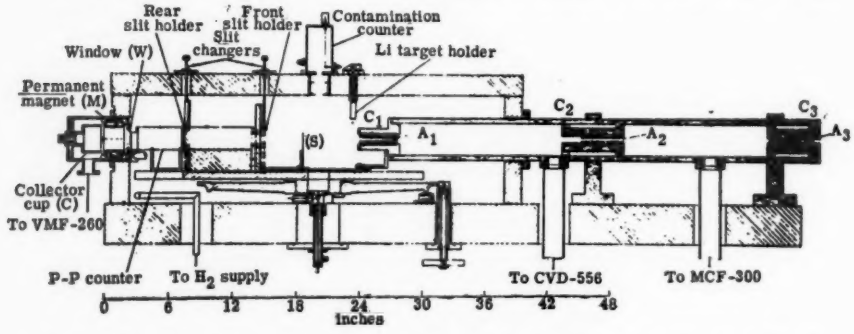

FIG. 8. Vertical section of the scattering chamber used by Worthington, Findley & McGruer (55) showing the long collimator using no foils, the contamination counter and the permanent magnet at the collector cup.

1 of dissertations of Findley & McGruer). Special features of the chamber are: (a) a long collimator employing no foils and eliminating spread of beam by multiple scattering in a foil, (*b*) a contamination counter and (*c*) a permanent magnet at the collector cup. The large size of the chamber as a whole should be noted.

The principal precautions, some of which have also been taken in the older work of Herb *et al.* (56) are:

(*a*) Correction for contamination. Since a small amount of air or of another impurity can cause relatively large fractional errors at small angles and since one of the objects of this work was to detect waves with $L>0$, special care was taken to make the correction for contamination as small as possible and to ascertain its value accurately. Tests were performed employing no hydrogen in the chamber and a special contamination counter was used during the regular runs. This counter viewed the incident beam at an angle of $\sim 90°$ with the direction of incident protons and the counter window was thick enough to stop protons scattered towards the counter. Tests on the variation of the contamination counts (90°) with energy were made before

each run. It was assumed that at a small scattering angle (20°) the contamination scattering varies with energy according to Rutherford's formula and the variation of the contamination scattering with angle was studied without hydrogen in the chamber by means of the counter used in the regular runs. The correction for scattering from contamination was then calculated on the assumption that the composition of the contamination is the same with and without hydrogen in the chamber. The experimenters are aware of the fact that this assumption is perhaps not completely justified. They point out in fact that approximately 75 per cent of the contamination counting rate was due to materials carried into the chamber by the hydrogen. The corrections for contamination were usually less than 0.1 per cent for scattering angles of 25° or larger. The probable error of the correction is considered to be about 30 per cent of the correction and the probable error of the yield for angles greater than 25° is accordingly about 0.03 per cent. The basis for assigning an uncertainty of 30 per cent to the contamination correction is the observation that during regular runs there occur occasional jumps in the contamination yield causing changes in counts at different angles which do not reproduce the angular variation expected from runs in the absence of hydrogen to better than 30 per cent. The correction increases rapidly at smaller angles. Thus at 1.855 Mev it is -0.71 at 15° and -0.02 at 45°; at 4.203 Mev it was -0.17 at 15° and -0.01 per cent at 35°. The uncertainty at small angles is of interest in the determination of scattering anomalies with $L>0$. Some improvements in the knowledge of the correction may result from studies of the scattering of protons from oxygen, nitrogen, and carbon.

(*b*) Energy definition and measurement. By means of the 90° electrostatic analyzer, previously referred to, the energy was defined to within 0.1 per cent. The reference standard was the $Li^7(p, n)Be^7$ threshold. The value for the threshold was used as $1.882 \pm .002$ Mev absolute as determined by Herb, Snowden & Sala (38). A small correction for energy loss in hydrogen was applied so as to obtain the energy at the scattering volume.

(*c*) Improvements in the measurement of charge in the primary beam. Among these are: the employment of a polystyrene four μf. condenser in the current integrator, precautions regarding leakage and operation of the current integrator circuit, precautions to eliminate secondary electron emission effects through the use of a magnet.

(*d*) Corrections for slit-edge scattering in the analyzer. Study of pulse-height distribution indicated the presence of low energy protons arising from slit-edge scattering in the analyzer. The corrections are known to within about 20 per cent of their value.

(*e*) Corrections for slit-edge scattering in the collimator. Pulse-height distribution as a function of counter gas pressure showed effects which are attributed to low energy protons in the incident beam and slit scattering in the collimator is held responsible for their production. Corrections have accordingly been applied. They are of roughly the same order as those for slit-edge scattering in the analyzer.

(*f*) Multiple scattering in counter assembly. Effects of multiple scattering in the slit system preceding the *p*-*p* scattering counter have been minimized by arranging for approximate compensation of protons scattered out of and into the beam.

An analysis of these careful observations has been made by Powell & Hall (58). They find that agreement with experiment can be improved through the inclusion of *p* wave scattering in the interpretation. On the assumption of equality of phase shifts for the three states $^3P_{0,1,2}$ the *p* wave phase shift K_1 is negative. Outstanding uncertainties in the data do not exclude other interpretations in terms of three unequal *p* wave-phase shifts for the three components of ^3P or of ^1D and ^3F waves. Hall & Powell (59) find that the *s* wave scattering anomaly fits expectation from older experiments and analyzes very well. An independent and later analysis of the data made by M. H. Hull and A. Herschman at Yale gave very similar results.

Some outstanding questions may be mentioned. At scattering angles of 6° to 8° in the laboratory system the observed scattering is greater than that calculated assuming only *s* and *p* phase shifts from $\Theta=15°$ to $\Theta=45°$. In many cases the discrepancy is not much greater than the supposed uncertainty in experimental results. Nevertheless it is strange that it appears consistently at all of the higher energies of the new Madison data. This discrepancy may be an indication of the presence of an unknown factor either in the theory of the elementary process or in the interpretation of the data. The discrepancy appears somewhat more strongly in the analysis of Hull & Herschman than in that of Powell & Hall. Hull & Herschman pay less attention to the smallest scattering angles in their determination of K_1. The discrepancies become accordingly more pronounced. A decision regarding the best interpretation appears to be premature. At the smallest scattering angles there is more difficulty in avoiding errors caused by finiteness of angular openings and coplanarity of lines defined by the beam collimator, and the counter slit system is also important.

The variation of K_1 with energy is slower than expected for the Yukawa potential with a range constant corresponding to the energy variation of K_0. It is disturbing that the apparent K_1 reaches a plateau and even decreases at the highest energy, 4.203 Mev, of the new set of data. The experimenters do not attach enough weight to the observations to justify a definite conclusion from the apparent anomaly in the energy behavior of K_1. Powell & Hall point out that with the exception of $E=4.203$ Mev, a monotonically increasing curve representing K_1 as a function of E could be drawn through the points within the experimental uncertainty.

According to Powell & Hall their value of K_1 is not in contradiction with the more general phenomenological fits of Feshbach & Schwinger (35), which allow the combination $.35+.65\ P_m$ of ordinary and coordinate exchange forces. In the ^3P state the repulsive potential is only slightly smaller than the lower limit set many years ago by Feenberg (60) from saturation arguments

and does not contradict the additional upper limit found in Breit & Wigner (61). Since the whole question of comparison with requirements for saturation of nuclear forces is bound up with differences in range of force and with velocity dependence (62) of potential well depths and since it may be connected with nonlinearity (63), it is probably premature to speculate on the significance of the comparisons just made. But whatever the ultimate conclusion, these developments appear to contain the first indication of the setting in of a deviation from a pure s scattering anomaly as the energy is increased. One may hope that it will provide the necessary certainty in the interpretation of data at higher energies where the presence of anomalies with $L>0$ may be expected to be more marked but also more difficult to unravel on account of the simultaneous presence of many effects.

A comparison of the experimental values of the differential cross section obtained by Worthington, Findley & McGruer (55) with previous experimental results of Herb *et al.* (56) and Blair and co-workers (79) is shown in Figure 9 (from the dissertations of D. E. Findley and J. N. McGruer). The internal consistency of the most recent Wisconsin data as well as the consistency with the previous experimental results is readily seen. A comparison of the experimental points with an s wave fit is given in Figure 10 (from the dissertation of J. N. McGruer), which shows a small but consistent deviation of the experimental points from the curve, suggesting the small negative p wave of Powell & Hall (58).

Observations at $E=18.2$ Mev have been made by Yntema & White (64). Through the courtesy of these authors their data, as of 16 April, 1952, is given in Table VI.

TABLE VI

PROTON-PROTON SCATTERING AT 18.2 MEV*

θ (degrees)	σ_Ω (millibarns/steradian)	Relative Probable Error (per cent)
90	27.32	.5
80	27.29	.5
70	27.47	.5
60	27.42	.6
50	27.27	.7
40	26.50	1.0
36	25.98	1.2
30	25.00	1.2

* According to Yntema & White (64).

Yntema & White believe that the cross sections are accurate to about 1 per cent in absolute value. They have obtained fits to their data by means of the following two combinations of phase shifts:

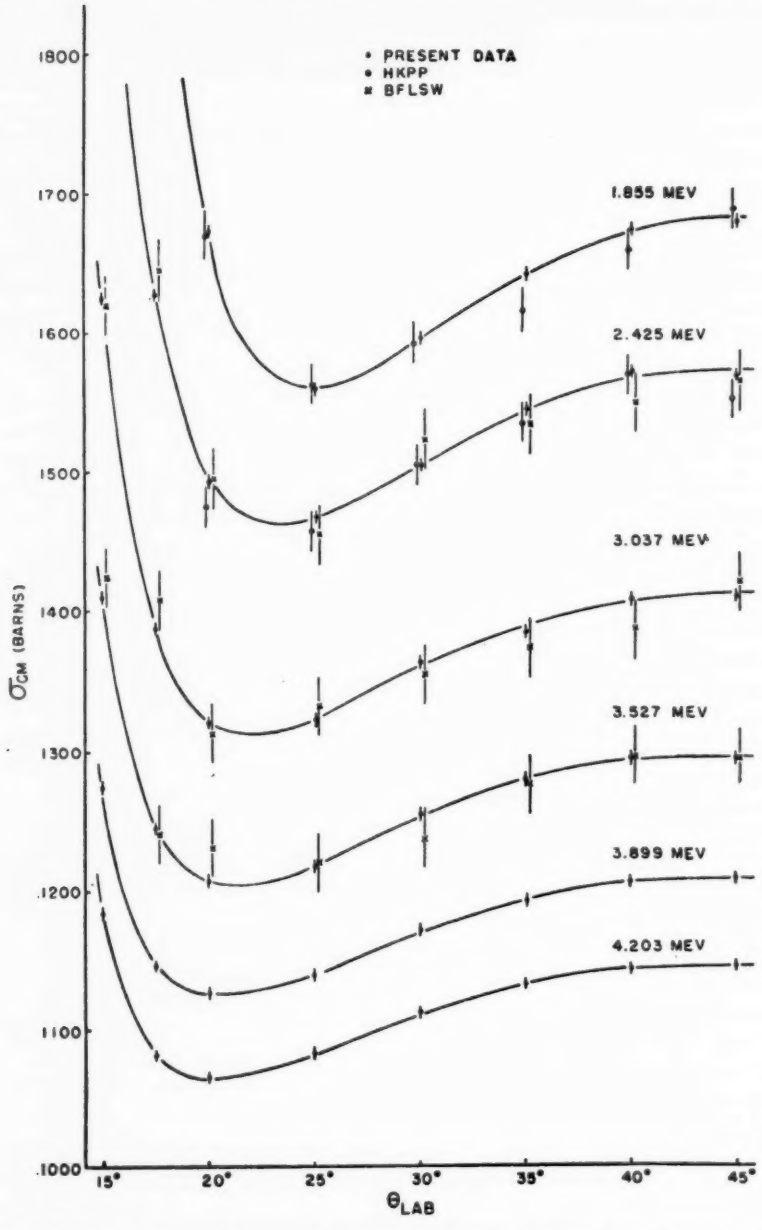

FIG. 9. Comparison of the experimental values of the p-p differential cross section, $\sigma(\theta)$, of Worthington, Findley & McGruer (55) with those of Herb, Kerst, Parkinson & Plain (56) and Blair, Freier, Lampi, Sleator & Williams (79).

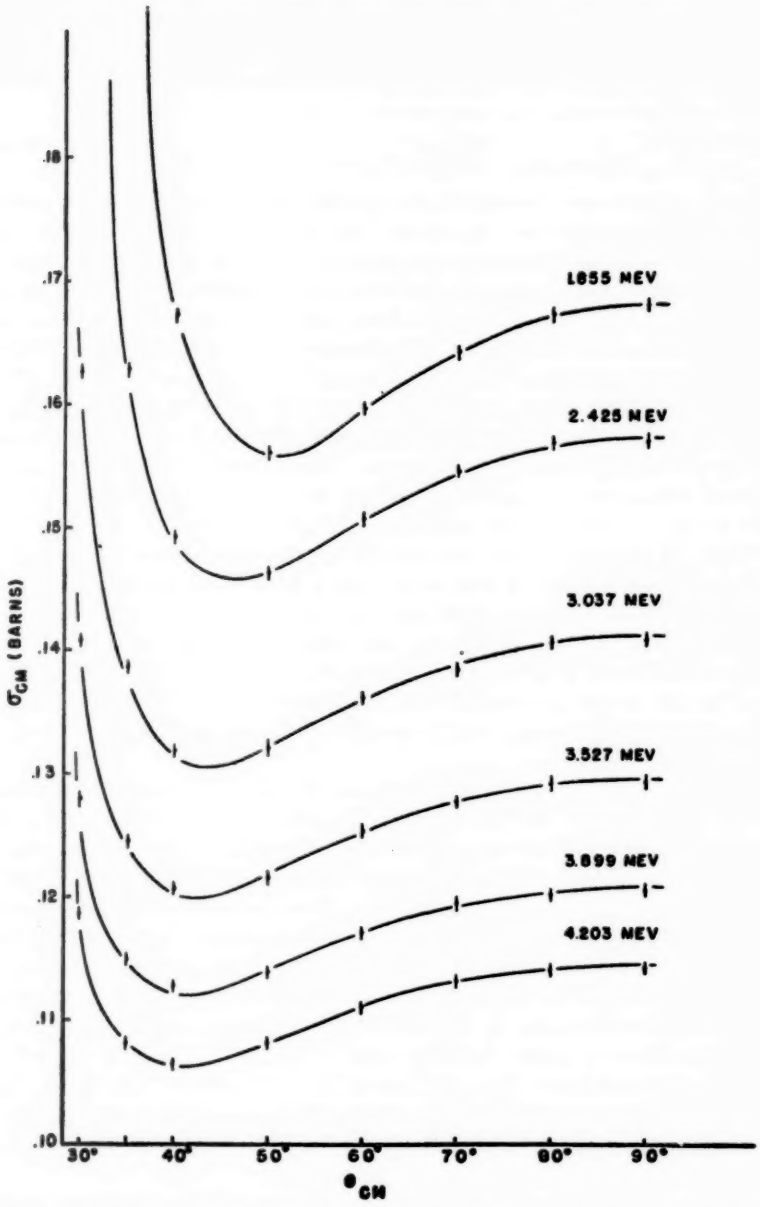

FIG. 10. Comparison of the experimental values of the *p-p* scattering data of Worthington, Findley & McGruer (55) with a pure *s* wave fit.

$(K_0 = 53.8°, K_2 = 0.3°)$, $(K_0 = 54.1°, K_1 = 1.0°, K_2 = 0.4°)$

and they believe that a Gauss error curve potential in the singlet state combined with a tensor interaction for triplet states is suggested by their results. These conclusions are of a preliminary character.

Advances in Phenomenological Treatments

Lack of space prevents a detailed account of advances in phenomenological treatments of the two and three body problem which have been made. The reader may be referred to the work of Pease & Feshbach (34) on the binding energy of H^3, to the work of Blatt & Biedenharn (65) on the rigorous treatment of forces not derivable from potentials by means of scattering parameters, and to the papers of Bethe (54), Bethe & Longmire (47), Salpeter (40) and Feshbach & Schwinger (35) for the consideration of best values of parameters on the basis of the binding energy of the deuteron, thermal neutron scattering lengths, intermediate energy n-p and p-p scattering, photodisintegration of the deuteron. The treatment of the latter involves consideration of the exchange moment which is also important in reconciling data on the static magnetic moments of H^3 and He^3 (66).

Pease & Feshbach (34) are able to obtain satisfactory fits practically without a term in $(\vec{\sigma}_1 \cdot \vec{\sigma}_2)$ and employing a tensor interaction instead. The possible importance of the latter may be connected with the results of Feingold & Wigner (27) which indicate that tensor forces may be responsible for the level structure of Li^6 and Li^7. Salpeter (40) arrives at an effective meson mass for the triplet interaction which is closely that of the π meson. In the singlet state his range constant is smaller corresponding to a meson mass of $(365 \pm 80)m$.

Hansson & Hulthén (50) and Hansson (67) have investigated the theory of the photoelectric and photomagnetic cross sections employing central forces. Feshbach & Schwinger (35) take into account the tensor force and employ different ranges for the central and tensor forces but do not distinguish between singlet and triplet ranges. They find it possible to account for the photodisintegration of the deuteron at low energies. A brief report to the same effect has been made by von Halban (68). In connection with the work of Poss, Salant & Yuan (69) on the total cross section for 14 Mev neutrons a theoretical consideration by G. A. Snow (70) presents some evidence to the effect that the n-p singlet intrinsic range is smaller than the p-p singlet intrinsic range but Snow does not regard the evidence as conclusive. Agreement of experiment with theory is on the whole satisfactory in all of the investigations perhaps as a consequence of the many adjustable parameters which may be introduced.

A refinement has been attempted by Schwinger (71), who shows that the consideration of relativistic and magnetic effects can be exploited so as to decrease the remaining discrepancies in potential well depth constants for n-p and p-p interactions which result if the ranges of these two interactions are assumed to be the same.

METHODS OF CALCULATION

Recent advances in methods of calculation are partly summarized by Breit (72), who also presents a way of generalizing the application of the f function to problems involving more than two bodies. The three body case has been previously treated by Verde (73). Breit & Yovits (74) show the relation of general properties of f to the considerations of Jackson & Blatt (53) and work out a general form for the coefficients of powers of E in expansions of f. For a study of methodology in the computation of phase shifts and the practical application of the variational method reference should be made to the paper by Blatt & Jackson (75) on neutron-proton scattering and of Jackson & Blatt (53) on proton-proton scattering. An ingenious method of a different type which has so far received little application has been worked out by Ferretti & Krook (76). It has been found very useful by Barker & Ravenhall (77) in their work on the scattering of like particles at 100 Mev. Space does not permit more explicit mention of the many other important advances (78) in mathematical techniques.

LITERATURE CITED

1. Chamberlain, O., Segrè, E., and Wiegand, C., *Phys. Rev.*, **83,** 923 (1951)
2. Segrè, E., *Proc. Intern. Conf. Nuclear Physics and Physics Fundamental Particles,* 87 (September, 1951)
3. Christian, R. S., and Hart, E. W., *Phys. Rev.*, **77,** 441 (1950)
4. Birge, R. W., Kruse, U. E., and Ramsey, N. F., *Phys. Rev.*, **83,** 274 (1951)
5. Oxley, C. L., and Shamberger, R. D., *Phys. Rev.*, **85,** 416 (1952)
6. Aamodt, L., Peterson, V., and Phillips, R., *UCRL*, 526 (1949)
7. Towler, O. A., Jr., *Phys. Rev.*, **85,** 1024 (1952)
8. Cassels, J. M., *Proc. Intern. Conf. Nuclear Physics and Physics Fundamental Particles,* 95 (September, 1951)
9. Wilson, R. R., and Creutz, E. C., *Phys. Rev.*, **71,** 339 (1947)
10. Rarita, W., and Schwinger, J., *Phys. Rev.*, **59,** 556 (1941)
11. Camac, M., and Bethe, H. A., *Phys. Rev.*, **73,** 191 (1948)
12. Wu, T. Y., and Ashkin, J., *Phys. Rev.*, **73,** 986 (1948)
13. Ashkin, J., and Wu, T. Y., *Phys. Rev.*, **73,** 973 (1948)
14. Cook, L. J., McMillan, E. M., Peterson, J. M., and Sewell, D. C., *Phys. Rev.*, **72,** 1264 (1947)
15. Barker, F. C., *Nature*, **161,** 726 (1948)
16. Chew, G. F., and Goldberger, M. L., *Phys. Rev.*, **73,** 1408 (1948)
17. Eisenstein, J., and Rohrlich, F., *Phys. Rev.*, **73,** 641 (1948)
18. Rohrlich, F., and Eisenstein, J., *Phys. Rev.*, **75,** 705 (1949)
19. Massey, H. S. W., Burhop, E. H. S., and Hu, T. M., *Phys. Rev.*, **73,** 1403 (1948)
20. Hu, T. M., and Massey, H. S. W., *Proc. Roy. Soc.* (*London*) [A]**196** (1949)
21. Burhop, E. H. S., and Yadav, H. H., *Proc. Roy. Soc.* (*London*) [A]**505** (1949)
22. Christian, R. S., and Noyes, H. P., *Phys. Rev.*, **79,** 85 (1950)
23. Case, K. M., and Pais, A., *Phys. Rev.*, **80,** 203 (1950)
24. Jastrow, R., *Phys. Rev.*, **79,** 389 (1950)
25. Mayer, M. G., *Phys. Rev.*, **75,** 1969 (1949); **78,** 16, 22 (1950)
26. Haxel, O., Jensen, J. H. D., and Suess, H. E., *Phys. Rev.*, **75,** 1766 (1949)
27. Feingold, A. M., and Wigner, E., *Phys. Rev.*, **79,** 221 (1950)
28. Jastrow, R., *Phys. Rev.*, **79,** 389 (1950); **81,** 165 (1951)
29. Parzen, G., and Schiff, L. I., *Phys. Rev.*, **74,** 1564 (1948)
30. Olsson, P. O., *Phys. Rev.*, **83,** 845 (1951)
31. Breit, G., *Proc. Intern. Conf. Nuclear Physics and Physics Fundamental Particles,* 102 (September, 1951)

31a. Hull, M. H., and Herschman, A., (Personal communication)

32. Guindon, W. G., *Phys. Rev.*, **74,** 145 (1948)
33. Broyles, A. A., and Hull, M. H., *Phys. Rev.*, **79,** 247 (1950)
34. Pease, R. L., and Feshbach, H., *Phys. Rev.*, **81,** 142 (1951)
35. Feshbach, H., and Schwinger, J., *Phys. Rev.*, **84,** 194 (1951)
36. Breit, G., *Phys. Rev.*, **84,** 1053 (1951); *Bull. Am. Phys. Soc.*, **27,** (3), 32 (1952); *Phys. Rev.*, **87,** 208 (1952); Breit, G., and Jones, H. M., *Phys. Rev.*, **84,** 1054 (1951)
37. Bell, R. E., and Elliott, L. G., *Phys. Rev.*, **79,** 282 (1950)
38. Herb, R. G., Snowden, S. C., and Sala, O., *Phys. Rev.*, **75,** 246 (1949)
39. Mobley, R. C., and Laubenstein, R. A., *Phys. Rev.*, **80,** 309 (1950)
40. Salpeter, E. E., *Phys. Rev.*, **82,** 60 (1951)

41. Taschek, R. F., Argo, H. V., Hemmendinger, A., and Jarvis, G. A., *Phys. Rev.*, **76,** 325 (1949)
42. Roberts, T. R., and Nier, A. O., *Phys. Rev.*, **77,** 746 (1950)
43. Hughes, D. J., Burgy, M. T., and Ringo, G. R., *Phys. Rev.*, **77,** 291 (1950); *Phys. Rev.*, **79,** 227 (1950); Ringo, G. R., Burgy, M. T., and Hughes, D. J., *Phys. Rev.*, **82,** 344 (1951)
44. Melkonian, E., *Phys. Rev.*, **76,** 1744 (1949)
45. Bishop, G. R., Halban, H., Shaw, P. F. D., and Wilson, R., *Phys. Rev.*, **81,** 219 (1951)
46. Whitehouse, W. J., and Graham, G. A. R., *Can. J. Research*, [A]**25,** 261 (1947)
47. Bethe, H. A., and Longmire, C., *Phys. Rev.*, **77,** 647 (1950)
48. Fermi, E., and Marshall, L., *Phys. Rev.*, **72,** 193 (1947)
49. Bishop, G. R., Collie, C. H., Halban, H., Hedgran, A., Siegbahn, K., du Toit, S., and Wilson, R., *Phys. Rev.*, **80,** 211 (1950)
50. Hansson, I. F. E., and Hulthén, L., *Phys. Rev.*, **76,** 1163 (1949)
51. Yovits, M. C., Smith, R. L., Hull, M. H., Bengston, J., and Breit, G., *Phys. Rev.*, **85,** 540 (1952)
52. Breit, G., Condon, E. U., and Present, R. D., *Phys. Rev.*, **50,** 825 (1936)
53. Jackson, J. D., and Blatt, J. M., *Rev. Mod. Phys.*, **22,** 77 (1950)
54. Bethe, H. A., *Phys. Rev.*, **76,** 38 (1949)
55. Worthington, H. R., Findley, D. E., and McGruer, J. N., *Bull. Am. Phys. Soc.*, **27**(3), 47 (1952); *Phys. Rev.*, **87,** 223 (1952)
56. Herb, R. G., Kerst, D. W., Parkinson, D. B., and Plain, G. J., *Phys. Rev.*, **55,** 998 (1939)
57. Warren, R. E., Powell, J. L., and Herb, R. G., *Rev. Sci. Instruments*, **18,** 559 (1947)
58. Powell, J. L., and Hall, H. H., *Bull. Am. Phys. Soc.*, **27**(3), 47 (1952); *Phys. Rev.*, **87** 223 (1952)
59. Hall, H. H., and Powell, J. L., *Bull. Am. Phys. Soc.*, **27**(3), 47 (1952); *Phys. Rev.*, **87,** 223 (1952)
60. Feenberg, E., *Phys. Rev.*, **52,** 667 (1937)
61. Breit, G., and Wigner, E. P., *Phys. Rev.*, **49,** 519 (1936)
62. Breit, G., and Yost, F. L., *Phys. Rev.*, **48,** 203 (1935); Breit, G., Thaxton, H. M., and Eisenbud, L., *Phys. Rev.*, **55,** 1018 (1939)
63. Schiff, L. I., *Phys. Rev.*, **84,** 1 (1951); *Phys. Rev.*, **84,** 10 (1951)
64. Yntema, J. L., and White, M. G., *Bull. Am. Phys. Soc.*, **27**(3), 47 (1952); *Phys. Rev.*, **87,** 223 (1952)
65. Blatt, J. M., and Biedenharn, L C., *Bull. Am. Phys. Soc.*, **27**(1), 35 (1952); *Phys. Rev.*, **86,** 610 (1952)
66. Avery, R., and Adams, N. E., *Phys. Rev.*, **75,** 1106 (1949); Sachs, R. G., *Phys. Rev.*, **69,** 611 (1946); Sachs, R. G., and Schwinger, J., *Phys. Rev.*, **70,** 41 (1946); Austern, N., and Sachs, R. G., *Phys. Rev.*, **81,** 710 (1951)
67. Hansson, I. F. E., *Phys. Rev.*, **79,** 909 (1950)
68. Halban, H. von, *Proc. Intern. Conf. Nuclear Physics and Physics Fundamental Particles*, 190 (September, 1951)
69. Poss, H. L., Salant, E. O., and Yuan, L. C. L., *Phys. Rev.*, **85,** 703 (1952)
70. Snow, G. A., *Phys. Rev.*, **85,** 703 (1952)
71. Schwinger, J., *Phys. Rev.*, **78,** 135 (1950)
72. Breit, G., *Rev. Mod. Phys.*, **23,** 238 (1951)

73. Verde, M., *Helv. Phys. Acta*, **22**, 339 (1949)
74. Breit, G., and Yovits, M. C., *Proc. Natl. Acad. Sci. U. S.*, **37**, 771 (1951)
75. Blatt, J. M., and Jackson, J. D., *Phys. Rev.*, **76**, 18 (1949)
76. Ferretti, B., and Krook, M., *Proc. Phys. Soc.* (*London*), **60**, 481 (1948)
77. Barker, F. C., and Ravenhall, D. G., *Nature*, **163**, 20 (1949)
78. Hulthén, L., *Transactions 10th Congr. Mathématiciens Scandinaves, Copenhagen*, 201 (1946); Hulthén, L., *Kgl. Fysiograf. Sällskap. Lund Förh.*, **14**, 8 (1944); **14**, 21 (1944); **15**, 22 (1945); Hulthén, L., *Arkiv Mat. Astron. Fysik*, [A]**35**, 1 (1948); Fröberg, C. E., *Arkiv Mat. Astron. Fysik*, [A]**34**, 1 (1947); [A]**35**, 1 (1948); [A]36, 1 (1948); Hansson, I., *Kgl. Fysiograf. Sällskab. Lund Förh.*, **18**, 1 (1948)
79. Blair, J. M., Freier, G., Lampi, E. E., Sleator, W., and Williams, J. H., *Phys. Rev.*, **74**, 553 (1948)
80. Rouvina, J., *Phys. Rev.*, **81**, 593 (1951)
81. May, A. N., and Powell, C. F., *Proc. Roy. Soc.* (*London*), [A]**190**, 170 (1947)
82. Meagher, R. E., *Phys. Rev.*, **78**, 667 (1950)
83. Mather, K. B., *Phys. Rev.*, **82**, 133 (1951)
84. Zimmerman, E. J., and Kreuger, P. G., *Phys. Rev.*, **83**, 218 (1950)
85. Wilson, R. R., *Phys. Rev.*, **71**, 384 (1947)
86. Faris, F., and Wright, B., *Phys. Rev.*, **79**, 577 (1950)
87. Wilson, R. R., Lofgren, E. J., Richardson, J. R., Wright, B. T., and Shankland, R. S., *Phys. Rev.*, **71**, 560 (1947)
88. Cork, B., *Phys. Rev.*, **80**, 321 (1950)
89. Panofsky, W. K. H., and Fillmore, F. L., *Phys. Rev.*, **79**, 57 (1950)
90. Ragan, G. L., Kanne, W. R., and Taschek, R. F., *Phys. Rev.*, **60**, 628 (1941)
91. Heydenburg, N. P., and Little, J. L. (Personal communication to authors in Ref. 51)
92. Heydenburg, N. P., Hafstad, L. R., and Tuve, M. A., *Phys. Rev.*, **56**, 1078 (1939)
93. Segrè, E., *Intern. Conf. Nuclear Physics, Physics Fundamental Particles* 94 (Chicago, Ill., September, 1951)
94. Kramers, H. A., and Bethe, H. A., *Ann Arbor Summer Symp.* (Ann Arbor, Mich., 1936)

HIGH ENERGY FISSION[1]

By R. W. Spence and G. P. Ford

University of California, Los Alamos Scientific Laboratory, Los Alamos, New Mexico

INTRODUCTION

Shortly after the discovery that U^{235} readily underwent fission with thermal neutrons, investigations were begun to determine what other nuclides could be made to fission. Neutrons of energy higher than thermal energy were used as well as γ-rays. As more intense sources of high energy particles were developed, fissionability studies were extended, until at the present time, particles with hundreds of million electron volts energy have been used to induce fission in elements as light as copper. In this article we survey the work done on fission using bombarding particles above thermal energies. The first section covers those experimental results which indicate at what energies neutrons, photons, and charged particles have been observed to induce fission in the elements so far studied; some idea of the fission cross sections is also given although in many cases only approximate values have been measured. For convenience, this first section on the fissionability of nuclides has been divided into two parts: the first part deals with heavy elements from thorium on up, while the second part deals with medium elements from bismuth on down. No fission studies have been reported as yet on elements between bismuth and thorium, and from the standpoint of ease of fissionability, the gap between the two groups is large. The second section of this article is concerned with the observed changes in modes of fission as the target element and the energy of the bombarding particle are changed.

FISSIONABILITY OF NUCLIDES

Heaviest Elements ($Z > 89$)

Neutron induced fission.—Aside from nuclides such as Pu^{239}, U^{235}, and U^{233}, which undergo fission with thermal neutrons, Np^{237}, U^{238}, Pa^{231}, and Th^{232} have all been observed to fission with somewhat more energetic neutrons. Klema (1) measured the Np^{237} fission cross section using neutrons from thermal energy to 3.0 Mev and observed the fission fragment pulses in an ionization chamber. The thermal cross section was apparently zero, but fissions were observed for 350-kev neutrons. The fission cross section rose rapidly with neutron energy up to about 1.0 Mev and stayed essentially constant at 1.45 barns from 1.0 to 3.0 Mev. Shoupp & Hill (2) found that U^{238} and Th^{232} fissioned with neutrons above 1.0 Mev, and Grosse, Booth &

[1] The survey of the literature pertaining to this review was concluded in June, 1952.

Dunning (3) fixed the threshold for neutron fission of Pa^{231} as being higher than thermal energy and less than 2.0 Mev.

Photon induced fission.—For the five nuclides Pu^{239}, U^{238}, U^{235}, U^{233}, and Th^{232}, the photofission thresholds are all 5.3 Mev within a few tenths of a million electron volt [Koch, McElhinney & Gasteiger (4)]. This result is not in accord with the predicted values calculated from the liquid drop model by Frankel & Metropolis (5). Photofission in uranium and thorium was first observed in 1941 by Haxby *et al.* (6) who used 6.3-Mev photons; their work was confirmed soon after by Arakatsu and co-workers (7). Later, Baldwin & Klaiber (8) studied the photofission of uranium and thorium with betatron x-rays of 100-Mev maximum energy. Because of the distribution of photon energies, they could not calculate fission cross sections as a function of photon energy, but for both uranium and thorium they could tell that the fission cross section went through a maximum somewhere between 10 and 20 Mev, dropping off to much smaller values at 30 Mev and above. Later work by Ogle & McElhinney (9) confirmed the existence of this resonance in the photofission of uranium. While Ogle & McElhinney could not arrive at a unique function for the change in fission cross section with photon energy, their data did show that the cross section went through a maximum at about 15 Mev. The photofission cross section for uranium is uniformly higher than for thorium by a factor of between two and four, depending on the method of observing fissions.

Fission induced by charged particles.—Various investigators in the years 1939 to 1941 observed that fission could be induced in uranium by bombardment with charged particles. In 1948, Jungerman & Wright (10) determined the excitation functions for the fission of uranium and thorium by α-particles and by deuterons. Their absolute values of the cross sections depended upon the assumption that the gross β-activity of the fission fragments produced was the same for charged particle fission as for thermal neutron fission. Therefore Jungerman (11) investigated the excitation functions by counting the ionization pulses of the fission fragments in an ionization chamber. He observed that beginning at deuteron energies of $\sim$10 Mev and α-particle energies of slightly over 20 Mev, the fission cross sections for U^{238}, U^{235}, and Th^{232} rose rapidly with incident particle energy. For deuterons on U^{238}, the fission cross section levelled off at $\sim$40 Mev and then stayed approximately constant at 1.3 barns for deuteron energies of 40 to 193 Mev. The excitation curves for deuterons on U^{235} and Th^{232} were similar, except that for Th^{232} a slow rise from $\sim$0.9 barn at 40 Mev to $\sim$1.2 barns at 193 Mev was observed, and for U^{235} a more pronounced rise from $\sim$1.3 barns at 40 Mev to $\sim$2.0 barns at 193 Mev was observed. The excitation curves using α-particles were similar, rising rapidly in the 20 to 40 Mev energy region, then levelling off and remaining roughly constant at $\sim$1.5 barns from 100 to 390 Mev. For Th^{232} in particular, there was some evidence for a dropping off of fission cross section at the highest energies. Jungerman suggested that it is likely that above $\sim$30 Mev other reactions begin to compete with fission.

O'Connor & Seaborg (12) bombarded uranium with 380-Mev α-particles

and then analyzed radiochemically for spallation and fission products. From the area under the fission yield curve, they could make a rough estimate of the fission cross section. Their value of 2.0 barns can be considered in essential agreement with the value of 1.5 barns reported by Jungerman, since O'Connor & Seaborg did not know accurately the intensity of their helium beam. Similarly, the work of Newton (13) on the fission of Th^{232} with 37.5-Mev α-particles gave a fission cross section of 0.6 barn, in fair agreement with the work of Jungerman.

Jungerman (11) obtained some preliminary results on proton induced fission by bombarding U^{238}, U^{235}, and Th^{232} with protons in the energy region 220 to 340 Mev; he found cross section values of $\sim$0.5 barn for U^{238}, 0.8 to 1.0 barn for U^{235}, and $\sim$0.35 barn for Th^{232}, all lower than the corresponding fission cross sections obtained in this energy region for α-particle and deuteron induced fission.

Meson induced fission.—The first reported study of meson induced fission was by Al-Salam (14), who loaded photographic emulsions with uranyl acetate and exposed the plates to mesons produced in the Berkeley 184-in. cyclotron. Of 2061 meson tracks observed, 22 terminated in fission tracks. It was calculated that 1 in 85 π^-mesons would be expected to enter a uranium nucleus, so the observed frequency of fission is in accord with the idea that every π^-meson entering a uranium nucleus causes fission.

Medium Heavy Elements ($Z < 84$)

Neutron induced fission.—Soon after the discovery of fission, numerous attempts were made to initiate fission in elements of atomic number 83 or less by irradiations with energetic neutrons. Negative results attended these early efforts, all of which used rather low intensity neutron sources. Magnan (15) reported probable fission pulses in an ionization chamber when gold, tungsten, and titanium were bombarded with Li-D neutrons. (About 10 per cent of these neutrons had an energy near 14 Mev.) However, Roberts, Meyer & Hafstad (16), also using Li-D neutrons, found that fission of seven elements in the tungsten to bismuth region amounted to no more than 1/1000 that of uranium. Broda & Wright (17) bombarded lead and bismuth with Li-D neutrons, then looked for radioactive iodine as a measure of the extent of the fission reaction. No positive evidence for the presence of iodine activity was found. Broda (18) also did a similar experiment but changed the method of detecting fissions by looking for fissions fragment tracks in Ilford α-sensitive emulsions; again no positive evidence for fission was obtained. Phillips, Rosen & Taschek (19) bombarded bismuth, lead, mercury, gold, iridium, and tungsten with 14-Mev neutrons and compared the number of fission tracks in a photographic emulsion with the number found in a similar emulsion in contact with uranium. Very few fission tracks were observed for elements tested, and these tracks could have been due to uranium contamination. The conclusion reached was that the highest fission cross section (for Pb^{203}) could not be greater than 1.3×10^{-3} barn while for the majority of the nuclides bombarded the cross sections must be no greater than 1×10^{-5} barn.

Meanwhile, experiments using neutrons up to 100-Mev energy from the 184-inch, frequency-modulated cyclotron at Berkeley obtained definite evidence for the fission of elements from platinum to bismuth. The first such evidence was reported by Perlman *et al.* (20), who irradiated bismuth and lead with 100-Mev neutrons and chemically identified radioactive fission products. Shortly thereafter, Kelley & Wiegand (21) published a report of their work on the fission of elements in the platinum to bismuth region with neutrons up to 84 Mev. Their method of detection was that of observing the ionization of the fission fragments in an ionization chamber. True excitation curves could not be obtained because of the energy spread of each neutron beam. However, if relative thick target fission yields were plotted against calculated mean neutron energies, the resulting "excitation curves" showed clearly that bismuth began fissioning first, followed by lead, thallium, mercury, gold, and platinum in that order. The data showed clearly that for 84-Mev neutrons bismuth was much more fissionable than lead, while differences in the rest of the elements tested were less marked.

Photon induced fission.—Baldwin & Klaiber (8) attempted to find photofission in bismuth, lead, thallium, gold, tungsten, and samarium by irradiating these elements with x-rays from a 100-Mev betatron and observing fission pulses in an ionization chamber. Whereas fissions in uranium and thorium were readily observed, no evidence was found for fissions in the lighter elements. Sugarman (22) identified fission-product activities when bismuth was irradiated with x-rays from a betatron operating at 85-Mev maximum energy, although he could not absolutely rule out the possibility that the fissions were caused by secondary fast particles. Similarly, Duffield & Gindler (23) have observed photofission in bismuth and gold, using x-rays of 315-Mev maximum energy; the fission cross section for bismuth appeared to be considerably higher than for gold.

Fission induced by charged particles.—At the same time that Perlman and co-workers (20) reported that bismuth and lead would undergo fission when bombarded with 100-Mev neutrons, they also reported that bismuth, lead, thallium, platinum, and tantalum could be fissioned by 400-Mev α-particles, and that bismuth, lead, and thallium could be fissioned by 200-Mev deuterons. They noted that for a given projectile the probability of fission dropped as the target atomic number decreased, and that for a given target the probability of fission increased with the energy of the projectile. Goeckermann & Perlman (24, 25), in a more extensive radiochemical study of the fission of bismuth with 200-Mev deuterons, obtained a rough value of 0.2 barn for the fission cross section.

Fissionability studies were extended to medium weight elements by Batzel & Seaborg (26, 27), who irradiated copper, silver, bromine, tin, and barium with 340-Mev protons. In such irradiations the size of the fragments produced varies continuously from small particles like neutrons, protons, and α-particles (in which case the reaction is called a spallation reaction) through intermediate sized particles like Be^7 and Li^8 [Wright (28); Marquez & Perlman (29)], and on up to fragments whose sizes resemble fission fragments. For example, Batzel & Seaborg found that two of the products formed

from the reaction of high energy protons on $Cu^{63,65}$ were Cl^{38} and Na^{24}. Both products were identified at a bombarding energy of about 70 Mev where the production cross sections were of the order of 10^{-8} barn. As the proton energy was increased, the production cross sections rose rapidly. The Cl^{38} production cross section flattened out above ~175 Mev and rose only slightly up to 340 Mev, where the cross section was about 4×10^{-5} barn. The Na^{24} production cross section rose sharply from $\sim4\times10^{-8}$ barn at 70 Mev to $\sim4\times10^{-7}$ barn at 100 Mev. The increase in cross section with proton energy then became somewhat less rapid, increasing steadily to $\sim3\times10^{-5}$ barn at 340 Mev. Batzel & Seaborg calculated thresholds for the production of Cl^{38} and Na^{24} by both spallation type reactions and by fission type reactions. The threshold for the spallation reaction $Cu^{63}(p,pn6\alpha)Cl^{38}$ was calculated to be about 110 Mev, while that for the extreme reaction $Cu^{63}+p\rightarrow Cl^{38}+Al^{25}+n$ was calculated to be about 50 Mev. Similarly, the threshold for the reaction $Cu^{63}(p,p3n9\alpha)Na^{24}$ was calculated to be about 170 Mev, while the threshold for the reaction $Cu^{63}+p\rightarrow Na^{24}+K^{39}+n$ was calculated to be about 50 Mev. In the same way, thresholds were calculated and compared with experiment for the production of Sc^{44} from bromine; Co^{61} from silver; Na^{24}, Ga^{66}, and Ga^{72} from tin; and Ga^{66} and Ga^{72} from barium. The spallation calculations were somewhat uncertain because the coulomb energy requirement for the emission of charged particles made up a fair contribution to the calculated threshold, and the coulomb barrier might well be effectively lowered at high excitation energies. Nevertheless, in the majority of the cases, the experimental thresholds were well below values which would reasonably be expected from the successive emission of α-particles. Also, observations on the range of recoil fragments from copper bombarded with 340-Mev protons indicated that the fragments were larger than α-particles. Therefore, Batzel & Seaborg suggested that a reaction in which the nucleus is split into several pieces of comparable size might properly be called "fission." They concluded that such reactions occur in all nuclei provided enough excitation energy is available. As the energy of the incident particle is increased, smaller fragments (such as Be^{7} and Li^{8}) are emitted more frequently, while at very high energies spallation reactions become more and more probable, so that a given product nuclide can be formed in a variety of ways from any one target element.

Greenberg & Miller (30) carried out similar work by bombarding copper with 370-Mev protons. They estimated cross sections (reliable to about a factor of two) of 3×10^{-5} barn for the production of C^{11}, F^{18}, and Na^{24}. The production cross section for K^{42} was estimated as 5×10^{-5} barn. They quoted data obtained by Belmont & Miller on the production of C^{11}, Na^{24}, and K^{42} from the reaction of 370-Mev protons on cobalt; the production cross sections for C^{11} and Na^{24} from cobalt are about the same as from copper, but the production cross section of K^{42} from cobalt is about 10 times greater than from copper. Greenberg & Miller suggest that perhaps C^{11} and Na^{24} are formed primarily as fission products while K^{42} is formed as a fission product from copper but primarily as a spallation product from cobalt.

Meson induced fission.—Sugarman (31) has reported fission in mercury

irradiated with 122-Mev π^--mesons; he identified bromine, strontium, yttrim, and ruthenium fission product activities.

EFFECT OF ENERGY ON MODES OF FISSION

Introduction

We have seen that fission can be induced in a wide range of nuclei provided that enough energy is imparted to the nucleus by the incident particle. The question then arises: in what ways does the fission process differ when high-energy particles are used to induce fission? Practically all of the evidence obtained to data has been on changes in the mass distribution and proton to neutron ratio of the fission fragments. In general, information on the mass distribution has been obtained in two ways: the ionization chamber technique, which measures the frequency of various kinetic energy releases, from which data a fission yield versus mass number curve can be deduced; and radiochemical identification of the fission fragments. Since the latter method is much more sensitive than the former, we shall confine ourselves chiefly to evidence produced by radiochemical techniques.

For incident particles of moderate energy, we adopt the familiar picture of the formation of a compound nucleus. This excited nucleus may emit various particles, the probability for emission of any given particle depending on the particular compound nucleus and its degree of excitation. For example, suppose we irradiate U^{235} with 16-Mev neutrons, forming excited U^{236} nuclei. The binding energy of a neutron entering a U^{235} nucleus is about 6 Mev, so each compound U^{236} nucleus formed has an excitation energy of about 22 Mev. We can neglect the probability that such a heavy compound nucleus will emit a charged particle, so we need only in this case consider the competition between neutron emission, fission, and γ-ray emission. If we assume for convenience that each neutron emitted carries away 7 Mev from its parent nucleus, we can picture the various reaction possibilities as follows:

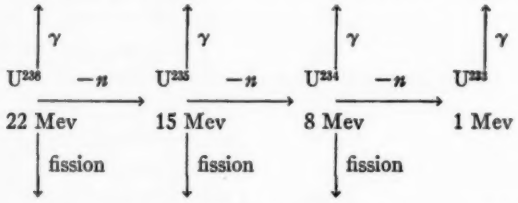

Some of the reaction possibilities shown will have low probabilities; for example, for U^{236} nuclei with 22 Mev excitation energy, γ-ray emission will not compete to any large extent with neutron emission and fission. A U^{233} nucleus with 1-Mev excitation can neither emit a neutron nor fission and, therefore, must become de-excited by γ-ray emission. Fission products from such a bombardment are the result of contributions from fission of U^{236} with 22-Mev excitation, U^{235} with 15-Mev excitation, and U^{234} with 8-Mev excitation, the extent of each contribution depending upon the values of the various branching ratios involved. If instead of 16-Mev incident neutrons we had

used 2-Mev neutrons, the only fission process occurring would have been the fission of U^{236} compound nuclei with 8-Mev excitation energy, since the emission of a neutron would leave behind a U^{235} nuclei whose excitation energy would be well below the ~5.3 Mev necessary to cause fission. As the incident neutron energy is increased, contributions by fission of excited U^{235}, U^{234}, etc., will become appreciable. We see, then, that only a relatively limited energy region is available for a study of the way in which the fission process is influenced by the excitation of the compound nucleus, uncomplicated by the fission of other nuclei with less excitation energy; for such a study, only those heavy elements with relatively low fission thresholds can be used.

When the energy of the incident particle is very high (~100 Mev or more), Serber (32) has pointed out that the idea of the formation of a compound nucleus is no longer valid. The first interaction of the incident particle is with a single nucleon in the target nucleus rather than with the nucleus as a whole, and the incident particle may lose perhaps one-fourth of its kinetic energy in the process. After this interaction, the incident particle may leave the nucleus (if it happened to pass through the edge of the nucleus) or it may interact with other nucleons (if it hit the nucleus more squarely). Thus the amount of energy lost by the incident particle will vary from little loss to complete loss. The struck particle would leave the nucleus only if it were near the edge and heading outwards; otherwise its energy would be distributed over the nucleus and the energy dissipated by successive evaporation of particles with a few million electron volts energy. The probability of an interaction leaving a given amount of excitation energy in the target nucleus will be determined by the nucleon mean free path which varies slowly with incident particle energy; therefore excitation functions should not change rapidly with energy at high energies.

Experimental Results

Moderate incident particle energies.—One of the outstanding features of thermal fission is that the most probable mode of fission is not a division into two fragments of equal mass; in fact, this mode of fission is extremely unlikely. As early as 1940, Nishina and co-workers (33) had examined fission product activities from fast fission of uranium, using Li-D neutrons, and had observed products of symmetrical fission which had not been previously found in thermal fission. One possible explanation was that the fast fission produced symmetrical fission products in higher yield than did thermal fission. Later, Engelkemeir and co-workers (34, 35) observed that the fission yield of Pd^{109} from fission of Pu^{239} with neutrons of roughly 600 kev was 50 per cent higher than the corresponding thermal yield. In 1947, Turkevich (36) showed beyond question that increasing the energy of the incident particle increased the probability of symmetrical fission. He irradiated thorium with ~2-Mev neutrons and with Li-D neutrons (12 to 19 Mev); in the former case, symmetrical fission was about 1/100 of the most probable mode, while in the latter case symmetrical fission was about 1/15 of the most probable mode. In an extension of this work, Turkevich & Niday (37) suggested that fission

of thorium with pile neutrons of 2.6 Mev average energy might be regarded as a combination of two modes of fission, one asymmetrical and the other symmetrical. Later work done at Los Alamos, utilizing neutrons of ~1 Mev from a Van de Graaff accelerator and also somewhat degraded fission spectrum neutrons, showed that for U^{235}, faster neutrons caused more symmetrical fission [Spence (38)].

Changes in the fission yield distribution (compared to thermal fission) when U^{235} was irradiated with 14-Mev neutrons were marked [Spence and co-workers (38, 39)]. First, symmetrical fission became much more probable; the ratio of peak fission yields to trough fission yields for thermal fission was about a factor of 600, while for 14-Mev fission, the corresponding ratio was about a factor of six. The rise in fission yields for elements (e.g., Cd^{115}) corresponding to symmetrical fission was accompanied by a drop in the fission yields of peak elements; thus the 14-Mev fission yield of Mo^{99} was about 15 per cent lower than the corresponding thermal yield. Second, the wings of the fission yield curve appeared to rise for the faster fission; the Br^{83}/Mo^{99} fission yield ratio increased by a factor of roughly 2.5, and the Eu^{156}/Mo^{99} yield ratio increased by a factor of about five in going from thermal to 14-Mev fission. Third, 14-Mev fission yields for products just beyond the heavy peak (Ba^{140}, Ce^{143}, Ce^{144}) were significantly lower than the corresponding thermal yields. Fourth, the yields of the shielded nuclides Br^{82}, Rb^{86}, and Cs^{136} were much higher for 14-Mev fission than for thermal fission. Since the shielded nuclides cannot be formed by β-decay but must be formed directly in the fission process, the observed rise in their production indicates that the neutron to proton ratio of the initial fission fragments is less for 14-Mev fission than for thermal fission; that is, that the primary products formed are closer to stability.

The observed changes listed above are the result of some fission of U^{236} nuclei with about 20-Mev excitation, plus some fission of U^{235} nuclei with perhaps 13-Mev excitation, plus some fission of U^{234} nuclei with perhaps 6-Mev excitation. The exact excitation of the U^{235} and U^{234} nuclei depends on the unknown amount of energy carried away by the neutrons emitted from the excited U^{236} and U^{235} nuclei. The fission of U^{234} nuclei with about 6-Mev excitation is just the reaction occurring when U^{233} is irradiated with thermal neutrons; the resulting fission yield curve shows the pronounced double-peaked curve characteristic of asymmetric fission. The observed shift toward symmetrical fission for 14-Mev neutrons can only mean that in the fission of U^{236} nuclei with 20-Mev excitation (and perhaps in the fission of U^{235} nuclei with 13-Mev excitation) the probability of symmetrical fission is comparable to the probability of asymmetrical fission.

Jones, Fowler & Paehler (40) bombarded uranium with protons in the energy region 11.2 to 17.5 Mev. In this energy region, the ratio of the Mo^{99} to Ba^{140} yields stayed almost constant at a value some 60 per cent higher than the value obtained by thermal fission of U^{235}. The ratio of Ag^{111} to Ba^{140} yields was 0.26 at 11.2 Mev, 0.36 at 14.3 Mev, and 0.48 at 17.5 Mev com-

pared to 0.0029 for thermal fission of U^{235}. The results are, therefore, in agreement with 14-Mev neutron fission of U^{235}, showing a rise in symmetrical fission which becomes greater as the incident particle energy is increased.

An extension to a higher energy was made by Newton (13), who irradiated Th^{232} with 37.5-Mev α-particles (forming the compound nucleus U^{236}) and then analyzed for fission product activities. He found that the ratio of peak to trough fission yields was only about a factor of two. Again we see that increasing the incident particle energy causes fission to become more symmetrical, for the ratio of peak to trough yields found by Newton from 37.5-Mev α's-fission of Th^{232} is substantially lower than the corresponding ratio found by Spence and co-workers for 14-Mev neutron fission of U^{235}.

High incident particle energy.—One of the most striking results obtained when elements from tantalum to uranium were irradiated with high energy (100 Mev or more) particles was that the fission product distribution became single-peaked, with abnormally high yields for the light fragments compared to thermal fission [Perlman *et al.* (20); Seaborg *et al.* (41)]. Measurements of the kinetic energy release in the fission of U^{238}, U^{235}, Th^{232}, and Bi^{209} by Jungerman & Wright (10) showed a single peak in the distribution of kinetic energy of fragments versus the number of fragments when 90-Mev neutrons were used, but double peaks appeared when 45-Mev neutrons were used. Thus for 90-Mev fission, the most probable mode of fission produces two fragments of equal kinetic energy, in contrast to thermal fission. The mean kinetic energy of the fragments from high energy fission of U^{235} differed little from thermal fission.

Studies by Goeckermann & Perlman (24, 25) of the fission product distribution from the fission of bismuth with 190-Mev deuterons showed that the fission yield curve had a single peak in the neighborhood of mass number 99 where the fission yield was about 5 per cent. The lighter fission products were β^--emitters while the heavier fission fragments decayed by β^+-emission or electron capture. Goeckermann & Perlman showed that these observations were consistent with the following picture: the excited nuclei formed in the irradiation boiled off neutrons until nuclides were reached for which fission could compete well with further neutron emission; when fission then occurred, the fission fragments had the same neutron to proton ratio as the fissioned nuclide. Both Jungerman & Wright and Goeckermann & Perlman agreed that most of the energy transmitted by the incident particle to the target nucleus was dissipated by neutron emission preceding fission. The situation is, of course, complicated, because there is a wide range of excitation of the target nuclei, therefore a variation in the number of neutrons emitted. In addition, fission probably competes reasonably well with neutron emission over a fair range of excited nuclei, so fissions come from quite a few different fissioning nuclides. The experimental results show that symmetrical fission outweighs asymmetrical fission, and furthermore, fissions in which there is no charge redistribution overshadow fissions which, like low-energy fission, require a charge redistribution. Goeckermann & Perlman estimated

that most of the fissions they observed from the reaction of 190-Mev deuterons on bismuth came from reactions in which 100 Mev or more of the incident particle energy was transferred to the target nucleus; only about 25 per cent of all the reactions led to transfer of less than 100 Mev in the first place, and in addition the fission cross section drops rapidly as the target excitation drops below 100 Mev.

Goeckermann & Perlman estimated the fission cross section for 190-Mev deuterons on bismuth as 0.2 barn, about one-tenth of the geometric cross section. Thus the fissions observed result from only about 10 per cent of all the incident particle interactions with the target nuclei. Presumably, the other interactions result in the emission of charged particles leading to the formation of nuclides for which the value of the fissionability parameter, Z^2/A, is low, and fission is not included in the chain of events. It perhaps should be pointed out that the experimental evidence does not distinguish between a process where neutrons are first boiled off before fission begins to compete with further neutron emission, and a process where fission first occurs and neutrons are then emitted from the fission fragments. However, the former process is considered to be much more probable.

Sugarman (22) found that when bismuth was irradiated with photons of 84-Mev maximum energy, the resulting fission fragment distribution was narrower than that found by Goeckermann & Perlman for 190-Mev deuterons on bismuth. In addition, Sugarman concluded that the photofission of bismuth yielded neutron-rich isotopes which decayed by β^--emission.

O'Connor & Seaborg (12) bombarded uranium with 380-Mev α-particles and found a single-peaked fission product distribution curve. There was an indication that the peak of the curve came at a mass number less than one-half the mass of the initial compound nucleus, although the data was not sufficiently accurate to prove that neutrons had boiled off prior to fission. Since uranium has a relatively low fission threshold, contributions to fission from target nuclei of a wide excitation range would be observed. In common with most high energy fission studies, it was noticed that very asymmetrical fission (giving fragments with abnormally low and high mass numbers) was more probable than in the case of low-energy fission. Further work by Wolfe & Ballou (42) on the production of platinum group isotopes from the irradiation of uranium with 380-Mev α-particles indicated no dip in the mass number region 103 to 140. From the yields of osmium, iridium, and platinum, the fission yield curve appeared to merge smoothly into the spallation yield curve, confirming similar observations by O'Connor & Seaborg.

Of the experiments on the fission of medium weight elements reported by Batzel & Seaborg (26, 27) and Greenberg & Miller (30), little can be added to the discussion already given earlier in this chapter. Such fission reactions are only slightly exoergic or even endoergic with respect to mass balance. Nuclides which can be formed by "fission" of medium weight elements can also be formed simultaneously by spallation-type reactions. The whole

gamut of reactions is so broad that it is extremely difficult to sort out the contributions to the formation of a given nuclide by the various ways it can be produced. At the present time, few products have been determined quantitatively from the high-energy fission of medium weight elements.

Summary.—We have seen that the fission process can be made to occur over a wide portion of the periodic table, provided enough excitation energy is supplied. For elements of atomic number below about 83 (bismuth) it is true that the cross section for actual fission of the original target nuclei may be very low, but fission can be accomplished nevertheless by first evaporating neutrons; when sufficient energy is provided to do this, fission cross sections may reach a few tenths of a barn. For the heaviest elements (thorium and above) fission can be induced relatively easily and fission cross sections in the neighborhood of a few barns are common.

We have also seen that one of the chief characteristics of high-energy fission is the increased probability of symmetrical fission as the incident particle energy is increased; this change is apparent for even small (1 Mev) increases in excitation. A second characteristic of high-energy fission is the appearance of a broader distribution of fission products; that is, the probability of very asymmetrical fission also increases with incident particle energy, although not to the same degree as does symmetrical fission. A third characteristic of high-energy fission is the trend toward less redistribution of charge during the fission process; in extreme cases, the fragments may have the same neutron to proton ratio as the fissioning nuclide. A fourth characteristic of high-energy fission is that such fission is invariably a mixture of contributions from at least several nuclides with varying excitation energies, since at high energies, the excited target nuclei will emit neutrons prior to fission; for very high excitations, fission probably does not compete appreciably with neutron emission, but as the neutron emission process continues, nuclides are reached for which fission can compete.

Finally, we cannot at the present time fit all of the observations on high-energy fission into a neat, coherent picture. In particular, an explanation of the increase in probability of symmetrical fission with energy will probably have to await a clarification of why low-energy fission favors asymmetrical fission.

LITERATURE CITED

1. Klema, E. D., *Phys. Rev.*, **72,** 88 (1947)
2. Shoupp, W. E., and Hill, J. E., *Phys. Rev.*, **75,** 785 (1949)
3. Grosse, A. V., Booth, E. T., and Dunning, J. R., *Phys. Rev.*, **56,** 382 (1939)
4. Koch, H. W., McElhinney, J., and Gasteiger, E. L., *Phys. Rev.*, **77,** 329 (1950)
5. Frankel, S., and Metropolis, N., *Phys. Rev.*, **72,** 914 (1947)
6. Haxby, R. O., Shoupp, W. E., Stephens, W. E., and Wells, W. H., *Phys. Rev.*, **59,** 57 (1941)
7. Arakatsu, B., Uemura, Y., Sonada, M., Shimizu, S., Kimura, K., and Muraoka, K., *Proc. Phys.-Math. Soc. Japan*, **23,** 440 (1941)
8. Baldwin, G. C., and Klaiber, G. S., *Phys. Rev.*, **71,** 3 (1947)

9. Ogle, W. E., McElhinney, J., *Phys. Rev.*, **81,** 344 (1951)
10. Jungerman, J., and Wright, S. C., *Phys. Rev.*, **74,** 150 (1948)
11. Jungerman, J., *Phys. Rev.*, **79,** 632 (1950)
12. O'Connor, P. R., and Seaborg, G. T., *Phys. Rev.*, **74,** 1189 (1948)
13. Newton, A. S., *Phys. Rev.*, **75,** 17 (1949)
14. Al-Salam, S. G., *Phys. Rev.*, **84,** 254 (1951)
15. Magnan, C., *Compt. rend.*, **208,** 742 (1939)
16. Roberts, R. B., Meyer, R. C., and Hafstad, L. R., *Phys. Rev.*, **55,** 416 (1939)
17. Broda, E., and Wright, P. K., *Nature*, **158,** 871 (1946)
18. Broda, E., *Nature*, **158,** 872 (1946)
19. Phillips, A. N., Rosen, L., and Taschek, R. F., *Phys. Rev.*, **75,** 919 (1949)
20. Perlman, I., Goeckermann, R. H., Templeton, D. H., and Howland, J. J., *Phys. Rev.*, **72,** 352 (1947)
21. Kelly, E. L., and Wiegand, C., *Phys. Rev.*, **73,** 1135 (1948)
22. Sugarman, N., *Phys. Rev.*, **79,** 532 (1950)
23. Duffield, R. B., and Gindler, J. (Personal communication)
24. Goeckermann, R. H., and Perlman, I., *Phys. Rev.*, **73,** 1127 (1948)
25. Goeckermann, R. H., and Perlman, I., *Phys. Rev.*, **76,** 628 (1949)
26. Batzel, R. E., and Seaborg, G. T., *Phys. Rev.*, **79,** 528 (1950)
27. Batzel, R. E., and Seaborg, G. T., *Phys. Rev.*, **82,** 607 (1951)
28. Wright, S. C., *Phys. Rev.*, **77,** 742 (1950)
29. Marquez, L., and Perlman, I., *Phys. Rev.*, **81,** 953 (1951)
30. Greenberg, D. H., and Miller, J. M., *Phys. Rev.*, **84,** 845 (1951)
31. Sugarman, N., *Phys. Rev.*, **86,** 604 (1952)
32. Serber, R., *Phys. Rev.*, **72,** 1114 (1947)
33. Nishina, Y., Yasaki, T., Kimura, K., and Ikawa, M., *Phys. Rev.*, **58,** 660 (1940)
34. Engelkemeir, D. W., Freedman, M. S., Seiler, J. A., Steinberg, E. P., Winsberg, L., in Coryell, C. D., and Sugarman, N., *Radiochemical Studies of the Fission Products*, Natl. Nuclear Energy Ser., Div. IV-9, Paper 204, 1331–33 (McGraw-Hill Book Co., Inc., New York, N. Y., 1951)
35. Steinberg, E. P., and Freedman, M. S., in Coryell, C. D., and Sugarman, N., *Radiochemical Studies of the Fission Products*, Natl. Nuclear Energy Ser., Div. IV-9, Paper 219, 1378–90 (McGraw-Hill Book Co., Inc., New York, N. Y., 1951)
36. Turkevich, A., *U. S. Atomic Energy Commission Document MDDC-1568* (1947)
37. Turkevich, A., and Niday, J. B., *Phys. Rev.*, **84,** 52 (1951)
38. Spence, R. W., *U. S. Atomic Commission Document, BNL-C-9* (1949)
39. Spence, R. W., Ford, G. P., Gilmore, J. S., Minkkinen, C. O., Barnes, J. W., Stanley, C. W. (Unpublished data)
40. Jones, W. H., Fowler, J. L., and Paehler, J. H., *Phys. Rev.*, **87,** 174 (1952)
41. Seaborg, G. T., Cunningham, B. B., Hopkins, H. H., Lindner, M., Miller, D. R., O'Connor, P. R., Perlman, I., and Thompson, R. C., *Phys. Rev.*, **72,** 740 (1947)
42. Wolfe, R. D., and Ballou, N. E., *Phys. Rev.*, **75,** 527 (1949)

AUTHOR INDEX

A

Aamodt, R. L., 164, 165, 175, 373
Aarts, W. H., 202
Abragram, A., 143
Abraham, B.M., 225, 348
Adair, R.K., 68, 250
Adams, E.N., 3rd., 239
Adams, N., 65, 344, 345
Adams, N.E., 394
Adams, R.V., 93
Addario, M.M., 99
Aeppli, H., 130, 131, 137, 141, 146, 147, 150, 152, 153, 155, 157, 244
Agarwala, B.K., 12
Agnew, H.M., 277
Albada, G.B. van, 11, 13, 16, 59
Albers-Schönberg, H., 130, 141, 147, 150, 151, 157, 244
Albert, R.D., 276
Alburger, D.E., 152, 153, 155, 240, 244, 291
Alder, K., 130, 131, 135, 136, 141, 142, 144, 157, 244
Alford, W.L., 180, 181
Alford, W.P., 261, 277, 278, 284
Alfvén, H., 349, 352, 354, 356
Allen, A.D., 211
Allen, A.J., 243
Allen, J.S., 245
Allen, K.W., 278
Allen, R., 21
Allen, R.A., 155, 156
Allen, T.L., 230
Aller, L.H., 2, 3, 44, 53
Almqvist, E., 278
Almy, G.M., 108, 120, 121
Alpher, R.A., 1-40; 1,2, 5, 6, 8, 9, 11, 12, 13, 14, 16, 17, 18, 19, 21, 22, 23, 24, 25, 26, 27, 28, 29, 31, 32, 34, 44, 49, 59, 60
Al-Salam, S.G., 401
Alvarez, L.W., 80, 88
Ames, D.P., 289
Anderson, C.D., 180
Anderson, E.B., 75
Anderson, E.C., 63-78; 63, 67, 69, 70, 71, 74, 75, 76
Anderson, G.W., Jr., 8, 65
Anderson, H.L., 84, 172, 173, 239
Andrade, E.N. da C., 200, 212
Angus, J., 261, 277, 278, 284
Annis, M., 182
Arakatsu, G., 400
Arendale, W.F., 234
Arfken, G.B., 134, 137, 138, 139, 153, 252
Argo, H.V., 384
Arley, N., 68
Armenteros, R., 180, 182
Arnold, J.R., 69, 74, 76
Arnold, R.D., 224, 225
Arnold, W.R., 80, 130, 244
Arx, A., von, 87
Ashkin, J., 376
Aston, F.W., 7
Aten, A.H.W., Jr., 5, 7, 72, 314
Atkinson, R., 41
Atkinson, R. E., 11
Atterling, H., 82
Austerman, S.B., 193, 194, 195, 196, 197, 198
Austern, N., 137, 253, 394
Avery, R., 394
Axel, P., 247

B

Baade, W., 2, 57, 60
Bacher, R.F., 241, 263, 309, 311
Backus, J., 276
Badger, R.M., 234
Bagge, E., 67, 346, 355
Baker, R.G., 108, 115
Bakker, C.J., 154
Baldinger, E., 242
Baldwin, G.C., 100, 107, 400, 402
Ballou, N.E., 408
Baltensberger, W., 144
Band, W., 11, 33
Bardeen, J., 226
Barden, S.E., 85
Barkas, W.H., 164
Barker, F.C., 377, 395
Barker, K.H., 180, 182
Barnes, J.W., 406
Barschall, H.H., 21, 68, 248
Bartell, F.O., 98, 100
Barton, G.W., 96
Batchelor, G.K., 350, 351
Battat, M.E., 68
Batzel, R.E., 95, 96, 98, 100, 101, 102, 402, 408
Bauchsbaum, R., 228
Beals, L.S., 360
Beard, D.B., 3
Becker, E.W., 225, 227
Becker, G.E., 89
Becker, M., 205, 210
Becker, R., 348
Becker, R.A., 85
Bederson, B., 253, 254, 255
Beenakker, J.J.M., 225
Behr, A., 17, 18
Beling, J.K., 153, 157, 244
Bell, P.R., 154, 291
Bell, R.E., 384
Bell, R.P., 232
Bellamy, E.H., 239, 240, 255, 256
Benedict, T.S., 126
Bengston, J., 385, 386
Bennett, W.H., 80
Benveniste, J., 113
Berestetski, V.B., 243
Bergstralh, T.A., 80
Beringer, R., 145
Berlin, T.H., 26, 245
Berman, A., 254
Berman, R., 212, 213, 214
Bernardini, G., 100
Bernstein, R.B., 233
Beskow, G., 10, 11, 12, 13, 14, 15, 16, 59
Bethe, H.A., 3, 11, 21, 25, 41, 47, 48, 49, 50, 67, 68, 112, 113, 117, 118, 123, 124, 241, 263, 311, 376, 377, 380, 385, 394
Beun, J.A., 241
Beyster, J.R., 152, 153, 154, 155, 156
Biddick, R.E., 232
Bidelman, W.P., 55
Biedenharn, L.C., 131, 134, 137, 138, 139, 153, 242, 267, 394
Biermann, L., 335-64; 346, 348, 350, 351, 355, 357
Bigeleisen, J., 221-38; 73, 226, 227, 229, 230
Billington, D.S., 195, 198
Birge, R.W., 371, 374
Bishop, A.S., 130, 131, 146, 152, 155, 157, 174, 175, 244
Bishop, G.R., 21, 384, 385
Bitter, F., 253

Blair, J.M., 386, 387, 391, 392
Blair, J.S., 163-86; 175
Blatt, J.M., 131, 137, 142, 176, 242, 385, 394, 395
Bleany, B., 241
Bleuler, E., 205, 272, 273
Blewett, J.P., 81
Blewitt, T.H., 198, 199, 202, 204, 216
Blin-Stoyle, R.J., 241
Blix, R., 72
Bloch, F., 252
Blocker, W., 107
Bloembergen, N., 143
Boas, W., 199, 216
Boehm, F., 152, 155
Boer, J., de, 225
Bohm, D., 53
Bohr, A., 252, 253, 254
Bohr, N., 96, 112, 123, 187, 309, 312, 314, 315, 328
Bok, B.J., 17
Boley, F.I., 278
Bolgiano, P., 245
Bondi, C.M., 56
Bondi, H., 34, 53, 56
Bonet-Maury, P., 215
Bönisch, A., 221
Bonner, N.A., 99, 102
Booth, E.T., 100, 166, 399, 400
Bopp, C.D., 215
Borowitz, S., 170
Borst, L., 58, 59
Bothner-By, A.A., 230
Bourns, A.N., 230
Bowen, D., 193, 196, 201, 202
Bowers, W.A., 31
Bowman, F., 198
Boyd, A.W., 234
Boyd, C.A., 232
Boyer, K., 81
Braddick, H.J.J., 345
Bradley, C.A., Jr., 9, 11
Bradley, L.C., 235
Bradner, H., 88
Bradt, H.L., 8, 359
Brady, E.L., 130, 145, 149, 150, 152, 153, 154, 155, 157, 244
Brattain, W.H., 208
Breit, G., 365-98; 172, 252, 366, 382, 383, 385, 386, 391, 395
Brickwedde, F.G., 231
Bridge, H.S., 182
Brightsen, R.A., 5, 314, 315, 319, 320, 321, 323, 324, 325, 326, 329
Brix, P., 235, 252
Broda, E., 401
Brody, J.K., 235
Brooks, H., 188, 196
Brown, A.B., 242, 250
Brown, F.W., 193, 201
Brown, H., 2, 4, 11, 14, 15, 17, 27, 27, 30, 276, 277, 278, 360
Brown, R., 179
Broyles, A.A., 383
Brueckner, K.A., 165, 173, 175, 178
Bryce, W.A., 233
Buliginski, D.G., 244
Bunker, M.E., 289
Burgy, M.T., 384
Burhop, E.H.S., 377
Burling, R.L., 17
Burrows, H.B., 234
Burton, M., 187, 215
Butement, F.D.S., 324
Butler, C.C., 180, 182
Butler, S.T., 243
Butler, T., 354
By, A.A.B., see Bothner-By, A.A.
Byerly, P.R., Jr., 108, 120, 121
Byfield, H., 166

C

Cachon, A., 180, 182
Caianello, E.R., 266
Caldin, E.F., 232
Calvin, M., 73, 229, 230
Camac, M., 376, 377
Camerini, U., 179
Cameron, A.G.W., 106, 108, 109, 110, 111, 115, 116, 117, 118, 121, 122
Carlsson, A., 155
Carson, A.N., 29
Cartwright, W.F., 164, 165
Carver, J.H., 119, 122
Case, K.M., 170, 175, 366, 378, 379, 380
Casher, R., 211
Cassels, J.M., 83, 375
Cassidy, J.M., 291
Caswell, D.A., 89
Cavanaugh, P.E., 130, 146
Chackett, K.F., 8
Chadwick, J., 105
Chalmers, T.A., 105
Chamberlain, J.W., 53
Chamberlain, O., 98, 166, 366, 367, 368, 369, 370, 372, 374
Chandrasekhar, S., 2, 11, 13, 17, 41, 44, 45, 49, 51, 55, 57, 351
Chao, C.J., 130
Chapman, A.H., 182
Chapman, S., 348
Charette, J., 234
Charpak, G., 154
Cherdyncev, V., 12, 13, 16, 32
Cheston, W.B., 164
Chew, G.F., 163-86; 175, 177, 178, 377
Chick, D.R., 90
Christian, R.S., 371, 372, 377, 378, 382
Chu, E.L., 79-92; 89
Chupp, W.W., 98
Clark, D.L., 165
Clarke, J.T., 224
Clay, J., 345
Cleland, J.W., 205, 206, 207, 209
Clendenin, W.W., 252
Clusius, K., 223
Cockroft, A.L., 261, 277, 278, 284
Cohen, K., 223
Cohen, S.G., 311
Cohn, H.O., 180
Collie, C.H., 79, 385
Collins, T.L., 221, 222, 312
Coltman, R.R., 198, 199, 202, 204, 216
Compton, A.H., 340, 341
Condon, E.U., 133, 135, 366, 385
Condon, F.E., 234
Cook, C.S., 276, 277
Cook, J.A., 121, 122
Cook, L.G., 195
Cook, L.J., 99, 377
Cooper, E.P., 143
Cork, B., 113, 386
Cork, J.M., 276
Cortini, G., 100
Coryell, C.D., 305-34; 314, 315, 319, 320, 321, 323, 324, 325, 326, 329, 330, 331
Cottingham, J.D., 82
Courant, E.D., 113, 119
Cowan, C.E., 147
Cowan, E.W., 180
Cowling, T.G., 348, 349
Cox, C.D., 155
Craggs, J.D., 75
Crane, H.R., 264
Crawford, B.L., Jr., 234
Crawford, J.H., 205, 206, 207, 209
Crawford, M.F., 254
Creutz, E.C., 375, 386
Critchfield, C.L., 2, 3, 9, 11, 13, 17, 29, 31, 41, 50, 266, 295
Crocker, I.H., 222
Crosby, E.H., 121, 122
Cunningham, B.B., 407
Cunningham, G.L., Jr., 234
Cunningham, J.A., 107, 108
Curie, I.J., see Joliot-Curie, I.
Curran, S.C., 75, 261, 277, 278, 284
Curtis, N.W., 109, 121

Cushing, R.L., 195
Cushman, B.E., 79

D

da C. Andrade, E.N., see Andrade, E.N., da C.
Dainton, A.D., 8, 336, 338, 339, 362
Dancoff, S.M., 170, 173, 247, 248
Daniels, J.M., 241
Danos, M., 113; 118, 123
Darby, E.K., 146, 156
Darling, B.T., 183
Daunt, J.G., 225
Davidson, J.P., Jr., 251, 252, 254, 291
Davidson, W.L., 216
Davis, L., 85, 352
Davis, L., Jr., 239
Davis, R.E., 205, 210
Davis, W.O., 65, 66, 67
Day, M.J., 216
DeBenedetti, S., 147
deBoer, J., see Boer, J. de
Decius, J.C., 234
Deevey, E.S., Jr., 76
de Groot, S.R., see Groot, S.R. de
de Hemptinne, M., see Hemptinne, M. de
Delbecq, E.J., 211
Dementi, V.S., 21
Demers, P., 21
Demeur, M., 11, 13
De Shalit, A., 146, 148, 252
de Toledo, P.S., see Toledo, P.S. de
Deutsch, M., 31, 130, 131, 145, 146, 147, 149, 150, 151, 152, 153, 154, 155, 156, 157, 241, 243, 244, 245
Deutschmann, M., 180
Devons, S., 243, 244
Dewan, J.T., 278
Dharmatti, S.S., 239
Dibeler, V.H., 232, 233
Dickel, G., 223
Dickinson, W.C., 239
Dickson, J.M., 83, 98
Dienes, G.J., 187-220; 191, 193, 198, 201, 202, 203, 204
Dirac, P.A.M., 33, 34
Diven, B.C., 108, 120, 121
Dokoupil, Z., 225
Dolbear, D.W.N., 341
Dole, M., 216, 222
Donahue, T.M., 361
Donnelly, F.K., 82
Donoghue, J.J., 193
Döpel, K., 17
Döpel, R., 17
Douglas, R.A., 106, 108, 115, 116
Drell, S.D., 170, 175
Duane, W., 215
Duckworth, H.E., 222, 312, 326
Duffield, R.B., 293, 402
Duke, F.R., 231
Duncan, D.B., 52
Dunn, G.E., 231
Dunning, J.R., 399, 400
Dunning, K.L., 80
Dunworth, J.W., 132, 146, 147, 156
Durand, E., 80
Durbin, R., 165, 177
du Toit, S., see Toit, S., du
Dutrannois, J., 90

E

Eatherly, W.P., 193
Edwards, R.R., 142
Eggler, C., 20, 21, 25, 291
Eggleston, R.R., 193, 194, 195, 196, 197, 198, 201, 216
Ehmert, A., 341, 345, 346, 354
Einstein, A., 19
Eisenbud, L., 391
Eisenstein, J., 377
Eisinger, J.T., 253, 254, 255
Elliot, K., 341
Elliot, L.G., 384
Ellison, C.H., 80
Elsasser, W.M., 5, 248, 347, 349
Engebretson, H.J., 82
Engelkemeir, A.G., 63
Engelkemeir, D.W., 405
Engler, H.D., 235
Engler, N., 311
Epstein, L, 51, 52, 53
Epstein, S., 228
Evans, G.E., 208
Ewald, H., 221
Eyges, L., 109, 116, 123, 124, 125
Eyring, H., 231

F

Falk, C.E., 243
Falkoff, D.L., 130, 132, 133, 134, 136, 137, 138, 139, 140, 141, 152, 155, 243, 244, 245
Fan, C.-Y., 277, 359
Fan, H.Y., 205, 210
Fano, L., 318, 320, 321, 328, 329, 331
Fano, U., 136
Faris, F., 386
Farkas, A., 231
Farkas, L., 9, 231
Feather, N., 328
Feeley, H.W., 71, 72, 76
Feenberg, E., 6, 21, 130, 172, 222, 245, 250, 252, 267, 273, 291, 311, 312, 314, 315, 328, 329, 330, 333, 361, 390
Feingold, A.M., 156, 245, 274, 380, 394
Feister, I., 272
Feld, B.T., 239-60; 153, 157, 239, 242, 244, 253, 254, 255
Feldman, L., 291, 299
Feldman, M., 193, 201
Félici, N.J., 90
Fermi, E., 22, 29, 170, 172, 173, 245, 311, 312, 313, 315, 330, 331, 351, 357, 360, 385
Fernbach, S., 98
Ferretti, B., 395
Feshbach, H., 178, 242, 383, 389, 394
Fierz, M., 135, 138, 139, 272
Fillmore, F.L., 386
Fincke, K., 67
Findley, D.E., 388, 391, 392
Fireman, E.L., 262, 311
Fishman, H., 100
Flammersfeld, A., 246, 318, 320, 321, 328, 329, 331
Fletcher, W.H., 234
Flint, R.F., 76
Flowers, B.H., 256
Flügge, S., 6, 11, 25, 63, 64, 311
Flum, R.S., 180
Foldy, L.L., 170, 252, 253
Foley, H.M., 251
Follin, J.W., Jr., 32
Fookson, A., 224
Foote, R.S., 86
Forbes, S.G., 80
Forbush, S.E., 341, 343, 354
Ford, G.P., 399-410; 406
Forsyth, P.A., 85
Fortescue, R.L., 79, 80, 82, 83
Foss, M.H., 83
Fowler, E.C., 171, 172
Fowler, J.L., 406
Fowler, P.H., 8, 179, 180, 336, 338, 339, 362
Fowler, R.H., 9
Fowler, W.A., 41, 51, 68, 221, 240, 242, 250, 312
Fowler, W.B., 171, 172
Frank, F.C., 8, 17
Frankel, S., 148, 149, 151, 153, 156, 400
Frauenfelder, H., 129-62;

130, 131, 137, 141, 143, 144, 146, 147, 150, 151, 152, 153, 155, 157, 244
Fred, M., 235, 239, 240
Freedman, M.S., 299, 405
Freier, G., 386, 387, 391, 392
Freier, P.S., 8
Fremlin, J.H., 79, 82, 83, 85, 87
Fretter, W.B., 180
Friedlander, G., 31, 100, 102, 112, 153, 244
Friedman, A.S., 224, 225
Friedman, H.L., 166
Friedman, L., 226, 229, 230
Friedman, M.H., 175
Frieman, E., 49
Fritz-Niggli, H., 87
Fröberg, C.E., 395
Fröhlich, H., 169, 226
Fry, D.W., 79, 88, 89
Fry, T.M., 212, 214
Fry, W.F., 166
Fuchs, M., 130, 134, 139, 156
Fujimoto, Y., 99, 175
Fulbright, H.W., 291, 299
Fuller, G., 318, 320, 321, 328, 329, 331
Furry, W.H., 262

G

Gaerttner, E.R., 116, 120, 123
Gailar, N., 234
Gallone, S., 252
Gamba, A., 266
Gamow, G., 2, 3, 9, 13, 17, 18, 25, 29, 31, 41, 57, 58, 245
Gaposchkin, C.P., see Payne Gaposchkin, C.
Gardner, E., 100, 164
Gardner, J.H., 239
Gardner, J.W., 135, 136, 138, 139, 243
Garth, R.C., 20, 21, 25
Garwin, R.L., 155, 156, 174
Gasteiger, E.L., 400
Gauer, G., 86
Géhéniau, J., 13
Geib, I.G., 216
Gerhart, J., 278, 285
Germain, L.S., 100
Geschwind, S., 239
Getting, I.A., 340, 341
Ghiorso, A., 96, 130, 262, 326
Ghormley, J.A., 211
Ghoshal, S.N., 115
Gibbs, J.W., 9, 10
Gibson, W.M., 243
Gill, R.G.S., see Summers-Gill, R.G.
Gilman, H., 231
Gilmore, J.S., 406
Gindler, J., 402
Ginzton, E.L., 89
Glasoe, G.W., 82
Gluckstern, R.L., 365-98
Glueckauf, E., 319
Goechermann, R.H., 100, 101, 402, 407
Goeddel, W., 193, 201
Goens, J., 90
Goeppert-Mayer, M., 262
Goertzel, G., 130, 131, 134, 135, 137, 141, 142, 243, 244
Goffin, E.S., see Sauvenier-Goffin, E.
Gold, T., 34
Goldberg, M.D., 170
Goldberger, M.L., 98, 177, 242, 377
Goldhaber, G.S., see Scharff-Goldhaber, G.
Goldhaber, M., 105, 112, 117, 123, 130, 137, 142, 153, 154, 244, 247, 250, 306, 321
Goldschmidt, V.M., 2, 5, 25
Goldsmith, H.H., 79, 251
Goldstein, N., 21, 22
Goldstein, W., 242
Good, M.L., 291
Good, R., 295
Good, W.M., 145
Gooden, J.S., 79, 82, 83, 85, 87
Goodman, C., 6, 66
Gordon, H., 88
Gordy, W., 239, 240, 251
Gorter, C.J., 225, 241
Goudsmit, S.A., 222
Goward, F.K., 79, 80, 82, 83, 85
Grace, H.A., 155, 156
Grace, M.A., 241
Graef, C., 340, 341
Graham, G.A.R., 384
Graham, R.P., 222
Graves, E.R., 80
Green, A.E.S., 311
Green, G.K., 82
Green, L., Jr., 193
Greenberg, D.H., 100, 102, 403, 408
Greenstein, J.L., 2, 3, 60, 61, 352
Gregg, E.C., 85
Greuling, E., 245, 289
Griffiths, J.H.E., 21
Grilly, E.R., 224, 225
Groot, S.R. de, 132, 241, 243, 266, 267
Gross, L., 149, 261, 277, 278, 284
Grosse, A.V., 63, 399, 400
Guggenheimer, K., 11
Guindon, W.G., 383
Gulbransen, E.A., 72
Gunther, P., 215
Gunther-Mohr, R., 239
Gurney, R.W., 144, 187, 193
Guth, E., 126
Gutowsky, H.S., 239
Gwathmey, E., 225
Gwinn, H.R., 222
Gwinn, W.D., 234

H

Haar, D. ter, 2, 3, 13, 41, 57, 60
Hadley, J., 164, 165, 175
Hafner, E.M., 240
Hafstad, L.R., 387
Hahn, E.L., 143
Halban, H., 21, 155, 156, 241, 384, 385, 394
Hales, R.W., 178
Hall, H.H., 390, 392
Halpern, J., 79, 87, 153, 157, 244, 311, 312, 313, 315, 330, 331
Halpern, O., 225
Hamermesh, M., 235
Hamill, W.H., 63
Hamilton, D.R., 132, 133, 134, 135, 136, 140, 141, 149, 243, 244, 245, 261, 276, 277, 278, 284
Hammack, K.C., 222, 250, 252
Hammel, E.F., 225
Hammond, G.S., 231
Hanna, G.C., 261, 277, 278, 284
Hansen, W.W., 89
Hansson, I.F.E., 385, 394, 395
Hardebol, J., 223
Harding, J.B., 179
Harding, J.G., 99
Harkins, W.D., 5, 6, 7, 9
Harman, W.D., 222
Harr, J., 130
Harris, D., 243
Harris, G.M., 226, 230
Harris, W.M., 285
Harrison, M.H., 45, 52
Hart, E.W., 371, 372, 377, 382
Harteck, P., 3, 9, 225
Harvey, J.A., 170, 312, 318, 327
Harvie, R.B.R.S., 89
Haslam, R.N.H., 85, 106, 108, 110, 111, 115, 116, 121, 122
Hastings, J.M., 17
Hauser, W., 242
Havens, W.W., 170

Haxby, R.O., 400
Haxel, O., 240, 248, 306, 308, 357, 379
Hayashi, C., 31
Hayden, D.C., 222
Hays, E.E., 222
Hebb, M.H., 86, 248
Hebert, G., 239, 240
Hedberg, K., 234
Hedgran, A., 385
Heer, E., 130, 153, 157, 244
Heidmann, J., 118
Heisenberg, W., 309, 335, 340, 349
Heitler, W., 169, 170, 173
Hellman, M., 230
Helmholz, A.C., 100
Hemmendinger, A., 384
Hemptinne, M., de, 234
Henderson, J.E., 82
Henkel, R.L., 21
Henning, G., 193
Henri, V.P., 166
Henrich, L.R., 11, 13
Herb, R.G., 384, 386, 387, 388, 390
Herman, R.C., 1-40; 1, 2, 6, 9, 11, 12, 13, 14, 16, 17, 18, 19, 21, 22, 23, 24, 25, 26, 27, 28, 29, 31, 32, 34, 44, 49, 59, 60
Herzberg, G., 2, 228, 234
Hess, R.J., Jr., 222
Hevesy, G. von, 2
Heydenburg, N.P., 387
Heyn, F., 83
Hibbs, R.F., 222
Hilberry, N., 336, 359
Hildebrand, R.H., 178
Hill, J.E., 399
Hill, R.D., 306, 321
Hilliger, R.E., 234
Hiltner, W.A., 352
Hintenberger, H., 224
Hintz, N.M., 98
Hirschfelder, J.O., 231
Hirzel, O., 75, 114, 120
Hiskey, C.F., 232
Hoang, T.-F., 8
Hodgson, P.E., 179
Hofstad, L.R., 401
Hoge, H.J., 224, 225
Holmes, D.K., 295
Holt, J.R., 243
Holt, R.B., 98
Holtzman, R.B., 277
Holzapfel, L., 215
Hopkins, H.H., Jr., 94, 95, 407
Horiuti, J., 232
Hornbostel, J., 109, 121
Hornig, D.F., 234
Hornyak, W.F., 41, 51, 68, 240, 242, 277
Horovitz, K.L., see Lark-Horovitz, K.
Horsley, R.J., 108, 110, 111, 115
Houtermans, F.G., 11, 41
Howerton, H.K., 80
Howland, J.J., 100, 402, 407
Howlett, J., 83
Hoyle, F., 13, 16, 34, 56, 58, 59
Hsiao, C., 180
Hu, T.M., 377
Hubble, E.P., 2, 3, 18
Huber, O., 146, 147, 148, 149, 150, 151, 156, 157
Huber, P., 242
Huddleston, C.M., 289
Hughes, D.J., 20, 21, 22, 25, 170, 291, 384
Hull, M.H., 382, 383, 385, 386
Hulthén, L., 385, 394, 395
Humbel, F., 146, 148
Hummel, H.H., 250
Hunt, J.P., 227
Huntington, H.B., 190
Hurwitz, H., Jr., 21
Hutchison, C.A., Jr., 212
Hynek, J.A., 43

I

Igelnitsky, J.M., 75
Ikawa, M., 405
Iloff, E., 164, 165
Inghram, M.G., 63, 222, 262, 311
Inglis, D.R., 250, 251, 283
Inskeep, R.G., 234
Isaacs, P., 172
Itoh, J., 145

J

Jaccarino, V., 239
Jackson, H.L., 250
Jackson, J.D., 385, 395
Jacobsohn, B.A., 180
Jahn, H.A., 135
Jakobson, M., 166, 178
James, H.M., 208, 209, 210
Jamison, R.E., 199, 216
Jarmie, W.N., 121, 124, 125
Jarvis, G.A., 384
Jastrow, R., 378, 380, 383
Jauch, J.M., 241
Jeans, J.H., 33
Jeffries, C.D., 239
Jennings, B., 243
Jensen, E.N., 289
Jensen, H., 5
Jensen, J.H.D., 5, 6, 9, 11, 12, 13, 16, 17, 113, 117, 123, 240, 248, 306, 308, 315, 317, 318, 319, 320, 321, 323, 326, 327, 379
Jensen, P., 31
Jentsch, C., 360
Johns, H.E., 85, 106, 108, 110, 111, 115, 116
Johns, M.W., 154, 155
Johnson, C.H., 68
Johnson, C.M., 239, 240
Johnson, F., 76
Johnson, M.H., 164
Johnson, R.D., 201
Johnson, V.A., 205
Johnson, W.E., 205
Johnson, W.H., Jr., 221, 222, 311, 312
Johnston, H.L., 224, 225
Johnston, W.H., 63
Joliot-Curie, I., 314
Jones, A.V., 234
Jones, L.W., 107, 121, 124, 125
Jones, W.H., 406
Jones, W.M., 230
Jordan, P., 34
Joyet, G., 87
Judd, D.L., 86
Jungerman, J., 101, 400, 401, 407
Jurgens, A., 318, 320, 321, 328, 329, 331

K

Kalkstein, M., 262
Kanne, W.R., 387
Kaplon, M.F., 166, 175, 336, 337, 339
Karplus, R., 239
Karraker, D.G., 96, 98
Karzmark, C.J., 180
Katcoff, S., 17
Katz, L., 85, 106, 108, 109, 110, 111, 115, 116, 117, 121, 122, 126
Keck, J.C., 125, 126
Keen, R., 193
Kegley, C.L., 312, 326
Keilson, J., 248
Keim, C., 223
Keister, G.L., 154
Keller, G., 57
Kelly, E.L., 101, 402, 408
Kemball, C., 227
Kemmer, N., 172
Kempton, A.E., 21
Kennedy, W.R., 89
Kenney, R.W., 107
Kent, D.W., 8, 336, 338, 339, 362
Kerr, E.C., 224
Kerst, D.W., 86, 116, 117, 119, 121, 124
Kessler, J., 166
Keston, A.S., 72

Kienle, H., 43
Kiepenheuer, K.,O., 356
Kikuchi, S., 124, 145
Kimura, K., 400, 405
King, J. G., 239
Kip, A. F., 212
Kirshenbaum, A. D., 63
Kirshenbaum, I., 225
Klaiber, G. S., 100, 107, 400, 402
Klein, A., 239
Klein, D., 59
Klein, O., 9, 10, 11, 12, 13, 14, 16, 267
Klema, E. D., 154, 399
Klemm, A., 244
Klemons, P. G., 212, 214
Klontz, E., 209, 210
Klüber, H. von, 2
Kluyver, J. C., 223
Knable, N., 178
Knipp, J. K., 166
Knox, W. J., 83, 100
Koch, H. W., 107, 108, 400
Koch, J., 211
Koester, L. J., 250
Kohman, T. P., 309, 314, 319, 321, 328
Kohn,W., 170
Kolsky, H. G., 239
Kondaiah, E., 294
Konneker, W. R., 147
Konopinski, E. J., 261-304; 130, 139, 245, 246, 263, 289, 294, 297, 305, 306, 311
Kopfermann, H., 143, 252, 253
Korff, S. A., 63, 65, 66, 67
Koster, G. F., 239
Kowarski, L., 21, 81, 319
Kramers, H. A., 380
Kraushaar, J. J., 152, 155
Kraushaar, W. L., 79, 87, 166
Krest, D. W., 386, 387, 388
Kreuger, P. G., 386
Kröger, F. A., 226
Kroll, N. M., 239
Krook, M., 395
Kropschot, R. H., 196, 201
Kruse, U. E., 371, 374
Kuiper, G. P., 2, 3
Kulchitski, L. A., 157, 244
Kulp, J. L., 71, 72, 75, 76
Kurath, D., 250, 256
Kurie, F. N. D., 246
Kurti, N., 241
Kusaka, S., 340, 341
Kusch, P., 239, 254
Kynch, G. J., 253

L

Lacroute, P., 13
Ladenburg, R., 68
Lampi, E. E., 386, 387, 391, 392
Lancaster, J. E., 234
Lange, I., 341
Langer, L. M., 261-304; 146, 246, 261, 276, 277, 278, 284, 289, 291, 293, 294, 299, 305, 306, 311
Lark-Horovitz, K., 188, 205, 206, 207, 208, 209, 210
Lasky, C., 82
Laslett, L. J., 289
Lattes, C., 12
Lattimore, S., 99
Latychev, G. A., 244
Laubenstein, R. A., 384
Lauritsen, C. C., 221, 242, 250, 312
Lauritsen, T., 41, 51, 68, 240, 242, 277
Lawson, J. L., 87, 100, 107, 112, 262, 276
Lax, H., 178
Le Couteur, K. J., 84, 99
Lederman, L. M., 166
Ledoux, P. J., 56
Ledrus, R., 90
Lee, D. D., 74
Lee, D. W., 109, 121
Lee, T. D., 56
Lefort, M., 215
Leighton, R. B., 180
Leitch, L. C., 234
Leith, C., 98
Lemaître, G., 32
Lennox, E. S., 139
Lepore, J. V., 86
Leprince-Ringuet, L., 75
Levi, H., 74
Levine, C. A., 262
Levinger, J. S., 112, 113, 117, 123, 124, 126
Levinthal, C., 120, 125, 126
Lewis, E. M., 53
Lewis, H. W., 178
Li, C. H., 221
Li, C. W., 312
Li, H., 56
Libby, W. F., 7, 63, 67, 69, 70, 71, 74, 75, 76, 262
Lidofsky, L., 278
Lieshout, R. van, 154
Liller, W. C., 53
Lind, S. C., 187
Lindenbaum, S. J., 100
Linder, M., 96, 97
Lindner, M., 407
Lindsay, J. G., 230
Lindsey, G. R., 244
Lindström, G., 82
Ling, D. S., Jr., 243
Lippmann, B. A., 132, 243
Lipps, F., 245
Lipscomb, W. N., 234
Littauer, R. M., 179
Little, J. L., 387
Little, R. N., 80
Livingood, J. J., 82
Livingston, M. S., 79, 82, 83, 85, 87, 88
Livingston, R., 239, 240
Livingston, R. S., 82
Lloyd, S. P., 130, 132, 135, 136, 137, 138, 141, 144, 157, 243, 244
Loar, H., 165, 177
Loebner, E. E., 193
Lofgren, E. J., 8, 386
Logan, R. A., 239, 254
Lohman, J. B., 234
Long, E. A., 172, 173
Longmire, C. L., 57, 276, 295, 297, 300, 385, 394
Loomis, C. C., 239
Lord, R. C., 234
Lossing, F. P., 233
Low, F. E., 239
Low, W., 251
Lowen, I. S., 248
Lowenstam, H., 228
Lukesh, J. S., 193
Lundby, A., 172, 173
Lunden, A., 224
Lüst, R., 347
Luttinger, J. M., 170
Lyttleton, R. A., 56

M

McCall, D. W., 239
MacCallum, C., 266, 267, 268
McCarthy, J. A., 311
McClelland, J. D., 193
McCrea, J. M., 226, 228
McCrea, W. H., 34
McDaniel, B. D., 116, 118
MacDonald, J. E., 141
McDonald, J. K., 53
McElhinney, J., 107, 108, 400
MacFarlane, R. B., 222
McGee, J. F., 193, 194, 195, 196, 197, 198
MacGillavry, C. H., 226
McGinnis, C. L., 152, 155
McGowan, F. K., 154
McGruer, J. N., 388, 391, 392
Machida, S., 178
McIntosh, L. R., 81
Mack, J. E., 251, 255
McKellar, A., 3
MacKenzie, K. R., 84
McKibben, J. L., 81
McKinney, C. R., 228
McMillan, E. M., 85, 88, 98, 99, 357, 377
McMullen, C. C., 155
McMurry, H. L., 234
McNally, J. R., Jr., 235
McNamara, A. G., 85
MacNamara, J., 21

Macnamara, J., 222
McVittie, G. C., 17, 34
Madansky, L., 146, 150, 153, 154, 155, 245
Magee, J. L., 231
Magnan, C., 401
Mahmoud, H., 294
Maienschein, F. C., 289
Majumdar, S. D., 223
Malenka, B. J., 248
Malmstrom, C., 193
Malpica, J. M., 90
Manfredini, A., 100
Mann, A. K., 109, 116, 119
Margenau, H., 251
Marinucci, N. J., 311
Marquez, L., 102 402
Mars, K. E., 72
Marshak, R. E., 41, 56, 163, 164, 166, 176, 297, 298
Marshall, J. F., 126
Marshall, L., 108, 126, 170, 385
Martell, E. A., 7, 75
Martin, A. B., 193, 194, 195, 196, 197, 198, 201
Martin, D. S., 100
Martin, G. R., 8
Martin, R., 172, 173
Mason, D. F., 232
Massey, H. S. W., 377
Mather, K. B., 386
Matsuda, H., 221
Mattauch, J., 6, 7, 11, 25, 311, 318, 320, 321, 328, 329, 331
Mauderli, W., 87
Maury, P. B., see Boney-Maury, P.
Maxwell, E., 226
May, A. N., 386
May, M. M., 180
Mayer, M. G., see Goeppert-Mayer, M.
Mayer, M. G., 7, 31, 32, 73, 222, 227, 240, 248, 250, 274, 277, 289, 294, 299, 306, 308, 321, 379
Mazur, P., 225
Meadows, J. W., 98
Meagher, R. E., 386
Meeks, M. L., 245
Meggers, W. F., 239, 240
Mei, J. Y., 289
Melkonian, E., 66, 67, 384
Mendez, V. P., see Perez-Mendez, V.
Menon, M. G. K., 179, 180
Menzel, D. H., 57, 357
Merat, P., 312
Mescheryakov, M. G., 21
Messiah, A. M. L., 66, 295, 297, 300
Metropolis, N., 311, 312, 318, 327, 400
Metzger, F., 130, 145, 152, 153, 154, 244
Meyer, B. J., 178
Meyer, R. C., 401
Michel, L., 266
Milatz, J. M. W., 223
Milford, F. J., 252
Millar, C. H., 121
Miller, D. H., 171, 172
Miller, D. R., 95, 96, 98, 100, 102, 407
Miller, J. F., 100
Miller, J. M., 100, 102, 403, 408
Miller, R. D., 124
Mills, M. M., 209
Milton, J. C. D., 291, 299
Minkkinen, C. O., 406
Minkowski, R., 57
Mitchell, A. C. G., 240, 289, 294, 299
Mittelman, P., 79
Miyazawa, H., 175, 252, 253
Mizushima, M., 251
Mobley, R. C., 384
Moffat, R. D., 146, 261, 276, 277, 278, 284, 289, 299
Mohr, R. G., see Gunther-Mohr, R.
Molenar, J., 202
Monk, G. S., 211
Montalbetti, R., 85, 108, 109, 110, 126
Montgommery, D. J. X., 75
Moon, J. H., 96
Moon, P. B., 243
Moore, M. J., 84
Morand, M., 82
Morgan, T. J., 82
Morpurgo, G., 178
Morrish, A. H., 245
Morrison, P., 3, 41, 51, 68, 240, 242, 247
Moses, A. J., 100
Moszkowski, S. A., 250, 272, 273, 274, 277, 284, 287, 289, 294, 299, 306, 321
Mott, N. F., 144, 187
Mottelson, B. R., 250
Motz, J. W., 276, 293, 294
Motz, L., 49
Mozley, R. F., 124, 166
Mrozowski, S., 193
Muether, H. R., 285
Muirhead, H., 179
Muller, G. J., 226
Murakawa, K., 235
Muraoka, K., 400
Murphey, B. F., 72, 73
Murray, G. T., 195, 196
Myers, R. J., 234

N

Nabarro, F. R. N., 200
Nachaj, J. F., 243
Nagle, D. E., 172, 173
Nakamura, S., 250, 291, 299
Nakane, R., 223
Naugle, J. E., 8, 65
Neal, R. B., 89
Neary, G. J., 246
Nelson, E., 248
Nesbitt, E. A., 195, 216
Nesbitt, L. B., 226
Neumann, H. M., 96
Meville, O. K., 230
Newkirk, L. I., 107
Newton, A. S., 401, 407
Ney, E. P., 8
Niday, J. B., 405
Nielsen, A. H., 234
Nielsen, E., 234
Nier, A. O., 72, 73, 221, 222, 312, 384
Nierenberg, W. A., 239
Nijgh, G. J., 154
Nishina, Y., 405
Noble, P. C., 86
Noddack, I., 7
Noddack, W., 7
Nordheim, L. P., 306, 308, 321
Nordheim, L. W., 222, 250, 255, 256, 274, 277, 289, 294, 299
Nordman, C. E., 234
North, E. D., 223
Novey, T. B., 153, 154, 156
Nowick, A. S., 200
Noyes, H. P., 377, 378
Nunan, C., 86
Nygard, J. C., 81

O

Ocampo, J., 234
O'Ceallaigh, C., 182
Ochs, S. A., 254
O'Connor, P. R., 100, 400, 407, 408
Oddo, G., 6
Ogata, K., 221
Ogle, W. E., 400
Okamoto, G., 232
Olson, J. M., 312, 326
Olsson, P. O., 382
Omer, G. C., Jr., 18
Ono, K., 250, 291
Opechowski, W., 146, 156
Öpik, E. J., 2, 54, 56, 58, 61
Oppenheimer, F., 8
Orear, J., 311, 312, 313, 315, 330, 331
Orr, W. C., 99
Osborn, R. K., 253
Osborne, D. W., 225
Osoba, J. S., 289
Owen, G. E., 276
Oxley, C. L., 373, 374

P

Pacjak, F.A., 243
Paehler, J.H., 406
Page, N., 99
Pais, A., 183, 366, 378, 379, 380
Paneth, H.R., 245
Panofsky, W.K.H., 88, 107, 164, 165, 174, 175, 356
Pappas, A.C., 314, 315, 319, 320, 321, 323, 324, 325, 326, 329
Parkins, W.E., 193, 201
Parkinson, D.B., 386, 387, 388
Parzen, G., 86, 382
Patterson, C., 2
Pauli, W., 170, 173, 179
Pavalow, M., 65, 66
Paxton, H.C., 246
Payne, C.H., 3
Payne-Gaposchkin, C., 57
Peacock, C.L., 289, 299
Pearson, G.L., 208
Pease, R.L., 383, 394
Pedersen, C.N., 75
Peierls, R.E., 32, 33
Penfold, A.S., 108, 121, 122
Pepkowitz, L.P., 102
Pepper, T.P., 278
Perez-Mendez, V., 277, 278
Perkins, D.H., 99, 102
Perlman, I., 5, 17, 96, 97, 100, 101, 102, 130, 326, 402, 407
Perlman, M.L., 31, 100, 102, 107, 112
Perry, A.M., 100
Perry, J.E., 52
Petch, H.E., 154, 239
Peters, B., 8, 166, 336, 337, 339, 359
Peters, R., 100, 122
Peterson, J.M., 99, 277
Peterson, V., 100, 164, 165, 373
Petree, B., 68
Petrie, D.P.R., 90
Petschek, A.G., 297, 298
Phillips, A.N., 401
Phillips, D.G., 200
Phillips, R., 373
Phipps, T.E., Jr., 239
Pick, H., 211
Pickavance, T.G., 79, 80, 82, 83
Pigg, J.C., 205, 206, 207, 209
Pinkerton, R.C., 231
Pitzer, K.S., 229
Placzek, G., 67, 68
Plain, G.H., 386, 387, 388
Ploch, W., 233
Plyer, E.K., 234
Pokrowski, G.I., 9, 11
Pollock, F., 239
Pollock, H.C., 86
Pomerantz, P., 224
Pontecorvo, B., 261, 277, 278, 284
Popolka, M., Jr., 6
Poppema, O.J., 241
Porter, G., 234
Poss, H.L., 121, 394
Post, B., 232
Post, R.F., 89
Potter, W.H., 53
Pound, R.V., 143, 241
Powell, C.F., 179, 180, 386
Powell, J.L., 390, 391
Present, R.D., 366, 385
Preston, M.A., 263
Preston, R.S., 222, 312, 326
Price, G.A., 116, 117, 119, 121, 124
Price, H.C., Jr., 146, 246, 276, 277, 289, 294
Prigogine, I., 13, 226
Primakoff, H., 147, 166, 262, 361
Pringsheim, P., 211
Probst, H., 225
Proctor, W.G., 239, 242
Pryce, M.H.L., 143, 311
Purcell, E.M., 143
Pursey, D., 294, 296
Putman, J.L., 75

Q

Quinton, A., 108, 110, 111, 115

R

Rabi, I.I., 170
Racah, G., 133, 135, 243
Raeth, C.H., 75
Ragan, G.L., 387
Rai, R.N., 11
Rainwater, J., 166, 252
Rainwater, L.J., 170
Rakestraw, N.M., 222
Ramsay, D.A., 234
Ramsey, N., 239
Ramsey, N.F., 239, 371, 374
Randle, T.C., 98
Randolph, B., 196, 202
Rankama, K., 2, 6, 7, 72, 73
Rarita, W., 376
Raskin, A., 82
Ravenhall, D.G., 395
Reding, F.P., 234
Redmond, J.W., 222
Reid, A.F., 63
Reitwiesner, G., 311, 312, 318, 327
Reitz, J.R., 276
Reynolds, C.A., 226
Reynolds, H.L., 336, 337, 339
Reynolds, J.H., 262, 311
Rich, E.H., 224
Richards, P.I., 222
Richardson, J.R., 246, 386
Richardson, R.S., 2, 3, 61
Richardson, W.S., 226
Richman, C., 88, 165
Richtmyer, R.D., 339, 353
Riddiford, L., 84, 354
Ridgway, S.L., 153, 156
Rifkin, E.B., 224
Ringo, G.R., 384
Ringuet, L.L., see Leprince-Ringuet, L.
Ritson, D.M., 166, 179, 336, 337, 339
Roberts, A., 165
Roberts, D.M., 152, 155
Roberts, R.B., 401
Roberts, T.R., 221, 384
Robinson, B.L., 146, 150, 153, 154, 155
Robinson, D.M., 81
Robinson, F.N.H., 241
Robson, J.M., 27, 64, 277, 278, 284
Rochat, O., 179, 180
Rochester, G.D., 93, 99
Roe, A., 230
Rohrlich, F., 377
Rollefson, G.K., 187
Ropp, G.A., 230
Rose, B., 244
Rose, M.E., 130, 131, 134, 137, 138, 139, 153, 241, 267, 276, 295
Rosen, L., 401
Rosenfeld, A.H., 108, 126, 311, 312, 313, 315, 330, 331
Rosenfeld, L., 11, 311
Ross, J.S., 235
Ross, M., 253
Rosseland, S., 57
Rosser, W.G.V., 93, 99
Rotblat, J., 79, 80, 82, 83, 85, 243
Rouvina, J., 386, 387
Rudd, D.P., 222
Ruderman, M., 86
Ruetschi, R., 153
Rusinov, L.I., 75
Russell, H.N., 3
Rustad, B.M., 278

S

Sachs, A., 172
Sachs, R.G., 68, 137, 253, 394
Sagane, R., 107, 116, 126
Saha, M.N., 9
Sahama, T.G., 2, 6, 7

Sakata, S., 167
Sala, O., 384, 390
Salam, S.G.A., see Al-Salam, S.G.
Salant, E.O., 109, 121, 394
Salisbury, W.W., 357
Salpeter, E.E., 41-62; 11, 49, 51, 54, 58, 239, 384, 394
Salvetti, C., 252
Salzman, F., 175
Sampson, M.B., 277
Sauvenier-Goffin, E., 56
Schaeffer, O.A., 17
Scharff-Goldhaber, G., 153, 241, 244
Schatzman, E., 56, 57, 58
Schecter, L., 243
Schein, B., 343, 354
Scherrer, P., 130, 141, 147, 150, 151, 157
Scheuer, O., 215
Schiff, D., 154
Schiff, L.I., 79-92; 86, 89, 107, 114, 119, 126, 167, 382, 391
Schlüter, A., 345, 347, 348, 350, 351, 356, 357, 360
Schluter, R.A., 311, 312, 313, 315, 330, 331
Schmid, E., 199, 216
Schmidt, F.H., 82, 154
Schmidt, H.W., 225
Schmidt, T., 250
Schneider, E.E., 211, 216
Schneider, H., 146, 148
Schönberg, H.A., see Albers-Schönberg, H.
Schönberg, M., 58
Schrader, R., 226
Schulz, A., 166
Schulz, A.G., 178
Schwartz, H.M., 142
Schwarzer, D., 311
Schwarzschild, M., 3, 52, 56, 61
Schwinger, J., 167, 239, 378, 383, 389, 394
Scott, M.R., 318, 320, 321, 328, 329, 331
Scott, R.B., 231
Seaborg, G.T., 2, 5, 95, 96, 98, 100, 101, 102, 130, 262, 326, 400, 402, 407, 408
Seagondollar, L.W., 81
Seaton, M.F., 2
Segall, B., 177
Segrè, E., 98, 366, 367, 368, 369, 370, 371, 372, 374, 383
Seiler, J.A., 405
Seitz, F., 187, 188, 190, 208, 210, 211
Senseman, R.W., 98
Serber, R., 96, 165, 405
Seriff, A.J., 180
Serin, B., 226
Sevold, B.J., 75
Sewell, D.C., 99, 377
Shaknov, I., 153, 156
Shamberger, R.D., 373, 374
Shankland, R.S., 386
Shanley, T.J.B., 336
Shaw, P.F.D., 384
Shawlow, A.L., 251, 254
Sheline, R.K., 277
Sher, R., 109, 110
Sheriff, R.E., 239
Sherman, D., 164, 165
Sherr, R., 278, 285
Sherrill, F.A., 198, 199
Sherwin, C.W., 130, 146, 245
Shimizu, S., 400
Shire, E.S., 79, 80, 82, 83, 85
Shortley, G.H., 133, 135
Shoupp, W.E., 399, 400
Shull, F.B., 291
Shutt, R.P., 171, 172
Siegbahn, K., 146, 149, 150, 153, 156, 385
Siegel, S., 189, 193, 195, 198, 205
Silsbee, H.B., 239
Silverman, A., 120, 125, 126, 174
Simon, A., 241
Simon, F.E., 212, 214, 241
Simpson, J.A., Jr., 64, 65, 68, 69
Singwi, K.S., 11, 12, 32, 33
Sisman, O., 215
Skyrme, T., 263
Slater, J.C., 79, 88, 89, 187, 189, 200
Slavin, W., 80
Sleator, W., 386, 389, 391, 392
Slotnick, M., 170
Smart, J.S., 22, 30, 31
Smellie, D.W., 239
Smith, A.M., 294, 300
Smith, A.W., 212
Smith, D.D., 235
Smith, F.M., 164
Smith, K.F., 239, 240, 255, 256
Smith, L.G., 222
Smith, R.L., 385, 386
Smits, A., 226
Smoller, B., 239
Snow, G.A., 394
Snowden, S.C., 384, 390
Snyder, C.W., 242, 250
Softky, S.D., 98, 100
Sonada, M., 400
Sonder, R.A., 5
Sorensen, B., 289
Sörensen, S.O.C., 102
Spatz, W.B., 21, 22
Spence, R.W., 399-419; 406
Spiers, J.A., 132, 134, 153, 241
Spinrad, B.I., 130
Spitzer, L., Jr., 3, 352
Spruch, L., 253
Staker, W.P., 65, 66, 68
Stanford, G.S., 312, 326
Stanley, C.W., 406
Staveley, L.A.K., 226
Stearns, M.B., 116, 118, 174
Stebbins, J., 18
Steenberg, N.R., 241
Steenland, M.J., 241
Steensholt, G., 11
Steffen, R.M., 131, 146, 152, 153, 154, 155
Stehl, O., 225
Stein, G., 216
Steinberg, E.P., 405
Steinberger, J., 165, 166, 167, 172, 174, 175, 177
Steinwedel, H., 9, 12, 13, 113, 117, 123
Steller, J., 165, 174
Stello, P.G., 203
Stephens, W.E., 108, 109, 110, 118, 119, 120, 121, 400
Stern, M., 312, 315, 321, 326
Sterne, T.E., 9, 11, 12
Sternheimer, R., 239
Stevenson, D.P., 232, 233
Stevenson, D.T., 130, 146, 150, 153, 155, 156, 157, 245
Stewart, D.B., 100
Stewart, D.W., 3, 223
Stinchcomb, T.B., 343, 354
Stoyle, R.J.B., see Blin-Stoyle, R.J.
Strandberg, M.W.P., 234, 239
Stranks, D.R., 226
Strauch, K., 105-28; 108, 109, 115, 118, 122, 123
Streib, J.F., 82
Strömgren, B., 11, 43, 44
Strong, P., 130
Stroud, W.G., 336
Struve, O., 2
Stukenbroeker, G.L., 235
Stump, R., 153, 156
Stumpff, P., 360
Suess, H.E., 3, 5, 6, 7, 8, 11, 12, 16, 17, 240, 248, 306, 308, 315, 317, 318, 319, 320, 321, 323, 324, 326, 327, 328, 379
Sugarman, N., 100, 101, 122, 402, 403
Sugimoto, A., 223
Summers-Gill, R.G., 122

Sun, K. H., 243
Sunyar, A. W., 130, 137, 142, 153, 154, 244, 247, 250
Suwa, S., 235
Suzor, F., 154
Suzuki, S., 9
Swann, W. F. G., 354
Swiatecki, W. J., 101
Swings, P., 3
Symonds, J. L., 243
Szilard, L., 105

T

Taconis, K. W., 225
Taimuty, S. I., 299
Takebe, H., 291, 299
Taketani, M., 250, 291
Talley, R. M., 234
Talmi, I., 250, 255, 256
Tamburino, S., 99
Tamor, S., 176
Tamura, T., 178
Tanikawa, Y., 167
Tarpinian, M., 193, 194, 195, 196, 197, 198
Taschek, R. F., 384, 387, 401
Taube, H., 227
Taylor, T. I., 232
Taylor, W., 202
Taylor, W. E., 195, 196
Telegdi, V. L., 111
Teller, E., 7, 31, 32, 68, 112, 117, 123, 245, 339, 353
Templeton, D. H., 93–104; 96, 100, 101, 102, 402, 407
Tendam, P. L., 205
Teng, L. C., 84
ter Haar, D., see Haar, D. ter
Terwilliger, K. M., 107, 121, 124, 125
Thaxton, H. M., 391
Thew, K., 151, 318, 320, 321, 328, 329, 331
Thirion, J., 138
Thode, H. G., 3, 21, 230
Thomas, D. G., 226
Thomas, E., 79
Thomas, J. E., 79, 87, 166
Thompson, A. L., 96
Thompson, N., 200
Thompson, R. C., 407
Thompson, R. W., 180
Thorndike, A. M., 171, 172
Thornton, R. L., 98
Thornton, V., 234
Tickner, A. W., 233
Tiers, G. V. D., 234
Timoshuk, D. V., 21
Tinkham, M., 212
Tiomno, J., 266
Titterton, E. W., 100
Toit, S., du, 385
Toledo, P. S. de, 12
Tolhoek, H. A., 132, 241, 243, 266, 267
Tolman, R. C., 9, 13, 17, 18
Tomkins, F. S., 235, 239, 240
Toms, M. E., 109, 118, 119, 120
Topley, B., 231
Towler, O. A., Jr., 374, 383
Townes, C. H., 143, 239, 251
Tralli, N., 248
Treffenberg, L., 10, 11, 12, 13, 14, 15, 16, 59
Trefftz, E., 347
Trigg, G. L., 130, 245, 267, 273, 285, 287
Tryon, L. E., 71, 72, 76
Tuck, J. L., 84
Tukey, J. W., 352
Turkevich, A., 22, 29, 405
Turkevich, J., 216
Turner, C., 278
Tuve, M. A., 387
Tyler, A., 276

U

Ubbleohde, A. R., 11
Ubisch, H. von, 72
Uemura, Y., 400
Uhlenbeck, G. E., 130, 132, 133, 134, 136, 137, 138, 139, 166, 243, 244, 245, 289, 294, 297
Umezawa, M., 250, 251, 291, 299
Unsöld, A., 3, 13, 352, 353, 360, 361
Urey, H. C., 2, 3, 9, 11, 72, 73, 228

V

Vaidya, P. C., 16
Vallarta, M. S., 340, 341
van Albada, G. B. see Albada, G. B. van
van Lieshout, R. see Lieshout, R. van
Van Meersche, M., 231
Van Vleck, J. H., 143
Verde, M., 395
Verster, N. F., 154
Villars, F., 253
Vogell, W., 227
Volkoff, G. M., 239
von Arx, A. see Arx, A. von
von Hevesy, G., see Hevesy, G. von
von Klüber, H. see Klüber, H. von
von Ubisch, H. see Ubisch, H. von
von Weizsäcker, C. F. see Weizsäcker, C. F. von

W

Wäffler, H., 75, 87, 114, 120
Wagner, C. D., 233
Wagner, F., Jr., 299
Wagner, G., 102
Walcher, W., 233
Walchli, H., 239, 240
Waldvogel, P., 87
Walke, H. J., 11, 17
Walker, D., 125, 157, 178
Walker, R. L., 116, 118
Walkinshaw, W., 79, 88, 89
Wallace, P. R., 193
Walter, M., 130, 131, 137, 146, 147, 148, 149, 150, 151, 152, 155, 156, 157, 244
Walton, H. F., 232
Wanlass, S. D., 180, 181
Wapstra, A. H., 221, 312, 314
Ward, A. H., 157
Warren, R. E., 390
Warrington, P. M., 230
Warshaw, S. D., 277
Wataghin, G., 12
Watanabe, T., 223
Watase, Y., 145
Watson, K., 165, 172, 175, 178
Way, K., 7, 151, 314, 318, 319, 320, 321, 328, 329, 330, 331
Weaver, B., 291
Weaver, H. E., Jr., 239
Weber, N. E., 53
Weigl, J. W., 73, 230
Weinberger, A. J., 230
Weinhouse, S., 63
Weinstock, B., 225
Weiss, M. T., 234
Weisskopf, V. F., 130, 131, 137, 142, 153, 176, 239, 242, 247, 248, 253, 254
Weizäcker, C., 41
Weizsäcker, C. F. von, 11, 17, 351
Wells, W. H., 400
Wentzel, G., 169
Westervelt, D., 212, 216
Whaling, W., 221, 312
Wheeler, A., 231
Wheeler, J. A., 309, 312, 314, 315, 328
White, D., 224, 225
White, M. G., 285, 391
White, R. R., 223
White, R. S., 178
Whitehead, M. N., 165

Whitehouse, W. J., 384
Whitford, A. E., 18
Wick, G. C., 169, 177
Wickman, J. E., 72
Wideröe, R., 87
Wiedenbeck, M. L., 152, 153, 154, 155, 156
Wiedling, T., 155
Wiegand, C. E., 98, 101, 165, 166, 366, 367, 368, 369, 370, 372, 374, 402, 408
Wightman, A., 266, 267, 268
Wightman, A. S., 176
Wigner, E. P., 25, 133, 187, 231, 251, 280, 282, 287, 312, 380, 391, 394
Wiig, E. O., 102
Wilcox, H. A., 165
Wildt, R., 3
Wilet, L., 235
Wilkins, J. J., 111
Wilkinson, D. H., 75, 89, 119, 122
Willard, H. B., 81
Williams, A. H., 154
Williams, D., 239
Williams, H. J., 195, 216
Williams, J. H., 88, 386, 391, 392
Wilson, A. H., 11
Wilson, A. R. W., 244
Wilson, E. B., Jr., 226, 234
Wilson, E. D., 7
Wilson, J. G., 335, 340
Wilson, R., 165, 384
Wilson, R. R., 375, 386
Winckler, J. J., 336
Winsberg, L., 405
Winter, R. G., 262
Wirtz, K., 226
Witzig, W. F., 200
Wolfe, R. D., 408
Wolfenden, J. H., 232
Wolff, P., 86
Wolfgang, R. L., 63
Wood, M., 151, 318, 320, 321, 328, 329, 330, 331
Woodbury, E. J., 51
Woodruff, E. P., 336, 339
Woodward, W. M., 126
Woodyard, J. R., 80, 88
Woolley, H. W., 231
Worthington, H. R., 388, 391, 392
Worthington, W. J., Jr., 96, 97
Wright, B. T., 386
Wright, P. K., 401
Wright, S. C., 101, 102, 108, 126, 400, 402, 407
Wroe, D., 32, 33
Wu, C. S., 130, 137, 246, 276, 278, 289, 291, 299
Wu, T. Y., 376

Y

Yadav, H. H., 377
Yagoda, H., 8
Yamaguchi, Y., 99, 101, 250, 291
Yang, C. N., 135, 165, 174, 177, 243, 266
Yankwich, P. E., 229
Yasaitis, E., 239
Yasaki, T., 405
Yeates, M. L., 116, 120, 123
Yenicay, F. E., 79
Yntema, J. L., 391
Yodh, G. B., 172, 173
Yost, F. L., 391
Young, C. T., 243
Young, F. W., Jr., 205, 206, 207, 209
Yovits, M. C., 385, 386, 395
Yu, F. C., 239
Yuan, L. C. L., 65, 66, 68, 69, 394
Yuster, P., 211

Z

Zabel, C., 239
Zacharias, J. R., 239
Zaffarano, D. J., 278, 289
Zimmerman, E. J., 386
Zinnes, I., 140, 141
Zünti, W., 111, 131, 146, 147, 148, 149, 150, 151, 152, 155, 156, 157, 244, 272, 273

SUBJECT INDEX

A

Abundances, isobaric
  cosmic relative, 2-9
  equilibrium theories of, 12-17
  nonequilibrium theories of, 17-32
Abundances, isotopic
  equilibrium theories of, 9-17
  nonequilibrium theories of, 17-32
  systematics of, 6-8
  terrestial variation of, 3
  See also Elements, abundances of
Accelerators, 79-90
  miscellaneous types of, 89-90
  proton
    travelling-wave helix, 90
  See also Cosmotron; Cyclotrons; Kevatrons; Linear accelerators; Synchrocyclotrons
Allowed beta transitions, see Beta-decay
Alloys, metallic
  radiation effects in, 193-204
Alpha particles
  capture of, 54-55
  in cosmic radiation, 359
  directional correlation with, 138, 157
  fission induced by, 400-2, 407
  radiation damage from, 193-95
  See also Helium
Angular correlation, see Nuclear radiations
Anticoincidence technique in counting, 73
Antimony
  spallation by high energy deuterons, 96-97
Antimony^{122}
  gamma cascade of, 153
Antineutrinos, 261-64
Arsenic
  spallation by high energy deuterons, 94-96
Asymmetric core nuclear model, 251-52
Atmosphere
  carbon^{14} in, 63-70
  neutron flux in, 63-65
Atomic displacement, theory of, 188-89
Atomic spectra
  isotope effects in, 234-35
Atomic weights, error in, 222
Atoms, field strengths in, 143

B

Beryllium^{7}, in supernovae, 59
Beryllium^{10}, beta spectrum of, 291
Beryllium nuclei
  in primary cosmic rays, 8, 339, 359
  in stellar energy production, 47-48
Beta-decay, 261-301, 305-32
  allowed transitions in, 269-77
    half lives data for, 273-76
    l-forbidden in, 274-76
    nuclear shell effects, 275
    spectra of, 276-77
    theoretical results, 271-73
  and angular correlation data, 130, 139-40, 156
  a priori theoretical basis of, 264-71
  comparative half lives in, 245-46, 273-74, 286
  double, 262, 311
  energetics of, 305-32
  energies of isodiapheres in, 316-19
  energy discontinuities at shell edges, 315-28
  favored transitions in, 278-87
    comparative half lives of, 286
    quantitative results for, 282-87
    shell model and, 282
    supermultiplet theory of, 278-82
  Fermi theory of, 264-66
  Fierz interference terms, 272, 277
  forbidden transitions in, 269-70, 288-300
    once-forbidden, 292-99
    shape factor for, 288, 292
    unique transitions of, 288-91
  interaction energy density in, 261, 264-68
    Critchfield-Wigner hypothesis, 266
    Fermi assumption, 264-66
    Talhoek-de Groot hypothesis, 266-67
  Kurie plot in, 272
  and maximum stability charge, 310, 321-28
  nature of neutrino in, 261-64
  normal allowed transitions in, 274
  once-forbidden transitions in, 290, 292-99
    abnormal spectra of, 296-99
    half lives of, 292-93
    normal spectra of, 293-96
  in origin of elements, 22, 30
  parabolic energy surface and, 310-11
  prediction of total energy of, 331
  selection rules in, 246, 268-71
  and spin term of statistical model, 319-20, 331
  subshell evidence from, 325-26
  table of favored transitions, 278
  twice-forbidden transitions in, 299-300
  universal Fermi interaction and, 261, 267-68
Beta-gamma cascades, directional correlation in, 155-56
Beta spectra
  allowed, 276-77
  forbidden, 288-300
  See also Beta-decay
Betatrons, 84-87
  beam energy control in, 85
  increase in duty cycle of, 86
  injection process in, 85
  target developments in, 85-86
Binding energies

in beta-decay energetics, 309
and origin of nuclides, 9
Bismuth, fission of, 101-2
Bismuth^{210}, (RaE), beta spectrum of, 296-99
Boron^{10}, in neutron counter calibration, 66
Boron^{12}, beta-decay spectrum of, 277
Boron nuclei
in primary cosmic rays, 8, 339, 359
in stellar energy production, 47
Bremsstrahlung, in photonuclear reaction studies, 105-9, 117

C

Cadmium^{111}
gamma cascade of, 152, 155
magnetic moment of, 244
Cadmium difference, calculation of, 66-69
Calcium^{43}, (d, p) reaction for, 222
Carbon^{11}, method for proton beam calibration, 373-75
Carbon^{12}, photonuclear reactions in, 110-11, 115-16, 120
Carbon^{14}
absolute specific activity of, 76
beta-decay and nuclear shells, 275
counting techniques in measurement of, 74-76
exchange equilibrium of, 69-70
exchange reservoir of, 70
natural occurrence of, 63-76
natural production of, 63-76
in photosynthesis, 73
in shells, 71
specific activity in atmosphere, 64-70, 76
in various woods, 70-72
Carbon dioxide, in carbon^{14} natural distribution, 69
Carbon isotopes, fractionation in nature, 71-74
Carbon-Nitrogen cycle in stars, 50-52
effect of helium on, 53
Cascade DC generators, see Kevatrons
Cascades, double
in angular correlation studies, 129-57
Charge independence principle
and pion-nucleon system, 172-74
Chemical equilibria, isotope effects in, 226, 29
Chemical kinetics, isotope effects in, 229-32
Cobalt^{60}, magnetic moment of, 241
Cockroft-Walton DC generators, see Kevatrons
Coincidence measurements
in angular correlation studies, 146
spurious counts in, 150-51
Conductivity of interstellar space, 354
Conversion electrons, see Electrons, conversion; Internal conversion
Copper, proton spallation of, 95-96
Corrections, in angular correlation measurements, 146-51
Correlation, angular, see Nuclear radiations, angular correlation of
Cosmic rays, 335-62
alpha particles in, 359
background in C^{14} measurements, 74-76
Compton-Getting effect in, 340-41
energy density of, 346
energy spectrum of, 335-38, 357-61
extragalactic origin of, 346-47
and interstellar magnetic fields, 346-62
isotropy of, 340-41
mass spectrum of, 335-38, 357-61
neutron component in, 63-65, 76, 344-45, 357
origin of, 346-62
pressure of, 352
primary acceleration of, 353-57
primary radiation in elements of, 8, 336-38
properties of, 335-46
vertical intensity of, 338-39
propagation of, 352-57
radio fade outs and, 344-45
solar origin of, 345-47
sudden increases in, 341-46
time variations in, 340-46
Cosmogony, 1-34
Cosmological models
and matter creation theories, 33-34
in nonequilibrium theory of element origin, 17-19
Cosmotron, 84, 87
Counters
beta, 74-76
boron trifluoride
cosmic ray neutron measurements and, 66
in carbon^{14} determinations, 74-76
gas-sample, 74
G. M., in angular correlation measurements, 145-51
scintillation
in angular correlation experiments, 145-51
and radiation effects, 211-12
screen-wall type, 74
Counter telescopes, in cosmic ray research, 341
Cross section
fission, 399-404
nucleon-nucleon scattering, 365-95
for photonuclear reactions, 106-26
for pion scattering by hydrogen, 171
of thermonuclear reactions, 50-52
Crystal counters, see Counters, scintillation
Cyclotrons
advances in design of, 82
use in radiation damage research, 189
frequency modulated, see Synchrocyclotrons

D

Damage, radiation, see Radiation effects
Decarboxylation reactions, 229-30
Delta-rays, cosmic ray measurements and, 336-38
Detectors
in angular correlation experiments, 145-51
neutron, calibration of, 65-69
soft beta, 74-76
See also Counters
Deuterium, thermal properties of, 224-25
Deuterons
angular correlation in stripping of, 242-43
binding energy of, 384

fission induced by, 400, 402, 407
interaction with pions, 177-78
and nuclear forces, 379, 384-85, 394
photodisintegration of, 385, 394
photomagnetic capture cross section of, 384, 394
in proton-proton energy chain, 49-50
Diffusion in solids, radiation effects on, 200-1
Dipole photon absorption, see Photonuclear reactions
Directional correlation, see Nuclear radiations, directional correlation of
Displacement production, theory of, 188-89
Doublets, mass determination of, 221-22

E

Earth, abundances of elements in, 2-9
Electrical resistivity, radiation effects on, 196-97, 204-9
Electrodynamics, cosmical, 347-52
Electromagnetic radiation
and betatron beam energy loss, 86
emission by stars of, 41-44
Electron loading, in electrostatic generators, 81
Electrons
corrections for scattering of, 149-51
conversion
directional correlation and, 138-39, 155-57
Electrostatic generators, 80-82
electron loading in, 81
Elements
abundance distribution of, 1-34
abundance distribution in nebulae, 3
cosmic relative abundance of, 2-9
equilibrium theories of origin of, 9-17
formation in stellar models, 13-16
heavy, origin of, 59
neutron capture theory of origin of, 19-32
nonequilibrium theories of origin, 17-32
origin of, 1-34
and beta-decay, 22, 30
polyneutron theory of origin of, 32-33
stellar abundance of, 2-9
Endothermic reactions in supernovae, 58-59
Energy production in stars, 41-61
Energy of beta-decay processes, 305-32
Equilibrium theories of element formation, 9-17
effect of excited states on, 13
stellar models for, 13
Exchange equilibria, in C^{14} occurrence, 69-70
Expanding universe, see Cosmological models
Extranuclear fields
in angular correlation studies, 141-44
table of values for, 143

F

Fermi interaction, 261
Fermi plot, 272
Fermi theory of beta-decay, 264-66
Fission
alpha particle induced, 400, 402, 407
deuteron induced, 400, 402, 407
of heavy elements, 399-401, 404-8
by high energy particles, 100-2, 399-409
of medium heavy elements, 401-4, 407-9
modes of, 404-9
neutron emission in, 407-8
neutron induced, 399, 404-6
of polyneutrons, 32-33
positron-emitting fragments in, 407
and spallation reactions, 402-3
symmetrical vs. asymmetrical, 405-9
yields, 405-9
Forbidden beta transitions, see Beta-decay
Fusion, see Thermonuclear reactions

G

Gamma rays
betatron production of, 85
calibration of beam monitor, 107
directional correlation of, 136-38, 152-57
and photoproduction of pions, 171, 174-76
polarization correlation in, 140-41
spallation induced by, 100
and spurious coincidences, 149-51
See also Photonuclear reactions
Gas, interstellar, 347-52
Geomagnetism, cosmic rays and, 336-37
Geometry, in coincidence detection, 148-49
Germanium
atomic weight of, 222
See also Semiconductors
Glass, radiation effects in, 211-12
Gravitation, contraction as energy source, 41, 44-46, 54-59
Group theory, use in angular correlation theory, 135

H

Hafnium^{177}, gamma cascade of, 154
Heavy water, properties of, 225-26
Helium
beryllium^{7} formation in supernovae, 59
conversion into carbon of, 54-55
in hydrogen depleted stars, 54
in stellar energy production, 46-57
Helium^{3}, properties of, 225-35
Helium^{4}
photodisintegration of, 113
see also Alpha particles
Helium^{6}, beta-decay spectrum of, 277
High energy reactions, 93-102
secondary reactions in, 102
Hydrogen
in carbon-nitrogen cycle, 50-52
exhaustion in stars of, 53-55
mean lifetime in stars, 48
ortho-para conversion in, 224, 231
photochlorination of, 230-31
thermal properties of, 224-25
Hyperfine structure, 235
anomaly in, 253-54

I

Independent particle model of nucleus, 248-56

asymmetric core modification in, 251-53
and hyperfine structure anomaly, 254
nucleon moment quenching hypothesis and, 252-53
Infrared spectroscopy, 223
Insulators, radiation effects on, 192, 211-15
Internal conversion
directional correlation and, 138-39, 156
in isomeric transitions, 246-48
Ion source, for negative hydrogen ions, 80
Ionized gases, and plasma, 347-52
Isobaric triads, 278-79
Isobars, Wigner or mirror, 278
Isodiapheres, 318
beta-decay energies of, 316-19
Isomers, nuclear
transitions of, 246-48
classification of, 247
and nuclear moments, 246-48
Isotopes, 221-35
abundances of, 222-23
atomic spectra effects of, 234-35
chemical equilibria effects of, 226-29
chemical kinetics effects of, 229-32
exchange equilibria of, 226-29
mass measurements of, 221-22
mass spectra effects of, 232-34
molecular spectra effects of, 234-35
phase equilibria effects of, 224-26
separation of, 223-24

K

K-capture, in angular correlation studies, 142-44
Kevatrons, 79-80
voltage doubling technique for, 80
Kurie plot, 272

L

Lattice disturbances, see Radiation effects
Lead, isotope abundances of, 6
Lead^{204}, gamma cascade of, 153
Lifetimes, nuclear
from angular correlation data, 130, 141-42, 147, 157
in beta-decay, 245-46, 273-74, 286
Light elements
origin of, 27-31, 33
in photonuclear process, 119-20
Linear accelerators, electron, 88-89
progress in construction of, 89
wave guide developments in, 89
Linear accelerators, proton, 87-88
focusing developments in, 88
Liquid drop model of nucleus, 309-10, 400
discrepancies in Fermi parameters for, 312
pairing term in, 309-10, 320, 331
shell closure effects, 314-15
Lithium, use as beam energy absorbers, 366-69
Lithium nuclei
in primary cosmic rays, 8, 339, 359
in stellar energy production, 47
Luminosity, stellar, 42-44

M

Magic numbers, see Nuclear shells
Magnetic fields
cosmic, 347-52
effect on directional correlation, 144
Magnetic moments, nuclear
in angular correlation studies, 143-44
and pion-nuclear model, 169-70
table for odd-odd nuclei, 255
Magnet design for Synchrocyclotrons, 83
Main sequence stars, 43-60
Marine animals, oxygen^{18} content of, 228-29
Mass, of isotopes, 221-22
Mass spectra, isotope effects in, 232-34
Matter creation theory, 33-34
Maxwellian distribution, in nuclear reaction calculations, 53
Mechanical properties, radiation effects on, 197-200
Mercury, meson induced fission of, 403
Mesons
fission induced by, 401, 403
in high energy photonuclear reactions, 124
in nucleon-nucleon interaction, 382-83, 394
κ-Mesons, 182
μ-Mesons, see Muons
π-Mesons, see Pions
τ-Mesons, 179-80
Metals
angular correlation in, 144
radiation effects in, 192-204
Meteorites, element abundances in, 2-9
Mirror isobars, 278
Molecular solids, radiation effects in, 192, 215-16
Molecular spectra, isotope effects in, 234-35
Molecular structure, isotope exchange and, 226-35
Muons
and universal Fermi interaction, 261, 267
See also Pions, decay of

N

Nebulae, element abundances in, 3
Neptunium, high energy fission of, 399
Neutrinos, 261-64, 305, 311
in stellar energy loss, 58
Neutron-proton scattering, 365-95
Neutrons
in atmosphere, 63-65
beta-decay of, 284
BF_3 counter calibration for, 66
binding energies of, 318
capture cross section data, 19, 22
in cosmic rays, 344-45, 357
and carbon^{14} production, 63-65
cosmogony and capture of, 19-32
emitted in fission, 407-8
excess in abundant nuclides, 8
fission with, 399, 401, 404-6
kevatron sources of, 79
magnetic moment of
and pion-nucleor model, 169-70
moderation in nitrogen of,

68
from photoexcited nuclei, 121
and radiation effects, 189
yield in photonuclear reactions, 117-19, 124-25
see also Polyneutron
Nickel^{60}, gamma cascade of, 153, 155
Nitrogen, moderation of neutrons by, 68
Nitrogen^{14}
in carbon^{14} production, 66-69
photonuclear reactions on, 110-11, 115-16
Nitrogen, see also Carbon-Nitrogen cycle in stars
Nonequilibrium theories of element formation, 17-32
Novae, 57
Nuclear excitation, photo absorption and, 119-22
Nuclear forces
charge independence of, 378, 380-83
in favored beta-transitions, 279
in nucleon-nucleon scattering, 376-87, 390-95
parameters of, 383-85
pion-nucleor interaction and, 168-70, 178-79
repulsive core potential, 380-83
Nuclear isomerism, see Isomers, nuclear
Nuclear levels
in angular correlation theory, 131-44
lifetime measurements of, 130, 141-42, 147, 157
Nuclear masses, liquid-drop model and, 312
Nuclear models
in decay of photoexcited nuclei, 120-21
in photonuclear reactions, 112-13, 118, 123
Nuclear moments, 239-56
and angular correlation data, 241-44
asymmetric core hypothesis and, 251-53
from beta-decay spectra, 244-46
and hyperfine structure anomaly, 253-54
and independent particle model, 248-56
in odd-odd nuclei, 254-56
Schmidt curves and, 250-51
of unstable nuclear states, 240-48
Nuclear photoeffect, see Photonuclear reactions
Nuclear radiations
angular correlation of, 129-58
data from, 130-31, 151-57
in deuteron stripping reactions, 242-43
extranuclear field effects on, 141-44
free nucleus theory for, 136-41
in gamma cascades, 154-55
Hamilton's theory of, 132-34
method and apparatus, 145-51
moment measurements and, 241-45
in successive decays, 243-44
theory of, 131-44
directional correlation of
for alpha particles, 138, 157
in beta-gamma cascades, 139-40, 155-56
electron shell effects in, 152-53
experimental corrections in, 151
in gamma cascades, 136-38, 152-55
magnetic field effects on, 144
measurement of, 151
table of data on, 156
from polarized nuclei, 241
Nuclear reactions
angular correlation in, 241-43
induced by high energy particles, 93-102
low energy types of, 93-94
spallation, 94-100
stellar and terrestial, 60
Nuclear reactors, see Reactors, nuclear
Nuclear resonance levels, thermonuclear reactions and, 51-52
Nuclear shells, 248-50, 307-8
and cosmic abundance data, 6-8
discontinuities in beta-decay energy and, 315-28
energetics of, 326-28
evidence for subshells in, 325-26
experimental data on, 222
and favored beta-transitions, 282
and forbidden beta-transitions, 275
neutron capture data and, 21, 31
and once-forbidden beta-transitions, 292
order of energy levels in, 249
term diagram for, 307
Nuclear spins, see Spins, nuclear
Nuclear stability
and origin of nuclides, 6-9
and spallation yields, 95-100
Nuclear states
in angular correlation theory, 131-44
supermultiplet theory and, 278-82
see also Isomers, nuclear
Nuclei, origin of, 1-35
Nucleon-nucleon interaction
and pions, 176-77
scattering, 365-95
angular isotropy of, 366, 383
calculation methods, 395
high energy data, 366-83
interaction potentials for, 375-83
interpretation for high energies, 376-83
low energy data, 383-95
phenomenological treatments of, 394
Nucleon-photon interaction, 114
Nucleon-pion interaction, 167-79
Nucleons
evaporation in spallation, 99
excited states of, 168-69
photoproduction of pions from, 171, 174-76
Nucleor, 168

O

Ocean, bicarbonate in, 69-70
Optical properties, radiation effects on, 210-12, 216
Order-disorder alloys, radiation effects on, 193-95, 203
Organic compounds, carbon isotopes effects in, 229-30, 232-34
Oxygen^{16}, photonuclear reactions in, 110-11, 115-16
Oxygen^{18}, terrestial variation of, 222-23, 228-29

P

Pair spectrometer, photon flux calibration with, 107
Paleotemperature research, 228-29
Palladium^{106}, gamma cascade of, 152-53
Paraffins, protio and deutero, 233
Phase equilibria, isotope effects in, 224-26
Photochlorination of hydrogen, 230-31
Photofission
  of heavy elements, 400, 408
  of medium heavy elements, 402
Photographic plates
  and cosmic ray studies, 336-38
  in cyclotron beam measurements, 374-75
  fission measurements with, 401
  in photonuclear reaction research, 111, 119-21
  in pion studies, 164, 166
  in spallation studies, 100
Photoneutrons, betatron production of, 85
Photosynthesis, and carbon^{14} studies, 73
Photonuclear reactions, 105-26
  in carbon^{12}, 110-11, 115-16, 120
  cross section calculation for, 105-9
    photon difference method, 106-7
    total spectrum method, 106-7
    transition curve method, 109
  decay of photoexcited nucleus in, 119-22
  dipole resonance absorption in, 112-13
  effective photon energy in, 107-9
  energies of, 105-9, 115-17
  experimental techniques for, 105-9
  with high energy photons, 122-26
  high order reactions in, 122-24
  low energy region of, 109-22
  multiple bombardment methods in, 106-7
  neutron yields in, 117-19, 124-25
  nuclear photoeffect in, 113-14
  photoneutron reactions, 114-19
  photoproton reactions, 114-17, 119, 125-26
  photo stars in, 124
  proton yield in, 119
  quadrupole absorption in, 110-11
  resonance effects in, 117, 123
  single bombardment method in, 107-9
  table of (γ, n) reactions, 108, 114-17
  table of (γ, p) reactions, 109, 114-17
Piles, see Reactors, nuclear
Pions
  charge independence principle and, 172-74
  decay of, 167-67
  fission induced by, 401, 403
  interaction with nucleor, 168-70
  interaction with single nucleon, 170-76
  interaction with two nucleons, 177-78
  masses of, 164
  and nucleon magnetic moment, 169-70
  and nucleon-nucleon interaction, 176-77
  parity of, 164-65
  photoproduction of, 171, 174-76, 178
  scattering in hydrogen, 170-72
  scattering on deuterons, 177-78
  spin of, 164-65
Plasma, cosmic magnetic fields and, 347-52
Plutonium, fission of, 400, 405
Polarization correlation, see Nuclear radiations, angular correlation of
Polyethylene, in scattering experiments, 366-70, 374
Polymers, radiation effects on, 215-16
Polyneutron, theory of fission of, 32-33
Polystyrene, in scattering experiments, 374
Positrons
  in angular correlation experiments, 147
  from fission fragments, 407
Potassium^{40}, beta spectrum of, 291
Potential fitting for p,p data, 386
Potentials
  Rarita-Schwinger classification of, 375-76
  repulsive core type, 380-83
Prometheum^{147}, beta spectrum of, 290, 293
Proton-neutron scattering, 365-95
Proton-proton chain, stellar energy production and, 48-53
Proton-proton scattering, 365-95
  corrections in low energy measurements, 388-90
  high energy data on, 366-75
  low energy data on, 385-94
  see also Nucleon-nucleon scattering
Protons
  beam measurement by C^{11} method, 373-75
  capture reactions in stars, 47
  in decay of photoexcited nuclei, 121
  fission induced by, 401-3, 406
  isomeric state of, 383
  in primary cosmic rays, 64-65, 336-37
  scattering of thermal neutrons by, 384
  yield in photonuclear reactions, 119, 125-26
  see also Hydrogen
Proton synchrotron, see Cosmotron

Q

Quadrupole photon absorption, see Photonuclear reactions
Quartz, radiation effects on, 212-15

R

Radiation effects
  atomic displacement theory in, 188-89
  cold work analogy in, 190-91
  on creep, 200
  and crystal structure of metals, 193-96
  on diffusion rates, 200-1
  in glass systems, 211-12
  in insulators, 192, 211-15
  interstitials and vacancies in, 190
  kinetic studies of, 191, 200-4

in metals, 192-204
in molecular solids, 192, 215-16
on optical properties, 210-12, 216
in order-disorder alloys, 193-95, 203
on polymers, 215-16
in precipitation-hardening alloys, 195
rate processes and, 191, 200-4
in semiconductors, 192, 204-11
in solids, 187-216
electrical properties and, 196-97
mechanical properties and, 197-200
physical properties and, 189-90
research summary of, 191-93
surface effects in, 212
on thermal properties, 212-15
thermal spike concept in, 188, 191
unit displacement energy in, 188
Radio, fade outs of, 344-45
Radio telescopes, in cosmic ray research, 344, 361
Radioactive sources
critical thickness of, 149-50
preparation of, 146
Radiocarbon, see $Carbon^{14}$
Radiochemistry
in fission studies, 402-4
in spallation studies, 100
Radium E, beta spectrum of, 296-99
Rare earths, isotope shifts in, 235
Rate processes, radiation effects and, 191, 200-4
Reactors, nuclear in radiation effects research, 200
Red giant stars, energy production in, 56-57
Resolving time, of coincidence circuits, 147-48
Resonance effects, in photonuclear reactions, 117, 123
Rubidium^{86}, gamma cascade of, 153

S

Scattering
experimental corrections for, 149-51
nucleon-nucleon, 365-95
Schmidt limits, 251
Scintillation spectrometers, in angular correlation experiments, 150
Selection rulse, in beta-decay, 268-71
Semiconductors, radiation effects in, 192, 204-11
Separation of isotopes, 223-24
Shielded nuclear species, 8, 31
Solar flares
cosmic ray intensity and, 343-45
cosmic ray neutrons and, 65
Solids
directional correlation of radiations in, 143, 152-54
field strengths in, 143
radiation effects in, 187-216
Solid-state physics, see also Radiation effects
Space charge, in a plasma, 347
Spallation, 94-100
and compound nucleus concept, 97-98
and fission, 100-2, 402-3
and "hit and run" model, 97-98
by photons, 100
yields of, 99-100
Spectrograph, magnetic, 146-150
Spectrometry, mass, 221-23
Spins, nuclear
from cross section at resonance, 242
table for odd-odd nuclei, 255
Stable nuclei, occurrence of, 311-15
Stars
carbon-nitrogen cycle in, 50-52
Chandrasekhar limit in, 46, 54-55
with convective core, 45-46
element abundances in, 2-9
empiral data on, 42-44
energy production in, 41-61
equilibrium relations in, 53-55
main sequence
energy production in, 52-53
properties of, 43-44
novae, 57
proton-proton chain in, 48-50
red giants, energy production in, 56-57
structure of, 44-46
supernovae, 57-59
surface composition of, 44
thermonuclear reactions in, 46-52
variable, 57
white dwarfs, energy production in, 55-56
Stars, nuclear
photon production of, 124
in spallation reactions, 100
Statistical theory of nucleus, see Liquid-drop model
Stellar models, 13-16
Subnuclear particles, 163-83
see also, K-Mesons, Pions, τ-Mesons, V-particles
Sun
cosmic rays and spots on, 344-47, 355-57
energy production in, 52
Superconductivity of separated isotopes, 226
Supermultiplet theory, 278-82
Supernovae, energy production in, 57-59
Synchrocyclotrons, 83-84
beam energy control in, 366-69
beam extractor development, 84
internal target effects, 83
primary beam measurement in, 366-68, 373-75
reduction in magnet cost for, 83-84
use in scattering research, 366-75
Synchrotrons, electron, 87
beam extraction in, 86
see also Betatrons
Systematics, beta-decay, 305-32

T

Thermal diffusion, isotope separation and, 223
Thermal properties
of hydrogen, 224-25
radiation effects on, 212-15
Thermal spikes, 188, 191
Thermonuclear reactions
effect on element abundances of, 3, 6, 29

rate of, 47, 50
Maxwell distribution effects, 53
in stars, 46-53
Thorium, fission of, 400, 407
Thorium^{228} (RdTh), gamma cascade of, 153
Three body problem, 395
Thulium^{170}, gamma cascade of, 153
Trees, carbon^{14} in, 71
Triads, isobaric, 278-79
Tritium, thermal properties of, 224-25
Turbulence, in interstellar gas, 349-52

U

Ultrasonic radiation, effect on exchange, 232
Universe, origin of, 1-34
Uranium
charged particle fission of, 399-401, 404-7
disproportionation in water, 231
high energy fission of, 399-401, 404-7
isotope shift in, 235
meson induced fission of, 401
photofission of, 400
Urca process, in supernovae, 58

V

Van de Graaff generators, see Electrostatic generators
Variable stars, energy production in, 57
V-particles, 180-81

W

White dwarf stars, energy production in, 55-56
Wood, carbon^{14} in, 70-72

X

Xenon^{131}, gamma cascade in, 154

Y

Yttrium^{91}, beta spectrum of, 289-90

Z

Zinc, spallation of, 96-97